

# 2006 Atomic, Molecular, Optical Sciences Research Meeting



**Airlie Conference Center  
Warrenton, Virginia  
September 10-13, 2006**



**Sponsored by:  
U.S. Department of Energy  
Office of Basic Energy Sciences  
Chemical Sciences, Geosciences & Biosciences Division**

**Cover Art Courtesy of Diane Marceau  
Chemical Sciences, Geosciences and Biosciences  
Division, Basic Energy Sciences, DOE**

**This document was produced under contract number DE-AC05-06OR23100  
between the U.S. Department of Energy and Oak Ridge Associated Universities.**

## Foreword

This volume summarizes the 2006 Research Meeting of the Atomic, Molecular and Optical Sciences (AMOS) Program sponsored by the U. S. Department of Energy (DOE), Office of Basic Energy Sciences (BES), and comprises descriptions of all of the current research sponsored by the AMOS program. The research meeting is held annually for the DOE laboratory and university principal investigators within the BES AMOS Program in order to facilitate scientific interchange among the PIs and to promote a sense of program identity.

In addition to presentations by our principal investigators, we have continued our tradition of inviting distinguished plenary speakers. Ned Sauthoff from Oak Ridge National Laboratory and Daren Stotler from the Princeton Plasma Physics Laboratory will join us to speak about the ITER project and related scientific challenges. We gratefully acknowledge the contributions of all of this year's speakers.

Despite perennial budget uncertainty, the BES/AMOS program continues to be vibrant and forward moving, thanks to our scientists and the outstanding research they perform. We were pleased to be able to initiate three new grants in the past year enhancing the program in areas of ultrafast chemical imaging using high field phenomena. Developments at two new ultrafast laboratory centers at Lawrence Berkeley and Stanford are presented for the first time in this volume. Many of our principal investigators have been involved in planning research and instrumentation for the Linac Coherent Light Source. Our community was central in shaping the recently released NAS study "AMO 2010: Controlling the Quantum World," which offers a compelling vision for AMO science.

We are indebted to all of the members of the scientific community who have contributed valuable time toward the review of proposals and programs, either by mail review of grant applications or on-site reviews of multi-PI programs. These thorough and thoughtful reviews have been central to the continued vitality the AMOS Program.

Thanks also to the staff of the Oak Ridge Institute for Science and Education, in particular Sophia Kitts, and Angie Lester, and to the Airlie Conference Center for assisting with the meeting. We thank our colleagues in the Chemical Sciences, Biosciences, and Geosciences Division - Diane Marceau, Robin Felder, and Michaelena Kyler-King - for indispensable behind-the-scenes efforts in support of the BES/AMOS program. Special thanks go to Diane for the beautiful photograph gracing our cover.

Michael P. Casassa  
Richard Hilderbrandt  
Eric A. Rohlfing  
Chemical Sciences, Geosciences and Biosciences Division  
Office of Basic Energy Sciences  
Department of Energy



# *Agenda*



**2006 Meeting of the Atomic, Molecular and Optical Sciences Program**  
**Office of Basic Energy Sciences**  
**U. S. Department of Energy**

**Airlie Center, Warrenton, Virginia, September 10-13, 2006**

**Sunday, September 10**

3:00-6:00 pm      \*\*\*\* Registration \*\*\*\*  
6:00 pm            \*\*\*\* Reception (Pub, No Host) \*\*\*\*  
7:00 pm            \*\*\*\* Dinner \*\*\*\*

**Monday, September 11**

7:00 am            \*\*\*\* Breakfast \*\*\*\*

8:00 am            *Welcome and Introductory Remarks*  
**Michael Casassa** BES/DOE

**Session I**            Chair: Dave Schultz

\*\*\*\* Plenary Talks \*\*\*\*

8:15 am            *The ITER Project*  
**Ned Sauthoff**, U.S. ITER Project Office, Oak Ridge National  
Laboratory

9:15 am            *Atomic Physics in ITER*  
**Daren Stotler**, Princeton Plasma Physics Laboratory

10:15 am            \*\*\*\* Break \*\*\*\*

10:45 am            *Low-Energy Ion-Surface Interactions*  
**Fred Meyer**, Oak Ridge National Laboratory

11:15 am            *Study of Ions Transmitted Through an Anodic Nanocapillary Array*  
**Herb Krause**, Oak Ridge National Laboratory

11:45 am            *Electron-Molecular Ion Interactions*  
**Mark Bannister**, Oak Ridge National Laboratory

12:15 pm            \*\*\*\* Lunch \*\*\*\*

**Session II**

Chair: Ali Belkacem

5:00 pm

*Ion Properties from Rydberg Fine Structure Studies:  
Eyes on the Actinides***Stephen Lundeen**, Colorado State University

5:30 pm

*Inner-Shell Electron Spectroscopy and Chemical Properties of  
Atoms and Small Molecules***Darrah Thomas**, Oregon State University

6:00 pm

\*\*\*\* Reception (Roof Terrace, No Host) \*\*\*\*

6:30 pm

\*\*\*\* Dinner \*\*\*\*

**Session III**

Chair: Ann Orel

7:30 pm

*Electron-Driven Processes in Polyatomic Molecules***Vincent McKoy**, California Institute of Technology

8:00 pm

*Giant Resonances in Photoionization of Ions:**Making Electrons Dance in Unison***Ronald Phaneuf**, University of Nevada, Reno**Tuesday, September 12**

7:00 am

\*\*\*\* Breakfast \*\*\*\*

**Session IV**

Chair: John Doyle

8:00 am

*Chemistry with Ultracold Molecules***Dudley Herschbach**, Harvard University

8:30 am

*Experiments in Ultracold Collisions***Phillip Gould**, University of Connecticut

9:00 am

*Formation of Ultracold Molecules***Robin Côté**, University of Connecticut

9:30 am

*Towards Ultra-Cold Molecules – Laser Cooling and Magnetic  
Trapping of Neutral, Ground-State, Polar Molecules for Collision  
Studies***Jun Ye**, University of Colorado, JILA

10:00 am

\*\*\*\* Break \*\*\*\*

10:30 am

*Exploiting Universality in Atoms with Large Scattering Lengths***Eric Braaten**, Ohio State University

11:00 am

*Quantum Dynamics of a Strongly-Interacting Fermi Gas***John Thomas**, Duke University

11:30 am

*Bose-Fermi Mixtures Near an Interspecies Feshbach Resonance***John Bohn**, University of Colorado, JILA

Noon

\*\*\*\* Lunch \*\*\*\*

**Session V**

Chair: Chandra Raman

4:30 pm

*Exploring Quantum Degenerate Bose-Fermi Mixtures*

**Deborah Jin**, University of Colorado, JILA

5:00 pm

*Cold Rydberg Atom Gases and Plasmas in Strong Magnetic Fields*

**Georg Raithel**, University of Michigan

5:30 pm

*Population Dynamics in Coherent Excitation of Cold Atoms*

**Brett DePaola**, Kansas State University

6:00 pm

\*\*\*\* Reception (Pavilion, No Host) \*\*\*\*

6:30 pm

\*\*\*\* Banquet (Pavilion) \*\*\*\*

**Wednesday, September 13**

7:00 am

\*\*\*\* Breakfast \*\*\*\*

**Session VI**

Chair: Lou DiMauro

8:30 am

*Development and Characterization of Replicable Tabletop*

*Ultrashort Pulse X-ray Sources for Chemical Dynamics Research*

**Christoph Rose-Petruck**, Brown University

9:00 am

*Monitoring Molecular Vibrations using Coherent Electrons  
from High-Harmonic Generation*

**Henry Kapteyn and Margaret Murnane**,

University of Colorado, JILA

9:30 am

*New Directions in Intense-Laser Alignment*

**Tamar Seideman**, Northwestern University

10:00 am

\*\*\*\* Break \*\*\*\*

10:30 am

*X-Ray Microprobe of Optical Strong-Field Processes*

**Linda Young**, Argonne National Laboratory

11:00 am

*Physics of Correlated Systems*

**Chris Greene**, University of Colorado, JILA

11:30 am

*Time-Dependent Treatment of Three-Body Systems in Intense  
Laser Fields*

**Brett Esry**, Kansas State University

Noon

*Closing Remarks*

**Michael Casassa** BES/DOE

12:10 pm

\*\*\*\* Lunch \*\*\*\*



# *Table of Contents*



## Invited Presentations (Ordered by Agenda)

The ITER Project <b>Ned Sauthoff</b> .....	1
<i>Atomic Physics in ITER – The Foundation for the Next Step to Fusion Power</i> <b>D. P. Stotler</b> .....	2
<i>Low Energy Chemical Sputtering of ATJ Graphite and HOPG by Atomic and Molecular D Projectiles</i> <b>F. W. Meyer</b> .....	3
<i>Study of Ions Transmitted Through an Anodic Nanocapillary Array</i> <b>Herb Krause</b> .....	4
<i>Electron-Molecular Ion Fragmentation</i> <b>M. E. Bannister</b> .....	7
<i>Inner-shell Electron Spectroscopy and Chemical Properties of Atoms and Small Molecules</i> <b>T. Darrah Thomas</b> .....	11
<i>Electron-Driven Processes in Polyatomic Molecules</i> <b>Vincent McKoy</b> .....	15
<i>Energetic Photon and Electron Interactions with Positive Ions</i> <b>Ronald A. Phaneuf</b> .....	19
<i>Slowing and Cooling Molecules via a Counter-Rotating Supersonic Nozzle</i> <b>Dudley Herschbach</b> .....	23
<i>Experiments in Ultracold Collisions</i> <b>Phillip L. Gould</b> .....	25
<i>Formation of Ultracold Molecules</i> <b>Robin Côté</b> .....	28
<i>Cold Molecules : Laser cooling and Magnetic Trapping of Neutral, Ground-state, Polar Molecules for Collision Studies</i> <b>Jun Ye</b> .....	32
<i>Exploiting Universality in Atoms with Large Scattering Lengths</i> <b>Eric Braaten</b> .....	34

<i>Quantum Dynamics of Optically-Trapped Fermi Gases</i> <b>John E. Thomas</b> .....	37
<i>Strongly Interacting Bose and Fermi Gases</i> <b>John L. Bohn</b> .....	41
<i>Exploring Quantum Degenerate Bose-Fermi Mixtures</i> <b>Deborah Jin</b> .....	44
<i>Cold Rydberg Atom Gases and Plasmas in Strong Magnetic Fields</i> <b>G. Raithel</b> .....	48
<i>Population Dynamics in Coherent Excitation of Cold Atoms</i> <b>B. D. DePaola</b> .....	52
<i>Development and Characterization of Replicable Tabletop Ultrashort Pulse X-ray Sources for Chemical Dynamics Research</i> <b>Christoph G. Rose-Petruck</b> .....	56
<i>Ultrafast Atomic and Molecular Optics at Short Wavelengths</i> <b>Henry C. Kapteyn and Margaret M. Murnane</b> .....	60
<i>New Directions in Intense-Laser Alignment</i> <b>Tamar Seideman</b> .....	63
<i>X-ray Microprobe of Optical Strong-Field Processes</i> <b>L. Young</b> .....	67
<i>Physics of Correlated Systems</i> <b>Chris H. Greene</b> .....	68
<i>Time-Dependent Treatment of Three-Body Systems in Intense Laser Fields</i> <b>B. D. Esry</b> .....	72

## **Laboratory Research Summaries (by institution)**

<b>AMO Physics at Argonne National Laboratory</b> .....	76
<i>X-Ray Microprobe of Optical Strong-Field Ionization Dynamics in Atoms</i> <b>Linda Young</b> .....	76
<i>Collective Behavior in Laser-Generated Plasmas</i> <b>E. P. Kanter</b> .....	77

<i>Photoionization of Laser-Aligned Molecules</i> <b>S. H. Southworth</b> .....	78
<i>Inner-Shell Decay Processes</i> <b>R. W. Dunford</b> .....	79
<i>Nondipolar Photoelectron Angular Distribution in Atoms and Molecules</i> <b>B. Krässig</b> .....	80
<i>Towards a Quantitative Understanding of High-Harmonic Generation</i> <b>R. Santra</b> .....	81
<i>Theory of X-ray Microprobe of strong-Field Processes</i> <b>R. Santra</b> .....	82
<b>Overview of J. R. Macdonald Laboratory Program for Atomic, Molecular, and Optical Physics</b> .....	87
<i>Structure and Dynamics of Atoms, Ions, Molecules, and Surfaces: Molecular Dynamics with Ion and Laser Beams</i> <b>Itzik Ben-Itzhak</b> .....	88
<i>Stabilizing the Carrier-Envelope Phase of the Kansas Light Source</i> <b>Zenghu Chang</b> .....	92
<i>Structure and Dynamics of Atoms, Ions, Molecules and Surfaces: Atomic Physics with Ion Beams, Lasers and Synchrotron Radiation</i> <b>C.L. Cocke</b> .....	96
<i>Theoretical Studies of Interactions of Atoms, Molecules and Surfaces</i> <b>C. D. Lin</b> .....	100
<i>COLTRIMS Studies of Strong-Field Laser-Matter Interactions</i> <b>I. V. Litvinyuk</b> .....	104
<i>Electronic Excitations and Dynamics in Carbon Nanotubes Induced by Femtosecond Pump-Probe LASER Pulses</i> <b>Pat Richard</b> .....	108
<i>Structure and Dynamics of Atoms, Ions, Molecules, and Surfaces: Atomic Physics with Ion Beams, Lasers and Synchrotron Radiation</i> <b>Uwe Thumm</b> .....	112

<b>Atomic, Molecular and Optical Science at Los Alamos National Laboratory.....</b>	<b>114</b>
<i>Multiparticle Processes and Interfacial Interactions in Nanoscale Systems Built from Nanocrystal Quantum Dots</i>	
<b>Victor Klimov .....</b>	<b>114</b>
<b>Atomic, Molecular and Optical Sciences at Lawrence Berkeley National Laboratory.....</b>	<b>118</b>
<i>Ultrafast X-ray Science Laboratory</i>	
<b>Ali Belkacem.....</b>	<b>119</b>
<i>Inner-Shell Photoionization of Atoms and Small Molecules</i>	
<b>Ali Belkacem.....</b>	<b>122.1</b>
<i>Electron-Atom and Electron-Molecule Collision Processes</i>	
<b>T. N. Resigno .....</b>	<b>123</b>
<i>Femtosecond X-ray Beamline for Studies of Structural Dynamics</i>	
<b>Robert W. Schoenlein.....</b>	<b>127</b>
<b>Atomic and Molecular Physics Research at Oak Ridge National Laboratory.....</b>	<b>131</b>
<i>The MIRF Upgrade Project</i>	
<b>Fred W. Meyer .....</b>	<b>131</b>
<i>Low-Energy Ion-Surface Interactions</i>	
<b>F. W. Meyer .....</b>	<b>132</b>
<i>Low-Energy Charge Exchange using the Upgraded Ion-Atom Merged-Beams Apparatu</i>	
<b>C. C. Havener .....</b>	<b>133</b>
<i>Electron-Molecular Ion Interactions</i>	
<b>M. E. Bannister .....</b>	<b>134</b>
<i>Grazing Surface Studies at Intermediate Energy</i>	
<b>H. F. Krause.....</b>	<b>136</b>
<i>Atomic Ion-Atom and Molecular Ion-Atom Electron Transfer</i>	
<b>C.R.Vane.....</b>	<b>137</b>

<i>Ion Beam Characterization and Preparation End Station</i> <b>C. R. Vane</b> .....	139
<i>Chemical Sputtering of Hydrocarbons by D and D2 Impact at Deuterated Carbon</i> <b>P.S. Krstic</b> .....	140
<i>Engineering High-n Rydberg States with Tailored Pulses</i> <b>C. O. Reinhold</b> .....	141
<i>Capture, Ionization, and Transport of Electronic States of Fast Ions Penetrating Solids</i> <b>C. O. Reinhold</b> .....	141
<i>Development of the LTDSE Method for Atomic Collisions and New Molecular Collision Calculations for Cool Plasmas</i> <b>D. R. Schultz</b> .....	142
<i>Computation of Sturmian States for <math>H_2^+</math>-Like Ions</i> <b>J. H. Macek</b> .....	142
<b>PULSE: The Stanford Photon Ultrafast Laser Science and Engineering Center</b> .....	148
<i>Structural Dynamics in Chemical Systems</i> <b>Kelly J. Gaffney</b> .....	151
 <b>University Research Summaries (by PI)</b>	
<i>Properties of Transition Metal Atoms and Ions</i> <b>Donald R. Beck</b> .....	155
<i>Molecular Structure and Electron-Driven Dissociation and Ionization</i> <b>Kurt H. Becker</b> .....	159
<i>Probing Complexity Using the Advanced Light Source</i> <b>Nora Berrah</b> .....	163
<i>Atomic and Molecular Physics in Strong Fields</i> <b>Shih-I Chu</b> .....	167
<i>Optical Two-Dimensional Fourier-Transform Spectroscopy of Semiconductors</i> <b>Steven T. Cundiff</b> .....	171

<i>Theoretical Investigations of Atomic Collision Physics</i> <b>A. Dalgarno</b> .....	175
<i>Coherent Control of Multiphoton Transitions in the Gas and Condensed Phases with Ultrashort Shaped Pulses</i> <b>Marcos Dantus</b> .....	178
<i>Interactions of Ultracold Molecules: Collisions, Reactions, and Dipolar Effects</i> <b>D. DeMille</b> .....	182
<i>Attosecond Science: Generation, Metrology, and Application</i> <b>Louis F. DiMauro</b> .....	185
<i>High Intensity Laser Driven Explosions of Homo-Nuclear and Hetero-Nuclear Molecular Clusters</i> <b>Todd Ditmire</b> .....	189
<i>Ultracold Molecules: Physics in the Quantum Regime</i> <b>John Doyle</b> .....	193
<i>Atomic Electrons in Strong Radiation Fields</i> <b>J. H. Eberly</b> .....	197
<i>Few-Body Fragmentation Interferometry</i> <b>James M Feagin</b> .....	201
<i>Studies of Autoionizing States Relevant to Dielectronic Recombination</i> <b>T.F. Gallagher</b> .....	205
<i>Strongly-Interacting Quantum Gases</i> <b>Murray Holland</b> .....	209
<i>Using Intense Short Laser Pulses to Manipulate and View Molecular Dynamics</i> <b>Robert R. Jones</b> .....	213
<i>Theory of Threshold Effects in Low-Energy Atomic Collisions</i> <b>J. H. Macek</b> .....	217
<i>Photoabsorption by Atoms and Ions</i> <b>Steven T. Manson</b> .....	221
<i>Electron/Photon Interactions with Atoms/Ions</i> <b>Alfred Z. Msezane</b> .....	225
<i>Theory and Simulations of Nonlinear X-Ray Spectroscopy of Molecules</i> <b>Shaul Mukamel</b> .....	229

<i>Nonlinear Photoacoustic Spectroscopies Probed by Ultrafast EUV Light</i> <b>Keith A. Nelson</b> .....	233
<i>Single Molecule Fluorescence in Inhomogeneous Environments</i> <b>Lukas Novotny</b> .....	237
<i>Electron-Driven Excitation and Dissociation of Molecules</i> <b>A. E. Orel</b> .....	241
<i>Low-Energy Electron Interactions with Interfaces and Biological Targets</i> <b>Thomas M. Orlando</b> .....	245
<i>Photoelectron-Vibrational Coupling in Nonlinear Molecules</i> <b>Erwin D. Poliakoff and Robert R. Lucchese</b> .....	249
<i>Control of Molecular Dynamics: Algorithms for Design and Implementation</i> <b>Herschel Rabitz</b> .....	253
<i>A Dual Bose-Einstein Condensate: Towards the Formation of Heteronuclear Molecules</i> <b>Chandra Raman</b> .....	257
<i>Ultrafast X-ray Coherent Control</i> <b>D. A. Reis and P. H. Bucksbaum</b> .....	260
<i>Atomic Physics Based Simulations of Ultra-cold Plasmas</i> <b>F. Robicheaux</b> .....	264
<i>High Harmonic Generation in Discharge-Ionized Plasma Channels</i> <b>Jorge J. Rocca</b> .....	268
<i>Dynamics of Few-Body Atomic Processes</i> <b>Anthony F. Starace</b> .....	272
<i>Femtosecond and Attosecond Laser-Pulse Energy Transformation and Concentration in Nanostructured Systems</i> <b>Mark I. Stockman</b> .....	276
<i>Laser Produced Coherent X-Ray Sources</i> <b>Donald Umstadter</b> .....	280



***Invited Presentations***  
***(ordered by agenda)***



## The ITER Project

Ned Sauthoff

Project Manager, U.S. ITER Project Office  
Oak Ridge National Laboratory

Decades of research on plasma physics and fusion technology have finally achieved the scientific and technological readiness necessary to proceed to the study of self-heated "burning" plasmas. The governments of China, the European Union, India, Japan, South Korea, the Russian Federation, and the United States have recently initialed an international agreement to construction ITER, a facility for this study, aimed at establishing the scientific and technological feasibility of fusion power by magnetically confined plasmas. ITER is a toroidal confinement device of the tokamak configuration that uses large superconducting magnets for plasma confinement and control, electromagnetic waves and neutral particle beams for external heating and non-inductive current drive, and injection of frozen hydrogen pellets for fueling. ITER presents both scientific/technological and management challenges. The dominant self-heating of the plasma is a new condition, with more opportunities for self-organization; the population of energetic charged particles can excite waves; and the large size of the system relative to the particle orbits and other plasma spatial scales affects the balance between surface and volume phenomena. Atomic and molecular processes are important in the plasma, in the diagnosis of plasma behavior, and in the heating/fueling/exhaust systems. The magnitude and complexity of the multinational project, especially with the large extent of "in-kind contributions," are driving the development of international arrangements and project management tools and approaches that may be applicable to other areas of large science.

## Atomic Physics in ITER – The Foundation for the Next Step to Fusion Power

D. P. Stotler<sup>1</sup>

<sup>1</sup> *Princeton Plasma Physics Laboratory, Princeton, NJ, 08543*

*dstotler@pppl.gov*

ITER represents the next step towards practical magnetic confinement fusion power [1]. Its primary physics objective is to study plasmas in which the fusion power exceeds the external heating power by a factor of 5 to 10. Among its technological objectives are the use of superconducting magnets and remote maintenance, the handling of high heat fluxes, and the testing of tritium breeding concepts. Atomic physics processes will play a fundamental role in facilitating the achievement of these objectives [2]. First, atoms and molecules generated by the interaction of the ITER plasma with surrounding material surfaces will impact and, in some respects, dominate the particle, momentum, and energy balances in both the adjacent and confined, core plasmas. High quality atomic physics data for the relevant species (including hydrogen atoms and molecules, as well as intrinsic impurities beryllium, tungsten, and carbon) will be required to interpret and predict their behavior as they travel into the plasma. Second, extrinsic impurity gases, such as neon and argon, will be introduced into the edge plasma so that their radiation will spread heat coming out from the core more uniformly over the surrounding material surfaces than it would otherwise. Third, many of the diagnostics used to monitor the dense ( $n_e \sim 10^{20} \text{ m}^{-3}$ ), hot ( $\sim 1 \times 10^8 \text{ K}$ ) core plasma leverage off of atomic physics effects. Beam emission and charge exchange recombination spectroscopy based on a dedicated diagnostic neutral atom beam will yield ion temperatures and rotation velocities as well as local impurity ion densities, including that of the helium ash generated by the fusion reactions. X-ray crystal spectrometers will provide independent and complementary measurements of the impurity ion temperatures and rotation velocities. A diagnostic based on the motional Stark effect will measure the local orientation of the magnetic field.

[1] ITER Technical Basis, ITER EDA Documentation Series No. 24, IAEA, Vienna (2002).

[2] ITER Physics Basis Editors, Nucl. Fusion 39, 2137 (1999).

# Low Energy Chemical Sputtering of ATJ graphite and HOPG by Atomic and Molecular D projectiles

F. W. Meyer\*

*Physics Division, Oak Ridge National Laboratory, Oak Ridge, TN 37831-6372 USA*

Because of its high thermal conductivity, excellent shock resistance, absence of melting, low activation, and low atomic number, there is significant technological interest in using graphite as a plasma-facing component on present and future fusion devices.

This interest extends to the use of different types of graphite or carbon fiber composites that contain tungsten, beryllium, or other refractory metals, for the ITER divertor. Although these materials have outstanding thermo-mechanical properties, they can suffer significant chemical erosion and sputtering by low energy hydrogen ion impact, which determines in large part the carbon-based-material lifetime.

Due to evolving divertor design, interest in the erosion characteristics of the carbon surfaces is shifting to progressively lower impact energies. Results are presented of chemical sputtering yields of ATJ graphite by impact of  $D^+$  and  $D_2^+$  and  $D_3^+$  in the energy range 5-250 eV/D.

Our experimental approach is based on the use of a quadrupole mass spectrometer to monitor partial pressure increases of selected mass species resulting from ion impact on the graphite surface [1]. The high  $D^+$  currents obtainable with our ECR ion source and the highly efficient beam deceleration optics employed at the entrance to our floating scattering chamber allowed us to compare the sputtering yields of atomic and molecular species at the same velocity for energies as low as 10 eV/D. Thus we could test the commonly made assumption that atomic and molecular species at the same speed lead to identical sputtering yields when normalized to the number of D atoms in the incident projectile [2]. As can be seen in Figure 1 below, the assumption was found to break down at energies below about 60 eV/D, suggesting caution in interpreting results obtained using molecular ions to simulate lower energy incident atomic projectiles in chemical sputtering measurements.

The measurements also serve as benchmarks for testing new MD simulations [3] of the chemical sputtering process that seek to incorporate more realistic many-body potentials and expand the reaction pathway to include vibrational and/or electronic excited states.

In addition to the ATJ graphite work, comparative results will be presented for chemical sputtering of two highly oriented pyrolytic graphite (HOPG) surfaces, one with basal planes parallel to the surface, and the other perpendicular. The latter is a much more open structure that is expected to enhance diffusion back to the surface of chemical sputtering products produced by more energetic incident projectiles at the end of their range after deeper penetration into the target bulk.

---

\* In collaboration with H. F. Krause, L. I. Vergara, and H. Zhang

# Study of Ions Transmitted through an Anodic Nanocapillary Array

*Herb Krause\**

*Physics Division, Oak Ridge National Laboratory, P. O. Box 2008, Oak Ridge, TN 37831*

## 1. Scope

Objects having nanometer to micron dimensions, such as nanoparticles, nanopores and nanotubes, provide a bridge between the atomic quantum and macroscopic classical worlds. By studying multiply charged ions transmitted through aligned nanopores, for example, we can investigate fundamental atomic collision processes such as charge exchange, angular scattering and energy loss phenomena in a mesoscopic ultra-grazing ion-surface setting under a wide variety of conditions. This knowledge may help to characterize the inside of nanopores or carbon nanotubes and lead to atomic physics-based diagnostics or future applications for the rapidly expanding field of nanotechnology. The arrays being studied are commonly used for biofiltration and chemical separations. This work is part of the ongoing beam-surface studies at the ORNL Multi-charge Ion Research Facility (MIRF) that seek to develop a fundamental understanding of neutralization, energy dissipation and sputtering processes when atomic and molecular ions interact with metal, semiconductor and insulator surfaces.

## 2. Recent Progress

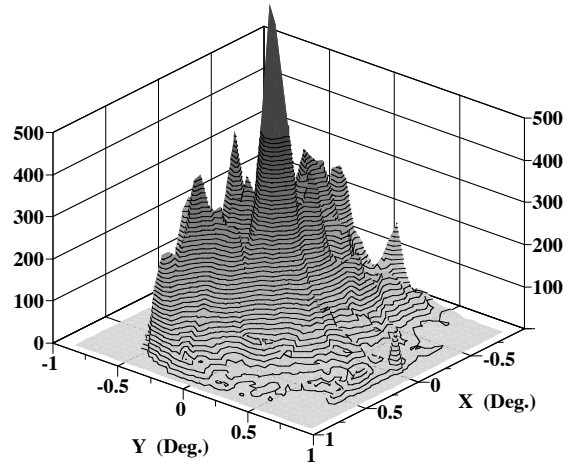
The nanocapillary array studied consists of a dense distribution ( $> 3 \times 10^9$  pores/cm<sup>2</sup>) of cylindrical nanopores typically 100 nm in diameter and 60  $\mu$  in length formed by anodic oxidation of aluminum. The Al<sub>2</sub>O<sub>3</sub> array [1], which is a rigid and self-supporting insulator, has been extensively characterized previously by other researchers using techniques such as scanning electron microscopy, gas absorption, deuterium-based nuclear magnetic resonance, and small-angle neutron scattering [2-3]. The nanopores, which are smooth, straight and hexagonally arranged, are six times longer than those used previously to guide 3-keV Ne<sup>7+</sup> ions through insulating PET or mylar films [4]. Heretofore, experimental high-resolution angular scattering studies have not been reported for any nanocapillary target.

The transmission of incident 200-MeV Ti<sup>12+</sup> ions and 10- to 20-keV/q Ar<sup>+</sup>, Ar<sup>3+</sup>, Ne<sup>3+</sup>, and Ne<sup>7+</sup> ions through the array was studied using two different methods [5]. Initially, tilting experiments measuring transmitted titanium ion energy loss at 200 MeV estimated the co-alignment of nanopores in the target. Later, charge-state-selected angular distributions were studied at low energy using a two-dimensional position sensitive detector (TDPSD). The principal transmitted q-state is the incident q-state in all cases. Yields in lower q-states and neutrals formed by electron capture are typically below 3% of the entrance q-state yield. The transmitted fraction of incident beam,  $\approx 2 \times 10^{-8}$ , is many orders of magnitude smaller than the array's surface porosity ( $\approx 40\%$ ). No evidence of significant energy loss was observed for the transmitted ions.

---

\*In collaboration with C. R. Vane and F. W. Meyer

Fig. 1. Q-state selected angular distribution for incident 140-keV  $\text{Ne}^{7+}$  ions ( $q=7$  out) transmitted by the nanocapillary array. The nanopores are tilted 0.1 Deg. from the beam direction (along the X axis) where observed structure is enhanced.



Observed angular distributions consist of well resolved, two-dimensional structures sitting on a continuum distribution. The distribution and sharp angular structures can be steered in the direction of the pores within about  $\pm 0.5^\circ$  without a significant loss of transmitted intensity by rotating the sample with respect to the incident beam. Analysis of the structure has allowed the identification of single, double and triple collisions inside the nanopores. All data suggest that the structure observed in the scattered-ion angular distributions arises when ions bounce at ultra-low grazing angles in very large impact parameter Coulomb collisions with electrically charged nanopore walls. Arrays with and without surface deposited 7- and 15-nm Au films have been investigated [6]. Films can increase the transmitted ion beam fraction 10 to 20 times. Some of the transmission characteristics of our thick arrays contrast sharply with those observed in the case of the low porosity and much thinner carbonaceous targets [4].

### 3. Future Plans

We will investigate ion transmission using arrays having much thicker deposited Au films (30-100 nm) to determine whether the transmitted fraction can be controlled over a much greater range ( $> 10^{-6}$ ). Studies in the intermediate energy range will be performed using a grazing beam line associated with a new ECR ion source located on a 250-kV platform at MIRF. We will also investigate molecular dissociation processes in nanocapillary arrays in the low to intermediate energy regime using a new molecular breakup detector available in the MIRF laboratory.

Condensed matter scientists at ORNL have been developing ways to produce aligned arrays of single- and double-wall carbon nanotubes. When a suitable research sample becomes available to us, we will attempt to study its transmission characteristics. Recent calculations by Burgdörfer and coworkers suggest that the substrate conductivity plays an important role in determining how well ions move through nanopores.

## References

- [1] Anopore membranes are available from Whatman Inc., 200 Park Avenue, Ste. 210, Florham Park, NJ 07932 USA.
- [2] G. P. Crawford, L. M. Steele, R. Ondis-Crawford, G. S. Iannacchione, C. J. Yeager, J. W. Doane, and D. Finotello, *J. Chem. Phys.* **96**, 7788 (1992).
- [3] D. Marchal and B. Demé, *J. Appl. Cryst.* **36**, 713 (2003).
- [4] N. Stolterfoht, J. H. Bremer, V. Hoffmann, R. Hellhammer, D. Fink, A. Petrov, and B. Sulik, *Phys. Rev. Lett.* **88**, 133201 (2002).
- [5] H. F. Krause, C. R. Vane and F. W. Meyer, submitted to *Physical Review A* (2006).
- [6] H. F. Krause, C. R. Vane, F. W. Meyer, and H. M. Christen, selected presentation, 13<sup>th</sup> International Conference on the Physics of Highly Charged Ions, Queens University Belfast (2006).

## Electron-Molecular Ion Fragmentation\*

M. E. Bannister

*Physics Division, Oak Ridge National Laboratory, P. O. Box 2008  
Oak Ridge, TN 37831*

In support of low-temperature plasma science, we are studying interactions of electrons with molecular ions leading to fragmentation. These collisions are important in determining the dynamics and chemistry of plasmas found in fusion energy, plasma processing, astrophysics, and aeronomy. In an effort to obtain a complete picture of molecular fragmentation, our experimental program focuses on the processes of dissociative excitation (DE), ionization (DI), and recombination (DR) and includes experiments at the Multicharged Ion Research Facility (MIRF) at ORNL and collaborative experiments at the CRYRING heavy-ion storage ring in Stockholm. Absolute cross section measurements of the DE and DI of the hydrocarbon ions  $\text{CH}_2^+$  and  $\text{CH}_3^+$  producing  $\text{C}^+$  and  $\text{CH}^+$  fragment ions will be presented. Results for dissociation of  $\text{N}_2\text{H}^+$  and  $\text{DCO}^+$  into heavy fragment ions will also be discussed. Experimental results for DR of di-hydride and similar molecular ions measured at CRYRING will be presented, including absolute cross sections, branching fractions, and fragment imaging studies for collisions at or near zero interaction energy. The systems investigated include the di-hydride ions  $\text{SH}_2^+$ ,  $\text{PD}_2^+$ , and  $\text{LiH}_2^+$  and the similar ions  $\text{O}_3^+$  and  $\text{D}_5\text{O}_2^+$  that are also expected to exhibit significant break-up into three-body channels. Present studies at ORNL using the merged electron-ion beams energy-loss (MEIBEL) technique for imaging studies of zero-energy DR of molecular ions will be highlighted. These experiments are made possible by the recent addition to the MIRF of a 250-kV high-voltage platform for accelerating both atomic and molecular ions. Future plans for our experimental program will be outlined, including continued DE/DI measurements on the ORNL crossed-beams apparatus, DR experiments employing the ORNL MEIBEL apparatus and the CRYRING heavy-ion storage ring, and development of a cold molecular ion source for use on the high-voltage platform.

\* Please also see the Research Summary for the ORNL AMOS program.

**Program Title:**

**"Properties of actinide ions from measurements of Rydberg ion fine structure"**

**Principal Investigator:**

Stephen R. Lundeen,  
Dept. of Physics  
Colorado State University  
Ft. Collins, CO 80523  
Lundeen@Lamar.colostate.edu

**Program Scope:**

Measurements of the fine structure of non-penetrating, high-L Rydberg states of atoms or ions can be used to deduce polarizabilities and permanent moments of the positive ions that form the cores of these Rydberg systems. Special experimental techniques developed under previous DOE support now make it possible to carry out such studies in a wide range of elements and charge states. The current focus of this project is the application of these techniques to measure some properties of chemically interesting actinide ions, such as  $U^{6+}$ ,  $Th^{4+}$ , and other open shell ions. Since *a-priori* prediction of the properties of such highly relativistic ions is very challenging but still much simpler than predicting their behavior in chemical compounds, it is hoped that such measurements will contribute to improved understanding of actinide chemistry.

**Recent Progress and Immediate Plans:**

Since a source of U and Th ions is not yet available, the current work on this project is taking two forms.

1) At Kansas State University, using an existing 3 GHz ECR source, an apparatus has been assembled to carry out studies of the  $Kr^{6+}$  ion that are analogous to the proposed studies of U and Th ions. The challenge is to demonstrate that ions with charge as high as six can be successfully studied with the methods that have previously been applied only to ions with charge one [1], two [2], and three [3]. Good progress has been made during the current grant period, clarifying important aspects of apparatus design that will be critical to the proposed actinide studies. One example of the results obtained in this work is shown in Fig. 1. It shows a partially resolved excitation spectrum of  $Kr^{5+}$  Rydberg ions from the  $n=55$  to the  $n=110$  level. The two resolved peaks correspond to the  $n=55$ ,  $L=6$  and  $L=7$  levels, which are separated from the large peak consisting of higher L levels because of the  $n=55$  fine structure. Their positions provide a preliminary value of the  $Kr^{6+}$  polarizability,  $\alpha_d = 0.9 a_0^3$ .

Based on these initial studies, plans are being made to incorporate several improvements of the apparatus that promise to improve the resolution and signal to noise. When a source of U and Th ions is obtained, it will be substituted for the current ECR source and we will move immediately to the study of closed shell ions,  $U^{6+}$  and  $Th^{4+}$ .

2) At Colorado State University, a similar apparatus is maintained that can study Rydberg atoms, but not Rydberg ions. Since many of the theoretical questions relating to Rydberg fine structure are common to atoms and ions, studies at this location are aimed at clarifying the connection between observed fine structure and ion properties.

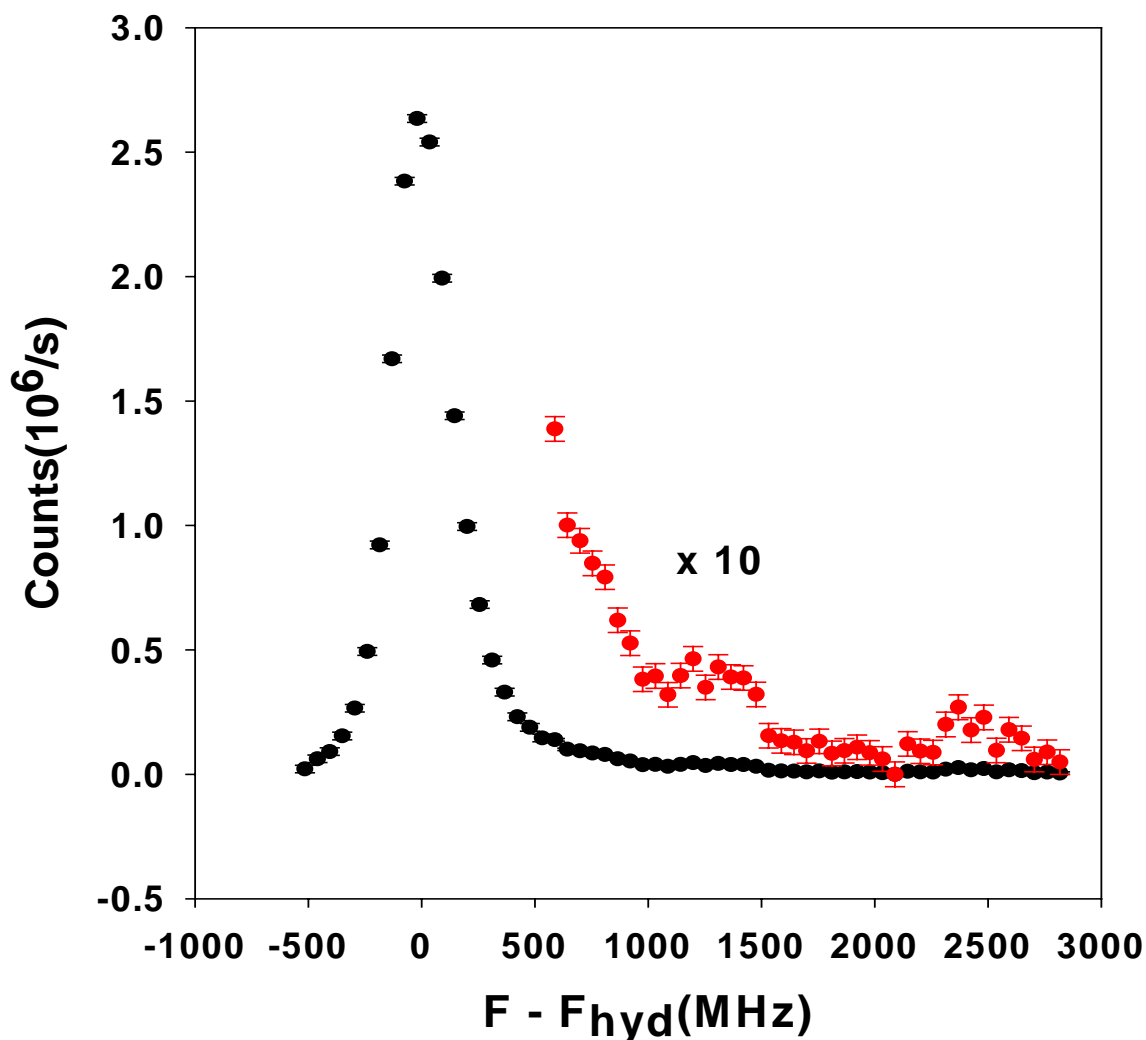


Fig. 1) Excitation spectrum for 55-110 transitions in  $\text{Kr}^{5+}$ . The vertical scale is the number of ions detected after Stark ionization of  $n=110$  states. The horizontal scale is the difference between the Doppler-tuned  $\text{CO}_2$  laser frequency and the hydrogenic 55-110 transition frequency. The points shown in red are magnified by a factor of ten, and show the resolved contributions of  $n=55$ ,  $L=6$  and  $L=7$  levels.

**2a)** Graduate student Erica Snow is carrying out a study of several heavier Rydberg atoms with  $^2S_{1/2}$  ion cores, Mg and Ba. This work is motivated by long-standing difficulties in extracting reliable quadrupole polarizabilities from Rydberg fine structure measurements. In contrast to dipole polarizabilities extracted in this way, which in several cases seem to be in very good agreement with *a-priori* calculations [3,4], the quadrupole polarizabilities indicated by naive interpretation of fine structure data have consistently failed to confirm calculations. This project involved both significant new experimental measurements in Mg and Ba, including intervals at much higher  $L$  than previous studies, and also a thorough reexamination of the theoretical framework used to

interpret the measurements. She has found that most inconsistencies can be explained by higher-order terms that had previously been neglected. Her PhD thesis reporting this work is nearly complete and several papers are in preparation.

**2b)** Graduate student Laura Wright is measuring the fine structure patterns in several levels of Rydberg Argon. Since  $\text{Ar}^+$  has a  $^2P_{3/2}$  ground state, these patterns are more complex than those of Mg and Ba, and reveal other core properties such as quadrupole moment and anisotropic polarizability. Open shell U and Th ions, such as  $\text{U}^{5+}$ , are expected to display even more complex fine structure patterns, so exploring such patterns in neutral atoms should help to build experience and understanding necessary for those studies. This work is nearly complete and a paper reporting the results is in preparation.

### References

- [1] "Fine Structure in High-L Rydberg states: A Path to Properties of Positive Ions", S.R. Lundeen, in *Advances in Atomic, Molecular, and Optical Physics*, Vol. 52 edited by Chun C. Lin and Paul Berman (Academic Press, 2005)
- [2] "Ion Properties from High-L Rydberg Fine Structure: Dipole Polarizability of  $\text{Si}^{2+}$ ", R.A. Komara, M.A. Gearba, C.W. Fehrenbach, and S.R. Lundeen, *J. Phys. B. At. Mol. Opt. Phys.* **38**, S87 (2005)
- [3] "Determination of the polarizability of Na-like Silicon by study of the fine structure of high-L Rydberg states of  $\text{Si}^{2+}$ ", R.A. Komara, M.A. Gearba, S.R. Lundeen, and C.W. Fehrenbach, *Phys. Rev A* **67**, 062502 (2003)
- [4] "Determination of dipole and quadrupole polarizabilities of  $\text{Ba}^+$  by measurement of the fine structure of high-L, n=9 and 10 Rydberg states of Barium" E.L. Snow, M.A. Gearba, W.G. Sturru, and S.R. Lundeen, *Phys. Rev A* **71**, 022510 (2005)

### Recent Publications:

"Ion Properties from High-L Rydberg Fine Structure: Dipole Polarizability of  $\text{Si}^{2+}$ " R.A. Komara, M.A. Gearba, C.W. Fehrenbach, and S.R. Lundeen, *J. Phys. B. At. Mol. Opt. Phys.* **38**, S87 (2005)

"Stark-induced X-ray emission from H-like and He-like Rydberg ions", M.A. Gearba, R.A. Komara, S.R. Lundeen, C.W. Fehrenbach, and B.D. DePaola, *Phys. Rev A* **71**, 013424 (2005)

"Determination of dipole and quadrupole polarizabilities of  $\text{Ba}^+$  by measurement of the fine structure of high-L, n=9 and 10 Rydberg states of Barium" E.L. Snow, M.A. Gearba, W.G. Sturru, and S.R. Lundeen, *Phys. Rev A* **71**, 022510 (2005)

"Fine Structure in High-L Rydberg states: A Path to Properties of Positive Ions" in *Advances in Atomic, Molecular, and Optical Physics*, Vol. 52 edited by Chun C. Lin and Paul Berman (Academic Press, 2005)

"Relative charge transfer cross section from  $\text{Rb}(4d)$ ", M.H. Shah, H.A. Camp, M.L. Trachy, X. Flechard, M.A. Gearba, H. Nguyen, R. Bredy, S.R. Lundeen, and B.D. DePaola, *Phys. Rev. A* **72**, 024701 (2005)

## Inner-shell electron spectroscopy and chemical properties of atoms and small molecules

T. Darrah Thomas, Principal Investigator  
[T.Darrah.Thomas@oregonstate.edu](mailto:T.Darrah.Thomas@oregonstate.edu)

Department of Chemistry  
153 Gilbert Hall  
Oregon State University  
Corvallis, OR 97331-4003

### Program scope

Many chemical phenomena depend on the ability of a molecule to accept (or donate) charge at (or from) a particular site in the molecule. Examples are acidity, basicity (proton affinity), rates and regioselectivity of electrophilic reactions, hydrogen bonding, and ionization. Among these, inner-shell ionization spectroscopy (ESCA or x-ray photoelectron spectroscopy) has proven to be a useful tool for investigating how a molecule responds to added or diminished charge at a particular site. The technique is element specific and is applicable to all elements except hydrogen. It is, in many cases site specific. As a result, x-ray photoelectron spectroscopy (XPS) can probe all of the sites in a molecule and identify the features that cause one site to have different chemical properties from another. In addition, the inner-shell ionization energies, as measured by XPS, provide insight into the charge distribution in the molecule – a property of fundamental chemical importance.

During the last 35 years, inner-shell electron spectroscopy has been a source of much useful chemical information. Until recently, however, the investigation of the carbon 1s photoelectron spectra of hydrocarbons (or the hydrocarbon portion of molecules containing a heteroatom) has been hampered by lack of resolution. Carbon atoms with quite distinct chemical properties may have carbon 1s ionization energies that differ by less than 1 eV, whereas historically the available resolution has been only slightly better than this. In addition, the vibrational excitation accompanying core ionization adds complexity to the spectra that has made analysis difficult.

The availability of third-generation synchrotrons coupled with high-resolution electron spectrometers has made a striking difference in this situation. It is now possible to measure carbon 1s photoelectron spectra with a resolution of about half the natural line width (~100 meV), with the result that recently measured carbon 1s spectra in hydrocarbons show a richness of chemical effects and vibronic structure.

During the last nine years this program has endeavored to exploit this capability in order to investigate systems where new features can be revealed by high-resolution carbon 1s photoelectron spectroscopy. The primary goal has been to determine carbon 1s ionization energies not previously accessible in order to use the relationships between these energies and other chemical properties to elucidate the chemistry of a variety of systems. Early work focused on understanding the features of the spectra: line shape, line width, vibrational structure, and vibronic coupling, since understanding these features is essential to unraveling the complex spectra that are found for molecules having several carbon atoms. Now that these features are (more or less) understood, emphasis has shifted to investigation of chemically significant systems and to gaining further insights into the relationships between core-ionization energies and chemical properties.

## Recent progress (2005-2006)

During the last 12 months, we have had 28 shifts of synchrotron time – 10 at the ALS in January 2006 and 18 at MAX II in May 2006. (A run at the ALS that was scheduled for October 2005 was scrubbed because of a failure of the beamline.) This time was devoted to acquiring carbon 1s photoelectron spectra for a number of compounds of interest. Particular emphasis was on substituted benzenes and on molecules in which there is an effect of the molecular conformation on the carbon 1s photoelectron spectra.

**Core-ionization energies, proton affinities, and reactivities in substituted benzenes.** Benzene plays a special role in chemistry as the building block for many important compounds. Its properties, reactivity, and spectroscopy are all strongly influenced by any substituents that are attached to the ring. As a consequence the study of substituent effects in the chemistry of benzene has a very long history, as does the study of substituent effects on the carbon 1s ionization energies in benzene. However, because of limitations of resolution, obtaining unequivocal experimental results on such effects on the carbon 1s ionization energies has been difficult. Now, with third-generation synchrotrons and advanced electronic structure theory, it is possible to assign carbon 1s ionization energies to all of the carbon atoms in a substituted benzene ring.

We have recently published results of our measurements and analysis of the fluorobenzenes.<sup>1</sup> In this work we have shown, first, that the effect of multiple substituents is additive, and, second, that there are linear correlations between carbon 1s ionization energies and proton affinities for these molecules. From these correlations we have obtained insight into the role of fluorine as a  $\pi$ -electron donor. Specifically, the results show that a fluorine substituent that is ortho or para to the site of ionization or protonation is a better  $\pi$ -electron donor to an added proton than it is to a core hole. This difference can be understood in terms of the specific structure of the protonated molecule, which has a more extensive system of  $\pi$  molecular orbitals than does the core-ionized species.

These studies have been supplemented by similar measurements on the methyl-substituted benzenes. Here the additivity model also holds and there are also linear correlations with proton affinities. However, the  $\pi$ -donor effect is smaller for the methyl group than it is for fluorine. A paper on this work is about to be submitted.

Measurements on molecules that have both fluoro and methyl substituents have been made to provide further insight into the additivity model. Preliminary results indicate that this model will work well for these mixed compounds. We are in the process of analyzing data taken in May 2006 for these molecules.

To extend our knowledge on substituent effects, we have made measurements on a variety of substituted benzenes, with one or more substituents. The substituents include Cl, Br, I, OH, OCH<sub>3</sub>, NH<sub>2</sub>, N(CH<sub>3</sub>)<sub>2</sub>, NO<sub>2</sub>, SH, C $\equiv$ CH, CH=CH<sub>2</sub>, and CN. Analysis of these results is in progress.

**Conformational effects on carbon 1s photoelectron spectra and ionization energies.** In general, there has been little reason to expect that different conformers of a molecule would give different photoelectron spectra, and, until recently, where this possibility has been investigated no conformational effects on the spectra have been observed. We have, however, found a number of examples in which conformational effects are very apparent in carbon 1s photoelectron spectra. Two different effects are seen. In one, the existence of more than one form is reflected in the degree of vibrational excitation that accompanies core-ionization. In the other the existence of more than one form leads to there being more than one carbon 1s ionization energy for a given carbon atom.

An example of the first effect is found in ethanol, which exists in two conformers in about equal abundance. In the *anti* form the hydroxyl group is pointed away from the methyl group, with an HOCC dihedral angle of 180°. By contrast, in the *gauche* form this angle is about 60°, with the

result that the hydroxyl group can interact strongly with the methyl group. Carbon 1s ionization at the methyl group leaves a localized positive charge at the methyl group, and this positive charge interacts repulsively with the positive charge on the hydroxyl group. In the *anti* form, these charges are far apart, and the interaction is weak. By contrast, in the *gauche* form, the interaction is strong and the *gauche* form is strongly destabilized. As a consequence, core ionization of the methyl group in *gauche* ethanol leads to considerable excitation of torsional motion, but ionization of the *anti* form leads to no excitation of this motion.<sup>2</sup>

The second effect is illustrated by molecules of the type  $\text{CH}_3\text{CH}_2\text{CH}_2\text{X}$ , where X is an electronegative group such as F,  $\text{C}\equiv\text{N}$ ,  $\text{C}\equiv\text{CR}$ , or O. These molecules typically exist in two conformations, one with X pointed more or less away from the terminal methyl group (with the XCCC dihedral angle greater than  $90^\circ$ ) and one with it pointed more or less towards the methyl group ( $\text{XCCC} < 90^\circ$ ). The distance between of the negatively charged electronegative group and the methyl carbon affects the carbon 1s ionization energy and hence the photoelectron spectrum. We have found that this hitherto unobserved effect has a noticeable influence on the spectra of a number of molecules of this type – butyronitrile, 1-fluoropropane, and propanal, for instance, as well as other related compounds. A paper reporting some of these results is in preparation.

### Future plans

The quality of the experimental data that can be obtained with third generation synchrotrons is so good that it presents significant challenges to theory. Although, we have had considerable success in understanding the carbon 1s spectra of hydrocarbons and fluorocarbons, these challenges are becoming more apparent as we consider more complex molecules. Thus, the program for the future must include, in addition to further measurements, a focus on how to include in our analysis such effects as anharmonicity, torsional motion, and large changes in geometry upon ionization. Through our collaboration with theoreticians, we are in a good position to explore these questions, and will do so in the coming year.

Experimental work will be concerned with several problems. (1) Continued work on substituent effects on carbon 1s ionization energies. This will include measurements on 1-fluoropentane, fluorocyclohexane, 1,3,5-trimethoxybenzene, the three isomers of phenylenediamine, and the three isomers of dichlorobenzene, among others. (2) Investigation of recoil effects on the vibrational profiles produced in core ionization.<sup>3</sup> A promising candidate for these studies is the boron 1s spectrum  $\text{BF}_3$ , which contains a very light central atom surrounded by heavier atoms. Preliminary measurements of this spectrum<sup>4</sup> show well-resolved vibrational structure. (3) Investigation of vibronic-coupling (symmetry-breaking) effects in fluorine 2s photoelectron spectra. In such molecules as  $\text{CH}_2\text{F}_2$ , the pairs of fluorine 1s and 2s orbitals form pairs of delocalized orbitals. Upon ionization from one of these orbitals, there is the possibility of vibronic coupling that leads to symmetry breaking. For the 1s electrons, where the two molecular orbitals are nearly degenerate, this effect is strong, and the core hole can be treated as delocalized. For the 2s electrons, on the other hand, the splitting of the two molecular orbitals in  $\text{CH}_2\text{F}_2$  is about 1.75 eV, and it is not clear whether the energy that can be gained by symmetry breaking can offset the energy cost of localization. Since this splitting depends critically on the fluorine-fluorine distance, it is possible to tune it by choosing different molecules. For instance in  $\text{CBr}_2\text{F}_2$ , the splitting is expected to be about 2.0 eV, whereas in  $\text{CH}_2=\text{CF}_2$  and *cis*- $\text{CHF}=\text{CHF}$  it is expected to be 1.9 eV and 0.3 eV, respectively. By tuning the splitting it is possible to tune the degree of vibronic coupling.

1. T. X. Carroll, T. D. Thomas, H. Bergersen, K. J. Børve, and L. J. Sæthre, *J. Org. Chem.* **71**, 1961 (2006).
2. M. Abu Samha, K. J. Børve, L. J. Sæthre, and T. D. Thomas, *Phys. Rev. Lett.*, **95**, 103002 (2005).
3. E. Kukk, K. Ueda, U. Hergenbahn, X.-J. Liu, G. Primper, H. Yoshida, Y. Tamenori, C. Makachekanwa, T. Tanaka, M. Kitajima, and H. Tanaka, *Phys. Rev. Lett.* **95**, 13301 (2005).
4. K. Ueda, unpublished results.

### **Publications involving DOE support, 2004-2006**

Carbon 1s photoelectron spectroscopy of halomethanes. Effects of electronegativity, hardness, charge distribution, and relaxation, T. D. Thomas, L. J. Sæthre, K. J. Børve, J. D. Bozek, M. Huttula, and E. Kukk, *J. Phys. Chem. A* **108**, 4983 (2004).

Carbon 1s photoelectron spectroscopy of six-membered cyclic hydrocarbons, V. M. Oltedal, K. J. Børve, L. J. Sæthre, T. D. Thomas, J. D. Bozek, and E. Kukk, *Physical Chemistry Chemical Physics PCCP*, **6**, 4254 (2004).

Reactivity and core-ionization energies in conjugated dienes. Carbon 1s photoelectron spectroscopy of 1,3-pentadiene, T. D. Thomas, L. J. Sæthre, K. J. Børve, M. Gundersen, and E. Kukk, *J. Phys. Chem. A*, **109**, 5085 (2005).

Conformational effects in inner-shell photoelectron spectroscopy of ethanol, M. Abu Samha, K. J. Børve, L. J. Sæthre, and T. D. Thomas, *Phys. Rev. Lett.*, **95**, 103002 (2005).

Fluorine as a  $\pi$  donor. Carbon 1s photoelectron spectroscopy and proton affinities of fluorobenzenes, T. X. Carroll, T. D. Thomas, H. Bergersen, K. J. Børve, and L. J. Sæthre, *J. Org. Chem.* **71**, 1961 (2006).

# PROGRESS REPORT

## ELECTRON-DRIVEN PROCESSES IN POLYATOMIC MOLECULES

**Investigator: Vincent McKoy**

A. A. Noyes Laboratory of Chemical Physics  
California Institute of Technology  
Pasadena, California 91125  
*email:* mckoy@caltech.edu

### PROJECT DESCRIPTION

The focus of this project is the application and development of accurate, scalable methods for the computational study of low-energy electron–molecule collisions, with emphasis on larger polyatomics relevant to materials-processing and biological systems. Because the calculations required are highly numerically intensive, efficient use of large-scale parallel computers is essential, and the computer codes developed for the project are designed to run both on tightly-coupled parallel supercomputers and on workstation clusters.

### HIGHLIGHTS

We have continued to focus on developing and applying methodology for accurate calculations of electron interactions with larger polyatomic molecules, especially those relevant to biological systems and to technological applications. Principal accomplishments in the past year include:

- Comparative study of elastic electron scattering by deoxyribose, deoxyribose monophosphate, and tetrahydrofuran
- Comparative study of elastic scattering by purine bases, nucleosides, and nucleotides
- Detailed study of elastic and inelastic scattering by uracil
- High-accuracy calculations on N<sub>2</sub>O using recently-developed approach to polarization
- Continued improvement of computational methods

### ACCOMPLISHMENTS

During 2006, we continued to focus on applications to biological systems and on methodological developments in support of those applications. We have largely completed our work on the purine and pyrimidine bases of DNA and RNA and are beginning follow-on work looking at the DNA backbone and at how scattering behavior changes when we consider larger subunits—for example, nucleosides or nucleotides instead of isolated bases. Our goal is to develop a better understanding of how results computed or measured for isolated fragments relate to electron interactions with DNA itself in the condensed phase.

We completed a study [1] of elastic and inelastic scattering by uracil, a pyrimidine base found in RNA. Previous calculations [2,3] have produced higher energies for the  $\pi^*$  resonances in the elastic cross section than those assigned by Burrow *et al.* [4,5] to features in their electron-transmission spectra, leading to some controversy [6]. Our results, which are based on extensive examination of both basis-set convergence and polarization effects, indicate that the lowest  $\pi^*$  resonance occurs near 0.3 eV, in agreement with the assignment proposed by Burrow *et al.* [4,5], and our second  $\pi^*$  resonance energy is also fairly consistent with the experimental assignment.

Along with elastic scattering, we looked at electron-impact excitation of uracil to the lowest singlet and triplet ( $\pi \rightarrow \pi^*$ ) states and found a particularly large cross section for the singlet excitation.

In a second line of work, we examined electron interactions with the DNA backbone, looking in particular to predict energies of shape resonances associated with the deoxyribose moiety [7]. To assess conformation effects on resonance positions, we computed electron cross sections for two realistic ring conformations ( $C_s$  and  $C_2$ ) of the deoxyribose analog tetrahydrofuran (THF) as well as for a planar ( $C_{2v}$ ) conformation; differences were small between  $C_s$  and  $C_2$  but rather larger for  $C_{2v}$ . Accordingly, calculations for deoxyribose itself were carried out for a nonplanar-ring conformation. We also examined the effect of appending a phosphate group to deoxyribose, as is found in the DNA backbone, and found that the two distinct resonance bands seen in THF or deoxyribose merge into a single broad maximum (Fig. 1). Comparison between high-level and lower-level calculations on THF yields a 2 eV downward shift due to polarization, allowing us to make predictions of temporary-anion energies for deoxyribose and deoxyribose monophosphate.

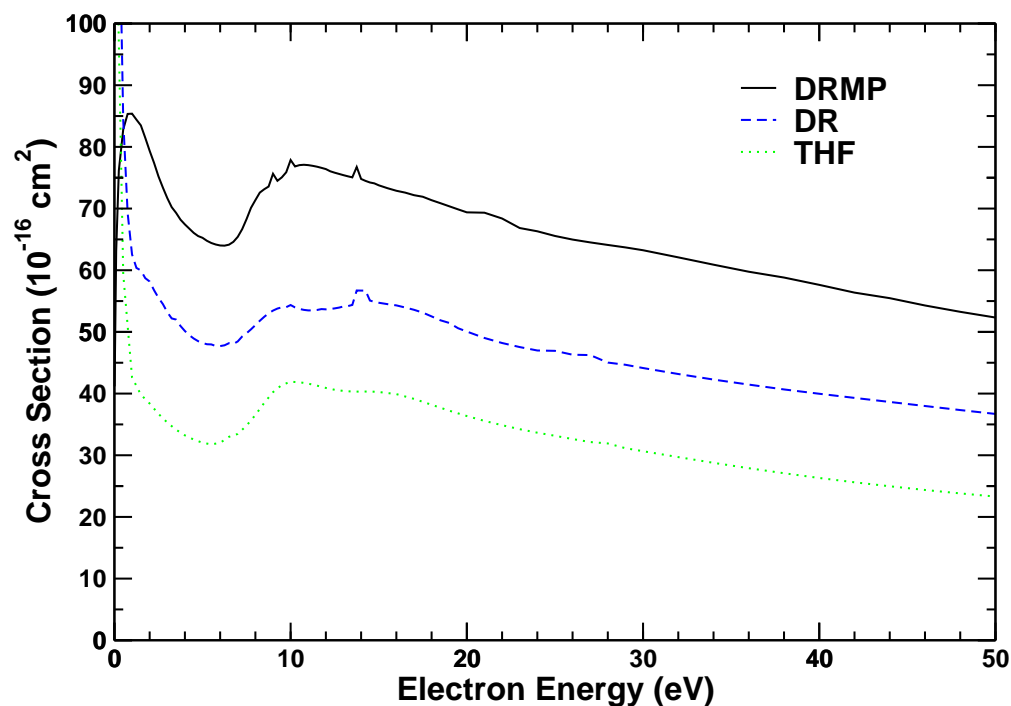


**Fig. 1** Integral elastic electron scattering cross sections for deoxyribose monophosphate (solid black line), deoxyribose (dashed blue line), and tetrahydrofuran (dotted green line) computed in the static-exchange approximation. Figure taken from Ref. [7].

We are taking a similar approach of working from the smallest subunits to larger assemblies in a study of the purine bases, adenine and guanine, that is being prepared for publication. Calculations including polarization effects were carried out to obtain  $\pi^*$  resonance positions for the isolated bases. Comparison of these high-level results with static-exchange results establishes energy

shifts that are then used to predict  $\pi^*$  resonance energies for the nucleosides deoxyadenosine and deoxyguanosine and for the nucleotide deoxyadenosine monophosphate. Complementary work on the pyrimidine bases and nucleosides is being carried out in collaboration with Sergio d'A. Sanchez.

Last year we reported the development of a promising approach to capturing polarization effects efficiently and thereby accelerating the convergence of electron–molecule collision calculations [8]. This year we further tested that approach on the  $N_2O$  molecule, where, over a certain range of scattering energies and angles, strong deviations were known to exist between previous high-level calculations and measurements of the elastic cross section. Our results [9] show that excellent agreement with experiment can be obtained with our new approach to polarization. Interestingly, though, and in contrast to previous work on ethylene [8], we found a more extensive one-electron basis set was also critical in the case of  $N_2O$ .

## PLANS FOR COMING YEAR

We intend to complete work on the DNA and RNA bases and nucleosides and move on to consideration of base pairs and/or nucleoside pairs in order to examine how the scattering behavior changes when bases are paired as they are in DNA. In particular, it will be interesting to see whether  $\pi^*$  resonance energies shift and to see how the scattering pattern changes with a smaller net dipole moment. We also plan exploratory calculations on the effects of solvation, in which one or more water molecules will be included along with a subunit of DNA. In support of this work, we will continue code development aimed at permitting larger and more efficient calculations. A parallel scheme for evaluating and transforming the energy-independent two-electron integrals needed in our scattering calculation is under development, as is a distributed-memory solver for the final linear system of equations. In implementing the latter, we will be working to incorporate refined mechanisms for distinguishing between real and spurious (numerical) resonances based on problem-specific diagnostics [10].

## REFERENCES

- [1] C. Winstead and V. McKoy, submitted to J. Chem. Phys.
- [2] S. Tonzani and C. H. Greene, J. Chem. Phys. **124**, 054312 (2006).
- [3] F. A. Gianturco and R. R. Lucchese, J. Chem. Phys. **120**, 7446 (2004).
- [4] K. Aflatooni, G. A. Gallup, and P. D. Burrow, J. Phys. Chem. A **102**, 6205 (1998).
- [5] A. M. Scheer, K. Aflatooni, G. A. Gallup, and P. D. Burrow, Phys. Rev. Lett. **92**, 068102 (2004).
- [6] P. D. Burrow, J. Chem. Phys. **122**, 087105 (2005).
- [7] C. Winstead and V. McKoy, J. Chem. Phys., in press.
- [8] C. Winstead, V. McKoy, and M. H. F. Bettega, Phys. Rev. A **72**, 042721 (2005).
- [9] M. H. F. Bettega, C. Winstead, and V. McKoy, Phys. Rev. A **74**, XXXXXX (2006).
- [10] C. Winstead and V. McKoy, Phys. Rev. A **41**, 49 (1990).

## PROJECT PUBLICATIONS AND PRESENTATIONS, 2003–2006

- 1. “Electron–Molecule Collisions in Processing Plasmas,” V. McKoy, Applied Materials, Santa Clara, California, 7 February, 2003 (*invited talk*).

2. "Electron–Molecule Collisions in Processing Plasmas," V. McKoy, Colloquium, Departments of Physics and Materials Science, University of Southern California, 28 April, 2003.
3. "Electron–Molecule Collision Calculations on Vector and MPP Systems," C. Winstead and V. McKoy, Cray Users' Group Conference, Columbus, Ohio, 12–16 May, 2003.
4. "Low-Energy Electron Scattering by Methylsilane," M. H. F. Bettega, C. Winstead, and V. McKoy, *J. Chem. Phys.* **119**, 859 (2003).
5. "Low-Energy Electron Collisions with Sulfur Hexafluoride, SF<sub>6</sub>," C. Winstead and V. McKoy, *J. Chem. Phys.* **121**, 5828 (2004).
6. "Elastic Electron Scattering by C<sub>2</sub>F<sub>4</sub>," C. Winstead and V. McKoy, *J. Chem. Phys.* **122**, 234304 (2005).
7. "Low Energy Electron Scattering by DNA Bases," S. d'A. Sanchez, C. Winstead, and V. McKoy, XXIV International Conference on Photonic, Electronic, and Atomic Collisions, Rosario, Argentina, 20–26 July, 2005.
8. "Recent Progress with the Schwinger Multichannel Method," C. Winstead, V. McKoy, and S. d'A. Sanchez, Fourteenth International Symposium on Electron–Molecule Collisions and Swarms, Campinas, Brazil, 27–30 July, 2005 (*invited talk*).
9. "Low-Energy Electron Scattering by N<sub>2</sub>O and C<sub>2</sub>H<sub>4</sub>," M. H. F. Bettega, C. Winstead, and V. McKoy, Fourteenth International Symposium on Electron–Molecule Collisions and Swarms, Campinas, Brazil, 27–30 July, 2005.
10. "Elastic Electron Scattering by Ethylene, C<sub>2</sub>H<sub>4</sub>," C. Winstead, V. McKoy, and M. H. F. Bettega, *Phys. Rev. A* **72**, 042721 (2005).
11. "Low-Energy Electron Collisions with Buckminsterfullerene, C<sub>60</sub>," C. Winstead and V. McKoy, *Phys. Rev. A* **73**, 012711 (2006).
12. "Total Dissociation Electron Impact Cross Sections for C<sub>2</sub>F<sub>6</sub>," D. W. Flaherty, M. A. Kasper, J. E. Baio, D. B. Graves, H. F. Winters, C. Winstead, and V. McKoy, submitted to *J. Appl. Phys.*
13. "Electron Collisions with Large Molecules: Computational Advances," V. McKoy, American Chemical Society National Meeting, Atlanta, March 28, 2006 (*invited talk, Symposium on Theoretical and Experimental Advances in the Study of Low-Energy Electron-Induced Processes in Complex Systems*).
14. "Low-Energy Electron Scattering by N<sub>2</sub>O," M. H. F. Bettega, C. Winstead, and V. McKoy, *Phys. Rev. A* (in press).
15. "Low-Energy Electron Collisions with Gas-Phase Uracil," C. Winstead and V. McKoy, submitted to *J. Chem. Phys.*
16. "Low-Energy Electron Scattering by Deoxyribose and Related Molecules," C. Winstead and V. McKoy, *J. Chem. Phys.* (in press).
17. "Electron Collisions with Large Molecules," C. Winstead, Colloquium, Department of Physics, Federal University of Paraná, Curitiba, Brazil, July 27, 2006.

# Energetic Photon and Electron Interactions with Positive Ions

Ronald A. Phaneuf,  
Department of Physics /220  
University of Nevada  
Reno NV 89557-0058  
phaneuf@physics.unr.edu

## Program Scope

This experimental program investigates processes leading to ionization of positive ions by photons and electrons. The objective is a deeper understanding of both ionization mechanisms and electron-electron interactions in ions of atoms and molecules. Monoenergetic beams of photons and electrons are crossed or merged with ion beams to probe their internal electronic structure as well as the interaction dynamics. Of particular interest are collective electron excitations that are manifested by giant resonances in the ionization cross sections. In addition to precision spectroscopic data for ionic structure, measurements of absolute cross sections for photoionization and electron-impact ionization of atomic ions provide critical benchmarks for the theoretical calculations that generate opacity databases. The latter are critical to models and diagnostics of astrophysical, fusion-energy and laboratory plasmas. Examples of particular relevance to DOE include the Z pulsed-power facility at Sandia National Laboratories, the world's brightest and most efficient x-ray source, and the National Ignition Facility at Lawrence Livermore National Laboratory, the world's most powerful laser. Both facilities are dedicated to high-energy-density science and fusion energy research.

## Recent Progress

The major thrust has been the application of an ion-photon-beam (IPB) research endstation to experimental studies of photoionization of singly and multiply charged positive ions using monochromatized synchrotron radiation. The high photon beam intensity and energy resolution available at ALS undulator beamline 10.0.1 make photoion spectroscopy a powerful probe of the internal electronic structure of atomic and molecular ions, permitting tests of sophisticated structure and dynamics codes at unprecedented levels of detail and precision. Measurements using the IPB endstation at ALS define the current state of the art in energy resolution available to studies of photon-ion interactions. This program has primary responsibility for maintenance and upgrade of this multi-user endstation.

- Fullerene ions are of special interest because they bridge the gap between molecules and solids, and their valence electrons may be excited collectively. Absolute cross sections for photoionization of  $C_{60}^+$ ,  $C_{70}^+$  and  $C_{84}^+$  were measured over the energy range 17-310 eV as part of a detailed investigation of the relative roles of localized and collective electron excitations. This research was conducted in collaboration with the University of Giessen. At photon energies below 100 eV, the cross sections are dominated by giant resonances associated with collective surface and volume plasmon excitations of the valence electrons [6, 7]. Above 280 eV, the localized K-shell excitation of carbon atoms dominates, and the cross sections become distinctly

molecular in character. Detailed reports on this work are being prepared for publication.

- An investigation of photoionization of ions of the xenon isonuclear sequence was conducted in collaboration with the NIST EBIT group, with a focus  $\text{Xe}^{4+}$ ,  $\text{Xe}^{5+}$  and  $\text{Xe}^{6+}$  for applications in the development of 13.5 nm light sources for EUV lithography. This work has recently been published [14].
- High-resolution absolute measurements of K-shell photoionization cross sections for  $\text{C}^{2+}$  were completed and published [5]. Resonance energies, linewidths and lineshape parameters determined from the measurements were compared to new R-matrix calculations.
- $\text{O}^+$  photo-fragment ion-yield spectra resulting from photo-fragmentation of  $\text{CO}^+$  were analyzed and published [10]. This work, led by collaborators from the University of Mexico, identified four distinct Rydberg series of autoionizing resonances as well as vibrational structure.
- In collaboration with Daresbury Laboratory and Århus University, high-resolution measurements were made of photoionization of the metallic ion  $\text{Al}^+$  [12]. This work complements absolute measurements made in Århus at lower spectral resolution.
- Complementary measurements of photoionization and electron-impact ionization of ions of the krypton isonuclear sequence were completed. Measurements on  $\text{Kr}^{3+}$ ,  $\text{Kr}^{4+}$  and  $\text{Kr}^{5+}$  constituted the Ph.D. dissertation of Miao Lu [15]. The  $\text{Kr}^{5+}$  measurements were published [13]. A manuscript is nearly ready for submission on the  $\text{Kr}^{3+}$  measurements, which indicate that the ionization potential tabulated in the NIST database is in error by nearly 2 eV.
- Measurements of photoionization of ions of the chlorine isoelectronic sequence were initiated as part of the Ph.D. thesis research of Ghassan Alna'Washi. Measurements for photoionization of  $\text{K}^{2+}$  and  $\text{Ca}^{3+}$  are in progress.
- Complementary measurements of photoionization and electron-impact ionization of  $\text{Ar}^{5+}$  are in progress and will constitute the M.S. thesis of J. Wang.
- Two additional translating-slit beam profile monitors were installed to improve the accuracy of beam-overlap measurements in the interaction region of the IPB endstation, reducing the uncertainty of photoionization cross-section measurements.
- A channeltron-based photo-ion detector designed by the Giessen group was installed in the IPB endstation. The increased gain assures near-unit detection efficiency of product ions and a negligibly low dark count rate. Installation of four-jaw slits in front of the detector now permits adjustment of the collection solid angle for product ions as well as the energy/charge and mass/charge resolution.

### Future Plans

In addition to the continuation of work already in progress on photoionization and electron-impact ionization of atomic ions, research is planned in two new directions.

- Experiments to date have concentrated mainly on decay of the photo-excited plasmon resonances in  $C_{60}^{9+}$ ,  $C_{70}^{+}$  and  $C_{84}^{+}$  molecular ions by ejection of an electron. Exploratory measurements indicate that these giant plasmon resonances may also decay by fragmentation, with ejection of a pair of carbon atoms being most probable. With the recent installation of four-jaw slits, the ion-photon-beam endstation at ALS is well-suited to investigation of photo-fragmentation channels that yield charged products. A systematic investigation is planned of the relative importance of fragmentation versus ionization as the initial charge state of the fullerene ion is increased. Measurements are planned for  $C_{60}^{9+}$ ,  $C_{70}^{9+}$  and  $C_{84}^{9+}$  ions in initial charge states  $q = 1, 2, 3$  over a broad photon energy range. Photoionization of the fullerene fragment ions such as  $C_{58}^{+}$  and  $C_{56}^{+}$  is of interest in exploring the effect of the size and symmetry of the molecular cage on the plasmon resonances, as well as the stability of these fragment ions.
- A number of studies have demonstrated that single atoms (e.g. of metals) may be stably trapped inside the hollow cage of a fullerene molecule. The technology to produce so-called endohedral fullerenes in macroscopic quantities has advanced to the stage that it may now become feasible to produce charged endohedral fullerene ions in a discharge and to accelerate them. A promising possibility for initial studies at ALS is the photoionization of ionized  $La@C_{84}$ . Prospects are encouraging that sufficient quantities may become available for ion beam production within the ECR source. Such experiments are planned in collaboration with A. Müller and S. Schippers of the University of Giessen, and L. Dunsch of the Institute for Solid State and Materials Research in Dresden, where the endohedral molecules would be produced. In addition to probing the influence of the fullerene cage on atomic resonances, an objective of such experiments is to investigate the possible influence of a caged atom on the properties of collective plasmon oscillations of the valence-shell electrons of fullerene molecular ion.

#### References to Publications of DOE-Sponsored Research (2004-2006)

1. *Lifetime of a K-shell vacancy in atomic carbon created by 1s-2p photoexcitation of  $C^{+}$* , A.S. Schlachter, M.M Sant'Anna, A.M. Covington, A. Aguilar, M.F. Gharaibeh, E.D. Emmons, S.W.J. Scully, R.A. Phaneuf, G. Hinojosa, I. Álvarez, C. Cisneros, A. Müller and B.M. McLaughlin, J. Phys. B 37, L103 (2004).
2. *Threshold truncation of a 'giant' dipole resonance in photoionization of  $Ti^{3+}$* , S. Schippers, A. Müller, R.A. Phaneuf, T. van Zoest, I. Álvarez, C. Cisneros, E.D. Emmons, M.F. Gharaibeh, G. Hinojosa, A.S. Schlachter and S.W.J. Scully, J. Phys. B 37, L209 (2004).
3. *Electron-impact ionization of  $Ti^{3+}$  ions*, T. van Zoest, H. Knopp, J. Jacobi, S. Schippers, R.A. Phaneuf and A. Müller, J. Phys. B 37, 4387 (2004).
4. *A complementary study of photoionization and electron-impact ionization of an atomic ion:  $Xe^{3+}$* , E.D. Emmons, M.S. Thesis, University of Nevada, Reno (2004).
5. *K-shell photoionization of Be-like carbon ions: experiment and theory for  $C^{2+}$* , S.W.J. Scully, A. Aguilar, E.D. Emmons, R.A. Phaneuf, M. Halka, D. Leitner, J.C. Levin,

- M.S. Lubbell, R. Püttner, A.S. Schlachter, A.M. Covington, S. Schippers, A. Müller and B.M. McLaughlin, *J. Phys. B* **38**, 1967 (2005).
6. *Photoexcitation of a volume plasmon in C<sub>60</sub> ions*, S.W.J. Scully, E.D. Emmons, M.F. Gharaibeh, R. A. Phaneuf, A.L.D. Kilcoyne, A.S. Schlachter S. Schippers, A. Müller, H.S. Chakraborty, M.E. Madjet and J.-M. Rost, *Phys. Rev. Lett.* **94**, 065503 (2005).
  7. *240 Electrons Set in Motion*, *Physics News Update* **722** #1 American Institute of Physics, (March 17, 2005).
  8. *Photoionization of ions of the nitrogen isoelectronic sequence: experiment and theory for F<sup>2+</sup> and Ne<sup>3+</sup>*, A. Aguilar, E.D. Emmons, M.F. Gharaibeh, A.M. Covington, J.D. Bozek, G. Ackerman, S. Canton, B. Rude, A.S. Schlachter, G. Hinojosa, I. Alvarez, C. Cisneros, B.M. McLaughlin and R.A. Phaneuf, *J. Phys. B At. Mol. Opt. Phys.* **38**, 343 (2005).
  9. *Photoionization and electron-impact ionization of Xe<sup>3+</sup>*, E.D. Emmons, A. Aguilar, M.F. Gharaibeh, S.W. J. Scully, R.A. Phaneuf, A.L.D. Kilcoyne, A.S. Schlachter, I. Alvarez, C. Cisneros and G. Hinojosa, *Phys. Rev. A* **71**, 042704 (2005).
  10. *Photofragmentation of ionic carbon monoxide*, G. Hinojosa, M.M. Sant'Anna, A.M. Covington, R.A. Phaneuf, I.R. Covington, I. Domínguez, A.S. Schlachter, I. Alvarez and C. Cisneros, *J. Phys. B.* **38**, 2701 (2005).
  11. *Systematic photoionization study along the iron isonuclear sequence*, M. F. Gharaibeh, Ph.D. Dissertation, University of Nevada, Reno (2005).
  12. *A theoretical and experimental study of the photoionization of Al II*, C.E. Hudson, J.B. West, K.L. Bell, A. Aguilar, R.A. Phaneuf, F. Folkmann, H. Kjeldsen, J. Bozek, A.S. Schlachter and C. Cisneros, *J. Phys. B: At. Mol. Opt. Phys.* **38**, 2911 (2005).
  13. *Photoionization and electron-impact ionization of Kr<sup>5+</sup>*, M. Lu, M.F. Gharaibeh, G. Alna'Washi, R.A. Phaneuf, A.L.D. Kilcoyne, E. Levenson, A.S. Schlachter, A. Müller, S. Schippers, J. Jacobi and C. Cisneros, *Phys. Rev. A* **74**, 012703 (2006).
  14. *Absolute photoionization cross sections for Xe<sup>4+</sup>, Xe<sup>5+</sup> and Xe<sup>6+</sup> near 13.5 nm: Experiment and theory*, A. Aguilar, J.D. Gillaspay, G.F. Gribakin, R.A. Phaneuf, M.F. Gharaibeh, M.G. Kozlov, J.D. Bozek and A.L.D. Kilcoyne, *Phys. Rev. A* **74**, 032717 (2006).
  15. *Photoionization and electron-impact ionization of multiply charged krypton ions*, Miao Lu, Ph.D. Dissertation, University of Nevada, Reno (2006).
  16. *Interaction of photons with ionized matter*, Ronald A. Phaneuf, p.p. 171-175 in McGraw-Hill Yearbook of Science and Technology 2006, McGraw-Hill, New York, 2006.
  17. *Doubly excited resonances in the photoionization spectrum of Li<sup>+</sup>: experiment and theory*, S.W.J. Scully, I. Álvarez, C. Cisneros, E.D. Emmons, M.F. Gharaibeh, D. Leitner, M.S. Lubbell, A. Müller, R.A. Phaneuf, R. Püttner, A.S. Schlachter, S. Schippers, W. Shi, C.P. Balance and B.M. McLaughlin, *J. Phys. B* (accepted for publication).

## Slowing and Cooling Molecules via a Counter-Rotating Supersonic Nozzle

Dudley Herschbach, Harvard University  
Department of Chemistry and Chemical Biology  
Harvard University, Cambridge, MA 02138  
herschbach@chemistry.harvard.edu

The advent of methods for cooling, trapping, and manipulating neutral alkali atoms with laser light provided access to intriguing hyperquantum phenomena, by virtue of achieving deBroglie wavelengths in the nanometer range [1]. To pursue such phenomena with molecules is an enticing prospect, since molecules offer many properties, particularly collisional and chemical interactions, not available with atoms. Dramatic examples involving quantum degeneracy have come from inducing formation of alkali dimer molecules within an alkali atom trap by photoassociation or Feshbach resonances [2]. For most molecules, however, formation from precooled atoms does not appear feasible, and the complexity of vibrational and rotational structure generally thwarts laser cooling. Over the past decade, several other means of slowing and cooling molecules have been undertaken. Yet results thus far remain very limited in scope [3].

This talk reports recent work in our lab that has finally attained a benchmark level of performance for a slow, cold beam source applicable to a wide variety of molecules. Our source, which exploits "inverse seeding" in xenon, can now provide  $\sim 10^{12}$  molecules/sec with velocities as low as  $\sim 15$  m/sec. That corresponds to translational kinetic energies of about 0.3K or less for molecules such as O<sub>2</sub>, NO, and CH<sub>3</sub>F, and deBroglie wavelengths  $\sim 7\text{\AA}$ . The method employs a supersonic nozzle, propelled by a high-speed rotor. Spinning the rotor with peripheral velocities of several hundred meters/sec, contrary to the direction of gas flow from the nozzle, markedly slows the emerging molecular beam in the laboratory frame. The supersonic expansion from the nozzle provides both high intensity and drastic cooling of internal states of the molecules. The high speed rotor also functions as a gas centrifuge, thereby enhancing the supersonic character of the gas flow. The device is applicable to a host of molecules, as it requires no special attributes (such as electric or magnetic moments) other than volatility.

Basic aspects of this method were examined in model calculations and assessed in exploratory experiments some years ago [4]. It remained tantalizing, however, as in practice until now the yield of slow molecules became too meager below about 70 m/sec. The major handicap was strong attenuation of slow molecules by scattering from background gas. Inputting gas into the spinning rotor ( $\sim 40,000$  RPM) is inevitably leaky, and the 360-degree spray of xenon from the whirling nozzle creates an even more important background. Reducing this by supplying improved pumping, liquid nitrogen cooled shielding, and charcoal absorption of xenon proved key improvements.

We expect that in its current incarnation our slow, cold molecule source should find many applications. It is relatively simple and inexpensive to assemble, as well as compact (rotor only 10 cm long) and versatile. At least for fairly light molecules, it provides translational energies adequately low for spatial trapping by now standard means. It also offers the advantage of cumulative loading of traps. The small size of the source makes it particularly suitable for augmenting experiments employing electric, magnetic, or laser fields to manipulate molecules. As deflections induced by such fields are inversely proportional to translational kinetic energy, using slow molecules can hugely increase the sensitivity and resolution. Indeed, it becomes practical to utilize feeble but ubiquitous interactions, especially the induced electric dipole due to molecular polarizability and magnetic moments resulting from molecular rotation or from nuclear spins [5]. In our future work, we are eager to exemplify some of these applications. As well as outlining our fond ambitions, the talk will conclude by exhibiting designs for a more universal counter-revolutionary supersonic source, capable of slowing a still wider range of molecules without the aid of inverse seeding.

The experiments discussed here were carried out chiefly by Dr. Michael Timko. Much of his work was aided by prior or concurrent contributions from Drs. Manish Gupta, Timothy McCarthy, Zhenhong Yu, Kelly Higgins, and especially from Bretislav Friedrich (differential pumping to civilize the leaky gas input into the rotor), and from Wes Campbell (loan of charcoal absorption trap).

## References

- [1] C.E. Wieman, D.E. Pritchard, and D.J. Wineland, *Rev. Mod. Phys.* 71, S253 (1999).
- [2] J. Goldwin, S. Inouye, M. L. Olsen and D. S. Lin, *Phys. Rev. A* 71, 043408 (2005).
- [3] J. Doyle, B. Friedrich, R.V. Krems, and F. Masnou-Seeuws, *Eur. Phys. J. D* 31, 149 (2004).
- [4] M. Gupta and D. Herschbach, *J. Phys. Chem. A* 103, 10670 (1999); *J. Phys. Chem. A* 105, 1626 (2001).
- [5] T.J. McCarthy, M.T. Timko, and D. Herschbach, *J. Chem. Phys.* (in press).

## Experiments in Ultracold Collisions

Phillip L. Gould  
Department of Physics U-3046  
University of Connecticut  
2152 Hillside Road  
Storrs, CT 06269-3046  
<phillip.gould@uconn.edu>

### Program Scope:

Ultracold atoms and molecules have come to play an increasingly important role in many of the research areas at the frontier of atomic, molecular and optical (AMO) physics. Examples of such applications include: Bose-Einstein condensation (BEC); degenerate Fermi gases; optical lattices; ultracold Rydberg gases and plasmas; quantum computing; photoassociative spectroscopy and ultracold molecule production; ultracold chemistry; precision spectroscopy and improved atomic clocks; studies of photoionization, electron scattering, and ion-atom collisions; and fundamental atomic and nuclear physics experiments with radioactive isotopes. At the high densities (e.g.,  $n > 10^{11} \text{ cm}^{-3}$ ) and low temperatures (e.g.,  $T < 100 \text{ } \mu\text{K}$ ) usually encountered in these studies, collisions between the ultracold atoms are important processes. They can be either detrimental or beneficial. For example, inelastic collisions can cause undesired heating and/or loss from high-density atom traps. By contrast, photoassociation and magnetic Feshbach resonances can be used to control the formation of ultracold molecules. The main motivations of our experimental program are to improve our understanding of ultracold collisions and to exploit our ability to control the collision dynamics with laser light. Since the colliding partners have low velocities, their motion can be significantly altered by laser excitation and the resulting long-range dipole-dipole interactions. An especially exciting prospect is to bring the elements of coherent control to the photoassociative formation of ultracold molecules.

Our ultracold collision experiments use a magneto-optical trap (MOT) to capture, cool, and confine rubidium atoms. Rb is our atom of choice for several reasons: 1) its resonance lines are well-matched to readily available diodes lasers; 2) there are two stable and abundant isotopes ( $^{85}\text{Rb}$  and  $^{87}\text{Rb}$ ); and 3) because of its favorable collisional properties,  $^{87}\text{Rb}$  has emerged as the most popular atom for BEC studies. In our experiments, a phase-stable MOT is loaded from a slow atomic beam and the subsequent decay of atoms from the trap is monitored. The density-dependent atomic loss rate yields the inelastic collisional rate constant.

### Recent Progress:

During the past year, we have carried out several ultracold collision experiments involving pulses of frequency-chirped laser light. Our ability to control the temporal variation of both the laser frequency (by chirping) and amplitude (by pulsing) opens up new opportunities in the manipulation of ultracold collisions. Prior to our recent work with chirped light, ultracold excited-state collision experiments used fixed-frequency

light applied either continuously (cw) or pulsed (e.g., pulse widths  $\sim 100$  ns). The detuning of the light relative to the atomic resonance determines the internuclear separation  $R$  at which the atom pair is excited to the attractive ( $1/R^3$ ) molecular potential. If the excited pair subsequently gains sufficient kinetic energy (e.g., 1 K) in rolling down the attractive potential, the atoms will escape from the trap. By “chirping” the light, i.e., changing its frequency as a function of time, atom pairs spanning a wide range of  $R$  can be excited nearly simultaneously and caused to undergo inelastic trap-loss collisions. One advantage of the chirp is that for sufficiently high intensities, the population transfer to the excited state can be adiabatic, and therefore efficient and robust. Our measurements of the intensity dependence show the collision rate does indeed saturate. Furthermore, the saturated rate is consistent with all collision pairs which are accessed by the chirp (and whose excitation survives to short range) undergoing an inelastic trap-loss collision. We have also measured the dependence on chirp rate and verified that the efficient excitation provided by a rapid chirp is important. Simply having a range of quasi-cw frequencies present is not sufficient.

We have compared the collision rates induced by positive (red-to-blue) and negative (blue-to-red) chirps at various center detunings. We find interesting differences in certain regimes. For the positive chirp, the collision rate is small at large negative detunings, increases smoothly as the detuning approaches zero (i.e., as the center frequency of the chirp approaches the atomic resonance), then drops sharply for positive detunings. We expect this smooth behavior because the separation  $R$  at which excitation occurs increases with time, while the resulting excited atom pair accelerates on the attractive potential in the opposite direction. Therefore, an atom pair, once excited, is unable to further interact with the positively chirped field. The negative chirp exhibits a rather different detuning dependence. In this case, the chirp and the excited atom pair trajectory both proceed toward decreasing  $R$  and further interactions between the two are therefore possible. The data show that for relatively large negative detunings (e.g., -700 MHz), fewer collisions occur with the negative chirp than with the positive chirp. Based on comparisons with Monte-Carlo simulations of the collisional trajectories, we attribute this reduction to “collision blocking”: an atom pair is initially excited to the attractive potential by the negative chirp, then a short time later is de-excited by the same chirp. This stimulated de-excitation occurs before the atom pair has gained sufficient kinetic energy to escape from the trap, and thereby prevents an observable collision. By contrast, for small negative detunings (e.g., -300 MHz), we find that the negative chirp yields more collisions than the positive chirp. We attribute this to “flux enhancement”. In this process, an atom pair is excited at long-range early in the chirp, but gains minimal kinetic energy before spontaneously decaying back to the ground state. This same pair, now moving towards each other, can be re-excited later in the chirp, this time at short range, where an observable inelastic collision is much more likely to occur. The first excitation enhances the collisional flux available for the second excitation. This cannot happen for the positive chirp where only one interaction is possible.

We have also investigated multiple-chirp effects. By varying the delay between successive chirped pulses, we measure how the collisions induced by a given pulse are influenced by the preceding pulse. In the limit of long delay (e.g., 1  $\mu$ s), the chirped pulses act independently. For shorter delays, we observe both enhancement and depletion effects. At a center detuning for the chirp of -300 MHz, an earlier chirp enhances the rate

of collisions induced by a later chirp. This is similar to the flux enhancement discussed above for a single chirp, but now involving two chirps. At a  $-600$  MHz center detuning, we observe depletion at the shortest delay (200 ns). The first chirp efficiently excites (and causes to collide) all available atom pairs within the chirp range, leaving none to be excited by the second chirp. This depleted pair distribution is eventually replenished by the thermal motion of the ultracold atoms.

#### Future Plans:

To date, we have generated the frequency-chirped light by a rapid ramp of the injection current of an external-cavity diode laser. To minimize the resulting intensity modulation, we use the chirped light from this “master” laser to injection-lock a separate “slave” laser. Although this method works well, it has speed limitations. We are developing a new technique based on a fiber-coupled electro-optic phase modulator driven by an arbitrary waveform generator. In this scheme, a pulse of light from a diode laser is sent through the modulator multiple times, acquiring the prescribed phase shift during each pass. Each time it emerges from the fiber loop, the light is re-injected into the initial laser to boost the power. We expect to realize not only higher chirp rates, but also the ability to produce chirps of arbitrary shape. We will use this capability to study the influence of chirp shape on the collisions. In a sense, this will be similar to short-pulse coherent control experiments, but on a slower time scale. Instead of dispersing the pulse, manipulating the phase of the various frequency components, and then reassembling the pulse, we can directly control the phase in the time domain. We have already seen dramatic effects due to multiple interactions between the chirped light and the colliding atom pair. Since these multiple interactions depend on the details of the chirp, we expect to be able to optimize the collisions by varying the chirp shape. All of our measurements to date have used chirped light tuned below the  $5P_{3/2}$  level (780 nm). However, the complicating aspects of hyperfine structure are considerably simpler below the  $5p_{1/2}$  level (795 nm), so we will adapt our chirped laser system to this wavelength. Finally, we will apply a separate fixed-frequency laser, tuned to a photoassociative resonance, and use the frequency chirp to transiently enhance the flux available for photoassociation.

#### Recent Publications:

“Landau-Zener Problem for Trilinear Systems”, A. Ishkhanyan, M. Mackie, A. Carmichael, P.L. Gould, and J. Javanainen, *Phys. Rev. A* **69**, 043612 (2004).

“Frequency-Chirped Light from an Injection-Locked Diode Laser”, M.J. Wright, P.L. Gould, and S.D. Gensemer, *Rev. Sci. Instrum.* **75**, 4718 (2004).

“Control of Ultracold Collisions with Frequency-Chirped Light”, M.J. Wright, S.D. Gensemer, J. Vala, R. Kosloff, and P.L. Gould, *Phys. Rev. Lett.* **95**, 063001 (2005).

“Probing Ultracold Collisional Dynamics with Frequency-Chirped Pulses”, M.J. Wright, J.A. Pechkis, J.L. Carini, and P.L. Gould, submitted to *Phys. Rev. A*.

# Formation of Ultracold Molecules

Robin Côté

Department of Physics, U-3046  
University of Connecticut  
2152 Hillside Road  
Storrs, Connecticut 06269

Phone: (860) 486-4912  
Fax: (860) 486-3346  
e-mail: [rcote@phys.uconn.edu](mailto:rcote@phys.uconn.edu)  
URL: <http://www.physics.uconn.edu/~rcote>

## Program Scope

Current experimental efforts to obtain ultracold molecules (*e.g.*, photoassociation (PA), buffer gas cooling, or Stark deceleration) raise a number of important issues that require theoretical investigations and explicit calculations.

This Research Program covers interconnected topics related to the formation of ultracold molecules. We propose to investigate schemes to form ultracold molecules, such as homonuclear alkali metal dimers using stimulated and spontaneous processes. We will also study heteronuclear molecules, in particular alkali hydrides; these polar molecules have very large dipole moments. In addition, we will investigate the enhancement of the formation rate via Feshbach resonances, paying special attention to quantum degenerate atomic gases. Finally, we will explore the possible formation of a new and exotic type of molecules, namely ultralong-range Rydberg molecules.

## Recent Progress

Since the start of this Program (August 1<sup>st</sup> 2005), we have worked on the following projects:

### • Formation of alkali hydrides

We explored the formation of alkali hydrides from one- and two-photon photoassociative processes. We found that the one-photon formation rate for LiH and NaH in their  $X^1\Sigma^+$  ground electronic state is sizable in the upper ro-vibrational states  $|v'', J = 1\rangle$ ; assuming conservative values for the atom densities ( $10^{12} \text{ cm}^{-3}$ ), temperature (1 mK), laser intensity ( $1000 \text{ W/cm}^2$ ), and the volume illuminated by it ( $10^{-6} \text{ cm}^3$ ), the rate coefficients are of the order  $3 \times 10^{-13} \text{ cm}^3/\text{s}$ , leading to about 30,000 molecules per second [1]. We also found that all of those molecules would populate a narrow distribution of  $J$ -states in the  $v'' = 0$  vibrational level by spontaneous emission cascading (see Fig.1); the momentum transfer due to the photon emission is not large enough for remove the molecules from traps deeper than  $10 \mu\text{K}$  or so. In the two-photon case, we calculated the formation rate of LiH into the singlet ground state via the  $B^1\Pi$  excited state. This excited electronic state has only three bound levels (in the  $J = 1$  manifold) and a fairly good overlap with the  $X^1\Sigma^+$  ground electronic state. We found rate coefficients about 1000 times larger [2].

### • Rydberg-Rydberg interactions

We began working on the Rydberg-Rydberg interactions to explain some spectral features observed in  $^{85}\text{Rb}$  experiments. We calculated the long-range molecular potentials between two atoms

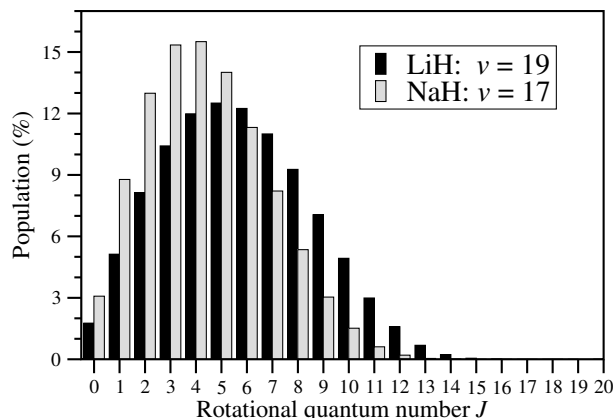


Figure 1: Distribution into the  $J$  states of the  $v = 0$  manifold starting from  $v = 19, J = 1$  for LiH and  $v = 17, J = 1$  for NaH. In both cases, we observe that the maximum population is achieved around  $J \sim 5$ .

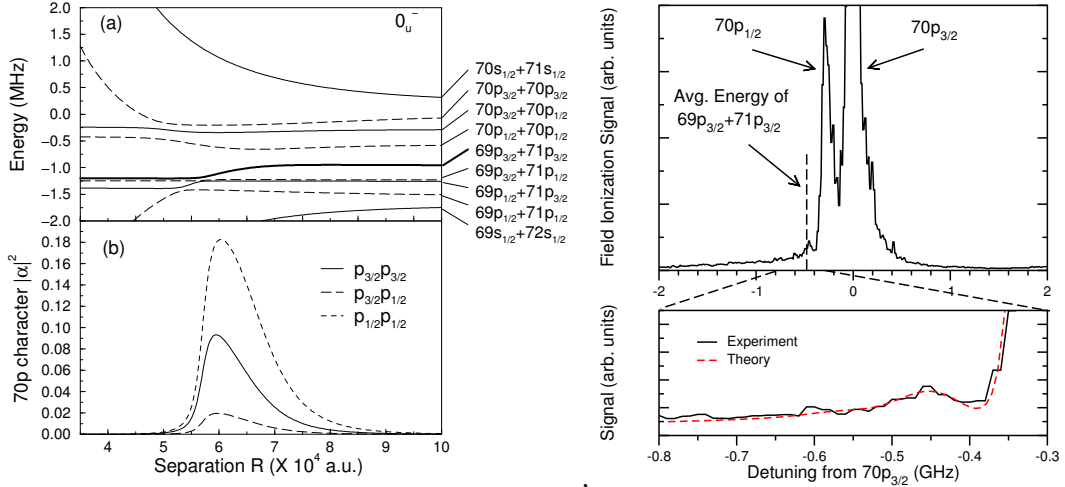


Figure 2: Left panel: (a) Potentials for the  $0_u^-$  symmetry for asymptotes between  $70s + 71s$  and  $69s + 72s$  (zero of energy set at the  $70p_{3/2} + 70p_{3/2}$  asymptote). (b) Fraction of  $70p$  character  $|\alpha|^2$  for  $p_{3/2}p_{3/2}$ ,  $p_{3/2}p_{1/2}$ , and  $p_{1/2}p_{1/2}$  mixtures of the  $69p_{3/2} + 71p_{3/2}$  curve. Right panel: Experimental spectrum near the  $70p$  atomic resonance. Zoom: comparison between experiment and theory (assuming a 120 MHz laser bandwidth, and contributions from the  $0_g^+$ ,  $0_u^-$ , and  $1_u$  symmetries).

in  $70p$  in Hund's case (c), by diagonalization of an interaction matrix. We included the effect of fine structure, and showed how the strong  $\ell$ -mixing due to long-range Rydberg-Rydberg interactions can lead to resonances in excitation spectra. Such resonances were first reported in S.M. Farooqi *et al.*, Phys. Rev. Lett. **91** 183002, where single UV photon excitations from the  $5s$  ground state occurred at energies corresponding to normally forbidden transitions or very far detuned from the atomic energies. We modeled a resonance correlated to the  $69p_{3/2} + 71p_{3/2}$  asymptote by including the contribution of various symmetries (see Fig. 2): the lineshape is reproduced within the experimental uncertainties [3].

### • Evanescent-wave mirrors

In [4], we investigated the interaction of an ultracold diatomic polar molecule with an evanescent-wave mirror (EWM). Several features of this system were explored, such as the coupling between internal rovibrational states of the molecule and the laser field (see Fig. 3). Using numerical simulations under attainable physical conditions, we found that the reflection/transmission coefficient depends on the internal (rovibrational) states of the

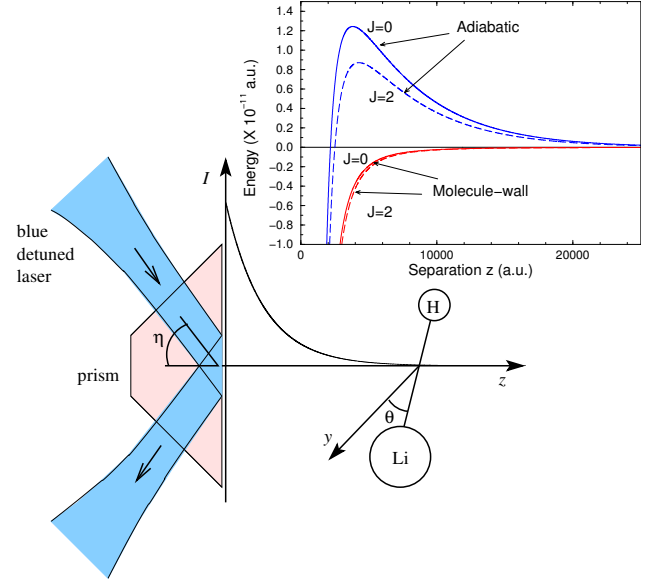


Figure 3: Setup: laser light enters a prism (index  $n$ , angle  $\eta$ ) and undergoes total internal reflection. At a distance  $z$  outside the prism, the evanescent field interacts with the polar molecule. *Inset*: Molecular-light and adiabatic potentials for  $J = 0$  and  $2$ .

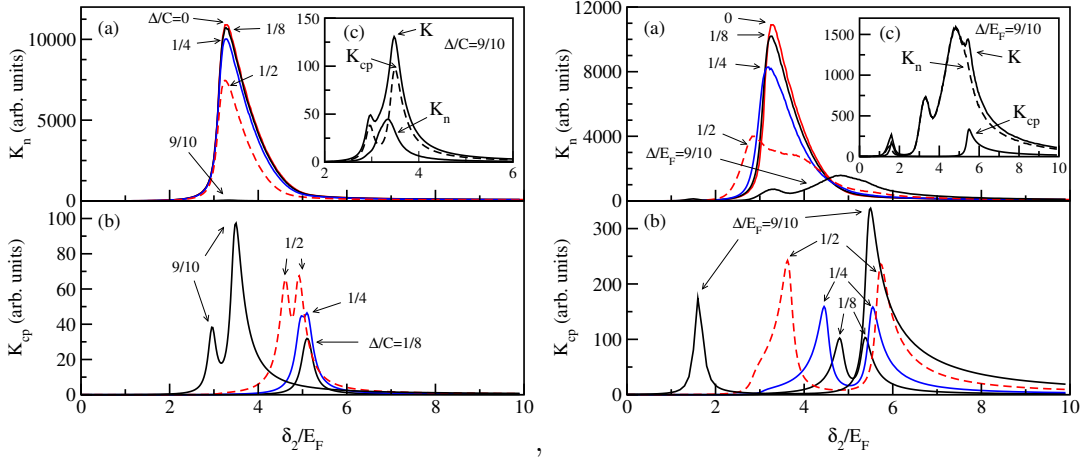


Figure 4: Left (weak coupling  $C = \frac{1}{8}E_F$ ): normal  $K_n$  (a) and correlated pair  $K_{cp}$  (b) signals for various BCS-gaps  $\Delta/C$ . (c) the double peak of  $K_{cp}$  becomes apparent in the total signal  $K$  for a large gap ( $\Delta/C = 0.9$ ). Right (strong coupling  $C = 87E_F$ ): same for various  $\Delta/E_F$ . ( $E_F = 1 \mu\text{K}$ ).

molecules. Such molecular optics components could facilitate the manipulation and trapping of ultracold molecules, and might serve in future applications in several fields, e.g., as devices to filter and select state for ultracold chemistry, to measure extremely low temperatures of molecules, or to manipulate states for quantum information processing.

#### • Degenerate Fermi gas

In [5], we worked on the spectroscopic signature of Cooper pairs in a degenerate Fermi gas, namely  ${}^6\text{Li}$ . We calculated two-photon Raman spectra for fermionic atoms with interactions described by a single-mode mean-field BCS-BEC crossover theory. By comparing calculated spectra of interacting and non-interacting systems, we found that interactions lead to the appearance of correlated atomic pair signal - due to Cooper pairs; splitting of peaks in the spectroscopic signal - due to the gap in fermionic dispersion; and attenuation of signal - due to the partial conversion of fermions into the corresponding single-mode dimer. By exploring the behavior of these features (see Fig. 4), one can obtain quantitative estimates of the BCS parameters from the spectra, such as the value of the gap as well as the number of Cooper pairs.

#### Future Plans

In the coming year, we plan to continue the alkali hydride work by exploring the formation of molecules in the  $a^3\Sigma^+$  electronic state [6]. It is predicted to support one ro-vibrational level, leading to a sample in a pure single ro-vibrational state. We also will extend this work to other polar molecules relevant to the experimental community, such as LiCs [7], LiRb, etc. We also plan to explore the enhancement of photoassociation rates associated with Feshbach resonances.

We expect to carry more calculations on Rydberg-Rydberg interactions and explore the possibility of forming metastable long-range doubly-excited Rydberg molecules as well as the experimental signature to be expected [8]. Finally, we will investigate the possibility of trapping and cooling molecules using evanescent-wave mirrors with time-dependent laser fields.

## Publications sponsored by DOE

1. E. Juarros, P. Pellegrini, K. Kirby, and R. Côté, *One-photon-assisted formation of ultracold polar molecules*. Phys. Rev. A **73**, 041403(R) (2006).
2. E. Juarros, K. Kirby, and R. Côté, *Laser-assisted Ultracold Lithium-hydride Molecule Formation: Stimulated vs. Spontaneous Emission*. Submitted to J. Phys. B on April 30 2006 (accepted).
3. J. Stanojevic, R. Côté, D. Tong, S.M. Farooqi, E.E. Eyler, and P.L. Gould, *Long-range Rydberg-Rydberg interactions and molecular resonances*. Eur. Phys. J. D (published online June 21, 2006).
4. K. Shimshon, B. Segev, and R. Côté, *Evanescence-Wave Mirror for Ultracold Diatomic Polar Molecules*. Phys. Rev. Lett. **95**, 163005 (2005).
5. M. Kořtrun and R. Côté, *Two-color spectroscopy of fermions in mean-field BCS-BEC crossover theory*. Phys. Rev. A **73**, 041607(R) (2006).
6. E. Juarros, K. Kirby, and R. Côté, *Formation of ultracold molecules in a single pure state:  $LiH$  in  $a^3\Sigma^+$* . In preparation.
7. P. Pellegrini and R. Côté, *Formation of ultracold  $LiCs$* . In preparation.
8. J. Stanojevic and R. Côté, *Molecular resonances in ultracold Rydberg gases*. In preparation.

Cold Molecules –  
Laser cooling and magnetic trapping of neutral, ground-state, polar  
molecules for collision studies

Jun Ye

JILA and Department of Physics, National Institute of Standards and Technology and  
University of Colorado, Boulder, CO 80309-0440  
Email: Ye@jila.colorado.edu

A main scientific goal of our work toward cold molecules is to achieve a significant improvement in the phase space density of cold, ground-state, polar molecules, opening the door for an external control by applied fields of dipolar interactions important for ultra-cold collisions, certain chemical reactions, and quantum control.

In the past year, three projects were carried out. First, we built on our success in producing slow and cold beams of hydroxide radicals (OH) in a Stark decelerator and used cold samples of OH molecules for precision spectroscopy [1]. Experimental resolution is significantly improved, leading to 25-fold increase in measurement precision of the ground-state structure of OH. The spectroscopy data has resulted in improved understandings of higher-order angular momentum couplings in OH, thanks to the collaboration with the theory group of John Bohn at JILA. Comparing the laboratory measured transition frequencies to those from OH megamasers in interstellar space will allow a test sensitivity of  $10^{-6}$  for a possible variation in the fine structure constant  $\alpha$  over  $10^{10}$  years.

In the second experiment, we successfully produced cold and slow beams of formaldehyde ( $\text{H}_2\text{CO}$ ) molecules [2], at a temperature of 100 mK and with a density of about  $10^6 \text{ cm}^{-3}$ , the first time an asymmetric rotor was decelerated.  $\text{H}_2\text{CO}$  holds a prominent position in molecular physics. As a four-atom asymmetric rotor,  $\text{H}_2\text{CO}$ 's rotational structure and six internal degrees of freedom give rise to the same complexities of much large molecules. However, as a relatively light molecule,  $\text{H}_2\text{CO}$  is still tractable at a high level of theory, making it an ideal proving ground for molecular physics. OH –  $\text{H}_2\text{CO}$  collision and reaction dynamics provide a novel paradigm for the study and control of cold chemical reactions. The energy resolution and tuning capability of the Stark decelerator make it an unprecedented tool to study chemical reactions with near zero barriers. Specifically, the hydrogen abstraction channel in the reaction  $\text{H}_2\text{CO} + \text{OH} \rightarrow \text{CHO} + \text{H}_2\text{O}$  is theoretically studied. By trapping OH and “bombarding” the trap with decelerated  $\text{H}_2\text{CO}$  packets, while monitoring OH trap loss and the production of the formyl CHO radicals, the OH -  $\text{H}_2\text{CO}$  total scattering and reaction rates can be mapped out as a function of collision energy.

The third project improved the Stark decelerator efficiency. A systematic study has been performed on the intrinsic properties of the Stark decelerator. Using a new electric field

switching sequence, we can now operate the decelerator in different resonant modes than the fundamental mode. The enhanced transverse guiding capabilities have allowed an increase of Stark decelerated molecular numbers by a factor of 5.

In the near future, we will continue with our experiment on magnetic trapping of OH. Furthermore, we are collaborating with Chris Greene's group in JILA on systematic modeling of cavity-assisted cooling of OH molecules before we start a full experimental investigation.

In related experiments on producing ultracold molecules based on ultracold atoms, we have performed narrow-line photoassociation spectroscopy using a weak intercombination transition of Sr atoms confined in an optical lattice [3]. The weak dipole coupling associated with the narrow transition leads to good Franck-Condon overlapping factors between the vibrational levels in the S + P excited and S + S ground state potentials, favoring decays of the excited molecules into tightly bound and stable ground-state molecules. Furthermore, with the goal to produce a dense ensemble of stable ultracold polar molecules, we have started theoretical investigations on a general scheme for performing narrowband Raman transitions between vibrational molecular states with efficiencies approaching unity using a coherent train of weak pump-dump pairs of shaped ultrashort pulses.

1. E. R. Hudson, H. J. Lewandowski, B. C. Sawyer, and J. Ye, "Cold molecule spectroscopy for constraining the evolution of the fine structure constant," *Phys. Rev. Lett.* **96**, 143004 (2006).
2. E. R. Hudson, C. Ticknor, B. C. Sawyer, C. A. Taatjes, H. J. Lewandowski, J. R. Bochinski, J. L. Bohn, and J. Ye, "Production of cold formaldehyde molecules for study and control of chemical reaction dynamics with hydroxyl radicals," *Phys. Rev. A* **73**, 063404 (2006).
3. T. Zelevinsky, M. M. Boyd, A. D. Ludlow, T. Ido, J. Ye, R. Ciurylo, P. Naidon, and P. S. Julienne, "Narrow line photoassociation in an optical lattice," *Phys. Rev. Lett.* **96**, 203201 (2006).

# Exploiting Universality in Atoms with Large Scattering Lengths

Eric Braaten

## Contact info

Physics Department  
Ohio State University  
191 W Woodruff Ave  
Columbus OH 43210-1117  
(braaten@mps.ohio-state.edu)

## Program scope

Atoms whose scattering lengths are large compared to the range set by their interactions exhibit universal behavior at sufficiently low energies. Recent dramatic advances in cooling atoms and in manipulating their scattering lengths have made this phenomenon of practical importance for controlling ultracold atoms and molecules. This research project is aimed at developing a systematically improvable method for calculating few-body observables for atoms with large scattering lengths starting from the universal results as a first approximation. The ultimate goal is to be able to predict and control the behavior of ultracold atoms and molecules near a Feshbach resonance.

## Recent Progress

Hans-Werner Hammer and I completed a lengthy review article (132 pages) entitled *Universality in Few-body Systems with Large Scattering Length* that was recently published in Physics Reports [1]. It provides an introduction to the concept of universality for atoms with large scattering length, summarizes the universal results that had been obtained to date, and lays the ground work for further progress in this direction.

I was the coorganizer of a workshop at the Institute for Nuclear Theory in Seattle in August 2005. At the workshop, I met Rudi Grimm and I communicated to him the results on Efimov states obtained by Hammer

and me. Grimm's group at Innsbruck used these results in the analysis of their data on 3-body recombination in cold  $^{133}\text{Cs}$  atoms that led to their announcement in March 2006 of the first experimental evidence for Efimov states [T. Kraemer et al., Nature 440, 315-318 (2006)].

In collaboration with a graduate student Dongqing Zhang, I developed a new factorization approximation for the break-up and recombination rates for loosely-bound molecules composed of atoms with a large scattering length  $a$  in processes with large collision energy  $E \gg \hbar^2/ma^2$ . The leading contributions to their rates can be separated into short-distance factors that are insensitive to  $a$  and long-distance factors that are insensitive to  $E$ . The short-distance factors are atom-atom cross sections at a lower collision energy. In simple cases, the long-distance factors simply count the number of atoms in the molecule. An example is an analytic formula for the 3-body recombination rate constant at a collision energy in the range  $\hbar^2/ma^2 \ll E \ll \hbar^2/mr_s^2$ , where  $r_s$  is the effective range:

$$K_3(E) = \frac{12288\sqrt{3}\pi^2\hbar^5}{3m^3E^2}. \quad (1)$$

After the paper was dramatically expanded from its original version to convince a skeptical referee of the validity of the results, it was published in Physical Review A [2].

I have understood how to use few-body calculations to determine parameters that govern the phenomenon of atom-molecule coherence in Bose-Einstein condensates of atoms with large scattering length. The method is based on the one-particle-irreducible (1PI) effective action formalism for quantum field theory. Unlike previous approaches to this problem, this new approach does not require a microscopic model with an explicit molecular field. It can be applied equally easily to models in which the shallow dimer is generated dynamically. Unfortunately I have been slow in writing this work up for publication.

### Future Plans

Universality relates 3-body results for large positive and negative scattering length on opposite sides of a Feshbach resonance. The recent evidence for Efimov states from the Grimm group involved large positive and negative scattering lengths on opposite sides of a zero in the scattering length for  $^{133}\text{Cs}$  atoms. An accurate model for the 2-body physics in this experiment

is the resonance model, with atom fields that couple to a molecular field and also have a zero-range interaction that gives a large background scattering length. I plan to calculate various 3-body observables using this model, including the Efimov spectrum and the 3-body recombination rate, in order to predict quantitatively how observables on opposite sides of a zero in the scattering length should be related.

A universal result for the 3-body recombination rate at threshold for identical bosons with a large scattering length has been derived by Petrov and by Gasaneo, Macek, and Ovchinnikov:

$$K_3(0) = \frac{768\pi^2(4\pi - 3\sqrt{3})\hbar a^4/m}{\sinh^2(\pi s_0) + \cosh^2(\pi s_0) \cot^2[s_0 \ln(a\kappa_*) + 1.16]}, \quad (2)$$

where  $s_0 = 1.00624$  and  $\kappa_*$  is a 3-body parameter. It should be possible to calculate  $K_3(E)$  in terms of  $a$  and  $\kappa_*$  only at all collision energies satisfying  $E \ll \hbar^2/mr_s^2$ . I would like to carry out this calculation and show that it interpolates between the universal result at threshold in Eq. (2) and the universal result at high energy in Eq. (1). The results would be compared with those from solving the 3-body Schroedinger equation for  $^4\text{He}$  atoms numerically which revealed dramatic variations of the contributions from various partial waves as a function of the collision energy [Suno et al., Phys. Rev. A **65** 042725 (1991)]. If these results can be reproduced using the universality approach, it should convince skeptics of the power of this method.

One great advantage of my method for using the 1PI effective action to determine parameters that govern atom-molecule coherence is that it can be extended rather straightforwardly to Efimov trimers. I plan to carry out these calculations to determine parameters that govern the coherent flow of atoms between Bose-Einstein condensates consisting of atoms, dimers, and Efimov trimers.

## Recent publications

1. *Universality in Few-body Systems with Large Scattering Length*, Eric Braaten and H.-W. Hammer, Physics Reports **428**, 259 (2006) [arXiv:cond-mat/0410417]
2. *Factorization in Break-up and Recombination Processes for Atoms with a Large Scattering Length*, E. Braaten and D. Zhang, Physical Review A **73**, 042707 (2006) [arXiv:cond-mat/0501510].

# Quantum Dynamics of Optically-Trapped Fermi Gases

Grant #DE-FG02-01ER15205  
Report for the Period: 11/1/05-10/31/06

John E. Thomas  
Physics Department, Duke University  
Durham, NC 27708-0305  
e-mail: jet@phy.duke.edu

## 1. Scope

The purpose of this program is to study the many-body quantum dynamics of a very general fermionic system: An optically trapped, strongly-interacting 50-50 mixture of spin-up and spin-down  ${}^6\text{Li}$  fermions, in the regime of quantum degeneracy. Strongly-interacting, highly degenerate samples are directly produced in an ultrastable  $\text{CO}_2$  laser trap by forced evaporation at a magnetic field tuned near a Feshbach resonance. The resonance permits wide tunability of the s-wave scattering length which determines the interaction strength.

Strongly-interacting mixtures of spin-up and spin-down atomic Fermi gases provide unique systems for stringent tests of competing quantum theories of superfluidity and high temperature superconductivity. In the controlled environment of an optical trap, such mixtures permit wide variation of temperature, density, spin composition and interaction strength. Indeed, strongly-interacting Fermi gases provide scale models of a variety of exotic systems in nature, not only high temperature superconductors, but neutron stars, strongly-interacting matter in general, and even a quark-gluon plasma. The scale is set by the Fermi temperature, which is a few  $\mu\text{K}$  in a quantum gas and about an electron volt in a metal or  $10^4$  K. Near a Feshbach resonance, spin-up and spin-down mixtures of atomic Fermi gases exhibit super-strong pairing interactions and are predicted to achieve superfluid transition temperatures which are a significant fraction of the Fermi temperature. Such high transition temperatures are consistent with recent experiments and correspond to achieving superconductivity in a metal at thousands of degrees, far above room temperature.

## 2. Recent Progress

During the past year, we achieved an important breakthrough in devising a model-independent method for measuring the energy of a strongly-interacting Fermi gas [11]. Using this method, we are currently measuring the entropy of the gas as a function

of energy. We are also measuring the velocity of sound in the gas, as a function of magnetic field, to explore sound propagation in molecular BEC's and Fermi superfluids. This study tests recent predictions of the zero temperature equation of state of the gas. In addition, we have brought a new second-generation apparatus online. The primary results are described briefly below.

### *Energy Measurement in a Strongly-Interacting Fermi Gas [11]*

Strongly-interacting Fermi gases provide a paradigm for strong interactions in nature. For this reason, measurements of the thermodynamic properties of this unique system are of paramount importance. Model-independent measurement of the energy is essential for exploring the dynamics and thermodynamics of the gas.

Model-independent energy measurement is a consequence of universality, which requires generally that a strongly-interacting gas obey the virial theorem. Near a broad Feshbach resonance, the s-wave scattering length diverges, and the only length scale is the interparticle spacing. In this case, the local pressure in the gas is a function only of the density and temperature. It then follows from elementary thermodynamics that the pressure is  $2/3$  of the local energy density. Using this result for a harmonically trapped gas, one finds that the potential energy of a strongly interacting gas is precisely half of the total energy, as for an ideal gas. This is a remarkable result, since the gas generally contains superfluid pairs, noncondensed pairs, and unpaired Fermi atoms, all strongly interacting.

Since the potential energy is proportional to the mean square cloud size, the energy can be determined in a model-independent manner simply by measuring the profile of the trapped cloud and trap oscillation frequencies. Further, the corrections arising from anharmonicity in the trap are readily computed.

### *Entropy Measurement*

To measure the entropy, we first create a superfluid, strongly-interacting Fermi gas of  ${}^6\text{Li}$  at broad Feshbach resonance by evaporative cooling at a magnetic field of 834 G. The gas is confined in a shallow trap to minimize heating arising from relaxation processes. Then we add energy by releasing and recapturing the cloud. After the gas reaches equilibrium over a period of a second, we measure the cloud size to determine the energy  $E$ . Then the experiment is repeated, except that the magnetic field is swept from 834 G to 1200 G before measuring the cloud size. At 1200 G, the cloud is weakly interacting, and the entropy is essentially equal to that of an ideal Fermi gas (the perturbative corrections are known). The cloud size at 1200 G determines the energy of the weakly interacting gas, and hence its entropy. The magnetic field sweep is shown to be adiabatic by a round trip sweep, which produces cloud radii and atom numbers which are identical to those obtained without a sweep. Then, the measured ideal gas entropy is that of the strongly-interacting gas for the

given initial energy  $E$ . Experiments to measure  $S(E)$  for a strongly-interacting Fermi gas are currently in progress. These measurements will also enable an experimental test of the calibration between our measured empirical temperature and the actual reduced temperature  $T/T_F$ , as used on our recent measurements of the heat capacity [9].

### *Sound Velocity Measurement*

We have made major progress measuring the propagation of first sound throughout the entire BEC-BCS crossover regime. As is well known, by tuning the magnetic field in the vicinity of a Feshbach resonance, it is possible to access a variety of superfluids including a BEC of molecules well below resonance, a strongly-interacting Fermi gas on resonance, and a weakly interacting Fermi gas above resonance. By measuring the sound velocity over a wide range of magnetic fields, we are able to test predictions for the zero temperature equation of state over a wide range of interaction strengths.

In the experiments, we use a 532 nm beam to excite a ripple in a cigar-shaped cloud, and to watch the ripple propagate along the axial direction, to determine the sound velocity. The ripple covers the 200  $\mu$  cloud in about 10 ms. The statistical error in the measurements is quite small. Our preliminary measurements are in good agreement with quantum Monte Carlo calculations and appear to rule out the Leggett ground state. Currently, we are trying to understand the systematic errors and hope to submit a paper in the near future.

### **3. Future Plans**

Our present plans include comprehensive measurement of the entropy, for both balanced and imbalanced spin mixtures, as a function of energy. Further, we hope to measure the dependence of the sound velocity on the energy. These measurements will test the best finite-temperature many-body predictions of the equation of state in the nonperturbative regime.

### **4. References to Publications of DOE Sponsored Research (Past 3 Years)**

- 1) M. E. Gehm, S. L. Hemmer, S. R. Granade, K. M. O'Hara, and J. E. Thomas, "Mechanical stability of a strongly interacting Fermi gas of atoms," *Phys. Rev. A* **68**, 011401(R) (2003).
- 2) M. E. Gehm, S. L. Hemmer, K. M. O'Hara, and J. E. Thomas, "Unitarity-limited elastic collision rate in a harmonically trapped Fermi gas," *Phys. Rev. A* **68**, 011603(R) (2003).
- 3) J. E. Thomas, S. L. Hemmer, J. Kinast, A. Turlapov, M. E. Gehm, and K. M. O'Hara, "Dynamics of a highly-degenerate, strongly-interacting Fermi gas of atoms," *Proceedings of the Quantum Fluids Conference 2003* (Albuquerque, NM, August 3-8, 2003); *J. Low Temp. Phys.* **104** (2003).

- 4) J. E. Thomas, S. L. Hemmer, J. M. Kinast, A. V. Turlapov, M. E. Gehm, and K. M. O'Hara, "Dynamics of a highly-degenerate, strongly-interacting Fermi gas," Proceedings of the 16<sup>th</sup> International Conference on Laser Spectroscopy, (Palm Cove, Australia, July 13-18, 2003), P. Hannaford, A. Sidorov, H. Bachor, and K. Baldwin, editors, p.137-144.
- 5) K. M. O'Hara, M. E. Gehm, S. R. Granade, M.-S. Chang, and J. E. Thomas, "Coherence in an optically trapped Fermi gas," in *Proceedings of the Eighth Rochester Conference on Coherence and Quantum Optics*, N. P. Bigelow, J. H. Eberly, C. R. Stroud, and I. A. Walmsley, editors, (Kluwer Academic/Plenum Publishers, New York, 2003), pp. 587.
- 6) J. Kinast, S. L. Hemmer, M. E. Gehm, A. Turlapov, and J. E. Thomas, "Evidence for superfluidity in a resonantly interacting Fermi gas," *Phys. Rev. Lett.* **92**, 150402 (2004).
- 7) J. E. Thomas and M. E. Gehm, "Optically trapped Fermi gases," *Amer. Sci.* **92**, 238-245 (2004).
- 8) J. Kinast, A. Turlapov, and J. E. Thomas, "Breakdown of hydrodynamics in the radial breathing mode of a strongly interacting Fermi gas," *Phys. Rev. A* **70**, 051401(R) (2004).
- 9) J. Kinast, A. Turlapov, and J. E. Thomas, "Heat capacity of a strongly-interacting Fermi gas," *Science* **307**, 1296 (2005).
- 10) J. Kinast, A. Turlapov, and J. E. Thomas, "Damping of a unitary Fermi Gas," *Phys. Rev. Lett.* **94**, 170404 (2005).
- 11) J. E. Thomas, J. Kinast and A. Turlapov, "Virial theorem and universality in a unitary Fermi gas," *Phys. Rev. Lett.* **95**, 120402 (2005).
- 12) J. Kinast, A. Turlapov, and J. E. Thomas, "Optically trapped Fermi gases model strong interactions in nature," *Opt. Phot. News*, **16**, 21 (December, 2005).
- 13) J. E. Thomas, J. Kinast, and A. Turlapov, "Thermodynamics and mechanical properties of a strongly-interacting Fermi gas," Proceedings of the 17th International Conference on Laser Spectroscopy, Aviemore, Scotland (June 19-24, 2005), E. A. Hinds, A. Ferguson and E. Riis editors, p.223-238 (World Scientific London 2005).
- 14) J. E. Thomas, J. Kinast, and A. Turlapov, "Universal thermodynamics of a strongly-interacting Fermi gas," Proceedings of the 24th International Conference on Low Temperature Physics, Orlando, Florida (August 10-17, 2005).

# Strongly Interacting Bose and Fermi gases

John L. Bohn  
JILA, UCB 440  
University of Colorado  
Boulder, CO 80309  
[bohn@murphy.clolorado.edu](mailto:bohn@murphy.clolorado.edu)

## Program Scope:

The work in this program revolves around the theory of novel few- and many-body systems that are now becoming experimentally feasible. One such system is an ultracold gas of alkali atoms whose interparticle interaction varies resonantly with a magnetic field. A second is an ultracold gas of polar molecules, where the strong and anisotropic dipole-dipole interaction introduces qualitatively new phenomena.

## Recent Progress:

Bose-Fermi Mixtures. The ability to tune interparticle interactions between atoms, via magnetic-field Feshbach resonances, has greatly enriched the phenomena available in ultracold quantum degenerate gases. For bosons, this has meant coherent atom-molecule oscillations and the rigged collapse of Bose-Einstein condensates. For fermions, it has allowed the study of the “crossover” regime between Cooper pairs of atoms on one side, and Bose-condensed molecules on the other. Now, experiments are also turning to mixtures of bosons and fermions, where the interaction can be tuned between the two. This summer, for example, several groups have reported creating  $^{40}\text{K}$ - $^{87}\text{Rb}$  molecules using a Feshbach resonance.

The standard many-body theory of such systems posits a separate quantum field that keeps track of pairs of atoms. For dealing with pairs of bosons or pairs of fermions, this theory is reasonable, indeed often quantitative, at the mean-field level. Last year we found that this is not the case for the boson-fermion mixture [1]. We showed that the mean-field version of the theory is unable to reproduce the molecular binding energy in the limit where the density of the gas is low. We further traced this difficulty to the way in which the theory treats three-body correlation functions [1].

We have therefore also approached this problem from another direction. In the perturbative, low density limit, we can evaluate the scattering T-matrix. If there were only one fermion and one boson present, the poles of this T-matrix would accurately identify both the true molecular binding energy, and the positions and widths of scattering resonances. The poles shift, however, in the many-body environment, in a way we can track perturbatively [2]. A main result

of this analysis is that the energetics and stability of the fermionic pairs in the gas depend strongly of the center-of-mass momentum of the pair. This is shown in the figure below.

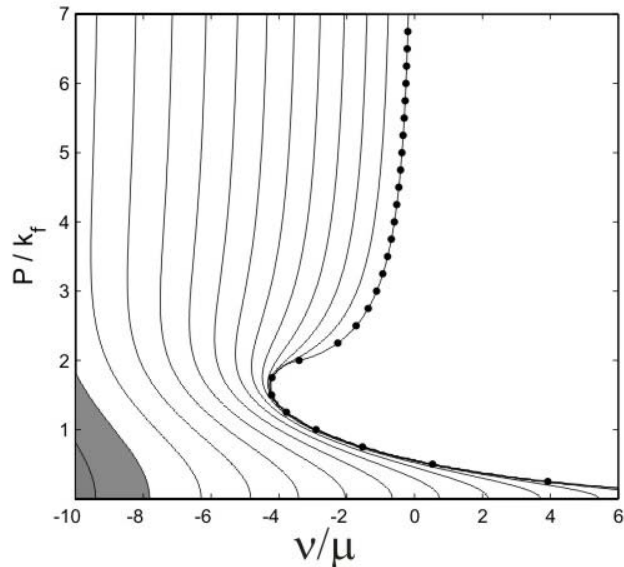


**Figure.** Contours of molecular population under various combinations of molecular center-of-mass momentum  $P$  and magnetic field detuning  $v/\mu$ , in a Bose-Fermi mixture. The dotted contour denotes the dividing line between stable molecules on the left, and unstable molecules on the right. For a single molecule, this contour would be a vertical line at  $v/\mu = 0$ . In the many-body environment, however, two things occur. First, for low center-of-mass momentum  $P$ , molecules that are not intrinsically stable are stabilized; and second, for intermediate values of  $P$ , molecules that would have been stable are de-stabilized [2].

Dipolar Bose-Einstein Condensates. We are also exploring the properties of Bose-Einstein condensates whose constituents interact via dipolar forces. This is relevant to the recently achieved BEC of chromium, and to the yet-to-be-achieved BEC of heteronuclear molecules. It had been assumed in the theoretical community that the usual Gross-Pitaevskii (GP) equation would adequately describe dipolar BEC, after modifying it to account for the nonlocal dipolar interaction, yet this assumption had not been tested rigorously. We therefore tested the GP equation against Diffusion Monte Carlo calculations performed by our collaborator, D. Blume at Washington State University. We found that the modified GP equation works well, provided that proper account is taken of the way in which the two-body scattering length depends on the dipole moment [3].

In doing this careful study, we became aware of an unexpected instability of the dipolar BEC. It has been long understood that if enough dipoles are added to the condensate, then ultimately the attractive part of the interaction overwhelms the repulsive part, and the condensate collapses. However, we found that long before this happens, the two-body interaction can ingest an additional bound state,

driving the scattering length negative and inducing a collapse. This collapse could be the dominant effect observed as experiments approach molecular BEC's.

In addition, we have computed, for the first time, the Bogoliubov excitation spectrum for a fully three-dimensional dipolar BEC [4]. This was a significant numerical challenge, which will allow a number of studies on the collective excitations, condensate collapse, and finite temperature effects.

### **Future Plans:**

Bose-Fermi Mixtures. We will continue to probe the theory of the BF mixture. Notably, the results in [1,2] assumed that the nonresonant scattering length is zero, for simplicity. For the real  $^{40}\text{K}$ - $^{87}\text{Rb}$  system, this is far from true, and the inclusion of the correct scattering length will likely impact the results. In spite of the deficiencies of the mean-field approach, we expect to probe the qualitative features of the system using mean-field theory, as a reference against which to understand more realistic theories later on. We should then be able to address realistic issues such as mechanical stability of a resonant Bose-Fermi mixture, creation heteronuclear fermionic molecules, and Bose-mediated fermionic superfluidity in these systems.

Dipolar BEC. We have already submitted results showing the unexpected richness of the stability diagram of dipolar BEC as the trap aspect ratio is varied. We are further exploring the excitation spectrum at nonzero temperatures. In the longer term, we expect to assess the influence of realistic molecular structure on the dipolar interaction, hence on the condensate as a whole.

P-wave superfluidity. An additional topic, mentioned in the original proposal, is the behavior of a gas of fermionic atoms interacting near a p-wave Feshbach resonance. This topic is of growing importance, as experimental efforts at JILA move in this direction.

### **DOE-Sponsored Publications:**

[1] *Bose-Fermi Mixtures Near an Interspecies Feshbach Resonance*

D. C. E. Bortolotti, A. V. Avdeenkov, C. Ticknor, and J. L. Bohn, *J. Phys. B.* **39**, 189 (2006).

[2] *Stability of Fermionic Feshbach Molecules in a Bose-Fermi Mixture*

A. V. Avdeenkov, D. C. E. Bortolotti, and J. L. Bohn, *Phys. Rev. A* **74**, 012709 (2006).

[3] *Dipolar Bose-Einstein Condensates with Dipole-Dependent Scattering Length*

S. Ronen, D. C. E. Bortolotti, D. Blume, and J. L. Bohn, *Phys. Rev. A* (accepted).

[4] *Bogoliubov modes of a dipolar condensate in a cylindrical trap*

S. Ronen, D. C. E. Bortolotti, and J. L. Bohn, *Phys. Rev. A* (accepted).

# Exploring Quantum Degenerate Bose-Fermi Mixtures

Deborah Jin  
JILA, UCB440  
University of Colorado  
Boulder, CO 80309  
[jin@jilaul.colorado.edu](mailto:jin@jilaul.colorado.edu)

## Program Scope

In this project we are exploring interaction dynamics in an ultracold, trapped gas of bosonic and fermionic atoms. Investigation of this new class of quantum degenerate gases concentrates on interaction dominated phenomena such as sympathetic cooling, phase separation, excitations, Feshbach resonances, and the effects of quantum degeneracy. In addition to exploring these new phenomena we seek to understand and ultimately control the interactions in the gas. In particular, effective interactions between the fermionic atoms will be explored in the context of the longer term goal of realizing Cooper pairing of atoms.

## Recent Progress and Future Plans

In the recent three year funding period we achieved a quantum degenerate Bose-Fermi mixture using evaporative cooling of the bosonic  $^{87}\text{Rb}$  atoms and sympathetic cooling of the fermionic  $^{40}\text{K}$  atoms. We characterized the interactions between bosons and fermions in this mixture by measuring the magnitude of the interspecies s-wave scattering length.<sup>1, 2</sup> We then implemented a far off resonance optical dipole trap to confine the ultracold gas mixture with atoms in spin states that cannot be magnetically confined. This allowed us to observe four distinct interspecies Feshbach in the ultracold  $^{87}\text{Rb}/^{40}\text{K}$  mixture.<sup>3</sup> These resonances open up exciting new possibilities for controlled exploration of interaction effects in ultracold Bose-Fermi gas mixtures. In recent work (unpublished) we have been further investigating the Feshbach resonances, with an emphasis on looking for evidence of heteronuclear molecule creation. Our results are discussed in more detail below.

### *Evaporative cooling in the optical trap*

With direct evaporation of the bosonic  $^{87}\text{Rb}$  atoms and sympathetic cooling of the  $^{40}\text{K}$  atoms we reached quantum degeneracy with the Bose-Fermi mixture in the magnetic trap. However, our first observation of Feshbach resonances used a relatively hot ( $T=14\ \mu\text{K}$ ) gas in the optical trap. For future experiments using an interspecies Feshbach resonance we clearly would require a gas cooled to a temperature below or near quantum degeneracy. For example, it has been shown that Feshbach molecule creation depends on the quantum degeneracy of the atom gas.<sup>4</sup>

Before attempting evaporative cooling in the optical trap we first improved our trap stability to reduce heating effects. We improved the pointing stability of the optical trap beam by implementing more stable mounting of the relevant optics. We also improved the intensity stability of the optical trap beam using active feedback.

Evaporation was then implemented by ramping down the beam intensity to lower the trap depth. This simultaneous evaporation of the  $^{87}\text{Rb}$  and  $^{40}\text{K}$  atom gases works well and with about 10 seconds of evaporation we can achieve quantum degeneracy of the mixture.

### *A p-wave Feshbach resonance*

Loss of trapped atoms near a Feshbach resonance, due to inelastic collisions, provides a very convenient method of detecting a Feshbach resonance. However, high temperatures can mask features of the resonance, such as in the case of a p-wave resonance. In Fig. 1 we see that at  $T \sim 300$  nK we can resolve the predicted double peak structure of a p-wave resonance between  $^{40}\text{K}$  atoms and  $^{87}\text{Rb}$  atoms.<sup>5</sup> These features correspond to different projections of the pair angular momentum onto the magnetic-field direction.

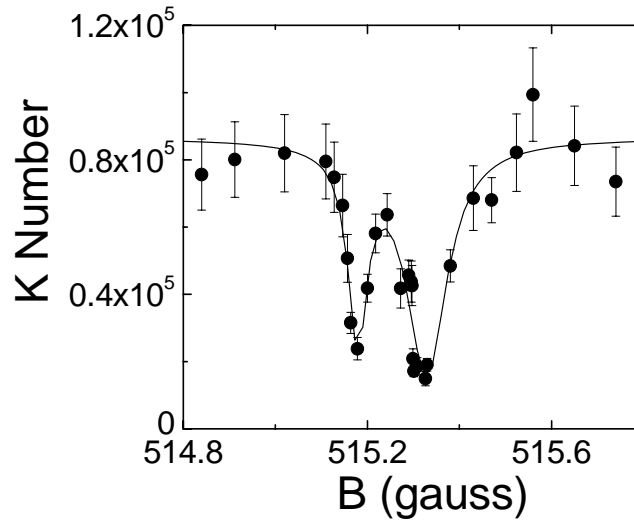


Fig. 1. Loss of K atoms near a p-wave Feshbach resonance. The two features correspond to different projections of the pair angular momentum,  $m_L = \pm 1$  and  $m_L = 0$ . The fact that the mixture is ultracold ( $T \sim 300$  nK) allows us to resolve the two features, which are separated by only 0.15 G.

### *Creating heteronuclear Feshbach molecules*

Since the observation of heteronuclear Feshbach resonances<sup>3, 6</sup> a number of experimental groups have been trying to create heteronuclear Feshbach molecules. Very recently this has been achieved for  $^{87}\text{Rb}$  and  $^{40}\text{K}$  atoms in an optical lattice<sup>7</sup>, as well as for a mixture of two Rb isotopes in an optical trap<sup>8</sup>. In this section, we discuss our preliminary results in creating  $^{87}\text{Rb}$ - $^{40}\text{K}$  Feshbach molecules in an optical trap.

For this work we added the capability to perform fast magnetic-field sweeps, using an auxiliary pair of coils whose current is provided by the controlled discharge of a large capacitor. When initially charged to a high voltage the capacitor can drive a fast current change in the coils and thus provide a fast change in the magnetic-field.

We tried making molecules using the relatively wide s-wave Feshbach resonance at about 545 G and sweeping the magnetic field from 5 G above the resonance to 5 G below the resonance. Since the Feshbach molecule state appears for magnetic field strengths below the resonance, this sweep should produce molecules. Moreover, one expects an exponential dependence for the number of molecules created as a function of sweep rate. Our results are shown in Fig. 2. We chose to work with a near degenerate gas, with  $T \sim 1.3 * T_c$  where  $T_c$  is the  $^{87}\text{Rb}$  BEC transition temperature, to avoid possible losses due to the high density of a BEC. When we sweep through the resonance we observe a loss of atoms; this is consistent with molecule production since molecules are not detected by our resonant absorption imaging. We find that the loss is exponentially dependent on the sweep rate, as expected for molecule creation. Also consistent with molecule creation is the fact that we see much less loss, for similar sweep speeds, when sweeping the magnetic field in the opposite directions (low to high).

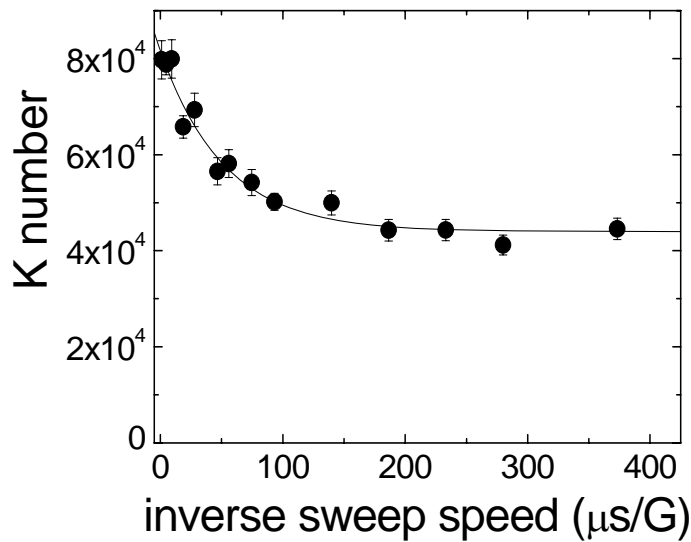


Fig.2. Measured number of  $^{40}\text{K}$  atoms as a function of the inverse sweep speed of a ramp across an s-wave Feshbach resonance. The data are consistent with the creation of about 40,000 heteronuclear Feshbach molecules. The error bars correspond to statistical fluctuations in repeated measurements. For this data  $T = 500$  nK and the number of  $^{87}\text{Rb}$  atoms was 5 times the initial number of  $^{40}\text{K}$  atoms.

We find that the observed atom loss, which we associate with molecule creation, depends critically on whether or not we actually cross the Feshbach resonance, as one would expect. This provides a precise measure of the resonance location, which we find to be  $B_0 = 546.44 \pm 0.12$  G.

Finally we have attempted to reverse the process and convert the molecules back to free atoms with an additional sweep back above the resonance. Preliminary results with such a double sweep experiment showed that we could recover about half the “lost” atoms. The conversion from atoms to Feshbach molecules should in principle be completely reversible and we are currently investigating why we are not able to recover more of the atoms. We can measure the lifetime of the molecules by inserting a variable

hold time at some magnetic field before the sweep back across the resonance. One such measurement gave a relatively short molecule lifetime,  $\tau = 25 \pm 9 \mu\text{s}$ , however we need to explore the dependence on the ultracold gas density, the ratio of the numbers of  $^{87}\text{Rb}$  and  $^{40}\text{K}$  atoms, and the value of magnetic field relative to the Feshbach resonance.

### DOE-supported Publications

1. "Measurement of the interaction strength in a Bose-Fermi mixture with Rb-87 and K-40", J. Goldwin, S. Inouye, M. L. Olsen, B. Newman, B. D. DePaola and D. S. Jin, *Phys. Rev. A* 70, 021601(R) (2004).
2. "Cross-dimensional relaxation in Bose-Fermi mixtures", J. Goldwin, S. Inouye, M. L. Olsen and D. S. Jin, *Phys. Rev. A* 71, 043408 (2005).
3. "Observation of heteronuclear Feshbach resonances in a mixture of bosons and fermions", S. Inouye, J. Goldwin, M. L. Olsen, C. Ticknor, J. L. Bohn and D. S. Jin, *Phys. Rev. Lett.* 93, 183201 (2004).

### Bibliography

4. "Production efficiency of ultra-cold Feshbach molecules in bosonic and fermionic systems", E. Hodby, *et al.*, *Phys. Rev. Lett.* 94, 120402 (2005).
5. "Multiplet structure of Feshbach resonances in nonzero partial waves", C. Ticknor, C. A. Regal, D. S. Jin and J. L. Bohn, *Phys. Rev. A* 69, 042712 (2004).
6. "Observation of Feshbach resonances between two different atomic species", C. A. Stan, M. W. Zwierlein, C. H. Schunck, S. M. F. Raupach and W. Ketterle, *Phys. Rev. Lett.* 93, 143001 (2004).
7. "Ultracold heteronuclear molecules in a 3D optical lattice", C. Ospelkaus, S. Ospelkaus, L. Humbert, P. Ernst, K. Sengstock and K. Bongs, *cond-mat/0607581* (2006).
8. "Observation of heteronuclear Feshbach molecules from a  $^{85}\text{Rb}$ - $^{87}\text{Rb}$  gas", S. B. Papp and C. E. Wieman, *cond-mat/0607667* (2006).

# Cold Rydberg Atom Gases and Plasmas in Strong Magnetic Fields

G. Raithel, FOCUS Center, Physics Department, University of Michigan  
450 Church St., Ann Arbor, MI 48109-1120, graithel@umich.edu  
<http://cold-atoms.physics.lsa.umich.edu/projects/highb/>

## 1 Program scope

In this project we investigate interactions in highly magnetized, cold Rydberg-atom gases and magnetized plasmas. Many Rydberg atoms present in these environments have large values of the magnetic quantum number  $|m|$ . The dynamics of strongly magnetized high- $|m|$  Rydberg atoms is regular and characterized by drift-orbit solutions, also known as guiding-center solutions (see, e.g., J. R. Guest, J.-H. Choi, G. Raithel, Phys. Rev. **A** **68**, 022509 (2003) and references therein). Drift-state atoms exhibit distinct cyclotron, bounce and magnetron motions of the Rydberg electron. These drift-orbit states have large densities of states and lifetimes, and can become populated via collisions and recombination.

In the experiments, we use a particle trap that operates at magnetic fields up to 6 Tesla and that can simultaneously function as a ground-state atom trap, Rydberg-atom trap and nested Penning ion and electron trap. Ground-state atom clouds collected in the trap are excited into clouds of magnetized Rydberg atoms or cold plasmas. In studies of low-angular-momentum Rydberg atoms directly excited by lasers, we are interested in coherent spin oscillations of the Rydberg electron induced by spin-orbit coupling. Using our capability to magnetically trap Rydberg atoms, we intend to determine properties such as polarizabilities, cyclotron quantum numbers, and decay rates of the trapped Rydberg atoms. Employing combinations of Rydberg-atom and electron Penning traps, collisions between Rydberg atoms and electrons as well as recombination in strong-magnetic-field environments are investigated. It is further planned to investigate spatial correlations in Rydberg-atom clouds that are due to coherent interactions.

## 2 Recent Results

### 2.1 Cold-plasma expansion dynamics in strong magnetic fields

Magnetized plasmas primarily expand in the degree of freedom parallel to the magnetic field. In our trap, both electrons and ions are confined longitudinally in a shallow, nested Penning-trap-like configuration. The magnetic field is approximately homogeneous ( $\mathbf{B} = B\hat{z}$ ). Near the trap center, the electric potential along the  $z$ -axis  $V(0, 0, z) \approx -1V + \alpha z^2 + V_{\text{hole}} \times (d/\sqrt{d^2 + z^2})^3$ , where the constants  $\alpha \sim 0.05$  V/cm<sup>2</sup>,  $V_{\text{hole}} \sim 0.05$  V, and  $d = 0.84$  cm. The term  $\alpha z^2$  in the potential is a weak ion-trapping potential applied via segmented electrodes. The ion-trapping potential confines Rb ions (initial energy  $\sim k_B \times 150$   $\mu$ K) to regions  $z < 5$  mm. The term  $V_{\text{hole}} \times (d/\sqrt{d^2 + z^2})^3$  in the potential is created by utilizing the effective electric dipole moments associated with the electrode holes that allow the trap laser beams to enter. This hole potential confines the plasma electrons (initial energy  $\sim k_B \times 50$  K) in a region  $z < 2$  mm. In this way, a nested trap configuration for both ions and electrons is achieved.

On time scales of order 1 ms and longer, the  $\mathbf{E} \times \mathbf{B}$  drift motion associated with the transverse components of the trapping electric field causes a slow alignment of the plasma along a diagonal with a known angle, and a slow escape of the plasma along that diagonal. The time scale of the plasma alignment and escape, shown in Fig. 1(a) and (b), amounts to values of order 1 ms. The plasma lifetime decreases with increasing “hole potential”  $V_{\text{hole}} \times (d/\sqrt{d^2 + z^2})^3$ , as shown in Fig. 1(c).

Immediately after photo-excitation, the ion component of the plasma performs breathing-mode oscillations parallel to the magnetic field ( $z$ -direction). This oscillation is equivalent to a space-charge oscillation, which in turn leads to a modulation of the net trapping potential for the electron component of the plasma. The modulation in electron-trap depth causes a periodic electron “shake-off” signal, which can be observed over a few hundred microseconds (see Fig. 1(d)). The shake-off signal exhibits reproducible structures that develop with increasing density (see Fig. 1(e)). We believe that these structures are a manifestation of ionic waves. We are able to explain most of the dynamics shown in Fig. 1.

### 2.2 Energy distribution of trapped electrons

In the scheme described in Sec. 2.1, the electron component of the strongly magnetized plasma is contained

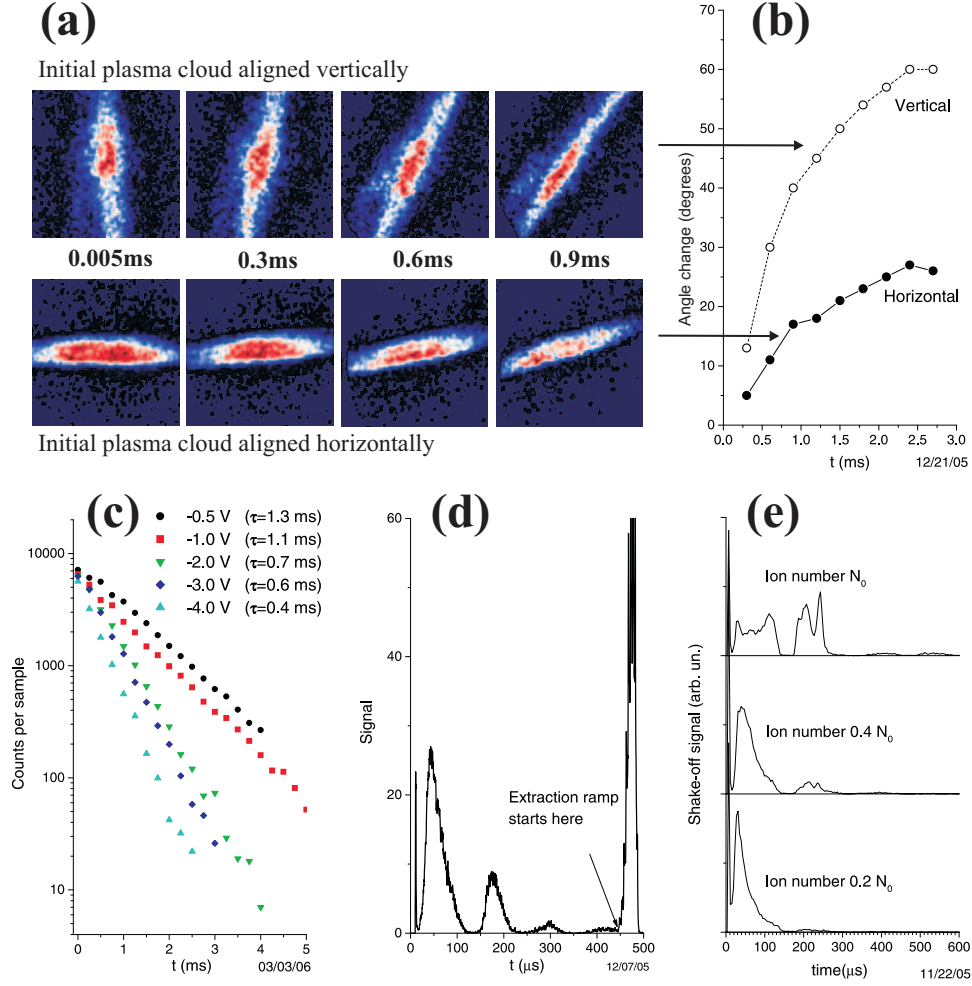


Figure 1: **(a)** Progressive alignment of a cold, magnetized plasma in the trapping potential described in the text. Initially, the plasma is prepared in either a vertical (upper row) or a horizontal (lower row) geometry. **(b)** Change in alignment angle vs time for initially vertical or horizontal alignment. **(c)** Number of detected plasma electrons vs time for different values of the applied ion-trapping voltage. **(d)** Periodic electron shake-off signal caused by oscillations of the ion component of the plasma. The signal past 450  $\mu$ s is due to an electron extraction pulse that is applied at the indicated time. **(e)** Effect of the initial ion number on the shake-off signal. Irregularities observed at high numbers are interpreted as ion pressure-wave effects.

in a well formed by a combination of the hole potential ( $V_{\text{hole}} \times (d/\sqrt{d^2 + z^2})^3$ ) and a space-charge potential produced by the ions (the ions oscillate in a larger well generated by the term  $\alpha z^2$  in the longitudinal potential). The energy distribution of the electrons is measured by application of a stepped electric-field electron extraction ramp. At each step of the extraction ramp, a fraction of the electrons is released (see Fig. 2(a)). The electron energy spectra reveal the overall potential depth and the electron temperature. A correlation between ionic oscillations and the electron energy distribution has been observed; this correlation reflects a space-charge modulation caused by the ionic oscillations (Fig. 2(b)). Over long time scales, we observe a significant lowering of the electron energy (Fig. 2(c)) that we attribute to evaporative cooling of the electron cloud.

### 2.3 Recombination and Rydberg-atom collisions

It is of interest how many drift-state Rydberg atoms are formed in a cold, strongly magnetized plasma, and how quickly these atoms percolate from high-lying Rydberg states down into the ground state. In our effort to answer some of these questions for a cold, magnetized plasma of electrons and rubidium ions, we have obtained state-selective field ionization spectra of Rydberg atoms for different values of the initial ion number, the electron temperature, the bias electric field, and the cold-plasma evolution time after photo-excitation.

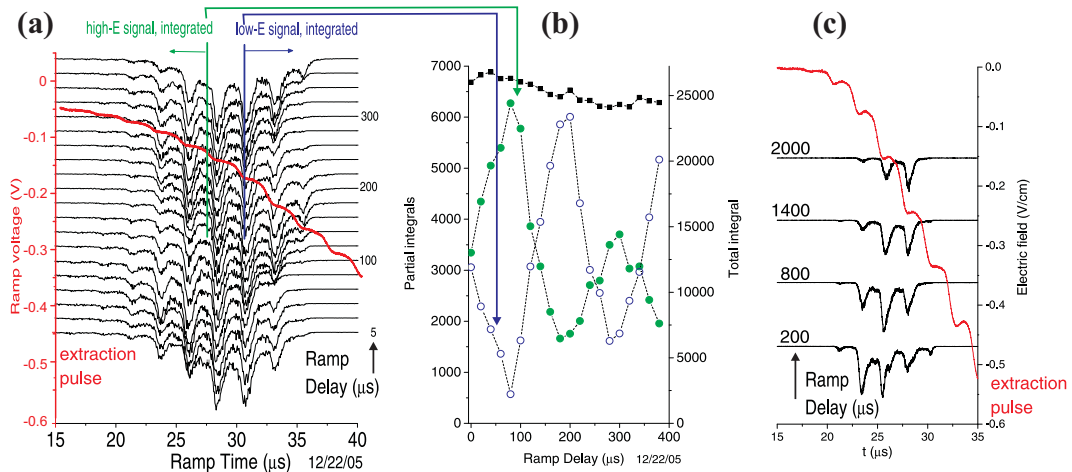


Figure 2: **(a)** Spectra of the electron-component of a strongly, magnetized plasma obtained with a stepped electron extraction ramp (overlaid curve, left axis) for the indicated values of the delay time between photo-excitation and application of the extraction ramp (ramp delay indicated on the right). **(b)** Integral over the most energetic (filled circles), the least energetic (open circles) and all (squares) electrons. The respective integration ranges are indicated in part (a). The modulations of the lower two curves in part (b) reflect the effect of ionic space-charge oscillations. **(c)** Long-term evolution of the electron energy spectra. The longer the delay time, indicated on the left, the more electric field is needed to extract the electrons from the plasma. Hence, the electron gas cools as a function of time. The overlaid curve shows the stepped electron extraction ramp (right axis).

We have observed that Rydberg atoms initially form in a broad energy distribution that peaks at very high-lying levels. Due to the interaction of the Rydberg atoms with the electron component of the plasma, the total number of detected Rydberg atoms declines with increasing delay time after photo-excitation, and the state-distribution shifts to lower states. A typical data set is shown in Fig. 3(a). We believe that the Rydberg atoms form due to three-body recombination, and that Rydberg-atom-electron collisions cause the gradual departure of atoms from high-lying states.

Using photo-excitation below the photo-ionization threshold, cold gases of strongly magnetized Rydberg atoms are obtained. If the Rydberg gas is created in a nested Penning trap, implemented as explained in Sec. 2.1, electrons originating in Rydberg-Rydberg collisions remain trapped in the Rydberg atom cloud and collide frequently with the remaining Rydberg atoms. We find that, under the utilized conditions and within about one millisecond, the energy distribution of the Rydberg-atom gas is significantly shifted towards lower-lying states, and that about a quarter of the atoms ionize (Fig. 3(b)). While these processes are somewhat reminiscent of similar dynamics in magnetic-field-free Rydberg-atom gases, the time-scale of the evolution in the high-magnetic-field case is much slower than it is in the magnetic-field-free case. Also, in the high-magnetic-field case the fraction of ionized atoms is lower than it is in corresponding magnetic-field-free cases. Both observations hint at a suppression of Rydberg-atom-electron collisions due to the magnetic field.

### 3 Plans

The work on Rydberg atom trapping will evolve towards using the Rydberg atom trap as an analytic tool to measure single-atom properties (electric polarizabilities, magnetic moments, cyclotron transition behavior).

In previous research, we have found that low-angular-momentum Rydberg atoms in strong magnetic fields at energies very close to the continuum still have significant spin-orbit coupling (of order  $h \times 1$  MHz). We have observed indications of spin-orbit oscillations caused by the coupling. Using narrow-linewidth excitation, we intend to study coherent spin oscillations in real-time.

We further plan to expand our studies of the expansion of cold, strongly magnetized plasmas and to illuminate the fate of Rydberg atoms that form via recombination in such plasmas. Exploiting our capability to trap both atoms and electrons at the same spatial location, we also consider to study collisions between cold-

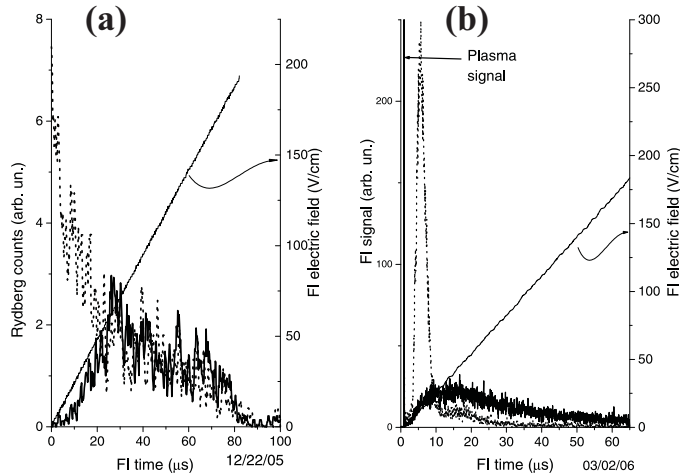


Figure 3: (a) State-selective field ionization spectra of Rydberg atoms observed after photo-ionization of a cold-atom cloud in a weak background electric field (dotted line) and in a nested electron/ion trap (solid). In both cases, Rydberg atoms in a broad distribution of states are observed. The absence of atoms in high-lying Rydberg states, observed in the case of the nested electron/ion trap, is attributed to Rydberg-atom-electron collisions. The linear curve shows the electric-field ionization ramp (right axis). (b) The effect of collisions on a strongly magnetized Rydberg-atom gas excited in a nested electron/ion trap. Initially, most Rydberg atoms ionize at a well-defined electric field (dotted curve). After an interaction time of 1 ms, about a quarter of the Rydberg-atom population has ionized (“plasma signal”), while the remaining Rydberg atoms have been shifted to lower-energy states with higher ionization electric fields (solid curve). The linear curve shows the electric-field ionization ramp (right axis).

electron clouds and Rydberg atoms implanted into these clouds. It is further planned to investigate the effects of coherent electric-quadrupole interactions between strongly magnetized Rydberg atoms.

#### 4 Publications in 2005 and 2006 which acknowledge DoE support

1. “Laser cooling and magnetic trapping at several Tesla,” J. R. Guest, J.-H. Choi, E. Hansis, A. P. Povilus and G. Raithel, *Phys. Rev. Lett.* **94**, 073003 (2005).
2. “Magnetic trapping of long-lived cold Rydberg atoms,” J.-H. Choi, J. R. Guest, A. P. Povilus, E. Hansis, and G. Raithel, *Phys. Rev. Lett.* **95**, 243001 (2005).
3. “Time dependence and Landau quantization in the ionization of cold, magnetized Rydberg atoms,” J.-H. Choi, J. R. Guest, E. Hansis, A. P. Povilus, and G. Raithel, *Phys. Rev. Lett.* **95**, 253005 (2005).
4. “A simple pressure-tuned Fabry-Perot interferometer,” E. Hansis, T. Cubel, J.-H. Choi, J. R. Guest, and G. Raithel *Rev. Sci. Instrum.* **76**, 033105 (2005).
5. “Magnetic Trapping of Strongly-Magnetized Rydberg Atoms,” J.-H. Choi, J. R. Guest, G. Raithel, *European Physics Journal D*, in print (2006).
6. “Cold Rydberg atoms”, J.-H. Choi, B. Knuffman, T. Cubel Liebisch, A. Reinhard, G. Raithel, in *Advances in Atomic, Molecular and Optical Physics* vol. 54, eds. E. Arimondo and P. Berman, (Elsevier, in print 2006).
7. “Coherent population transfer of ground-state atoms into Rydberg states”, T. Cubel, B. K. Teo, V. S. Malinovsky, J. R. Guest, A. Reinhard, B. Knuffman, P. R. Berman, and G. Raithel *Phys. Rev. A* **72**, 023405 (2005). (J. R. Guest supported by DoE).

# Population Dynamics in Coherent Excitation of Cold Atoms

B. D. DePaola

J. R. Macdonald Laboratory Department of Physics  
Kansas State University  
Manhattan, KS 66056  
depaola@phys.ksu.edu

## Introduction

A summary of the entire scope of the Kansas State University AMO program is contained in the J. R. Macdonald Laboratory abstract. The present document is limited to a discussion of recent progress in the MOTRIMS projects.

MOTRIMS, or magneto optical trap recoil ion momentum spectroscopy, is a methodology originally developed for the study of ion-atom or photon-atom collisions. Following the basic “inverse kinematics” idea underlying COLTRIMS (cold target recoil ion momentum spectroscopy) MOTRIMS combines well-established techniques for cooling and trapping atoms with the equally well-established techniques for measuring the momenta of product ions in the above-mentioned collision types. Several years ago it was realized that the whole idea of MOTRIMS could be turned around and charge transfer is now being used as a probe of population dynamics in cold, trapped atomic samples.

The key idea behind MOTRIMS is that in an ionizing collision, the recoiling target ion’s momentum carries with it detailed information about the collision process. For example, in the single electron transfer process of this work, the Q-value, or energy defect of a collision is given by

$$Q = -\frac{1}{2}m_e v_p^2 - p_{\parallel} v_p, \quad (1)$$

where  $m_e$  is the mass of the electron,  $v_p$  is the velocity of the projectile, and  $p_{\parallel}$  is the component of the recoil ion velocity that lies parallel to the initial direction of the projectile ion. The energy defect,  $Q$ , can be thought of as the difference between the initial and final potential energies of the transferred electron. (The transverse component of the recoil momentum is related to the projectile scattering angle, but that is not relevant to the studies described here.) So, a measurement of the recoil ion’s  $p_{\parallel}$  gives the Q-value of the collision which, in turn, gives the initial and final states associated with that collision. Taken together with the previously measured relative cross sections of the different collision channels, a measurement of the relative count rates for the different collision channels then yields the relative initial populations of the different states of the target before the collision. For example, for a 2-level system in which the two states of the system are designated by the subscripts  $s$  and  $p$ , the fraction of atoms in the  $p$  state is given by

$$f_p = \frac{n_p}{n_s + n_p} = \frac{A_p/\sigma_p}{A_s/\sigma_s + A_p/\sigma_p} = \frac{A_p}{RA_s + A_p}, \quad (2)$$

where  $n_s$  and  $n_p$  are the relative numbers of atoms in the indicated states,  $A_s$  and  $A_p$  are the measured rates for charge transfer from the indicated initial states, and  $\sigma_s$  and  $\sigma_p$  are the relative cross sections for charge transfer from the indicated states. The term  $R$  is defined as  $\sigma_p/\sigma_s$ .

In the remaining sections of this abstract, a brief summary of two MOTRIMS projects will be given. In the first, the steady-state, average excited fraction in a MOT was measured as a function of trapping laser detuning and intensity. The results were compared with predictions of simple models. In the second project, the population *dynamics* of a 3-level ladder system undergoing coherent 2-color excitation was measured.

## Excited State Fraction in an “Active” Magneto Optical Trap

At some time or other most groups using a MOT need to know the what fraction of atoms in the MOT are in an excited state. This is because the most convenient way to determine the total number of atoms in a MOT is to make a measurement of the total number of atoms in the excited state (via a fluorescence measurement) and then to divide this number by the excited fraction. Knowing the total number of atoms in a MOT is important for several reasons. The most common one is so that one can determine the density of atoms in the MOT. Researchers are interested in knowing this because many processes, including cold collisions, depend on the density. Until now, however, the MOT community has had to rely on untested simple models to estimate the excited fraction of atoms in their MOTs. The most commonly used expression for the excited fraction is

$$f_{ex} = \frac{I/I_s}{1 + 2I/I_s + (2\delta/\Gamma)^2}, \quad (3)$$

where  $I$  is the total trapping laser intensity (the incoherent sum of the intensities of all the trapping laser beams),  $\delta$  is the trapping laser’s detuning from resonance,  $\Gamma$  is the full linewidth of the atomic transition, and  $I_s$  is the so-called saturation intensity, often given by

$$I_s = \frac{2\pi h c \Gamma}{3\lambda^3}, \quad (4)$$

where  $h$  is Planck’s constant and  $\lambda$  is the transition wavelength. Note that Eq. (3) does not contain dependencies on several important MOT parameters, including B-field gradient, repump laser intensity, and the intensity balance between the different trapping laser beams. This equation is exact for a single travelling optical wave, interacting with a true 2-level system, in the absence of external fields, and at low enough target densities so as to be able to neglect radiation trapping. However, in a MOT one typically does *not* have a 2-level system due to the presence of Zeemann splitting from the magnetic field gradient. Furthermore, radiation trapping is nearly always taking place, and instead of a single travelling wave, the atoms in a MOT are typically subjected to 3 pairs of counter-propagating waves whose relative phases are typically not fixed. Thus, in a MOT one typically has spatially and temporally varying pump laser beam intensities interacting with a spatially-varying Zeemann-split system, of unknown m-distribution that can trap some fraction of the spontaneously emitted radiation. Under these conditions, the use of Eq. (3) as an accurate predictor of excited fraction does not seem promising. Nevertheless, an experiment was carried out using the MOTRIMS apparatus to study  $^{87}\text{Rb}$ , in which the excited state fraction was directly measured, while the trap laser detuning and total intensity were continuously varied. Remarkably, it was found that Eq. (3) does indeed work, over a wide range of B-field gradients, intensity balances of the trapping laser beams, and repump laser intensities. However, instead of using Eq. (4), which gives a value of 3.2 mW/cm<sup>2</sup> for  $I_s$ , a fitted value of 9.2 mW/cm<sup>2</sup> had to be used. Using this value

for  $I_s$  in Eq. (3), along with the measured trap laser detuning and total intensity, our study shows that one can confidently estimate the excited fraction of  $^{87}\text{Rb}$  in a MOT to within  $\pm 1\%$ .

## Population Dynamics During STIRAP

Developing the ability to efficiently control populations would benefit many areas of science and technology. For example, if one could efficiently place reactants in certain states, one could potentially control the speed of a desired chemical reaction. In the area of quantum information, much depends on the efficiency with which one can create or interact with individual qubits. Over the past decade, one of the developments in coherent interaction of light with matter is the particular excitation scheme known as stimulated Raman adiabatic passage, or STIRAP. Although both theory and experiment has made progress in characterizing STIRAP, until now the temporal evolution of populations in a system undergoing this form of excitation has not been observed. Now, using the methodology described above, such population dynamics have been observed on the few nanosecond time scale.

In the experimental procedure,  $^{87}\text{Rb}$  was trapped and cooled in the usual manner. The trapping lasers were then turned off for a period of 500 ns, allowing the excited atoms to decay to the ground state. Then, while the trapping lasers were still off, 50 ns pulses of optical excitation were allowed to interact with the rubidium, one tuned just to the red of the  $\text{Rb}(5s) \rightarrow \text{Rb}(5p)$  transition, and the other tuned to the blue, by the same amount, of the  $\text{Rb}(5p) \rightarrow \text{Rb}(4d)$  transition. This process was repeated at a frequency of 200 kHz with the continuous accumulation of Q-value spectra. The resulting 2-dimensional spectra (counts versus Q-value and time) were then analyzed by dividing the number of counts in each charge capture channel by the corresponding relative cross section, as described above in the section on MOT excitation fraction. In this case, there were 3 levels of interest:  $\text{Rb}(5s)$ ,  $\text{Rb}(5p)$ , and  $\text{Rb}(4d)$ . The relative excited state fractions were normalized to unity and plotted versus time.

In this excitation scheme there were essentially 5 experimental parameters that could be varied. These are the peak intensities of the two optical excitation pulses, the temporal widths of the pulses, and the relative timing between these pulses. In the work presented here, only the intensities and relative timing were varied. Because the temporal evolution of all three levels were measured, the effects of changing these parameters were readily observed, including the effects of changing the excitation from the completely adiabatic to partially diabatic regimes.

## Summary

The emphasis of the work presented here has been on measuring the relative populations of atoms that have been cooled and trapped in a MOT. In one case, the temporal evolution of the populations were measured with a resolution of a few nanoseconds. Although it is believed that the examples presented here are already of great value to the greater scientific community, it is also believed that this represents only the beginning of what will eventually be accomplished using the MOTRIMS methodology. For example, presently in the Macdonald lab experiments are under way in which photo-association with subsequent excitation along a ladder of molecular states is being measured. In addition, a second MOTRIMS apparatus has been constructed and installed on the Macdonald Lab EBIS, under the direction of Dr. C. Fehrenbach. This will allow more flexibility in the choice of projectile ions used in this sort of measurement. For example, until now, only alkali ions have been used with MOTRIMS to probe population dynamics. However, due to spin-orbit interactions lifting the  $l$ -degeneracy in the projectile energy structure, the Q-value spectra are more “crowded”

than one would wish. Also, the use of singly charged projectiles limits the charge capture rate to a lower level than is desired. By using the EBIS, we will have fully stripped highly charged ions available, reducing both of these limitations. Thus, the future of MOTRIMS as a tool for measuring population dynamics in a variety of systems looks promising.

## Recent Publications

- “State Selective Charge Transfer Cross Sections for  $\text{Na}^+$  with Excited Rubidium: A Unique Diagnostic of Population Dynamics of a Magneto-Optical Trap”, X. Fléchar, H. Nguyen, R. Brédy, S. R. Lundeen, M. Stauffer, H. A. Camp, C. W. Fehrenbach, and B. D. DePaola, *Phys. Rev. Lett.* **91** 243005 (2003).
- “Measurement of the Interaction Strength in a Bose-Fermi Mixture with  $^{87}\text{Rb}$  and  $^{40}\text{K}$ ” J. Goldwin, S. Inouye, M. L. Olsen, B. Newman, B. D. DePaola, and D. S. Jin, *Phys. Rev. A* **70** 021601 (2004).
- “Recoil Ion Momentum Spectroscopy Using Magneto-Optically Trapped Atoms”, H. Nguyen, X. Fléchar, R. Brédy, H. A. Camp, and B. D. DePaola, *Rev. Sci. Instrum.* **75** 2638 (2004).
- “Differential Charge-Transfer Cross Sections for Systems with Energetically Degenerate or Near-Degenerate Channels”, H. Nguyen, R. Brédy, H. A. Camp, T. Awata, and B. D. DePaola *Phys. Rev. A* **70** 032704 (2004).
- “Three-Dimensional Spatial Imaging in Multiphoton Ionization Rate Measurements”, R. Brédy, H. A. Camp, H. Nguyen, T. Awata, B. Shan, Z. Chang, and B. D. DePaola, *J. Opt. Soc. Am. B* **21** 2221 (2004).
- “Numerical Exploration of Coherent Excitation in Three-Level Systems”, H. A. Camp, M. H. Shah, M. L. Trachy, O. L. Weaver, and B. D. DePaola, *Phys. Rev. A* **71** 053401 (2005).
- “Entropy Lowering in Ion-Atom Collisions”, H. Nguyen, R. Brédy, T. G. Lee, H. A. Camp, H. Awata, and B. D. DePaola, *Phys. Rev. A* **71** 062714 (2005).
- “Relative Charge Transfer Cross Section from  $\text{Rb}(4d)$ ”, M. H. Shah, H. A. Camp, M. L. Trachy, X. Fléchar, M. A. Gearba, H. Nguyen, R. Brédy, S. R. Lundeen, and B. D. DePaola, *Phys. Rev. A* **72** 024701 (2005).
- “A Novel Method for Laser Beam Size Measurement”, G. Veshapidze, M. L. Trachy, M. H. Shah, and B. D. DePaola, *Appl. Opt.* (2006) (Accepted).
- “Model-Independent Measurement of the Excited Fraction in a Magneto-Optical Trap”, M. H. Shah, M. L. Trachy, G. Veshapidze, M. A. Gearba, and B. D. DePaola, *Phys. Rev. A* (2006) (Submitted).

# Development and Characterization of Replicable Tabletop Ultrashort Pulse X-ray Sources for Chemical Dynamics Research

**Christoph G. Rose-Petruck**

*\* Department of Chemistry, Box H, Brown University, Providence, RI 02912*

*phone: (401) 863-1533, fax: (401) 863-2594, [Christoph.Rose-Petruck@brown.edu](mailto:Christoph.Rose-Petruck@brown.edu)*

## 1 Program Scope

Advanced x-ray sources based on accelerator technology and sources based on laser technology form a symbiotic community with each source type addressing specific needs of the scientific community, for instance, average and peak x-ray flux, x-ray pulse lengths, or available beam time. This work focuses on the development and characterization of laser-driven tabletop, ultrashort pulse, hard-x-ray sources with high brightness for x-ray absorption spectroscopy and x-ray diffraction. This requires the generation of continuum radiation while x-ray line radiation is not important. Primary applications are the measurements of the structural dynamics of molecules during chemical and physical transformations. The constructed x-ray source is based on a liquid mercury target and operates over long periods at kilohertz repetition rates with x-ray wavelengths in the range of single Å and x-ray pulse durations that have been simulated to be equal or shorter than 50 fs. The sources use high power, femtosecond laser pulses with kilohertz repetition rate to generate x-ray emitting plasmas from solid and liquid metal targets. This research focuses entirely on the sources' optimization and characterization and relies on an existing laser system that has been upgraded to 40-fs laser pulse with an average power of 16-W on target at 5-kHz repetition rate. It was the specific goal of this project, to develop a source that is modular, compact, and robust enough to be replicable by many scientists with diverse experimental backgrounds.

Integral parts of the project are experiments that serve multiple purposes: First, the data allow the measurements of the sources' pulse lengths over a large spectral range with sub-hundred femtosecond temporal resolution. Second, performance parameters of the entire x-ray spectroscopic system, consisting of source, x-ray imaging optics, spectrometer, and detector, can be determined for electronic or structural dynamics experiments in the gas or liquid phases.

## 2 Recent Progress

### 2.1 Development of an ultrafast, high-flux x-ray source and spectrometer

The design and machining of the new laser-driven plasma x-ray source has been completed and the source module has been constructed as proposed. A picture of the x-ray source is shown in Figure 1. The entire source is fully shielded. An electronic rotation stage and an optical bench system are directly attached to the source unit. This permits the quick and reproducible selection of the desired x-ray spectral range.

One of the goals of this work is to make the source construction data available to other researchers. While we are working on the web-publication of all construction files, we have already distributed the Solidworks models to another colleague, Dr. Dong Hee Son, Texas A&M Univ. Dr. Son has replicated the liquid mercury source. Recently, we began to transfer the construction models to Dr. Martin M. Nielsen, Director of the Danish National Research Foundation Centre for Molecular Movies, University of Copenhagen.

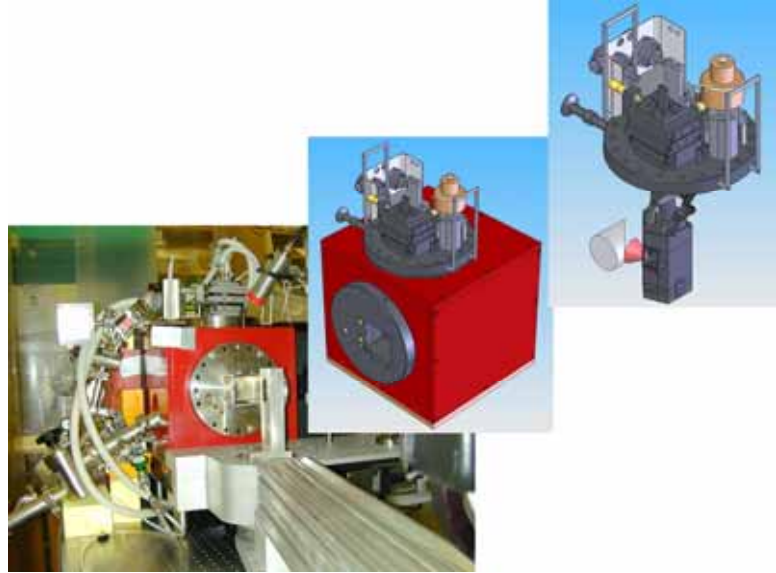


**Figure 1:** X-ray source design models and constructed x-ray source. The upper left image depicts the inner chamber containing the liquid metal target. The middle image shows the target flange inserted into the vacuum chamber. The left image shows the x-ray source and the XAFS spectrometer.

### 2.2 X-ray emission from source

The x-ray emission spectrum of the source has been measured and is shown in Figure 2. The driving laser has been upgraded during the last year to 16-W compressed power and the x-ray source is driven with 3-mJ, 40-fs, 5-kHz laser pulses. The shown radiation has been generated without any prepulse which will enhance the flux by a factor 5. However, the prepulse generation unit has been installed in the laser system. Flux optimization has not been carried out yet but is currently in progress. Nevertheless, the current flux already is the largest continuum-flux ever measured

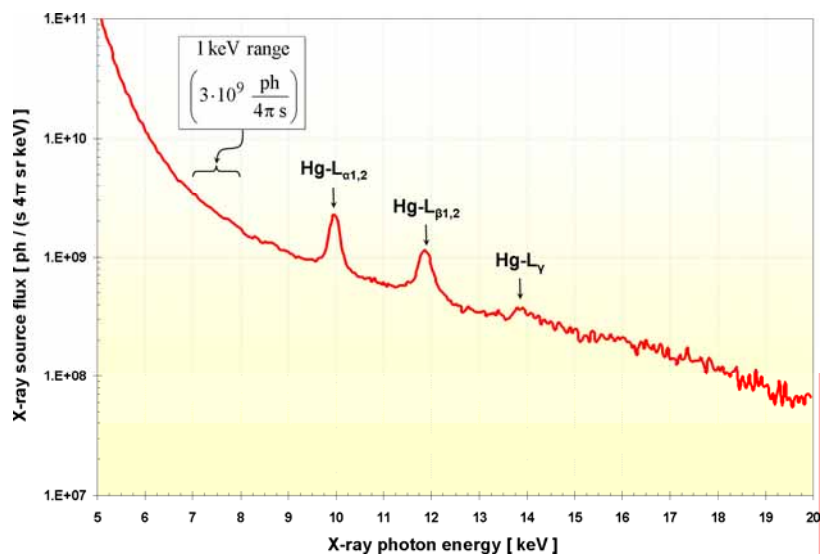


**Figure 2:** Absolutely calibrated x-ray emission spectrum from the source shown in Figure 1.

from a liquid target.

### 2.3 Simulations of 50-fs x-ray pulse generation from Hg targets:

The x-ray pulses emitted from the Hg-target have been theoretically investigated by a combination of particle-in-cell (PIC) and Monte-Carlo (MC) simulations of the laser target interaction and the resulting electron dynamics. A two-step approach was applied to determine the x-ray emission. First, 1D, oblique incidence PIC simulations of the laser-plasma interaction were performed to obtain the energy distribution of the hot electrons generated during the laser plasma interaction. All calculations were performed for p-polarized, 100-fs, 800-nm laser pulses with an incidence angle of 45 degrees. An exponential plasma density profile with a scale length  $L/\lambda = 0.2$  for a laser wavelength  $\lambda = 800$  nm was used. This scale length corresponds approximately to an interaction where a laser pre-pulse or pedestal generates a small amount of preformed plasma. Second, a Monte-Carlo electron-photon transport code was used to compute

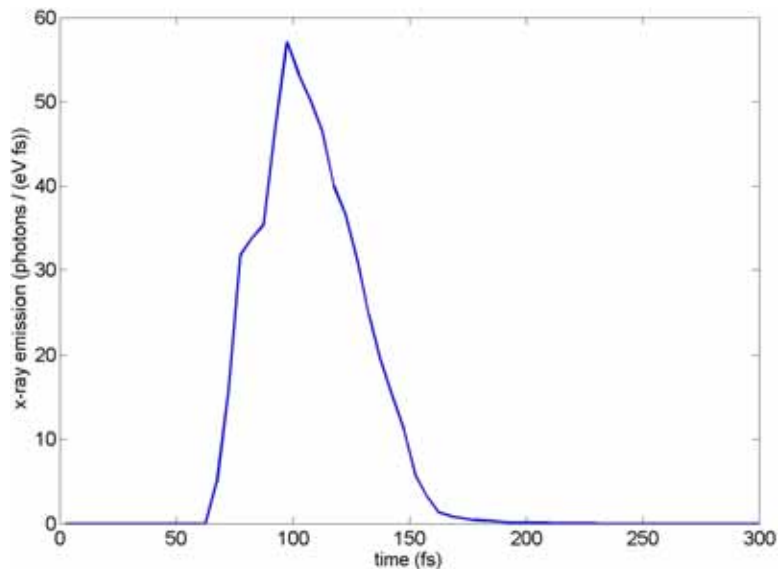


**Figure 3:** Simulated x-ray pulse in the spectral range from 7.1 to 7.2 keV emitted from a mercury target illuminated with an 800-nm, 100-fs laser pulse with an intensity of  $10^{17}$  W/cm<sup>2</sup> and 5-mJ pulse energy.

the electron trajectories in the mercury target. Figure 3 shows a simulated x-ray pulse emitted from a mercury target illuminated with laser pulse with an intensity of  $10^{17}$  W/cm<sup>2</sup> and 5-mJ pulse energy. The full width at half maximum (fwhm) of the emitted x-ray pulse in the spectral range between 7.1 and 7.2 keV is 50 fs. This short pulse duration is due to the short electron penetration depth into the target material in combination with the large x-ray absorption cross section of the target material. At lower x-ray photon energies, the pulse lengths are expected to be substantially below 50 fs! This radiation is shorter than the driving laser pulse! If confirmed experimentally, these x-ray pulses would be the shortest ever produced from any hard x-ray source.

Furthermore, the simulations demonstrate that the lengths of x-ray pulses emitted from other targets, such as copper, depend on the x-ray wavelengths and on the laser pulse intensity. For instance, at  $10^{17}$  W/cm<sup>2</sup>, continuum x-radiation below the Cu K-absorption edge as well as  $K\alpha$  radiation have 90%-pulse lengths of nearly one picosecond. Simultaneously continuum x-rays emitted above the K-absorption edge have 90%-pulse lengths of about 150 femtoseconds, which corresponds to 75 fs (fwhm).

### 2.4 Current experiments

Current experiments have begun that aim at the measurements of the x-ray pulse length by cross-correlation with 800-nm laser pulses in Xe-gas that is contained at 1 bar in a 5-mm diameter glass tube with 10- $\mu$ m wall thickness. The x-ray absorption spectrum of the Xe L-edges are measured while the gas is irradiated by laser pulses of approx.  $10^{14}$  W/cm<sup>2</sup>. This leads to dressed atom states with a ponderomotive shift of the continuum of about 7.5 eV. Given the spectral resolution of our spectrometer of 1.1 eV, such shifts can be easily detected. Since the bound electronics states are very little influenced by the laser field, the measurement might be considered x-ray pump – laser probe experiments. In any

case, both, the laser and the x-ray pulses have to be present to detect the signal and the resulting time-resolved spectra are cross-correlations and yield the x-ray pulse length without differentiation of the signal. This is in contrast to the additionally present x-ray edge shifts caused by photo-ionization of the gas.

## 2.5 Future plans

The X-ray Absorption Fine Structure (XAFS) spectra of  $Fe(CN)_6^{4-}$  solvated in water have been measured before photoexcitation and tens of picoseconds after photoexcitation with ultrashort UV laser pulses. The XAFS spectra after photoexcitation exhibits a chemical shift as well as indications for the increase of the iron-ligand distances. Reference spectra measured at a synchrotron source yield structural data that show bond length changes of the metal complex due to solvation. The pump-probe delay times are not indicative of the temporal resolution of the experimental setup. The most likely temporal resolution is in the sub-picosecond regime. Once the “dressed atom” measurement have been complete, we will resume the measurements with high temporal resolution of this chemical system.

## 3 References

1. "Ultrafast XAFS of transition metal complexes," T. Lee, C. Reich, C. M. Laperle, X. Li, M. Grant, C. G. Rose-Petruck and F. Benesch-Lee, in *Ultrafast Phenomena 15*, (Springer, 2006).
2. "Ultrafast laser-pump x-ray probe measurements of solvated transition metal complexes," T. Lee, F. Benesch, C. Reich and C. G. Rose-Petruck, in *Femtochemistry VII*, edited by Jr. A.W. Castleman and M. Kimble (Elsevier, 2005), p. 23 - 33.  
"Ultrafast table-top laser pump - x-ray probe measurement of solvated  $Fe(CN)_6^{4-}$ ," T. Lee, Y. Jiang, C. Rose-Petruck and F. Benesch, *J. Chem. Phys.* 122 (8), 084506/1 - 084506/8 (2005).
3. Ultrafast table-top laser pump - x-ray probe measurement of solvated  $Fe(CN)_6^{4-}$ , T. Lee, Y. Jiang, C. Rose-Petruck and F. Benesch, Selected for re-publication by: *Virtual Journal of Ultrafast Science*, Vol. 4 (3), <http://www.vjulfast.org/ultrafast/>, edited by P. H. Bucksbaum (American Institute of Physics, American Physical Society, 2005), ISSN: 1553-9601, Original Publication: *J. Chem. Phys.* (2005), 122(8), 084506/1 - 084506/8.
4. Ultrafast table-top laser pump - x-ray probe measurement of solvated  $Fe(CN)_6^{4-}$ , T. Lee, Y. Jiang, C. Rose-Petruck and F. Benesch, Selected for re-publication by: *Virtual Journal of Biological Physics Research*, Vol. 9 (5), <http://www.vjbio.org/bio/>, edited by R. H. Austin (American Institute of Physics, American Physical Society, 2005), ISSN: 1553-9628, Original Publication: *J. Chem. Phys.* (2005), 122(8), 084506/1 - 084506/8.
5. "Acoustically Modulated X-ray Phase Contrast and Vibration Potential Imaging," A. C. Beveridge, C. J. Bailat, T. J. Hamilton, S. Wang, C. Rose-Petruck, V. E. Gusev and G. J. Diebold, in *Photons Plus Ultrasound: Imaging and Sensing 2005*, edited by A.A. Oraevsky and L.V. Wang (SPIE Publishing, Bellingham, WA, 2005), Vol. 5697, p. in press.
6. "Acoustic radiation pressure: a "phase contrast" agent for x-ray phase contrast imaging," C. J. Bailat, T. Hamilton, C. Rose-Petruck and G. J. Diebold, *Applied Physics Letters* 85 (19), 4517-4519 (2004).
7. "Acoustically Modulated X-ray Phase Contrast Imaging," T. Hamilton, C. J. Bailat, C. Rose-Petruck and G. J. Diebold, *Physics in Medicine and Biology* 49, 4985-4996 (2004).

## Ultrafast Atomic and Molecular Optics at Short Wavelengths

P.I.s: Henry C. Kapteyn and Margaret M. Murnane  
Department of Physics and JILA  
University of Colorado at Boulder, Boulder, CO 80309-0440  
Phone: (303) 492-8198; FAX: (303) 492-5235; E-mail: kapteyn@jila.colorado.edu

### PROGRAM SCOPE

The goal of this work is to study of the interaction of atoms and molecules with intense and very short (<20 femtosecond) laser pulses, with the purpose of developing new short-wavelength light sources. Novel short wavelength probes of materials and molecules are also being developed. We are also developing novel optical pulse shaping techniques to enable this work.

### RECENT PROGRESS

A number of recent experiments have used the process of high harmonic generation to probe molecular structure. In high harmonic generation, an atom or molecule is first field-ionized by an intense femtosecond laser. The ionized electron then propagates in the optical field, and can recollide with its parent ion after a fraction of an optical cycle of the driving field. In this picture, the energy of the high harmonic emission can be related to the energy of the recolliding electron, and therefore to its de Broglie wavelength. For electron energies of 20-100 eV, corresponding to the extreme-ultraviolet (EUV) region of the electromagnetic spectrum where HHG emission is relatively strong, the de Broglie wavelength is in the range of  $\sim 1-3$  Å. This corresponds well to the distances between atoms in a molecule. Recent experimental and theoretical studies have exploited this relationship to show that high harmonic emission from a molecule is sensitive to the structure and orientation of a molecule. These studies make use of the fact that the orientation distribution of gas-phase molecules can be readily manipulated by impulsively exciting rotational wave packets using an ultrashort pulse. This ensemble of aligned molecules can then be used as the medium for generating high harmonics. The symmetry, shape and orientation of the molecular orbital relative to the polarization of the driving laser field, and therefore to the propagation direction of the recolliding electron, determine the probabilities of ionization and recombination, and thus high harmonic emission.

In recent work, we obtained new and unexpected data that show that high-order harmonic generation is strongly modulated by small changes in the configuration of atoms within a molecule and as a result, is extremely sensitive to intramolecular vibrational dynamics. In our experiment, we first excite vibrations in an SF<sub>6</sub> molecule using impulsive stimulated Raman scattering (ISRS). We then observe oscillations in the intensity of the EUV high-order harmonic emission generated from the vibrationally excited SF<sub>6</sub>. SF<sub>6</sub> was chosen as a spherically-symmetric molecule that has been previously studied using ISRS. A simple Fourier transform of the oscillations shows that all the Raman-active modes of SF<sub>6</sub> can be detected, with an asymmetric breathing mode most visible. In the case of conventional stimulated Raman scattering, only the strong symmetric breathing mode has been observed. Based on our experimental data, we determine that the HHG process is sensitive to the relative position of atoms within the molecule with milliAngstrom sensitivity. Simulations of high harmonic generation in excited molecules confirm that HHG is an exceedingly sensitive probe of molecular configuration, and that in general we might expect it to be sensitive to any molecular dynamics; for example to all vibrational modes including both Raman- and non-Raman-active modes. Furthermore, our data show that the observed oscillations vary in amplitude with observed harmonic order, and that different vibrational modes exhibit different behavior. Our

data show evidence of relaxation dynamics and sensitivity to reorientation of the vibrationally excited molecules.

These observations collectively demonstrate that monitoring high harmonic generation from vibrationally excited molecules yields useful data on intra-molecular dynamics that can be directly interpreted independent of complex models or tomographic deconvolution techniques. In particular, this work extends Raman spectroscopies in new directions, adding new capabilities that are not addressed by any other spectroscopic approach because of the potential sensitivity to all vibrational modes in a molecule (both infrared and Raman-active), the ultrafast duration of the probe, and because all vibrational modes are observed simultaneously and coherently. In the future, this approach can be applied to complex and important phenomena such as dissociation dynamics, vibrational mode coupling, fast configuration changes, nuclear and electron dynamics during structural changes in molecules – including highly excited states and dissociating molecules. Moreover, by monitoring the change in the HHG modulation signal as a function of harmonic order (i.e. recolliding electron wavelength), it may also be possible to extend this technique to monitor dynamic molecular structure. As a result, this technique could become a broadly applicable probe of chemical dynamics, combining the ultrahigh time-resolution of conventional optical pump-probe experiments, with the potential for obtaining structural information complimentary to techniques such as femtosecond electron diffraction, or proposed experiments using ultrashort-pulse x-rays as a probe of molecular dynamics.

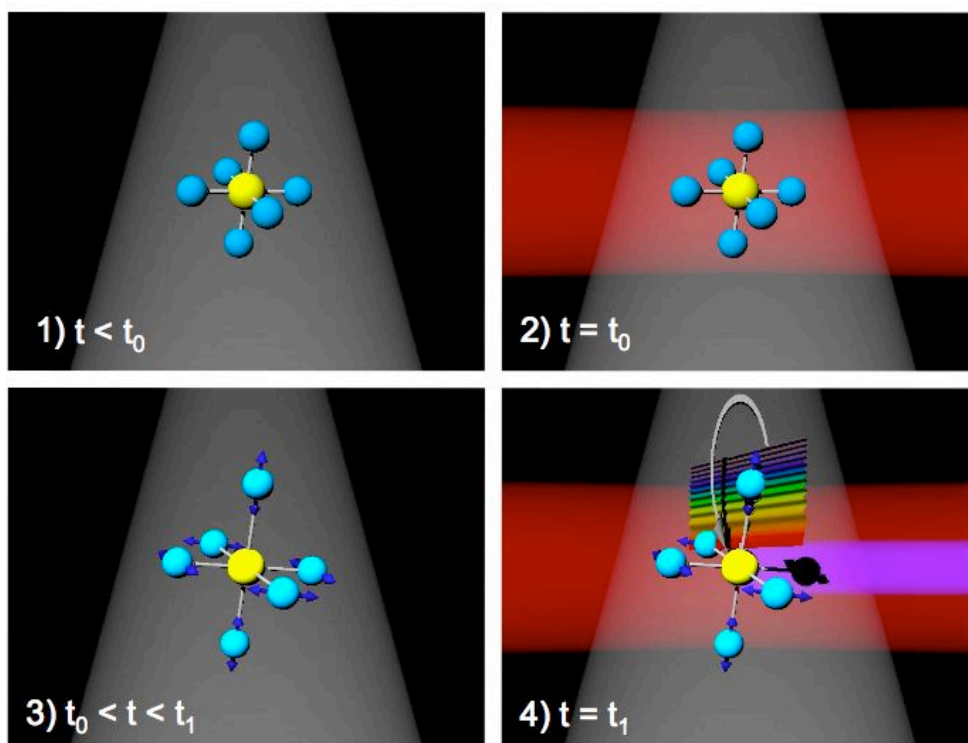


**Figure 1:** Schematic of experiment. At time zero ( $t_0$ ) the femtosecond laser excites the Raman-active vibrations in  $\text{SF}_6$  by impulsive stimulated Raman scattering. The vibrational wavepacket then evolves in time, until times  $t=t_1$  when a probe femtosecond laser pulse generates high-order harmonics from the vibrationally excited molecule.

Very recently, we observed dynamics in a non-spherically symmetric molecule  $\text{CClF}_3$  (Freon 13). We observe strong modulation of the harmonic emission by the vibrational wavepacket, and also decay of different vibrational modes over time.

We are working with Chris Greene and his students as well as Ivan Christov from Sofia, in modeling high harmonic generation from excited molecules. We are also working collaboration with Tamar Seideman to understand high harmonic generation form rotationally aligned molecules. In the future, we will expand on this work in several ways to study the dynamics of structural changes in molecules through monitoring the HHG yield from excited molecules.

### **Publications (refereed) as a result of DOE support since 2002**

1. R. Bartels, T. Weinacht, N. Wagner, M. Baertschy, C. Greene, M. Murnane, H. Kapteyn , “Phase Modulation of Ultrashort Light Pulses using Molecular Rotational Wavepackets”, *Phys. Rev. Lett.* **88**, 019303 (2002).
2. C. Durfee, L. Misoguti, S. Backus, R. Bartels, M. Murnane and H. Kapteyn, “Phase Matching in Cascaded Third-Order Processes, *JOSA B* **19** (4): 822-831 (2002).
3. S. Christensen, H.C. Kapteyn, M.M. Murnane, S. Backus, "Simple, high power, compact, intracavity frequency-doubled Q-switched Nd:YAG laser," *Rev. Sci. Instrum.* **73** (5): 1994-1997 (2002).
4. R. Bartels, N. Wagner, M. Baertschy, J. Wyss, M. Murnane, H. Kapteyn, "Phase-matching conditions for nonlinear frequency conversion by use of aligned molecular gases," *Opt. Lett.* **28**, 346 (2003).
5. Ariel Paul, Randy Bartels, Ivan Christov, Henry Kapteyn, Margaret Murnane, Sterling Backus, “Multiphoton photonics: quasi phase matching in the EUV”, *Nature* **421**, 51 (2003).
6. E. Gibson, A. Paul, N. Wagner, R. Tobey, I. Christov, D. Attwood, E. Gullikson, A. Aquila, M. Murnane, H. Kapteyn, “Generation of coherent soft x-rays in the water window using quasi phase-matched harmonic generation”, *Science* **302**, 95 (2003).
7. E. Gibson, A. Paul, N. Wagner, R. Tobey, I. Christov, M. Murnane, H. Kapteyn, “Very High Order Harmonic Generation in Highly Ionized Argon”, *Physical Review Letters* **92**, 033001 (2004).
8. R. Tobey, E. Gershgoren, M. Siemens, M.M. Murnane, H.C. Kapteyn, T. Feuerer, K. Nelson, “Photothermal and Photoacoustic Transients probed with Extreme Ultraviolet Radiation”, *Appl. Phys. Lett.* **85**, 564 (2004).
9. David M. Gaudiosi, Amy Lytle, Pat Kohl, Margaret M. Murnane, Henry C. Kapteyn, Sterling Backus, “Downchirped Pulse Amplification”, *Optics Letters* **29**, 2665-2667 (2004).
10. Randy A. Bartels, Margaret M. Murnane, Herschel Rabitz, Ivan P. Christov, and Henry C. Kapteyn , “Using learning algorithms to study attosecond dynamics”, *Phys. Rev. A* **70**, 112409 (2004).
11. N. Wagner, E. Gibson, T. Popmintchev, I. Christov, M. Murnane, H. Kapteyn, “Self-compression of ultrashort pulses through ionization-induced spatio-temporal reshaping”, *PRL* **93**, 173902 (2004).
12. E. A. Gibson, I. P. Christov, M. M. Murnane, and H. C. Kapteyn, "Quantum Control of High Harmonic Generation: Applied Attosecond Science," in *Femtosecond Optical Frequency Comb: Principle, Operation, and Applications*, J. Ye, Ed.: Kluwer Publishing Company, 2004.
13. E. Gibson, X. Zhang, T. Popmintchev, A. Paul, N. Wagner, A. Lytle, I. Christov, M. Murnane, H. Kapteyn, “Extreme Nonlinear Optics: Attosecond Photonics at Short Wavelengths”, **invited**, *JSTQE* **10**, 1339 (2004).
14. Henry C. Kapteyn, Margaret M. Murnane and Ivan P. Christov, “Coherent X-Rays from Lasers: Applied Attosecond Science”, **invited article**, *Physics Today*, page 39 (March 2005).
15. L. Misoguti, I.P. Christov, S. Backus, M. M. Murnane, and H. C. Kapteyn, “Nonlinear wavemixing processes in the extreme ultraviolet”, *Physical Review A* **72**, 063803 (2005).
16. A. Paul, E.A. Gibson, X. Zhang, A. Lytle, T. Popmintchev, X. Zhou, M.M. Murnane, I.P. Christov, H.C. Kapteyn “Phase matching techniques for coherent soft-x-ray generation”, **invited paper**, *IEEE Journal of Quantum Electronics* **42**, 14 - 26 (2006).
17. D.. Gaudiosi, B. Reagan, T. Popmintchev, M. Grisham, M. Berril, O. Cohen, B. Walker, M. Murnane, H. Kapteyn, J. Rocca, “High harmonic generation from ions in a capillary discharge”, *Phys. Rev. Lett.* **96**, 203001 (2006).
18. R.I. Tobey, M.E. Siemens, M. M. Murnane, H. C. Kapteyn, and K.A. Nelson, “Ultrasensitive Transient Grating Measurement of Surface Acoustic Waves in Thin Metal Films with Extreme Ultraviolet Radiation “, to be published in *Applied Physics Letters* (2006).
19. N. Wagner, A. Wüest, I. Christov, T. Popmintchev, X. Zhou, M. Murnane, H. Kapteyn, “Monitoring Molecular Dynamics using Coherent Electrons from High-Harmonic Generation”, to be published in *PNAS* (August 2006).
20. M.E. Siemens, R.I. Tobey, M. M. Murnane, H. C. Kapteyn, and K.A. Nelson, “Femtosecond X-Ray Holography“, submitted to *Optics Letters* (2006).

## New Directions in Intense-Laser Alignment

*Tamar Seideman*

*Department of Chemistry, Northwestern University*

*2145 Sheridan Road, Evanston, IL 60208-3113*

*t-seideman@northwestern.edu*

### 1. Program Scope

Nonadiabatic molecular alignment by short intense pulses has been the topic of rapidly growing activity during the past few years. This activity owes both to the fascinating fundamental physics associated with rotational wavepacket dynamics and to a variety of already demonstrated and projected applications in fields ranging from molecular spectroscopy and laser optics through reaction dynamics and stereochemistry, to quantum storage and information processing.<sup>1</sup> In this approach, a moderately intense laser pulse of duration short with respect to the rotational periods aligns a given molecular axis (axes) to the field polarization vector(s). Nonadiabaticity (rapid turn-off as compared to the system time scales) guarantees that the alignment will survive subsequent to the pulse turn-off, under field-free conditions.

Our DOE-sponsored research introduces two main new directions in the area of nonadiabatic intense laser alignment and explores them theoretically and numerically. One part of the research extends the concepts of alignment and 3D alignment from the isolated molecule limit to condensed phase environments. Applications of the extended scheme that have been explored during the past year include the development of an approach to control charge transfer reactions in solutions,<sup>2</sup> the introduction of a method of probing the dissipative properties of dense media and quantifying the system-bath interactions,<sup>3,4</sup> and the development of an optimal control approach to enhance the alignment in dissipative media and tailor its time evolution.<sup>5</sup>

The second part of the research extends the theory of rotational revivals from linear systems to molecules of arbitrary symmetry and explores practical and experimental implications. In this area, research carried out during the past year has developed the theoretical framework<sup>1,6,7</sup> and has applied it in several theory-experiment collaborative projects.<sup>6,8</sup> Included in this research is an ongoing effort to develop and contrast different modes of establishing field-free (post-pulse) 3D alignment so as to guide ongoing and future experiments.<sup>9</sup>

The DOE AMOP meetings of September 04 and September 05 have inspired a third research direction within the general theme of nonadiabatic intense-laser alignment. Here we collaborate with the group of Keptyne and Murnane to understand high harmonics generation (HHG) spectra from nonadiabatically aligned molecules and apply them to derive new insights into molecular systems. This research has motivated the development of a theoretical framework for the calculation of HHG spectra that goes beyond several oversimplified approximations of the current model.

## 2. Recent Progress

We focus on three projects (Secs. 2.1–2.3) within the first part of the program, addressing alignment in dissipative media, and on three projects within the second part, addressing alignment of isolated complex polyatomic systems (Secs. 2.4–2.6).

### *2.1 Intense laser alignment in dissipative media as a route to solvent dynamics*

In Refs. 3,4 we extend the concept of alignment by short intense pulses to dissipative environments within a density matrix formalism and illustrate the application of this method as a probe of the dissipative properties of dense media. In particular, we propose a means of disentangling rotational population relaxation from decoherence effects via strong laser alignment. We illustrate also the possibility of suppressing rotational relaxation through choice of the field parameters, so as to prolong the alignment lifetime.

### *2.2 Alignment of torsional motions. Application to the design of a molecular switch*

In recent and ongoing research we extend three-dimensional alignment from a means of controlling solely the overall rotations of molecules with respect to the space-fixed axes, to a means of simultaneously controlling also their torsional motions. The approach is applied to control of charge transfer reactions in solution, potentially a route to a light-triggered molecular switch. We find extensive control over the charge transfer rate, depending, however, on both the solvent and solute properties.<sup>2</sup>

### *2.3 Optimal control theory of alignment in dissipative media*

In ongoing work<sup>5</sup> we apply a density matrix variation of optimal control theory to the problem of molecular alignment in dense environments. Our major goal is to use optimal control as a coherence spectroscopy, to gain new insights into the dissipative properties of the medium. A second goal is to time the post-pulse (field free) alignment to a specific instance while controlling also its duration. A third goal is to construct superposition states that would live long in a gas cell environment, as required, for instance, for quantum information applications. Figure 1 illustrates the application of optimal control theory both as a coherence spectroscopy of the medium properties and as a practical tool for timing of the alignment.

### *2.4 Nonperturbative quantum theory of alignment and 3D alignment*

Much of our effort in the domain of alignment of isolated polyatomic molecules has been devoted to the development of an efficient and accurate numerical framework to predict the alignment and 3D alignment characteristics of asymmetric tops. We are motivated by the rapidly growing interest in nonadiabatic alignment of polyatomic systems, the qualitative questions posed by experiments,<sup>6,8,9</sup> and the variety of anticipated applications.<sup>1</sup> Our methods are summarized in Ref. 6 and discussed in detail in a recent review article.<sup>1</sup> In brief, we solve the time-dependent Schrödinger equation nonperturbatively, transforming between basis sets of symmetric and asymmetric tops to maximize the code efficiency.

Recent work<sup>7</sup> on the form of the interaction Hamiltonian in the case of nonresonant, intense

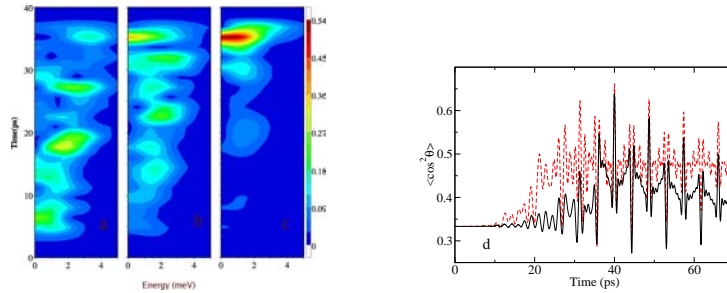


FIG. 1: Application of optimal control theory to understand and control molecular alignment in solutions. We seek to maximize the alignment of CO molecules subject to a gaseous Ar bath at a predetermined instance (here 40 ps). Left: Short-time Fourier transforms of the optimal fields that time the alignment at different Ar pressures; (a) 0 Torr, (b) 100 Torr, and (c) 200 Torr. The most efficient excitation mechanism in isolated molecules (panel a) is seen to be a sequence of short pulses with increasing center frequency. As pressure increases, the dissipation time scale approaches and surpasses the target time and coherence established earlier in the pulse is increasingly deteriorated before the target time. Consequently, the multiple pulse mechanism is gradually replaced by a single late pulse. Right: The averaged alignment induced by an optimal field in the presence of population relaxation (solid curve) and in the presence of pure decoherence (dashed curve). The dissipation timescale is 40 ps in both cases. The target is clearly reached in both media but the mechanism differs in an instructive way.<sup>5</sup>

field has re-derived the theory of Ref. 1 using a qualitatively different theoretical framework, obtaining an identical expression. This work resolves a longstanding puzzle in the theoretical literature on laser alignment, where two different and non-equivalent forms of the interaction have been consistently used by different researchers.

### 2.5 Applications to isolated polyatomic molecules

The formalism of Ref. 1 has been applied in several collaborative studies with the experimental group of H. Stapelfeldt, which uses femtosecond time-resolved photofragment imaging to probe the time-evolving alignment. In Ref. 6 we explore the nonadiabatic alignment of symmetric top molecules induced by linearly polarized, moderately intense picosecond laser pulses. Good agreement is found between the experimental and numerical results, allowing us to use the theory to provide insight into the origin of the experimental findings.

In ongoing work we apply similar experimental and theoretical methods to study the nonadiabatic alignment of asymmetric top molecules. Our numerical results explain several counter-intuitive experimental observations and generalize them to other molecules. We show that the rotational revival patterns of asymmetric tops differs qualitatively from the linear and symmetric top cases and explore the information content of these patterns. One of the intriguing predictions of our theoretical studies, which was not verified experimentally as yet, is a remarkable simplification of the revival spectrum of asymmetric tops by the moderately intense laser field. The strong field renders weak molecular interactions, such as the asymmetric top coupling, a perturbation. As a result, with increasing intensity the revival spectrum gradually converges to a symmetric top spectrum.

In Ref. 8 we study the alignment dynamics of polyatomic molecules subject to two temporally overlapping nonresonant laser pulses. We illustrate the advantage of combining a long (compared to the molecular rotational periods) with a short pulse, theoretically, numerically

and experimentally. In particular, significant enhancement of the alignment attainable under nondestructive conditions is predicted and found. Reference 9 develops an approach for 3D alignment of general polyatomic molecules based on extension of the long+short pulse combination.

### 2.6 Coherent control applications of molecular orientation

A related theoretical project, to be completed shortly, applies nonadiabatic orientation as the first step in two coherent control studies. One study considers ignition of electronic toroidal ring current around an oriented linear molecule. The second uses orientation for selective bond-breaking in polyatomic molecules.

### 3. Future Plans

- One goal of future work will be the extension of 3D alignment and torsional control (Sec. 2.2) to guided molecular assembly. Our numerical approach will apply classical molecular dynamics to describe molecular assembly subject to the combination of the molecular Hamiltonian and the external field.

- Our work on torsional control in general, and its application to charge transfer reactions in particular (Sec. 2.2) will be continued, as current experimental interest in realizing this scheme offers new questions for theoretical research. The same concept will be extended from the static (long-pulse-induced, adiabatic alignment) domain to the case of short pulses, where the alignment dynamically entangles with the reaction dynamics and new opportunities arise.

- Our collaborative research with the group of Murnane and Kapteyn will expand from the domain of isolated diatomics to polyatomic molecules and to dense gases. We expect to be able to learn much more from HHG spectra than what has been possible so far.

### 4. Articles from DOE sponsored research; 08/05–07/06

1. T. Seideman and E. Hamilton, *Nonadiabatic Alignment by Intense Pulses. Concepts, Theory, and Directions*, Ad.At.Mol.Opt.Phys. **52**, 52, 289 (2006) (**invited**).
2. S. Ramakrishna and T. Seideman, *Torsional Alignment by Intense Pulses as a Means of Controlling Charge Transfer Events*, to be submitted for publication in Phys. Rev. Lett.
3. S. Ramakrishna and T. Seideman, *Intense Laser Alignment in Dissipative Media as a Route to Solvent Properties*, Phys. Rev. Lett. **95**, 113001 (2005).
4. S. Ramakrishna and T. Seideman, *Dissipative Dynamics of Laser Induced Nonadiabatic Molecular Alignment*, J. Chem. Phys. **124**, 034101 (2006).
5. A. Pelzer, S. Ramakrishna and T. Seideman, *An Optimal Control Approach to Nonadiabatic Alignment in Dissipative Media*, to be submitted for publication in J. Chem. Phys.
6. E. Hamilton, T. Seideman, T. Ejdrup, M.D. Poulsen, S.S. Viftrup and H. Stapelfeldt, *Alignment of symmetric top molecules by short laser pulses*, Phys. Rev. A **72**, 043402 (2005).
7. N. Moiseyev and T. Seideman, *Alignment of Molecules by Lasers: Derivation of the Hamiltonian within the  $(t, t')$  Formalism*, J.Phys. B:At.Mol.Opt.Phys. **39** L211–L216 (2006).
8. M.D. Poulsen, T. Ejdrup, H. Stapelfeldt, E. Hamilton and T. Seideman, *Alignment Enhancement by the Combination of a Short and a Long Laser Pulse*, Phys. Rev. A **73**, 033405 (2006).
9. S.S. Viftrup, C.Z. Bisgaard, V. Kumarappan, H. Stapelfeldt, E. Hamilton and T. Seideman, *Three Dimensional Alignment of Molecules Using a Long and a Short Laser Pulse*, to be submitted for publication in Phys. Rev. Lett.

## **X-ray microprobe of optical strong-field processes**

L. Young, D. A. Arms, E. M. Dufresne, C. Höhr, E. R. Peterson, R. W. Dunford,  
D. L. Ederer, E. P. Kanter, B. Krässig, E. C. Landahl,  
N. Rohringer, J. Rudati, R. Santra, S. H. Southworth

*Argonne National Laboratory, Argonne, IL 60439*

The study of atoms in strong electromagnetic fields ( $\sim 10\text{V}/\text{\AA}$ ) has led to the discovery of phenomena with significant fundamental and technological interest, such as high-order harmonic generation and the production of attosecond pulses. Experimental studies to date have concentrated on detection of the ejected particles (photons, electrons, ions) from the focal volume. We have developed an alternate approach, an x-ray microprobe, to view the atoms/molecules directly in the focus of an intense, ultrafast laser. The methodology employs microfocused, tunable, monochromatic, polarized x-ray radiation from Argonne's Advanced Photon Source (APS) to provide a quantum-state specific probe of atoms (ions) in the laser focal volume. Using the x-ray microprobe we have established that, and to what degree, ions produced by a strong laser field are aligned. We further studied the time evolution of the orbital alignment in the plasma environment and found that disalignment was induced by electron-ion binary collisions. Application of a magnetic field was found to preserve the alignment and induce coherent spin precession of the laser-produced ions. Theoretical analysis yields insight into the dominant interactions leading to disalignment and suggests directions for future work. A summary of the work on strong-field ionization of atoms as well as future plans in a lower intensity regime to study dressed atoms and aligned molecules will be presented.

Physics of Correlated Systems  
Chris H. Greene  
Department of Physics and JILA  
University of Colorado, Boulder, CO 80309-0440  
chris.greene@colorado.edu

### Program Scope

The quantum physics of atomic and molecular systems that interact with each other, and with incident photons, electrons, and ions, controls the transformation of energy from one form into another in a broad variety of contexts. In some systems, an adequate theoretical description of the interacting bodies can be achieved through independent particle approximations, in which one degree of freedom has little effect on other degrees of freedom. However, for the class of processes of particular interest to energy control, these approximations are invariably inadequate and must be treated at a more realistic level of approximation.

The aim in this research effort is to develop theoretical tools that permit a description of the complex phenomena that occur when different degrees of freedom in an atomic system exchange energy with one another. The systems studied frequently possess many interacting channels or pathways through which energy can flow. The application of quantum mechanics to such systems raises nontrivial complications, especially in regimes where energy exchange occurs readily. In such regimes, resonances often proliferate and perturbative, weak-coupling methods are inadequate. We formulate nonperturbative techniques and approximations that encapsulate the key physics, and then apply these techniques at a practical level to systems of experimental interest through numerical computations. This strategy has been applied to many different atomic and molecular systems in the course of this project. These include the detonation of rare gas atomic clusters following their exposure to vacuum-ultraviolet radiation from a free-electron laser; identification of the quantum mechanical pathways relevant to vibrational excitations that accompany the high-harmonic generation process in polyatomic molecules; resonant excitation of the bases, phosphate, and sugar components of DNA and RNA, relevant to developing an understanding of how secondary electrons causes strand breaks in the context of radiation damage.

### Recent Progress

A new thrust for this project during the past two years has been a study of the resonant excitation of the DNA and RNA bases subjected to low energy ( $<20\text{eV}$ ) electron collisions. When high energy radiation interacts with matter, most of the chemical damage is triggered not by the primary particle, but rather by the lower energy secondary electrons. Until recently, it has been beyond existing capabilities to describe the chemical rearrangements triggered by these low energy electrons. In fact, most such electrons simply collide and scatter without causing serious damage to the molecule. But some of them, when their energy coincides with one of the resonance energies of the compound system, become trapped long enough for the molecule to become vibrationally excited or even to dissociate into smaller fragments. The crucial role of such resonances has been

particularly stressed in the work of Leon Sanche and his collaborators. Theoretical progress in electron collisions with polyatomic molecules has primarily been restricted to smaller species than are relevant in radiation damage to biologically interesting molecules.

A breakthrough came during the past two years, however, when an advanced student funded by this project, Stefano Tonzani, developed a three-dimensional finite-element R-matrix scattering program capable of treating molecules as large as the DNA and RNA bases, the two purines adenine( $C_5H_5N_5$ ), guanine( $C_5H_5N_5O$ ), and the pyrimidines thymine( $C_5H_6N_2O_2$ ), cytosine( $C_4H_5N_3O$ ), and uracil( $C_4H_4N_2O_2$ ).[1-4] The shape resonances in these bases are of importance for understanding single and double strand breaks that are caused by collisions with low energy secondary electrons; this has become realized through the important work of the Sanche group. Our most recent work along these lines has been an application [3] of these techniques to the other major parts of DNA other than the aforementioned bases, namely to predict electron scattering resonances in tetrahydrofuran (THF,  $C_4H_8O$ ), which is similar to deoxyribose, and phosphoric acid ( $H_3PO_4$ ). The work to date has concentrated on solving the clamped nucleus part of the problem, and it remains a future goal to describe the transformation of this electronic resonance energy into bond breakage in these complicated species. Eventually we plan to build on the progress we have made in recent years on the description of dissociative recombination in polyatomic molecules, including the role of the Jahn-Teller and Renner-Teller effects.[5-10] For such studies, we anticipate that our improved understanding of Siegert pseudostates, achieved in the course of paper [11] below, should prove to be very useful. Tonzani will defend his doctoral thesis before the end of August, after which he will assume a postdoctoral appointment in the group of George Schatz at Northwestern University.

The past year also saw headway on our efforts to develop a theoretical description of xenon clusters exposed to intense VUV radiation, of the type provided by the free-electron laser at the TESLA Test Facility (TTF) in Hamburg. This is a new regime of strong photon-cluster interactions, very different from the physics of infrared laser pulses that are directed at such clusters. Our first theoretical treatment showed that linear physics is able to explain why approximately 30 photons per atom are absorbed, in a 100 femtosecond pulse of intensity  $7.3 \times 10^{13}$  W/cm<sup>2</sup>. [The experimental research was published by H. Wabnitz *et al.*, Nature **420**, 482 (2002).] Our calculations suggest that this absorption of this many VUV photons, one at a time, can be understood once realistic screened potentials are used to describe the behavior of the electrons, in addition to plasma screening effects. Another experimental study by the same group measured multiphoton ionization processes. Robin Santra also was instrumental in developing a detailed theoretical calculation of the multiphoton ionization rates of single ions by these VUV photons. During the past year, graduate student Zachary Walters has made a number of improvements to the initial model calculations reported in our 2003 Physical Review Letter on this subject, which have provided a more complete and quantitative description of this new regime of laser-cluster interaction dynamics. This theoretical project culminated in the publication of another long article that includes a reasonably successful

model for understanding the distribution of ejected electron energies in those VUV laser-cluster experiments.[13]

### Immediate Plans

During the past year, the two aforementioned projects, namely electron scattering by polyatomic molecules and strong laser interactions with atomic and molecular systems, have been fruitfully combined to treat a new class of challenging problems that arise in high-harmonic generation experiments with polyatomic molecules. A popular topic in the field originated with the idea that such experiments could be used to actually “image” the lowest unoccupied molecular orbital of the polyatomic positive ion, but our calculations have shown that this idea is based on inaccurate approximations. This will be important to firm up into definite predictions this coming year, because several experimental groups around the world are attempting to apply similar ideas to image other systems, and it will be important to see if the existing theoretical interpretation is unsound, and if that is the case, to see whether it can be improved to a useful level by our analysis. Another recent development has been the demonstration by the group of M. Murnane and H. Kapteyn that molecular vibrations can be observed in high-harmonic spectra, e.g. in the SF<sub>6</sub> molecule. [See, e.g., their very recent publication in Proceedings of the National Academy of Sciences.] We have formulated a preliminary analysis of this phenomenon that appears to roughly account for the main observations, and it will be a major goal during the coming year to solidify this treatment and develop it into a more comprehensive and quantitative methodology.

### **Papers published since 2004 that were supported at least in part by this grant**

[1] *Low energy electron scattering from DNA and RNA bases: shape resonances and radiation damage*, S. Tonzani and C. H. Greene, J. Chem. Phys. 124, 054312-1 to -11 (2006).

[2] *Electron-molecule scattering calculations in a 3D finite element R-matrix approach*, S. Tonzani and C. H. Greene, J. Chem. Phys. **122**, 014111-1 to -8 (2005).

[3] *Radiation damage to DNA: electron scattering from the backbone subunits*, S. Tonzani and C. H. Greene, J. Chem. Phys. (in press 2006, see also arXiv: physics/0607063).

[4] *FERM3D: A finite element R-matrix general electron molecule scattering code*, S. Tonzani, Comp. Phys. Commun. (submitted, nearly accepted in final form, 2006).

- [5] *Theoretical progress and challenges in  $H_3^+$  dissociative recombination*, C. H. Greene and V. Kokoouline, Proc. Roy. Soc. Lond. (in press 2006, supported partially by DOE and partially by NSF).
- [6] *Photofragmentation of the  $H_3$  molecule, including Jahn-Teller coupling effects*, V. Kokoouline and C. H. Greene, Phys. Rev. A **69**, 032711-1 to -16 (2004).
- [7] *Dissociative recombination of polyatomic molecules: A new mechanism*, C. H. Greene and V. Kokoouline, Phys. Scr. **T110**, 178-182 (2004).
- [8] *Triatomic dissociative recombination theory: Jahn-Teller coupling among infinitely many Born-Oppenheimer surfaces*, V. Kokoouline and C. H. Greene, Faraday Discuss. **127**, 413-423 (2004).
- [9] *Theoretical study of the  $H_3^+$  ion dissociative recombination process*, V. Kokoouline and C. H. Greene, J. Phys. Conf. Series 4, 74-82 (2005).
- [10] *Dissociative recombination of  $HCO^+$* , A. Larson, S. Tonzani, R. Santra, and C. H. Greene, J. Phys. Conf. Series 4, 148-154 (2005).
- [11] *Siegert pseudostates: Completeness and time evolution*, R. Santra, J. M. Shainline, and C. H. Greene, Phys. Rev. A 71, 032703-1 to -12 (2005).
- [12] *Properties of metastable alkaline-earth-metal atoms calculated using an accurate effective core potential*, R. Santra, K. V. Christ, and C. H. Greene, Phys. Rev. A **69**, 042510-1 to -10 (2004).
- [13] *Interaction of intense VUV radiation with large xenon clusters*, Z. B. Walters, R. Santra, and C. H. Greene, Phys. Rev. A (in press 2006, see also arXiv:physics/0510187).

# TIME-DEPENDENT TREATMENT OF THREE-BODY SYSTEMS IN INTENSE LASER FIELDS

**B.D. Esry**

*J.R. Macdonald Laboratory, Kansas State University, Manhattan, Kansas 66506*

esry@phys.ksu.edu

<http://www.phys.ksu.edu/personal/esry>

## Program Scope

The primary goal of this program is to understand the behavior of  $\text{H}_2^+$  in an intense laser field. Because the system has more degrees of freedom than can be directly treated, past theoretical descriptions have artificially reduced the dimensionality of the problem or excluded one — or more — important physical processes such as electronic excitation, ionization, vibration, or rotation. One component of this work is thus to systematically include these processes in three dimensions and gauge their importance based on actual calculations. Further, as laser pulses get shorter and more intense, approaches that have proven useful in the past may become less so. A second component of this program is thus to develop novel analytical and numerical tools to describe  $\text{H}_2^+$ . The ultimate goal is to understand the dynamics of these strongly coupled systems in quantum mechanical terms.

## Recent progress

The above-stated goal presupposes that the behavior of  $\text{H}_2^+$  in an intense field is not already completely understood. Many in this field, though, claim just the opposite — that everything is understood. Some recent measurements, however, belie this claim ([R1], [P14], and see I. Ben-Itzhak's abstract). These two experiments — at NRC in Canada [R1] and JRML at Kansas State [P14] — revealed structure in the relative nuclear kinetic energy spectrum following single and double ionization of  $\text{H}_2^+$  and  $\text{H}_2$ , respectively, that neither was expected nor has an accepted explanation. In fact, there are at least three distinct models being discussed with no resolution imminent.

One of those models was put forward by my collaborators and me in [P14] where we successfully applied it to explain essentially all of the features of our measurements. Our model is described in I. Ben-Itzhak's abstract which also shows its fit of the data, but I will summarize it again here for the clarity of the following discussion. Our model imagines that ionization is initiated by dissociation. At a sequence of internuclear distances, ionization channels for  $n, n-1, \dots$  photon transitions open. The dissociating nuclei pass through these channel-opening distances, leading to the observed peaks. For each dissociation mechanism — bond-softening and above threshold dissociation, for instance — there will thus be a sequence of peaks separated by a photon's energy. In analogy to above threshold ionization and above threshold dissociation, we have labeled this phenomenon above threshold Coulomb explosion.

Our model is most easily visualized using the Floquet potentials [R2] shown in Fig. 1. This figure shows the main non-standard piece of our model: diabatic Floquet ionization-threshold potentials. These potentials are just  $1/R - n\omega$  in atomic units and represent  $n$ -photon ionization with zero total energy electrons. They are shifted by  $n\omega$  in accord with the Floquet representation. One advantage of this picture is that it treats dissociation and ionization on an equal footing. Another advantage is that total energy is conserved within roughly the bandwidth of the laser pulse. The nuclear dynamics in an intense field can thus be completely followed just as for any other set of Born-Oppenheimer potentials. Time-dependent predictions follow from the time the system takes to travel along a given potential.

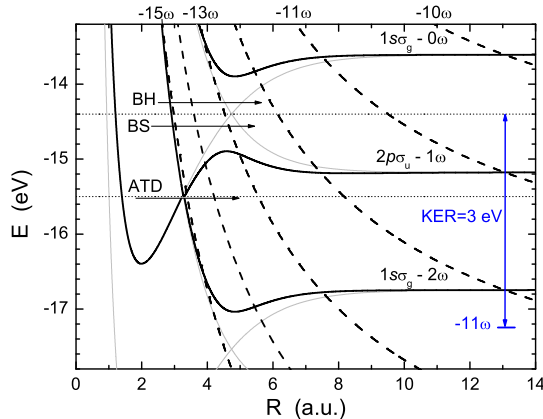


Figure 1: Floquet potentials for  $\text{H}_2^+$  at 800 nm: adiabatic dissociation potentials at  $10^{13} \text{ W/cm}^2$  (solid lines) and diabatic ionization potentials (dashed lines). The latter are simply  $1/R - n\omega$  in atomic units. The approximate total energy available for the main initiating dissociation mechanisms are indicated: bond-softening (BS), bond-hardening (BH), and above threshold dissociation (ATD). The kinetic energy release (KER) expected for BS-initiated,  $11\omega$  ionization is indicated at the right (blue). The molecular axis was assumed aligned with the linearly polarized field and fixed in space.

In terms of the kinetic energy release (KER) spectrum, Fig. 1 allows us to predict the peak positions for each dissociation process. It also allows us to predict which peaks should appear by comparing the pulse duration with the travel times to each crossing. We can further make reasonable arguments about the relative magnitudes of the various peaks. In fact, nearly all of the qualitative trends observed can be explained within our model.

Unknown to us and essentially simultaneously with our work, Andre Staudte in Reinhard Dörner’s group was measuring Coulomb explosion of  $\text{H}_2$  and  $\text{D}_2$  using the intense laser facilities at the NRC in Ottawa in collaboration with Paul Corkum’s group. As Paul Corkum later told me, they were very surprised to find structure in their KER spectrum. After careful analysis to eliminate any spurious sources of the structure, they were confident it was real but had no satisfactory physical explanation for it [1]. When we learned of their data, we applied our model to try to explain it.

Their data is shown in Fig. 2(a)-(d) for linear and circular polarization at two different intensities. Our fit, one to a linear polarization spectrum and one to a circular, is also shown in the figure in panels (e) and (f). As with our own experimental data, the model produced an excellent fit. The details of this fitting process are essentially the same as described in [P14]. The key point is that we fit both spectra simultaneously and that the consistency requirements of our model more than halved the number of free parameters.

One key difference between their measurements and ours is that they began from neutral  $\text{H}_2$  rather than  $\text{H}_2^+$ . So, the  $\text{H}_2^+$  was created when the laser intensity was already high. One consequence is that there are no peaks from bond-hardening, and above threshold dissociation dominates over bond-softening. The latter effect is consistent with the higher intensities experienced. Our model further explained the differences between the isotopes and the differences between the polarizations.

## Future plans

It would seem that our model explains the structure observed for both  $\text{H}_2$  and  $\text{H}_2^+$  quite well. There are, however, some fundamental assumptions in it that are best tested by comparison with solutions of the time-dependent Schrödinger equation. These tests are one component of the

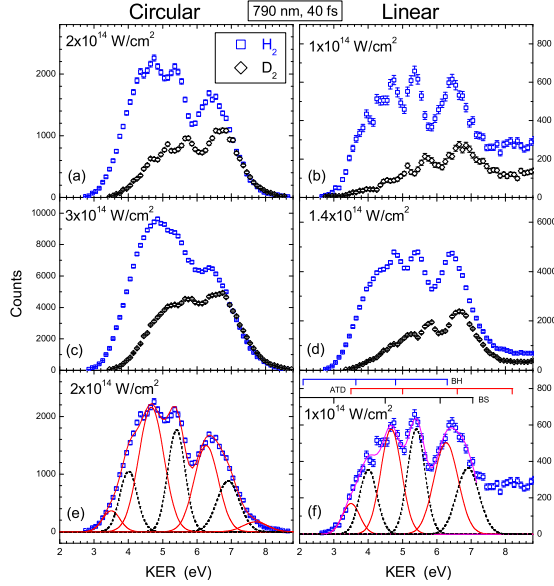


Figure 2:  $\text{H}_2$  and  $\text{D}_2$  Coulomb explosion KER spectra from Staudte *et al.* [1]. Panels (e) and (f) show our model fit, both for individual peaks and total. The bars in (f) indicate the diabatic peak positions grouped by mechanism. We expect an intensity-dependent shift of the peaks downward from these positions. (Data courtesy of A. Staudte.)

future direction of this work. Whether rigorously supported or not, our model seems to have descriptive and predictive power for this low intensity KER structure where no other explanation has yet proven satisfactory.

My broader future efforts will be to continue to develop the theoretical tools to make quantitative comparisons between theory and experiment. Despite the long history of this problem, very few calculations have been done for the purpose of quantitative comparison (see [R3]). We will also continue to study carrier-envelope phase effects in  $\text{H}_2^+$  [P5,P6] and look for other novel effects in these simple systems. I will also expand my group's efforts to effective one-electron molecules and simple two-electron molecules. Our goal in these efforts will be the same as for  $\text{H}_2^+$ : to make quantitative predictions that can be directly compared with experiment.

## References

- R1. A. Staudte, D. Pavicic, D. Zeidler, M. Meckel, H. Niikura, M. Schöffler, S. Schössler, B. Ulrich, P.P. Rajeev, Th. Weber, T. Jahnke, D.M. Villeneuve, S. Chelkowski, A.D. Bandrauk, C.L. Cocke, P.B. Corkum, and R. Dörner, *Phys. Rev. Lett.* (submitted) (2006).
- R2. A. Giusti-Suzor, F.H. Mies, L.F. DiMauro, E. Charron, and B. Yang, *J. Phys. B* **28**, 309 (1995); J.H. Posthumus, *Rep. Prog. Phys.* **67**, 623 (2004); D. Telnov and S.I. Chu, *Phys. Rep.* **390**, 1 (2004).
- R3. V.N. Serov, A. Keller, O. Atabek and N. Billy, *Phys. Rev. A* **68**, 053401 (2003).

## Publications

- P14. "Above threshold Coulomb explosion of molecules in intense laser pulses," B.D. Esry, A.M. Sayler, P.Q. Wang, K.D. Carnes, and I. Ben-Itzhak, *Phys. Rev. Lett.* **97**, 013003 (2006).
- P13. "Laser-assisted charge transfer in  $\text{He}^{2+} + \text{H}$  collisions," F. Anis, V. Roudnev, R. Cabrera-Trujillo, and B.D. Esry, *Phys. Rev. A* **73**, 043414 (2006).
- P12. "Isotopic preference of O-H over O-D bond cleavage following HDO ionization by fast ions," A.M. Sayler, M. Leonard, K.D. Carnes, R. Cabrera-Trujillo, B.D. Esry, and I. Ben-Itzhak *J. Phys. B* **39**, 1701 (2006).
- P11. "Lattice approach for  $\alpha + \text{H}_2^+$  collisions," S.C. Cheng and B.D. Esry, *Phys. Rev. A* **72**, 022704 (2005).
- P10. "Highlighting the angular dependence of bond softening and bond hardening of  $\text{H}_2^+$  in an ultrashort intense laser pulse," P.Q. Wang, A.M. Sayler, K.D. Carnes, J.F. Xia, M.A. Smith, B.D. Esry, and I. Ben-Itzhak, *J. Phys. B* **38**, L251 (2005).
- P9. "Bond rearrangement caused by sudden single and multiple ionization of water molecules," I. Ben-Itzhak, A.M. Sayler, M. Leonard, J.W. Maseberg, D. Hathiramani, E. Wells, M.A. Smith, J. Xia, P. Wang, K.D. Carnes, and B.D. Esry, *Nucl. Instrum. Meth. B* **233**, 284 (2005).
- P8. "Dissociation and ionization of molecular ions by ultra-short intense laser pulses probed by coincidence 3D momentum imaging," I. Ben-Itzhak, P. Wang, J. Xia, A.M. Sayler, M.A. Smith, K.D. Carnes, and B.D. Esry, *Nucl. Instrum. and Meth. B* **233**, 56 (2005).
- P7. "Disentangling volume effect through intensity-difference spectra: Application to laser-induced dissociation of  $\text{H}_2^+$ ," P. Wang, A.M. Sayler, K.D. Carnes, B.D. Esry, and I. Ben-Itzhak, *Optics Letters* **30**, 664 (2005).
- P6. " $\text{HD}^+$  photodissociation in the scaled coordinate approach," V.R. Roudnev and B.D. Esry, *Phys. Rev. A* **71**, 013411 (2005).
- P5. "Controlling  $\text{HD}^+$  and  $\text{H}_2^+$  dissociation with the carrier-envelope phase difference of an intense ultrashort laser pulse," V. Roudnev, B.D. Esry, and I. Ben-Itzhak, *Phys. Rev. Lett.* **93**, 163601 (2004).
- P4. "Localized component method: application to scattering in a system of three atoms," V. Roudnev, *Proceedings of the Seventeenth International IUPAP Conference on Few-Body Problems in Physics*, Elsevier (2004), p. S292.
- P3. "Split diabatic representation," B.D. Esry and H.R. Sadeghpour, *Phys. Rev. A* **68**, 042706 (2003).
- P2. "Hyperspherical close coupling calculations for charge transfer cross sections in  $\text{He}^{2+} + \text{H}(1s)$  collisions at low energies," C.N. Liu, A.T. Le, T. Morishita, B.D. Esry and C.D. Lin, *Phys. Rev. A* **67**, 052705 (2003).
- P1. "Ultraslow  $\bar{p}$ -H collisions in hyperspherical coordinates: Hydrogen and protonium channels," B.D. Esry and H.R. Sadeghpour, *Phys. Rev. A* **67**, 012704 (2003).



***Laboratory Research Summaries***  
***(by institution)***



## AMO Physics at Argonne National Laboratory

R. W. Dunford, E. P. Kanter, B. Krässig, R. Santra, S. H. Southworth, L. Young  
*Argonne National Laboratory, Argonne, IL 60439*

dunford@anl.gov, kanter@anl.gov, kraessig@anl.gov, rsantra@anl.gov,  
southworth@anl.gov, young@anl.gov

Our central goal is to establish a quantitative understanding of x-ray interactions with free atoms and molecules. With the advent of hard x-ray FELs, exploration of nonlinear and strong-field phenomena in the hard x-ray regime becomes accessible for the first time. For example, strong focusing can lead to a situation where photoabsorption rates exceed Auger rates to create large ensembles of hollow atoms. Understanding and tracking the vacancy cascade process initiated by hollow atoms in complex systems is of intrinsic interest and will be of importance in assessing radiation damage. With respect to strong-field phenomena at longer wavelengths, we have developed a synchrotron-based x-ray microprobe for understanding the transient behavior of atoms and molecules in strong optical fields ( $\sim 10^{15}$  W/cm<sup>2</sup>). The x-ray microprobe incorporates all the attributes of synchrotron radiation (broad tunability, polarization, focusability, short pulses) to achieve a time-resolved quantum-state-specific probe of atoms/molecules in strong laser fields. Our development has led to the first direct evidence of orbital hole alignment in strong-field ionization. It further allows us to probe ion dynamics in complex plasma environments with  $\sim 10$ -micron spatial and  $\sim 100$ -ps temporal resolution. Such studies of atoms and molecules in strong-optical fields will be relevant for pump/probe experiments at next generation sources. Foundational to these experiments is the detailed understanding of x-ray photoionization, where our recent and earlier studies have provided a firm basis for understanding higher order effects, such as non-dipolar photoelectron angular distributions. The major program change during the past year has been the addition of a fully integrated theoretical component, which has been instrumental in kindling new initiatives. Recent progress and future plans are described below.

### **X-ray microprobe of strong-field ionization dynamics in atoms**

L. Young, C. Höhr, E. R. Peterson, R. W. Dunford, D. L. Ederer, E. P. Kanter,  
B. Krässig, N. Rohringer, J. Rudati<sup>1</sup>, R. Santra, S. H. Southworth,  
D. A. Arms<sup>1</sup>, E. M. Dufresne<sup>1</sup>, E. C. Landahl<sup>1</sup>

Strong-field ionization of atoms by ultrafast optical lasers is of both fundamental and technological interest because this process represents the first step in the production of compact, coherent soft x-ray sources and in attosecond pulse generation. Earlier studies of strong-field ionization phenomena have typically observed ejecta (ions, electrons and photons). We have developed methodology to probe free atoms directly in the focus of an intense, ultrafast laser at intensities up to  $\sim 10^{15}$  W/cm<sup>2</sup>, i.e. those used for the above applications. The methodology employs tunable, monochromatic, polarized x-ray radiation from Argonne's Advanced Photon Source (APS) to provide a quantum-state specific probe of atoms (ions) in the laser focal volume. Microfocusing to 1-10  $\mu\text{m}$

diameter spot size provides the following advantages: 1) elimination of the volume (intensity) averaging associated with single laser beam experiments, 2) access to multiple wavelength excitation because of the extremely efficient use of laser power, 3) the ability to study micron-sized, rare samples, and, 4) a mitigation of sample damage.

With the x-ray microprobe methodology, we have established that, and to what degree, ions produced in a strong laser field are aligned [23]. Reference [23] introduced the new methodology and provided the first direct evidence for orbital alignment in strong-field ionization. How long is the alignment preserved in the plasma environment in which the ions are embedded? We addressed this question in Ref. [27]. Using microfocused, tunable x-rays from the APS, the evolution of orbital alignment in a Kr plasma was measured as a function of the time delay between laser and x-ray pulses. For target densities of the order of  $10^{14}$  cm<sup>-3</sup>, the alignment was found to decay within a few nanoseconds. We developed a quantitative model that explains the decay in terms of electron-ion collisions in the plasma [27]. The key ingredient in this model is that e<sup>-</sup>-Kr<sup>+</sup> collisions induce transitions among the j,m states of the ion. An electron scattering on Kr<sup>+</sup> 4p<sub>3/2</sub><sup>-1</sup> sees a non-spherical charge distribution, with a leading quadrupole contribution in addition to the -1/r potential. The scattering calculation employs a distorted-wave Born approximation. We also observed that by applying an external magnetic field of just a few hundred gauss, it became possible to suppress the disalignment and induce coherent spin precession of the Kr ions [27]. It remains a challenge for theory, to be tackled in the upcoming year, to explain how such a relatively weak field can noticeably influence the outcome of a collision of a krypton ion with an electron. Experimentally, a detailed investigation of disalignment dynamics as a function of applied magnetic field is planned.

Significant infrastructure improvements were made during the past year, September 2005-August 2006. Most notably, through extensive efforts by Eric Landahl, Harold Gibson, Emily Peterson and Cindy Chaffee, the new Ultrafast Laser Laboratory at APS Sector 7-ID was commissioned in October 2005. It features a regeneratively-amplified Ti:sapphire laser system (2.5 W average power, <50 fs, 1-5 kHz) in a 7.8 × 3.7 m laser laboratory. This provides ample space for “laser-only” experiments which can be performed during APS maintenance periods (~3-months/year). Such preliminary experiments are essential to commission complex apparatus, such as 3D ion imaging detectors, prior to use during x-ray beamtimes. Of central importance to the AMOP group is the establishment of a dedicated location for experiments at the end of the 7-ID undulator beamline. In addition, the AMOP group and Sector 7 beamline scientists have devised a simple method for time-resolved x-ray fluorescence experiments [31] which will permit timing experiments during the standard 24-bunch fill pattern at the APS and thus expand available beamtime by a factor of 4 to 5. Finally, the AMOP group is actively engaged in the planning for the APS upgrade, which will include the production of ~1-ps pulses by the rf-deflection method originally proposed by Zholents.

### **Collective behavior in laser-generated plasmas**

E. P. Kanter, R. W. Dunford, D. L. Ederer, C. Höhr, B. Krässig, E. C. Landahl<sup>1</sup>,  
E. R. Peterson, J. Rudati<sup>1</sup>, R. Santra, S. H. Southworth, L. Young

In our experiments in which strong optical lasers are focused on gas-phase atoms and molecules, we necessarily produce transient underdense plasmas when the target atoms are ionized by the laser. The densities are fairly high ( $\sim 10^{14}/\text{cm}^3$ ), while the laser-ionized electrons are fairly hot ( $\sim U_p = 12 \text{ eV}$ ). The Debye length is large ( $\sim 2\mu\text{m}$ ) compared to the interparticle spacing ( $\sim 0.1\mu\text{m}$ ). These are weakly coupled plasmas ( $\Gamma \sim 0.6$ ) and the electron thermalization time is large compared to the timescale of our experiments ( $< 100 \text{ nsec}$ ). As a result of these considerations, the hot electrons leave the volume explored by our x-ray microprobe comparatively fast (typically 10-20 nsec) leaving behind the colder positive ions which then expand due to their mutual Coulomb repulsion. In order to properly understand our data probing this complex environment, we have developed a computer code to simulate the electron and ion dynamics in this plasma.

Simulations have been carried out with a highly specialized computer code which follows the trajectories of 10,000 particles ( $\text{Kr}^+$ ,  $\text{Kr}^{++}$ , and  $e^-$ ) using 4th-order Runge-Kutta numerical integrator of the equations of motion with adaptive step control based on conservation of energy. The initial conditions were given by a Stark-ionization calculation using Herman-Skillman wavefunctions, a complex absorbing potential and numerical integration of rate equations. Using effective masses and charges scaled to give the Coulomb energy and particle accelerations corresponding to the actual experimental Kr density, we are able to deduce final kinetic energies as well as the time-dependent spatial densities of both charge states from the simulated results. While highly successful at computing those quantities, the computations take several hours and cannot be used for simulating collisional processes at higher densities.

In the past year, we have simulated depolarizing collisions by limiting our calculations to a much smaller volume than that probed in the experiments (which typically view a volume containing  $\sim 10^6$  ions). This is a severe limitation which we plan to address in the near future. By parallelizing the force computation, the most cpu-intensive part of the calculation, we plan on porting this work to Argonne's 350-node Jazz computing cluster. Such a development would easily permit 200,000 particles to be simulated in the same time frame used presently and within a few days of computation, 2 million would be amenable. This would become comparable to experimental densities. Additional future plans include a detailed experimental investigation of parameter space (we can control the electron temperature via the strong-field ionization conditions) including higher densities and longer time scales. Finally, we plan to explore real-time absorption imaging to further visualize the ion dynamics suggested by the simulations.

### **Photoionization of laser-aligned molecules**

S. H. Southworth, E. R. Peterson, C. Höhr, C. Buth, R. W. Dunford, D. L. Ederer,  
E. P. Kanter, B. Krässig, E. C. Landahl<sup>1</sup>, S. T. Pratt, R. Santra, L. Young

Due to their anisotropic polarizabilities, molecules exposed to a strong, linearly-polarized laser field can spatially align along the polarization direction. There are many potential applications of aligned molecules including reactive collisions, photoionization and fragmentation, and structural determination of macromolecules by x-ray diffraction. By reducing loss of information due to averaging over molecular orientations, studies using aligned molecules can provide a more direct and detailed comparison with theory. We are developing instrumentation and methods to study photoionization and ion

fragmentation of aligned molecules using an ultrafast 800 nm laser alone or in combination with tunable x-rays at the APS.

Supersonic expansion through a pinhole and skimmer produces a beam of cold molecules that can be aligned adiabatically by interaction with focused "long pulses" ( $\sim 110$  ps,  $\sim 10^{12}$  W/cm<sup>2</sup>, 1 kHz) of laser light. The aligned molecules can then be photoionized either by focused "short pulses" ( $\sim 50$  fs,  $\sim 10^{14}$  W/cm<sup>2</sup>, 1 kHz) from the same laser or by focused x rays ( $\sim 100$  ps, 271 kHz) from the adjacent beamline. A half-wave plate can rotate the polarization direction of the long pulses and hence rotate the molecular alignment direction. The *K*-shell ionization energy of Br  $\approx 13.5$  keV is a good match to the beamline, so we have chosen CF<sub>3</sub>Br for initial experiments. We calculated the anisotropic polarizability of CF<sub>3</sub>Br using the coupled cluster method to be  $\alpha_{\parallel} = 35a_0^3$  and  $\alpha_{\perp} = 20a_0^3$ . With these parameters we performed rotational wavepacket calculations of the laser alignment process which indicate the suitable parameter space (rotational temperature, laser intensity) for efficient alignment of CF<sub>3</sub>Br. A strong, pre-*K*-edge resonance of CF<sub>3</sub>Br has its transition dipole moment along the C–Br axis. We expect to observe enhancement (depletion) of the x-ray absorption probability at that resonance by aligning molecules parallel (perpendicular) to the polarization direction of the x-ray beam. An initial attempt at this experiment is in progress.

An ion-velocity-imaging spectrometer has also been constructed to study photoionization and fragmentation by the short laser pulses. The spectrometer features a large microchannel plate detector with delay-line anode and associated processing electronics and software for multi-hit, event mode, time- and position-sensitive ion detection. Interesting results have been obtained with this instrument on cold (not yet aligned) CF<sub>3</sub>Br. Cold molecules are readily distinguished from warm background gas through their times of flight and small transverse momenta. The angular distributions of fragment ions such as CF<sub>3</sub><sup>+</sup> and Br<sup>+</sup> also exhibit patterns characteristic of their kinetic-energy releases.

Future work will involve developing methods for precise temporal and spatial overlap of long and short laser pulses, enhancing the cooling, density, and differential pumping of the molecular beam, and utilizing the position sensitivity and event-mode capability of the delay-line detector for x-ray ionization studies. Future plans also include extending this work to measure the structure of laser-aligned molecules.

### Inner-shell decay processes

R. W. Dunford, E. P. Kanter, B. Krässig, S. H. Southworth, L. Young, P. H. Mokler<sup>2,3</sup>,  
Th. Stöhlker<sup>2</sup>, S. Cheng<sup>4</sup>, A. G. Kochur<sup>5</sup> and I. D. Petrov<sup>5</sup>

In preparation for working with hard x-ray FELs, we are developing an understanding of the production of hollow atoms and the vacancy cascade processes following inner-shell ionization using the APS. This work typically utilizes the coincidence detection of x-rays to identify the processes of interest. Recent work has involved the study of heavy atoms, but in the near future it will be extended to more complex systems.

We recently reported a comprehensive study of double *K*-photoionization of Ag [17] at photon energies from just below the double *K*-ionization threshold (51.782 keV) to the region of the expected maximum in the cross-section ( $\sim 90$  keV). The energy dependence

of those data was fitted to a model which determined both the scattering contribution and the shakeoff contribution. The results showed a significantly larger scattering contribution than in lighter atoms and we developed a model which quantitatively describes these observations. We are currently working toward extending the measurements to 300 keV, well above the expected peak of the cross section, in order to confirm this model. Achieving this goal will require more x-ray intensity at 300 keV.

In other work, photon coincidences were used to study two processes in the decay of Au atoms following *K*-shell photoionization. One is the two-photon decay of *K*-holes via virtual intermediate states and the other is the cascade decay via real intermediate states. These measurements provide tests of theory where many-electron effects, relativistic effects, and strong field strengths prevail and provide a challenge to theory. In two-photon decay, the individual photon energies form a continuum while the sum-energy of the two photons equals the transition energy. The differential measurement of the shape of the continuum radiation provides a sensitive test of the details of the theory. The most recent measurement [15] determined the continuum shapes for the transitions  $2s \rightarrow 1s$ ,  $3s \rightarrow 1s$ ,  $3d \rightarrow 1s$ , and  $(4s+4d) \rightarrow 1s$ . There is general agreement with theory except for the  $3s \rightarrow 1s$  transition where anomalously high values are found near  $y=0.35$ , where  $y$  is the fraction of the transition energy carried by the lower energy photon. Analysis of the cascade data following *K*-shell photoionization of Au has allowed a study of a three step process involving emission of two photons accompanied by a Coster-Kronig rearrangement in the intermediate state. This has provided a precise measurement [25] of the Coster-Kronig transition probability  $f_{23}$  in Au. Our result is smaller than the calculations of McGuire [PRA **3**, 587 (1981)] and Puri *et al.* [X-ray Spectrom. **22**, 358 (1993)] but agrees with our own single-configuration Pauli-Fock calculation [25].

For the future, we plan to extend this work to more complex systems including molecules, size-selected clusters and, possibly, endohedral fullerenes. Following initial inner-shell photoionization of one of the atoms in these systems, the vacancy cascades can migrate to other atoms of the structure resulting in a complicated pattern which can be studied using coincidence techniques similar to those used in the work with single atoms. In addition to the patterns of the decay radiation we can study the final charge state distributions and determine how the structures break apart. This work would initially use existing facilities at the APS.

### **Nondipolar photoelectron angular distributions in atoms and molecules**

B. Krässig, E. P. Kanter, S. H. Southworth, L. Young, R. Wehlitz<sup>6</sup>

Photoelectron angular distributions that are not symmetric with respect to reversal of the photon propagation direction cannot be treated in the usual dipole approximation. Such an asymmetry is an indicator of mixing between multipole components of opposite parities. In general this effect becomes more prominent at higher photon energies, but it is also observable at low photon energies – especially in situations, e.g. Cooper minima or resonances, where the normal dipole contribution is suppressed or a higher multipole contribution is enhanced. In the parametrization of the photoelectron angular distribution the asymmetry is commonly characterized by two nondipolar asymmetry parameters  $\gamma$  and  $\delta$  (for ionization from an *s* shell  $\delta=0$ ). In previous years we reported strong

nondipolar asymmetries in inner-shell ionization of Ar, Kr and Br<sub>2</sub> [22], using photon energies from 2-22 keV at NSLS and APS. We found that these effects in atoms at high photon energies are well accounted for in the theoretical calculations if the appropriate higher-order terms are included. Our recent experiments at the University of Wisconsin's Synchrotron Radiation Center have focused on measurements of  $\gamma$  and  $\delta$  in the low energy region between 20 and 150 eV and in outer shells where electron correlation and intershell couplings are important. This is prominently seen in our work on low-energy nondipolar asymmetries in photoionization of Xe 5s [Hemmers *et al.*, PRL **91**, 53002 (2003)]. We have also studied the variations of the nondipolar parameters in the region of the dipole  $2snp$  and quadrupole  $2p^2$  autoionization resonances in helium ( $n=2-7$ , in collaboration with N.L.S. Martin and B. A. de Harak, University of Kentucky), and of the  $2s-3p$ ,  $2s-4p$  dipole and  $2s-3d$  quadrupole resonances in the neon  $2p$  cross section. In all of these cases we observed pronounced deviations from the nonresonant values of the asymmetry parameter. The results in neon are in good agreement with the prediction of Dolmatov and Manson [PRL **83**, 939 (1999)]. With our method it is possible to characterize pure quadrupole-excited resonance states that are not accessible otherwise. We also performed a survey of the photoelectron nondipolar asymmetry from near threshold to 150 eV for photoionization of H<sub>2</sub> and the valence shell of N<sub>2</sub> (in collaboration with O. Hemmers, R. Guillemin and D. W. Lindle, University of Nevada, Las Vegas). The data of the N<sub>2</sub> measurement, with additional data points from the Nevada group, and concomitant calculations by B. Zimmermann and V. McKoy (Caltech) and P. Langhoff (University of California, San Diego) are the subject of a manuscript currently under consideration by Phys. Rev. Letters [26]. On the basis of these and earlier investigations we conclude that the understanding of non-dipolar effects in atomic photoionization is rather solid and sufficient to predict angular distribution patterns at LCLS.

### **Towards a quantitative understanding of high-harmonic generation**

R. Santra, N. Rohringer, A. Gordon<sup>7</sup>, F. X. Kärtner<sup>7</sup>

In a recent landmark paper [Nature **432**, 867 (2004)], Corkum, Villeneuve, and co-workers made the remarkable claim that the phenomenon of high-order harmonic generation (HHG) in a strong laser field may be exploited to tomographically image the highest occupied molecular orbital (HOMO). This interpretation of HHG is based on the so-called three-step model. Intrigued by the idea of orbital imaging, we formulated a many-electron extension of the three-step model [18]. Employing many-body perturbation theory based on canonical Hartree-Fock orbitals, we derived correction terms to the standard three-step model. Essentially, we found that formally, even at the effective one-particle level, an HHG experiment *does not* provide sufficient information to fully reconstruct the HOMO of a molecule. One reason for this is that the wave function of the recollision electron in HHG must remain orthogonal to all occupied molecular orbitals. Therefore, in order to reconstruct the HOMO from HHG data, the occupied orbitals must already be known.

This limitation of HHG can be overcome [21]. Guided by the relationship between the amplitude for one-photon-induced electron emission and the electron-ion

recombination amplitude in the three-step model of high-order harmonic generation, it was argued that synchrotron-based photoionization might be a superior approach to imaging molecular orbitals. Within the Hartree-Fock independent-particle picture, the molecular-frame photoelectron angular distributions, measured as a function of photon energy, could be used to reconstruct all orbitals occupied in the Hartree-Fock ground state of the molecule investigated. It was suggested that laser alignment techniques could be employed to facilitate the measurement of the molecular-frame photoelectron angular distributions. The possibility of imaging molecular orbitals using photoionization might offer interesting new opportunities for experimental research at Argonne's Advanced Photon Source (APS). In this context, it should be mentioned that the ANL AMOP group is currently developing the methodology to study laser-aligned molecules using hard x-rays from the APS.

Still the primary and most important application of HHG is the production of coherent, ultrashort (down into the attosecond regime) XUV and soft x-ray pulses. The process, however, is plagued by a notoriously low conversion efficiency. An improved theoretical understanding of HHG, as provided, for example, by Ref. [18], is therefore crucial. Recently, we took another important step in this direction. In Ref. [16], we demonstrated the breakdown of the frozen-core single-active-electron approximation, which predicts roughly the same HHG radiation amplitude in all noble gases. This is in contradiction with experiments, where heavier noble gases are known to emit much stronger HHG radiation than lighter ones. We could qualitatively reproduce the experimental behavior of the noble gases when many-electron dynamics, within a simple approximation, was taken into account.

### **Theory of x-ray microprobe of strong-field processes**

R. Santra, R. W. Dunford, L. Young, C. Buth

A detailed account of the theory underlying the x-ray microprobe experiment on strong-field-ionized krypton is the topic of Ref. [29]. We showed that the degree of alignment of  $\text{Kr}^+$  is strongly overestimated by nonrelativistic strong-field ionization models. An effective one-electron model of strong-field ionization was utilized that includes the effect of spin-orbit interaction. The method makes use of a flexible finite-element basis set and determines ionization rates in this square-integrable basis using a complex absorbing potential. We find that even at the electric-field strength corresponding to the saturation intensity for the ionization of Kr, there is very little mixing between the  $4p_{3/2}$  and  $4p_{1/2}$  outer-valence orbitals. This shows that the uncoupled  $m_l, m_s$  projection quantum numbers are inappropriate to describe the  $\text{Kr}^+$  states that are populated by strong-field ionization of krypton. This realization challenges views held in the community of strong-field laser physicists. We developed a description of the x-ray probe step using a density-matrix formalism, which allowed us to demonstrate that the inclusion of spin-orbit interaction in the ionization process provides satisfactory agreement with the experimental observation. This research indicates future possibilities for time-resolved studies utilizing fs and sub-fs laser pulses. One possibility that we plan to explore is the degree of alignment that may be expected for  $\text{Kr}^{++}$ . What is the shape of the electron cloud in the doubly charged ion

after a strong laser pulse has removed two electrons from the initially neutral atom? The fundamental difference in comparison to the singly charged species is that the alignment of  $\text{Kr}^+$  is determined by spin-orbit coupling, while in  $\text{Kr}^{++}$  it is determined by the much stronger hole-hole interaction. This cannot be described in terms of simple mean-field theories. A second possibility is to employ an ultrashort laser pulse and use strong-field ionization to launch a spin-orbit wave packet in the valence shell of an atom. In neon, the spin-orbit period is about 40 femtoseconds. This should be long enough to allow for direct observation of the intraatomic wave-packet dynamics using a pump-probe configuration.

In order to describe the strong-field ionization of Kr [29], we wrote a computer program that calculates the atomic ionization rate in the tunneling limit, i.e., the laser electric field is assumed to be so strong that field ionization is faster than the oscillation period of the radiation field. This assumption makes calculations extremely efficient. However, it can only be justified in the long-wavelength limit. We therefore developed a second computer program that makes use of the strong-field (or Floquet) limit of quantum electrodynamics. This new code is again based on a finite-element basis. However, in contrast to an earlier Floquet code that one of us (R.S.) had written, the square-integrability of the wave function of the ionized electron is now enforced using a complex absorbing potential derived from smooth exterior scaling. This ensures higher accuracy of the numerical results and adds to the computational efficiency. Most importantly, in contrast to the tunneling code, the Floquet program can be applied to strong-field problems at any photon energy. There is no limitation to long wavelengths. This code, with further refinements, will allow us to calculate multiphoton absorption cross sections in the soft and hard x-ray regimes. Another important application of our Floquet code, which is of immediate interest in connection with ongoing experiments of the ANL AMOP group at the APS, is the calculation of the near-K-edge x-ray absorption spectrum of a laser-dressed atom. In this case, the laser is not sufficiently intense to ionize any of the valence electrons. The final-state manifold of the core-excited electron, however, becomes severely modified by the dressing laser field (via multiphoton absorption and emission). The detailed theory we have developed and calculations we have performed on krypton will be described in a manuscript we are currently preparing. Preliminary studies on neon, which we plan to extend further, indicate that the laser-dressing effect on the near-K-edge absorption spectrum is very dramatic. Finally, the x-ray microprobe technique is currently being extended to study laser-aligned molecules. Therefore, another future goal is to develop the theory for this experiment.

<sup>1</sup>Advanced Photon Source, Argonne National Laboratory, Argonne, IL 60439

<sup>2</sup>GSI, Planckstrasse 1, D64291 Darmstadt, Germany

<sup>3</sup>Justus-Liebig Univ., D35392 Giessen, Germany

<sup>4</sup>Dept. of Physics, Univ. of Toledo, Toledo, OH 43606

<sup>5</sup>Rostov State Univ. of Trans. Comm., Rostov-na-Donu, 344038, Russia

<sup>6</sup>Synchrotron Radiation Center, Stoughton, WI

<sup>7</sup>Massachusetts Institute of Technology, Cambridge, MA 02139

## Publications 2004 - 2006

- [1] An atom trap system for practical  $^{81}\text{Kr}$ -dating  
X. Du, K. Bailey, Z.-T. Lu, P. Mueller, T. P. O'Connor and L. Young, *Rev. Sci. Instrum.* **75**, 3224 (2004).
- [2] Nonvanishing  $J=1 \rightarrow 0$  Equal-Frequency Two-Photon Decay: E1M2 Decay of the He-like  $2^3\text{S}_1$  state,  
R. W. Dunford, *Phys Rev A* **69**, 062502, 1-5 (2004).
- [3] Higher-order processes in x-ray photoionization and decay,  
R. W. Dunford, E. P. Kanter, B. Krässig, S. H. Southworth and L. Young, *Radiat. Phys. Chem.* **70**, 149-172 (2004).
- [4] Two-photon decay in heavy atoms and ions,  
P. H. Mokler and R. W. Dunford, *Physica Scripta* **69**, C1-9 (2004).
- [5] Two-photon decay of K-shell vacancies in silver atoms,  
P. H. Mokler, H. W. Schäffer and R. W. Dunford, *Phys Rev A* **70**, 032504, 1-5 (2004).
- [6] Counting individual  $^{41}\text{Ca}$  atoms with a magneto-optical trap,  
I. D. Moore, K. Bailey, J. Greene, Z.-T. Lu, P. Mueller, T. P. O'Connor, C. Geppert, K. D. A. Wendt and L. Young, *Phys. Rev. Lett.* **92**, 153002, 1-4 (2004).
- [7] Inner-shell photoionization in weak and strong radiation fields,  
S. H. Southworth, R. W. Dunford, D. L. Ederer, E. P. Kanter, B. Krässig and L. Young, *Radiat. Phys. Chem.* **70**, 655-660 (2004).
- [8] One million years of Nubian Aquifer groundwater history,  
N. C. Sturchio, X. Du, R. Purstchert, B. E. Lehmann, M. Sultan, L. J. Patterson, Z.-T. Lu, P. Mueller, T. Bigler, K. Bailey, T. P. O'Connor, L. Young, R. Lorenzo, R. Becker, Z. El Alfy, B. El Kaliouby, Y. Dawood and A. M. A. Abdallah, *Geophys. Res. Lett.* **31**, L05503 (2004).
- [9] Lifetime of the  $2^3\text{P}_0$  state of He-like  $^{197}\text{Au}$ ,  
S. Toleikis, B. Manil, E. Berdermann, H. F. Beyer, F. Bosch, M. Czanta, R. W. Dunford, A. Gumberidze, P. Indelicato, C. Kohuharov, D. Liesen, X. Ma, R. Marrus, P. H. Mokler, D. Schneider, A. Simionovici, Z. Stachura, T. Stöhlker, A. Warczak and Y. Zou, *Phys. Rev. A* **69**, 022507, 1-5 (2004).
- [10] Nondipole effects in molecular nitrogen valence shell photoionization,  
O. Hemmers, R. Guillemin, D. Rolles, A. Wolska, D. W. Lindle, E. P. Kanter, B. Krässig, S. H. Southworth, R. Wehlitz, B. Zimmermann, V. McKoy and P. W. Langhoff, *J. Elec. Spec.* **144-147**, 155-156 (2005).
- [11] Photo double ionization of helium 100 eV and 450 eV above threshold : C. gerade and ungerade amplitudes and their relative phase,

A. Knapp, B. Krässig, A. Kheifets, I. Bray, T. Weber, A. L. Landers, S. Schössler, T. Jahnke, J. Nickles, S. Kammer, O. Jagutzki, L. P. H. Schmidt, M. Schöffler, T. Osipov, M. H. Prior, H. Schmidt-Böcking, C. L. Cocke and R. Doerner, *J. Phys. B* **38**, 645-657 (2005).

[12] Extreme-ultraviolet wavelength and lifetime measurements in highly ionized krypton, K. W. Kukla, A. E. Livingston, C. M. V. Vogt, H. G. Berry, R. W. Dunford, L. J. Curtis and S. Cheng, *Can. J. Phys.* **83**, 1127-1139 (2005).

[13] Time-resolved activities at the advanced photon source requiring the pulsed structure of the x-ray beam, J. Wang, E. Landahl, T. Graber, R. Pahl, L. Young, L. X. Chen and E. E. Alp, *Synch. Rad. News* **18**, 24 (2005).

[14] Photo double detachment of  $\text{CN}^-$ : electronic decay of an inner-valence hole in molecular anions, R. C. Bilodeau, C. W. Walter, I. Dumitriu, N. D. Gibson, G. D. Ackerman, J. D. Bozek, B. S. Rude, R. Santra, L. S. Cederbaum and N. Berrah, *Chem. Phys. Lett.* **426**, 237-241 (2006).

[15] Two-photon decay in gold atoms, R. W. Dunford, E. P. Kanter, B. Krässig, S. H. Southworth, L. Young, P. H. Mokler, T. Stöhlker and S. Cheng, *Phys Rev A* **74**, 012504, 1-11 (2006).

[16] Role of many-electron dynamics in high harmonic generation, A. Gordon, F. X. Kärtner, N. Rohringer and R. Santra, *Phys. Rev. Lett.* **96**, 223902 (2006).

[17] Double *K*-shell photoionization of silver, E. P. Kanter, I. Ahmad, R. W. Dunford, D. S. Gemmell, B. Krässig, S. H. Southworth and L. Young, *Phys. Rev. A* **73**, 022708, 1-11 (2006).

[18] Three-step model for high harmonic generation in many-electron systems, R. Santra and A. Gordon, *Phys. Rev. Lett.* **96**, 073906 (2006).

[19] Higher-order processes in x-ray photoionization of atoms, E. P. Kanter, R. W. Dunford, B. Krässig, S. H. Southworth and L. Young, *Radiat. Phys. Chem.* (in press).

[20] Double *K*-photoionization of heavy atoms, E. P. Kanter, R. W. Dunford, B. Krässig, S. H. Southworth and L. Young, *Radiat. Phys. Chem.* (in press).

[21] Imaging molecular orbitals using photoionization, R. Santra, *Chem. Phys.* (in press).

[22] Nondipole asymmetries of *K*-shell photoelectrons of Kr, Br<sub>2</sub>, and BrCF<sub>3</sub>, S. H. Southworth, R. W. Dunford, E. P. Kanter, B. Krässig, L. Young, L. A. LaJohn and R. H. Pratt, *Radiat. Phys. Chem.* (in press).

- [23] X-ray microprobe of orbital alignment in strong-field ionized atoms, L. Young, D. A. Arms, E. M. Dufresne, R. W. Dunford, D. L. Ederer, C. Höhr, E. P. Kanter, B. Krässig, E. C. Landahl, E. R. Peterson, J. Rudati, R. Santra and S. H. Southworth, Phys. Rev. Lett. (in press).
- [24] X-ray microprobe of optical strong-field processes, L. Young, R. W. Dunford, C. Höhr, E. P. Kanter, B. Krässig, E. R. Peterson, S. H. Southworth, D. L. Ederer, J. Rudati, D. A. Arms, E. R. Dufresne and E. C. Landahl, Radiat. Phys. Chem. (in press).
- [25] Coster-Kronig transition probability  $f_{23}$  in gold atoms, R. W. Dunford, E. P. Kanter, B. Krässig, S. H. Southworth, L. Young, P. H. Mokler, T. Stöhlker, S. Cheng, A. G. Kochur and I. D. Petrov, Phys Rev A (submitted).
- [26] Low-energy nondipole effects in molecular nitrogen valence-shell photoionization, O. Hemmers, R. Guillemin, D. Rolles, A. Wolska, D. W. Lindle, E. P. Kanter, B. Krässig, S. H. Southworth, R. Wehlitz, B. Zimmermann, V. McKoy and P. W. Langhoff, Phys. Rev. Lett. (submitted).
- [27] Dynamics of orbital alignment in a laser-generated plasma, C. Höhr, E. R. Peterson, N. Rohringer, J. Rudati, D. A. Arms, E. M. Dufresne, R. W. Dunford, D. L. Ederer, E. P. Kanter, B. Krässig, E. C. Landahl, R. Santra, S. H. Southworth and L. Young, Phys Rev Lett. (submitted).
- [28] Why complex absorbing potentials work : a DVR perspective, R. Santra, Phys Rev A (submitted).
- [29] Spin-orbit effect on strong-field ionization of krypton, R. Santra, R. W. Dunford and L. Young, Phys Rev A (submitted).
- [30] Interaction of intense vuv radiation with large xenon clusters, Z. B. Walters, R. Santra and C. H. Greene, Phys. Rev. A (submitted).
- [31] A simple short-range point-focusing spatial filter for time-resolved x-ray fluorescence, C. Höhr, E. R. Peterson, E. Landahl, D. A. Walko, R. W. Dunford, E. P. Kanter and L. Young, Proceedings of the 9<sup>th</sup> International Conference on Synchrotron Radiation Instrumentation, 2006, AIP Conference Proceedings (submitted).

## OVERVIEW 2006

The J.R.Macdonald Laboratory (JRML) has now reached a mature stage in the transition from collisions to intense-laser interactions with matter. In 2005 more than 70% of our publications were on laser-related work. At the same time, we continue to make use of our accelerators in conjunction with the Kansas Light Source (KLS), our central laser facility.

Most of the laser-related work is associated with one or more of five major themes:

**1) Attosecond physics** (*Chang, Cocke, Lin, Litvinyuk*): the ultimate goal of this work is to develop pulses so short and so strong that we will be able to follow, in real time, the electronic motion in atoms and molecules. We are using polarization gating and other techniques to try to produce pulses as short as tens of attoseconds. We are developing our ability to characterize these pulses using combined XUV and infrared fields, and to use the accompanying technology to carry out related pump/probe experiments. Theoretical work guides the experimental work.

**2) Time-resolved dynamics of heavy-particle motion in neutral molecules** (*Cocke, Esry, Litvinyuk, Lin, Thumm*): We follow in real time, using pump/probe techniques, the evolution of heavy particle motion in light molecules from  $H_2$  to heavier systems such as  $N_2$  and  $CO_2$ . The mechanisms whereby molecules “Coulomb explode” when exposed to intense short pulses are being explored. Theoretical analysis of these and related systems is being carried out, including the study of long-time vibrational motion in  $H_2^+$  and studies in multi-electron systems.

**3) Control, from the femtosecond to the nanosecond time scale** (*Chang, Cocke, DePaola, Esry, Lin, Litvinyuk, Thumm*): The ultimate goal of AMO ultrafast is to see the motion in real time and to control it. This requires the ability to control the shape of the pulse. We have recently achieved carrier-envelope-phase (CEP) stabilization of our laser and are beginning to do AMO experiments with this capability. In the near future we (*DePaola*) will be installing a “dazzler” on the KLS to shape the pulses from the KLS to control ionization pathways in ultra-cold atoms (in a MOT) and for other “AMO ultrafast” experiments. We will also use the MOT to explore and control multi-photon mediated ionizing collisions in cold atoms. Theoretical work will continue on the effects of CEP stabilized pulses on  $H_2^+$  dissociation, on attosecond spectra and harmonic generation.

**4) Studies involving simultaneous use of laser and accelerators** (*Ben-Itzhak, Carnes, Chang, Cocke, DePaola, Esry*): We continue to exploit our ability to combine our laser and accelerator facilities. We use the Kansas Light Source (KLS) to dissociate and ionize slow molecular ion beams ( $H_2^+$ ,  $O_2^+$ , ..) from our ECR source. We are exploring the possibility of delivering pico-second pulses of fast ion beams produced in our Tandem accelerator using the KLS.

**5) Photons from the KLS interacting with solids and clusters** (*Richard, Thumm*): We will continue to study the interactions of photons from the KLS with nanotubes and with surfaces, both experimentally and theoretically.

In the area of stand-alone collisions our main program involves low-energy ions from the EBIS interacting with a MOT target, (*Fehrenbach*) and user collaborations. We continue to host outside users in a collaborative mode, and to participate in outside collaborations.

Details of the above projects are provided in the individual contributions which follow.

**Structure and Dynamics of Atoms, Ions, Molecules, and Surfaces:  
Molecular Dynamics with Ion and Laser Beams**

*Itzik Ben-Itzhak, J. R. Macdonald Laboratory, Kansas State University  
Manhattan, Ks 66506; ibi@phys.ksu.edu*

*The goal of this part of the JRML program is to study the different mechanisms for molecular dissociation initiated by ultrashort intense laser pulses or following fast or slow collisions. To that end we typically use molecular ion beams as the subject of our studies.*

Below we give a couple of examples of our recent work<sup>1</sup>.

**Above threshold Coulomb explosion (ATCE) of  $\text{H}_2^+$  in intense fs laser pulses, Itzik Ben-Itzhak, Pengqian Wang, A. Max Saylor, Kevin D. Carnes, and Brett D. Esry**

*This work is the direct result of close collaboration between theory and experiment. Theory suggested a model that was simpler to test experimentally than from first principles. As a consequence, a new mechanism of molecular dissociation was uncovered: above threshold Coulomb explosion.*

In talks on the intense field ionization of  $\text{H}_2^+$ , it is common to see a plot that shows the lowest two  $\text{H}_2^+$  Born-Oppenheimer potentials,  $1s\sigma_g$  and  $2p\sigma_u$ , along with the ionization potential  $1/R$ . The  $2p\sigma_u$  state is shifted downward by the photon energy in accord with the Floquet picture [1], but ionizing transitions are indicated by a stack of arrows representing photons. Not liking this mixture of representations — the Floquet picture already includes the photons, after all — we asked ourselves how to describe dissociation and ionization within the same conceptual framework while retaining the benefits of the Floquet picture for dissociation. The simplest answer was to simply include the ionization potentials in the Floquet picture, shifting  $1/R$  by integer multiples of the photon energy. These curves, along with the dissociation curves, are shown in the left hand side of Fig. 1(b). Such curves really represent the lower edge of the ionization continuum and assume the ionized electron has zero total energy. But, where they cross the appropriately shifted  $1s\sigma_g$  and  $2p\sigma_u$  potentials, that ionization channel opens. At low laser intensities near the ionization appearance intensity, these channel openings should translate into structure in the nuclear kinetic energy release (KER) spectrum. No such structure had been reported experimentally, however.

So, with this new picture in mind, we re-analyzed the low-intensity ionization KER data available from our application of the intensity difference spectrum (IDS) method [Pub. #12]. Typical data is shown in the right hand side of Fig. 1 in (a) and (b) [Pub. #19]. The bars at the top of each panel show the peak positions expected from our model and the fit produced by placing a Gaussian at these positions allowing for intensity-induced shifts. Panels (a) and (b) were fit simultaneously using constraints suggested by our model that reduced the total number of free parameters by a factor of two.

Our model also allows us to predict the angular distribution, since we know the number of photons leading to each peak. The idea is that each photon absorbed will contribute a factor of  $\cos^2\theta$ , since primarily parallel transitions are involved. Thus, for the 800 nm data shown in panels (a) and (b) that require 12-13 photons to ionize, the angular distribution should be  $\cos^{24}\theta$  or  $\cos^{26}\theta$ . Panel (d) shows a  $\cos^{2n}\theta$  fit to the data in (a) and (b) with the result that  $n=12.5\pm 1.0$ , in good agreement with our model.

---

<sup>1</sup>Some of our studies are done in collaboration with Z. Chang's group, C.W. Fehrenbach, and others.

It occurred to us that a good test of our model would be to change the laser wavelength. Doubling the frequency was a convenient choice and would give a spectrum clearly distinct from the 800 nm result. We then performed the measurement, and the data is shown in panel (c) with the new predictions for the peak positions. Again, our model gives a good fit of the data. The more convincing test of the model, though, is the angular distribution. For 400 nm light, our model predicts ionization primarily with 6-7 photons. The  $\cos^{2n}\theta$  fit gave  $n=6.5\pm 1.0$  in good agreement as before.

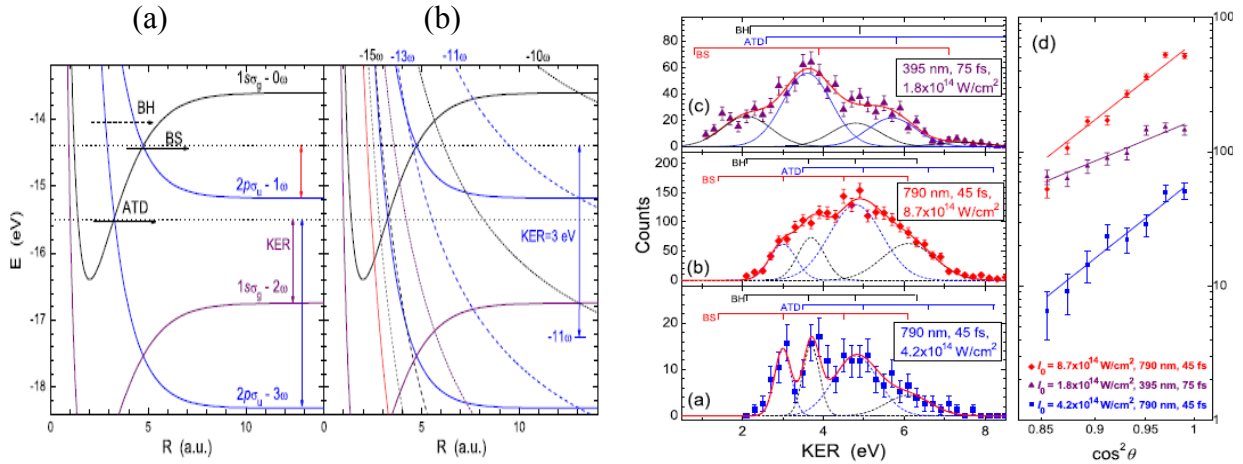


**Figure 1.** *Left:* (a) The diabatic Floquet potentials for  $H_2^+$ . Besides the molecular quantum numbers, each curve carries a photon number label. (b) The same as (a), but including the ionization threshold potentials. *Right:* (a)–(c) Experimental ionization KER spectra. The vertical bars indicate the predicted KER peak locations, grouped by initiating mechanism. (d) Experimental log-log angular distributions corresponding to the spectra (a)–(c).

We have also successfully applied this model to explain the surprising structure in the double ionization of  $H_2$  reported recently by Staude *et al.* – see the report of Brett Esry for details.

**Enhanced ionization of  $H_2^+$  (CREI)** – *I. Ben-Itzhak, P.Q. Wang, A.M. Sayler, K.D. Carnes, M. Leonard, B.D. Esry, A.S. Alnaser, B. Ulrich, X.M. Tong, I.V. Litvinyuk, C.M. Maharjan, P. Ranitovic, T. Osipov, S. Ghimire, Z. Chang and C.L. Cocke*

*The goal for this JRML “super-group” effort was to reveal the predicted structure in the CREI spectrum of  $H_2^+$ . Our data shows no such structure mainly due to the nuclear motion of the stretching molecule and intensity averaging in the interaction region.*

The research conducted at JRML on the interaction of intense short-pulse lasers with molecular ion beams and with molecular targets is complementary to each other. In an effort to improve our understanding of enhanced ionization we teamed up. Zuo and Bandrauk suggested that this enhancement in ionization is due to charge resonance enhanced ionization (CREI) around some critical internuclear distances that are larger than the bond length of  $H_2^+$ . Their calculations predicted two prominent peaks in the ionization rate centered about an internuclear distance,  $R$ , of 7 and 10 a.u. [2], which initiated further theoretical work on the structure of CREI (e.g. Refs. [3-4]). Furthermore, this intriguing structure motivated experimental work trying to reveal it [5-9]. The fact that ionization of  $H_2^+$  is enhanced at some large  $R$  is well established. However, evidence for the second CREI peak around 10 a.u. is still in dispute. Using the pump-probe technique we selected the ionization of  $D_2^+$  dissociating on the  $2p\sigma_u - 1\omega$  curve and converted the time delay to the internuclear distance where ionization occurred, as shown in Fig. 2(Left). We also converted the KER distribution of an ionized  $H_2^+$  beam, shown in Fig. 2(Right),

to  $R$  using a similar classical model for the propagation. Both measured distributions clearly show a single broad enhanced-ionization peak and do not support the predicted second CREI peak at 10 a.u. We suggested that the CREI structure predicted by “frozen nuclei” calculations [2-4,10] is washed out by nuclear motion during the stretch prior to ionization [10] and by intensity averaging effects. We hope that these recently submitted results will bring to an end the “hunt” for the double peak structure in enhanced ionization.

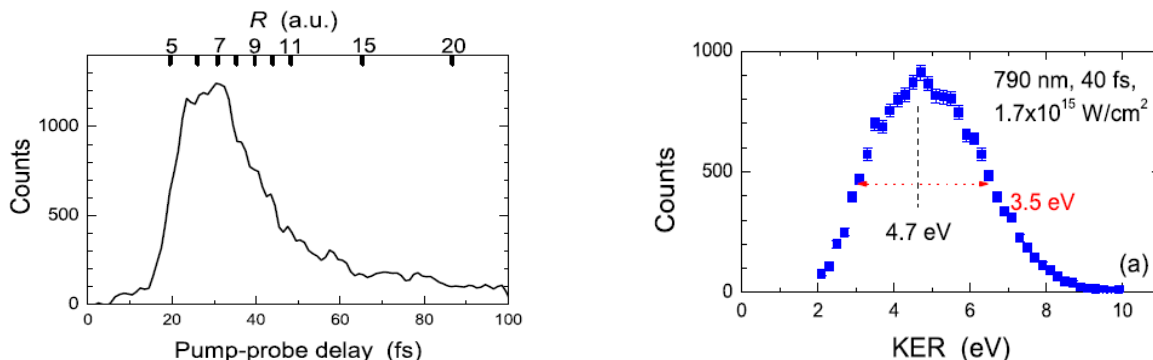


**Figure 2.** *Left:* measurements. (a) Measured pump-probe time-delay distribution of  $D_2$ , the associated value of  $R$  is marked on the top axis. *Right:* Measured KER distribution for an  $H_2^+$  beam. Note that a KER of about 4.6 is expected for ionization at  $R=7$  a.u. (including the dissociation energy gained to that point), while ionization at  $R=10$  a.u. should yield 3.4 eV.

In addition to the projects described in some detail above, we have studied a few other molecular-ion beams with our short-pulse laser and extended our studies to include few-cycle pulses. Furthermore, we have conducted a few ion-molecule collision experiments [see, for example Pub. #17-18]. In parallel, we are upgrading our molecular dissociation imaging setup for upcoming studies of collisions of a few keV molecular ion beams with atomic targets.

**Future plans:** We are in the process of analyzing recent measurements of  $H_2^+$ ,  $O_2^+$  and  $N_2^+$  beams interrogated by intense sub-10 fs FWHM pulses. First attempts to measure the predicted effects of the carrier envelop phase (CEP) on  $HD^+$  laser induced dissociation (see Pub. #7) have recently been carried out. Further improvements are required to bring this project to completion. Progress has been made on the understanding of the dissociation and ionization of more complex diatomic molecules, such as  $O_2^+$  and  $N_2^+$ , and we will continue our efforts in this direction. Finally, we hope to finish the upgrade of our new experimental setup, which will enable kinematically complete studies of dissociative capture at keV energies.

1. J.H. Posthumus, Rep. Prog. Phys. **67**, 623 (2004).
2. T. Zuo and A.D. Bandrauk, Phys. Rev. A **52**, R2511 (1995).
3. M. Plummer and J.F. McCann, **29**, 4625 (1996).
4. L.Y. Peng *et al.*, J. Phys. B **36**, L295 (2003).
5. G.N. Gibson *et al.*, Phys. Rev. Lett. **79**, 2022 (1997).
6. I.D. Williams *et al.*, J. Phys. B **33**, 2743 (2000).
7. Th. Ergler *et al.*, Phys. Rev. Lett. **95**, 093001 (2005); and J. Phys. B **39**, S493 (2006).
8. A.S. Alnaser *et al.*, J. Phys. B **39**, S485 (2006).
9. D. Pavičić *et al.*, Phys. Rev. Lett. **94**, 163002 (2005); and Eur. Phys. J. D **26**, 39 (2003).
10. S. Chelkowski, C. Foisy, A.D. Bandrauk, Phys. Rev. A **57**, 1176 (1998).

#### Publications of DOE sponsored research in the last 3 years:

19. “Above threshold Coulomb explosion of molecules in intense laser pulses”, B.D. Esry, A.M. Saylor, P.Q. Wang, K.D. Carnes, and I. Ben-Itzhak, Phys. Rev. Lett. **97**, 013003 (2006).

18. "Preference for breaking the O-H bond over the O-D bond following HDO ionization by fast ions", A.M. Sayler, M. Leonard, K.D. Carnes, R. Cabrera-Trujillo, B.D. Esry, and I. Ben-Itzhak, *J. Phys. B* **39**, 1701 (2006).
17. "Measurement of alignment dependence in single ionization of hydrogen molecules by fast protons", Nora G. Johnson, R.N. Mello, Michael E. Lundy, J. Kapplinger, Eli Parke, K.D. Carnes, I. Ben-Itzhak, and E. Wells, *Phys. Rev. A* **72**, 052711 (2005).
16. "One- and Two-electron processes in collisions between hydrogen molecules and slow highly charged ions", E. Wells, K.D. Carnes, H. Tawara R. Ali, E.Y. Sidky, C. Illescas, and I. Ben-Itzhak, *Nucl. Instrum. and Methods B* **241**, 101 (2005).
15. "Proton-Carbon Monoxide Collisions From 10 keV to 14 MeV", I. Ben-Itzhak, E. Wells, Vidhya Krishnamurthi, K.D. Carnes, N.G. Johnson, H.D. Baxter, D. Moore, K.M. Bloom, B.M. Barnes, and H. Tawara, *Phys. Rev. A* **72**, 022726 (2005).
14. "Dissociation and ionization of  $H_2^+$  by ultrashort intense laser pulses probed by coincidence 3D momentum imaging", I. Ben-Itzhak, P.Q. Wang, J.F. Xia, A.M. Sayler, M.A. Smith, K.D. Carnes, and B.D. Esry, *Phys. Rev. Lett.* **95**, 073002 (2005).
13. "Highlighting the angular dependence of bond softening and bond hardening of  $H_2^+$  in an ultrashort intense laser pulse", P.Q. Wang, A.M. Sayler, K.D. Carnes, J.F. Xia, M.A. Smith, B.D. Esry and I. Ben-Itzhak, *J. Phys. B* **38**, L251 (2005). *Chosen to appear in the J. Phys. B. Highlights of 2005* <http://herald.iop.org/jphysb-highlights2005/m51/crk/164563/link/211>.
12. "Intensity-selective differential spectrum: Application to laser-induced dissociation of  $H_2^+$ ", P.Q. Wang, A.M. Sayler, K.D. Carnes, B.D. Esry, and I. Ben-Itzhak, *Opt. Lett.* **30**, 664 (2005).
11. "Dissociation and ionization of molecular ions by ultra-short intense laser pulses probed by coincidence 3D momentum imaging", I. Ben-Itzhak, P.Q. Wang, J.F. Xia, A.M. Sayler, M.A. Smith, K.D. Carnes, and B.D. Esry, *Nucl. Instrum. and Methods B* **233**, 56 (2005).
10. "Bond rearrangement caused by sudden single and multiple ionization of water molecules", I. Ben-Itzhak, A.M. Sayler, M. Leonard, J.W. Maseberg, D. Hathiramani, E. Wells, M.A. Smith, J.F. Xia, P.Q. Wang, K.D. Carnes, and B.D. Esry, *Nucl. Instrum. and Methods B* **233**, 284 (2005).
9. "Electrostatic Ion Beam Trap for Electron Collision Studies", O. Heber, P.D. Witte, A. Diner, K.G. Bhushan, D. Stasser, Y. Toker, M.L. Rappaport, I. Ben-Itzhak, D. Schwalm, A. Wolf, N. Alstein and D. Zajfman, *Rev. Sci. Instrum.* **76**, 013104 (2005).
8. "Electron impact detachment of small negative clusters", D. Zajfman, O. Heber, A. Diner, P.D. Witte, D. Stasser, Y. Toker, M.L. Rappaport, I. Ben-Itzhak, O. Guliamov, L. Kronik, D. Schwalm, and A. Wolf, *Electron and Photon Impact Ionization and Related Topics 2004*, Institute of Physics conference series **183**, 173 (2005).
7. "Controlling  $HD^+$  and  $H_2^+$  dissociation with the carrier-envelope phase difference of an intense ultrashort laser pulse", V. Roudnev, B.D. Esry, and I. Ben-Itzhak, *Phys. Rev. Lett.* **93**, 163601 (2004).
6. "Ionization of atoms by the spatial gradient of the pondermotive potential in a focused laser beam", E. Wells, I. Ben-Itzhak, and R.R. Jones, *Phys. Rev. Lett.* **93**, 023001 (2004).
5. "Size dependent electron impact detachment of internally cold  $C_n^-$  and  $Al_n^-$  clusters", A. Diner, Y. Toker, D. Stasser, O. Heber, I. Ben-Itzhak, P.D. Witte, A. Wolf, D. Schwalm, M.L. Rappaport, K.G. Bhushan, and D. Zajfman, *Phys. Rev. Lett.* **93**, 063402 (2004).
4. "Electrostatic Ion Beam Trap", O. Heber, N. Alstein, I. Ben-Itzhak, A. Diner, M.L. Rappaport, D. Strasser, Y. Toker, and D. Zajfman, *proceedings of the IEEE conference* (2004).
3. "Reexamining if long-lived  $N^-$  anions are produced in fast dissociative electron-capture collisions" I. Ben-Itzhak, O. Heber, I. Gertner, A. Bar-David, and B. Rosner, *Phys. Rev. A* **69**, 052701 (2004).
2. "Interference effects in double ionization of spatially aligned hydrogen molecules by fast highly charged ions", A.L. Landers, E. Wells, T. Osipov, K.D. Carnes, A.S. Alnasser, J.A. Tanis, J.H. McGuire, I. Ben-Itzhak, and C.L. Cocke, *Phys. Rev. A* **70**, 042702 (2004).
1. "Bond-Rearrangement in Water Ionized by Ion Impact", A.M. Sayler, J.W. Maseberg, D. Hathiramani, K.D. Carnes, and I. Ben-Itzhak, *Application of Accelerators in Research and Industry*, edited by J.L. Duggan and I.L. Morgan (AIP press, New York 2003), vol. **680**, p. 48.

# Stabilizing the carrier-envelope phase of the Kansas Light Source

Zenghu Chang

J. R. Macdonald Laboratory, Department of Physics,  
Kansas State University, Manhattan, KS 66506, chang@phys.ksu.edu

The goals of this aspect of the JRML program are (1) to generate high power, few-cycle laser pulses with stabilized carrier-envelope phase, (2) to increase the brightness of attosecond x-ray sources based on the polarization gating of high-order harmonic generation, and (3) to improve ultrafast x-ray streak cameras.

## 1. Stabilizing the carrier-envelope phase of amplified laser pulses – C. Li, E. Moon, Z. Duan and Z. Chang

The high intensity laser facility, the *Kansas Light Source*, produces 25 fs pulses with 2.5 mJ energy by using the principle of chirped pulse amplification [1]. It also provides 6.2 fs pulses with 0.6 mJ energy by using an improved hollow-core fiber/chirped mirror compressor [2]. The dynamics in atoms [3], molecules [4, 5] and nanotubes [6] have been extensively studied using the facility. Since there are only few-cycle field oscillations under the 6 fs pulse envelope, it is crucial to control their carrier-envelope (CE) phase for strong field atomic physics studies. The CE phase errors can originate inside the oscillator, CPA amplifier, and the hollow-core fiber compressor of a laser system. We focused on the effects of the stability of the grating separation in the stretcher and compressor on the CE phase variation [7, 8], which have been overlooked so far.

For most stretcher and compressor designs, the incident angle is close to the Littrow angle. Considering the gratings with grating constant  $d_s \approx \lambda$ , It can be shown that amount of CE phase errors,  $\Delta\varphi_{CE}$ , introduced by the variation of the effective linear grating separation,  $\Delta l_{eff}$ , is,

$$\frac{\Delta\varphi_{CE}}{\Delta l_{eff}} = 2\pi \frac{\lambda}{d_s^2} \approx \frac{2\pi}{\lambda}. \quad (1)$$

It reveals that the CE phase change is significant when the variation of linear separation of the gratings is on the order of the laser wavelength.

The dependence of CE phase on the grating separation was measured experimentally by driving one of the telescope mirrors. To observe the phase shift caused by the variation of  $l_{eff}$ , we introduced a small change  $\Delta l_{eff}$  by moving the mirror in the grating based stretcher with a PZT driven mount. For a t mirror motion of  $\Delta$ , it was estimated that  $\Delta\varphi_{CE} / \Delta \approx 6 \text{ rad}/\mu\text{m}$ . When a sinusoidal wave with 60 volts peak to peak was applied to the PZT, the mirror moves back and forth with a 3.6  $\mu\text{m}$  displacement amplitude. The measured CE phase variation is shown in Fig. 1 (a) and (b). It was deduced that  $\Delta\varphi_{CE} / \Delta \approx \Delta\varphi_{CE} / \Delta l_{eff} \approx 6 \text{ rad}/\mu\text{m}$ , which agrees with the calculated results.

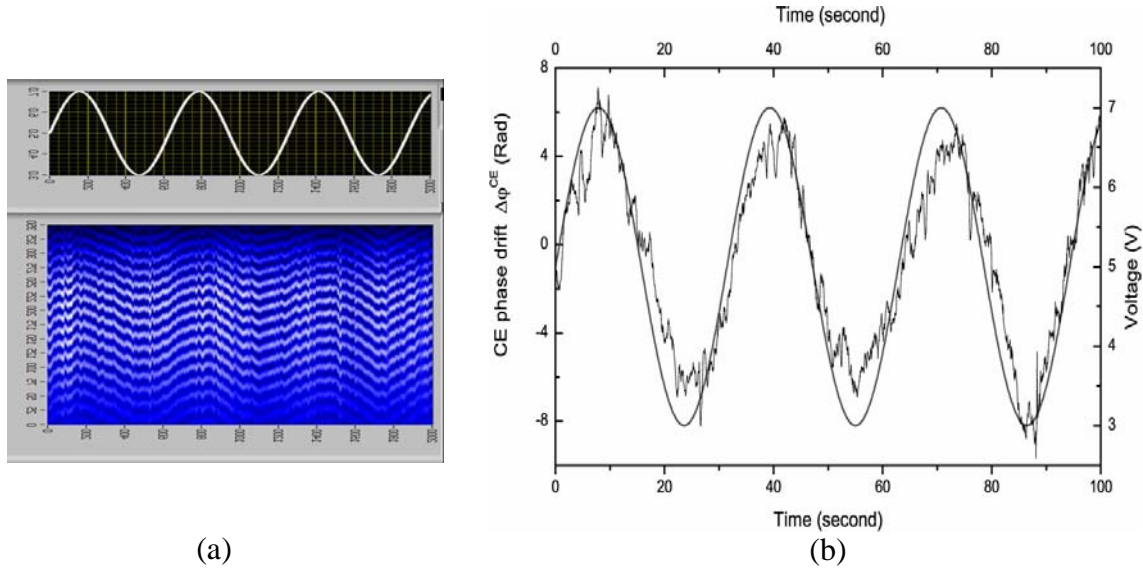
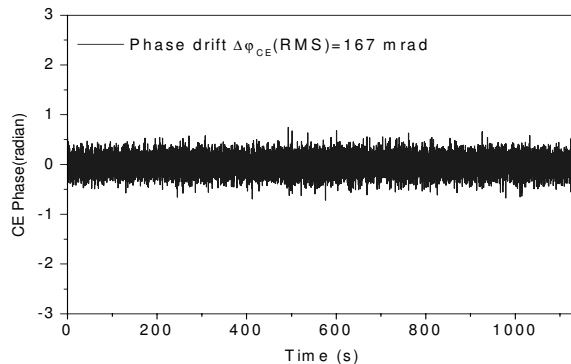


Fig. 1 . The dependence of the CE phase of the amplified pulses on the grating separation. (a) and (b), the fringe pattern of the collinear  $f$ -to- $2f$  interferometer and the corresponding relative carrier-envelope phase obtained with a 4 volts peak to peak sinusoidal voltage, which caused the PZT to move  $3.6 \mu\text{m}$ .

Since the gratings in the stretchers and compressor are not interferometrically stable, its vibration and thermal drift contributes to the variation of the CE phase. To produce CE phase stabilized pulses from a CPA system, one either has to fix the grating separation with an interferometrical accuracy, or correct the phase error. Stabilization the separations of the gratings and mirrors in the stretcher and compressor need three feedback loops which can be costly and complicated, we thus took the latter approach. Previously, the slow CE phase drift introduced by the CPA amplifiers was precompensated by adding a feedback loop to the oscillator offset frequency locking electronics using the measured CE phase from the collinear  $f$ -to- $2f$  as the input. We chose to feedback control the grating separation in the stretcher instead. The advantage of our method is that it does not disturb the oscillators, which should yield more stable output power from the oscillator since it reduces the pump power modulation. The relative CE phase with the feedback control is shown in Fig. 2. The RMS phase error is 167 mrad over 18 minutes. This can be improved further in the future.

Fig. 2. The CE phase of the amplified pulses stabilized by feedback controlling the grating separation. The RMS phase error in 18 minutes is 167 mrad.



**2. Dependence of attosecond spectra on the CE phase of the driving laser – M. Shakya, S. Gilbertson, H. Mashiko and Z. Chang.** We demonstrated that attosecond XUV supercontinuum can be generated by polarization gating of high harmonic generation [9]. Our numeric simulation predicted that the change of the CE phase of the driving laser pulse can result in either single or double electron ion recollisions in the gated harmonic generation process [10]. If the XUV spectrum can be measured and analyzed for every laser shot, then it is possible to determine the shot to shot variation of the CE phase. The measurement of the single shot CE phase is important for studying CE phase effects in many experiments when the CE phase of the few-cycle laser pulses are not locked. For a CE phase locked laser system, the measurement gated harmonic spectra are useful for observing fast variations of the CE phase. It is worth mentioning that the conventional  $f$ -to- $2f$  setup measures the relative CE phase change, while it is possible to determine the absolute CE phase from the XUV spectrum. The major challenge for measuring the single shot XUV spectrum was to obtain enough XUV photons per laser shot, which is what we plan to work on. In the mean time, we are also trying to measure the attosecond pulse duration by measuring the momentum shift and of the photoelectrons [11, 12].

**3. Calibration of an accumulative x-ray streak camera with high harmonic pulses—Mahendra Shakya, S. Gilbertson and Z. Chang.** We show experimentally that the deflection dispersions are a major limiting factor for streak cameras with resolutions approaching 100 fs [13]. The deflection aberrations can be reduced by reducing the beam size of the electron in the deflection plates. We demonstrated that a resolution of 280 fs FWHM was achieved when with a 5  $\mu\text{m}$  wide slit was used, as shown in Fig. 3. To the best of our knowledge, this is the highest resolution ever achieved with an accumulative streak camera. The high resolution is critical in experiments with synchrotrons [14, 15].

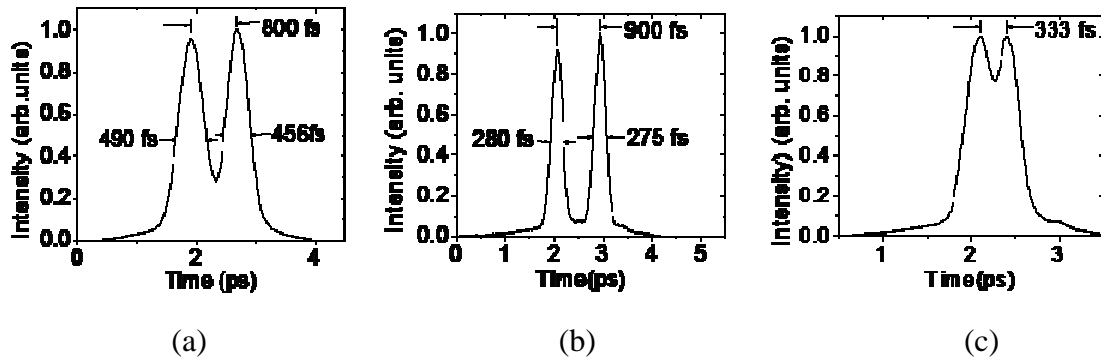


Fig. 3. The measured temporal resolution with various slits. (a) The slit width is 50 $\mu\text{m}$ . (b) and (c) The slit width is 5 $\mu\text{m}$ . The two pulses are produced by a Mach-Zehnder interferometer.

We plan to characterize the camera using the soft x-ray pulses from the high order harmonic generation. We will continue the collaboration with Prof. J. Rocca at Colorado State University. The x-ray streak camera is an idea too for studying the dynamics of the x-ray laser [16]. Progress is also made on applying the camera to the pico-pulse project, i.e., accelerating the ultrashort ion pulses producing by intense laser pulses in a tandem accelerator.

## **PUBLICATIONS (2005-2006):**

1. Bing Shan, Chun Wang and Zenghu Chang, "High peak-power kilohertz laser systems employing single-stage multi-pass amplification", U. S. Patent No. 7,050,474, issued on May 23, 2006.
2. S. Ghimire, B. Shan, C. Wang, and Z. Chang, "High-Energy 6.2-fs Pulses for Attosecond Pulse Generation," *Laser Physics*, **15**, No. 6, 838-842(2005).
3. C. M. Maharjan, A. S. Alnaser, X. M. Tong, B. Ulrich, P. Ranitovic, S. Ghimire, Z. Chang, I. V. Litvinyuk, and C. L. Cocke, "Momentum imaging of doubly charged ions of Ne and Ar in the sequential ionization region," *Phys. Rev. A* **72**, 041403(R) (2005).
4. A. S. Alnaser, C. M. Maharjan, X. M. Tong, B. Ulrich, P. Ranitovic, B. Shan, Z. Chang, C.D. Lin, C. L. Cocke, and I. V. Litvinyuk, "Effects of orbital symmetries in dissociative ionization of molecules by few-cycle laser pulses," *Phys. Rev. A* **71**, 031403(R) (2005).
5. A. S. Alnaser, B. Ulrich, X. M. Tong, I. V. Litvinyuk, C. M. Maharjan, P. Ranitovic, T. Osipov, R. Ali, S. Ghimire, Z. Chang, C. D. Lin, and C. L. Cocke, "Simultaneous real-time tracking of wave packets evolving on two different potential curves in  $H_2^+$  and  $D_2^+$ ," *PHYSICAL REVIEW A* **72**, 030702(R)(2005).
6. M. Zamkov, N. Woody, B. Shan, Z. Chang, P. Richard, "Lifetime of charge carriers in multiwalled nanotubes," *Phys. Rev. Lett.*, **94**, 056803 (2005).
7. Zenghu Chang, "Carrier envelope phase shift caused by grating-based stretchers and compressors," *Applied Optics*, accepted (2006).
8. Chengquan Li, Eric Moon, and Zenghu Chang, "Carrier-envelope phase shift caused by variation of grating separation," *Optics Letters*, accepted (2006).
9. Bing Shan, Shambhu Ghimire, and Zenghu Chang, "Generation of attosecond XUV supercontinuum by polarization gating," *Journal of Modern Optics* **52**, 277 (2005).
10. Zenghu Chang, "Chirp of the attosecond pulses generated by a polarization gating," *Phys. Rev. A*, **71**, 023813 (2005).
11. Z. X. Zhao, Zenghu Chang, X. M. Tong, and C. D. Lin, "Circularly-polarized laser-assisted photoionization spectra of argon for attosecond pulse measurements," *Optics express*, **13**, 1966 (2005).
12. Z. X. Zhao, Zenghu Chang, X. M. Tong, and C. D. Lin, "Measuring attosecond pulses generated from polarization gating," *Proc. SPIE Int. Soc. Opt. Eng.* **5920**, 592007 (2005).
13. Mahendra Shakya and Zenghu Chang, "Achieving 280 fs resolution with a streak camera by reducing the deflection dispersion," *Appl. Phys. Lett.* **87**, 041103 (2005).
14. Jinyuan Liu, Eric Landahl, Jing Wang, and Zenghu Chang, "Single-pulse measurement of synchrotron radiation using an ultrafast x-ray streak camera," *Proc. SPIE Int. Soc. Opt. Eng.* **5920**, 592007 (2005).
15. S. L. Johnson, P. A. Heimann, A. G. MacPhee, A. M. Lindenberg, O. R. Monteiro, Z. Chang, R. W. Lee, and R. W. Falcone, "Bonding in liquid carbon studied by time-resolved x-ray absorption spectroscopy," *Phys. Rev. Lett.*, **94**, 057407 (2005).
16. M. A. Larotonda, Y. Wang, M. Berrill, B. M. Luther and J. J. Rocca, Mahendra Man Shakya, and Zenghu Chang, "Pulse duration measurements of grazing incidence pumped table-top Ni-like Ag and Cd transient soft x-ray lasers," *Optics Letters*, accepted (2006).

## Structure and Dynamics of Atoms, Ions, Molecules and Surfaces: Atomic Physics with Ion Beams, Lasers and Synchrotron Radiation

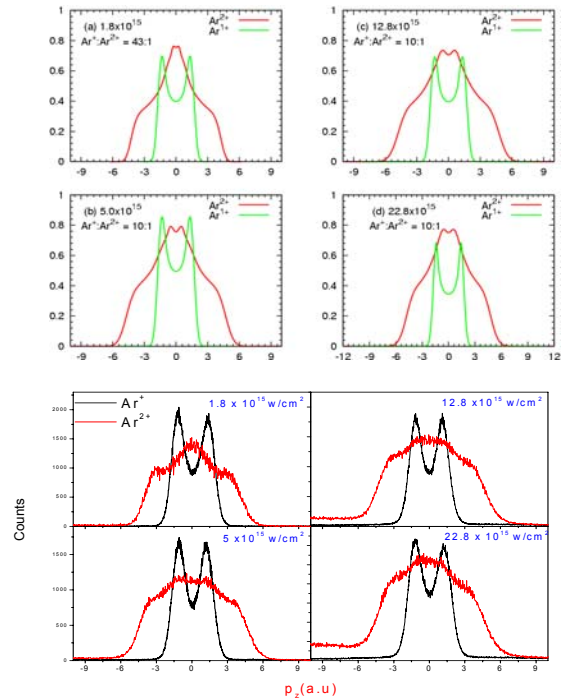
C.L.Cocke, Physics Department, J.R. Macdonald Laboratory, Kansas State University,  
Manhattan, KS 66506, [cocke@phys.ksu.edu](mailto:cocke@phys.ksu.edu)

*The goals of this aspect of the JRML program are to explore mechanisms of ionization of atoms, ions and small molecules by intense laser pulses and ions and to investigate the dynamics of photoelectron emission from small molecules interacting with x-rays from harmonic generation and synchrotron radiation.*

### Recent progress:

**1) Momentum imaging of doubly charged ions of Ne and Ar in the sequential ionization region,** *C. M. Maharjan, A. S. Alnaser, X. M. Tong, B. Ulrich, P. Ranitovic, S. Ghimire, Z. Chang, I. V. Litvinyuk, and C. L. Cocke.* One theme of “AMO ultrafast” science is to develop “clocks” for following the dynamics of atomic and molecular processes in real time. The project described here developed from our attempt to use the rotation of the electric field vector in circular polarization to measure the time interval between the emission of two electrons when an atom is doubly ionized by a short intense laser pulse. The plan was to measure the azimuthal angle between the momentum vectors of the two emitted electrons, using COLTRIMS and measuring the doubly charged ion and the two electrons in coincidence. This experiment has not yet been successful, due largely to the limitation of the repetition rate of our laser (1 kHz). However, we were able to gain important information concerning the sequential ionization process from the momentum spectra of the singly and doubly charged recoil ions of Ar and Ne when neutral gas targets of these elements were ionized by 8 fs pulses of circularly polarized 800 nm radiation at intensities approaching  $10^{16}$  w/cm<sup>2</sup>. The recoil momentum spectra of the singly charged ions, taken in the plane of the electric field vector, show the expected “donut” pattern, reflecting the momentum corresponding to the vector potential of the laser at the time of emission. The projections of these donuts onto the axis along which we have our best resolution are shown in fig. 1 for argon. A similar projection of the momenta of doubly charged ions, also shown in fig. 1, shows considerably more interesting and more informative structure. This structure can be interpreted as the folding together of two “donuts”, each with a radius corresponding to the magnitude of the vector potential at the time of emission of the electrons. Roughly speaking, the outer peak in the projection corresponds to the sum of the magnitudes of the vector potentials at the times of first and second ionization, and the inner peak corresponds to the magnitude of the difference of these vector potentials. This information, when combined with knowledge of the time-profile of the pulse, allows the deduction of the approximate times of ionization of the two electrons, although not with the resolution which the angular measurement would provide. The experimental momentum spectra were interpreted quantitatively by a model calculation of X.-M. Tong. This work is described in publication 3.

Fig. 1. (Lower half) Spectra of the momenta of singly and doubly ionized Ar ions projected onto the z-axis (along the collection field of the spectrometer) for circularly polarized radiation at four different peak laser intensities. (Upper half) Model calculations by X.-M.Tong of the  $p_z$  distributions, corresponding to the ionization data.



## 2) Wavelength dependence of momentum-space images of low-energy electrons generated by short intense laser pulses at high intensities, C. M. Maharjan, A. S. Alnaser, I. Litvinyuk, P. Ranitovic, and C. L. Cocke.

Recent measurements of the momentum spectra of low energy electrons released from atomic targets by intense laser pulses, in an intensity region where tunneling ionization was expected to dominate, have shown marked structure in both electron energy and angle. The exact origin of this structure has not yet been unambiguously identified. Both “Freeman resonances” and diffraction are thought to play a role. In an attempt to provide experimental data on this subject, we used COLTRIMS to measure electron momentum spectra over wavelength range between 400 and 800 nm at high enough intensities that one might naively expect tunneling to dominate over multi-photon ionization. Complex structure was observed, as shown in fig. 2. By following individual features over a range of wavelengths, some of the energy structure could be associated with particular Rydberg resonances in the atom. Some could not. The angular structure was observed to maintain a preference for an angular momentum of 6 over a range of energy structures. The observed structures are too complex to be easily interpreted without a complete solution to the Schrödinger equation. Integration of theoretical calculations over the interaction volume is crucial in the interpretation. At least two groups, including that of C.D.Lin, are presently making progress in quantitatively interpreting this structure. See publication 3.

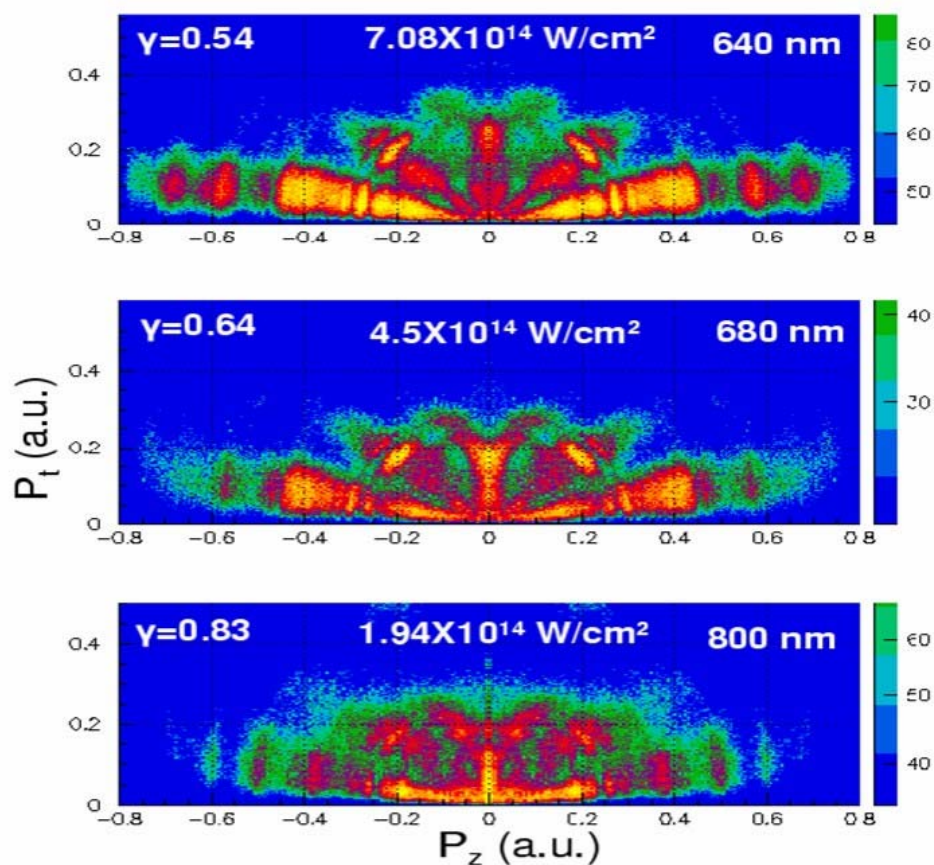


Fig. 2. 3D electron momentum distributions measured for single ionization of Ar. Horizontal axis corresponds to momentum component along the polarization direction, vertical axis represents value of electron momentum perpendicular to laser polarization.

### Future plans:

**3) Infrared pump/XUV probe work** discussed in last year's progress report has continued. We have successfully produced photoelectrons from harmonics up to approximately 45 eV in a COLTRIMS geometry and are building a two-component mirror to allow time-resolved photoelectron spectroscopy. One of the initial experiments will be to try to launch a wave packet into the dissociative  $2p\sigma_u$  potential curve of  $D_2^+$  with an infrared pulse and to photoionize this state at a known later time with the XUV probe. This work is an extension of our infrared pump-probe work on  $H_2^+$  and  $D_2^+$  discussed in last year's progress report and in publication 5. We will also use photoelectron spectra generated by the harmonics in the presence of the infrared field to characterize the time structure of the attosecond pulse trains represented in the harmonics.

**4) Other future projects:** We will continue our infrared pump-probe work using CEP stabilized pulses and investigate ways to control the dissociation/ionization routes in  $H_2$ ,  $D_2$  and other light molecules.

**Publications appearing in 2005-2006 not previously listed:**

1. "Photon-ion collisions and molecular clocks", T. Osipov, A. L. Alnaser, S. Voss, M. H. Prior, T. Weber, O. Jagutzki, L. Schmidt, H. Schmidt-Böcking, R. Dörner, A. Landers, E. Wells, B. Shan, C. Maharjan, B. Ulrich, P. Ranitovic, X. M. Tong, C. D. Lin, and C. L. Cocke, *J. of Modern Optics* 52, 439 (2005).
2. "Simultaneous real-time tracking of wave packets evolving on two different potential curves in  $H_2^+$  and  $D_2^+$ ", A. S. Alnaser, B. Ulrich, X. M. Tong, I. V. Litvinyuk, C. M. Maharjan, P. Ranitovic, T. Osipov, R. Ali, S. Ghimire, Z. Chang, C. D. Lin, and C. L. Cocke, *Phys. Rev. A* 72, 30702 (2005)
3. "Momentum imaging of doubly charged ions of Ne and Ar in the sequential ionization region," C. M. Maharjan, A. S. Alnaser, X. M. Tong, B. Ulrich, P. Ranitovic, S. Ghimire, Z. Chang, I. V. Litvinyuk, and C. L. Cocke, *Phys. Rev. A* 72 041403 (R) (2005).
4. "Resonant excitation during strong-field dissociative ionization," A. S. Alnaser, M. Zamkov, X. M. Tong, C. M. Maharjan, P. Ranitovic, C. L. Cocke, and I. V. Litvinyuk, *Phys. Rev. A* 72 041402 (R) (2005)
5. "Wavelength dependence of momentum-space images of low-energy electrons generated by short intense laser pulses at high intensities," C. M. Maharjan, A. S. Alnaser, I. Litvinyuk, P. Ranitovic, and C. L. Cocke, *J. Phys. B: At. Mol. Opt. Phys.* 39 1955 (2006).
6. "Momentum-imaging investigations of the dissociation of  $D_2^+$  and the isomerization of acetylene to vinylidene by intense short laser pulses," A.S. Alnaser, I. Litvinyuk, T. Osipov, B. Ulrich, A. Landers, E. Wells, C. M. Maharjan, P. Ranitovic, I. Bocharova, D. Ray and C. L. Cocke, *J. Phys. B: At. Mol. Opt. Phys.* 39, S485(2006).

## Theoretical Studies of Interactions of Atoms, Molecules and Surfaces

**C. D. Lin**

J. R. Macdonald Laboratory  
Kansas State University  
Manhattan, KS 66506  
e-mail: cdlin@phys.ksu.edu

### **Program Scope:**

We investigate the interaction of intense lasers and attosecond light pulses with atoms and molecules, including high-order harmonic generation, energy and momentum spectra of the electrons or ions, from the breakup of atoms or molecules, with the goal of interpreting and/or guiding experimental observations. References to our published papers or preprints (the full list is given at the end of this report) are given in bold letters in the text.

### **1. Alignment dependence of high-order harmonic generation (HHG) and two-center interference**

#### *Recent progress*

In the last two years, a number of experimental groups have made measurements of high-order harmonic generation (HHG) from aligned molecules. The procedure is rather straightforward: A weak laser pulse is first used to partially align molecules, and another probe laser is later used to generate HHG at different time delays, especially at the short time intervals when the molecules undergo "rotational revival", i.e., when their angular distributions undergo rapid changes. The polarization directions of the two pulses can be either parallel or varied.

There is no reliable theoretical calculations of HHG from aligned molecules. In general, one expects that the HHG from molecules would depend on the symmetry of the molecular orbital of the outermost electron, or the highest occupied molecular orbital (HOMO). To test to what extent the recent experiments can be explained with the simple Lewenstein model, we generalized this model to molecular systems where the molecular wavefunctions were calculated by using the GAMESS code. Initially we have tested our calculations for N<sub>2</sub> and O<sub>2</sub> targets (see **A9**, **A10**) and we were able to show that the experimental results are well explained by our calculations. The calculations and experiments both show that the ionization rates and the HHG yields for N<sub>2</sub> peak in the forward direction, while for O<sub>2</sub> they tend to peak at large angles near 45°. To compare with experimental data, we also calculated the angular distributions of the molecules at different time delays, using laser parameters and gas temperature suggested by the experiments.

The situation is different for CO<sub>2</sub>. The first experiment on CO<sub>2</sub> by Kanai et al [Nature, 435, 470, 2005] observed that the ionization rates and the HHG yields are inverted in that when one is maximum the other is minimum, at least for some harmonics. Since the first step of HHG is the tunneling ionization, this inversion was interpreted as evidence of two-center interference in the recombination process. The latter was proposed by Lein et al [Phys. Rev. A88,183903, 2002] earlier. They argued that the wave packet from the returning electron reaches the atomic centers at different time or different phase such that under proper condition, the harmonics from the two atomic centers can interfere destructively and a minimum in the HHG can be observed if the standard two-center interference condition is satisfied. Note that in this interference model, the position of the HHG minimum does not depend on the laser intensity. Similar experiment with somewhat different laser parameters was carried out by Vozzi *et al* [Phys. Rev. Lett. 95, 153902, 2005]. Inversion was observed but it is at a different HHG order. In a private communication, the HHG from CO<sub>2</sub> is also being studied in Colorado. Inversion has been observed also but again at

different HHG orders. Thus the situation is quite confusing. What is the origin of the inversion in CO<sub>2</sub>? Can the inversion be interpreted in terms of two-center interference?

We have made a theoretical investigation of HHG from CO<sub>2</sub> using the Lewenstein model, see **A4**. In the calculation, we accounted for the depletion effect -- i.e., when a molecule is ionized it does not contribute to the generation of HHG. We found inversion in our calculation, but the position of the HHG minimum depends on the laser intensity, and the inversion has nothing to do with the two-center interference. In other words, we found an alternative interpretation of the inversion of HHG and the result is intensity dependent.

*Future plans:*

All of our calculations were carried out in the length gauge for the dipole matrix element. Because of the gauge dependence of the calculated HHG and the approximate nature of the Lewenstein model, we cannot conclude precisely whether the inversion is indeed due to two-center interference or not. This project will be further pursued in the coming grant period.

## **2. Attosecond pulses probing atomic and molecular dynamics**

*Recent Progress:*

We have carried out numerical calculations to illustrate that attosecond pulses can be used to probe the time dependence of the motion of atoms in a small molecule, as well as the correlated motion of two excited electrons. We assume that a vibrational wave packet of D<sub>2</sub><sup>+</sup> is created at time t=0. The subsequent motion of this wave packet can be probed accurately by using an attosecond xuv pulse of duration of about 300 as to ionize D<sub>2</sub><sup>+</sup>. From the D<sup>+</sup> energy one can recover the wave packet, revealing detailed spreading and interference of the vibrational wave packet. Analysis of the time evolution of such a wave packet would allow experimentalists to extract the amplitude and phase of each vibrational state in the wave packet. (**A3**). This is an extension of the experiment of Alnaser et al [Phys. Rev. A72, 030702(R), 2005] where an 8 fs laser pump is used to generate the wave packet and its time evolution is probed by another 8 fs pulse.

We have also investigated the time evolution of a wave packet made of a coherent sum of doubly excited states. The wave packet is then probed by using an attosecond pulse to doubly ionize the atoms. From the momentum distributions of the two ionized electrons partial information about the initial wave packet can be probed. A preliminary result of such a study was published in **A1**.

*Future plans:*

In the coming year we will make further calculations to probe electron-electron dynamics. We will first study the rovibrational motion of two excited electrons in the time domain. For the probe, an xuv attosecond pulse will be used to double ionize the atom. We will use products of Coulomb wavefunctions to represent the two ionized electrons. We will begin to develop a time-dependent two-electron code in hyperspherical coordinates which would allow us to perform calculations for pump-probe experiments with attosecond pulses which can be compared to actual experiments in the future. The code would also allow us to study nonlinear processes using xuv or soft-x-ray light pulses from high-order harmonic generation, as well as from x-ray free electron lasers.

## **3. Electron energy and momentum spectra of atoms and molecules induced by intense short laser pulses**

*Recent progress:*

Motivated by the experimental observations of the electron momentum spectra carried out at Kansas State University and elsewhere, we initiated a new theoretical study along this same line last year. While ionization of atoms by intense lasers in the multiphoton ionization regime is considered to be well understood, the situation is different in the tunneling ionization region. In the latter, the electron distribution was expected to be rather smooth with a strong peak at the zero momentum. Experiments from the Frankfurt group, which were later confirmed by the experiments from Kansas State University, showed that there are still numerous structures in the electron energy and momentum distributions, even for laser intensities well into the tunneling ionization region.

We have calculated the electron momentum spectra from Ar atoms by a short intense laser pulse by directly solving the time-dependent Schrodinger equation (TDSE) and by using the strong field approximation (SFA). We found that the two theories give rather similar electron spectra, and the spectra show the familiar multiphoton peaks even in the tunneling ionization region. For the short pulses, there also exist many substructures which have been attributed to the rapidly changing ponderomotive potential in the pulse. In the two-dimensional momentum spectra, the major features from the two theories are the same, but for low energy electrons, we noticed substantial differences. The positions of the ATI peaks and the substructures are sensitive to the laser intensities but the structures for the low energy electrons are rather insensitive to it.

#### *Future plans:*

Up to now we have not tried to compare the calculated ATI spectra with experimental measurements. We intend to do so in the coming year. For the high laser intensities used in the experiments where the laser is highly focused, the intensity within the gas volume is not constant. In order to compare with experiments, electron momentum spectra have to be calculated over a large range of laser intensities with small steps and the total yield is then calculated. Major contribution to the electron spectra in this case does not come from the peak intensity, but rather from the lower intensities. Since depletion could be quite severe for high laser intensities, its effect has to be included as well. After these factors are considered we will be able to compare with experimental measurements. In the future we will also examine the ATI electrons from aligned molecules.

#### **4. Other activities**

In the last year we carried out a few other projects which do not fall under the three categories above but are within the general scope of this program. Among them, **A2** is a review article, **A6** and **B2** are invited papers from two conferences. The rest of them are one-time projects that may be pursued further only if needed.

### **Publications**

#### **A. Published papers**

A1. C. D. Lin, X. M. Tong and Toru Morishita, "Direct experimental visualization of atomic and electronic dynamics with attosecond pulses", *J. Phys.* **B39**, S419 (2006)

A2. C. D. Lin and X. M. Tong, "Probing orbital symmetries and ionization dynamics of simple molecules with femtosecond laser pulses," in *ADVANCES IN MULTI-PHOTON PROCESSES AND SPECTROSCOPY*, VOL **17**, Ed. S. H. Lin, A. A. Villaeys and Y. Fujimura, World Scientific, 2006.

A3. X. M. Tong and C. D. Lin, "Attosecond xuv pulses for complete mapping of the time-dependent wave packet of  $D_2^{++}$ ", *Phys. Rev.* **A73**, 042716 (2006).

- A4. A. T. Le, X. M. Tong and C. D. Lin, "Evidence of two-center interference in high-order harmonic generation from CO<sub>2</sub>", Phys. Rev. A73, 041402(R), (2006).
- A5. M. Wickenhauser, X. M. Tong and C. D. Lin, "Laser induced substructures in above-threshold-ionization spectra from intense few-cycle laser pulses", Phys. Rev. A73, 011401(R) (2006).
- A6. C. D. Lin, X. M. Tong and Z. X. Zhao, "Effects of orbital symmetries on the ionization rates of aligned molecules by short intense laser pulses", J. of Mod. Optics, 53, 21 (2006).
- A7. A. T. Le, Toru Morishita, X. M. Tong and C. D. Lin, "Signature of chaos in high-lying doubly excited states of the helium atom," Phys. Rev. A72, 032511 (2005)
- A8. A. S. Alnaser, B. Ulrich, X. M. Tong, I. V. Litvinyuk, C. M. Maharjan, P. Ranitovic, T. Osipov, R. Ali, S. Ghimire, Z. Chang, C. D. Lin and C. L. Cocke, "Simultaneous real-time tracking of wave packets evolving on two different potential curves in H<sub>2</sub><sup>+</sup> and D<sub>2</sub><sup>+</sup>" Phys. Rev. A72, 030702(R) (2005).
- A9. X. X. Zhou, X. M. Tong, Z. X. Zhao and C. D. Lin, "Alignment dependence of high-order harmonic generation from N<sub>2</sub> and O<sub>2</sub> molecules in intense laser fields", Phys. Rev. A72, 033412(R) (2005).
- A10. X. M. Tong and C. D. Lin, "Empirical formula for static field ionization rates of atoms and molecules by lasers in the barrier-suppression regime", J. Phys. B38, 2593 (2005).
- A11. Z. X. Zhao and C. D. Lin, "Theory of laser-assisted autoionization by attosecond light pulses", Phys. Rev. A71, 060702(R) (2005).
- A12. X. X. Zhou, X. M. Tong, Z. X. Zhao and C. D. Lin, "Role of molecular orbital symmetry on the alignment dependence of high-order harmonic generation with molecules", Phys. Rev. A71, 061801(R) (2005).
- A13. Z. X. Zhao, Z. H. Chang, X. M. Tong and C. D. Lin, "Circularly-polarized laser-assisted photoionization spectra of argon for attosecond pulse measurements", Optics Express 13, 1968 (2005).
- A14. X. M. Tong and C. D. Lin, "Double photoexcitation of He atoms by attosecond XUV pulses in the presence of intense few-cycle infrared lasers", Phys. Rev. A71, 033406 (2005).

## **B. Papers accepted for publications**

- B1. X. M. Tong, Z. X. Zhao and C. D. Lin, Comment on "Correlation quantum dynamics between an electron and D<sub>2</sub><sup>+</sup> molecules with attosecond resolution", Phys. Rev. Lett.
- B2. C. D. Lin and X. M. Tong, "Dependence of tunneling ionization and harmonic generation on the structure of molecules by short intense laser pulses", J. photochemistry and photobiology.
- B3. M. Wickenhauser, X. M. Tong, D. G. Arbo, J. Burgdorfer and C. D. Lin, "Signature of multiphoton and tunneling ionization in the electron momentum distributions of atoms by intense few-cycle laser pulses", Phys. Rev. A.

## COLTRIMS studies of strong-field laser-matter interactions

**I.V. Litvinyuk**

J. R. Macdonald Laboratory  
Physics Department, Kansas State University  
Manhattan, KS 66506  
[ivl@phys.ksu.edu](mailto:ivl@phys.ksu.edu)

*We use coincident momentum imaging technique (“reaction microscope” or COLTRIMS) to study experimentally interactions of intense ( $10^{13}$ - $10^{16}$  W/cm<sup>2</sup>) ultrashort (6-60 fs) laser pulses with atoms and molecules in gas phase. In particular, we are interested in such aspects of laser-matter interactions as (i) interplay between non-resonant and resonant pathways of electronic excitation and ionization; (ii) ultrafast dynamics of strong-field processes; and (iii) interactions of strong-field with aligned molecules. To explore these aspects we (i) measure wavelength dependence of various strong-field processes; (ii) conduct pump-probe studies with short intense pulses; and (iii) employ rotational wavepacket technology to produce strongly anisotropic ensembles of molecules to interrogate.*

### **1. Multi-photon resonant effects in strong-field ionization: origin of the dip in experimental longitudinal momentum distributions - A.S. Alnaser, C.M. Maharjan, P. Wang and I.V. Litvinyuk**

We studied ionization of neon and argon by intense linearly polarized femtosecond laser pulses of different wavelengths (400 nm and 800 nm) and peak intensities, by measuring momentum distributions of singly charged positive ions in the direction parallel to laser polarization. For Ne the momentum distributions exhibited a characteristic dip at zero momentum at 800 nm and a complex multi-peak structure at 400 nm. Similarly, for Ar the momentum distributions evolved from complex multi-peak structure with a pronounced dip in the center at 400 nm, to a smooth distribution characteristic of pure tunneling ionization (800 nm high intensities). In the intermediate regime (800 nm, medium to low intensities), for both atoms we observed recoil ion momentum distributions modulated by quasi-periodic structures usually seen in the photoelectron energy spectra in multi-photon regime (ATI spectra). Ne did show a characteristic “dip” at low momentum, while the longitudinal momentum distribution for Ar exhibited a spike at zero momentum instead. The spectra did dramatically change at 400 nm, where both ions show the pronounced dip near zero momentum. Based on our results, we conclude that the structures observed in Ne and Ar momentum distributions reflect the specifics of atomic structure of the two targets and should not be attributed to effects of electron re-collision, as was suggested earlier. Instead, as our results indicate, they are due to effects of multi-photon resonant enhancement of strong-field ionization. The report of these studies is submitted for publication in J. Phys. B [1].

### **2. Resonant excitation during strong-field dissociative ionization - A. S. Alnaser, M. Zamkov, X. M. Tong, C. M. Maharjan, P. Ranitovic, C. L. Cocke, and I. V. Litvinyuk**

We studied dissociative ionization of oxygen by intense femtosecond laser pulses with central wavelengths between 550 and 1800 nm. We measured kinetic energy release spectra and angular distributions of fragments resulting from symmetric dissociation of doubly charged molecular ions ( $O_2^{2+} \rightarrow O^+ + O^+$  channel). In the kinetic energy release spectra we identified a number of distinct excited states of the molecular ion. Angular distributions for all but one of those states were consistent with re-collision excitation following single ionization of  $O_2$ . For the remaining ( $B\ 3\ \Pi_g$ ) excited state we observed a characteristic resonant dependence of its relative yield on the central optical frequency of the pulse, with the yield peaking at around 890 nm. This presents unambiguous evidence in support of importance of resonant excitation channels in strong field ionization of molecules. This study is reported in [2].

**3. Momentum-imaging investigations of the dissociation of  $D_2^+$  and the isomerization of acetylene to vinylidene by intense short laser pulses** - *A. S. Alnaser, I.V. Litvinyuk, T. Osipov, B. Ulrich, A. Landers, E. Wells, C. M. Maharjan, P. Ranitovic, I. Bocharova, D. Ray and C.L. Cocke.*

We measured momentum-images of the ionic products from the ionization of  $D_2$  and  $C_2H_2$  by short laser pulses. For  $D_2$  we use a pump-probe approach to investigate the dependence of the enhanced ionization on the internuclear distance. Evidence for two (not well separated) regions of enhancement are found near internuclear distances of 6 and 10 atomic units. In the case of acetylene we report clear evidence for the production of both acetylene and vinylidene dications with kinetic energy releases similar to those reported earlier by core electron removal. We also find very different angular distributions for the fragments in the two channels, consistent with a finite time for the isomerization. These studies are reported in [3].

**4. Strong-field ionization of dynamically aligned molecules** – *C.M. Maharjan, A.S. Alnaser, I. Bocharova, P. Ranitovic, D. Ray, C.L. Cocke and I.V. Litvinyuk*

This study is motivated by the recent molecular tomography experiment of Corkum and co-workers. In this experiment they reconstruct complete the HOMO wave-function of  $N_2$  (including phase) from a series of high harmonics spectra measured with molecules aligned at various angles to the laser polarization. The reconstruction procedure uses normalization to the high harmonics spectra of a companion atom (Ar), and it is based on the assumption that re-colliding electron wavepacket has the same 3D structure for  $N_2$  and Ar, and also for  $N_2$  this electron wavepacket is independent of molecular orientation. The hypothesis is that molecular structure and orientation do not affect the momentum distribution of tunneling electrons (“all tunnels are alike”). We undertook to directly verify this assumption. We measured full 3D electron momentum distributions for aligned  $N_2$  and  $O_2$  molecules. In a pump-probe experiment we first created rotational wavepackets in target molecules with a weak pump pulse and then ionized molecules with a stronger probe pulse around the wavepacket revival time, when most molecules are aligned either parallel or perpendicular to the polarization direction of the pump. The probe polarization was perpendicular to the pump polarization. We measured high-resolution electron energy spectra and complete 3D momentum distributions of electrons

using COLTRIMS. In summary, for aligned  $N_2$  and  $O_2$  we did not observe a significant dependence of the electron energy spectra and 3D momentum distributions on the alignment of the molecular axis. Our results seem to provide experimental validation for the “all tunnels are alike” hypothesis behind the molecular tomography technique. However, for both molecules we did observe small but definite difference in momentum distribution projections on the two axes perpendicular to polarization direction – one along the alignment axis, another perpendicular to it. Along the alignment axis the 1D projection of 3D momentum distribution showed more pronounced cusp structure at zero momentum, than similar projection on the perpendicular axis. Such cusp structure is usually associated with “Coulomb focusing” of the electron wavepacket by the ion core potential. We attribute observed differences to different Coulomb focusing in the two directions due to the two-center attractive potential which breaks the cylindrical symmetry of the problem. Also in the electron energy spectra for both molecules, in addition to the usual ATI peaks with photon energy (1.55 eV) periodicity we observe multiple non-ATI peaks at low energy (0-5 eV) indicative that some resonance or resonance-enhanced ionization processes also playing a role. These peaks seem to be related to similar structures observed in Ar (see abstract by C.L. Cocke and [4]). The exact nature and production mechanism for these low energy electron peaks remains unexplained and will be a subject of further studies. The publication of these results is being prepared.

**5. Time-resolved Coulomb explosion imaging of small molecules - F. Légaré, K. F. Lee, I. V. Litvinyuk, P. W. Dooley, A. D. Bandrauk, D. M. Villeneuve, P. B. Corkum**

This is continued collaboration with Ottawa and Sherbrooke groups aimed at developing Coulomb explosion imaging as probe of time-dependent molecular structure. The experiments were conducted in Ottawa awhile ago, with collaborative work on data analysis and presentation resulting in two publications in 2005. In [5] we use intense few-cycle laser pulses to ionize molecules to the point of Coulomb explosion. We use Coulomb’s law or *ab initio* potentials to reconstruct the molecular structure of  $D_2O$  and  $SO_2$  from the correlated momenta of exploded fragments. For  $D_2O$ , a light and fast system, we observed about 0.3 Å and 15° deviation from the known bond length and bond angle. By simulating the Coulomb explosion for equilibrium geometry, we showed that this deviation is mainly caused by ion motion during ionization. Measuring three-dimensional structure with half bond length resolution is sufficient to observe large-scale rearrangements of small molecules such as isomerization processes. In [6] we image the dynamics of diatomic and triatomic molecules with sub- 5 fs and sub-Å resolution using laser Coulomb explosion imaging with 8 fs pulses. We obtain image information by measuring the vector momenta of all atomic ions produced by explosion of a single molecule. We image vibrating  $D_2^+$  and of dissociating  $SO_2^{2+}$  and  $SO_2^{3+}$ . Images taken at 0 and 60 fs show that the dissociation of  $SO_2^{2+}$  produces an  $SO^+$  rotational wave packet.

## Publications (2005-06 and pending)

1. A.S. Alnaser, C.M. Maharjan, P.Q. Wang and I.V. Litvinyuk, “*Multi-photon resonant effects in strong-field ionization: origin of the dip in experimental longitudinal momentum distributions*”, submitted to J. Phys. B
2. A.S. Alnaser, M. Zamkov, X.M. Tong, C.M. Maharjan, P. Ranitovic, C.L. Cocke, and I.V. Litvinyuk, “*Resonant excitation during strong-field dissociative ionization*”, Phys. Rev. A **72**, 041402 (2005)
3. A.S. Alnaser, I.V. Litvinyuk, T. Osipov, B. Ulrich, A. Landers, E. Wells, C.M. Maharjan, P. Ranitovic, I. Bocharova, D. Ray and C.L. Cocke, “*Momentum-imaging investigations of the dissociation of  $D_2^+$  and the isomerization of acetylene to vinylidene by intense short laser pulses*”, J. Phys. B: At. Mol. Opt. Phys. **39**, S485 (2006)
4. C.M. Maharjan, A.S. Alnaser, I.V. Litvinyuk, P. Ranitovic and C.L. Cocke “*Wavelength dependence of momentum-space images of low-energy electrons generated by short intense laser pulses at high intensities*”, J. Phys. B: At. Mol. Opt. Phys. **39**, 1955 (2006)
5. F. Légaré, K.F. Lee, I.V. Litvinyuk, P.W. Dooley, S.S. Wesolowski, P.R. Bunker, P. Dombi, F. Krausz, A.D. Bandrauk, D.M. Villeneuve, and P.B. Corkum, “*Laser Coulomb-explosion imaging of small molecules*”, Phys. Rev. A **71**, 013415 (2005)
6. F. Légaré, K.F. Lee, I.V. Litvinyuk, P.W. Dooley, A.D. Bandrauk, D.M. Villeneuve, and P.B. Corkum, “*Imaging the time-dependent structure of a molecule as it undergoes dynamics*”, Phys. Rev. A **72**, 052717 (2005)
7. A.S. Alnaser, C.M. Maharjan, X.M. Tong, B. Ulrich, P. Ranitovic, B. Shan, Z. Chang, C.D. Lin, C.L. Cocke, and I.V. Litvinyuk, “*Effects of orbital symmetries in dissociative ionization of molecules by few-cycle laser pulses*”, Phys. Rev. A **71**, 031403 (2005)
8. A.S. Alnaser, B. Ulrich, X.M. Tong, I.V. Litvinyuk, C.M. Maharjan, P. Ranitovic, T. Osipov, R. Ali, S. Ghimire, Z. Chang, C.D. Lin, and C.L. Cocke, “*Simultaneous real-time tracking of wave packets evolving on two different potential curves in  $H_2^+$  and  $D_2^+$* ” Phys. Rev. A **72**, 030702 (2005)
9. C.M. Maharjan, A.S. Alnaser, X.M. Tong, B. Ulrich, P. Ranitovic, S. Ghimire, Z. Chang, I.V. Litvinyuk, and C.L. Cocke, “*Momentum imaging of doubly charged ions of Ne and Ar in the sequential ionization region*”, Phys. Rev. A **72**, 041403 (2005)
10. I.V. Litvinyuk, F. Légaré, P.W. Dooley, D.M. Villeneuve, P.B. Corkum, J. Zanghellini, A. Pegarkov, C. Fabian, and T. Brabec, “*Shakeup Excitation during Optical Tunnel Ionization*”, Phys. Rev. Lett. **94**, 033003 (2005)
11. A.S. Alnaser, C.M. Maharjan, X.M. Tong, B. Ulrich, P. Ranitovic, B. Shan, Z. Chang, C.D. Lin, C.L. Cocke, and I.V. Litvinyuk, “*Effects of orbital symmetries in dissociative ionization of molecules by few-cycle laser pulses,*” Phys. Rev. A **71**, 031403(R) (2005).

# Electronic Excitations and Dynamics in Carbon Nanotubes Induced by Femtosecond Pump-Probe LASER Pulses

Pat Richard

JR Macdonald Laboratory, Physics Department, Kansas State University  
Manhattan, Kansas 66506

[richard@phys.ksu.edu](mailto:richard@phys.ksu.edu)

We have continued our efforts in the J. R. Macdonald Laboratory directed toward the study of electronic excitations and dynamics in carbon nanotubes excited by femtosecond pump-probe laser pulses generated by the ultra-fast Ti:Sapphire Kansas Light Source, KLS. We use time-of-flight of electrons emitted from carbon nanotubes to deduce the energy and temporal behavior of the electronic states of the nanotubes. Experiments have been performed on multiwalled carbon nanotubes, MWNT, and more recently on both double walled carbon nanotubes, DWNT, and single walled carbon nanotubes, SWNT.

---

**MWNT: Quasi-ballistic transport of charge carriers in multi walled carbon nanotubes.** *M. Zamkov, A. Alnaser, N. Woody, S. Bing, Z. Chang, and P. Richard*

Our initial motivation for studying carbon nanotubes was to search for the Rydberg-like tubular image potential states in carbon SWNT predicted by the Harvard group of Granger, Kral and Sadegpour (PRL **89**, 135506 (2002)). These interesting and unique states have a tubular presence surrounding the nanotube cylinder. The term “tubular image states” are reserved for the high angular momentum states that are bound at large distances from the surface in a shallow well formed by the combination of the image attraction and the angular momentum barrier. Following the ideas of Granger et al, we calculated the energy spectra of circular image potential states as well as tubular image potential states for both SWNT and MWNT. The “circular image states” are the more tightly bound low angular momentum states which have similar spatial profiles to the tubular states. Our predictions (Publication #1) demonstrated that the energetics of electron emission were more favorable for observing circular image potential states in MWNT than for tubular states in SWNT. We observed the excitation energies and lifetimes of the circular states produced around MWNT (Publication #2) and reported the results last year in the AMOS research meeting - **Time-resolved photo imaging of image-potential states in carbon nanotubes** *Experimental Group: M. Zamkov, N. Woody, B Shan, Z. Chang, and P. Richard Theory Group: H.S. Chakraborty and U. Thumm.*

The second phase of the research on MWNT involves the study of the charge carriers in MWNT. The image potential states are formed by pumping the MWNT with the third harmonic (4.71 eV) of the KLS laser beam and probing the states with the primary beam (1.57 eV), see top schematic in Fig. 1. We are able to study the charge carriers in the nanotubes by reversing the role of the pump and probe. The excited image potential states can be seen in the upper end of the electron time of flight spectrum in Fig. 1b whereas the excitation of the charge carriers can be seen at the lower end of the spectrum. The image potential spectrum is the difference between the pump-probe and pump spectra whereas

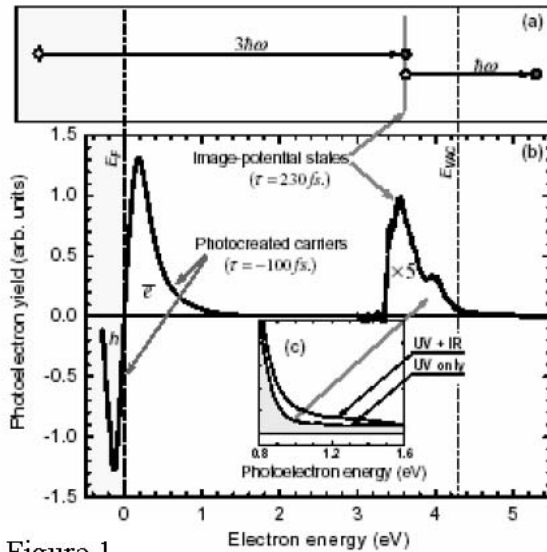


Figure 1

**-Lifetime of Charge Carriers in Multi-walled Nanotubes** *M. Zamkov, N. Woody, B Shan, Z. Chang, and P. Richard.* We observed that the e-e decay curves were in the range of 200 to 700 fs and followed a  $(E-E_F)^{-n}$  with  $n \approx 2.07 \pm 0.1$  behavior which is consistent with a two or three dimensional Fermi-liquid behavior as opposed to a one-dimensional Luttinger Liquid behavior as was observed for SWNT.

The final phase of our study of MWNT is the investigation of the long lived e-ph

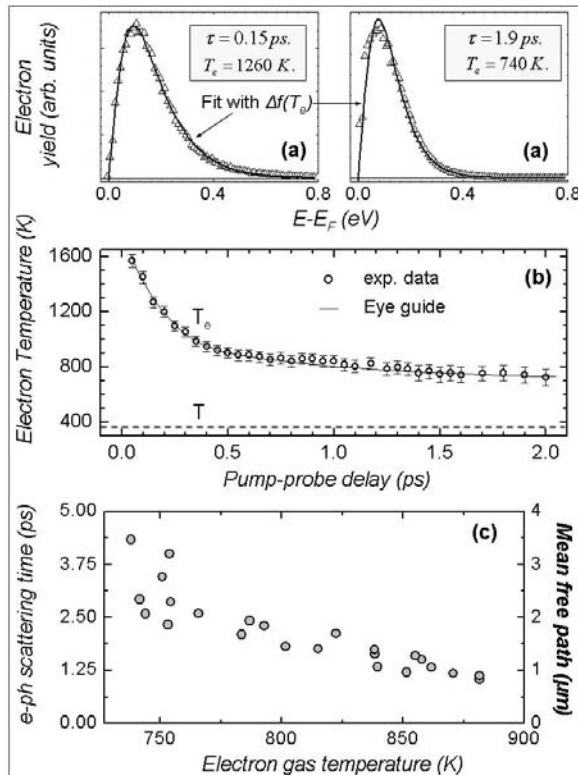


Figure 2

the carrier spectrum is the difference between the pump-probe and probe spectra. The bipolar shape of the charge carrier difference spectrum is characteristic of the hole and the promoted electron as seen by the probe pulse. The lifetimes of the excited electrons is probed by the delay between the pump and probe just as in the case of the study of the image potential states. Lifetime plots show a two component curve. The fast part of the decay curve is due to the e-e interactions and the slow decay is due to e-phonon interactions, as published (Publication #3) and reported last year in the AMOS research meeting

interaction, which brings us to the subject of quasi-ballistic transport of charge carriers in multi-walled carbon nanotubes. The basic idea in this experiment is that the time of flight difference spectra can be fit to the difference in a Fermi-Dirac, FD, distribution at some intermediate cooling temperature to that at room temperature. The effect of the laser pump-pulse is to promote the electrons into the conduction band and thus increase the thermal energy of the electronic system. In this case the thermal equilibrium between the unperturbed lattice and the excited carriers will be realized by the energy exchange through e-ph coupling. By fitting the data to

the non equilibrium minus the equilibrium FD calculation, we can determine the temperature  $T_e$  of the system for every delay  $\tau$  (see upper panel in Fig. 2). We then use the two temperature model (TTM) adapted to the case of carbon nanotubes by Hertel and Moos PRL **84**, 5002(2000) to the e-ph decay rate

$$\tau_{e-ph}(T_e) = \tau_E(T_e) \times A \times \frac{1 - (T/T_e)^2}{1 - (T/T_e)^5}, \text{ where } A = 0.9534. \text{ The resulting e-ph scattering}$$

times, obtained within the thermalization approach, are shown in Figure 2(c) along with the associated electron mean-free paths. The latter is found to be within 0.8 and 4  $\mu\text{m}$ , which agrees well with the range of  $l$  inferred from the direct measurements of  $\tau_{e-ph}$ . This agreement provides additional support to the fact that a collision-free distance for an electron in a MWNT is comparable to the nanotube length. In particular, close to the Fermi level, where the electron mean-free path extends up to 3-4  $\mu\text{m}$ , the charge transport is believed to be ballistic. The result of this work has recently been submitted for publication (see Publication # 4).

---

**DWNT: Do the charge carriers in DWNT behave as a Fermi-Liquid as observed in MWNT or as a Luttinger Liquid as reported for SWNT?** *I. Chatzakis, A. Habib, M. Zamkov, and P. Richard*

We have undertaken the task of measuring the lifetimes of the charge carries (Fermi-Dirac type?) and the electron mean free path (ballistic motion?) in DWNT. The first efforts in this project were to use DWNT formed on a plastic backing. These targets are known to form nanotubes in ropes, which is not ideal for this experiment. We have, however, recently obtained isolated DWNT in the form of “bucky” paper from NanoLab Inc, Newton, MA. These are isolated nanotubes of a similar form to those used in our MWNT work reported above. The apparatus for this experiment is presently being moved out of the KLS lab into an isolated laser hutch serviced by a laser beam transport. This move is necessitated due to the interference of this experiment with the work on development and use of the carrier envelope phase locking. Preliminary results have been obtained using the original targets, but we have no results using the new targets. We anticipate that our apparatus move to the new hutch will be complete at the end of August and that the experiment will be running during the fall 2007.

---

**SWNT: Exciton Dynamics in Bundles of Single Walled Carbon Nanotubes.** *Mikhail Zamkov, Ali S. Alnaser, Bing Shan, Zenghu Chang, and Patrick Richard*

Systems exhibiting one-dimensional (1D) electron confinement have long fascinated scientists due to their unusual electrical and optical properties. The microscopic origin underlying this behavior is the significant enhancement in the Coulomb interaction that only permits collective multi-particle excitations, which leads to the formation of strongly correlated electron-hole ( $e-h$ ) pairs, known as excitons. Semiconductive SWNT are one of the most interesting representations of such systems where the excitonic nature of optical excitations was manifested by the emission of fluorescence (FL) arising from the recombination of bound  $e-h$  pairs. FL emission in SWNT, however, can be observed only when a nanotube is isolated from its environment by encapsulating in a SDS micelle. On

the other hand, when their natural surroundings are not chemically suppressed, smooth-sided SWNT readily aggregate into bundles, in which case no FL signal is detected. The quenching of optical emission poses considerable experimental challenges for studying the dynamics of excitons in interacting SWNT, raising a question if strongly bound  $e-h$  pairs even exist in nanotube bundles. According to several experimental reports the intertube interaction in aggregated SWNT unlocks the carrier tunneling ability and, could, in principal, wipe out the reduced dimensionality of  $e-h$  excitations. In this case, some basic photoelectrical properties of bundled SWNT such as the carrier photogeneration and the spatial separation of opposite charges would be substantially different from those of isolated nanotubes. Resolving these issues, for the most part, depends on our ability to probe the character of optical excitations in non-fluorescing bundles, favoring an experimental approach that does not rely on FL emission.

Therefore in this work we have turned our attention to SWNT. Sample production of nanotubes, at best, isolates single wall, double wall and sets of multi-wall nanotubes. In each of these types of samples a distribution of nanotubes diameters is produced as well as a mixture of semi-conductive (*S*) and metallic (*M*) nanotubes. In some processes the nanotube samples are free standing, some form bundles of nanotubes, and in some processes they are created in a dielectric environment such as in a micelle-suspension or in an aqueous solution.

In this study time-resolved photoemission was used to differentiate between excitons and free carriers in non-fluorescing bundles of SWNT. In summary, by monitoring the electron emission from non-fluorescing nanotube bundles, we have demonstrated that the primary excitations in aggregated *S* SWNTs are strongly bound excitons. In particular, our findings indicate that the van-der-Waal forces between the interacting nanotubes do not destroy the 1D character of optical excitations. We also show that the excitonic stability against non-radiative annihilation in bundles could be weakened due to robust tunneling of carriers from *M* into *S* nanotubes. This intertube charge exchange may play a decisive role in lowering the quantum efficiency for fluorescence emission in aggregated SWNTs and will merit further investigation. First results of this work are being submitted for publication.

Publication # 1: **Image Potential States of single- and multi-walled Carbon Nanotubes**, M. Zamkov, N. Woody, B. Shan, H. S. Chakraborty, Z. Chang, U. Thumm, and P. Richard, Phys. Rev. B **70**, 115419 (2004).

Publication # 2: **Time-Resolved Photoemission of Image-Potential States in Carbon Nanotubes**, M. Zamkov, N. Woody, B. Shan, H. Chakraborty, Z. Chang, U. Thumm, and P. Richard, Phys. Rev. Lett. **93**, 156803 (2004).

Publication # 3: **Lifetime of Charge Carriers in Multi-walled Nanotubes** M. Zamkov, N. Woody, B. Shan, Z. Chang and P. Richard, Phys. Rev. Lett. **94**, 056803 (2005).

Publication # 4: **Quasi-ballistic transport of charge carriers in multi walled carbon nanotubes**. M. Zamkov, A. Alnaser, N. Woody, S. Bing, Z. Chang, and P. Richard, submitted for publication.

Publication # 5: **Exciton Dynamics in Bundles of Single Walled Carbon Nanotubes**. Mikhail Zamkov, Ali S. Alnaser, Bing Shan, Zenghu Chang, and Patrick Richard submitted for publication.

# Structure and Dynamics of Atoms, Ions, Molecules and Surfaces: Atomic Physics with Ion Beams, Lasers and Synchrotron Radiation

Uwe Thumm, J.R. Macdonald Laboratory, Kansas State University  
Manhattan, KS 66506 [thumm@phys.ksu.edu](mailto:thumm@phys.ksu.edu)

## 1. Laser-molecule interactions (with T. Niederhausen and B. Feuerstein)

**Project scope:** We seek to develop numerical and analytical tools to efficiently predict the effects of a strong laser field on the bound and free electronic and nuclear dynamics in small molecules [1] and in laser-assisted collisions [2].

**Recent progress:** We continued our investigation of the dissociation and ionization of  $H_2^+$  in short intense laser pulses by applying wave-packet propagation methods. We have started to extend our wave-packet propagation calculation to the single and double ionization of neutral  $H_2$ . As a complementary approach, we are developing a close-coupling method that coherently includes both ionization steps.

**Example:** Vibrational Wave-Packet Revivals in  $D_2^+$ . Figure 1 (a) illustrates our reduced-dimensionality calculations [1] for the nuclear wave packet dynamics in  $D_2^+$  following ionization of  $D_2$  ( $v = 0$ ) in a 5 fs,  $10^{15}$  W/cm<sup>2</sup> pulse. After a few optical cycles, the wave packet collapses due to the dephasing of its stationary vibrational state components. The autocorrelation function shows quarter and half revivals of the wave packet 100 and 200 optical cycles, respectively, after the wave packet has been launched (Fig.1 (b)). A second laser pulse, short and strong enough to ensure instantaneous and complete ionization of  $D_2^+$ , can probe the time evolution of the wave packet. Pump-probe

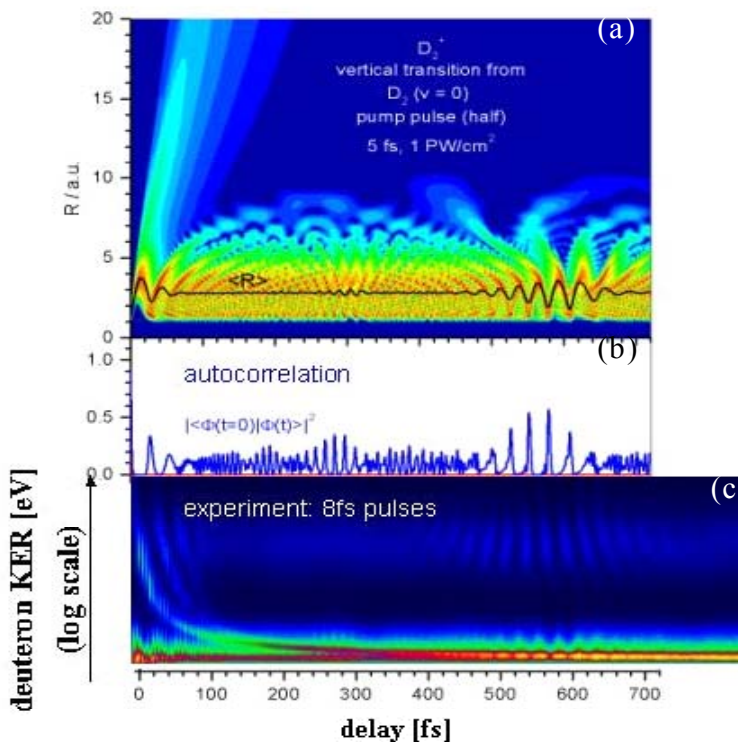


**Fig. 1.** Coherent motion of the nuclear vibrational wave packet in and dissociation of  $D_2^+$ .

(a) Probability density and expectation value  $\langle R \rangle$  of the internuclear distance.

(b) Autocorrelation function.

(c) Measured kinetic energy release, showing quarter and half revivals [3].

experiments with 8 fs laser pulses on  $D_2$  recorded the delay-dependent kinetic energy

release of the deuteron fragments [3] and reproduce the first quarter, half, and full wave packet revivals of our model calculation.

**Future plans:** For delays beyond the first full revival, the comparison between theory and preliminary experiments becomes inconclusive. We intend to investigate whether this discrepancy is due to insufficient experimental resolution or originates in the onset of rotational dephasing.

## **2. Neutralization of negative hydrogen ions near vicinal metal surfaces (with Himadri Chakraborty, Thomas Niederhausen, and Boyan Obreshkov)**

**Project scope:** We attempt to understand the resonant transfer of a single electron, initially bound to the projectile, during the reflection of a slow ion or atom at an arbitrarily shaped, nanostructured metal surface as a function of the collision parameters, the surface electronic structure, and crystal orientation of the surface [4].

**Recent progress:** We developed a new set of computer programs to calculate the ground-state electronic structure of arbitrarily shaped metallic surfaces and tested our codes in applications to flat and vicinal Al, Cu, Na, and K surfaces [5]. We modeled the surface electronic structure within a statistical Thomas-Fermi approach, including a gradient (von Weizsäcker) correction to the kinetic energy and a local density approximation for the exchange and correlation energy. We self-consistently calculated the projected density of states (PDOS) of the ion-surface system for arbitrary (but fixed) positions of the ion by direct numerical propagation of the time-dependent Schrödinger equation for the motion of the active electron. From the PDOS, we obtained the static shift and width of the ion-affinity level. Our results for the work function changes of vicinal (vs. flat) metal surfaces agree with experiments and Kohn-Sham calculations.

We derived the negative ion-survival probability near vicinal surfaces by integrating a rate equation including both electron capture and loss processes. Our results show a pronounced "step-up" versus "step-down" scattering asymmetry, even if averaged over many scattering trajectories, that is caused by enhanced electron loss along the outgoing part of ion trajectories, which approach a step from below.

**Future plans:** We will investigate resonance formation and charge exchange near vicinal and other structured surfaces. In particular, we will investigate the importance of lateral confinement effects (evidence for which was found in photo-emission experiments).

[1] B. Feuerstein and U. Thumm, Phys. Rev. A **67**, 063408 (2003); Phys. Rev. A **67**, 043405 (2003); J. Phys. B **36**, 707-716(2003).

I. Ben-Itzhak, Z. Chang, I. Litvinyuk, U. Thumm, and C.L. Cocke, submitted to J. Phys. B.

[2] T. Niederhausen, B. Feuerstein, and U. Thumm, Phys. Rev. A **70**, 023408 (2004).

T. Niederhausen and U. Thumm, Phys. Rev. A **73**, 041404(R) (2006).

[3] R. Moshhammer and J. Ullrich 2006, private communication.

[4] H.S. Chakraborty, T. Niederhausen, and U. Thumm, Phys. Rev. A **69**, 052901 (2004);

Phys. Rev. A **70**, 052903 (2004); Nucl. Instrum. Methods B **241**, 43 (2005).

[5] B. Obreshkov and U. Thumm, Phys. Rev. A **74**, 012901 (2006) and submitted to Surf. Sci.

**Other DoE-sponsored publications (2003-2006):** A.A. Khuskivadze, I.I. Fabrikant, and U. Thumm, Phys. Rev. A **68**, 063405 (2003). M. Zamkov, H.S. Chakraborty, A. Habib, N. Woody, U. Thumm, and P. Richard, Phys. Rev. B **70**, 115419 (2004). M. Zamkov, N. Woody, S. Bing, H.S. Chakraborty, U. Thumm, and P. Richard, Phys. Rev. Lett. **93** 156803 (2004).

# Multiparticle Processes and Interfacial Interactions in Nanoscale Systems Built from Nanocrystal Quantum Dots

Victor Klimov

Chemistry Division, C-PCS, MS-J567, Los Alamos National Laboratory  
Los Alamos, New Mexico 87545, klimov@lanl.gov, <http://quantumdot.lanl.gov>

## 1. Program Scope

By exploiting the effects of quantum confinement, one can control electronic and optical properties of matter at the most fundamental, electronic-wavefunction level. The approach explored most extensively involves the use of nanoscale semiconductor structures such as size/shape-controlled semiconductor nanocrystals. While being a powerful tool for engineering spectral responses, size control at the nanoscale has limited applicability for engineering the dynamical and nonlinear responses of nanostructures or for introducing new functionality to a material. In this project, we explore novel approaches for controlling carrier-carrier nonlinear interactions and carrier dynamical behavior using multicomponent nanocrystals. Specifically, we study multishell, multicomponent nanocrystals based on both semiconductor and metal materials that allow us to independently control spectral characteristics (by engineering confinement energies), dynamical responses (by engineering electron-hole wavefunction overlap and the exciton spin structure), and nonlinear, multiexciton interactions (by engineering Coulomb coupling). Our studies in this project address such important and interesting problems as the realization of low-threshold nanocrystal lasing in the single-exciton regime via the use of repulsive exciton-exciton interactions, highly efficient exciton multiplication for a new generation of solar cells, and novel, multifunctional behaviors from hybrid, semiconductor/metal nanoscale materials.

## 2. Recent Progress

One topic studied by us during the past year was light emitting properties of semiconductor nanocrystals in the regimes of both optical and electrical pumping for the cases when either single- or multiple excitons are created in a nanocrystal. We showed that by using shape-controlled nanoparticles or multi-shell heterostructures, we could almost independently control carrier confinement energies (i.e., emission wavelength) and their recombination dynamics. This capability was particularly important for achieving the optical amplification regime. We used different types of “engineered” II-VI and IV-VI nanocrystals to demonstrate amplified spontaneous emission with colors tunable from the near infrared to the blue.

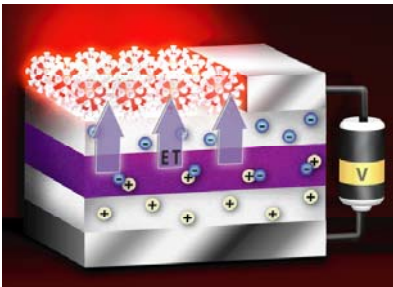


Figure 1. Light emission from nanocrystals is activated by nonradiative energy transfer from a proximal InGaN quantum well.

We also explored two novel approaches for injection of charges into semiconductor nanocrystals by using device architectures comprised of nanocrystals and traditional GaN and InGaN epitaxial structures. In one approach we used “excitonic” injection mechanism mediated by high-efficiency energy transfer from a proximal quantum well. In the other one, nanocrystal were activated via direct electrical injection from epitaxial *p*- and *n*-layers of wide-gap semiconductors.

In the “energy-transfer” structures, we combine nanocrystal mono- and multi-layers with InGaN quantum wells (Fig. 1). In these hybrid devices, charge injection into nanocrystals occurs via *nonradiative energy transfer*, which is enabled by strong electrostatic coupling between the emitting dipole of the quantum well and the absorbing dipole of the nanocrystals. We observe that the rate of nonradiative exciton transfer exceeds that of carrier recombination in the quantum

well, which results in high (greater than 50%) transfer efficiencies.

In the “direct-injection” structures, nanocrystals are incorporated as an *i*-layer into GaN *p-n* junctions (Figure 2) using novel, room-temperature, epitaxial technique that employs a beam of neutral energetic atoms. This method allows for encapsulation of nanocrystals into GaN without adversely affecting either their integrity or luminescence properties. The fabricated *p-i-n* devices show good injection efficiencies and low turn-on voltages.

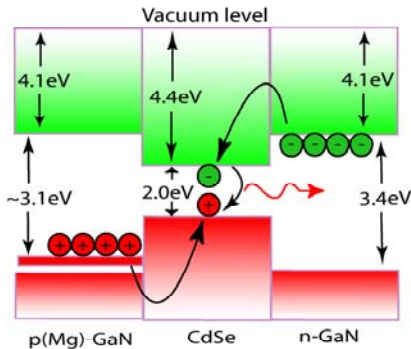


Figure 2. *P-i-n* structure comprised of semiconductor nanocrystals and *p*- and *n*-GaN injection layers

Both “energy-transfer” and “direct-injection” structures show stable, multi-hour operation under ambient conditions and long shelf lifetimes. The analysis of injection/recombination mechanisms in these devices indicates the feasibility of a significant improvement in their efficiencies by optimizing, e.g., device architecture and contact geometry/compositions.

Another topic studied by us in this project was photogeneration of multiple excitons in nanocrystals from single photons via carrier multiplication. A usual assumption is that absorption of a single photon by a semiconductor produces a single electron-hole pair (exciton), while the photon energy in excess of the energy gap is dissipated as heat by exciting lattice vibrations. In 2004, we reported for the first time that nanocrystals

of PbSe, could respond to absorption of a single photon by producing two or more electron-hole pairs with the 100% efficiency. In our most recent experiments, we observed the formation of seven excitons per photon per nanocrystal, which corresponds to the stunning value of 700% for quantum efficiency that describes conversion of photons into electrical charges (Figure 3). Using carrier multiplication we also demonstrated “exotic” *non-Poissonian* distributions of carrier populations. Specifically, by selecting certain photon energies, we could produce photoexcited NC ensembles with a nearly pure single multiplicity that can be tuned from 1 to 7. To

explain these observations, we developed a new model, in which direct photogeneration of multiexcitons occurs via *virtual* single-exciton states. This process relies on confinement-enhanced Coulomb coupling between single excitons and multiexcitons and also takes advantage of a large spectral density of multiexciton resonances in nanosized semiconductor crystals.

The controlled production of multiexcitons can benefit numerous technologies that rely on conversion of light quanta into electrical charges. One important application is in photovoltaics. Based on measured carrier-multiplication efficiencies, we can project that a “new” power-conversion limit of a single-junction solar cell can be increased up to approximately 42%, which is roughly a 40% improvement compared to the limit for a traditional solar cell operating without multiple-charge generation. Carrier multiplication can also significantly improve the performance of photoelectrolytic devices, in which photogenerated electrons and holes are utilized to

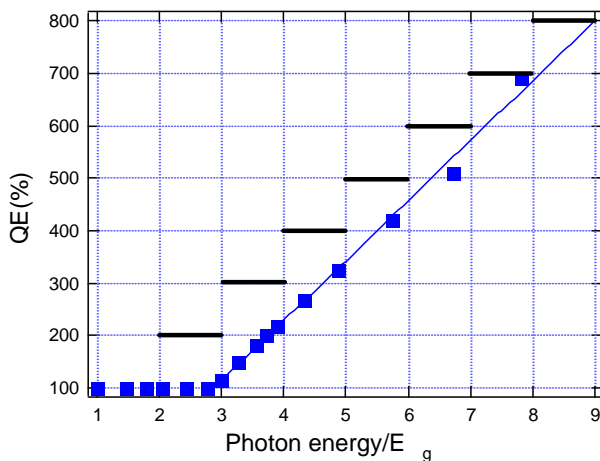


Figure 3. “Ideal” quantum efficiencies (QEs) derived from energy conservation (horizontal bars) and experimental QEs measured for PbSe NCs (solid squares) as a function of pump-photon energy,  $\hbar\omega$  normalized by energy gap. Experimental QEs approach the limit determined by energy conservation at  $\hbar\omega \approx 3E_g$ , for which  $QE \approx 700\%$ . The line is a linear fit (slope =  $115\%/E_g$ ) to experimental data in the range of energies  $>3E_g$ ; it indicates that complete filling of the 1S quantized state (8 electron-hole pairs) produced by a single photon is expected at  $\hbar\omega \approx 8E_g$ .

drive useful chemical reactions. Carrier multiplication can be particularly beneficial for chemical transformations that require localization of multiple reducing (oxidizing) equivalents at a single chemical site. One important reaction where this is required is photolysis of water to hydrogen and oxygen, which is a four-electron, four-proton process:  $2\text{H}_2\text{O} \rightarrow \text{O}_2 + 4\text{H}^+ + 4\text{e}^-$ . The use of carrier multiplication can reduce the number of photons required to drive this reaction. Other potential applications of this phenomenon include nonlinear optics, lasing, and quantum information.

### 3. Future Plans

In our future work, we will perform systematic studies of the effects of quantum and dielectric confinements on the strength/sign of exciton-exciton interactions and optical gain performance of core/shell hetero-nanocrystals. One goal of these studies will be the demonstration of nanocrystal lasing in the low-threshold, single-exciton regime, which will be achieved through the realization of strong exciton-exciton repulsion. We will begin our studies with ZnSe(core)/CdSe(shell) nanocrystals, in which the core is characterized by a wider energy gap than the shell. An interesting feature of these hetero-nanocrystals is that by changing the shell width one can continuously tune localization regimes from Type I (electrons and holes confined in the core) to Type II (electrons and holes separated between the core and the shell) and then back to Type I (electrons and hole are confined in the shell). We have performed preliminary calculations of exciton-exciton interactions in these heterostructures. An encouraging result of this theoretical modeling is that the interaction energy becomes positive (exciton-exciton repulsion) in the case of Type-II localization. We will use the time-resolved photoluminescence experiment to directly measure the exciton-exciton interaction energy through the transition between Type-I and Type-II localization. The results of these measurements together with our theoretical studies will provide feedback for our synthetic work on optimizing the geometry of hetero-nanocrystals.

In addition to tunable ZnSe/CdSe structures, we will investigate hetero-nanocrystals with a fixed Type II localization (e.g., CdS/ZnSe), which will allow us to reduce uncertainties associated with co-existence of different localization regimes within the nanocrystal ensemble. We will also use PbSe- and PbS-based Type II heterostructures to study the feasibility of single-exciton lasing in the infrared. For these compositions, the work on single-exciton gain is particularly important. Because of the 8-fold degeneracy of the ground electron and hole states, lasing in PbSe and PbS monocomponent nanocrystals requires more than 4 excitons per nanoparticle on average, which makes the problem of Auger recombination particularly severe.

We will continue our studies of carrier multiplication. Since the issue of toxicity may become important in practical applications of nanocrystal-based solar cells, we will study nanoparticles of such nontoxic materials as Si. To detect carrier multiplication and to measure its efficiency, we will use our newly developed dynamical method, which is based on a comparative analysis of population dynamics recorded for pump-photon energies below and above the carrier multiplication threshold.

An important issue associated with the practical use of carrier multiplication is highly efficient Auger recombination that can lead to rapid recombination of multiexcitons created via this effect. In order to overcome this problem, we will engineer Type-II heterostructures, which will allow us to quickly separate electrons and holes spatially before Auger recombination occurs. We will pursue rod and branched (e.g., tetrapods) hetero-nanocrystals, in addition to nanoparticles with concentric geometries, in order to promote charge separation and improve charge extraction efficiencies and transport in photovoltaic devices. As a practical step toward a real world photovoltaic device, we will investigate hybrid structures in which nanocrystals are interfaced with an external electrical circuit using a proximal quantum well. In these structures strong dipole-dipole interactions between nanocrystal excitations and the quantum well absorbing dipole will be used to extract charges from the nanocrystals via the energy transfer process.

#### 4. Publications (2005 - 2006)

1. V. I. Klimov, Mechanisms for photogeneration and recombination of multiexcitons in semiconductor nanocrystals: Implications for lasing and solar energy conversion, *J. Phys. Chem. B, Feature Article* (August, 2006)
2. M. Sykora, M. A. Petruska, J. Alstrum-Acevedo, I. Bezel, T. J. Meyer, and V. I. Klimov, Photoinduced charge transfer between CdSe nanocrystalline quantum dots and Ru-polypyridine complexes, *J. Am. Chem. Soc.* **128**, 9984 (2006).
3. M. Achermann, A. P. Bartko, J. A. Hollingsworth, and V. I. Klimov, The effect of Auger heating on intraband relaxation in semiconductor quantum rods **2**, 557 *Nature Physics* (2006).
4. M. Achermann, M. A. Petruska, D. D. Koleske, M. H. Crawford, and V. I. Klimov, Nanocrystal-based light emitting diodes utilizing high-efficiency nonradiative energy transfer for color conversion, *Nano Lett.* **6**, 1396 (2006).
5. R. D. Schaller and V. I. Klimov, Non-Poissonian exciton populations in semiconductor nanocrystals via carrier multiplication, *Phys. Rev. Lett.* **96**, 097402 (2006).
6. J. Nanda, S. A. Ivanov, H. Htoon, I. Bezel, A. Piryatinski, S. Tretiak, and V. I. Klimov, Absorption cross sections and Auger recombination lifetimes in inverted core/shell nanocrystals: Implications for lasing performance, *J. Appl. Phys.* **99**, 034309 (2006).
7. R. D. Schaller, M. Sykora, J. M. Pietryga, and V. I. Klimov, Seven excitons at a cost of one: Redefining the limits for conversion efficiency of photons into charge carriers, *Nano Lett.* **6**, 424 (2006).
8. G. R. Maskaly, M. A. Petruska, J. Nanda, I. V. Bezel, R. D. Schaller, H. Htoon, J. M. Pietryga, and V. I. Klimov, Enhancements to the stimulated light emission of semiconductor nanocrystals due to a photonic crystal pseudogap, *Advanced Materials* **18**, 343 (2006).
9. M. Furis, H. Htoon, M. A. Petruska, V. I. Klimov, T. Barrick, and S. A. Crooker. Bright-exciton fine structure and anisotropic exchange in CdSe nanocrystal quantum dots, *Phys. Rev. B* **73**, 241313 (R) (2006)
10. R. D. Schaller, V. M. Agranovich, and V. I. Klimov, High-efficiency carrier multiplication through direct photogeneration of multi-excitons via virtual single-exciton states, *Nature Physics* **1**, 189 (2005)
11. R. D. Schaller, M. A. Petruska, and V. I. Klimov, The effect of electronic structure on carrier multiplication efficiency: A comparative study of PbSe and CdSe nanocrystals, *Appl. Phys. Lett.* **87**, 253102 (2005).
12. R. D. Schaller, J. M. Pietryga, S. V. Goupalov, M. A. Petruska, S. A. Ivanov, and V. I. Klimov, Breaking the phonon bottleneck in semiconductor nanocrystals via multiphonon emission induced by intrinsic nonadiabatic interactions, *Phys. Rev. Lett.* **95**, 196401 (2005).
13. M. Furis, J. A. Hollingsworth, V. I. Klimov, and S. A. Crooker, Time- and polarization-resolved optical spectroscopy of colloidal CdSe nanocrystal quantum dots in high magnetic fields, *J. Phys. Chem. B* **109**, 15332 (2005).
14. S. Jeong, M. Achermann, J. Nanda, S. Ivanov, V. I. Klimov, and J. A. Hollingsworth, Effect of the thiol-thiolate equilibrium on the photophysical properties of aqueous CdSe/ZnS nanocrystal quantum dots, *J. Am. Chem. Soc.* **127**, 10126 (2005).
15. A. H. Mueller, M. A. Petruska, M. Achermann, D. J. Werder, E. A. Akhadov, D. D. Koleske, M. A. Hoffbauer, and V. I. Klimov, Multicolor light-emitting diodes based on semiconductor nanocrystals encapsulated in GaN charge injection layers, *Nano Lett.* **5**, 1039 (2005).
16. S. Kos, M. Achermann, V. I. Klimov, and D. L. Smith. Different regimes of Förster energy transfer between an epitaxial quantum well and a proximal monolayer of semiconductor nanocrystals, *Phys. Rev. B* **71**, 205309 (2005).

## Atomic, Molecular and Optical Sciences at LBNL

**A. Belkacem, M. Hertlein, C.W. McCurdy, T. Rescigno**

Chemical Sciences Division, Lawrence Berkeley National Laboratory, Berkeley, CA 94720

Email: [abelkacem@lbl.gov](mailto:abelkacem@lbl.gov), [mphertlein@lbl.gov](mailto:mphertlein@lbl.gov), [cwmccurdy@lbl.gov](mailto:cwmccurdy@lbl.gov), [tnrescigno@lbl.gov](mailto:tnrescigno@lbl.gov)

### Objective and Scope

The AMOS program at LBNL is aimed at understanding the structure and dynamics of atoms and molecules using photons and electrons as probes. The experimental and theoretical efforts are strongly linked and are designed to work together to break new ground and provide basic knowledge that is central to the programmatic goals of the Department of Energy. The current emphasis of the program is in three major areas with important connections and overlap: inner-shell photo-ionization and multiple-ionization of atoms and small molecules; low-energy electron impact and dissociative electron attachment of molecules; and time-resolved studies of atomic processes using a combination of femtosecond X-rays and femtosecond laser pulses. This latter part of the program is folded in the overall research program in the Ultrafast X-ray Science Laboratory (UXSL).

The experimental component at the Advanced Light Source makes use of the Cold Target Recoil Ion Momentum Spectrometer (COLTRIMS) to advance the description of the final states and mechanisms of the production of these final states in collisions among photons, electrons and molecules. Parallel to this experimental effort, the theory component of the program focuses on the development of new methods for solving multiple photo-ionization of atoms and molecules. This dual approach is key to break new ground and solve the problem of photo double-ionization of small molecules and unravel unambiguously electron correlation effects.

The relativistic collisions part of the program has been phased out in favor of branching into dissociative electron attachment measurements using COLTRIMS in support of the theoretical effort in the area of electron driven chemistry. These studies make use of the group's expertise at performing "complete" experiments using COLTRIMS. The theoretical project seeks to develop theoretical and computational methods for treating electron driven processes that are important in electron-driven chemistry and that are beyond the grasp of first principles methods.

## Ultrafast X-ray Science Laboratory

Ali Belkacem, Roger Falcone, Thornton E. Glover, Martin Head-Gordon, Stephen Leone, C. William McCurdy, Daniel M. Neumark, Robert W. Schoenlein

*Chemical Sciences, Lawrence Berkeley National Laboratory, Berkeley, CA 94720*

[ABelkacem@lbl.gov](mailto:ABelkacem@lbl.gov), [rwf@berkeley.edu](mailto:rwf@berkeley.edu), [TEGlover@lbl.gov](mailto:TEGlover@lbl.gov), [MHead-Gordon@lbl.gov](mailto:MHead-Gordon@lbl.gov), [SRLeone@lbl.gov](mailto:SRLeone@lbl.gov), [CWMcCurdy@lbl.gov](mailto:CWMcCurdy@lbl.gov), [DMNeumark@lbl.gov](mailto:DMNeumark@lbl.gov), [RWSchoenlein@lbl.gov](mailto:RWSchoenlein@lbl.gov)

**Program Scope:** This program seeks to bridge the gap between the development of ultrafast X-ray sources and their application to understand processes in chemistry and atomic and molecular physics that occur on both the femtosecond and attosecond time scales. Current projects include: 1) The construction of a new high repetition rate high harmonic source and its application in chemical physics, 2) Applications of a new ultrafast X-ray science facility at the Advanced Light Source at LBNL to understand solution-phase molecular dynamics, 3) Time-resolved studies and non-linear interaction of femtosecond x-rays with atoms and molecules using high-intensity HHG sources as well as femtosecond X-rays at the Advanced Light Source 4) Theory and computation treating the dynamics of two electrons in intense short pulses, and extending electronic structure methods so that they can be used in nonadiabatic direct dynamics calculations on the femtosecond time scale.

**Recent Progress and Future Plans:** This is a new program, and in its first year the experimental facilities are being constructed and new personnel are being hired. Two new Divisional Fellows and three Postdoctoral Fellows will be in the laboratory at the beginning of the next fiscal year. Two high harmonic generation sources are under construction, to produce VUV and soft X-ray harmonics in different regimes of repetition rate and intensity, and equipment is being purchased for experiments on the new undulator-based ultrafast x-ray beamline at the ALS. Computational methods breaking new ground for time-dependent studies of multiple ionization are being developed.

### 1. Soft X-ray high harmonic generation and applications in chemical physics

This part of the laboratory will combine the utilization of ultrashort pulses in the VUV and near X-ray regime with state-of-the-art photoelectron and photoion detection schemes in order to investigate fundamental chemical dynamics phenomena. An extended version of time resolved photoelectron spectroscopy (TRPES), the recently developed femtosecond time resolved photoelectron-photoion coincidence imaging spectroscopy (TRCIS), delivers a kinematically complete picture of unimolecular photochemical reactions. By measuring the complete, 3-dimensional momentum vectors of both photoelectrons and (fragment) photoions in coincidence, TRCIS gives access to photoelectron angular distributions in the molecular frame and correlated photoelectron-photoion kinetic energy distributions. These highly differential measurements reveal details of the molecular dynamics that are not accessible with methods that integrate over all molecular orientations in space and/or fragment ion kinetic energies.

The generation of high harmonics (HHG) of a fundamental wavelength from a femtosecond laser pulse is one of the most active fields of research in ultrafast science. In recent years great progress was made in the understanding and characterization of the HHG process itself. The next logical step is the utilization of ultrashort HH pulses for time resolved studies in the VUV and near X-ray energy regimes, thereby closing the gap between "traditional" time domain studies in the photon energy range from IR to near UV and energy domain studies in the VUV to hard X-ray regime.

We will employ ultrashort HH pulses in combination with TRPES and TRCIS detection schemes to address a wide variety of molecular dynamics phenomena. Examples are transitions between delocalized and localized behavior of electrons during a molecular dissociation, intramolecular energy redistribution processes, and the real-time observation of structural dynamics during a molecular dissociation. Aside from the immediate scientific impact of these investigations, many of the studies will provide valuable information for experiments on near and mid-term future 4th generation light sources like the linac coherent light source (LCLS) in Stanford CA. Furthermore, the inclusion of various target preparation techniques, like a pulsed molecular beam source and a He-droplet source will ensure that the laboratory's facilities can be used for a broad range of experiments.

## **2. Applications of the new femtosecond undulator beamline at the Advanced Light Source to solution-phase molecular dynamics**

Charge-transfer processes in solvated transition-metal complexes are of fundamental interest due to the strong interaction between electronic and molecular structure. In particular, Fe<sup>II</sup> molecular complexes exhibit strong coupling between structural dynamics, charge-transfer, and spin-state interconversions. These processes are closely related to the electron transfer reactions in heme proteins and are of practical interest for opto-magnetic storage via light-induced excited spin-state trapping (LIESST).

Our first objective on the femtosecond undulator beamline at the ALS will be to extend EXAFS studies of Fe<sup>II</sup> molecular complexes to the sub-picosecond time scale in order to discern the dynamic coupling between the spin transition and the structural changes of the ligands. We will develop techniques for solution-phase soft X-ray spectroscopy measurements (at the Fe L-edge), to provide more direct information about the influence of the ligand field dynamics on the Fe *d*-electrons.

An important goal is to apply time-resolved X-ray techniques to understand the structural dynamics of more complicated reactions in a solvent environment. Of current interest is the photochemical reaction dynamics of aqueous chlorine dioxide (O-Cl-O) which exists in stratospheric polar clouds and plays a significant role in sunlight-induced atmospheric chemistry due to its ability to produce atomic Cl. We will apply time-resolved EXAFS and XANES techniques in an effort to follow the changing oxidation state of the Cl, and thereby distinguish between various competing reaction pathways that cannot be unambiguously identified through visible spectroscopy but appear to be solvent dependent.

### **3. Time-resolved studies and non-linear interaction of femtosecond x-rays with atoms and molecules:**

*Development of a high intensity high harmonic source:* While the strong interaction regime has typically been inaccessible to (low peak power) synchrotron sources, it can be accessed with recently developed and with foreseeable sources. X-ray Free Electron Lasers will offer high flux ( $\sim 10^{12}$  photons/pulse) while high harmonics sources have recently been demonstrated to achieve focal intensities up to  $\sim 10^{14}$  W/cm<sup>2</sup>. We plan to study fundamental high field and nonlinear interactions with simple atomic and molecular systems using a high harmonics source optimized for high peak power. We are finishing constructing a high harmonic source based on a 40 mJ, 10 Hz, 800 nm laser system (10 Hz, 800 nm). The laser drives high harmonic generation, and we measured an initial photon flux exceeding  $10^{10-11}$  photons/pulse and expect peak intensities in the range  $10^{12}-10^{14}$  W/cm<sup>2</sup> after micro-focusing. The harmonics are generated in a long ( $\sim 10$  cm) gas cell and directed into an existing experimental chamber. We fabricated a parabolic mirror with multilayer coating to select and focus a single harmonic to micron size spot. The initial experiment will focus on studying two-photon triple ionization of Xenon and two-photon double ionization of He.

*Inner-shell photoionization of laser excited potassium:* The goal of this study is to modulate the interaction of hard or soft x-rays with the inner-shells of an atom by controlling the excitation of the atom with a sequence of short laser pulses. The binding energy of a core electron of an atom is influenced by the presence and configuration of other electrons in the atom, due to electron correlation effects such as charge screening and coupling. The fact that core electrons are tightly bound and have high (classical) speed allows them to follow adiabatically valence electron configuration changes. The change of the inner-shell excitation energy is induced by the sudden change of the Coulomb screening when the valence electron population is modified. We performed the preliminary experiments at beamline 5.3.1 at the Advanced Light Source using 70 ps x-ray pulses. Due to its low binding energy (4.3 eV) the excitation and ionization of the potassium 4s valence electron is accessible to existing femtosecond lasers. We developed a time-of-flight detection system in a rapidly but adiabatically decreasing magnetic field (inverse of a magnetic bottle) to detect KLL Auger electrons following K-shell ionization. We found that the 1s-4p excitation energy and the K-shell edge of potassium are modified when the outer 4s-electron is ionized or excited with a femtosecond laser. We also measured a cross correlation between the femtosecond laser and the ALS x-ray pulse. This cross correlation reflects the pulse length of the ALS x-rays and shows the ability of our set up to synchronize both in space and time the laser and the x-rays. This technique that uses the detection of KLL Auger electron via time-of-flight can work equally well with femtosecond x-rays at beamline 6 or the LCLS when available.

#### 4. Theory and computation

An initial focus of our work is the development of computational methods that will allow the accurate treatment of multiple ionization of atoms and molecules by short pulses in the VUV and soft X-ray regimes. Our recent calculations on the complete photofragmentation of  $H_2$ , reported recently in *Science*, demonstrated that in time-independent calculations we can solve such problems essentially exactly. The basic theoretical approach combines a reformulation of the ionization problem using exterior complex scaling (ECS) with a finite element implementation of the discrete variable representation (FEM-DVR) to produce an efficient numerical method for describing double ionization. We have now extended this approach to the time domain, thereby allowing calculations using a few hundred computer processors to produce accurate descriptions of highly correlated electronic wave packets. These methods allow the complete treatment of two active electrons, and they are capable of treating the electron dynamics of two electron systems accurately for comparison with benchmark level experiments. For many-electron systems we will use a more limited treatment of all but the two ionizing electrons.

A central challenge for the theory of time-dependent multiple ionization processes, that we have recently solved, is the rigorous extraction of the amplitudes for ionization from these wave packets, and the separation of single and double ionization probabilities. The integral formulation that successfully surmounted this difficulty in our time-independent calculations now forms the basis of a new time-dependent approach that avoids the ambiguities concerning the correct characterization of the final state that have characterized essentially all time-dependent descriptions of multiple ionization.

These developments put the investigation of attosecond pump and probe processes in atoms, including multiphoton absorption, within reach. For molecules the challenge remains to include nuclear motion in calculations that accurately treat correlated electronic motion so that processes occurring over 10s of femtoseconds can be treated accurately.

#### **Publications:**

“Inner-shell ionization of potassium atoms ionized by femtosecond laser”, M.P. Hertlein, H. Adaniya, J. Amini, C. Bressler, B. Feinberg, M. Kaiser, N. Neumann, M.H. Prior and A. Belkacem, *Phys. Rev. A* 73, 062715 (2006).

# Inner-Shell Photoionization of Atoms and Small Molecules

A. Belkacem and M. P. Hertlein

Chemical Sciences Division, Lawrence Berkeley National Laboratory, Berkeley, CA 94720

Email: abelkacem@lbl.gov

## Objective and Scope

The goal of this part of the LBNL AMOS program is to understand the structure and dynamics of atoms and molecules using photons as probes. The current research carried at the Advanced Light Source is focused on studies of inner-shell photoionization and photo-excitation of atoms and molecules, as well as breaking new ground in the interaction of x-rays with atoms and molecules dressed with femto-second laser fields. The low-field photoionization work seeks new insight into atomic and molecular processes and tests advanced theoretical treatments by achieving new levels of completeness in the description of the distribution of momenta and/or internal states of the products and their correlations. The intense-field two-color research is designed to provide new knowledge of the evolution on a femto-second time scale (ultimately atto-second) of atomic and molecular processes as well as the relaxation of atomic systems in intense transient fields. This latter part of the program is folded in the overall research program in the new LBNL's Ultrafast X-ray Science Laboratory (UXSL).

## K-shell photoionization of acetylene and isomerization to vinylidene

In this study we investigate the K-shell photoionization of acetylene and the dynamics of the following breakup pathways by measuring the momenta of the positively charged ions in coincidence with Auger electrons. The photoionization and the subsequent Auger process lead to the formation of the doubly charged  $C_2H_2^{2+}$  ion that dissociates into two or more fragments. We observe two clearly separated Auger electron peaks correlated with different kinetic energies taken by the fragments. The result of this analysis in the 2-D plot (Auger energy – kinetic energy of ions) shows that the isomerization to vinylidene is associated with a very sharp peak around 255 eV Auger energy and 4.5 eV ion kinetic energy. This gives a clear insight on the isomerization process. Following the emission of the 255 eV Auger electron  $\{C_2H_2^+ \rightarrow C_2H_2^{2+} + e_A (255 \text{ eV})\}$  the di-cation ends up in the lower lying states  $^1\Sigma_g^+$ ,  $^1\Delta_g$  and  $^3\Sigma_g^-$ . The di-cation is trapped behind a high (3-4 eV) and wide barrier preventing it from directly dissociating along the C-C bond or C-H bond. The dissociation appears to be achieved after an isomerization to vinylidene first followed by dissociation along the C-C bond forming  $C^+ + CH_2^+$  fragments.

## Double-photoionization of CO few eV above threshold.

We measured double photoionization of CO molecules at 48 eV photon energy. The double ionization of CO produces mostly  $C^+ + O^+$  fragments with non-measurable amounts of  $CO^{2+}$ . The formation of  $C^+ + O^+$  can proceed through two possible channels: a) Direct ionization of two electron into the continuum – similar to the  $H_2$  double ionization – direct channel. b) Ionization of one electron into the continuum followed by

autoionization of a second electron – Indirect channel. The electron distribution measured with a COLTRIMS shows a very clear distinction of the direct and indirect channels. The kinetic energy release spectrum shows a series of peaks corresponding to the transient vibrational states of the various electronic states of  $(\text{CO}^{2+})^*$ . These states are similar to previous measurements at higher energies (K-shell photoionization).  $(\text{CO}^{2+})^*$  is found to predissociate through a  $^3\Sigma^-$  and  $^1\Delta$  dissociative states leading to considerably faster dissociation times than natural lifetimes of the electronic bound states. We plan to improve our current measurement by detecting both electrons in coincidence. We will be able to estimate the dissociation time of these states by using an analysis technique similar to that used to estimate the time of the isomerization of acetylene to vinylidene.

### **Photoionization and double excitation in $\text{H}_2$ and $\text{D}_2$**

We crossed a supersonic jet of  $\text{H}_2$  and  $\text{D}_2$  with synchrotron radiation and examined the fragments resulting from ionization ( $\text{H}_2 + h\nu \rightarrow \text{H}_{(n=1,2,\dots)} + e^- + \text{p}$ ) using the COLTRIMS method. The photon energy was scanned from 29 to 60 eV, in order to get a comprehensive overview of the processes taking place during single ionization in  $\text{H}_2$  and  $\text{D}_2$ . The  $2p\sigma_u$  state is easily distinguished from the higher excited states. The data clearly shows regions, which correspond to excitation of the Q1 and Q2 band. A small ion kinetic energy release (KER) is observed and can be explained by a process in which the molecule is excited to the Q1 band. At a certain internuclear distance, the molecule autoionizes and decays back to the stable  $1s\sigma_g$  state. However, the atomic nuclei gained sufficient energy through the dissociation to move out of the potential minimum. The KER in the final state is hence reduced by the potential energy, and therefore relatively small (<2 eV). Photon energies around 31 to 41 eV are also used to excite the potential curves of the Q2 band. In this case the molecule separates for a while before it decays down to the  $2p\sigma_u$  potential curve and continues to dissociate. This later starting point therefore results in a slightly smaller KER than what would result through the direct population of the  $2p\sigma_u$  state. In addition, we observe a significant difference in the angular distribution between the Q2 band and the  $2p\sigma_u$  state.

### **Double-slit interference of photoelectrons from hydrogen molecules**

Electrons with de Broglie wavelengths  $\lambda_e$  close to the size (0.72 Å) of the  $\text{H}_2$  (or  $\text{D}_2$ ) molecule can be expected to show effects similar to Young's double slit diffraction of light. In a naïve view, one thinks of photo-electron emission arising coherently from near two identical centers leading to a far field interference modulation in the molecular frame angular distribution. In the case of double ionization with photon energies well above the threshold (e.g. 300 eV) the electrons have strongly asymmetric sharing of the excess energy. The higher energy electron (say 250 eV,  $\lambda_e = 0.78$  Å) shows interference perturbed by the presence of a slower few eV partner. One can select the inter-nuclear separation within the spread of the  $v=0$  vibrational wavefunction by selecting narrow regions of kinetic energy release in the  $\text{H}^+$ ,  $\text{H}^+$  explosion. The electron emission is not from two well localized sites in this case, but is spread over the extent of the initial electron wavefunction, thus the pattern might resemble more the interference from two wide slits...i.e. a combination of interference modulated by diffraction.

## **Dissociative electron attachment of small molecules.**

A Coltrims method is developed for measuring the angular distribution of fragment negative ions arising from dissociative electron attachment of molecules. A low energy pulsed electron gun is used in combination with pulsing the extraction plates of the Coltrims spectrometer. The angular distribution measurements are particularly important for dissociative electron attachment, due to the selection rules, which connects the states of the neutral molecule to the negative ion resonant states and the orientation of the neutral molecule with respect to the momentum vector of the incoming electron. Thus the angular distribution contains information on the symmetry of the negative ion state and the angular momentum of the captured electron. The formation of the resonant dissociative negative molecular states typically peak at electron energies below 10 eV. Thus a major technical problem is the production of a controlled, defined low electron beam that can strike the molecular jet within the uniform electric field of the COLTRIMS spectrometer. Our approach uses the uniform field and an orthogonal uniform magnetic field. This ExB field steers the electrons along the directions of the gas jet without (or minimally) affecting the electron energy. The low magnetic field (~10 G) used has a minimal effect on the motion of the slow heavy negative ion. This COLTRIMS configuration allowed us the injection of a usable low electron beam into the interaction region of the spectrometer. Earlier studies of DEA found in the literature measured angular distributions of negative ion products, however the COLTRIMS approach will result in higher sensitivity and simultaneous coverage of a wide range of negative ion final momenta. We applied this modified Coltrims technique to the measurement of dissociative electron attachment of O<sub>2</sub>. The formation of O<sup>-</sup> from O<sub>2</sub> is known to appear as a broad peak centered at 6.5 eV. These negative ions are formed with considerable kinetic energy making O<sub>2</sub> a very good test of the apparatus. The 3D angular distribution of O<sup>-</sup> changes as the energy of the electrons is swept across the broad resonance. At the maximum of cross section (6.5 eV) the angular distribution shows clear minima both when the O<sub>2</sub> molecule is aligned parallel or perpendicular to the electron beam direction. The maximum yield is observed at 450 degree angles which is interpreted as a strong signature of a  $\Pi$  contribution.

## **Future Plans**

We plan to continue application of the COLTRIMS approach to achieve complete descriptions of the single photon double ionization of CO and its analogs. New measurements will be made close to the double ionization threshold and approaching the regime where the outgoing electrons and the ions have nearly the same velocities. Our earlier observations of the isomerization of acetylene to the vinylidene configuration forms a basis for possible further studies of this phenomena perhaps using deuterated acetylene to alter the relative time scales of molecular rotation and the dissociation dynamics.

## **Recent Publications**

"Inner-shell ionization of potassium atoms ionized by femtosecond laser", M.P. Hertlein, H. Adaniya, J. Amini, C. Bressler, B. Feinberg, M. Kaiser, N. Neumann, M.H. Prior and A. Belkacem, Phys. Rev. A 73, 062715 (2006)

“The pair-production channel in atomic processes”, A. Belkacem and A. Sorensen, *Radiation Physics and Chemistry* **75**, 656-695 (2006).

“Electron correlation during photoionization and relaxation of potassium and argon after K-shell photoexcitation”, M. Hertlein, H. Adaniya, K. Cole, B. Feinberg, J. Maddi, M. Prior, R. Schriel and A. Belkacem, *Phys. Rev. A* **71**, 022702 (2005)

A. Knapp, B. Krassig, A. Kheifets, I. Bray, Th. Weber, A. Landers, S. Schossler, T. Jahnke, J. Nickles, S. Kammer, O. Jagutzki, L. Ph. H. Schmidt, M. Schoffler, T. Osipov, M. Prior, H. Schmidt-Bocking, C.L. Cocke and R. Dorner, *J. Phys. B: At. Mol. Opt. Phys.* **38**, 615 (2005)

A. Knapp, B. Krassig, A. Kheifets, I. Bray, Th. Weber, A. Landers, S. Schossler, T. Jahnke, J. Nickles, S. Kammer, O. Jagutzki, L. Ph. H. Schmidt, M. Schoffler, T. Osipov, M. Prior, H. Schmidt-Bocking, C.L. Cocke and R. Dorner, *J. Phys. B: At. Mol. Opt. Phys.* **38**, 635 (2005)

A. Knapp, B. Krassig, A. Kheifets, I. Bray, Th. Weber, A. Landers, S. Schossler, T. Jahnke, J. Nickles, S. Kammer, O. Jagutzki, L. Ph. H. Schmidt, M. Schoffler, T. Osipov, M. Prior, H. Schmidt-Bocking, C.L. Cocke and R. Dorner, *J. Phys. B: At. Mol. Opt. Phys.* **38**, 645 (2005)

“Vibrationally resolved K<sub>-</sub>shell photoionization of CO with circularly polarized light”, T. Jahnke, L. Foucar, J. Titze, R. Wallauer, T. Osipov, E. P. Benis, A. Alnaser, O. Jagutzki, W. Arnold, S. K. Semenov, N. A. Cherepkov, L. Ph. H. Schmidt, A. Czasch, A. Staudte, M. Schöffler, C. L. Cocke, M. H. Prior, H. Schmidt-Böcking, and R. Dörner, *Phys. Rev. Lett.* **93**, 083002 (2004)

“Complete photo-fragmentation of the deuterium molecule” T. Weber, A. O. Czasch, O. Jagutzki, A. K. Mueller, V. Mergel, A. Kheifets, E. Rotenberg, G. Meigs, M. H. Prior, S. Daveau, A. Landers, C. L. Cocke, T. Osipov, R. Diez Muiño, H. Schmidt-Böcking and R. Dörner, *Nature*, **431**, 437 (2004)

“Fully Differential Cross Sections for Photo-Double-Ionization of D<sub>2</sub>”, Th. Weber, A. Czasch, O. Jagutzki, A. Müller, V. Mergel, A. Kheifets, J. Feagin, E. Rotenberg, G. Meigs, M.H. Prior, S. Daveau, A.L. Landers, C.L. Cocke, T. Osipov, H. Schmidt-Böcking and R. Dörner, *Phys. Rev. Lett.* **92**, 163001 (2004).

“Metal-insulator transitions in an expanding metallic fluid: particle formation kinetics”, T.E. Glover, G. D. Ackerman, A. Belkacem, P. A. Heimann, Z. Hussain, R. W. Lee, H. A. Padmore, C. Ray, R. W. Schoenlein, W. F. Steele, and D. A. Young, *Phys. Rev. Lett.* **90**, 23102-1 (2003)

“Measurement of vacuum-assisted photoionization at 1 GeV for Au and Ag targets”, D. Dauvergne, A. Belkacem, F. Barrue, J. P. Bocquet, M. Chevallier, B. Feinberg, R. Kirsch, J. C. Poizat, C. Ray, and D. Rebreyent, *Phys. Rev. Lett.* **90**, 153002 (2003)

“Auger electron emission from fixed-in-space CO”, T. Weber, M. Weckenbrock, M. Balsler, L. Schmidt, O. Jagutzki, W. Arnold, O. Hohn, M. Schoffler, E. Arenholz, T. Young, T. Osipov, L. Foucar, A. de Fanis, R. D. Muino, H. Schmidt-Bocking, C.L. Cocke, M.H. Prior, and R. Dorner, *Phys. Rev. Lett.* **90**, 153003 (2003)

“Photoelectron-photoion momentum spectroscopy as a clock for chemical rearrangements: isomerization of the Di-cation of acetylene to vinylidene configuration”, T. Osipov, C.L. Cocke, M. Prior, A. Landers, T. Weber, O. Jagutzki, L. Schmidt, H. Schmidt-Bocking and R. Dorner, *Phys. Rev. Lett.* **90**, 233002 (2003)

## Electron-Atom and Electron-Molecule Collision Processes

T. N. Rescigno and C. W. McCurdy

Chemical Sciences, Lawrence Berkeley National Laboratory, Berkeley, CA 94720

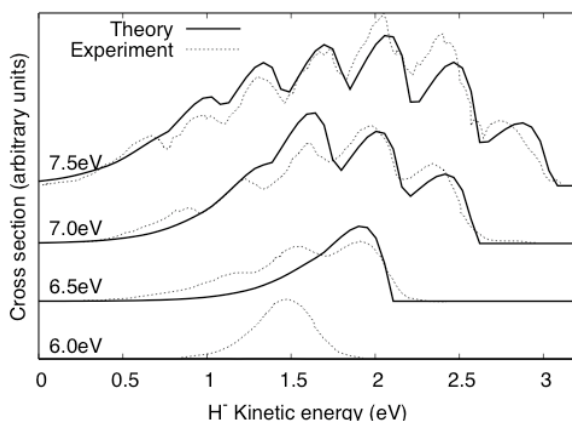
[tnrescigno@lbl.gov](mailto:tnrescigno@lbl.gov), [cwmccurdy@lbl.gov](mailto:cwmccurdy@lbl.gov)

**Program Scope:** This project seeks to develop theoretical and computational methods for treating electron collision processes that are important in electron-driven chemistry and physics and that are currently beyond the grasp of first principles methods, either because of the complexity of the targets or the intrinsic complexity of the processes themselves. New methods are being developed and applied for treating low-energy electron collisions with polyatomic molecules and clusters. A state-of-the-art approach is used to treat multidimensional nuclear dynamics in polyatomic systems during resonant electron collisions and predict channeling of electronic energy into vibrational excitation and dissociation. A second focus is the development of new methods for solving multiple photoionization and electron-impact ionization of atoms and molecules.

**Recent Progress and Future Plans:** We report progress in two areas covered under this project, namely electron-polyatomic molecule collisions and molecular double photoionization.

### 1. Electron-Molecule Collisions

We have continued our work on dissociative electron attachment (DEA) to water, which proceeds via formation of negative ion, Feshbach resonances of  $^2B_1$ ,  $^2A_1$  and  $^2B_2$  symmetry and is governed by complex nuclear and electronic resonance dynamics. The first phase of our study, DEA through the  $^2B_1$  resonance, has been extended with a study of the angular dependence of the observed products (ref. 22). We have detailed the complicated topology of the water anion surfaces in a paper that has appeared in *Phys. Rev. A* (ref. 14). There is a conical intersection between the  $^2A_1$  and  $^2B_2$  surfaces which significantly influences the dynamics that leads to production of  $O^-$ . There are also strong Renner-Teller couplings between the  $^2B_1$  and  $^2A_1$  states, which become degenerate in



DEA to water. Comparison of theory and experiment showing structure in the production of  $H^+$  as a function of the nuclear kinetic energy released for four values on incident electron energy.

linear geometry. The complex-valued surfaces and their couplings have been fit and the wavepacket calculations that determine the DEA cross sections and branching ratios have been completed. This benchmark study of DEA is the first to treat, from first principles, all aspects of

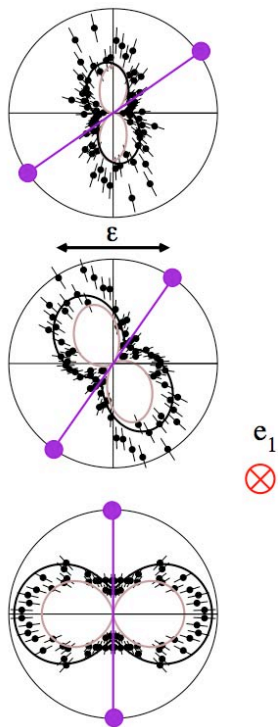
an electron polyatomic collision, including not only the determination of the fixed-nuclei electronic cross sections, but also a treatment of the nuclear dynamics in full dimensionality.

In collaboration with Prof. A.E. Orel of UC Davis, we have begun to look at electron interactions with biologically relevant molecules. We unraveled the mechanism for dissociative electron attachment to formic acid (HCOOH), which has been observed experimentally to fragment to produce formate ions ( $\text{HCOO}^-$ ) plus hydrogen atoms, showing that the dynamics are intrinsically polyatomic, involving two negative ion surfaces connected by a conical intersection. The results were published in *Physical Review Letters* (ref. 21). We also carried out a study of electron scattering by tetrahydrofuran ( $\text{C}_4\text{H}_8\text{O}$ ) and verified the presence of shape resonances in the 8-10 eV range that have been seen in experiment, but not in earlier theoretical calculations. These findings we also published in *Physical Review A* (ref. 23).

Finally, we have completed the first phase of a study aimed at examining the underpinnings and limitations of the local complex potential model, which has formed the basis of much of the work on resonant electron-molecule scattering, by studying a model 2-dimensional problem which can be solved without making the Born-Oppenheimer approximation. This first study was published in *Physical Review A* (ref. 20).

## 2. Double Photoionization

We have continued with our work on double photoionization of molecular hydrogen. In 2005, we completed an initial study of the triply differential double ionization cross sections for oriented  $\text{H}_2$ , using exterior complex-scaled B-splines and single-center expansions: the results were published in *Science* (ref. 18). This was the first precise quantum mechanical calculation of triply differential cross sections (TDCS) for double photoionization ever carried out for a molecular target and gave conclusive evidence that the observed patterns of photoejection, which depend both on bond distance and orientation, are a clear signature of changes in molecular electron correlation. We have since developed an independent check on these initial results using finite elements and the discrete variable representation and have succeeded in obtaining fully converged results. An initial analysis of both the **COLTRIMS** experiments which were performed at the ALS, as well as recent experiments from Paris by Huetz and coworkers, has been carried out which includes an averaging over the finite ranges of acceptance angles and energy sharings as in the experiments. This study has uncovered certain errors in the data analysis which have been corrected and has now produced excellent agreement between theory and experiment. We have submitted a long paper on this work to *Physical Review A* for publication (ref. 24).



Triple differential cross sections for double photoionization of aligned  $H_2$ . The fixed electron, with 50% of the available energy, is perpendicular, coming out of the page, while the molecule is oriented in the plane at (left to right)  $35^\circ$ ,  $55^\circ$ , and  $90^\circ$  to the polarization direction (horizontal). Our calculations, unaveraged (light curves) and averaged (dark curves), indicated an error in the experimental data analysis, which is shown here in corrected form.

### 3. Future Plans

We will turn to an analysis of the R-dependence of the TDCS for aligned  $H_2$  and the observed dependence of the cross sections on nuclear kinetic energy release. We will also be involved in a joint theoretical/experimental study of the doubly differential cross sections. With a view to extending these studies to more complex molecular targets, we will continue to work on a hybrid approach (ref. 16) that combines the use of molecular Gaussian basis sets with finite-element/DVR grid-based methods and exterior complex scaling. Such an approach avoids the use of single-center expansions, simplifies the computation of two-electron integrals and will pave the way for studies of double photoionization of more complex molecules.

The analysis of our benchmark study of DEA to water will be completed and published in two long papers. We will continue to examine resonant electron interactions with biologically relevant molecules and look for practical ways to extend the studies to more complex targets. We will focus on systems that overlap experimental efforts in the LBL AMO program, as well as with our collaborators at the Australian National University. We will complete the second phase of our study of formal molecular resonance models by extending the work to look at non-local resonance models.

#### Publications (2004-2006):

1. W. Vanroose, Z. Zhang, C. W. McCurdy and T. N. Rescigno, "Threshold Vibrational Excitation of  $CO_2$  by Slow Electrons", *Phys. Rev. Letts.* **92**, 053201 (2004).
2. C. W. McCurdy and F. Martin, "Implementation of Exterior Complex Scaling in B-Splines to Solve Atomic and Molecular Collision Problems", *J. Phys. B* **37**, 917 (2004).
3. C. W. McCurdy, D. A. Horner, T. N. Rescigno and F. Martin, "Theoretical Treatment of Double Photoionization of Helium Using a B-spline Implementation of Exterior Complex Scaling", *Phys. Rev. A* **69**, 032707 (2004).
4. Z. Zhang, W. Vanroose, C. W. McCurdy, A. E. Orel and T. N. Rescigno, "Low-energy Electron Scattering by NO: Ab Initio Analysis of the  $^3\Sigma^-$ ,  $^1\Delta$  and  $^1\Sigma^+$  shape resonances in the local complex potential model", *Phys. Rev. A* **69**, 062711 (2004).

5. D. J. Haxton, Z. Zhang, C. W. McCurdy and T. N. Rescigno, "Complex Potential Surface for the  $^2B_1$  Metastable State of the Water Anion", *Phys. Rev. A* **69**, 062713 (2004).
6. D. J. Haxton, Z. Zhang, H.-D. Meyer, T. N. Rescigno and C. W. McCurdy, "Dynamics of Dissociative Attachment of Electrons to Water Through the  $^2B_1$  Metastable State of the Anion", *Phys. Rev. A* **69**, 062714 (2004).
7. C. S. Trevisan, A. E. Orel and T. N. Rescigno, "Ab initio study of Low-Energy Electron Collisions with tetrafluoroethene, C<sub>2</sub>F<sub>4</sub>", *Phys. Rev. A* **70**, 012704 (2004).
8. C. W. McCurdy, M. Baertschy and T. N. Rescigno, "Solving the Three-Body Coulomb Breakup Problem Using Exterior Complex Scaling", *J. Phys. B* **37**, R137 (2004).
9. D. A. Horner, J. Colgan, F. Martin, C. W. McCurdy, M. S. Pindzola and T. N. Rescigno, "Symmetrized Complex Amplitudes for He Double Photoionization from the Time-Dependent Close Coupling and Exterior Complex Scaling Methods", *Phys. Rev. A* **70**, 064701 (2004).
10. D. A. Horner, C. W. McCurdy and T. N. Rescigno, "Electron-Helium Scattering in the S-wave Model Using Exterior Complex Scaling", *Phys. Rev. A* **71**, 012701 (2005).
11. W. Vanroose, F. Martin, T. N. Rescigno and C. W. McCurdy, "Nonperturbative Theory of Double Photoionization of the Hydrogen Molecule", *Phys. Rev. A* **70**, 050703 (R) (2004).
12. D. A. Horner, C. W. McCurdy and T. N. Rescigno, "Electron Impact Excitation-Ionization of Helium in the S-Wave Limit", *Phys. Rev. A* **71**, 010701 (2005).
13. C. S. Trevisan, K. Houfek, Zh. Zhang, A. E. Orel, C. W. McCurdy and T. N. Rescigno, "A Nonlocal, Ab Initio Model of Dissociative Electron Attachment and Vibrational Excitation of NO", *Phys. Rev. A* **71**, 052714 (2005).
14. D.J. Haxton, T. N. Rescigno and C. W. McCurdy, "Topology of the Adiabatic Potential Energy Surfaces for the Resonance States of the Water Anion", *Phys. Rev. A* **72**, 022705 (2005).
15. F. Martín, D. A. Horner, W. Vanroose, T. N. Rescigno and C. W. McCurdy, "First Principles Calculations of the Double Photoionization of Atoms and Molecules using B-splines and Exterior Complex Scaling", Proceedings of the Thirteenth International Symposium on Polarization and Correlation in Electronic and Atomic Collisions and the International Symposium on (e,2e), Double Photoionization and Related Topics, Buenos Aires, 2005 (American Institute of Physics, 2006).
16. T. N. Rescigno, D. A. Horner, F. L. Yip and C. W. McCurdy, "A Hybrid Approach to Molecular Continuum Processes Combining Gaussian Basis Functions and the Discrete Variable Representation", *Phys. Rev. A* **72**, 052709 (2005).
17. C. S. Trevisan, A. E. Orel and T. N. Rescigno, "Resonant Electron-CF Collision Processes", *Phys. Rev. A* **72**, 062720 (2005).
18. Wim Vanroose, F. Martín, T. N. Rescigno and C. W. McCurdy, "Complete Photofragmentation of the H<sub>2</sub> Molecule as a Probe of Molecular Electron Correlation", *Science* **310**, 1787 (2005).
19. T. N. Rescigno and C. W. McCurdy (with B. C. Garrett *et al.*), "Role of Water in Electron-Initiated Processes and Radical Chemistry: Issues and Scientific Advances" *Chemical Reviews* **105**, 355-389 (2005).
20. K. Houfek, T. N. Rescigno and C. W. McCurdy, "A Numerically Solvable Model for Resonant Collisions of Electrons with Diatomic Molecules", *Phys. Rev. A* **73**, 032721 (2006).
21. T. N. Rescigno, C. S. Trevisan and A. E. Orel, "Dynamics of Low-Energy Electron Attachment to Formic Acid", *Phys. Rev. Lett.* **96**, 213201 (2006).
22. D. J. Haxton, C. W. McCurdy and T. N. Rescigno, "Angular Dependence of Dissociative Electron Attachment to Polyatomic Molecules: Application to the  $^2B_1$  Metastable State of the H<sub>2</sub>O and H<sub>2</sub>S Anions", *Phys. Rev. A* **73**, 062724 (2006).
23. C. S. Trevisan, A. E. Orel and T. N. Rescigno, "Elastic scattering of low-energy electrons by tetrahydrofuran", *J. Phys. B* **39**, L255 (2006).
24. Wim Vanroose, D. A. Horner, F. Martín, T. N. Rescigno and C. W. McCurdy, "Double Photoionization of Aligned Molecular Hydrogen", *Phys. Rev. A* (submitted).
25. T. N. Rescigno, Wim Vanroose, D. A. Horner, F. Martín and C. W. McCurdy, "First Principles Study of Double Photoionization of H<sub>2</sub> Using Exterior Complex Scaling", *J. Elec. Spectros., Rel. Phenom.* (submitted).

# Femtosecond X-ray Beamline for Studies of Structural Dynamics

Robert W. Schoenlein

Materials Sciences Division  
Lawrence Berkeley National Laboratory  
1 Cyclotron Rd. MS: 2-300, Berkeley, CA 94720  
rwschoenlein@lbl.gov

Roger W. Falcone (co-PI)

Physics Department, University of California, Berkeley  
rwf@physics.berkeley.edu

## Background and Program Scope

A grand challenge in condensed matter research is to understand the dynamic interplay between electronic structure (energy levels, charge distributions, bonding, spin) and atomic structure (coordination, bond distances, atomic arrangements) on the fundamental, ultrafast time-scales of atomic vibrational periods, electron-phonon, and electron-electron interactions. X-rays are ideal probes of atomic structure, and they also offer important advantages for probing electronic structure via transitions from element-specific core levels with well-defined symmetry. Thus, femtosecond x-rays are powerful tools for understanding chemical reaction dynamics (formation/dissolution of bonds, conformational changes), phase transitions in solids (involving atomic structure and/or electronic properties), and complex systems in which atomic and electronic degrees of freedom are strongly correlated. The development of ultrafast x-ray science to date has been limited by the lack of suitable tunable x-ray sources for probing structural dynamics on the femtosecond time scale. This research program is based on a novel approach for generating  $\sim 100$  fs x-ray pulses from a synchrotron storage ring by using femtosecond optical pulses to modulate the energy (and time structure) of a stored electron bunch.

The first phase of this program included the development of a simple femtosecond bend-magnet beamline (and associated time-resolved detection and measurement techniques) to serve as a proving ground for time-resolved x-ray science incorporating femtosecond laser systems and end stations suitable for x-ray diffraction, EXAFS, XANES, and photoionization. An important component of this initial phase has been the development of scientific applications using ultrafast x-rays focusing on: (i) ultrafast atomic and electronic phase transitions in crystalline materials, and (ii) light-induced structural changes in solvated molecules. The first phase of this research program culminates in FY06 with the construction and commissioning of a femtosecond undulator-based beamline at the Advanced Light Source, providing  $\sim 10^3$  increase in average femtosecond x-ray flux. The future focus of this research program (as part of the LBNL Ultrafast X-ray Science Laboratory) will be on understanding molecular dynamics and transition-state species of photoexcited molecules in solution.

## Recent Progress

### *Time-resolved XAS of Solvated Transition-Metal Complexes*

During the past year, we have completed and published the first picosecond time-resolved x-ray absorption (XAS) measurements of a spin-crossover reaction in a solvated transition-metal complex. The goal is to quantify the dynamic changes in the ligand bond distance and understand their role in facilitating the ultrafast the spin transition. Time-resolved

XAS measurements were made on the spin-crossover complex  $[\text{Fe}(\text{tren}(\text{py})_3)](\text{PF}_6)_2$ , dissolved in acetonitrile using ALS bend-magnet beamline 5.3.1. Static XAS measurements, at the Fe K-edge, on the low-spin parent compound and a high-spin analog,  $[\text{Fe}(\text{tren}(6\text{-Me-py})_3)](\text{PF}_6)_2$ , reveal distinct spectroscopic signatures for the two spin states in the x-ray absorption near edge structure (XANES) and in the x-ray absorption fine structure (XAFS). For the time-resolved studies, 100 fs pulses at 400 nm are used to initiate a charge transfer transition in the low spin complex. The subsequent electronic and geometric changes associated with the formation of the high-spin excited state are probed with 70 ps x-ray pulses tunable near 7.1 keV. Modeling of the transient XAS data reveals that the average Fe–N bond is lengthened by  $0.21 \pm 0.03 \text{ \AA}$  in the high-spin excited state relative to the ground state, and that the bond dilation occurs within 70 ps. This structural modification causes a change in the metal-ligand interaction reflected by the altered density of states of the unoccupied metal orbitals. Our results constitute the first direct measurements of the dynamic atomic and electronic structural rearrangements occurring during a photo-induced Fe(II) spin crossover reaction in solution.

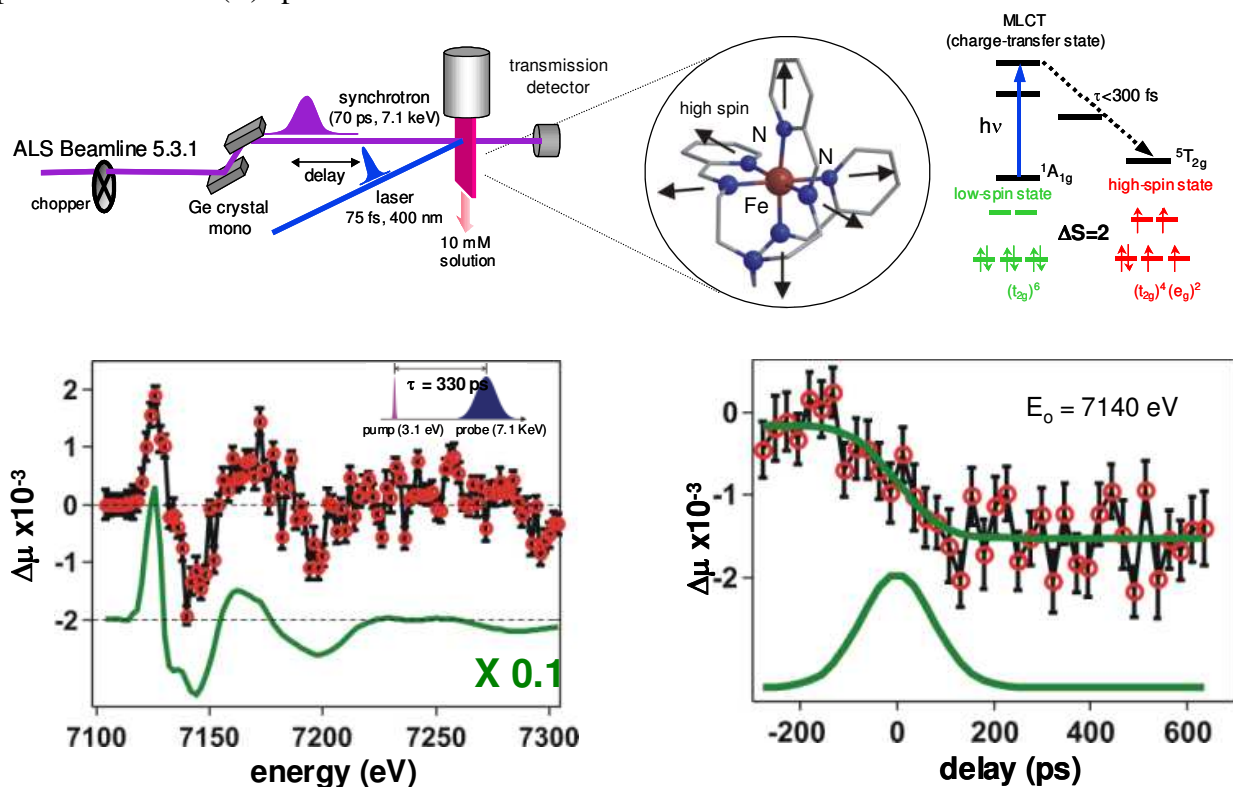


Figure 1. Top: experimental set up for time-resolved XAS measurements of  $\text{Fe}(\text{tren})_3$  in acetonitrile, model of the molecular complex, and simplified energy diagram of the low-spin and high-spin states, and the metal-ligand charge-transfer state. Bottom left: differential XAFS spectra at 300 ps delay, solid line is the differential EXAFS from the chemically stabilized high spin and low spin states. Observed changes are accounted for by a  $0.2 \text{ \AA}$  change in the Fe-N bond distance. Bottom right: time-resolved absorption at 7.14 KeV, indicating that the bond dilation occurs within the 70 ps resolution of the experiment.

### Ultrafast Soft X-ray Spectroscopy of Correlated Materials

We have completed the first direct observation of terahertz polariton propagation in  $\text{LiTaO}_3$  via femtosecond x-ray diffraction. Below  $\sim 900 \text{ }^\circ\text{C}$ ,  $\text{LiTaO}_3$  is ferroelectric, with a permanent  $c$ -axis structural distortion coupled to a permanent electric dipole. At terahertz frequencies, light couples with periodic lattice distortions around the ferroelectric equilibrium

positions, resulting in a phonon-polariton mode of  $A_1$  symmetry. Because of the reduced symmetry of the ferroelectric phase,  $\text{LiTaO}_3$  also has a large optical nonlinearity, thus femtosecond visible pulses can be used to generate terahertz radiation by means of impulsive stimulated Raman scattering (ISRS). We have applied time-resolved x-ray diffraction (using femtosecond x-rays from ALS bend-magnet beamline 5.3.1) to directly measure the transient ion displacements associated with the propagating polaritons. Thus, amplitude and phase of all degrees of freedom in a light field are directly measured in the time domain.

### ***Ultrafast X-ray Beamline Development***

A new undulator-based ultrafast x-ray beamline is now being constructed and commissioned at the ALS. The beamline consists of a 1.5 T undulator/wiggler providing femtosecond x-rays for two branchlines: a soft x-ray branchline operating in the 0.3-2 keV range, and a hard x-ray branchline operating in the 2-10 keV range. The soft x-ray branchline includes a spectrograph providing  $<0.5$  eV resolution for single-wavelength experiments, and  $\sim 100$  eV bandwidth for dispersive spectroscopic measurements. The hard x-ray branchline includes a double-crystal monochromator providing  $\sim 2$  eV resolution. Associated with the beamlines is a high repetition rate (20 KHz) femtosecond laser system with an average power of  $\sim 50$  W. The average flux from this beamline is expected to be  $\sim 10^7$  ph/sec/0.1% BW (with roughly 100x increase in flux from the insertion device relative to the current bend-magnet, and another 10x increase over the present laser repetition rate). The beamline will provide  $\sim 200$  fs duration x-ray pulses for a wide range of experiments in ultrafast x-ray science.

Commissioning of the soft x-ray beamline is nearly complete. The performance of the undulator and spectrometer (flux, throughput, energy resolution, tuning etc.) has been characterized. Femtosecond x-rays have been generated from the beamline, and further characterization (flux, background etc.) is in progress.

### **Future Plans**

The near-term priority is the construction of the hard x-ray branchline, expected to be complete in September 2006. Commissioning of the hard x-ray branchline, and remaining commissioning work on the soft x-ray branchline, will be done in the fall of 2006. The soft x-ray branchline will enable XANES studies of transition-metal molecular complexes. Initial experiments will focus on studies of electronic structural dynamics in  $\text{Fe}^{\text{II}}$  at the Fe L-edge, which will provide direct information about hybridization of the Fe  $d$  orbitals and influence of the ligand field. A particular challenge for these studies will be the development of thin ( $<1$   $\mu\text{m}$ ) liquid cell, necessary to allow transmission of soft x-rays. This capability will be directly relevant for other soft-x-ray absorption studies of solvated molecules.

Completion of the hard x-ray branchline will enable femtosecond EXAFS measurements of solvated molecules. Initial work will focus on transition-metal spin-crossover complexes. With femtosecond resolution, we can directly probe the dynamic distortion of the ligand bonds and begin to understand how the atomic structural dynamics are correlated with the electronic spin dynamics. EXAFS studies of photodissociation in Co-based metal carbonyls will be used to understand the transient solvent substitution in the intermediate molecular structures. Related hard x-ray and soft x-ray spectroscopy studies in aqueous  $\text{ClO}_2$  and halogen-bridge complexes will reveal transient molecular species in the transition state region. Also of future interest are linear-chain mixed-valence transition-metal molecular complexes (e.g.  $[\text{Pt}(\text{C}_2\text{H}_8\text{N}_2)_2\text{I}_2][\text{Pt}(\text{CN})_4]$ ). Here time-resolved diffraction may be used to understand the

coherent Pt-I vibration (Peierls distortion) associated with photoexcitation and subsequent formation of the self-trapped exciton.

### Publications from DOE Sponsored Research (2003-2006)

- T.E. Glover, G.D. Ackerman, A. Belkacem, P.A. Heimann, Z. Hussain, R.W. Lee, H.A. Padmore, C. Ray, R.W. Schoenlein, W.F. Steele, and D.A. Young, "Metal-insulator transitions in an expanding metallic fluid: particle formation kinetics," *Phys. Rev. Lett.*, **90**, pp.236102/1-4, (2003).
- A.Cavalleri and R.W. Schoenlein, "Femtosecond x-ray studies of lattice dynamics in solids," in **Ultrafast Dynamical Processes in Semiconductors**, ed. by K.T. Tsen, *Topics in Applied Physics Series No. 92*, Springer Verlag, (2004).
- M. Saes, C. Bressler, F. van Mourik, W. Gawelda, M. Kaiser, M. Chergui, D. Grolimund, R. Abela, T.E. Glover, P.A. Heimann, R.W. Schoenlein, S.L. Johnson, A.M. Lindenberg, and R.W. Falcone, "A setup for ultrafast time-resolved x-ray absorption spectroscopy", *Rev. Sci. Inst.*, **75**, pp. 24-30, (2004).
- P. A. Heimann, H. A. Padmore, and R. W. Schoenlein, "ALS Beamline 6.0 For Ultrafast X-ray Absorption Spectroscopy", in **Synchrotron Radiation Instrumentation**, T. Warwick, J. Author, H.A. Padmore, and J. Stohr Eds., AIP Conf. Proc. 705, 1407 (2004).
- R. W. Schoenlein, A. Cavalleri, H. H. W. Chong, T. E. Glover, P. A. Heimann, A. A. Zholents, and M. S. Zolotarev, "Generation of Femtosecond Synchrotron Pulses: Performance and Characterization", in **Synchrotron Radiation Instrumentation**, T. Warwick, J. Author, H.A. Padmore, and J. Stohr Eds., AIP Conf. Proc. 705, 1403 (2004).
- A. Cavalleri, H.H.W. Chong, S. Fourmaux, T.E. Glover, P.A. Heimann, J.C. Kieffer, B.S. Mun, H.A. Padmore, and R.W. Schoenlein, "Picosecond soft x-ray absorption measurement of the photo-induced insulator-to-metal transition in VO<sub>2</sub>," *Phys. Rev. B*, **69**, 153106 (2004).
- A. Cavalleri, H.H.W. Chong, S. Fourmaux, T.E. Glover, P.A. Heimann, J.C. Kieffer, H.A. Padmore, R.W. Schoenlein, "Femtosecond Near Edge X-ray Absorption Measurement of the VO<sub>2</sub> Phase Transition", in **Ultrafast Phenomena XIV**, Springer Series in Chemical Physics **79**, T. Kobayashi, T. Okada, T. Kobayashi, K.A. Nelson, S. De Silvestri, Eds., Springer-Verlag, p. 343, (2004).
- A.Cavalleri, M. Rini, H.H.W. Chong, S. Fourmaux, T.E. Glover, P.A. Heimann, J.C. Kieffer, R.W. Schoenlein, "Band-Selective Measurements of Electron Dynamics in VO<sub>2</sub> Using Femtosecond Near-Edge X-Ray Absorption," *Phys. Rev. Lett.*, **95**, 067405 (2005).
- M. Zolotarev, R.W. Schoenlein, A.A. Zholents, "Beam slicing by femtosecond laser" in **Femtosecond Beam Science**, M. Uesaka Ed., Imperial College Press, p. 202 (2005).
- M. Khalil, M.A. Marcus, A.L. Smeigh, J.K. McCusker, H.H.W. Chong, and R.W. Schoenlein, "Picosecond x-ray absorption spectroscopy of a photoinduced iron(II) spin crossover reaction in solution," *J. Phys. Chem. A*, **110**, pp. 38-44 (2006).
- A.Cavalleri, M.Rini, R.W. Schoenlein, "Ultra-broadband femtosecond measurements of the photo-induced phase transition in VO<sub>2</sub>: From the mid-IR to the hard x-rays" *J. Phys. Soc. Jap.*, **75**, p. 011004, (2006).
- J.M. Byrd, Z. Hao, M.C. Martin, D.S. Robin, F. Sannibale, R.W. Schoenlein, A.A. Zholents, and M.S. Zolotarev, "Tailored Terahertz Pulses from a Laser-Modulated Electron Beam," *Phys. Rev. Lett.*, **96**, 164801, (2006).
- A. Cavalleri, S. Wall, C. Simpson, E. Statz, D.W. Ward, K.A. Nelson, M.Rini, and R.W. Schoenlein, "Femtosecond X-ray Diffraction from Phonon-polaritons in LiTaO<sub>3</sub>: Lattice Dynamics in the Electronic Ground State of a Ferroelectric," *Nature*, in press, (2006).
- J. M. Byrd, Z. Hao, M. C. Martin, D.S. Robin, F. Sannibale, R.W. Schoenlein, A. A. Zholents, M.S. Zolotarev, "Laser seeding of the storage ring microbunching instability for high-power coherent terahertz radiation," *Phys. Rev. Lett.*, in press, (2006).

**ATOMIC AND MOLECULAR PHYSICS RESEARCH  
AT  
OAK RIDGE NATIONAL LABORATORY**

David R. Schultz, Group Leader, Atomic Physics  
[schultzd@ornl.gov]  
ORNL, Physics Division, P.O. Box 2008  
Oak Ridge, TN 37831-6372

**Principal Investigators**

H. Aliabadi,\* E. Bahati,\* M. E. Bannister, M. R. Fogle, Jr.\* C. C. Havener,  
H. F. Krause, J. H. Macek, F. W. Meyer, C. Reinhold, D. R. Schultz,  
C. R. Vane, L. I. Vergara,\* and H. Zhang\*

\*Postdoctoral Fellow

The OBES atomic physics program at ORNL has as its overarching goal the understanding of states and interactions of atomic-scale matter. These atomic-scale systems are composed of multiply-charged ions, charged and neutral molecules, atoms, atomic ions, electrons, solids, and surfaces. Particular species and interactions are chosen for study based on their relevance to gaseous or plasma environments of basic energy science interest such as those in fusion energy, atmospheric chemistry, and plasma processing. Towards this end, the program has developed and operates the Multicharged Ion Research Facility (MIRF) which has recently undergone a broad, multi-year upgrade. Work is also performed as needed at other facilities such as ORNL's Holifield Radioactive Ion Beam Facility (HRIBF) and the CRYRING heavy-ion storage ring in Stockholm. Closely coordinated theoretical activities support this work as well as provide leadership in complementary or synergistic research.

**The MIRF Upgrade Project** – *F. W. Meyer, M. E. Bannister, M. R. Fogle, J. W. Hale, C. C. Havener, H. F. Krause, and C. R. Vane*

A major facility upgrade of the ORNL Multicharged Ion Research Facility (MIRF) has been completed during the past year.<sup>1</sup> The installation of the 250-kV high-voltage platform with a new all-permanent magnet ECR ion source, and a new beamline switchyard for transporting the higher energy beams to on-line experiments was completed in January 2005. Routine delivery of high-energy beams to online experiments commenced shortly thereafter. The relocation and reconfiguration of the present CAPRICE ECR ion source for injecting extracted beams into a floating beamline to permit deceleration to energies as low as a few eV x q was completed in February 2006. Routine operation of the low energy beamline started the following month. With the two sources, the range of energies available at MIRF has been expanded to more than five orders of magnitude.

The energy range between 25 – 250 x q keV is at present virtually inaccessible for highly charged ion collision experiments requiring beam intensities in the particle- $\mu$ A range. With the completion of the MIRF upgrade, a broad range of new experiments involving high charge state ions are now possible in this energy range. In addition, all the currently online experiments at MIRF benefit from the higher energy beam capability developed by this project.

With the new floating beamline, keV-energy beams can be transported with high efficiency to end stations at ground potential and then decelerated there to a few eV x q (where q is the charge state of the ion of interest), using efficient ion optics already developed for the MIRF floating ion-surface interaction experiment.

Monitoring and control functions for the floating beamline are achieved via Group 3 ControlNet hardware originally used for the EN Tandem control system, and a Dell Optiplex PC-hosted PCI loop controller. HV isolation is achieved via fiber optic cables. All devices are integrated into a Labview-based distributed supervisory control and data analysis (SCADA) system which provides device independent, uniform access to all hardware via a LuaView real-time database. A complete LabVIEW/LuaVIEW database driven SCADA system is freely available as open source and was therefore straightforward to implement.

The enhanced low-energy capability provided by the new beamline makes possible investigations of many new low-energy heavy particle interactions. These include single, multiple, and dissociative low-energy electron capture, lifetime studies of metastable electronically excited MCI's, measurements of X-ray emission and surface modification in low energy MCI-surface interactions, and investigations of plasma wall interactions of relevance to present and future fusion plasma experiments.

1. F. W. Meyer, M. E. Bannister, D. Dowling, J. W. Hale, C. C. Havener, J. W. Johnson, R. C. Juras, H. F. Krause, A. J. Mendez, J. Sinclair, A. Tatum, C. R. Vane, E. Bahati Musafiri, M. Fogle, R. Rejoub, L. Vergara, D. Hitz, M. Delaunay, A. Girard, L. Guillemet, and J. Chartier, Nucl. Instrum. Meth. Phys. Res. **B242**, 71 (2006).

**Low-Energy Ion-Surface Interactions** – *F. W. Meyer, H. F. Krause, L. I. Vergara, and H. Zhang*

There is significant technological interest in using graphite as a plasma-facing component on present and future fusion devices, and in using different types of graphite or carbon fiber composites (CFC's), together with tungsten, beryllium, or other refractory metals, in the ITER divertor. Motivated in part by this interest, an experimental research program was recently started at the ORNL Multicharged Ion Research Facility (MIRF) to investigate chemical sputtering of graphite surfaces in the limit of very low impact energies (i.e. below 10 eV/D), where there is currently no available experimental data, and which is the anticipated regime of operation of the ITER divertor.

The experimental approach uses a sensitive quadrupole mass spectrometer which monitors the partial pressures of selected mass species in the range 1 – 60 amu present in the scattering chamber. A Macintosh-based data acquisition system is used to measure mass distributions at fixed intervals in time, or alternatively, to follow the intensities of selected mass peaks as function of beam exposure times. The evolution of the detected intensities of hydrocarbon species such as CD, CD<sub>2</sub>, CD<sub>3</sub>, CD<sub>4</sub>, C<sub>2</sub>D<sub>2</sub>, C<sub>2</sub>D<sub>4</sub>, and C<sub>2</sub>D<sub>6</sub> is followed as a function of accumulated beam dose until saturation in their intensities occurs. Calibrated hydrocarbon leaks are used to determine absolute yields of the sputtering products of interest.

The energies investigated so far span the range 4 – 250 eV/D. At the lower energies, comparisons have been made of the methane and acetylene production yields for equal velocity D<sup>+</sup>, D<sub>2</sub><sup>+</sup>, and D<sub>3</sub><sup>+</sup> incident on ATJ graphite, currently used on the DIII-D machine. We found factors of two differences below 60 eV/D, with the atomic projectile, i.e. D<sup>+</sup>, having the smallest yields and D<sub>3</sub><sup>+</sup> projectiles the biggest. At higher energies, where immediate dissociation of incident molecular projectiles is highly probable, the observed yields for equivelocity incident atomic and molecular ions are the same. It is speculated that at the lower energies, dissociation most likely occurs later in the projectile slowing in the bulk. The higher mass of the undissociated molecules may enhance the kinetically assisted desorption of sputter products, thereby increasing the observed yields. Similar mass effects have been observed when comparing yields for equivelocity H<sup>+</sup> and D<sup>+</sup> incident projectiles.

In addition to ATJ graphite, we have investigated chemical sputtering of HOPG in the energy range 12 – 100 eV/D. Comparative measurements were performed for surfaces oriented parallel

and perpendicular to the graphite basal planes, thereby probing the effect on sputter yields of differences of sputter product diffusion back to the surface, and the extent of amorphization that occurs during the hydrogenation phase. While no differences in sputter yields were found below 25 eV/D, at the higher energies, the methane production yield for an HOPG sample having the basal plane orientation perpendicular to the surface became progressively larger than that for a sample having basal planes parallel to the surface. This suggests that complete amorphization of the samples has not occurred, and that diffusion of methane produced at the end-of-range depths of the incident projectiles is enhanced in the direction along the 3.3 Å separated basal planes. These results will also serve to benchmark in-house molecular dynamics simulations efforts using REBO and AIREBO interatomic potentials that were initiated during the past year by P. Krstic and R. Reinhold of our group.

**Low-Energy Charge Exchange using the Upgraded Ion-Atom Merged-Beams Apparatus** –  
*C. C. Havener and C. R. Vane*

The Ion-Atom Merged-Beams Apparatus is used to measure benchmark absolute charge exchange cross sections for multicharged ions on neutral atoms from keV/u down to meV/u.<sup>1</sup> The apparatus has been upgraded and moved to accept beams from the High Voltage Platform. Upgrades to the merged-beams apparatus include a dual rotating-wire scanner which provides more accurate beam profiles and a shortened merge-path to increase the angular acceptance of the apparatus. The beam profiles from the dual wire scanner, developed at MIRF, give a real-time position and divergence of the overlapped beams and have proven critical tool for beam tuning. The upgraded apparatus can now collect the unusually high angular scattering of the reaction products recently found for He<sup>2+</sup> + H collisions.<sup>2</sup> A high transmission beam line from the HV Platform and the new spherical sector electrostatic mergers provide an observed factor of four decrease in the angular divergence of the ion beam. This translates into a significant improvement in the collision energy uncertainty and allows access to lower energies with higher resolution. The higher velocity ion beams permit charge exchange measurements with heavier ions and measurements with both H and D at eV/u energies and below to directly observe the isotope effect.<sup>3,4</sup> The new apparatus is being tested using the N<sup>2+</sup> + H (and D) collision system. N<sup>2+</sup> ion currents of 35 uA have been tuned through the apparatus, a factor of five greater than the previous configuration using the Caprice ECR ion source. Measurements will be made with both H and D to explore an unusual prediction of recent molecular coupled-channel theory. For this system the cross section is predicted to decrease below ~10 meV/u with little or no isotope effect.

ECR source development is underway to provide the required intense H-like and fully-stripped ion beams. Up to 5 uA of H-like O has been produced on the HV platform. The intense beams will be used to perform a benchmark study of low-energy charge exchange for fully stripped and H-like ions on atomic hydrogen. While there have been numerous studies at keV/u energies there is a real lack of state-selective data and appropriate quantal theory at eV/u energies and below. X-ray emission measurements are planned for a variety of bare and H-like ions (e.g., C, N, O) + H. For charge transfer at low energies, capture to non-statistical angular momentum states leads to observable signatures in the subsequent X-ray emission. Such measurements are possible using a high efficiency detector mounted directly above the merge path. The sounding rocket X-ray calorimeter at the University of Wisconsin<sup>5</sup> is being considered for these measurements. The X-ray detector is characterized by a high-energy resolution (5 – 12 eV FWHM) along with high throughput (1000 times greater than dispersive X-ray detectors).

1. C. C. Havener, *The Physics of Multiply Charged Ions*, Vol. 2, Kluwer Academic Publishers, The Netherlands, 2003, pp. 193-21.
2. C. C. Havener, R. Rejoub, P. S. Krstic, and A. C. H. Smith, *Phys. Rev. A* **71**, 042707 (2005).

3. C. C. Havener, R. Rejoub, C. R. Vane, H. F. Krause, D. W. Savin, M. Schnell, J. G. Wang, and P. C. Stancil, *Phys. Rev. A* **71**, 034702 (2005).
4. C. C. Havener and R. Rejoub, to be published in the invited *Proceedings, International Conference on Photonic, Electronic, and Atomic Collisions*, Rosario, (World Scientific).
5. McCammon *et al.*, *Astrophys. J* **576**, 188 (2002).

**Electron-Molecular Ion Interactions** – *M. E. Bannister, C. R. Vane, E. Bahati, M. Fogle, and H. Aliabadi*

Electron-molecular ion recombination, dissociation, and excitation and ionization processes are important from a fundamental point of view, especially in that they provide a testable platform for investigating and fully developing our understanding of the mechanisms involved in electronic energy redistribution in fragmenting many-body quantum mechanical systems. These processes are also important practically in that electron-ion collisions are in general ubiquitous in plasmas and molecular ions can represent significant populations in low to moderate temperature plasmas. Neutral and charged radicals formed in dissociation of molecules in these plasmas represent some of the most highly reactive components in initiating and driving further chemical reaction pathways. Thus electron-molecular ion collisions are important in determining populations of some of the most reactive species in a wide variety of environments, such as the diverter edge regions in fusion reactors, plasma enhanced chemical vapor deposition reactors, environments where chemistries are driven by secondary electron cascades, for example in mixed radioactive waste, the upper atmospheres of planets, and cooler regions of the solar or other stellar atmospheres. To correctly model these environments it is absolutely essential to know the strengths (cross sections and rates), branching fractions, and other kinematical parameters of the various possible relevant collision processes.

***Dissociative Excitation and Ionization:*** Measurements of cross sections for electron-impact dissociative excitation (DE) and dissociative ionization (DI) of molecular ions have continued using the MIRF crossed-beams apparatus.<sup>1</sup> The dissociation of  $N_2H^+$  ions forming  $NH^+$  and  $N^+$  fragments has been investigated in a complementary experiment to dissociative recombination (DR) studies undertaken by our collaborators at CRYRING.<sup>2</sup> The cross sections are fairly flat in the 30-100 eV range, but some structure is apparent around 20 eV. In addition, experiments have continued for the  $CH_3^+$  target ion with measurements completed for the  $CH^+$  and  $C^+$  ion fragment channels; cross sections for the  $C^+$  channel exhibited a smooth energy dependence over the 3–100 eV range of the measurements with no apparent resonance features. However, a resonance-like feature is observed near 20 eV in the  $CH^+$  fragment channel, similar to the structure observed in the cross section for dissociation of  $DCO^+$  ions producing  $CO^+$  ions<sup>3</sup> and for the production of  $CH^+$  from the dissociation of  $CH_2^+$ .<sup>4</sup>

The dissociation experiments discussed above used molecular ions produced by the ORNL MIRF Caprice ECR ion source,<sup>5</sup> but other cooler sources will also be used in order to understand the role of electronic and ro-vibrational excited states. A second ion source, a hot-filament Colutron ion source, is presently online and expected to produce fewer excited molecular ions. An even colder pulsed ion source, very similar to the one used for measurements<sup>6</sup> on the dissociative recombination of rotationally cold  $H_3^+$  ions at CRYRING, is under development for use at the ORNL MIRF. Additionally, work continues on a similar supersonic source that uses a piezoelectric mechanism for more reliable pulsed valve operation. With this range of ion sources, one can study dissociation with both well-characterized cold sources and with hotter sources that better approximate the excited state populations in plasma environments found in applications such as fusion, plasma processing, and aeronomy.

1. M. E. Bannister, H. F. Krause, C. R. Vane, N. Djuric, D. B. Popovic, M. Stepanovic, G. H. Dunn, Y.-S. Chung, A. C. H. Smith, and B. Wallbank, *Phys. Rev. A* **68**, 042714 (2003).
2. W. D. Geppert, R. Thomas, J. Semaniak, A. Ehlerding, T. J. Millar, F. Österdahl, M. af Ugglas, N. Djuric, A. Paál, and M. Larsson, *Astrophys. J.* **609**, 459 (2004).
3. E. M. Bahati, R. D. Thomas, C. R. Vane, and M. E. Bannister, *J. Phys. B* **38**, 1645 (2005).
4. C. R. Vane, M. E. Bannister, and R. Thomas, XXIII ICPEAC Abstracts, Stockholm, Sweden (2003).
5. F. W. Meyer, in *Trapping Highly Charged Ions: Fundamentals and Applications*, edited by J. Gillaspay (Nova Science, Huntington, NY, 1997), p. 117.
6. B. J. McCall *et al.*, *Nature* **422**, 500 (2003).

**Dissociative Recombination:** The process of dissociative recombination (DR) of relatively simple three-body molecular ions is being studied in our ongoing collaboration with Prof. Mats Larsson and colleagues at the Manne Siegbahn Laboratory (MSL), Stockholm University. Absolute cross sections, branching fractions, and measurements of the dissociation kinematics, especially of the three-body breakup channel, are being investigated at zero relative energy for a variety of light and heavy vibrationally-cold triatomic di-hydrides and other molecular ions with three-body channels. This research is carried out using the MSL CRYRING heavy ion storage ring facility, which is still expected to continue to be available for our electron-molecular ion measurements at least into calendar year 2007.

In the last year, we have continued studies of the systems  $D_5O_2^+$  and  $O_3^+$ . These experiments are a continuation of previous measurements concerning the DR of similar molecules, such as  $H_2O^+$ ,  $NH_2^+$ ,  $CH_2^+$ , and  $SD_2^+$  that have all revealed three-body break-up as the dominant reaction channel.<sup>1-5</sup> In order to study the three body break-up dynamics in detail, a high-resolution imaging technique is used to measure the displacement of the fragments from the center of mass of the molecule.<sup>6</sup> The displacement is related to the kinetic energy of the fragments and therefore information about the dynamics involved in the process can be obtained, i.e., the internal state distribution of the fragments. These event-by-event measurements yield information about how the kinetic energy is distributed between the two light fragments and the angular distribution of the dissociating molecules. In all of the triatomic di-hydride systems previously studied, the branching fractions showed very roughly (7:2:1) ratios for ( $X + H + H$ ;  $XH + H$ ;  $X + H_2$ ), while the observed energy sharing and angular distributions of the three-body breakup product channel could depend heavily on the structure, bonding and charge centre of the parent molecular ion. In contrast to these previously studied di-hydride systems,  $D_5O_2^+$  provides an excellent opportunity for investigating the role played by internal states of fragments in the DR process. The branching results indicate that the  $D_2O + D + D_2O$  channel contributes more than 95% of the DR. This is significantly higher than for the comparable channel in the DR of  $H_5O_2^+$ . One possible explanation is that the DR of  $D_5O_2^+$  can proceed through the  $D_2O + D_3O$  channel, whereas the  $H_3O$  channel is not possible for  $H_5O_2^+$ . For the DR of  $D_5O_2^+$ , the energy available to the products is approximately 5 eV; for ground state fragments this would mean 5 eV of kinetic energy, mostly given to the single D atom. Analysis of our imaging measurements, however, suggests that this is not the case, but instead that a significant portion (up to 3 eV) of the available energy is used in internal excitation of the  $D_2O$  molecules. Since this is below the first electronic excited state of  $D_2O$ , the internal energy must be in ro-vibrational levels of the ground state. For the  $O_3^+$  system, branching fractions show that approximately 94% of DR events lead to three separate O atoms, consistent with the dominance of the three-body channels observed in DR of di-hydride ions. This finding would have a significant impact on models of atmospheric chemistry where DR plays a crucial role by producing excited O atoms. Analysis of the imaging data for the  $O_3^+$  system indicates that the process yielding two  $^3P$  ground-state O atoms and one  $^1D$  excited O atom occurs almost half the time, with the other dissociations leading to either three ground-state

O atoms (30%) or one ground-state and two  $^1\text{D}$  excited O atoms (23%). Absolute DR cross sections have also been measured in the 0-1 eV range for both  $\text{D}_5\text{O}_2^+$  and  $\text{O}_3^+$ .

Preliminary investigations of DR of molecular ions using the fragment imaging technique have commenced on the merged electron-ion beams energy-loss apparatus<sup>7</sup> at ORNL. Future experiments will also include measurements of absolute DR cross sections using solid-state detectors. These studies are made possible by the recent construction of a 250-kV high-voltage platform with an all-permanent magnet ECR ion source at the ORNL MIRF. The cold molecular ion sources discussed above are also being adapted for use on the HV platform.

1. R. Thomas *et al.*, Phys. Rev. A **71**, 032711 (2005).
2. M. Larsson and R. Thomas, Chem. Phys. **3**, 4471 (2001).
3. Å. Larson *et al.*, Astrophys. J. **505**, 459 (1998).
4. S. Rosén *et al.*, Faraday Discussions **115**, 295 (2000).
5. F. Hellberg *et al.*, J. Chem. Phys. **122**, 224314 (2005).
6. R. Thomas *et al.*, Phys. Rev. A **66**, 032715 (2002).
7. E. W. Bell *et al.*, Phys. Rev. A **49**, 4585 (1994).

### **Grazing Surface Studies at Intermediate Energy** – *H. F. Krause, C. R. Vane, and F. W. Meyer*

This work is part of the larger beam-surface effort at the ORNL MIRF that seeks to develop a fundamental understanding of neutralization, energy dissipation and sputtering processes that occur when singly and multiply charged atomic and molecular ions interact with metal, semiconductor, and insulator surfaces.

We have performed experimental investigations of the transport, angular scattering, charge exchange and energy loss of low-energy (5-20 keV/q), multicharged ions in anodic nanocapillary arrays. Our studies of ions transmitted through aligned nanopores in an  $\text{Al}_2\text{O}_3$  insulator substrate have yielded some surprising new information that can be explained simply<sup>1</sup> (see abstract of H. F. Krause in this document). The arrays can be used to attenuate and steer highly charged ion beams.<sup>2</sup>

A new high-voltage platform installed at the ORNL Multicharged Ion Research Facility (MIRF) has extended the energy range of ions available for experimental investigations of their interactions with electrons, atoms, molecules, and solid surfaces.<sup>3</sup> We are installing a new beamline and end station that will enable multiple-parameter coincidence grazing surface studies to be performed at energies up to 250 keV/q. It will be possible to uniquely identify scattered charge states, emitted electrons, states involved in Auger processes, photons, and products sputtered from the surface that arise in the same collision event.

Initial studies will focus on the interaction of ions near crystalline insulator surfaces where less detailed information is available. We plan to probe “hollow atom” states formed in the proximity of a LiF surface using fast multiply charged projectiles (e.g.,  $\text{He}^{2+}$  and  $\text{Li}^{3+}$ ) in the 25–100-keV/u range. Using time-coincidence techniques, the ultra-grazing experiments will also provide state-selected information about coherent and incoherent processes such as projectile excitation, de-excitation and electron emission induced by projectile motion in the periodic electric fields<sup>4</sup> near the crystal surface (e.g., resonant coherent excitation resonances by a repetitive pulse train in the femtosecond to attosecond regime). This technique should allow a small portion of the full ion-surface grazing path length to be selectively probed. Singly and doubly excited states of ions formed above the surface will be investigated.

The beamline will be used also to extend our previous studies of  $\text{Al}_2\text{O}_3$  nanoscale capillaries and to investigate arrays of aligned carbon nanotubes using multiply charged atomic ions in a broad range of incident energies up to 250 keV/q. These coincidence studies will yield fundamental information on electron or photon production processes in addition to the ion

scattering, energy transfer, and charge-changing processes studied in our recent nanocapillary research.

1. H. F. Krause, C. R. Vane and F. W. Meyer, submitted to Phys. Rev. A (2006).
2. H. F. Krause, C. R. Vane, F. W. Meyer, and H. M. Christen, *13<sup>th</sup> International Conference on the Physics of Highly Charged Ions*, Belfast, N.I., 2006 (in press).
3. F. W. Meyer *et al.*, Nucl. Instrum. Meth. Phys. Res. B **242**, 71 (2006).
4. Herbert F. Krause and Sheldon Datz, "Channeling Heavy Ions through Crystalline Lattice," *Advances in Atomic, Molecular, and Optical Physics*, Ed. B. Bederson, Academic Press, Inc. (1966), pp. 139-180.

**Atomic Ion-Atom and Molecular Ion-Atom Electron Transfer** – C. R. Vane, H. Aliabadi, E. Bahati, M. E. Bannister, M. R. Fogle, C. C. Havener, and H. F. Krause

In low- to moderate-energy ion-atom collisions electron transfer from target to projectile bound states dominates ionization. Access to accurate, reliable data for such processes is central to understanding and accurate modeling of many important plasma environments. Formation of excited final states produced in electron capture from the neutral beams injected into fusion plasma devices leads to radiative cascades and the photon emission is routinely used to diagnose impurity ion concentrations and velocity profiles in fusion plasmas.<sup>1-3</sup> Similarly, x-ray diagnostics of upper terrestrial atmospheric, as well as astrophysical and cometary, photoionized plasmas depend on reliable cross sections.<sup>4</sup> Essential to all of these applications and many others is the accurate prediction of state-selective electron capture cross sections involving highly charged ions.

Projectile energy gain spectroscopy has historically been the most commonly used technique to measure the inelastic energy transfer (the  $Q$ -value) in a collision, which is directly related to the target and projectile initial and final states.<sup>5</sup> Within the last decade, however, cold-target recoil-ion momentum spectroscopy (COLTRIMS) has developed into a rather mature technology and is now the method of choice for many investigations of electron capture and ionization processes.<sup>6-11</sup> COLTRIMS enables simultaneous  $Q$ -value and projectile scattering angle measurements, both obtained with  $4\pi$  solid angle efficiency through momentum spectroscopy of the target recoils. This technique can be used to perform kinematically complete experiments for electron-capture processes, especially at low collision energy. Since the resolution depends only to second order on the momentum spread of the incoming projectile, COLTRIMS permits relatively simple high-resolution  $Q$ -value measurements. With sufficient resolution, events involving projectiles carrying excess energy (metastable excited-state ions) can be separated, enabling independent studies of electron capture with ground-state versus metastable ions, as well as providing a means for examination of the incident metastable fractions. Another important and unique feature of the COLTRIMS technique is its intrinsic capability to measure prompt characteristics of the collision. The recoil ion final vector momentum is determined by the collision dynamics from the very beginning of the interaction, relatively unaffected by various postcollision effects occurring in separated components, such as radiative decay or autoionizing evolution of the projectile or target after the collision. All these features make COLTRIMS a very powerful tool, which we will exploit for high resolution measurements of differential cross sections in state-selective electron capture.

The ORNL COLTRIMS apparatus, originally developed for use in high-energy atomic collisions research at the EN Tandem facility,<sup>12</sup> has been modified and installed on a relatively mobile, multi-purpose end station for studies employing both the high- and low-energy ion beam sources at the upgraded MIRF facility. It will be employed in a variety of experiments, including measurements of state-selective ion-atom electron capture, as well as measurements of dissociative electron transfer by molecular ions interacting with atomic targets. The former is

complimentary to our merged ion-atom electron capture work at lower energies, while the latter compliments our ongoing research involving interactions of free electrons with molecular ions.

***State-Selective Electron Capture by Multiply-Charged Ions:*** Multiply-charged low-energy ions from the Caprice ECR source, or higher energy ions from the 250-kV high-voltage platform ECR will be crossed at 90 degrees with cold supersonic He, Ne, and Ar targets, (or with highly-collimated H, Na, or Cs atomic target beams) in the COLTRIMS apparatus. Charge-changed projectiles will be electrostatically separated and counted downstream, in either a position-sensitive MCP detector or a fast, high-count rate (MHz), discrete dynode electron multiplier detector. X-rays emitted from charge-changed projectile ions formed by electron capture to excited states ( $n,l$ ) will be measured in a windowless x-ray detector. Recoil ions formed by electron capture to the projectiles will be analyzed using the COLTRIMS apparatus and counted in a MCP position-sensitive recoil detector. Extra electrons ejected into the continuum in target multiply-ionizing processes can also be measured. By analyzing the COLTRIMS data and identifying particular  $Q$ -value collision events, the cross sections for electron transfer to specific states of the projectiles will be measured as a function of collision energy. Similarly, studies of metastable fractions in the incident ECR-produced ion beams will be implemented as a diagnostic technique using high-resolution  $Q$ -value measurements for identification of electron-capture fractions proceeding via these states. Knowledge of the inherent metastable ion fractions present in the incident ions is important in a number of the MIRF studies outlined here.

***Dissociative Electron Capture of Molecular Ions:*** This research will involve measurements of electron capture from target atoms by projectile molecular ions, leading to molecular dissociation to neutral and/or ionic fragments. The process, labeled dissociative charge exchange or Dissociative Electron Capture (DEC) of molecular ions, has a long history, and has been pursued using a number of techniques.<sup>13-17</sup>

Cool, dense sub-regions of plasmas, far from equilibrium, present complex environments in which there may be significant populations of all the available components; i.e., of the constituent neutral atoms, molecules, and their ions, as well as a variety of their neutral and ionic fragments. Such environments naturally arise in a number of plasma-to-gas or plasma-to-surface transition regions, such as in plasma processing reactors and at the diverter edges of fusion plasma containment devices. The neutral components can present significant target densities for collisions with electrons and both atomic and molecular ions. Fragmentation of molecular ions through DEC processes provides a channel for production of highly reactive neutral and ionic species.

There have been several studies of DEC and DECI (in which the target atom is multiply ionized) of molecular hydrogen ions. Saito *et al.*,<sup>16</sup> have used a COLTRIMS-like, recoil-time-of-flight technique along with simultaneous 3D neutral fragment imaging to measure DECI of 20-keV  $H_2^+$  with an Ar target. The measurements for simple DEC indicate that the H-atom fragments dissociate isotropically in the center of mass. However, DECI dissociation is observed to yield highly anisotropic emission of the H-atom fragments, indicating a DECI preference for specifically oriented molecular ions at the time of collisional neutralization, interpreted as evidence for DECI proceeding primarily through three-body close collisions among the fragments and target atoms.

The ORNL COLTRIMS end station has been fitted with a fragment imaging detector system permitting multi-hit detection and position sensitive capability for studies of DEC. Measurements will be performed for DEC by diatomic and simple tri-atomic molecular ions, and the results compared with branching fractions and kinematics observed for dissociative recombination, dissociative excitation and dissociative ionization measured for similar ion species. Atomic beams sources will also be added later to the apparatus to permit DEC from

highly collimated beams of H, H<sub>2</sub>, Li, Na, and Cs. The COLTRIMS technique will be employed to differentiate events arising according to the initial states of the bound target electrons.

These measurements are made possible by the higher available energies per unit mass afforded by the new high-voltage platform and beamlines. Higher energy facilitates complete collection of a much broader range of kinetic energy of release systems, using the advantage of greater kinematic compression onto the beam axis in the lab frame. It also permits highly efficient, mass selective detection of even light molecular fragments (e.g., H ions and atoms) in ultra-thin window Si detectors. We will initially concentrate on the following systems - molecular projectile ions: H<sub>2</sub><sup>+</sup>, HD<sup>+</sup>, H<sub>3</sub><sup>+</sup>, and CH<sub>2</sub><sup>+</sup> with target atoms: H, H<sub>2</sub>, Cs, Na, He, Ne, and Ar.

1. R. C. Isler, *Plasma Phys. Controlled Fusion* **36**, 171 (1994).
2. E. Wolfrum *et al.*, *Rev. Sci. Instrum.* **64**, 2285 (1993).
3. M. Von Hellermann *et al.*, *Plasma Phys. Controlled Fusion* **33**, 1805 (1991).
4. T. R. Kallman, *Atomic Processes in Plasmas*, AIP Conf. Proc. **322** (AIP, New York 1994), pp. 36–52.
5. M. Barat *et al.*, *J. Phys. B* **25**, 2205 (1992).
6. H. Cederquist *et al.*, *Phys. Rev. A* **51**, 2169 (1995).
7. P. Jardin *et al.*, in *Recoil Ion Kinetics*, AIP Conf. Proc. No. 274 (AIP, New York, 1993), p. 291.
8. P. Jardin *et al.*, *Nucl. Instrum. Meth. Phys. Res. B* (to be published).
9. J. Ullrich *et al.*, *Comments At. Mol. Phys.* **30**, 235 (1994).
10. C. L. Cocke *et al.*, *Phys. Rep.* **205**, 153 (1991).
11. V. Mergel *et al.*, *Phys. Rev. Lett.* **74**, 2200 (1995).
12. M. A. Abdallah *et al.*, *Phys. Rev. Lett.* **85**, 278 (2000).
13. G. W. McClure, *Phys. Rev.* **140** A769 (1965).
14. B. Meierjohann and Volger M., *J. Phys. B: At. Mol. Phys.* **9** 1801 (1976).
15. D. P. de Bruijn *et al.*, *Chem. Phys.* **85** 215 (1984).
16. M. Saito *et al.*, *J. Phys. B* **36**, 699 (2003), and references therein.
17. C. M. Laperle *et al.*, *Phys. Rev. Lett.* **93**, 153202 (2004).

**Ion Beam Characterization and Preparation End Station** – C. R. Vane, M. E. Bannister, M. R. Fogle, J. W. Hale, C. C. Havener, H. F. Krause, and F. W. Meyer

A new apparatus for atomic and molecular ion preparation using ion cooling in an electrostatic storage apparatus is being developed for use at the newly upgraded MIRF. This new apparatus will be mounted on the high-energy beamline at the MIRF for cooling and characterization of the internal state populations of atomic and molecular ion beams provided by the new all-permanent magnet ECR ion source, or by cold molecular ion sources currently also under development. These ion sources will also operate on the MIRF Upgrade Project high-voltage platform, providing ion energies up to 250 keV x q. The new end station will be configured to ultimately permit interrogation and characterization of ions by co-linear and crossed interactions with electron, laser, and atomic beams. The apparatus development involves design, construction, and integration within the MIRF of a new ultra-high vacuum beamline, with computer controlled, fast-reaction electrostatic deflection and focusing elements, including a cryogenic (4°K) electrostatic trap and a number of spectroscopic beam diagnostic and characterization components. The electrostatic mirror ion trap is being assembled primarily from components of a system previously developed and used for atomic ion lifetime studies at the ORNL EN Tandem facility.<sup>1,2</sup> Recent design and technological developments at the Stockholm University DESIREE project and the Heidelberg CSR cryogenic storage ring are being used

to leverage efficient implementation of this project, especially through our ongoing close collaborations with members of the DESIREE staff.

Ultimately, this end-station is planned for use in developing a more sophisticated preparation and characterization technique in which atomic and molecular ions can be held for several seconds, radiatively cooled to ground states, and then used or selectively re-excited to chosen excited states for controlled studies of state-specific collisional interactions with photons, electrons, and other atomic and molecular systems. Establishment of this apparatus is in direct support of our mission goal of developing a facility for state-selectively producing and manipulating atomic and molecular ions to implement studies of a broad range of plasma relevant ion-interactions in as controlled a manner as possible.

1. H. F. Krause, C. R. Vane, and S. Datz, AIP Conf. Proc. 576 (AIP, New York 1994), pp. 126-129.
2. O. Heber *et al.*, Rev. Sci. Instrum. **76**, 013104 (2005).

### **Chemical Sputtering of Hydrocarbons by D and D<sub>2</sub> Impact at Deuterated Carbon – P. S. Krstic and C. O. Reinhold**

Bombardment of carbon-based deuterated surfaces by low-energy ( $E < 50$  eV) D atoms and D<sub>2</sub> molecules (and ions) induces chemical reactions which ultimately lead to emission of stable hydrocarbons. Though poorly understood, these chemical sputtering processes are an important source of erosion of plasma-facing materials (limiters/divertor plates, vacuum vessel walls) and degradation of fusion performance in fusion reactors. Thus, there is a strong need within the fusion community for quantitative predictions of the corresponding yields. Motivated by this need and recent experiments at ORNL,<sup>1</sup> we have undertaken a series of large-scale classical molecular dynamics (MD) simulations of chemical sputtering of carbon surfaces. We have performed MD simulations of D and D<sub>2</sub> impinging on deuterated amorphous carbon surfaces in the energy range of 7.5-30 eV/D using reactive empirical bond-order potentials (REBO) potentials,<sup>2</sup> which provides a good empirical description of the covalent bond for non polar systems. While previous MD simulations have focused on the total sputtering yield of carbon, we have centered our work on the description of the methane yield. Mimicking the experimental conditions requires careful control of the time scales of the sputtering process; specifically the fluence and the relaxation time after each impact. A number of surfaces were prepared by D or D<sub>2</sub> impact at each impinging energy, with up to 2000 deuterons on an initial deuterated simulation cell of about 2500 atoms for a time period of up to 2ns. For a constant D flux a “quasi steady state” in the hydrocarbon sputtering yield is reached which depends on the particular hydrocarbon. We find that the sputtering yield in the quasi-steady-state regime differs considerably from that obtained for a non-irradiated simulation cell, emphasizing the importance of modeling the experimental system, rather than an idealized one. The calculated yields of methane are directly related to the sp<sup>2</sup>/sp<sup>3</sup> densities at the topmost layers. We are also studying for the first time the dependence of the chemical sputtering on the vibrational state of the impinging D<sub>2</sub> molecules. Calculated sputtering yields per deuteron obtained for D and D<sub>2</sub> agree quantitatively with each other (within the statistical uncertainty) and that the methane and acetylene sputtering yields are in very good agreement with experiment.<sup>1</sup>

1. F. W. Meyer, L. I. Vergara, and H. F. Krause, Phys. Scr. **T124**, 44 (2006); L. I. Vergara, F. W. Meyer, H. F. Krause *et al.*, J. Nucl. Mat. (2006), in press.
2. S. J. Stuart, A. B. Tutein, and J. A. Harrison, J. Chem. Phys. **112** 6472 (2000).

## **Engineering High- $n$ Rydberg States with Tailored Pulses – C.O. Reinhold**

Rydberg states with large values of principal quantum number  $n$  provide a valuable laboratory in which to explore control of the quantum states of mesoscopic systems. Recent advances have stimulated the investigation of possible protocols to manipulate the dynamics of Rydberg atoms using, for example, tailored pulsed unidirectional electric fields, termed half-cycle pulses (HCPs). A remarkable degree of control over Rydberg wavepackets can be achieved using HCP trains. The underlying classical phase space features stable islands surrounded by a chaotic sea. Placing a wavepacket in a stable island gives rise to “dynamical stabilization”, i.e., to creation of a non-dispersive wavepacket. Conversely, placing a wavepacket in the chaotic sea results in rapid spreading and, eventually, in ionization. Rydberg wavepackets can, in principle, be “steered” to different regions of phase space (coordinate and momentum space) and even focused, by adiabatically chirping the amplitude and/or frequency of the HCP train. A critical first step is the production of a wavepacket that is strongly localized within an island. We have recently demonstrated that starting with very-high- $n$  quasi-one-dimensional (quasi-1D) Rydberg atoms it is possible to create localized wavepackets and position them either near the periphery (the “shore”) of an island or near its center. The ensuing evolution of the wavepacket gives rise to periodic transient phase space localization at locations that can themselves vary periodically with time providing the opportunity for optimal transfer to other islands. The latest protocols for selectively loading an island are remarkably efficient with 90% of the initial quasi-1D Rydberg atoms becoming trapped within it.

The ubiquitous coupling of any wavepacket to its environment (*noise*) tends to destroy the coherent superposition by randomly dephasing the wavepacket. This *decoherence* is considered to be a fundamental limitation to coherent quantum manipulation. Decoherence induced by dephasing converts a coherent superposition into an incoherent statistical mixture and is, therefore, often invoked in facilitating the quantum-to-classical transition of microscopic and mesoscopic dynamics. Rydberg atoms provide a bridge of the quantum-to-classical transition because of their *quasi-classical* behavior for large quantum numbers, even in the absence of noise. The quantum break time where classical and quantum dynamics diverge can reach times of the order of microseconds (for  $n \sim 400$ ). We are currently investigating noise induced dephasing and damping of quantum (or classical) beats in Stark wavepackets. Experimentally, it is possible to electronically synthesize colored noise with a spectral distribution that matches characteristic frequencies of the system. We are investigating the dependence of dephasing on the frequency and amplitude of noise. We also plan to use as environment a gas of polar molecules (whose density can be varied) and to utilize the rate of decoherent dephasing as a tool to measure cross sections for quasi-elastic electron-atom (or molecule) collisions at energies extending down to micro electron volts.

## **Capture, Ionization, and Transport of Electronic States of Fast Ions Penetrating Solids –**

*C. O. Reinhold, D. R. Schultz, and T. Minami*

The passage of an atom or ion through a solid involves a rich variety of physical phenomena. Theoretical description of such interactions remains a challenge, in part due to large number of degrees of freedom involved. Systems of such complexity are ideal candidates for applications of open quantum system approaches, within which only the (sub) system, in the present case the electronic degrees of freedom of the projectile, are treated explicitly. The rest of the system, here the solid (its electronic and ionic degrees of freedom) and the radiation field are treated as an environment. For the transport of projectile states in the solid, extensions beyond standard approaches are necessary. The interaction with the reservoir can not only destroy but also transiently induce coherences. Moreover, electron loss (i.e. ionization) represents a net flux of probability out of the subsystem that can be represented in a given basis: i.e. the system is not

only open with respect to energy transfer but also with respect to probability flux. Finally, probability flux into the system also occurs as the highly charged ion captures electrons from the solid. We have developed an inhomogeneous non-unitary Lindblad master equation that allows for a description of open quantum systems with both sinks (electron loss) and sources (capture). We are currently applying this theoretical framework to study line-emission intensities resulting from the transmission of 13.6 MeV/amu Ar<sup>18+</sup> ions through amorphous carbon foils. The calculated results are compared with experimental data obtained through high resolution X-ray spectroscopy in which individual fine structure components were resolved.<sup>1</sup> A considerable effort is devoted to performing a robust calculation of the electron capture density matrix by numerically solving on a three-dimensional lattice the time-dependent Schroedinger equation (LTDSE).

1. E. Lamour, B. Gervais, J. Rozet and D. Vernhet, Phys. Rev. A, in press.

### **Development of the LTDSE Method for Atomic Collisions and New Molecular Collision Calculations for Cool Plasmas – D.R. Schultz, T. Minami, and T-G. Lee**

Over the past decade we have applied a novel approach to treating atomic collisions through solution of the time-dependent Schrödinger equation on a numerical lattice using high-order methods, the so-called lattice, time-dependent Schrödinger equation (LTDSE) approach. During the last review period we have considered systems which have been motivated by applications in fusion energy research but which have also provided new fundamental tests of the LTDSE approach. In particular, we have treated collisions of protons with excited hydrogen atoms, a potentially important process in plasmas where multi-step excitation, ionization, or charge transfer occurs and have completed study of fusion relevant collisions of beryllium ions with hydrogen. We have also undertaken work to support the modeling of low-temperature plasmas such as those in fusion and astrophysical environments that involve energy transfer in collisions of atoms and molecules, e.g. He + H<sub>2</sub>, H<sub>2</sub> + H<sub>2</sub>. This work is part of a new collaboration involving a number of partners and is aimed at providing a comprehensive treatment of processes involving H, H<sub>2</sub>, and He.

### **Computation of Sturmian States for H<sub>2</sub><sup>+</sup>-Like Ions – J. H. Macek and S. Y. Ovchinnikov**

Benchmark computations of ionization in proton-hydrogen atom collisions applicable to plasma diagnostics are needed over a wide energy range, namely, from 1 keV to a tens of MeV. The Born theory is applicable at MeV energies but at low energies and at the cross section maxima near 25 keV only essentially exact methods such as the Lattice Time Dependent Schrödinger Equation (LTDSE) are reliable. Even here discrepancies between theory and experiment are of the order of 20%. More troublesome is the 20% discrepancy between H<sub>2</sub><sup>+</sup> Sturmian calculations<sup>1</sup> and LTDSE cross sections. This may be due to problems in treating high-Rydberg states since the box size of the LTDSE method limits the n value of the Rydberg state that can be accurately represented, while the accuracy of the Sturmian states decreases with increasing n. For that reason, we have developed a more accurate program for solving integral equations in three dimensions to compute H<sub>2</sub><sup>+</sup>-like Sturmian functions, and have verified that states with n of the order of 6 or 7 are accurately represented.

We will compute total ionization cross sections using our new 3-D integral equation solver for proton impact on one electron ions. As an additional test we will compare cross sections for excitation and capture of high-Rydberg states with those computed using standard methods. Finally, we will develop methods to propagate wave functions to infinite times that can be used at intermediate energies<sup>2</sup> where ionization maximizes.

1. S. Yu Ovchinnikov, G. N. Ogurtsov, J. H. Macek, and Yu. S. Gordeev, *Physics Reports* **389**, 119 (2004).
2. J. H. Macek and S. Yu. Ovchinnikov *Phys. Rev. A*, **70**, 052702 (2004).

#### References to Publications of DOE Sponsored Research from 2004-2006 (descending order)

“Methane Production from ATJ Graphite by Slow Atomic and Molecular D Ions: Evidence for Projectile Molecule-Size-Dependent Yields at Low Energies,” L. I. Vergara, F. W. Meyer, H. F. Krause, P. Träskelin, K. Nordlund, and E. Salonen, to be published in *J. Nucl. Mater.* (2006).

“Dipole Polarization Effects on Highly-Charged Ion-Atom Electron Capture,” C. C. Havener and R. Rejoub, [Invited] *Proceedings, International Conference on Photonic, Electronic, and Atomic Collisions*, Rosario, (World Scientific), 2006.

“Laser Ion Source Tests at the HRIBF on Stable Sn, Ge, and Ni Isotopes,” Y. Liu, C. Baktash, J. R. Beene, H. Z. Bilheux, C. C. Havener, H. F. Krause, D. R. Schultz, D. W. Stracener, C. R. Vane, K. Breuck, Ch. Geppert, T. Kessler, K. Wendt, *Nucl. Instrum. Meth. Phys. Res. B* **243**, 442-452 (2006).

“The ORNL Multicharged Ion Research Facility Upgrade Project,” F. W. Meyer, M. E. Bannister, D. Dowling, J. W. Hale, C. C. Havener, J. W. Johnson, R. C. Juras, H. F. Krause, A. J. Mendez, J. Sinclair, A. Tatum, C. R. Vane, E. Bahati Musafiri, M. Fogle, R. Rejoub, L. Vergara, D. Hitz, M. Delaunay, A. Girard, L. Guillemet, and J. Chartier, *Proceedings, 14th International Conference on Ion Beam Modification of Materials*, Asilomar, Calif., Sept. 5-10, 2004, *Nucl. Instrum. Meth. Phys. Res. B* **242**, 71-78 (2006).

“Realization of the Kicked Atom at High Scaled Frequencies,” C. O. Reinhold, S. Yoshida, J. Burgdörfer, W. Zhao, J. J. Mestayer, J. C. Lancaster, and F. B. Dunning, *Phys. Rev. A* **73**, 033420 (2006).

“Influence of a DC Offset Field on Kicked Quasi-One-Dimensional Rydberg Atoms: Stabilization and Frustrated Field Ionization,” S. Yoshida, C. O. Reinhold, J. Burgdörfer, W. Zhao, J. J. Mestayer, J. C. Lancaster, and F. B. Dunning, *Phys. Rev. A* **73**, 033411 (2006).

“Bidirectionally Kicked Rydberg Atoms: Population Trapping near the Continuum,” W. Zhao, J. J. Mestayer, J. C. Lancaster, F. B. Dunning, C. O. Reinhold, S. Yoshida, and J. Burgdörfer, *Phys. Rev. A* **73**, 015401 (2006).

“The Kicked Rydberg Atom,” F. B. Dunning, J. C., Lancaster, C. O. Reinhold, S. Yoshida, and J. Burgdörfer, *Adv. At. Mol. Phys.* **52**, 49 (2006).

“Lattice, Time-dependent Schrödinger Equation Approach for Charge Transfer in Collisions of  $\text{Be}^{4+}$  with Atomic Hydrogen,” T. Minami, M. S. Pindzola, T. G. Lee, and D. R. Schultz, *J. Phys. B* **39**, 2877 (2006).

“Methane Production by Deuterium Impact at Carbon Surfaces,” S. J. Stuart, P. S. Krstic, C. O. Reinhold, and T. A. Embry, to be published in *Nucl. Instrum. Meth. Phys. B* (2006).

“Collisions of Slow Highly Charged Ions with Surfaces,” J. Burgdörfer, C. Lemell, C. O. Reinhold, K. Schiessl, B. Solleder, K. Tokesi, and L. Wirtz, to be published in 2005 ICPEAC proceedings of invited papers.

“State-to-State Rotational Transitions in H<sub>2</sub>+H<sub>2</sub> Collision at Low Temperatures,” T. G. Lee, N. Balakrishnan, R. C. Forrey, P. C. Stancil, D. R. Schultz, and G. J. Ferland, to be published in J. Chem. Phys. (2006).

### Year 2005 publications

“Path Dependence of the Charge-State Distributions of Low-Energy F<sup>q+</sup> Ions Back-scattered from RbI(100),” L. I. Vergara, F. W. Meyer, and H. F. Krause, Nucl. Instrum. Methods Phys. Res. **B 230**, 379 (2005).

“Charge Transfer in Low-Energy Collisions of He<sup>2+</sup> with Atomic Hydrogen,” C. C. Havener, R. Rejoub, P. S. Krstic, and A. C. H. Smith, Phys. Rev. A **71**, 042707 (2005).

“Electron Capture by Ne<sup>4+</sup> Ions from Atomic Hydrogen,” C. C. Havener, R. Rejoub, C. R. Vane, H. F. Krause, D. W. Savin, M. Schnell, J. G. Wang, and P. C. Stancil, Phys. Rev. A **71**, 034702 (2005).

“Electron-Impact Dissociation of D<sup>13</sup>CO<sup>+</sup> Molecular Ions to <sup>13</sup>CO<sup>+</sup> Ions,” E. M. Bahati, R. D. Thomas, C. R. Vane, and M. E. Bannister, J. Phys. B **38**, 1645 (2005).

“Engineering Very-High-n Polarized Rydberg States Using Tailored HCP Sequences,” W. Zhao, J. J. Mestayer, J. C. Lancaster, F. B. Dunning, C. O. Reinhold, S. Yoshida, and J. Burgdörfer, Phys. Rev. Lett. **95**, 163007 (2005).

“Collisional Decoherence in Very-High-n Rydberg Atoms,” C. O. Reinhold, J. Burgdörfer, and F. B. Dunning, Nucl. Instrum. Meth. Phys. Res. B **233**, 48 (2005).

“The Periodically Kicked Atom: Effect of the Average DC Field,” W. Zhao, J. C. Lancaster, F. B. Dunning, C. O. Reinhold, and J. Burgdörfer, J. Phys. B **38**, S191 (2005).

“Three-Body Fragmentation Dynamics of Amidogen and Methylene Radicals via Dissociative Recombination,” R. Thomas, F. Hellberg, A. Neau, S. Rosen, M. Larsson, C. R. Vane, M. E. Bannister *et al.*, Phys. Rev. A **71**, 032711 (2005).

“Investigating the Breakup Dynamics of Dihydrogen Sulfide Ions Recombining with Electrons,” F. Hellberg, V. Zhaunerchyk, A. Ehlerding, W. D. Geppert, M. Larsson, R. D. Thomas, M. E. Bannister, E. Bahati, C. R. Vane, F. Österdahl, P. Hlavenka, and M. af Ugglas, J. Chem. Phys. **122**, 224314 (2005).

“The Effect of Bonding on the Fragmentation of Small Systems,” R. Thomas, A. Ehlerding, W. Geppert, F. Hellberg, M. Larsson, V. Zhunerchyk, E. Bahati, M. E. Bannister, C. R. Vane, A. Petrigiani, W. J. van der Zande, P. Andersson, and J. B. C. Pettersson, J. Phys. Conf. Ser. **4**, 187 (2005).

“Target Orientation Dependence of the Charge Fractions Observed for Low-Energy Multicharged Ions Ne<sup>q+</sup> And F<sup>q+</sup> Backscattered from RbI(100),” L. I. Vergara, F. W. Meyer, and H. F. Krause, Surf. and Coatings Tech. **196**, 19 (2005).

“An All-Permanent Magnet ECR Ion Source for the ORNL MIRF Upgrade Project,” D. Hitz, M. Delaunay, A. Girard, L. Guillemet, J. M. Mathonnet, J. Chartier, and F. W. Meyer, AIP Conference Proceedings **749**, 123 (2005).

“Traveling Wave Vs. Cavity RF Injection for the ORNL HRIBF ‘Volume-Type’ ECR Ion Source,” Y. Liu, F. M. Meyer, and J. M. Cole, AIP Conference Proceedings **749**, 187 (2005).

“Non-Unitary Master Equation for the Internal State of Ions Transversing Solids,” M. Seliger, C. O. Reinhold, T. Minami, and J. Burgdörfer, Nucl. Instrum. Meth. Phys. Res. B **230**, 7-11 (2005).

“Non-Unitary Quantum Trajectory Monte Carlo Method for Open Quantum Systems,” M. Seliger, C. O. Reinhold, T. Minami, and J. Burgdörfer, Phys. Rev. A **71**, 062901 (2005).

“Steering Rydberg Wave Packets Using a Chirped Train of Half-Cycle Pulses,” S. Yoshida, C. O. Reinhold, E. Persson, J. Burgdörfer, and F. B. Dunning, J. Phys. B **38**, S209-S217 (2005).

“Performances of ‘Volume’ vs ‘Surface’ ECR Ion Sources,” Y. Liu, F. M. Meyer, H. Bilheux, J. M. Cole, and G. D. Alton, AIP Conference Proceedings **749**, 191 (2005).

“Measurements of Chemical Erosion of ATJ Graphite by Low Energy  $D_2^+$  Impact,” F. W. Meyer, H. F. Krause, and L. I. Vergara, *Proceedings, International Conference on Plasma Surface Interactions*, Portland, Maine, May 24-28, 2004, J. Nucl. Mater. **337-339**, 922 (2005).

“The ORNL Multicharged Ion Research Facility (MIRF) High Voltage Platform Project,” F. W. Meyer, M. E. Bannister, J. W. Hale, J. W. Johnson, and D. Hitz, 2005 Particle Accelerator Conference, Knoxville, TN, May 16 – 20, 2005, Joint Accelerator Conf. Web Proceedings (2005).

“Control System for the ORNL Multicharged Ion Research Facility High-Voltage Platform,” M. E. Bannister, F. W. Meyer, J. Sinclair, 2005 Particle Accelerator Conf., Knoxville, TN, May 16 – 20, 2005, Joint Accelerator Conferences Web Proceedings (2005).

“Isobar Suppression by Photodetachment in a Gas-filled RF Quadrupole Ion Guide,” Y. Liu, J. R. Beene, C. C. Havener, and J. F. Lang, Appl. Phys. Lett. **87**, 113504 (2005).

“Isobar Suppression by Photodetachment in a Gas-Filled RF Quadrupole Ion Guide,” Y. Liu, J. R. Beene, C. C. Havener, J. F. Liang, A. C. Havener, pp. 3250-3252 in *Proceedings, Particle Accelerator Conference (PAC'05)*, Knoxville, Tenn., May 16-20, 2005, published on CD, IEEE Cat. No. 05CH37623C, IEEE, Piscataway, NJ, 2005.

“Chemical Sputtering of ATJ Graphite Induced by Low-Energy  $D_2^+$  Bombardment,” L. I. Vergara, F. W. Meyer, and H. F. Krause, J. Nucl. Mater. **337-339**, 922 (2005).

“Experiments on Electron-Impact Ionization of Atomic and Molecular Ions,” M. E. Bannister, pp. 172-179, *Proceedings of the 4<sup>th</sup> ICAMDATA Conference, Oct. 5-8, 2004, Toki, Japan*, AIP Conf. Proceedings 730, Woodbury, NY (2005).

“Excitation and Charge Transfer in p+H(2s) Collisions,” M. S. Pindzola, T. G. Lee, T. Minami, and D. R. Schultz, Phys. Rev. A. **72**, 062703 (2005).

“Close-Coupling Calculations of Low-Energy Inelastic and Elastic Processes in  $^4\text{He}$  Collisions with  $\text{H}_2$ : A Comparative Study of Two Potential Energy Surfaces,” T. G. Lee, C. Rochow, R. Martin, T. K. Clark, R. C. Forrey, N. Balakrishnan, P. C. Stancil, D. R. Schultz, A. Dalgarno, and G. J. Ferland, *J. Chem. Phys.* **122**, 024307 (2005).

“Recent ORNL Measurements of Chemical Sputtering of ATJ Graphite by Slow Atomic and Molecular D Ions,” F. W. Meyer, L. I. Vergara, and H. F. Krause, [Invited] *Workshop on New Directions for Advanced Computer Simulations and Experiments in Plasma Surface Interactions*, March 21-23, 2005, *Phys. Scripta* **T124**, 44 (2005).

“Nonadiabatic Processes near Barriers,” J. Burgdörfer, N. Rohringer, P. S. Krstic, and C. O. Reinhold, Book Chapter in ‘*Nonadiabatic Transition in Quantum Systems*’ edited by V. I. Osherov, L.I. Ponomarev, Chernogolovka, Russia p. 205 (2004). 2004 Institute of Chemical Physics RAS ISBN 5-901675-48-7.

“In-situ Electron Cyclotron Resonance (ECR) Plasma Potential Determination Using an Emissive Probe,” H. J. You, Y. Liu, and F. W. Meyer, 2005 Particle Accelerator Conference, Knoxville, TN, May 16 – 20, 2005, Joint Accelerator Conferences Web Proceedings (2005).

“Laser Ion Source Development for ISOL Systems at RIA,” Y. Liu, C. Baktash, J. R. Beene, H. Z. Bilheux, C. C. Havener, H. F. Krause, D. R. Schultz, D. W. Stracener, C. R. Vane, K. Brück, Ch. Geppert, T. Kessler, and K. Wendt, pp. 1640-1642 in *Proceedings, Particle Accelerator Conference (PAC'05)*, Knoxville, TN, May 16-20, 2005, published on CD, IEEE Cat. No. 05CH37623C, IEEE, Piscataway, NJ, 2005.

#### **Year 2004 publications**

“Multi-Electron Dynamics for Neutralization of Highly Charged Ions Near Surfaces,” J. Burgdörfer, L. Wirtz, C. O. Reinhold, and C. Lemell, *Vacuum* **73**, 3 (2004).

“Classical and Quantum Scaling for Localization of Half-Cycle Pulse-Driven Rydberg Wavepackets,” D. G. Arbo, C. O. Reinhold, and J. Burgdörfer, *Phys. Rev. A* **69**, 023409 (2004).

“Characterization of Quasi One-Dimensional Rydberg Atoms Using Half-Cycle Pulse Applied Perpendicular to the Atomic Axis,” W. Zhao, J. C. Lancaster, F. B. Bunning, C. O. Reinhold, J. Burgdörfer, *Phys. Rev A* **69**, 041401 (2004).

“Dynamics of Ionization in Atomic Collisions,” S. Yu. Ovchinnikov, G. N. Ogurtsov, J. H. Macek, and Yu. S. Gordeev, *Phys. Rep.* **389**, 119 (2004).

“Tailoring and Controlling Wave Packets In Multi-Photon Atom Collisions,” S. Yoshida, E. Persson, C. O. Reinhold, J. Burgdörfer, B. E. Tannian, C. L. Stokely, and F. B. Dunning, *Proceedings of XXIII International Conference on Photonic, Electronic, and Atomic Collisions (ICPEAC)*, Stockholm, Sweden, July 23-29, 2003, *Physica Scripta* **T110**, 424 (2004).

“Electron Capture by  $\text{Ne}^{3+}$  Ions from Atomic Hydrogen,” Rejoub, R., M. E. Bannister, C. C. Havener, D. W. Savin, C. J. Verzani, J. G. Wang, and P. C. Stancil, *Phys. Rev. A* **69**, 052704 (2004).

“Charge Changing Interactions of Ultrarelativistic Pb Nuclei,” C. Scheidenberger, I. A. Pshenichnov, K. Summerer, A. Ventura, J. P. Bondorf, A. S. Botvina, I. N. Mishustin, D. Boutin,

S. Datz, H. Geissel, P. Grafstrom, H. Knudsen, H. F. Krause, B. Lommel, S. P. Moller, G. Munzenberg, R. H. Schuch, E. Uggerhøj, U. Uggerhøj, C. R. Vane, Z. Z. Vilakazi, and H. Weick, *Phys. Rev. C* **70**, 014902 (2004).

“Site-Specific Neutralization of Slow Multicharged Ions Incident on Solid Surfaces,” F. W. Meyer, H. F. Krause, V. A. Morozov, C. R. Vane, and L. I. Vergara, *Phys. Scripta* **T110**, 403 (2004).

“Analysis of Structures in the Cross Sections for Elastic Scattering and Spin Exchange in Low Energy  $H^+ + H$  Collisions,” P. S. Krstic, J. H. Macek, S. Yu. Ovchinnikov, and D. R. Schultz, *Phys. Rev. A* **70**, 042711 (2004).

“Regge Oscillations in Integral Cross Sections for Proton Impact on Atomic Hydrogen,” J. H. Macek, P. S. Krstic, and S. Yu. Ovchinnikov, *Phys. Rev. Lett.* **93**, 183203 (2004).

“Energy and Angular Distributions of Electrons Ejected from Atomic Hydrogen by Low Energy Proton Impact,” J. H. Macek and S. Yu. Ovchinnikov, *Phys. Rev. A* **70**, 052702 (2004).

“Response of Highly Polarized Rydberg States to Trains of Half-Cycle Pulses,” C. O. Reinhold, W. Zhao, J. C. Landcaster, F. B. Dunning, E. Persson, D. G. Arbo, S. Yoshida, and J. Burgdörfer, *Phys. Rev. A* **70**, 033402 (2004).

“Coherence Parameters for Charge Transfer in Collisions of Protons with Helium Calculated Using a Hybrid Numerical Approach,” T. Minami, C. O. Reinhold, D. R. Schultz, and M. S. Pindzola, submitted to *J. Phys. B* **37**, 4025 (2004).

“Low Energy Charge Transfer with Multicharged Ions Using Merged Beams,” C. C. Havener, pp. 235-244, Proceedings, American Physical Society Spring Meeting on Atomic Processes in Plasmas, Santa Fe, New Mex., April 19-22, 2004, AIP Conference Proceedings 730, Woodbury, N.Y. (2004).

## **PULSE: The Stanford Photon Ultrafast Laser Science and Engineering Center**

Members and affiliates: Y. Acremann, N. Berrah, J. Bozek, P.H. Bucksbaum, H. Chapman, P. Emma, R. Falcone, M. Fayer, D. Fritz, J. Hajdu, S. Harris, J. Hastings, B. Hedman, P. Heimann, K. Hodgson, K. Gaffney, J. Isberg, M. Kasevich, P. Krejcik, R. Lee, A. Lindenberg, J. Luning, A. Nilsson, A. Nilsson, D. Reis, H. Siegmann, J. Stohr, D. van der Spoel, P. Weber

The Stanford PULSE Center conducts research in areas of ultrafast science at SLAC that support the research program of the LCLS. PULSE has initiated research in ultrafast materials science, condensed matter physics, molecular physics, physical chemistry, atomic physics, structural biology, electron beams and x-ray laser physics. PULSE also maintains close links to areas of ultrafast science that are critically served by LCLS, but which lie outside the scope of mission activities in BES. These include plasma physics and high energy density physics.

The PULSE Center participated in the recently completed SPPS project at SLAC, which produced and used the world's brightest beams of sub-100 fs x-rays during its two-year run. PULSE scientists also are involved in several projects at FLASH, the soft-x-ray FEL at DESY. Here is a very brief summary of PULSE activities:

**Ultrafast Optics: Electro-Optic Sampling of Relativistic Beams** (A. Cavalieri, SPPS collaboration, Published in Phys. Rev. Lett., 94:114801, 2005.) We have explored the electro-optic response of thin nonlinear crystals to the fields generated by relativistic electron beams at SLAC. This effect will be a principle timing diagnostic for experimental pump-probe spectroscopy at LCLS.

**X-Ray Scattering from Optical Phonons.** (D. Fritz, SPPS Collaboration) Optical phonons in crystalline solids have been suggested as ultrafast modulators for x-rays. SPPS pulse durations permitted us to test this concept using undulator radiation for the first time. Valence electrons are excited into conduction bands when a laser pulse is absorbed in a semi-conductive or semi-metallic solid. If the excitation pulse is short in duration, a brief window exists (~1-2 ps) subsequent to photoexcitation where the excited electrons are not in equilibrium with the lattice. The existence of excited state electrons can induce an alteration to the interatomic potential energy surface of the solid, particularly in bismuth and other group-V semi-metals. If the change in potential energy surface is impulsive, a coherent phonon mode of the crystal lattice can be induced. The details of the excited state potential, which on the microscopic level determines the properties of the material, may be inferred through observation of the coherent atomic motion. These observations, particularly the oscillation frequency and displacement from the equilibrium structure, were measured for the first time in photoexcited bismuth using ultrafast x-ray diffraction. These measurements quantified the curvature and equilibrium position of the excited state potential energy surface as a function of carrier excitation density.

**Towards Attosecond Physics.** (Bucksbaum and coworkers) We have established a new laboratory at Stanford and SLAC, which will be used for research on few-femtosecond or sub-femtosecond processes in molecular gases. Strong field ultrafast processes will be driven by a FemtoPower kilohertz laser and amplifier, which delivers

5.5 fsec 0.3 mJ carrier-stabilized pulses. We have recently installed a high harmonics chamber, and will be making and characterizing high harmonics in the next few months. At the same time, we have initiated two smaller projects on this source as well: on field ionization of carbon nanotubes, and ultrabroad continuum generation in molecular gases.

**Atomic-scale visualization of inertial dynamics.** (Lindenberg and SPPS collaboration, Published in Science, **308**, 392 (2005)). The motion of atoms on interatomic potential energy surfaces is fundamental to the dynamics of liquids and solids. An accelerator-based source of femtosecond x-ray pulses allowed us to follow directly atomic displacements on an optically modified energy landscape, leading eventually to the transition from crystalline solid to disordered liquid. We show that, to first order in time, the dynamics are inertial, and we place constraints on the shape and curvature of the transition-state potential energy surface. Our measurements point toward analogies between this nonequilibrium phase transition and the short-time dynamics intrinsic to equilibrium liquids.

**Time-resolved measurements of the structure of water at constant density.** (Nilsson and coworkers, Published in J. Chem. Phys., **122**, 204507 (2005)). Dynamical changes in the structure factor of liquid water,  $S(Q,t)$ , are measured using time-resolved x-ray diffraction techniques with 100 ps resolution. On short time scales following femtosecond optical excitation, we observe temperature-induced changes associated with rearrangements of the hydrogen-bonded structure at constant volume, before the system has had time to expand. We invert this data to extract transient changes in the pair correlation function associated with isochoric heating effects, and interpret these in terms of a decrease in the local tetrahedral ordering.

**Soft x-ray measurements of bond-breaking dynamics in water** (Lindenberg and coworkers) We are preparing for soft x-ray spectroscopic experiments at the Advanced Light Source femtosecond slicing beamline in order to probe changes in short-range order in liquid water. Measurements in transmission near the oxygen K-edge using ultrathin nanofluidic sample cells enable one to capture snapshots of local bonding configurations. Experiments using an optical parametric amplifier to generate near infrared light resonant with the OH-stretching mode vibration are in progress. Our goal is to directly measure femtosecond bond-breaking dynamics under resonant vibrational excitation. We have performed initial static measurements at the Advanced Light Source beamline 6.3.2. and demonstrated that our new design for the nanofluidic cells allow for high signal to noise measurements of the NEXAFS region around the oxygen K-edge.

**Femtosecond diffuse scattering from the liquid state** (Lindenberg, Gaffney, and SPPS). We have performed the first femtosecond diffuse scattering measurements probing the non-equilibrium evolution of the structure of liquid semiconductors. We observe at short times the formation of an unusual intermediate state, characterized by large amplitude density fluctuations. At 10 ns, the structure agrees well with the known equilibrium structure. At short times, large deviations from the equilibrium state are observed.

**Ultrafast magneto-dynamics.** (Stohr and coworkers) As of April 2006, the Final Focus Test Beam (FFTB) facility at the end of the 3 km long Stanford Linear Accelerator has closed to make way for construction of the LCLS. Prior to its closing we carried out several ultrafast magnetization switching experiments. Following earlier experiments in

2003 and 2004 [Phys. Rev. Lett. **94**, 197603 (2005), Nature **428**, 831 (2004)], the latest results obtained in August 2005 and January 2006 serve as the background for planned experiments in the years to come. Fast and efficient magnetic switching is one of the basic requirements in advanced technological applications of magnetism.

**Single Shot X-Ray Imaging of Magnetic Phase Transitions.** (Stohr and coworkers) The scientific goal is to further develop and prepare snapshot imaging with a single LCLS x-ray pulse of critical magnetic fluctuations at the ferro- to paramagnetic phase transition in a thin, quasi 2-dimensional film. Proposing this ambitious goal has been motivated by our successful demonstration of lensless imaging of a magnetic domain structure with about 50 nm spatial resolution by x-ray Fourier transform spectro-holography in 2004. One important finding of this experiment has been that a single x-ray pulse of LCLS should be sufficiently intense for imaging of a magnetic domain structure with sub 100 nm spatial resolution.

**Toward Single Molecule Imaging** (Hajdu and coworkers) The FLASH facility, at DESY in Hamburg, is the world's first soft-X-ray FEL. Our team has carried out successful experiments as part of its first user operations in February 2006, During those experiments the FEL operated at a wavelength of 32 nm with pulse duration of about 25 fs. This is the only source that has the requisite peak power and short wavelength to directly test models of the dynamics of samples in intense FEL beams. During our two weeks of beamtime at FLASH, we carried out a series of experiments that included the first demonstration of single-pulse coherent diffraction imaging, whereby we reconstructed an image at a resolution of 60 nm. The object was completely destroyed by the pulse, as was evidenced by the diffraction of a large hole by a subsequent pulse.

# Structural Dynamics in Chemical Systems

## Principal Investigator

**Kelly J. Gaffney**, PULSE Center, Photon Sciences, Stanford Linear Accelerator Center,  
Stanford University, Menlo Park, CA 94025

Telephone: (650) 926-2382

Fax: (650) 926-4100

Email: kgaffney@slac.stanford.edu

**I. Program Scope:** This grant will investigate the fundamental structural and dynamical properties that influence light harvesting efficiency and solar energy conversion in photocatalysis. A natural connection exists between ultrafast experimental techniques with sub-picosecond resolution and photochemical reactivity because the initial events in molecular light harvesting invariably occur on the ultrafast time scale. Acquiring a better understanding of the fundamental events that shape photochemical reaction mechanisms will assist in the development of affordable and renewable energy sources.

Developing and utilizing ultrafast x-ray pulses for the study of chemical dynamics represents the core technical objective of this research program. Initial efforts focused on the Sub-Picosecond Pulse Source (SPPS), a linear accelerator derived femtosecond hard x-ray source at the Stanford Linear Accelerator Center (SLAC). With the decommissioning of the SPPS in Spring 2006, our efforts turn to preparing for the arrival of the Linac Coherent Light Source (LCLS), an x-ray free electron laser being built at SLAC. We will complement these ultrafast x-ray studies with ultrafast vibrational and electronic spectroscopic studies of electron transfer dynamics, as well as equilibrium x-ray absorption and emission studies of electronic structure.

**II. Infrastructure development:** The past year has seen significant development of the infrastructure necessary for conducting experimental studies of chemical dynamics at SLAC. SLAC has begun building laboratory space for the PULSE Center, a Center for Pulsed Ultrafast Laser Science and Engineering founded by the Department of Energy (DOE) in 2004. The 'Structural Dynamics in Chemical Systems' component of the PULSE Center received initial funds in 2005. Completion of the laboratory construction has been scheduled for Fall 2006. The major laser components for generating independently tunable UV/visible and mid-IR femtosecond laser pulses have been purchased, as have the optics, mechanics, and detectors for conducting time resolved electronic and vibrational spectroscopy.

Spring of 2006 saw the completion of the SPPS experiment at SLAC. The SPPS provided a focal point for ultrafast science activities supported by the DOE at SLAC up to its completion. The decommissioning of the SPPS allows us to focus on preparing for the LCLS and developing an experimental program designed to utilize its unique attributes.

**III. Scientific Progress:** The successful achievement of the scientific objectives of the 'Structural Dynamics in Chemical System' grant requires the development of experimental techniques and tools applicable to a wide range of ultrafast x-ray science. The SPPS experimental program has demonstrated that the timing jitter between the laser and x-ray pulses can be measured on a shot-to-shot basis and used to collect data with a time resolution an order of magnitude better than the jitter averaged time resolution.<sup>1,4</sup> We have also demonstrated the tremendous capacity of x-ray diffraction to characterize the shape of the excited state potential energy surface for complex materials with a detail previously unachievable.<sup>2-6</sup> The ability to determine the shape of the potential energy surface with unprecedented detail represents one of the most significant attributes of ultrafast x-ray science.

Our efforts in photo-initiated electron transfer chemistry have focused on three areas: designing the layout and purchasing the equipment for our laser laboratory, developing

organometallic sample preparation and characterization expertise, and preparing for time resolved x-ray emission studies. The unique attributes of the LCLS make x-ray emission spectroscopy (XES), and to a lesser extent x-ray absorption near edge spectroscopy (XANES) and resonant inelastic x-ray scattering (RIXS), the preferred spectroscopic techniques for the LCLS. These techniques are ideally suited to studying electron transfer in organometallic compounds because they provide easily interpretable information about the oxidation state, spin multiplicity, and the local coordination of the metal centers in these complexes.

**III.A. Femtosecond x-ray diffraction studies of laser driven melting in InSb:** Ultrafast laser melting of a semiconductor differs from thermal melting because the initial atomic disordering results from modifications of the inter-atomic potential energy surface, not from high levels of atomic core kinetic energy. The valence electrons in tetrahedral semiconductors, like InSb, dictate the chemical bonding and the crystal structure of the material. Photo-excitation of the valence electrons weakens the bonding forces and transforms the material from a semi-conducting crystal into a liquid metal. Understanding how the inter-atomic potential varies with carrier density represents one of the key goals to understanding how intense laser fields can be used to modify material structure. Prior work at the SPSS demonstrated that the initial stage of crystal disordering results from inertial motion on a laser softened potential energy surface.<sup>2-6</sup> The atoms initially sample the modified potential with velocities determined by the lattice temperature prior to laser excitation. For the carrier density range studied previously, these inertial dynamics dominate for the first half picosecond (ps) following laser excitation, indicating that inter-atomic forces minimally influence atomic excursions from the equilibrium lattice positions, even for motions in excess of an Å. While these results represented a significant advance in our understanding of laser driven melting, no experiment had observed the carrier density dependent onset for lattice softening or the accelerated disordering predicted by theory.

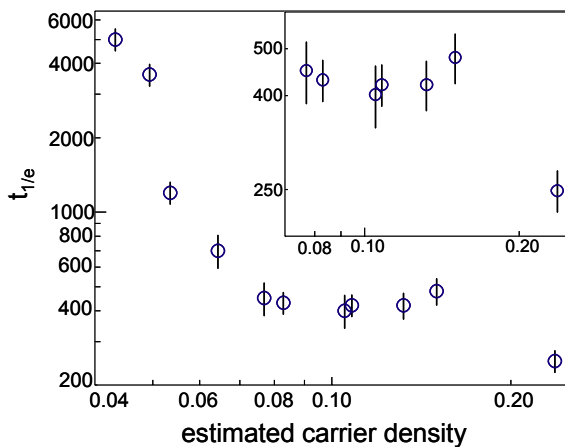


**Fig. 1:** log plot of the time required for the (111) Bragg peak intensity to drop to 35% of the initial value,  $t_{1/e}$ , versus the estimated carrier density. See text for a description of the data.

By extending the carrier density range investigated by a factor of three, we have succeeded in observing both the onset of lattice softening and the appearance of accelerated lattice disordering at extremely high carrier densities. The resultant carrier density dependence of the disordering appears in Fig. 1, and can be summarized as follows. For an estimated carrier density of less than 5% of the valence electron density, laser excitation of electronic carriers had no measurable influence on the inter-atomic potential. In the low carrier regime the rate of phonon emission by the excited carriers determines the disordering rate. From roughly 5% to 15%, inertial disordering dominates, as seen previously, but for a carrier density of 24%, we observe clear evidence for accelerated disordering, disordering faster than

the constant velocity disordering observed at lower carrier densities.

While x-ray diffraction provides direct evidence about the loss of crystalline order and the nature of the initial excited state potential, it does not monitor the structure of the liquid phase that results from laser melting. To access the formation time and structure of the liquid phase, we have used time resolved diffuse x-ray scattering. Figure 2 shows the ultrafast rise in the time dependent diffuse x-ray scattering signal following intense laser excitation of InSb. The rise in diffuse x-ray scattering intensity occurred with the same time dependence as the decay in the

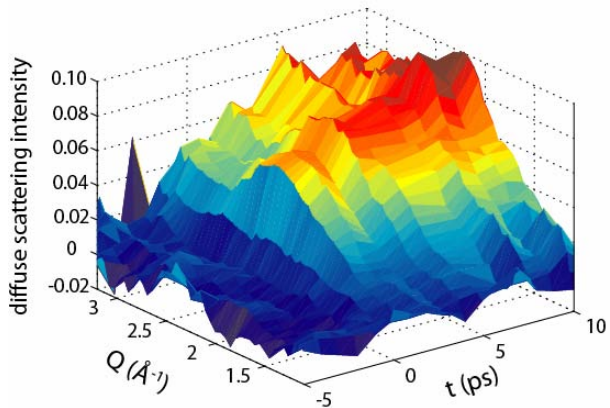


**Fig. 2:** Time dependent rise in diffuse scattering signal following laser excitation of InSb crystal. See text for description of data.

position of this first peak can be roughly correlated with the nearest neighbor distance in the liquid, where a larger  $Q$  corresponds to closer nearest neighbors. The larger  $Q$  for the peak in the structure factor at early delays is consistent with the closer nearest neighbor distance in the crystal phase than the liquid phase.

The most interesting and perplexing phenomena occurs on the tens to hundreds of picoseconds (ps) time scale. We observe a significant rise in the scattering intensity below a  $Q$  of  $\sim 1.75 \text{ \AA}^{-1}$ . This lower  $Q$  scattering has a maximum intensity for a time delay of roughly 100 ps, and then decays away by a 1 ns time delay. The appearance of increased scattering intensity below the first peak in the structure factor indicates that the InSb has formed a compressible fluid. The nature of this fluid phase and the physics that govern its formation and decay have yet to be determined.

**III.B. Photo-induced electron transfer dynamics:** Our research focuses on charge transfer in mixed valence organometallic complexes. Our current understanding of electron transfer reactions has resulted in large part from investigations of mixed valence compounds. Mixed valence organometallic structures also catalyze a wide range of chemical reactions, most prominently in metalloenzymes. Given their prominence and diversity, as well as the compatibility of Fe and Mn x-ray absorption K-edges with the energy range of the LCLS, we have decided to emphasize iron and manganese mixed valence compounds. The goal of these studies is to use XES, XANES, and RIXS to investigate the electronic degrees of freedom during a photochemical reaction. Organometallic compounds have sufficiently complex excited state potential energy surfaces that the interpretation of time dependent valence electronic spectra rarely proves conclusive. The time evolution of the spin multiplicity represents one of the critical aspects of metal center photochemistry that can be difficult to extract from valence electronic spectroscopy. XES spectroscopy provides a powerful and unambiguous probe of a metal atoms spin multiplicity, as shown in Fig. 3.

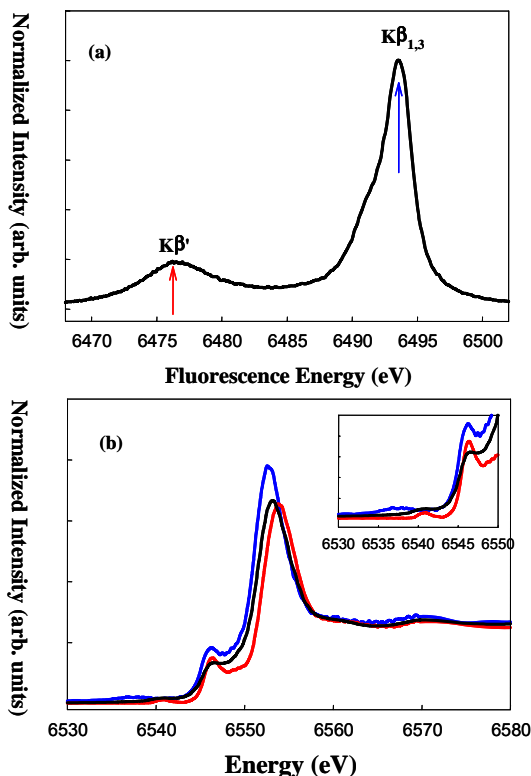
This research program will investigate  $\text{RbMnFe}(\text{CN})_6$ , a model photoelectron transfer system for developing time resolved XES spectroscopy.  $\text{RbMnFe}(\text{CN})_6$  undergoes a thermal phase transition from the  $\text{Mn}^{2+}(S=5/2)\text{-NC-Fe}^{3+}(S=1/2)$  cubic high temperature (HT) phase to the  $\text{Mn}^{3+}(S=2)\text{-NC-Fe}^{2+}(S=0)$  tetragonal low temperature (LT) phase caused by the electron transfer between Mn to Fe and a Jahn-Teller distortion around the  $\text{Mn}^{3+}$  ion. The high temperature phase can also be transiently photo-excited to the high temperature phase well below the phase transition temperature. This photo-induced phase transition has been attributed to a metal-to-

Bragg diffraction intensity, when integrated over the entire detector area. This result conforms to expectations, since disordering does not modify the scattering power of the atoms, but rather disperses the scattering more uniformly in space. The angle dependence of the scattering intensity, however, evolved for tens of nanoseconds (ns) before resembling the liquid structure factor at atmospheric pressure and the melting point temperature. The initial peak in the structure factor occurs at the reciprocal lattice vector  $Q = 2.4 \text{ \AA}^{-1}$ , instead of the  $2.3 \text{ \AA}^{-1}$  value, measured for the equilibrium liquid at atmospheric pressure and temperatures near the melting point. Only for time delays of 20 ns or longer does the scattering pattern peak at  $2.3 \text{ \AA}^{-1}$ . The

metal photoelectron transfer from  $\text{Fe}^{2+}$  to  $\text{Mn}^{3+}$ . We have chosen a solid state photo-induced phase transition system, rather than a solution phase chemical system, to investigate initially because it will optimize the concentration of excited states and consequently the transient changes in the XES spectrum. At the LCLS, where the laser coincident x-ray flux greatly exceeded that achievable at current synchrotrons, solution phase studies will be possible and we will be able to observe the time evolution of the spin multiplicity of photon induced spin crossover complexes.

We have initiated steady state XES and RIXS investigations of the phase dependent electronic structure, and will be initiating optical transient absorption measurements following the construction of our laser laboratory. The equilibrium and photo-excited phases have distinct spectra in the visible and the mid-IR, making these promising measurements that will effectively complement the time resolved x-ray studies. By combining a variety of time resolved techniques and methods, including time resolved powder diffraction, we have the potential to track structural and electronic degrees of freedom,

**Fig. 3:** Room temperature spectra for Mn in  $\text{RbMnFe}(\text{CN})_6$ . (a) XES  $\text{K}\beta$  spectrum. (b) Mn transmission XANES and emission channel selective for XANES. The (—) corresponds to transmission XANES, the (—) to the spin parallel XANES and (—) to the spin anti-parallel XANES. Since Mn resides in the high spin state at room temperature, there is no unoccupied spin parallel  $d$ -density of states, as shown in the inset.



making it possible to investigate their interdependence.

### References:

1. Clocking Femtosecond X-rays: A.L. Cavalieri, *et al. Phys. Rev. Lett.* **94**, 114801(2005).
2. Atomic-scale Visualization of Inertial Dynamics: A.M. Lindenberg, *et al. Science* **5720**, 392 (2005).
3. Observation of Structural Anisotropy and the Onset of Liquid-like Motion During the Nonthermal melting of InSb: K.J. Gaffney, *et al., Phys. Rev. Lett.* **95**, 125701 (2005).
4. Ultrafast X-ray Science at the Sub-Picosecond Pulse Source: K.J. Gaffney for the SPPS Collaboration, *Synchro. Rad. News* **18**, 32 (2005).
5. Ultrafast X-ray Studies of Structural Dynamics at SLAC: K.J. Gaffney, *et al., Proc. SPIE* **5917**, 59170D1 (2005).
6. D.A. Reis, K.J. Gaffney, G.H. Gilmer, B. Torralva, *Mat. Res. Soc. Bull.* **31**, 1 (2006).



*University Research Summaries*  
*(by PI)*



# Properties of Transition Metal Atoms and Ions

Donald R. Beck  
Physics Department  
Michigan Technological University  
Houghton, MI 49931  
e-mail: donald@mtu.edu

## Program Scope

Transition metal atoms are technologically important in plasma physics (e.g., as impurities in fusion devices), Atomic Trap Trace Analysis (detection of minute quantities of radioactive species), astrophysical abundance (e.g., Fe II) and atmospheric studies, deep-level traps in semiconductors, hydrogen storage devices, etc. The more complicated rare earths which we are beginning to study are important in lasers, high temperature superconductivity, advanced lighting sources, magnets, etc.

Because of the near degeneracy of  $nd$  and  $(n+1)s$  electrons in lightly ionized transition metal ions and the differing relativistic effects for  $d$  and  $s$  electrons [1], any computational methodology must simultaneously include the effects of correlation and relativity from the start. We do this by using a Dirac-Breit Hamiltonian and a Relativistic Configuration Interaction (RCI) formalism to treat correlation. Due to the presence of high- $l$  ( $d$ ) electrons, computational complications are considerably increased over those in systems with just  $s$  and/or  $p$  valence electrons. These include the following: (1) larger energy matrices (5-10x larger) because the average configuration can generate many more levels [2]. Multi-root RCI calculations with matrices of order 20,000 are becoming common. With the use of REDUCE [3], these can be equivalent to calculations 10 times (or more) larger, (2) increased importance of interactions with core electrons ( $d$ 's tend to be more compact, and there can be more of them), (3) a significant variation of the  $d$  radial functions with level ( $J$ ), which may require the presence of second order effects.

Methodological improvements are needed: (i) in the treatment of second order effects, (ii) to speed convergence, (iii) to more accurately treat Rydberg series-perturber interaction, and (iv) to improve overall efficiency (computer and human) in dealing with the complicated rare earths. Progress has been made in all these directions, during this project year.

## Recent Progress

[A]  $4f^7 J=7/2$  and  $4f^6 5d J=9/2$  Gd IV Energy Levels and Oscillator Strengths

This ion is of tremendous complexity for the *ab initio* computationalist, because of the large energy matrix required (well above 20 000), and the large size of the basis functions (over 100000 determinants in some cases) needed to create its elements. Higher angular momentum (e.g.  $l=6$ ) symmetries are also important. The ion is of potential interest for determination of the electron electric dipole moment [4] and in  $PbF_2:Gd$  scintillators [5]. An ultimate goal is to make *ab initio* treatments fully competitive with current semi-empirical

treatments for very complicated atomic states. This would then allow the extension of computational treatments to states where little or no observation is available.

First, by dividing the  $4f^7$  energy matrix up into about 50 pieces, we were able to identify the major contributions to energy differences within  $4f^7$ . Our RCI energy differences, at this stage, agree with observation [4] to  $\sim 1300 \text{ cm}^{-1}$  on average, comparable to the best semi-empirical results available [4]. When the important pieces are reassembled into a single matrix, this error increases to  $2852 \text{ cm}^{-1}$ , mainly due to the presence of pair-pair interactions.

Analysis shows that the principle losses are due to the interaction of  $4f^2 \rightarrow vf^2 + vg^2$  as well as  $4d \rightarrow vg$  with  $4d^2 \rightarrow 4f^2$ . The former seems to be mainly an “unlinked” cluster effect, whereas the latter seems to be a “linked” effect. Inclusion of the quadruple excitation  $4f^4 \rightarrow vf^2vg^2$  (26613 functions) and the triple excitation  $4d^3 \rightarrow 4f^2vg$  (33822 functions) did little to recover the above losses.

In order to carry out these demanding calculations, several methodological improvements were made: (i) replacement of 2 older computers with 2 2.4GHZ AMD CPUs (\$2K each); speed gain: 6x; (ii) Not computing matrix elements between different triple (quadruple) excitations, e.g., setting  $H(Q, Q') = 0$  when  $Q \neq Q'$ . Speed gain up to 10x (iii) Creating a code to automate data preparation for T and Q excitations (human speed gain 3x), (iv) improving convergence by using a non-relativistic concept that the bi-virtual correlation energy may be expressed as a sum of terms which are products of a group factor, and a radial pair energy that is nearly independent of moderate changes in  $Z$  and ionicity [6]. One can then extract these radial pair energies from the simpler closed shell system (e.g. Yb I [7]), and compare them to what is obtained in Gd IV, to see where basis set “weaknesses” are.

Our  $f$ -value study is initially focused on the electric dipole transition  ${}^8S$  (odd)  $7/2 \rightarrow 4f^65d$   $J=9/2$ . The  $4f^65d$  configuration is even more complicated than  $4f^7$ . It has 377 (not 50) references, but the bottom 9 levels have  $4f^6$  mostly coupled to  ${}^7F$ . While  $\sim 6.7 \text{ eV}$  of the excitation energy (out of  $\sim 11.9 \text{ eV}$ ) is due to correlation effects, most of this is due to the decreased number of  $4f$  electrons (e.g.,  $\sim 1.3 \text{ eV}$  is due to changes in  $4f^2$  pair correlation) in the upper state. Another illustration:  $\sim 0.6 \text{ eV}$  is due to lowering of  $4d^2 \rightarrow 4f^2$  exclusion effects (14186 functions were replaced with 27 functions, using REDUCE [3] in obtaining this). Most of these effects are not expected to influence the transition probability matrix element; however, another source for a reliable excitation energy needs to be found, if they’re not explicitly included.

## [B] Fe II Energy Levels and Oscillator Strengths

Fe II Oscillator Strengths are of great interest to astrophysicists for determination of stellar abundances and Fe II and its homologs are perhaps the most difficult transition metals to deal with. This is because some of the most dominant pair correlation (“first order”) effects leaves one with the most complicated “core”, viz  $d^5$ . Additionally, same symmetry adjacent levels can be very close together (a few thousand  $\text{cm}^{-1}$  on average), making the thorough inclusion of both correlation and relativity essential. Last year, we completed a study [8] of the Fe II  $9/2 \rightarrow 9/2$  (odd) transitions which were generally in good agreement with two extensive semi-empirical data bases.

This year, we have chosen to add the Fe II  $9/2 \rightarrow 11/2$  (odd) transitions. Several of the upper states exhibit strong near degeneracy effects ( $200\text{-}300 \text{ cm}^{-1}$ ), making it sometimes

difficult to properly label the levels (i.e. which coupling “dominates”). We have identified two new levels  $3d^5(^4G)4s4p\ ^6G$  and  $^6H$  which “sandwich” the  $y\ ^6F$  level. Improvements in convergence, using the methods described above, have been helpful. To illustrate, in Fe III  $3d^4J=4$ , the published [8] energy error relative to the ground state has been reduced from 1250 to 900  $\text{cm}^{-1}$ . The absolute adjacent energy difference error (a better figure of merit) has been reduced from 452  $\text{cm}^{-1}$  (12.2%) to 159  $\text{cm}^{-1}$  (9.4%).

#### [C] Br I, II Excitation, Ionization Energies and $f$ -values

Last year, we completed a study of Kr I and Kr II  $1s$  excitation, ionization energies and  $f$ -values (excitation) [9] in conjunction with experimental work done at Argonne National Lab using the Advanced Photon Source. Our  $f$ -values are quite consistent with observation, and our  $1s$  ionization potential for Kr I is in very good agreement with an existing theoretical result. There is a  $\sim 1$  eV difference with experiment, which at the time we felt was mainly due to the relatively crude treatment of QED effects ( $\sim 10\%$  error would be needed) [10].

This year ANL expressed an interest in similar calculations for Br I and Br II to be used as part of their fragmentation studies of  $\text{CF}_3\text{Br}$  molecules [11]. We have now completed these, and are about to write them up. While our  $1s$  IP in Br I agrees well with existing theory [12], comparison with experiment is more difficult, because the result is quite dependent on the state of matter in which the measurement is made [ $\text{Br}_2$  gas, XBr solids]. As part of this work, we also compared the QED methods we use with the more thorough ones of Drake *et al* [13] for the ionization potential of  $\text{Kr}^{34+}$ . The two results agreed quite well, which may indicate the bulk of the Kr I  $1s$  IP difference may not lie with QED.

#### [D] Mo VI Energy Levels and Oscillator Strengths

In the Mo VI odd  $J=5/2$  and  $J=7/2$  states, there is a strong interaction between  $4p^64f$  and  $4p^54d^2$  basis functions, which complicates both the experimental and computational work. Experimentally, two measurements are available [14,15] with sometimes quite different (up to a few thousand  $\text{cm}^{-1}$ ) energies. Only semi-empirical  $f$ -values are available. There is an ongoing re-analysis of the observations to resolve these differences [16].

Computationally the difficulty mainly arises because the two basis functions share a limited “common” core, viz  $KLM$  shells, so that much more correlation energy needs to be explicitly included. Generally, we are in better agreement with the newer measurement [15], although the top two  $4p^54d^2(J=5/2)$  levels are more uncertain due to their strong interaction with the nearby  $4p^65f$  and  $4p^66f$  levels. These results have now been published [17].

### DOE Publications mid 2003-mid 2006

In addition to items 2, 8, 9, 17 in the publication list already referred to, we have published calculations for energy levels and  $f$ -values in Zr III and Nb IV [18], and separately, Mo V [19].

## Future Plans

Near future applications include completion and publication of the work on Gd IV, Fe II and Br I, II. We will markedly improve the efficiency of the REDUCE program. This would be of considerable value for Gd IV, where the treatment of  $4d^2 \rightarrow 4f^2$  in  $4f^65d$  took  $\sim 18$  hrs with a 2.4GHZ AMD CPU. We think we can reduce this particular time to  $\sim 2$  hours.

## References

- [1] R. L. Martin and P. J. Hay, J. Chem. Phys. **75**, 4539 (1981).
- [2] S. M. O'Malley and D. R. Beck, Phys. Scr. **68**, 244 (2003). Drafts of all the PIs recent publications are available from [www.phy.mtu.edu](http://www.phy.mtu.edu) (under *faculty*).
- [3] The RCI program suite consists of 3 unpublished programs written by D. R. Beck over a period of years. RCI calculates the bound state wavefunctions, hyperfine structure, and Landé  $g$ -values. RFE uses RCI wavefunctions and computes E1, E2, M1 and M2  $f$ -values, including the effects of non-orthonormality. REDUCE minimizes the number of eigenvectors needed for a correlation manifold by rotating the original basis to maximize the number of zero matrix elements involving the reference functions; only rotated vectors having non-zero reference interactions are retained.
- [4] V. A. Dzuba *et al*, Phys. Rev. A **66**, 032105 (2002).
- [5] H. Jiang, private communication. H. Jiang *et al*, J. Phys. Cond. Matt. **16**, 3081 (2004) contains related work.
- [6] D. R. Beck and C. A. Nicolaides in *Excited States in Quantum Chemistry*, C. A. Nicolaides and D. R. Beck, editors, D. Reidel (1978), p.105ff.
- [7] K. Jankowski *et al*, Int. J. Quant. Chem. XXVII, 665 (1985).
- [8] D. R. Beck, Phys. Scr. **71**, 447 (2005).
- [9] L. Pan and D. R. Beck, J. Phys. B **38**, 3721 (2005).
- [10] the method of Welton [Phys. Rev. A. **46**, 2426 (1948)] is used, as implemented by J. P. Desclaux, *Methods and Techniques in Computational Chemistry*, Vol. A, E. Clementi, editor (Cagliari, Italy, STEF) 1994.
- [11] e.g. E. Peterson *et al*, Bull. Am. Phys. Soc. **51**, 120 (2006); S. Southworth, Bull. Am. Phys. Soc. **46**, 95 (2001).
- [12] P. Indelicato *et al*, Eur. Phys. J. D **3**, 29 (1998).
- [13] G. Drake, Can. J. Phys. **66**, 586 (1988).
- [14] A. Tauheed, K. Rahimullah, and M. S. Z. Chaghtai, Phys. Rev. A **32**, 237 (1985).
- [15] A. Kancerevicius *et al*, Lith. J. Phys. **31**, 143 (1991).
- [16] J. Reader, private communication.
- [17] L. Pan and D. R. Beck, Phys. Scr. **73**, 607 (2006).
- [18] D. R. Beck and L. Pan, Phys. Scr. **69**, 91 (2004).
- [19] L. Pan and D. R. Beck, Phys. Scr. **70**, 257 (2004).

## Molecular Structure and Electron-Driven Dissociation and Ionization

Kurt H. Becker and Vladimir Tarnovsky

Department of Physics and Engineering Physics and Center for Environmental Systems,

Stevens Institute of Technology, Hoboken, NJ 07030

phone: (201) 216-5671; fax: (201) 216-5638; [kbecker@stevens.edu](mailto:kbecker@stevens.edu)

### **Program Scope:**

This program is aimed at investigating the molecular structure and the collisional dissociation and ionization of selected molecules and free radicals. The focus areas are (1) ionization studies of selected molecules and free radicals and (2) the study of electron-impact induced neutral molecular dissociation processes – this part of the work is being phased out. Targets of choice for ionization studies include  $\text{SiCl}_4$  and  $\text{BCl}_3$  and their radicals, the molecular halogens  $\text{Br}_2$  and  $\text{F}_2$  and the compounds  $\text{SF}$ ,  $\text{SF}_2$ , and  $\text{SF}_4$ . The choice of target species is motivated on one hand by the relevance of these species in specific technological applications involving low-temperature processing plasmas and, on the other hand, by basic collision physics aspects. The scientific objectives of the research program can be summarized as follows:

- (1) provide the atomic and molecular data that are required in efforts to understand the properties of low-temperature processing plasmas on a microscopic scale
- (2) identify the key species that determine the dominant plasma chemical reaction pathways
- (3) measure cross sections and reaction rates for the formation of these key species and to attempt to deduce predictive scaling laws
- (4) establish a broad collisional and spectroscopic data base which serves as input to modeling codes and CAD tools for the description and modeling of existing processes and reactors and for the development and design of novel processes and reactors
- (5) provide data that are necessary to develop novel plasma diagnostics tools and to analyze more quantitatively the data provided by existing diagnostics techniques

### **Recent Progress and Ongoing Work:**

***Upgrade of the Fast-Beam Apparatus:*** Two major modifications were recently made to the fast-beam apparatus in an effort to improve the performance and sensitivity of this technique. First, we installed a new electron gun with a dispenser-type cathode, which consists of a porous tungsten matrix of about 20% porosity as a base interspersed uniformly with a mixture of barium and calcium aluminate as the electron emitting material. The total beam current produced by the new electron emitter is almost a factor of 10 higher than before with a maximum beam current of close to 4 mA at energies above 50 eV. At beam energies of 10 eV and 4 eV, the total current is still around 20  $\mu\text{A}$  and 5  $\mu\text{A}$ , respectively. In addition, the size (i.e. cross section) of the electron beam produced by the new emitter in the interaction region is about 0.2  $\text{cm}^2$  compared to a beam size of 0.6  $\text{cm}^2$  from the old electron gun. Thus, the current density delivered by the new emitter of up to 25  $\text{mA}/\text{cm}^2$  (for dc operation) exceeds that of the old gun by about a factor of 25.

We also replaced the channel electron multiplier (CEM), which served as ion detector with a position-sensitive, triple multichannel plate (MCP) detector in a Z-stack arrangement for maximum gain. This allows us to monitor the distribution of the product ions that emerge from the hemispherical analyzer on the face of ion detector. The ability to obtain the product ion distribution in addition to the total ion count is important in situations where fragment ions that are close in their mass-to-charge ratio are formed with broad excess kinetic energy distributions,

which causes the individual ion distributions to overlap on the face of the detector (as was the case for NO, NO<sub>2</sub> and N<sub>2</sub>O, where we could not resolve the ion signals corresponding to N<sup>+</sup> and O<sup>+</sup> and only reported a cross sections for the combined (N<sup>+</sup> + O<sup>+</sup>) formation). The experimental determination of the ion distribution on the detector face in conjunction with SIMION ion trajectory simulations allow us to deconvolute such overlapping ion distributions.

**Ionization of SiCl<sub>4</sub>:** SiCl<sub>4</sub> has a similar structure to fluorinated and hydrogenated targets that we studied in the past (SiF<sub>4</sub>, SiH<sub>4</sub>). No ionization cross section data are available for the molecule. We measured absolute partial cross sections for the formation of the SiCl<sub>x</sub><sup>+</sup> (x=1-4), Si<sup>+</sup>, and Cl<sup>+</sup> singly charged as well as the SiCl<sub>x</sub><sup>++</sup> (x=1-4) and Si<sup>++</sup> doubly charged positive ions following electron impact on SiCl<sub>4</sub>. Dissociative ionization was found to be the dominant process. The SiCl<sub>3</sub><sup>+</sup> fragment ion has the largest partial ionization cross section with a maximum value of slightly above 6 x 10<sup>-20</sup> m<sup>2</sup> at about 100 eV (see fig. 1). The cross sections for the formation of SiCl<sub>4</sub><sup>+</sup>, SiCl<sup>+</sup>, and Cl<sup>+</sup> have maximum values around 4 x 10<sup>-20</sup> m<sup>2</sup>. Some of the cross section curves exhibit an unusual energy dependence with a pronounced low-energy maximum at an energy around 30 eV followed by a broad second maximum at around 100 eV. This is similar to what has been observed earlier for other Cl-containing molecules of similar structure (TiCl<sub>4</sub> and CCl<sub>4</sub>) as well as for the Cl<sup>+</sup> partial ionization cross section from Cl<sub>2</sub>. The structure is most likely due to the presence of indirect ionization channels that compete with direct ionization. We note that evidence for the presence of indirect ionization was also found in the ionization of the TiCl<sub>x</sub> radicals as shown in fig. 2. The maximum cross sections for the formation of the doubly charged

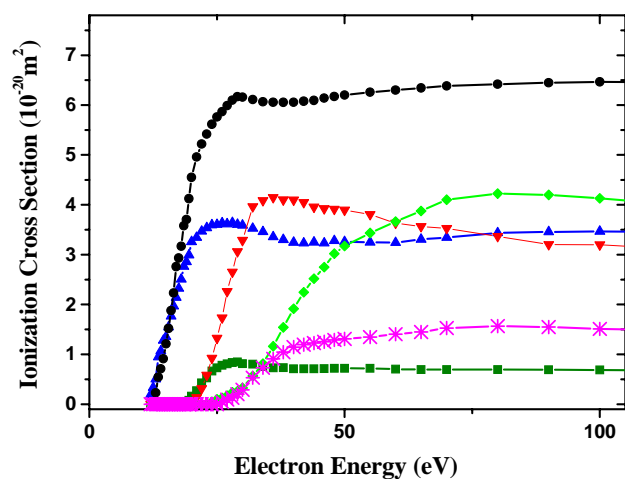


Fig. 1. Absolute cross sections for the formation of singly charged ions following electron impact on SiCl<sub>4</sub> from threshold to 100 eV: SiCl<sub>4</sub><sup>+</sup> (up triangles), SiCl<sub>3</sub><sup>+</sup> (circles), SiCl<sub>2</sub><sup>+</sup> (squares), SiCl<sup>+</sup> (down triangles), Si<sup>+</sup> (stars), Cl<sup>+</sup> (diamonds).

ions (except for SiCl<sub>3</sub><sup>++</sup>) are 0.05 x 10<sup>-20</sup> m<sup>2</sup> or less. The experimentally determined total single ionization cross section of SiCl<sub>4</sub> is compared with results of semi-empirical calculations and good agreement is found in terms of the absolute cross section value, but minor discrepancies exist in the cross section shape (fig. 3).

**Ionization Cross Section Calculations.** All experimental ionization studies were also supported by our continuing effort to extend and refine our semi-classical approach to the calculation of

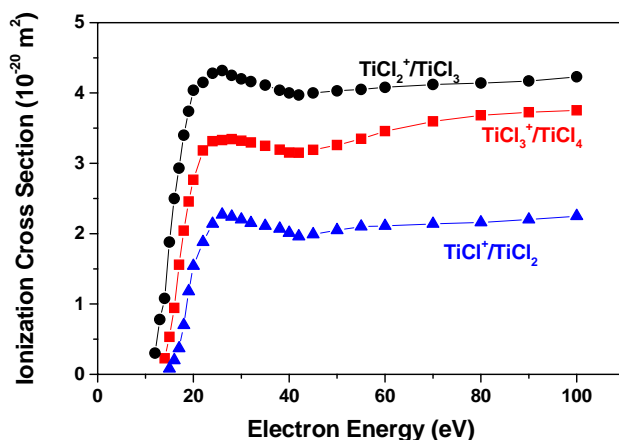


Fig. 2. Absolute partial ionization cross sections for the formation of  $\text{TiCl}_3^+$  from  $\text{TiCl}_4$  (red squares),  $\text{TiCl}_2^+$  from  $\text{TiCl}_3$  (black circles), and  $\text{TiCl}^+$  from  $\text{TiCl}_2$  (blue triangles) from threshold to 100 eV.

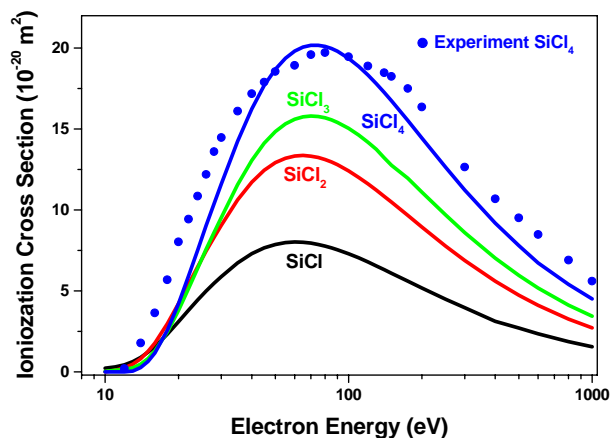


Fig. 3. Calculated absolute total (single) ionization cross sections for  $\text{SiCl}_4$  (blue line),  $\text{SiCl}_3$  (green line),  $\text{SiCl}_2$  (red line), and  $\text{SiCl}$  (black line) from threshold to 1000 eV. Also shown is the experimentally determined total single cross section for  $\text{SiCl}_4$  (blue circles).

total single ionization cross sections for atoms, molecules, free radicals, and ions. Recent calculations were carried out for Na Rydberg atoms, the  $\text{C}_2\text{H}_2^+$  ion, excited Ne atoms, and calculations are underway for the  $\text{CO}^+$  ion and the lanthanides

**Ionization of other Organic and Biologically Relevant Molecules:** Polycyclic aromatic hydrocarbons (PAHs) are important in environmental applications because of their toxicity in conjunction with their appearance as by-products in the combustion of organics. Two PAH compounds, coronene ( $\text{C}_{24}\text{H}_{12}$ ) and corannulene ( $\text{C}_{20}\text{H}_{10}$ ) are of special interest. There remains a rather large uncertainty in the ionization energies that have been reported for these two prototypical PAH compounds. We carried out electron impact ionization studies using a high resolution electron monochromator in conjunction with quadrupole mass spectrometry. The mass spectra determined at 100 eV show a rich fragmentation pattern (particularly for coronene) including the presence of multiply charged molecular cations for both compounds. For the singly and multiply charged parent ions of coronene and corannulene we determined the ionization

efficiency curves near threshold from which the corresponding appearance energies (AEs) were determined using a nonlinear least squares fitting routine and compared where available with previous values reported for both compounds using electron impact ionization and photoionization as well as with theoretical predictions.

**Neutral Molecular Dissociation Studies.** We completed the cross-comparison of neutral dissociation cross sections for SiH<sub>4</sub>, SiF<sub>4</sub>, and several Si-organic compounds (TMS, HMDSO, TEOS) with particular emphasis on the determination of final-state specific cross sections for the formation of Si(<sup>1</sup>S) and Si(<sup>1</sup>D) atoms. In the case of the formation of Si(<sup>1</sup>S) atoms from SiH<sub>4</sub> and SF<sub>4</sub> we found cross sections of about  $5 \times 10^{-21} \text{ m}^2$  (SiH<sub>4</sub>) and  $2.8 \times 10^{-21} \text{ m}^2$  (SiF<sub>4</sub>) at 60 eV. This part of the research is now being phased out.

#### **Publications Acknowledging DOE Support (since 2004)**

1. H. Deutsch, P. Scheier, K. Becker, and T.D. Märk, “Revised High-Energy Behavior of the DM Formula for the Calculation of Electron Impact Ionization Cross Sections of Atoms”, *Int. J. Mass Spectrom.* **233**, 13-7 (2004)
2. R. Basner, M. Schmidt, and K. Becker, “Measurement of Absolute Partial and Total Electron Ionization Cross Sections of Tungsten Hexafluoride”, *Int. J. Mass Spectrom.* **233**, 25-31 (2004)
3. W.Huo, V. Tarnovsky, and K. Becker, “Electron Impact Ionization Cross Sections of SF<sub>5</sub> and SF<sub>3</sub>”, *Int. J. Mass Spectrom.* **233**, 111-6 (2004)
4. S. Feil, K. Gluch, P. Scheier, K. Becker, and T.D. Märk, “The Anomalous Shape of the Cross Section for the Formation of SF<sub>3</sub><sup>+</sup> Fragment Ions Produced by Electron Impact on SF<sub>6</sub> Revisited”, *J. Chem. Phys.* **120**, 11465-8 (2004)
5. H. Deutsch, K. Becker, A.N. Grum-Grzhimailo, K. Bartschat, H. Summers, M. Probst, S. Matt-Leubner, and T.D. Märk, “Calculated Cross Sections for the Electron Impact Ionization of Excited Ar Atoms Using the DM Formalism”, *Int. J. Mass Spectrom.* **233**, 39-43 (2004)
6. S. Feil, K. Gluch, S. Matt-Leubner, P. Scheier, J. Limtrakul, M. Probst, H. Deutsch, A. Stamatovic, K. Becker, and T.D. Märk, “Absolute Partial and Total Cross Sections for Positive and Negative Ion Formation Following Electron Impact on Uracil”, *J. Phys. B* **37**, 3013-20 (2004)
7. S. Matt-Leubner, S. Feil, K. Gluch, J. Fedor, A. Stamatovic, O. Echt, P. Scheier, K. Becker, and T.D. Märk “Energetics, Kinetics, and Dynamics of Decaying Metastable Ions Studied with a High Resolution Three-Sector-Field Mass Spectrometer”, *Plasma Sources Sci. Techn.* **14**, 26-30 (2005)
8. H. Deutsch, P. Scheier, S. Matt-Leubner, K. Becker, and T.D. Märk “A Detailed Comparison of Calculated and Measured Electron-Impact Ionization Cross Sections of Atoms Using the Deutsch-Märk (DM) Formalism”, *Int. J. Mass Spectrom.* **243**, 215-21 (2005)
9. H. Deutsch, K. Becker, A.N. Grum-Grzhimailo, M. Probst, S. Matt-Leubner, and T.D. Märk, “Calculated Electron Impact Ionization Cross Sections of Excited Ne Atoms Using the DM Formalism”, *Contr. Plasma Phys.* **7**, 494-499 (2005)
10. R. Basner, M. Gutkin, J. Mahoney, V. Tarnovsky, H. Deutsch, and K. Becker, “Electron Impact Ionization of Silicon Tetrachloride”, *J. Chem. Phys.* **123**, 05313 (2005)
11. H. Deutsch, K.B. MacAdam, K. Becker, H. Zhang, and T.D. Märk, “Calculated Cross Sections for the Electron Impact Ionization of Na(ns) and Na(nd) Rydberg Atoms”, *J. Phys. B* **39**, 343-353 (2005)
12. S. Denifl, B. Sonnweber, J. Mack, L. T. Scott, P. Scheier, K. Becker, and T.D. Märk, “Appearance Energies of Singly, Doubly, and Triply Charged Coronene and Corannulene Ions Produced by Electron Impact”, *Int. J. Mass Spectrom.* **249/250**, 353-358 (2006)
13. H. Deutsch, K. Becker, P. Defrance, M. Probst, J. Limtrakul, and T.D. Märk, “Newly Calculated Absolute Cross Sections for the Electron Impact Ionization of C<sub>2</sub>H<sub>2</sub><sup>+</sup>”, *Europ. Phys. J. D* **38**, 489 (2006)
14. K. Becker, J. Mahoney, M. Gutkin, V. Tarnovsky, and R. Basner, “Electron Impact Ionization of SiCl<sub>x</sub> and TiCl<sub>x</sub> (x = 1-4): Contributions from Indirect Ionization Channels”, *Jap. J. Appl. Phys.* (2006), accepted for publication

# PROBING COMPLEXITY USING THE ADVANCED LIGHT SOURCE

Nora Berrah

Physics Department, Western Michigan University, Kalamazoo, MI 49008  
e-mail:nora.berrah@wmich.edu

## Program Scope

The objective of the research program is to carry out experiments that will further our understanding of *fundamental interactions between photons and complex systems* using the Advanced Light Source (ALS). The unifying theme of this program is to probe the frontiers of *complexity* by investigating quantitatively how two classes of systems, negative ions as well as molecules and clusters, respond to x-ray radiation. The proposed studies include investigation of multi-electron interactions and of energy transfer processes within gas-phase systems. Both will advance our understanding of the general many-body problem.

We have added to our experimental detection systems a momentum imaging apparatus which was commissioned this year. In addition, progress in the building of a movable ion beamline is underway. It will be used in the collinear and cross geometry with several photon beamlines at the Advanced Light Source. We present here results completed and in progress this past year and plans for the immediate future.

## Recent Progress

### 1) Inner-Shell Photodetachment of Negative Ions

#### 1.1 Photodetachment of He<sup>-</sup> near the 1s threshold: Absolute cross section measurements and post-collision interactions (Ref. 1)

He<sup>-</sup> is the smallest prototype negative ion, and offers an important model system that is accessible to advanced theoretical treatment. As such, He<sup>-</sup> has been the subject of extensive theoretical study [a] and was studied experimentally recently [b]. The experimental work [b] suggested that the cross section near the He<sup>-</sup>  $1s2s2p^4P^0 \rightarrow He\ 2s2p^3P^0$  threshold may be considerably smaller than expected. However, direct measurements of the absolute cross section were not available in this photon energy region, and comparison with theoretical studies relied on data scaled at 42 eV to theoretical cross sections calculated by Zhou *et al.* [c]. Later [a] it was noted that recapture of the photoelectron (i.e. the threshold electron) through post-collision interaction (PCI) effects could account for the apparent reduction of the cross section just above the threshold.

We have measured the absolute photodetachment cross section over a region covering 1.3 eV near to and above the He  $2s2p^3P^0$  threshold and compared it to calculations [1]. A greatly improved agreement with the shape of the cross section is found when PCI effects are included, underlining the importance of this process in near-threshold photodetachment. These new measurements were also found to be consistent with recent theory [a], within the semi-classical approximation that included photoelectron recapture due to PCI effects. Photoelectron recapture is most significant nearer to the threshold and would be observed as a large feature in neutral He production which will be difficult to measure.

## **1.2 High-charge-state formation following inner-shell photodetachment from S<sup>-</sup> (Ref 2)**

The formation of S<sup>+</sup>, S<sup>2+</sup>, S<sup>3+</sup>, and S<sup>4+</sup> have been measured following inner-shell photodetachment of S<sup>-</sup>. The absolute photodetachment cross sections for all possible ionic products were measured over a large photon energy region covering both the 2*p* and 2*s* thresholds [2]. Although S<sup>5+</sup> is energetically allowed at the higher photon energies, it was not observed. Our measurements also enabled us to determine neutral atomic excited states. The 2*s* threshold energy was measured to be 224.6(5) eV, allowing the determination of the neutral atomic S 2*s*<sup>-1</sup> 3*s*<sup>2</sup>3*p*<sup>5</sup> inner-shell excited state energy for the first time. Furthermore, the S<sup>-</sup> 2*s*<sup>-1</sup>3*s*<sup>2</sup>3*p*<sup>6</sup> <sup>2</sup>S<sub>1/2</sub> state is observed as a Feshbach resonance 2.3(5) eV below the 2*s* threshold in the S<sup>+</sup>, S<sup>2+</sup>, and S<sup>3+</sup> product channels unlike the case in T<sup>-</sup> [d].

## **2) Study of Auger decay in core-excited HBr by angle-resolved two-dimensional photoelectron spectroscopy (Ref. 3)**

Angle-resolved two-dimensional photoelectron spectroscopy was used in HBr in the vicinity of the Br 3*d* thresholds. In particular, 3*d*→σ\* resonances, 3*d*→*nl*λ Rydberg resonances and 3*d*→ε*l* continuum have been measured. The two 3*d*<sub>5/2,3/2</sub>→σ\* resonances have been measured for the first time and found to be at 70.84±0.03 eV and 71.87±0.05 eV, respectively, giving a spin-orbit splitting of 1.03±0.07 eV for the two 3*d*<sub>5/2,3/2</sub> components. Their angular distribution asymmetry parameters β have also been determined. For the two fine structure component, their respective β values are similar. Based on these β values, the intrinsic anisotropy parameter α<sub>2</sub> were derived and found similar to those of the corresponding M<sub>2,3</sub>NN normal Auger decay lines in the isoelectronic counterpart Kr. Resonant enhancements of the valence photolines, the 4*s*σ<sup>-1</sup> main line, the 4*p*σ<sup>-1</sup> and the 4*p*π<sup>-1</sup>, at the σ\* resonance have been observed and are attributed to molecular Auger decay from the intermediate dissociative state to some final dissociative states. A semiempirical potential energy curve for the antibonding σ\* state was derived and the potential curves for some of the final dissociative molecular states are quantitatively proposed. We also find that the resonant enhancements from both the σ\* resonances and the Rydberg resonances have different effects on the angular distribution parameters β of the three valence photolines [3].

## **3) An alternative explanation for the spectral hole attributed to continuum-continuum interference in HCl (Ref. 4)**

Photoelectron spectra in the vicinity of the 2*p*<sub>3/2,1/2</sub>→σ\* dissociative resonances in HCl and DCI have been measured using two-dimensional photoelectron spectroscopy. The comprehensive data suggests that the explanation for the negative spectral contribution observed in an atomic line, which arises from autoionisation following dissociation, might be more complex than the one proposed by Feifel *et al.* [e]. These authors attributed this feature solely to continuum-continuum interference between resonant atomic and molecular Auger contributions, the latter occurring prior to complete dissociation but resulting in an electron with the same kinetic energy as one produced in the atomic decay. Our data reveal a similar spectral feature in a region of the spectrum where this type of interference cannot occur. Consequently, an interference mechanism that does not require that the energy of the resonant Auger electron be the same whether it is emitted before or after the molecule dissociates is indicated. Alternatively, the two-dimensional resonant enhancements, observed in the region of the negative spectral contribution, could be

attributed to Auger decay to multiple final ion states, before the dissociating molecule has fragmented completely [4].

#### 4) **CI-induced spin polarization of the $\text{Ar}^* (2p^{-1} 4s)_{j=1}$ resonant Auger decay (Ref. 5, 6)**

Spin-resolved measurements of the  $\text{Ar}^* (2p^{-1}_{1/2,3/2} 4s_{1/2})_{j=1}$  resonantly excited  $L_{2,3}M_{2,3}M_{2,3}$  Auger decay have been carried out using our Mott-TOFs detectors [5,6]. The low resolution Auger spectrum should exhibit virtually zero dynamic spin polarization, due to cancellation between different multiplet components. However, it reveals an unexpected nonvanishing polarization effect. Calculations within a relativistic distorted wave approximation [5,6] explain this effect as configuration-interaction (CI) induced. The CI generates experimentally unresolved fine structure components with low and high total angular momentum, giving rise to asymmetric cases where the high  $J$  part of certain multiplets is suppressed by internal selection rules for diagram lines. In this case, only the low  $J$  components survive with no partner for spin-polarization cancellation.

#### **Future Plans.**

The principal areas of investigation planned for the coming year are to: 1) Continue the analysis of the photoelectron studies of van der Waals clusters. 2) Analyze the momentum imaging data generated this year from the fragmentation of molecules. 3) Study the dissociation of clusters using our new momentum imaging detector. 4) Continue the analysis of our photodetachment experiments in small anions clusters ( $\text{B}^-$  and  $\text{Si}^-$ ).

#### **References**

- [a] J.L. Sanz-Vicario, E. Lindroth, and N. Brandefelt, Phys. Rev. A 66, 052713(2002) and references therein.
- [b] N. Berrah, J. D. Bozek, G. Turri, G. Ackerman, B. Rude, H.-L. Zhou, and S. T. Manson, Phys. Rev. Lett. 88, 093001 (2002) and references therein.
- [c] [5] H.L. Zhou, S.T. Manson, L. Vo Ky, A. Hibbert, and N. Feautrier, Phys. Rev. A 64, 012714 (2001)
- [d] H. Kjeldsen, F. Folkmann, T. S. Jacobsen, and J. B. West, Phys. Rev. A 69, R050501 (2004)
- [e] Feifel et al. Phys. Rev. Lett. 85 3133 (2000)

#### **Publications from DOE sponsored research.**

- [1] R. C. Bilodeau, J. D. Bozek, A. Agular, G. D. Ackerman, and N. Berrah, "Photodetachment of  $\text{He}^-$  near the 1s threshold: Absolute cross section measurements and post-collision interactions" Phys. Rev. A 73, 034701 (2006).
- [2] R. C. Bilodeau, J. D. Bozek, G. D. Ackerman, N. D. Gibson, C. W. Walter, A. Aguilar, G. Turri, I. Dumitriu and N. Berrah "High-charge-state formation following inner-shell photodetachment from  $\text{S}^-$ " Phys. Rev. A 72, 050701(R), (2005).
- [3] X. Feng, A. A. Wills, E. Sokell, M. Wiedenhoef, and N. Berrah, "Study of Auger decay in core-excited HBr by angle-resolved two-dimensional photoelectron spectroscopy Phys. Rev. A 73 012716 (2006).
- [4] E. Sokell, A A Wills, M Wiedenhoef, X Feng, S E Canton, D Rolles and N Berrah "An alternative explanation for the spectral hole attributed to continuum-continuum interference in HCl" J. Phys. B.38, 1535 (2005).
- [5] B. Lohmann, B. Langer, G. Snell, U. Kleiman, S. Canton, A. Martins, U. Becker and N. Berrah, "CI-Induced Spin Polarization of the  $\text{Ar}^* (2p^{-1} 4s)_{j=1}$  Resonant Auger decay", Phys. Rev. A 71, R020701 (2005).

- [6] B. Lohmann, B. Langer, G. Snell, U. Kleiman, S. Canton, A. Martins, U. Becker and N. Berrah, Publisher's Note: "Configuration-interaction-induced dynamic spin polarization of the Ar\* ( $2p_{1/2,3/2}^{-1} 4s_{1/2}$ )<sub>J=1</sub> resonant Auger decay", *Phys. Rev. A* **71**, 020701 (2005).
- [7] J. Nikkinen, H. Aksela, S. Heinasmaki, E. Kukkk, N. Berrah and S. Aksela, "Strong Electron Correlation in Ca 2p, Sr 3d and Ba 4d Core Hole States Investigated by Means of Photoelectron Spectroscopy and MCDP Calculations", *Physica Scripta*. Vol. T115, 119–121, (2005).
- [8] J. Nikkinen, H. Aksela, S. Fritzsche, S. Heinasmaki, R. Sankari, E. Kukkk, N. Berrah and S. Aksela, "Photoionization and Auger decay of the 3d vacancy state of atomic strontium: Electron-electron correlations" *Phys. Rev. A* **72**, 042706 (2005).
- [9] X. Feng, A. A. Wills, T. Gorczyca, M. Wiedenhoeft, E. Sokell, and N. Berrah "Photoelectron recapture investigation in Ar using two-dimensional photoelectron spectra" *Phys. Rev. A* **72**, 042712 (2005).
- [10] N. Berrah, R. C. Bilodeau, J. D. Bozek, G. Turri and G.D. Ackerman, "Double photodetachment in He<sup>-</sup>: Feshbach and triply excited resonances, *J. Elect. Spec. and Relat. Phen.* **144-147**,19 (2005).]
- [11] R. C. Bilodeau, J. D. Bozek, N. D. Gibson, C. W. Walter, G. D. Ackerman, I. Dumitriu, and N. Berrah, "Inner-shell Photodetachment Thresholds: Unexpected Long-range Validity of the Wigner Law", *Phys. Rev. Lett.* **95**, 083001 (2005).
- [12] S. E. Canton, E. Kukkk, J. D. Bozek, D. Cubaynes, and N. Berrah "Imaging Wavepacket Interferences using Auger Resonant Raman Spectroscopy", *Chem. Phys. Lett.* **402**, 143, (2005).
- [13] N. Berrah, J. D. Bozek, R. C. Bilodeau and E. Kukkk, "Studies of Complex Systems: From Atoms to Clusters", *Radiat. Phys. Chem.* **70**, Issue 1, 57 (2004).
- [14] G. Turri, G. Snell, B. Langer, M. Martins, E. Kukkk, S. E. Canton, R. C. Bilodeau, N. Cherepkov, J. D. Bozek, and N. Berrah, "Probing the Molecular Environment using Spin-Resolved Photoelectron Spectroscopy" *Phys. Rev. Lett.* **92**, 013001 (2004).
- [15] B. Lohmann, B. Langer, G. Snell, U. Kleiman, S. Canton, M. Martins, U. Becker and N. Berrah, "Angle and Spin Resolved Analysis of the Resonantly Excited Ar\* ( $2p_{3/2}^{-1} 4s_{1/2}$ )<sub>j=1</sub> Auger Decay, AIP (American Institute of Physics) conference proceedings **697**, pp 133, ed: G.F. Hanne, L. Malegat, H. Schmidt-Boecking (2004).
- [16] N. Berrah, R. C. Bilodeau, G. Ackermann, J. D. Bozek, G. Turri, E. Kukkk, W. T. Cheng, and G. Snell "Probing atomic and Molecular Dynamics from Within" *Radiat. Phys. Chem.*, **70**, 491 (2004).
- [17] G. Turri, G. Snell, B. Langer, M. Martins, E. Kukkk, S. E. Canton, R. C. Bilodeau, N. Cherepkov, J. D. Bozek, and N. Berrah, "Probing the Molecular Environment using Spin-Resolved Photoelectron Spectroscopy" AIP (American Institute of Physics) conference proceedings **697**, pp 133, ed: G.F. Hanne, L. Malegat, H. Schmidt-Boecking (2004).
- [18] D. Cubaynes, M. Meyer, A. Grum-Grzhimailo, J.-M. Bizau, E. T. Kennedy, J. Bozek, M. Martins, S. Canton, B. Rude, N. Berrah, and F. J. Wuilleumier, "Dynamically and quasiforbidden lines in photoionization of open-shell atoms: a combined two-color experiment and theoretical study", *Phys. Rev. Lett.* **92**, 233002 (2004).
- [19] N. Berrah, R. C. Bilodeau, G. Ackermann, J. D. Bozek, G. Turri, B. Rude, N. D. Gibson, C. W. Walter and A. Aguilar, "Probing Negative Ions from Within", *Physica Scripta* **T110**, 51 (2004).
- [20] G. Turri, G. Snell, B. Langer, M. Martins, E. Kukkk, S.E. Canton, R.C. Bilodeau, N. Cherepkov, J.D. Bozek, A.L. Kilcoyne and N. Berrah "Spin and Angle Resolved Spectroscopy of S 2p Photoionization in Hydrogen Sulfide Molecule", *Phys. Rev. A* **70**, 022515 (2004).
- [21] R. C. Bilodeau, J. D. Bozek, G. Turri, G. D. Ackerman, and N. Berrah, Simultaneous 3-electron Decay and Triply Excited Quartet States in He<sup>-</sup>, *Phys. Rev. Lett.* **93**, 193001 (2004).
- [22] B. Lohmann, B. Langer, G. Snell, U. Kleiman, S. Canton, M. Martins, U. Becker and N. Berrah, "Angle and Spin Resolved Analysis of the Resonantly Excited Ar\* ( $2p_{3/2}^{-1} 4s_{1/2}$ )<sub>j=1</sub> Auger Decay, AIP (American Institute of Physics) conference proceedings **697**, pp 133, ed: G.F. Hanne, L. Malegat, H. Schmidt-Boecking (2004).

# Atomic and Molecular Physics in Strong Fields

Shih-I Chu

Department of Chemistry, University of Kansas

Lawrence, Kansas 66045

E-mail: sichu@ku.edu

## Program Scope

In this research program, we address the fundamental physics of the interaction of atoms and molecules with intense ultrashort laser fields. The main objectives are to develop new theoretical formalisms and accurate computational methods for *ab initio* nonperturbative investigations of multiphoton quantum dynamics and very high-order nonlinear optical processes of one-, two-, and many-electron quantum systems in intense laser fields, taking into account detailed electronic structure information and many-body electron-correlated effects. Particular attention will be paid to the exploration of novel new physical mechanisms, time-frequency spectrum, and coherent control of high-harmonic generation (HHG) processes for the development of table-top x-ray laser light sources. Also to be explored is the ionization mechanisms of molecules in intense laser fields and attosecond physics.

## Recent Progress

1. *Ab Initio* Nonperturbative Approach for the Exploration of the Coulomb Explosion Dynamics through Excited Molecular Vibrational States

The study of ionization and molecular fragmentation is a subject of considerable interest in strong-field molecular physics. In particular, the response of the simplest prototype molecular systems  $\text{H}_2^+$  ( $\text{D}_2^+$ ) and  $\text{H}_2$  ( $\text{D}_2$ ) in intense laser fields have been experimentally studied in the recent past. In intense laser fields, the electron of  $\text{H}_2^+$  can be excited and/or ionized. If the electron is ionized, the  $\text{H}_2^+$  ion breaks up via direct Coulomb explosion (DCE), producing  $\text{H}^+$  ions. If the electron is excited to continuum vibrational states,  $\text{H}_2^+$  can dissociate directly or be further ionized by the laser. The latter process, which will be called *excitation-ionization-dissociation* (EID) is a two-step process, in which  $\text{H}_2^+$  in intermediate continuum vibrational states induces CE. Recent experiments of ion-induced molecular fragments showed that the excited states of the transient molecular ions can have strong influence on kinetic-energy release (KER) spectra.

In a recent work [1], we investigate the fragmentation dynamics of  $\text{H}_2^+$  molecular ions in intense laser fields by means of an *ab initio* method beyond the Born-Oppenheimer approximation. Special attention is paid to the exploration of the Coulomb explosion (CE) mechanisms and quantum dynamics through *excited* vibrational states of  $\text{H}_2^+$ . A novel KER spectrum and CE phenomenon are predicted for the first time, in which the kinetic-energy distribution of  $\text{H}^+$  ions exhibits a series of peaks separated by one photon energy. A proposed scheme for the experimental observation of the KER spectrum and CE dynamics is presented in [1].

2. Recent Development of Generalized Floquet Formalisms for Nonperturbative Treatment of Multiphoton Processes in Intense One-Color or Multi-Color Laser Fields

a) In the last several years, we have continued the development of generalized Floquet formalisms and complex quasi-energy methods for *nonperturbative* treatment of multiphoton and high-order nonlinear optical processes in intense monochromatic (periodic) or polychromatic (quasi-periodic) laser fields. An extensive review article on these new developments & their applications has been recently published [2].

b) Precision Calculation of High-Order Harmonic Generation Spectrum of  $H_2^+$  in Intense Laser Fields: Time-Dependent Non-Hermitian Floquet Approach

The generalized Floquet approaches developed in the past involved the determination of the complex quasi-energies from a *time-independent* non-Hermitian Floquet matrix [2]. Recently we have introduced an alternative method, the *time-dependent* non-Hermitian Floquet approach [3,4]. The procedure involves the complex-scaling generalized pseudospectral spatial discretization of the time-dependent Hamiltonian and non-Hermitian time propagation of the time-evolution operator in the *energy* representation. The approach is designed for effective treatment of multiphoton processes in very intense and/or low-frequency laser fields, which are generally more difficult to treat using the *time-independent* Floquet matrix techniques.

The procedure is applied to the precision calculation of multiphoton ionization (MPI) and HHG calculations of  $H_2^+$  [4] for the wavelength 532 nm and several laser intensities, as well as various internuclear distances  $R$  in the range between 2.0 and 17.5 a.u. We found that both the MPI and HHG rates are strongly dependent on  $R$ . Further, at some internuclear separations  $R$ , the HHG productions are strongly enhanced and this phenomenon can be attributed to the resonantly enhanced MPI at these  $R$ . Finally, the enhancement of higher harmonics is found to take place mainly at larger  $R$ . Detailed study of the correlation between the behavior of MPI and HHG phenomena is presented. The time-dependent non-Hermitian Floquet approach has been also recently applied to the study of very high-order above-threshold ionization (ATI) of  $H^-$  system [3].

3. Generalized Strong-Field-Approximation Approach for the Study of HHG and MPI of Light Homonuclear Diatomics in Intense Laser Fields

A generalized strong-field approximation (GSFA) method recently developed for the treatment of atomic HHG is extended to the nonperturbative treatment of MPI and HHG of diatomic molecular systems in intense laser fields [5,6]. The GSFA approach incorporates the rescattering effects, beyond the conventional Keldysh model and saddle-point approximation. We are currently extending the molecular GSFA approach to the exploration of the quantum interference effect from aligned molecular systems.

4. Development of *Self-Interaction-Free* Time-Dependent Density Functional Theory (TDDFT) for Nonperturbative Treatment of Multiphoton Processes of Many-Electron Systems in Strong Fields

To study multiphoton processes of many-electron quantum systems in intense laser fields using the fully *ab initio* wave function approach, it is necessary to solve the time-dependent Schrödinger equation of  $3N$  spatial dimensions and  $1D$  in time ( $N$  = the number of electrons). This is well beyond the capability of current supercomputer technology for  $N > 2$ . Recently we have initiated a series of new developments of *self-interaction-free* TDDFT for probing strong-field physics of many-electron systems, taking into account electron correlations and detailed electronic structure [7-12]. Given below is a brief summary of some recent progress.

a) *Role of the Electronic Structure and Multi-electron Response in Ionization Mechanisms of Diatomic Molecules in Intense Laser Fields*

Recently, there is considerable interest in the study of the ionization mechanism of diatomic molecules in intense laser fields. Most theoretical studies of strong-field molecular ionization in the recent past are based on approximate models such as the charge-screening correction to tunneling theory [13], interference mechanism [14], and molecular ADK model [15], etc. For example, in the interference model, the destructive interference between electrons emitted from the vicinity of two distinct ionic cores leads to suppressed ionization in diatomic species with anti-bonding HOMO. Such a mechanism correctly describes the ionization suppression of  $O_2$ , and the absence of suppression in  $N_2$ . However, it also

predicts strong ionization suppression of  $F_2$ , which is in contradictory to the experimental observations [16]. The molecular ADK model [15] has encountered the similar difficulty. Thus currently no theoretical models can account for the absence of ionization suppression of  $F_2$ .

Recently we extend the self-interaction-free TDDFT[10,11] for nonperturbative investigation of the ionization mechanisms of diatomic molecules ( $N_2$ ,  $O_2$ , and  $F_2$ ) in intense short-pulsed lasers [17]. Our results indicated that the detailed electron structure and correlated multielectron responses (*not* considered by approximated models) are important factors for the determination of the strong-field ionization behavior. Further, we found that it is not adequate to use only the highest occupied molecular orbital (HOMO) for the description of the ionization behavior since the inner valence electrons can also make significant or even dominant contributions. To our knowledge, the *self-interaction-free* TDDFT study[17] is the first all-electron *ab initio* treatment that can account for all the experimental observations so far.

#### b) *Very- High-Order Harmonic Generation of Ar Atoms and Ar<sup>+</sup> Ions in Intense Laser Pulses*

To explore the underlying quantum dynamics responsible for the production of the very-high-order harmonics observed in a recent experiment [18], we performed an *all-electron* treatment of the response of Ar and Ar<sup>+</sup> systems to superintense laser fields [19] by means of the self-interaction-free TDDFT. In our study, all the valence electrons are treated explicitly & their partial contributions to the ionization are analyzed. Further, by introducing an effective charge concept, we can study at which laser intensity the contribution to the high-energy HHG from Ar<sup>+</sup> ions precede over the Ar atoms. Comparing the HHG power spectrum from Ar and Ar<sup>+</sup>, we conclude that the high-energy HHG observed in the recent experiment [18] originated from the ionized Ar atoms.

c) An invited review article for a special issue of the Journal of Chemical Physics, entitled “Recent development of self-interaction-free time-dependent TDDFT for nonperturbative treatment of atomic and molecular multiphoton processes in intense laser fields,” has been published [20] in this funding period.

#### 5. Effect of Electron Correlation on High-Order Harmonic Generation of He Atoms in Intense Laser Fields

Recently we present a time-dependent generalized pseudospectral (TDGPS) approach in *hyperspherical* coordinates (HSC) for *ab initio* 6D nonperturbative treatment of HHG processes of two-electron atomic systems in intense laser fields [21]. In this approach, the GPS technique [22] is extended to the HSC for *non-uniform* and optimal spatial discretization of the hyper-radius  $R (= (r_1^2 + r_2^2)^{1/2})$  and hyper-angle  $\alpha (= \tan^{-1}(r_1/r_2))$  [21,23]. A second-order split-operator method in the *energy* representation [24] is extended for efficient and accurate time propagation of the wave function in the HSC. The procedure is applied to the investigation of HHG of He atoms in ultrashort laser pulses at a KrF wavelength of 248.6 nm. Using this approach, we have achieved converged HHG results as indicated in the good agreement of the length- and acceleration- form HHG power spectra [21]. The effects of electron correlation and doubly excited states on HHG are also explored in details. A HHG peak with Fano-like line profile is identified which can be attributed to a broad resonance of doubly excited states. To our knowledge, this is the first fully *ab initio* 6D calculation showing the delicate electron correlation effect imprinted on the HHG power spectrum. Comparison of the HHG power spectrum of the *ab initio* two-electron calculations with that of the conventional single-active-electron (SAE) model is also made. It is shown that while the SAE model is capable of providing reasonable prediction of the first few harmonics for this case, it fails to exhibit the existence of the higher harmonics as well as the broad resonance peak with Fano-like line profile. Further study is to be continued in the next funding period.

#### 6. Creation and Control of Single Attosecond XUV Pulse by Few-Cycle Intense Laser Pulse

We present an *ab initio* quantum and classical investigations of the production and control of a single attosecond pulse using few-cycle intense laser pulses as the driving field [25]. The HHG power spectrum

is calculated by solving accurately and efficiently the time-dependent Schrödinger equation using the TDGPS method [24]. The time-frequency characteristics of the attosecond XUV laser pulse are analyzed in details by means of the wavelet transform of the time-dependent induced dipole acceleration. In addition, we perform classical trajectory simulation of the strong-field electron dynamics and electron return map. We found that the quantum and classical results provide complementary and consistent information regarding the underlying mechanisms responsible for the production of the attosecond laser pulse. For few-cycle (5 fs) driving pulses, it is shown that the emission of the consecutive harmonics in the supercontinuum cutoff regime can be synchronized and locked in phase, resulting in the production of a coherent attosecond pulse. Moreover, the time-frequency profile of the attosecond laser pulses can be controlled by the adjustment of the carrier envelope phase (CEP) [25].

### Future Research Plans

In addition to continuing the ongoing researches discussed above, we plan to initiate the following several new project directions: (a) Development and extension of the Floquet formulation of TDDFT to the more complex molecular systems. (b) Development and extension of self-interaction-free TDDFT to diatomic molecular systems including the vibrational degrees of freedom for the study of the ionization mechanism and HHG and Coulomb explosion phenomena in strong fields. (c) Development of spin-dependent *localized* Hartree-Fock (LHF)-DFT method for the study of singly, doubly, and triply excited states of Rydberg atoms and ions [26]. (d) Fully *ab initio* treatment of HHG and MPI processes of H<sub>2</sub> (D<sub>2</sub>) molecules. e) *Ab initio* exploration of sub-laser-cycle molecular dynamics at attosecond resolution.

### References Cited (\* Publications supported by the DOE program in the period of 2004-2006.)

- \*[1] Z. Y. Zhou and S. I. Chu, Phys. Rev. **A71**, 011402 (R) (2005).
- \*[2] S. I. Chu and D. Telnov, Physics Reports **390**, 1-131 (2004).
- \*[3] D. Telnov and S. I. Chu, J. Phys. B **37**, 1489 (2004).
- \*[4] D. Telnov and S. I. Chu, Phys. Rev. **A71**, 013408 (2005).
- \*[5] V. I. Usachenko and S. I. Chu, Phys. Rev. **A71**, 063410 (2005).
- \*[6] V. I. Usachenko, P. E. Pyak, and S. I. Chu, Laser Phys. (in press, 2006)
- [7] X. M. Tong and S. I. Chu, Phys. Rev. **A57**, 452 (1998).
- [8] X. M. Tong and S. I. Chu, Int. J. Quantum Chem. **69**, 305 (1998).
- [9] X. M. Tong and S. I. Chu, Phys. Rev. **A64**, 013417 (2001).
- [10] X. Chu and S. I. Chu, Phys. Rev. **A63**, 023411 (2001).
- [11] X. Chu and S. I. Chu, Phys. Rev. **A64**, 063404 (2001).
- [12] A. K. Roy and S. I. Chu, Phys. Rev. **A65**, 043402 (2002).
- [13] C. Guo, Phys. Rev. Lett. **85**, 2276 (2000).
- [14] J. Muth-Bohm, A. Becker, and F. H. M. Faisal, Phys. Rev. Lett. **85**, 2280 (2000).
- [15] X. M. Tong, Z. X. Zhao, and C. D. Lin, Phys. Rev. **A 66**, 033402 (2002).
- [16] M. J. DeWitt, E. Wells, and R. R. Jones, Phys. Rev. Lett. **87**, 153001 (2001).
- \*[17] X. Chu and S. I. Chu, Phys. Rev. **A70**, 061402 (R) (2004).
- [18] E. A. Gibson, *et al.*, Phys. Rev. Lett. **92**, 033001 (2004).
- \*[19] J. Carrera, X. M. Tong, and S. I. Chu, Phys. Rev. **A71**, 063813 (2005).
- \*[20] S. I. Chu, J. Chem. Phys. **123**, 062207 (2005).
- \*[21] X. Guan, X. M. Tong, and S. I. Chu, Phys. Rev. **A 73**, 023403 (2006).
- [22] G. Yao and S. I. Chu, Chem. Phys. Lett. **204**, 381 (1993);
- [23] X. M. Tong and C. D. Lin, Phys. Rev. **A 71**, 033406 (2005).
- [24] X. M. Tong and S. I. Chu, Chem. Phys. **217**, 119 (1997)
- \*[25] J. Carrera, X. M. Tong, and S. I. Chu, Phys. Rev. **A** (in press, 2006).
- \*[26] Z. Y. Zhou and S. I. Chu, Phys. Rev. **A71**, 022513 (2005).

# Optical Two-Dimensional Fourier-Transform Spectroscopy of Semiconductors

Steven T. Cundiff

JILA, University of Colorado and National Institute of Standards and Technology

Boulder, CO, 80309-0440

[cundiffs@jila.colorado.edu](mailto:cundiffs@jila.colorado.edu)

**Program Scope:** The goal of this program is to implement optical 2-dimensional Fourier transform spectroscopy and apply it to semiconductors. Specifically of interest are quantum wells that exhibit disorder due to well width fluctuations and quantum dots. In both cases, 2-D spectroscopy will provide information regarding coupling among excitonic localization sites.

**Progress:** During the past year, three papers resulting from this project have appeared [1-3]. As these papers had been submitted when last year's abstract was written, their contents were covered in detail then.

The basic apparatus has not been extensively modified over the last year. The only significant change has been the acquisition and incorporation of a new  $\frac{3}{4}$  meter spectrometer and a new CCD camera. The new spectrometer improved the resolution by close to an order of magnitude and the new camera greatly reduced the acquisition time for each spectral interferogram. The resulting speed up not only increased the rate at which 2D spectra are acquired, but also greatly increased the success rate for acquiring 2D spectra as the servo loops do not need to hold lock for as long. In addition, we obtained a new 10 period multiple quantum well sample (grown by Richard Mirin at NIST-Boulder). This sample displays less inhomogeneous broadening and a much stronger signal than the sample used for the data presented last year.

Transient four-wave-mixing (TFWM) studies from the early 90's showed that there was a surprising interplay between the polarization of the incident pulses and presence of localization in the sample due to disorder [4]. As the long term goal of this program is to study excitons localized in quantum dots, understanding the polarization dependence of 2D spectra from excitons is necessary first step. In figure 1, the 2D spectrum for a rephasing pulse sequence with all pulses co-linearly polarized is shown. Note that we have adopted the convention that the emission frequency ( $\omega_t$ ) has a positive frequency. Thus for a rephasing spectrum, the absorption frequency ( $\omega_r$ ) has a negative frequency. These results are comparable to those for the older sample, showing a strong cross peak and "dispersive" like features in the real spectrum.

As a first comparison, we took 2D spectra (both rephasing and non-rephasing sequences) for co-circularly polarized excitation. From the level diagram of the magnetic substates, the naïve expectation is that co-linearly polarized excitation would result in cross peaks because both valence bands couple to the same conduction band (e.g., the  $-3/2$  heavy hole and the  $+1/2$  light hole both couple to the  $-1/2$  conduction band, although with opposite circular polarizations) whereas co-circular polarized excitation would not result in cross peaks as the valence bands are

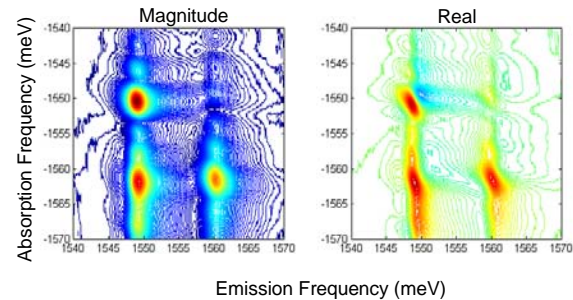


**Fig. 1** 2D spectrum of heavy- and light-hole excitons for collinearly polarized excitation.

apparently uncoupled. Previous TFWM and transient absorption studies have shown that the two valence bands are coupled, even for co-circularly polarized excitation, so it should not be surprising that there is still a cross-peak in the 2D spectra shown in Figure 2. However, it is surprising that the cross peak becomes the strongest peak in the rephasing 2D spectrum for co-circular excitation. The ability to observe the strengths of the peaks, and thus gain insight into the underlying microscopic coupling mechanisms is unique to 2D spectroscopy. Explanation of this observation will require help from theory.

The previous work on polarization showed surprising differences between co- and cross-linearly-polarized excitation (for three pulse excitation, the polarization of the first two beams is cross-polarized, the polarization of the third pulsed does not matter). Naturally, we have taken 2D spectra for cross-polarized excitation (Fig. 3). For the first two pulses cross-polarized, it is not clear what polarization configuration to use the spectrally resolve transient absorption measurement used for determining the overall phase, thus we only show the magnitude spectrum. We observe that the heavy-hole diagonal peak is elongated in the horizontal direction. We attribute this feature to the incoherent excitation of biexcitons, which results in a new peak shifted by the biexciton binding energy of approximately 1 meV. Previous theory, with some indirect support from experiment, has suggested that cross-polarization suppresses the exciton and reveals biexcitonic features. Although we have not yet conclusively assigned the new peak to biexcitons, this 2D spectrum does provide the best experimental evidence for this hypothesis.

As somewhat of an aside from primary goals of this program, we have also looked at the 2D spectrum of continuum states (unbound e-h pairs). The nature of the e-h continuum transitions in semiconductors has been puzzling for a number of years. Early measurements treated then a simple inhomogeneously broadened ensemble of 2 level systems that would produce a photon echo. However, these measurements did not time-resolve the signal and verify that it was indeed an echo. Later time-resolved measurements yielded mixed results, with some echo-like components, but not a pure echo. Our theory collaborators have performed calculations that show interesting polarization dependences to continuum coherent-excitation-spectra. We have taken 2D spectra of the continuum in a bulk GaAs layer (Fig. 4). As of yet we are still trying to understand the spectra, which show interesting evolution as  $T$  is varied as well as distinctions between rephasing and non-rephasing spectra.

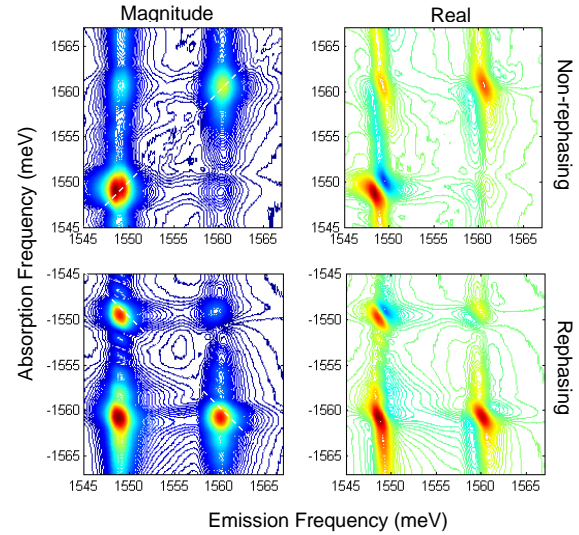


**Fig. 2.** Non-rephasing (upper) and rephasing (lower) spectra for co-circular polarized excitation.

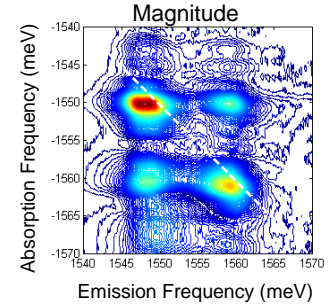


**Fig. 3.** Rephasing magnitude 2D spectrum for cross-linearly-polarized excitation.

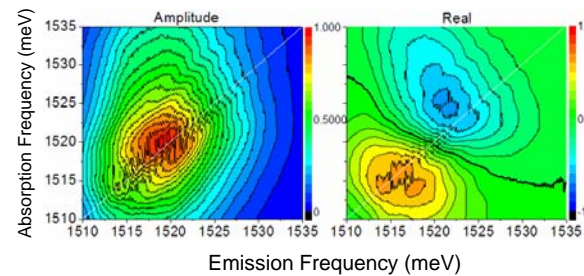


**Fig. 4.** Non-rephasing 2D spectrum of continuum states in bulk GaAs.

The ability to determine coupling between resonances is one of the strengths of 2D spectroscopy. One unique advantage of semiconductor heterostructures is the ability to “engineer” the relevant states. We have combined these by looking at the 2D spectra of coupled quantum wells. We have had a series of samples grown with pairs of 9 nm and 8 nm wells separated by varying thickness barriers. The linear absorption spectra of 3 of these samples are shown in Fig. 5. For the thick barrier, where the wells are completely uncoupled, it is possible to assign the peaks in the spectra. However, for thinner barriers, where the wavefunctions extend across both wells, the spectra become complicated and assignment of the peaks in the linear spectra is problematic.

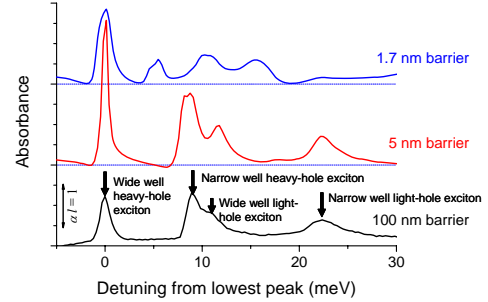


**Fig 5.** Absorption spectra of coupled quantum wells for 3 different barrier thicknesses.

2D spectra help significantly with identification of the peaks observed in the 1D spectrum. Fig. 6. shows 2D spectra of the 100 nm barrier sample for two tunings of the incident laser. First the laser is tuned to overlap with the lowest two peaks, which show no cross peaks, confirming the assignment as being the heavy-hole excitons in the wide well (lowest peak) and narrow well (second peak). Tuning the laser to higher energy allows the upper three peaks to be excited. Their 2D spectra reveals strong coupling between the 2<sup>nd</sup> and 4<sup>th</sup> peaks, consistent with their assignment as heavy and light holes of the narrow quantum well. The third peak does not couple to the 2<sup>nd</sup>, but does appear to couple weakly to the fourth peak, although the cross peaks are asymmetric. This coupling is, in principle, unexpected although unexpectedly strong coupling between quantum wells has often been observed in previous luminescence experiments.

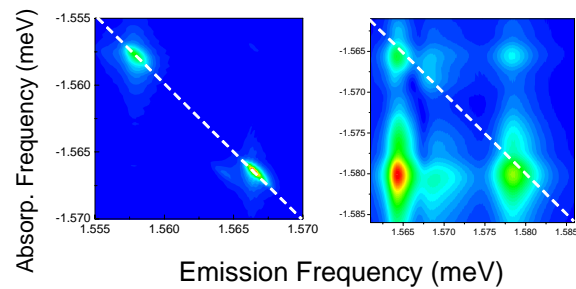


**Fig 6.** Rephasing 2D spectra of thick barrier sample for two tuning of the laser. Left panel

The 2D spectrum of the sample with the thin barrier displays a full set of cross peaks between the 4 resonances (Fig. 7). Simple analysis of allowed transitions yields 10 cross-peaks, not the 12 that are observed. We attribute the “extra” cross peaks to many-body interactions, however, a full explanation requires help from theory.

During the process of building the three pulse TFWM apparatus several years ago, we spent some time comparing the dephasing of the optical coherences and the Raman coherence between the heavy- and light-hole excitons. At the time we could not get good agreement between the experiment and calculations. Since then, we discovered that the including of “inhomogeneous dephasing” (also known as “frequency dependent linewidth”) is critical to getting an accurate match between experiment and theory. Although it is well known that the dephasing rate varies across the inhomogeneous line, its signatures in the quantum beats between the excitons had not been identified. Specifically, it results in a beat frequency that varies with delay as well as incompatible delays as a function of  $\tau$  and  $T$ . We have now reanalyzed the data and prepared a manuscript [5] that will be submitted shortly.

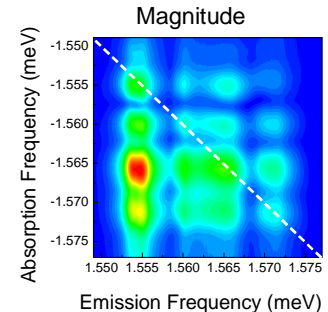


**Fig. 7.** Magnitude 2D spectrum of the sample with a thin barrier between wells.

**Future Plans:** We currently have a large collection of 2D data that show many interesting features. To help understand those features, we have established collaborations with two theory groups. The group of Peter Thomas at the University of Marburg, Germany, has modified their existing code to produce 2D spectra. They have a long history of working on the polarization dependence of TFWM and its interplay with disorder/localization. Their first effort will be to model our polarization dependence results. They expect to have polarization dependent results in the next few months. They also have a model for the continuum that they plan to apply to our results. The group of Shaul Mukamel at UC-Irvine is also interested in working with us. They have extensive experience in calculating 2D spectra for molecular systems, however need to develop a model for semiconductors. Their approach is best suited to the coupled quantum well case. (Note that these two groups are interacting with each other as well.)

We plan to take some more polarization dependent data to clarify the origin of some of the features shown in the 2D spectra. We also plan to take data on a new set of coupled InGaAs quantum wells. InGaAs quantum wells have large inherent strain that shifts the light-hole exciton so that the spectra will be simpler. Beyond these, further experiments on these two projects will be in response to the theory results.

To reveal the effects of localization and inhomogeneous broadening, as occurs in quantum dot ensembles, we will begin a series of experiments with narrower excitation bandwidth and lower excitation density. Both are required in order to avoid excessive scattering from optically excited carriers.

Although the current apparatus is routinely producing high quality 2D spectra, it has two serious disadvantages, 1) the phase between the second and third excitation pulses cannot be locked and 2) the overall phase is ambiguous. Based on our experience with the current setup, we have developed a design for an improved apparatus that will not have the current disadvantages. In addition, we anticipate the new apparatus will have much higher intrinsic phase stability, thus improving the quality of the data. We have begun building the new improved apparatus and anticipate having it operational by the end of the year. This apparatus will allow us to produce phase-resolved 2D spectra for any polarization configuration and identify 2 quantum coherences.

- [1] T. Zhang, C.N. Borca, X. Li and S.T. Cundiff, "Optical two-dimensional Fourier transform spectroscopy with active interferometric stabilization," *Optics Express* **13**, 7432 (2005).
- [2] C.N. Borca, T. Zhang, X. Li and S.T. Cundiff, "Optical Two-dimensional Fourier Transform Spectroscopy of Semiconductors," *Chemical Physics Letters* **416**, 311 (2005).
- [3] X. Li, T. Zhang, C.N. Borca and S.T. Cundiff, "Many-body Interactions in Semiconductors Probed by Optical Two-Dimensional Fourier Transform Spectroscopy," *Physical Review Letters* **96**, 057406 (2005).
- [4] S.T. Cundiff, H. Wang and D.G. Steel, "Polarization-dependent picosecond excitonic nonlinearities and the complexities of disorder," *Phys. Rev. B* **46**, 7248 (1992).
- [5] A.G. VanEngen Spivey and S.T. Cundiff, "Inhomogeneous dephasing of heavy-hole and light-hole exciton coherences in GaAs quantum wells," to be submitted to the *Journal of the Optical Society of America B* (2006).

**Bold number:** publications from this program. Other publications to result from this program in the last 3 years

- C. N. Borca, T. Zhang, and S. T. Cundiff, Two-dimensional fourier transform optical spectroscopy of GaAs quantum wells in *Ultrafast Phenomena in Semiconductors and Nanostructure Materials VIII*ed., (SPIE - The International Society for Optical Engineering, Bellingham, WA, 2004), Vol. 5352, p. 257-265.
- C. N. Borca, A. G. V. Spivey, and S. T. Cundiff, "Anomalously fast decay of the LH-HH exciton Raman coherence," *Physica Status Solidi B-Basic Research* **238**, 521-524 (2003).

## Theoretical Investigations of Atomic Collision Physics

A. Dalgarno

Harvard-Smithsonian Center for Astrophysics  
Cambridge, MA 02138  
adalgarno@cfa.harvard.edu

The research develops and applies theoretical methods for the interpretation of atomic, molecular and optical phenomena and for the quantitative prediction of the parameters that characterize them. The program is responsive to experimental advances and influences them. A particular emphasis has been the study of collisions in ultracold atomic and molecular gases.

Long range forces occupy a central role in the physics of atomic and molecular collisions at low and ultralow temperatures. At large distances the interaction potential can be expanded as a series in inverse powers of the internuclear distance  $R$  in which the leading term in the case of ground state neutral atoms varies as the inverse sixth power. The coefficients of the individual terms can be expressed as integrals over frequency of the products of dynamic multipole polarizabilities of the interacting species evaluated at imaginary frequencies. The leading term  $C_6$  is obtained as the integral of the product of the dynamic dipole polarizabilities. Xi Chu and I have employed a version of time-dependent density functional theory (TDDFT) to calculate the isotropic part of  $C_6$  for an extensive range of atom pairs and of atoms with helium. However as was demonstrated long ago inelastic scattering, which can lead to trap loss, is controlled by the separations of the potential curves of molecular states of different symmetries because of the difference in phase that results as the particles scatter along the potentials. For example the quenching of the excited fine-structure level of  $C^+(2P)$  in collisions with helium is determined by the separation of the doublet sigma and pi states of the molecule  $CHe^+$ . Thus to determine if inelastic loss is likely we need to calculate the long range  $C_6$  coefficients of the sigma and pi states. Xi Chu, Gerrit Groenenboom and I have extended the theory which expresses  $C_6$  in terms of polarizabilities and applied TDDFT to calculate the anisotropy of the long range coefficients for atoms in states of non-zero orbital angular momentum. The rare earths are of particular immediate interest. Some values of the isotropic  $C_6(0)$  and anisotropic  $C_6(2)$  coefficients in atomic units for rare earths in the  $^2D$  state are listed in the Table.

**Table 1**

$C_6(0)$  and  $C_6(2)$  in a.u.

Atom	Configuration	$C_6(0)$	$C_6(2)$
La	[Xe]6s <sup>2</sup> 5d	46.6	-1.8
Gd	[Xe]6s <sup>2</sup> 4f <sup>7</sup> 5d	40.2	-1.6
Lu	[Xe]6s <sup>2</sup> 4f <sup>14</sup> 5d	35.6	-1.3

Some measure of the overall accuracy of the procedures can be obtained by comparison with the results of Buchachenko, Szczesniak and Chalasinski (J.Chem.Phys. 124,114301,2006) who carried out extensive calculations of the potential energy curves and derived values of the coefficients by fitting the potentials at long range. For Tm-He they inferred values for  $C_6(0)$  and  $C_6(2)$  of 41.2 au and 0.10 au respectively compared to our estimates of 37.9 and 0.47 au. For Yb(1S) they obtained 45.0 for  $C_6(0)$  whereas we calculated 37.3. Whichever values are the more accurate they indicate as do the results in the Table that the inelastic cross sections will be small and the elastic will probably be large. The atoms are excellent candidates for trapping. We are now extending the formal theory to the interactions between pairs of rare earth atoms. We have discovered that an additional polarizability of rank 1 appears to be needed for the evaluation of the  $C_6$  coefficients.

We have initiated a study of the long range exchange energy that is responsible for the difference between the gerade and ungerade symmetry states of a pair of similar atoms. Approximate formulas are available but they are of limited accuracy. We are seeking a systematic method whose precision can be improved (as in variational calculations). We have tested it for the simple cases of the diatomic molecular ions of the alkali metals and believe we have achieved high accuracy. The method has also been tested on the slightly more complicated case of  $\text{He}^+-\text{He}$  for which multiconfiguration interaction calculations have been reported. The comparison shows clearly the failure at large distances of the variational calculations (which involve the subtraction of two large numbers to determine a small number). We have in progress a study of charge transfer in collisions at low energies of high lying levels of atomic hydrogen and antihydrogen with ground state hydrogen atoms and we are examining again the collisions of excited  $n=2$  hydrogen atoms at ultracold temperatures. The molecular states are resonance states undergoing autoionization. There occurs a long range coupling of  $\text{H}(2s)-\text{H}(2s)$  and  $\text{H}(2s)-\text{H}(2p)$  that will modify the cross section.

We have developed a procedure that makes possible an accurate evaluation of the cross section for Raman scattering of molecules as a function of the frequency of the incident photon for a pair of atoms in the vibrational continuum of the molecule. The variation of the resulting population of discrete vibrational levels with the incident frequency may be predicted. The process involving hydrogen atoms was used as a test case. It happens to play a role in the formation of hydrogen molecules in the early Universe.

## Publications 2004-2006

- P. Froelich, B. Zygelman, A. Saenz, S. Jonsell, S. Eriksson and A. Dalgarno, Hydrogen-antihydrogen Molecule and Its Properties, Few-Body Systems 34, 63, 2004.
- S. Jonsell, A. Saenz, P. Froelich, B. Zygelman and A. Dalgarno, Hydrogen-Antihydrogen Scattering in the Born-Oppenheimer Approximation, J. Phys. B. 37, 1195, 2004.
- R. V. Krems and A. Dalgarno, Quantum Mechanical Theory of Atom Molecule and Molecular Collisions in a Magnetic Field: Spin Polarization, J. Chem. Phys. 120, 2296, 2004.
- E. Bodo, F. A. Gianturco, N. Balakrishnan, and A. Dalgarno, Chemical Reactions In The Limit Of Zero Kinetic Energy: Virtual States And Ramsauer Minima in  $\text{F} + \text{H}_2 \rightarrow \text{HF} + \text{H}$ , J Phys. B 37 3641, 2004.
- X. Chu and A. Dalgarno, Linear Response Time-Dependent Density Functional Theory for Van Der Waals Coefficients, J. Chem. Phys. 121, 4083, 2004.
- C. Zhu, A. Dalgarno, A., S. Porsev, and A. Derevianko, Dipole Polarizabilities of Excited Alkali-Metal Atoms and Long Range Interactions with Helium Atoms, Phys. Rev. A 70, 03722, 2004.
- X. Chu and Shih-I Chu, Role of the electronic structure and multielectron responses in ionization mechanisms of diatomic molecules in intense short-pulse lasers: An all-electron *ab initio*

- study, Phys. Rev. A, 70, 061402 (R), 2004.
- R. Krems, G. Groenenboom, and A. Dalgarno, Electronic Interaction Anisotropy between Atoms in Arbitrary Angular Momentum States, J. Phys Chem A, 108, 8941, 2004.
- R. V. Krems, J. Klos, M.F.Rode, M.M.Szczesniak, G.Chalasinski and A. Dalgarno., Suppression of Angular Forces in Collisions of Non-S-State Transition Metal Atoms, Phys. Rev.Lett. 94, 013202, 2005.
- Teck-Ghee Lee, C. Rochow, R. Martin, T. K. Clark, R. C. Forrey, N. Balakrishnan, P. C. Stancil, D. R. Schultz, A. Dalgarno and Gary J. Ferland, Close-coupling calculations of low-energy inelastic and elastic processes in  $^4\text{He}$  collisions with  $\text{H}_2$ : A comparative study of two potential energy surfaces, J. Chem. Phys. 122, 024307, 2005.
- G. Barinovs, M.C. van Hemert, R. Krems and A. Dalgarno, Fine-structure Excitation of  $\text{C}^+$  And  $\text{Si}^+$  by Atomic Hydrogen, ApJ 620, 537, 2005.
- M. Bouledroua, A. Dalgarno and R. Côté, Viscosity and Thermal Conductivity of Li, Na, and K Gases, Physica Scripta, 71, 519, 2005.
- H. Cybulski, R. V. Krems, H.R. Sadeghpour, A. Dalgarno, J. Klos, G.C. Groenenboom, A. van der Avoird, D. Zgid and G. Chalasinski, Interaction of  $\text{NH } X^3\Sigma^-$  with He: Potential Energy Surface, Bound States and Collisional Zeeman Relaxation, J. Chem. Phys. 122, 094307, 2005.
- X. Chu, A. Dalgarno, and G. C. Groenenboom, Polarizabilities of Sc and Ti Atoms and Dispersion Coefficients for their Interaction with Helium Atoms, Phys. Rev. A. 72, 032703, 2005.
- C. Zhu, J. F. Babb and A. Dalgarno, Theoretical Study of Pressure Broadening of Lithium Resonance Lines by Helium Atoms. Phys. Rev. A, 71, 052710, 2005.
- X. Chu and A. Dalgarno, Polarizabilities of  $^3\text{P}$  atoms and van der Waals coefficients for their interaction with helium atoms, Adv. Atom. Mol. Opt., 51, 032703, 2005.
- X. Chu, A. Dalgarno, and G. C. Groenenboom, Polarizabilities of Sc and Ti Atoms and Dispersion Coefficients for their Interaction with Helium Atoms, Phys. Rev. A 72, 032703, 2005.
- C.M. Dutta, C. Oubre, P. Nordlander, M. Kimura and A. Dalgarno, Charge Transfer Cross Sections in Collisions of Ground State Ca and  $\text{H}^+$ , Phys. Rev. A 73, 032714, 2006.
- M.P.J. van der Loo, G.C. Groenenboom, M. J. Jamieson and A. Dalgarno, Raman Association of  $\text{H}_2$  in The Early Universe, Disc. Farad Soc. in press 2006.
- Y. V. Vanne, A. Saenz, A. Dalgarno, R.C. Forrey, P. Froelich and S. Jonsell, Doubly Excited Autoionizing States of  $\text{H}_2$  Converging to the  $\text{H}(n=2)+\text{H}(n'=2)$  Limit, J. Chem. Phys. in press 2006.
- A. Dalgarno and M.P.J. van der Loo, Recombination of  $\text{H}_2$  by Raman Association in the Early Universe, ApJ Letters, in press 2006.

# Coherent Control of Multiphoton Transitions in the Gas and Condensed Phases with Ultrashort Shaped pulses

DOE Grant No. DE-FG02-01ER15143

Marcos Dantus

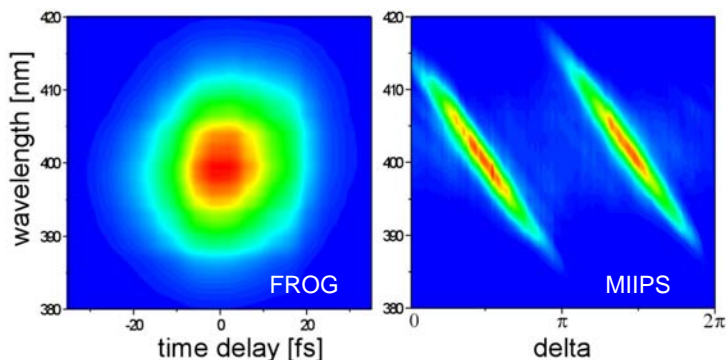
Department of Chemistry and Department of Physics, Michigan State University, East Lansing MI 48824  
[dantus@msu.edu](mailto:dantus@msu.edu)

## 1. Program Scope

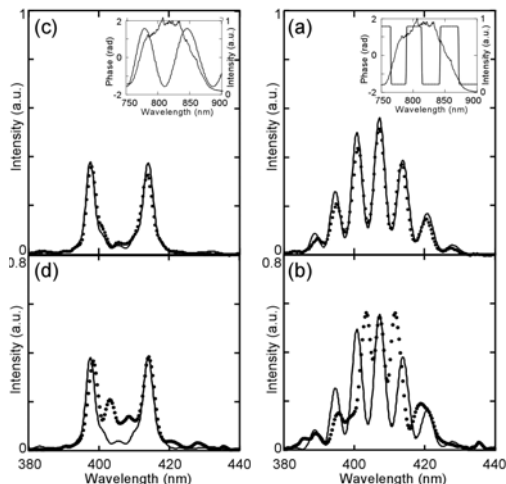
Controlling laser-molecule interactions has become an integral part of developing future devices and applications in spectroscopy, microscopy, optical switching, micromachining and photochemistry. Coherent control of multiphoton transitions could bring a significant improvement of these methods. In microscopy, multi-photon transitions are used to activate different contrast agents and suppress background fluorescence; coherent control could bring selective probe excitation. In photochemistry, different dissociative states are accessed through two, three, or more photon transitions; coherent control could be used to select the reaction pathway and therefore the yield specific products. For micromachining and processing a wide variety of materials, femtosecond lasers are now used routinely. Understanding the interactions between the intense femtosecond pulse and the material could lead to technologically important advances. Pulse shaping could then be used to optimize the desired outcome. The scope of our research program is to develop efficient strategies to control nonlinear laser-matter interactions using ultrashort shaped pulses in gas and condensed phases [1-17].

## 2. Recent Progress

Our research on accurate and reproducible pulse shaping led us to the development of multiphoton intrapulse interference phase scan (MIIPS) [2, 7, 10]. MIIPS has turned out to be an extremely accurate method for measuring arbitrary phase distortions in the spectral phase of femtosecond pulses. Because MIIPS uses a pulse shaper, it can compensate spectral phase distortions to produce routinely transform limited pulses within 1% of the theoretical limit. We have compared MIIPS to other widely used methods for phase retrieval and MIIPS has been found to be as accurate as SPIDER, an order of magnitude more accurate than FROG, and as accurate as white-light interferometry for measuring group velocity dispersion [10]. MIIPS is now integrated in our laser systems for automatically optimizing the output until it is transform limited, and then carrying out phase shaping projects. The figure on the right shows an SHG FROG trace on the left and a MIIPS scan for the same 18 fs, transform-limited pulses. The MIIPS technology was recently launched by Coherent in their new line of pulse shapers called Silhouette.

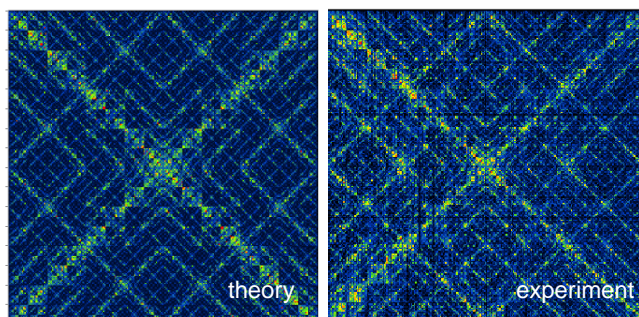


We subjected the MIIPS method to a number of rigorous tests to determine if it could accurately yield phase shaped pulses in a number of conditions, such as when the beam traverses thick substrates, scattering media, and high numerical aperture microscope objectives. MIIPS performed better than other well established methods for pulse characterization [10]. For example, the figure on the right shows theoretical prediction (line) and experimental measurement (dots) for two types of phase functions imposed on 12 fs pulses, continuous and binary phase. Notice that we are able to deliver at the sample the desired phase with remarkable precision (top). When we turn off the MIIPS compensation, the agreement between experiment and theory is lost, demonstrating the importance of being able to deliver accurately shaped pulses at the sample.



Projects using selective multiphoton excitation on large molecules led us to demonstrate selective two-photon microscopy. In these projects we demonstrated selective excitation of two different chromophores or a single chromophore but in different environments [1, 3, 5]. The latter experiment sparked the idea of using phase shaping for functional imaging. The goal was to use a two-photon active chromophore that was sensitive to a chemical gradient such as pH. We then use phase shaping to control the excitation of the chemically sensitive chromophore. Results from the initial measurements were very encouraging, especially when working with HPTS, a large organic molecule with a pH dependent two-photon cross section spectra that always emits at the same wavelength [1, 8, 9].

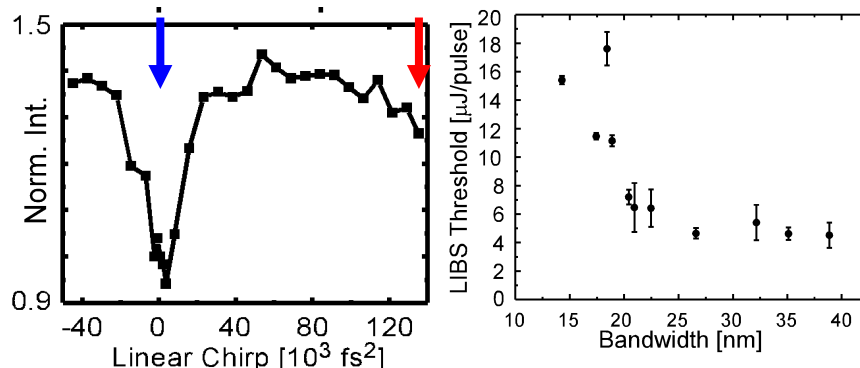
We embarked on a systematic study of the effects of phase shaping on multiphoton transitions [11]. This study primarily focused on selective two-photon excitation, the competition of two- versus three-photon transitions, and on selective CARS excitation. This study explores the most efficient methods for controlling multiphoton transitions. Starting from first principles we review a number of different phase functions and conclude with very valuable lessons. The most valuable being that selective excitation requires the pixels of the pulse shaper to take only two phase values, and not a whole range of values as previously believed. Binary phase shaping, when the difference between the two phase values is  $\pi$ , represents a quantum leap in our progress towards controlling multiphoton processes and the design of robust applications using coherent control [6, 7, 11]. Theoretical work in our laboratory has progressed at the same rate as our experiments. We are presently able to calculate optimum phase functions using a computer operating at 3 GHz, and then implement those phase functions in the lab. We can



alternatively make experimental measurements and also simulate them accurately using theory. To demonstrate our present capabilities we evaluated  $2^{16}$  different 16-bit binary phase functions for their ability to generate SHG intensity at 400 nm within a narrow 0.5 nm spectral width, while keeping the background SHG outside that spectral window to a minimum. The results from that research project are mapped on the left (theoretical prediction on the left and experimental result on the right). The measured figure of merit ranged from red (factor of 2.5 signal-

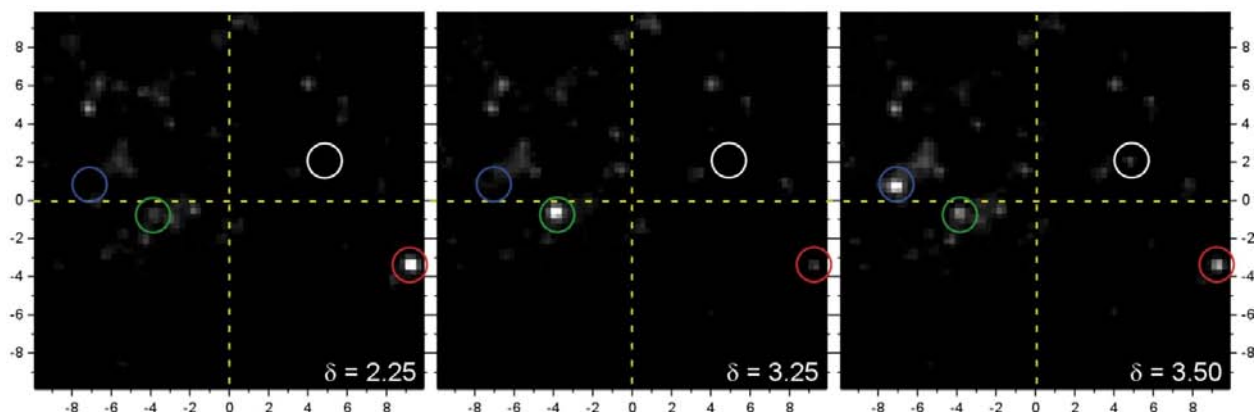
to-background) to black (factor of 0.5 signal-to-background) in the figures on the left. The systematic evaluation of binary phase functions and mapping the results has now become a standard in our group that we have applied to a number of projects such as the identification of chemical warfare agents.

Our ability to control nonlinear optical excitation at low and intermediate intensities had to be tested at higher laser intensities ( $10^{14}$  to  $10^{18}$  W/cm<sup>2</sup>) where perturbation theory is no longer applicable. This research started by exploring the interaction of intense femtosecond pulses on metallic surfaces [12]. We focused the beam on a continuously refreshed surface (rotating the target) and measured the laser induced breakdown spectroscopy (LIBS) atomic emission. Because we used 30 fs pulses, we noticed that the threshold for LIBS was very low, far lower than the threshold reported by groups using longer pulses. Instead of requiring  $\sim 100$  mJ of pulse energy we were able to obtain stable signals with  $\sim 5$   $\mu$ J of energy per pulse. When we explored different pulse shaping strategies we found very small effects compared to those found earlier for multiphoton excitation. Although some degree of selectivity between copper and aluminum surfaces was found when using binary phase shaping, the extent of the effect was very modest ( $\sim 30$  %). The most intriguing finding, illustrated in the left panel in the figure below. As the 35 fs pulses (blue arrow) were stretched to a pulse duration of 10 ps (red arrow), the overall LIBS signal did not disappear; it actually was  $\sim 20\%$  higher than for transform limited pulses. This was a surprising finding because the laser intensity was near threshold and we had assumed peak intensity was critical to observe LIBS near threshold. If the pulse duration of ultrashort pulses was not responsible for the very low LIBS threshold we observed, then it had to be their broad bandwidth. We



tested this conclusion and found that the LIBS threshold depends on the inverse of the bandwidth of the pulses (see right panel of figure). We believe this observation will have important implications in the field of micromachining and surface processing by lasers and we plan to explore this further.

Having developed all the tools necessary for selective nonlinear optical microscopy, we turned our attention to the study of multiphoton excitation of silver nanoparticles [17]. Our first finding was that dendritic silver nanoparticles have a very large cross section for two-photon induced luminescence. When excited at 800 nm they exhibit strong two-photon induced luminescence near 550 nm. When imaging the dendritic silver nanoparticles in the microscope, we noticed that excitation at one location resulted in emission from multiple nanoparticles, some at distances greater than 40 $\mu$ m, or approximately 100 focal-spot diameters away. The dendritic nanoparticles are interconnected during the deposition of a thin film during sample preparation. The remote emission results from surface plasmon waveguiding. What is most intriguing is that the remote emission spots can be controlled through the phase or polarization of the excitation beam. Control by phase shaping is shown in the figure below. To be able to obtain these images we had to use MIIPS to compensate all phase distortions introduced by the 60X 1.45 NA objective, and we also had to attenuate the beam to 0.1 pJ/pulse to avoid damaging the nanoparticles. The positions of the sample and laser were fixed, with the laser focused to a spot of about 0.5  $\mu$ m diameter at the center of the crosshairs. A sinusoidal phase function was introduced to shape the  $\sim$ 12 fs pulses. We see that different phases preferentially cause two-photon luminescence at locations far from the focal spot (colored circles). This phenomenon, its implications to plasmon waveguiding, and energy transfer between molecules at long distances (up to 100  $\mu$ m) will be studied in detail.



### 3. Future Plans

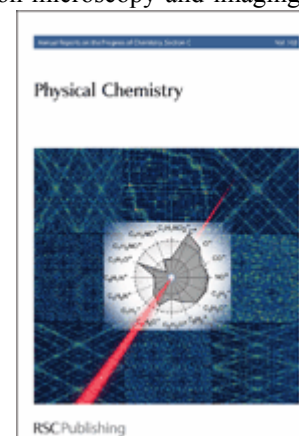
We plan to bring the state of the art in ion imaging to solve some of the prevalent questions in the observed changes in fragment ion yield resulting from laser-molecule interactions in the gas phase when controlled by pulse shaping. Experiments on transparent media will be imaged using time-resolved shadowgraphy to visualize changes in the laser-matter interactions that are brought about by pulse shaping. Finally, the interaction of intense shaped pulses with metals and semiconductors will be explored. Results from these interactions will be imaged using time-resolved reflectometry. These efforts will be complemented by critical analysis of the results using search space mapping and computer simulations.

### 4. Scientists Supported:

This grant has partially supported two postdocs, two undergraduate students, and five graduate students since 2004.

## Publications Resulting from this Grant 2004-2006:

1. J. M. Dela Cruz, I. Pastirk, V. V. Lozovoy, K. A. Walowicz and M. Dantus, "Multiphoton Intrapulse Interference 3: probing microscopic chemical environments," *J. Phys. Chem.* 108, 53 - 58, (2004) Our results were featured in the cover.
2. V. V. Lozovoy, I. Pastirk, M. Dantus, "Multiphoton intrapulse interference 4; Characterization and compensation of the spectral phase of ultrashort laser pulses", 29, 7, 775-777, *Optics Letters* (2004)
3. J. Dela Cruz, I. Pastirk, V.V. Lozovoy, K.A. Walowicz, and M. Dantus, "Control of nonlinear optical excitation with multiphoton intrapulse interference," *Ultrafast Molecular Events in Chemistry and Biology*, M. M. Martin and J.T. Hynes Eds. Elsevier, p. 95 (2004)
4. V.V. Lozovoy, M. Comstock, I. Pastirk, and M. Dantus, "Femtosecond Photon Echo Measurements of Electronic Coherence Relaxation of I2 in the presence of He, Ar, N2, O2, C3H8," *Ultrafast Molecular Events in Chemistry and Biology*, M. M. Martin and J.T. Hynes Eds. Elsevier, p. 33 (2004)
5. M. Dantus and V.V. Lozovoy, "Experimental Coherent Laser Control of Physicochemical Processes", *Chem. Reviews*, Special Issue on Femtochemistry, A. H. Zewail and M. Dantus Eds. 104, 1813-1860, (2004)
6. M. Comstock, V. V. Lozovoy, I. Pastirk, and M. Dantus, "Multiphoton intrapulse interference 6; binary phase shaping", 12, 6, 1061-1066, *Optics Express* (2004)
7. V. V. Lozovoy and M. Dantus, "Systematic control of nonlinear optical processes using optimally shaped femtosecond pulses," *Chem. Phys. Chem.* Invited Review, 6, 1970 (2005)
8. J. M. Dela Cruz, I. Pastirk, M. Comstock, and M. Dantus, "Coherent control through scattering tissue, Multiphoton Intrapulse Interference 8," *Optics Express*, 12, 4144 (2004)
9. J. M. Dela Cruz, I. Pastirk, M. Comstock, V. V. Lozovoy, and M. Dantus, "Use of coherent control methods through scattering biological tissue to achieve functional imaging", *Proceedings of the National Academy of Sciences USA* 101, 16996-17001 (2004)
10. B. Xu, J. M. Gunn, J. M. Dela Cruz, V. V. Lozovoy, M. Dantus, "Quantitative investigation of the MIIPS method for phase measurement and compensation of femtosecond laser pulses," *J. Optical Society B* 23, 750-759 (2006).
11. V. V. Lozovoy, B. Xu, J. C. Shane and M. Dantus, "Selective nonlinear excitation with pseudorandom Galois fields," (Submitted to PRA, 2006)
12. T. Gunaratne, M. Kangas, S. Singh, A. Gross, and M. Dantus, "Influence of bandwidth and phase shaping on laser induced breakdown spectroscopy with ultrashort laser pulses." *Chem. Phys. Letters* 423, 197-201 (2006)
13. J. M. Gunn, B. Xu, J. M. Dela Cruz, V. V. Lozovoy, M. Dantus, "The MIIPS method for simultaneous phase measurement and compensation of femtosecond laser pulses and its role in two-photon microscopy and imaging." *Proc. SPIE Vol. 6108*, pgs. 61-68, *Commercial and Biomedical Applications of Ultrafast Lasers VI*; Joseph Neev, Stefan Nolte, Alexander Heisterkamp, Christopher B. Schaffer; Eds. (2006)
14. J. M. Gunn, B. Xu, J. M. Dela Cruz, V. V. Lozovoy, M. Dantus, "Quantitative phase characterization and compensation by multiphoton intrapulse interference phase scan (MIIPS)." *Femtochemistry VII*, W. Castelman Ed. Elsevier in press (2006)
15. M. Dantus V. V. Lozovoy, I. Pastirk, J.M. Dela Cruz, "Converting Concepts and Dreams of Coherent Control into Applications." *Femtochemistry VII*, W. Castelman Ed. Elsevier in press (2006)
16. Vadim V. Lozovoy and Marcos Dantus, *Laser control of Physicochemical Processes; Experiments and Applications*, Annual Reports C, 102, DOI: 10.1039/b417201a (2006). Our review was featured in the cover.
17. J. M. Gunn, M. Ewald and M. Dantus, "Properties of Two-Photon Induced Emission from Dendritic Silver Nanoclusters," *Ultrafast Phenomena* 2006.



## Interactions of ultracold molecules: collisions, reactions, and dipolar effects

D. DeMille

*Physics Department, Yale University, P.O. Box 208120, New Haven, CT 06520*

e-mail: david.demille@yale.edu

**Program scope:** The primary goal of our project is to study the reactive, inelastic, and elastic collisions of polar molecules (specifically, RbCs) in the ultracold regime. A variety of physical effects associated with the low temperatures and/or the polar nature of the molecules should be observable for the first time. These include phenomena such as chemical reactions at vanishing temperature,<sup>1</sup> ultra-long range “field-linked” states of polar molecules in an external electric field,<sup>2</sup> extraordinarily large ( $\sim 10^8$  Å<sup>2</sup>) elastic collision rates in the presence of a polarizing electric field,<sup>3,4</sup> etc. In addition, the study of inelastic (e.g., vibrationally or rotationally quenching) collisions will make it possible to produce optimized sources of ultracold polar molecules for a variety of applications. Finally, as a spin-off to this main effort, we have investigated the energy level structure of deeply-bound vibrational levels of the  $a^3\Sigma_u^+$  levels of Cs<sub>2</sub>, motivated by the possibility to use these levels in a sensitive search for possible variations in fundamental constants.

**Recent progress:** Our group recently demonstrated the ability to produce and state-selectively detect ultracold heteronuclear molecules. These techniques yielded RbCs molecules at translational temperatures  $T < 100$  μK, in any of several desired rovibronic states—including the absolute ground state, where RbCs has a substantial electric dipole moment. Our method for producing ultracold, ground state RbCs consisted of several steps. In the first step, laser-cooled and trapped Rb and Cs atoms were bound together into an electronically excited state, via the process known as photoassociation.<sup>5</sup> These initially-created molecules decayed rapidly into a few, weakly bound vibrational levels in the ground electronic state manifold.<sup>6</sup> Specifically, by proper choice of the photoassociation resonance, we formed metastable molecules exclusively in the  $a^3\Sigma^+$  level. This sample had significant population in only a small number of rotational levels.

We state-selectively detected these long-lived molecules with a two-step, resonantly-enhanced multiphoton ionization process (1+1 REMPI) followed by time-of-flight mass spectroscopy.<sup>7</sup> This unique detection capability (for ultracold molecules) was enabled by our spectroscopic characterization of RbCs in a previously inaccessible range of energy levels. Our method made it possible to determine the distribution of population among vibrational levels; under typical conditions, the  $a(v=37)$  level (bound by  $\sim 5$  cm<sup>-1</sup>) was most highly populated, although this distribution could be changed considerably (towards higher or lower vibrational levels) by the choice of photoassociation resonance.

In the final stage of this work, we demonstrated the long-sought ability to transfer population from these high vibrational levels, into the lowest vibronic states  $X^1\Sigma^+(v=0,1)$  of RbCs.<sup>8</sup> The technique was based on a laser “pump-dump” scheme. Two sequential laser pulses (each  $\sim 5$  ns in duration,  $\sim 100$  μJ pulse energy) drove population first “upward” into an electronically excited level, then “downward” into the vibronic ground state. The vibronic ground-state molecules were spread over a small number (2-4) of the lowest rotational levels, determined by the finite spectral resolution of the pump/dump lasers. These ground-state molecules were also detected with 1+1 REMPI.

In parallel with a major rebuilding of our experiment (see below), we have used our existing apparatus to perform precision spectroscopy of deeply-bound levels of the  $\text{Cs}_2$   $a^3\Sigma_u^+$  electronic state. These experiments were motivated by a new idea to amplify the effect of a possible variation in the electron-to-proton mass ratio,  $\mu$ . This amplification arises when a highly-excited vibrational level of one electronic state (e.g., the  $X^1\Sigma_g^+$  state of  $\text{Cs}_2$ ) is nearly degenerate with a deeply bound vibrational level of another electronic state (e.g. the  $\text{Cs}_2$   $a^3\Sigma_u^+$  state). Using the technique of two-color photoassociation spectroscopy,<sup>9</sup> we have probed  $\text{Cs}_2$   $a^3\Sigma_u^+$  state vibrational levels with binding energies as large as 1500 GHz ( $\sim 30\times$  more strongly bound than levels accessed in previous work of this type<sup>10</sup>). We have identified a clear case of the desired near-degeneracy, which appears as a hyperfine-induced perturbation of the  $a^3\Sigma_u^+$  state substructure. We have received crucial theoretical guidance from E. Tiesenga (NIST) on state assignments in our spectra, and from T. Bergeman (Stony Brook) on a global fit to all  $\text{Cs}_2$  data; we expect to write a paper with them on these results over the next months. Based on this analysis, we infer that this system of nearly-degenerate levels in  $\text{Cs}_2$  could be used to search for variations in  $\mu$  at the level of  $\delta\mu/\mu \sim 10^{-18}/\text{year}$ , a factor of  $\sim 1000$  more sensitive than any existing laboratory or cosmological test of such variations.

**Future plans:** We are nearing the end of a major rebuilding of our apparatus, as needed to implement our plan to optically trap dense samples of RbCs molecules with a single, low-lying rovibronic state populated. A new vacuum system has been assembled which will allow us to trap both the precursor Rb and Cs atoms and the resulting molecules (regardless of internal state) in a  $\text{CO}_2$  laser trap with long lifetimes. This apparatus also makes it possible to apply various electric fields and field gradients, in order to manipulate the ground-state molecules. New, higher-power trapping lasers have also been installed. A new postdoc (Eric Hudson) recently joined the group and we expect to see our first trapped atoms in the new apparatus shortly. Our present plan is to begin by trapping Rb and Cs in the  $\text{CO}_2$  trap, and cooling them to  $T \sim 10$   $\mu\text{K}$ . Next we will apply the photoassociation laser beam to form and accumulate vibrationally-excited RbCs. The initial goal is to observe simple processes such as vibrational quenching by collisions with precursor atoms.

The next phase of our work will focus on transferring population to the rovibronic ground state  $X^1\Sigma^+(v=0, J=0)$  in the trapped RbCs sample, and then “distilling” the sample so that only these ground-state molecules remain. With a simple system using two CW diode lasers and a Stimulated Raman Adiabatic Passage excitation scheme, we expect to have high efficiency and excellent state selectivity for the transfer process. In addition, we have worked out a plausible protocol for the distillation, which takes advantage of the large DC electric polarizability characteristic of the rovibronic ground state (and of no other states or species present in the trap). The pure sample of dense, ultracold, strongly polar molecules we anticipate producing will represent a near-ideal starting point for studying the new phenomena mentioned above.

## References

- <sup>1</sup>E. Bodo, F. A. Gianturco, N. Balakrishnan, and A. Dalgarno, *J. Phys. B: At. Mol. Opt. Phys.* **37**, 3641 (2004), and references therein.; R.V. Krems, in *Recent Research Developments in Chemical Physics*, vol. 3 pt. II, p. 485 (2002).
- <sup>2</sup>A.V. Avdeenkov and J. L. Bohn, *Phys. Rev. Lett.* **90**, 043006 (2003); A.V. Avdeenkov, D.C.E. Bortolotti and J.L. Bohn, *Phys. Rev. A* **69**, 012710 (2004).

- 
- <sup>3</sup>D. DeMille, D.R. Glenn, and J. Petricka, *Eur. Phys. J. D* **31**, 275 (2004).
- <sup>4</sup>M. Kajita, *Eur. Phys. J. D* **20**, 55 (2002).
- <sup>5</sup>A.J. Kerman *et al.*, *Phys. Rev. Lett.* **92**, 033004 (2004).
- <sup>6</sup>T. Bergeman *et al.*, *Eur. Phys. J. D* **31**, 179 (2004).
- <sup>7</sup>A.J. Kerman *et al.*, *Phys. Rev. Lett* **92**, 153001 (2004).
- <sup>8</sup>J.M. Sage, S. Sainis, T. Bergeman, and D. DeMille, *Phys. Rev. Lett.* **94**, 203001 (2005).
- <sup>9</sup>E. R. I. Abraham, W. I. McAlexander, C. A. Sackett, and R. G. Hulet, *Phys. Rev. Lett.* **74**, 1315 (1995).
- <sup>10</sup>N. Vanhaecke, Ch. Lisdat, B. T'Jampens, D. Comparat, A. Crubellier, and P. Pillet, *Eur. Phys. J. D* **28**, 351 (2004).

## ATTOSECOND SCIENCE: GENERATION, METROLOGY, AND APPLICATION

Louis F. DiMauro  
Department of Physics  
The Ohio State University  
Columbus, OH 43210  
dimauro@mps.ohio-state.edu

### 1. PROJECT DESCRIPTION

#### 1.1 PROGRESS IN FY06

##### 1.1.1 LABORATORY OPERATIONS

This document is a request for continuing funding of BES funded project entitled “Attosecond Science: Generation, Metrology & Application” at The Ohio State University (OSU). Over the past year significant progress has been made in initiating high harmonic experiments using long wavelength laser sources and developing the theoretical tools for guidance. All the work in FY06 is intended at meeting the objectives of the attosecond project while building the future foundation for the production of *light pulses with both the time-scale and the length-scale each approaching atomic dimension*. In other words, the formation of kilovolt x-rays bursts with attosecond ( $10^{-18}$  s) duration.

The original DOE proposal discussed the detailed strategy of utilizing the strong-field phenomenon of high harmonic generation for producing a broadband frequency comb of short wavelength radiation. In the frequency domain the harmonic comb is a powerful laboratory source of short wavelength coherent light. In the time-domain, proper synthesis of the frequency comb will yield a train of pulses or a single pulse with attosecond ( $10^{-18}$  s) durations. The scientific importance of breaking the femtosecond barrier is obvious: the time-scale necessary for probing the motion of an electron(s) in the ground state is attoseconds (atomic unit of time  $\equiv 24$  as). The availability of such attosecond pulses would allow, for the first time, the study of the time-dependent dynamics of correlated electron systems by freezing the electronic motion, in essence exploring the structure with ultra-fast snapshots, then following the subsequent evolution using pump-probe techniques. The explicit dynamics of excited states of atoms could be followed characterizing, for example, processes like autoionization or non-adiabatic transitions during atomic collisions. These pulses also would allow investigations of the dynamics of bond breaking and formation during chemical reactions. Such studies would lead ultimately to developing new more fundamental methods for the complete quantum control of electron dynamics. All of these areas of science are well centered in the scientific scope of DOE Basic Energy Sciences (BES).

The efforts in FY06 focused on building both the experimental and theoretical tools needed to perform the work outlined above. The progress included:

1. Complete the majority of infrastructure renovations in the DiMauro laboratories in the newly constructed Physics Research Building (PRB) at The Ohio State University.
2. Reestablish the functionality of the laboratory apparatus moved from Brookhaven National Laboratory (BNL) to OSU and initiate new experimental capabilities at OSU.
3. Develop theoretical methods for testing and guiding the attosecond experiments.
4. Initiate experiments of atoms in large ponderomotive potentials with 2  $\mu\text{m}$  and 4  $\mu\text{m}$  excitation.
5. Generated high harmonics in argon using 2  $\mu\text{m}$  excitation.

The PI and the majority of the group (3 Stony Brook physics graduate students and one post-doctoral research associate) moved to OSU from BNL in October 2004. The new laboratories in PRB were

anticipated for completion at that time but an unexpected failure in the buildings mechanical systems delayed the completion of the construction for several months. The PRB did not receive occupational safety certification until February 2005. Nonetheless the DiMauro group was given special dispensation by the University Architectural Office to begin establishing some of the laboratories infrastructure prior to this date although with significant constraints. At the time of this writing, the basic infrastructure (HVAC, processed chilled water, computer networking, cable trays, electrical and safety systems) needed for laboratory operation is available.

The laboratory space consists of three rooms totaling 3,000 ft<sup>2</sup>. The rooms are configured to allow optical access from the main laser clean room area (1,800 ft<sup>2</sup>) to the adjacent target rooms (600 ft<sup>2</sup> each) where the experiments are conducted. As seen in Fig. 1, the main laser room consists of three optical bench setups totaling 325 ft<sup>2</sup> of vibrationally damped table space. In the photograph the blue semi-transparent curtains surround each table set for environmental control and laser safety. Each table set supports a laser systems and associated diagnostics that provide one of the three colors (0.8  $\mu\text{m}$ , 2  $\mu\text{m}$  and 4  $\mu\text{m}$ ) of intense ultra-short pulses needed for this project. All the laser systems operate at a minimum of one kilohertz repetition rate. The 0.8  $\mu\text{m}$ , 2  $\mu\text{m}$  and 4  $\mu\text{m}$  laser systems are functional at OSU and will be described in the next paragraph.

**4  $\mu\text{m}$  source:** The back table set houses the 4  $\mu\text{m}$  laser system which consists of a synchronized titanium sapphire and Nd:YLF amplified laser systems, the 4  $\mu\text{m}$  light is derived as the difference frequency between these two colors. As shown in the center inset in Fig. 1, the new additions to this systems include a new Nd:YLF oscillator (Time-Bandwidth Lasers) for more stable performance and shorter pulse, 80 fs, titanium sapphire operation (the BNL system was 2 ps) and a multi-pass titanium sapphire amplifier for improved energy output. The major operational objectives of this system were achieved in January 2006. The current 1 kHz performance of the 4  $\mu\text{m}$  system is  $\sim 175 \mu\text{J}$  at a measured 80 fs pulse duration. As will be discussed later, the maximum focused intensity, estimated from photoelectron studies, is approximately  $10^{14} \text{ W/cm}^2$ ; an improvement by a factor of 100 over the previous system that existed at Brookhaven.



Figure 1: From left to right the photos are the main laser clean room, the 4  $\mu\text{m}$  mid-infrared system and one of the target rooms for conducting the attosecond experiments discussed in this grant. Photographs were taken in April 2006.

**2  $\mu\text{m}$  source:** Located on the near left table set in Fig. 1 is an intense, ultra-fast 2  $\mu\text{m}$  laser system which was a new experimental capability developed at OSU. The 2  $\mu\text{m}$  source was constructed by modifying an existing titanium sapphire laser system using OSU startup funds. A 100 fs titanium sapphire oscillator was replaced with a new 8 fs oscillator (Nanolayers Venteon broadband oscillator). The CPA was redesigned and constructed with a band-pass for 25 fs amplification. A multi-pass titanium sapphire power amplifier was added to the system for 5 mJ pulse operation after compression. The 2  $\mu\text{m}$  pulses are generated using a modified commercial optical parametric amplifier (Quantronix Topas OPA visible in

lower left-hand corner of figure). The specification of the 2  $\mu\text{m}$  source is 50 fs, 0.6 mJ pulse energy at a 1 kHz repetition rate. The focused intensity, estimated from photoelectron studies, is  $\geq 1 \text{ PW}/\text{cm}^2$ .

In the main laser room photograph the near right optical table set houses a commercial (Femtolasers Lasers) titanium sapphire amplifier laser system with carrier-envelope phase stabilized output. The system is operational and produces 23 fs, 0.8 mJ pulses at a 3 kHz repetition rate.

The photograph on the right in Fig. 1 shows the attosecond target room. A harmonic test-stand is operational for characterizing the frequency comb of the high harmonic light interacting with a long wavelength (2  $\mu\text{m}$  and 4  $\mu\text{m}$ ) fundamental field. The vacuum box with the Plexiglas covered flange is a 0.7 m Hettrick x-ray imaging spectrometer on loan from the AMOP group (L. Young-group leader) at Argonne National Laboratory (ANL). The Hettrick is equipped with an x-ray CCD camera. The cylindrical vacuum chamber closes to the optical table is the harmonic source chamber. A separate apparatus for performing applications with attosecond pulses is being designed under the supervision of Prof. DiMauro and Prof. Agostini. The apparatus will consist of a harmonic source chamber, a transport section with XUV focusing optics and an experimental science chamber for conducting attosecond experiments. The science chamber will incorporate a COLTRIMS design for both electron and ion detection.

The scaled interaction target room (not shown) contains the apparatus for continuing the scaled interactions of alkali atoms with an intense long wavelength fundamental field started at BNL. The required apparatus needed for the first set of experiments is complete.

### 1.1.2 TWO-CYCLE CARRIER-ENVELOPE PHASE STABILIZED 2 $\mu\text{m}$ PULSES

The output of the 50 fs, 2  $\mu\text{m}$  OPA has been temporally compressed resulting in a measured pulse duration of 12 fs. The pulse reduction is achieved by forming a plasma filament in a high pressure xenon cell using the focused 2  $\mu\text{m}$  OPA beam. The plasma filament shown in Fig. 2(a) provides two crucial elements: (1) new frequencies (bandwidth) are generated around the 2  $\mu\text{m}$  central wavelength via self-phase modulation and (2) the interplay of self-focusing and electron density dispersion provides wave guiding of the 2  $\mu\text{m}$  light. In the experiment 2-octaves of white-light bandwidth are measured on the output of the filament. Pulse compression is achieved by passing the chirped 2  $\mu\text{m}$  light through a prescribed thickness of optical glass (negative GVD at 2  $\mu\text{m}$ ). Figure 2(b) shows a 12 fs interferometric autocorrelation measured after the xenon cell. The 6.6 fs optical period of the 2  $\mu\text{m}$  light is equal to a  $< 2$ -cycle pulse. We also measure that the carrier-envelope phase (CEP) of the 2  $\mu\text{m}$  light is preserved with long-term stability through the filament propagation process. This is the first demonstration of a filament compressor for the production of 2-cycle CEP mid-infrared pulses and a manuscript is in preparation.

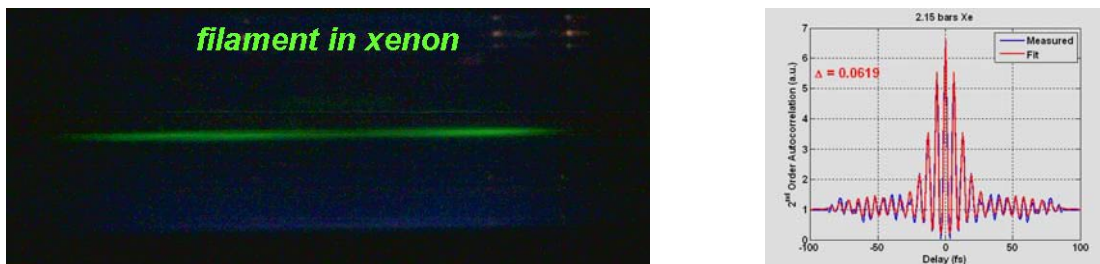


Figure 2: (a) The fluorescence from an intense 2  $\mu\text{m}$  pulse propagating through a few centimeter long plasma filament. (b) The measured and fitted interferometric autocorrelation of a 12 fs, 2  $\mu\text{m}$  pulse.

### 1.1.3 HIGH HARMONIC GENERATION WITH A 50 FS, 2 $\mu\text{M}$ PULSE

An important accomplishment for FY06 is the observation of strong-field excitation of inert gas atoms using mid-infrared sources. This result is a major experimental breakthrough for enabling our attosecond studies. The studies have been performed using both TOF methods for electron/ion detection and photon detection for harmonic generation.

Figure 3 is the high harmonic spectrum resulting from 2  $\mu\text{m}$  excitation of argon. The spectrum shows the comb of odd-order harmonics extending to the aluminum filter absorption edge at 73 eV. A zirconium filter reveals that the spectrum extends to at least 150 eV. Our photoionization studies performed under similar conditions indicate that argon is experiencing a ponderomotive potential of 70 eV placing the cutoff energy near 250 eV. Contrast this to 0.8  $\mu\text{m}$  excitation of argon which produces harmonics only to 50 eV or the 29<sup>th</sup>-order.

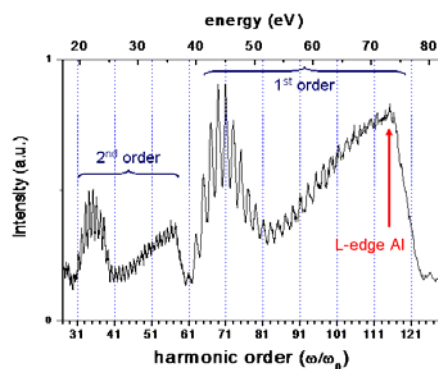


Figure 3: High harmonic spectrum resulting from excitation of argon with intense 2  $\mu\text{m}$  ultra-short pulses. The odd-order harmonic peaks are spaced by twice the fundamental frequency. The harmonic spectrum cuts off at  $\sim 73$  eV due to the absorption of the aluminum filter.

## 1.2 PROPOSED STUDIES IN FY07

The following is a brief description of experimental plans in FY07:

1. Study conditions for optimized harmonic generation at 2  $\mu\text{m}$ , e.g. yield and cutoff energy.
2. Explore the physics of attosecond generation using CEP 2-cycle, 2  $\mu\text{m}$  light.
3. Begin studies of scaled atomic systems using 4  $\mu\text{m}$  excitation.
4. Construct apparatus for science-driven attosecond experiments.

## 1.3 PROJECT PERSONNEL

As part of this proposal a post-doctoral research associate, Dr. Jennifer Tate and two graduate students, Mr. Jonathan Wheeler and Ms. Emily Sistrunk have been supported on the DOE contract. Two additional Stony Brook (SB) physics graduate students (Phil Colosimo and Anne Marie March) who relocated with Prof. DiMauro are supported on startup funds and work on this project. In the autumn 2005, Pierre Agostini was appointed professor of physics at OSU on a half-time basis.

## 1.4 PUBLICATIONS

Nine publications (3 PRL) have resulted from this DOE contract. Two additional papers have been submitted (PRL) or accepted (J. Mod. Optics).

# High Intensity Laser Driven Explosions of Homo-nuclear and Hetero-nuclear Molecular Clusters

Project DE-FG02-03ER15406

Abstract (Summer 2006)

Principal Investigator:

Todd Ditmire

*The Texas Center for High Intensity Laser Science*

*Department of Physics*

*University of Texas at Austin, MS C1600, Austin, TX 78712*

*Phone: 512-471-3296*

e-mail: [tditmire@physics.utexas.edu](mailto:tditmire@physics.utexas.edu)

## Program Scope:

The nature of the interactions between high intensity, ultrafast laser pulses and atomic clusters of a few hundred to a few thousand atoms has come under study by a number of groups world wide. Such studies have found some rather unexpected results, including the striking finding that these interactions appear to be more energetic than interactions with either single atoms or solid density plasmas and that clusters explode with substantial energy when irradiated by an intense laser. It is now well established that the explosions of low-Z molecular clusters such as hydrogen or deuterium clusters explode mainly by a Coulomb explosion. Our program under the last three year cycle studied the interplay between a traditional Coulomb explosion description of the cluster disassembly and a plasma-like hydrodynamic explosion, particularly for small to medium sized clusters (<1000 atoms) and clusters composed of low-Z atoms. In this program we have extended these studies, particularly with an eye toward the optimization of cluster explosions for use in a high flux, laser driven neutron source. We are examining the details of the Coulomb explosion of molecular clusters and we are studying the temporal dynamics of the electron ejection and ion expansion through pump probe techniques. We have also studied in detail the dynamics of explosions of mixed species clusters, such as methane (and deuterated methane) where it was conjectured that dynamic effects play an important role in the ejection of the lighter ions. We are looking at a number of diagnostics but mainly have been concerned with examining ion energy spectra and fusion neutron yield in deuterated cluster plasmas. In the past year, we wrapped up experiments on hydrogen and mixed species clusters having examined anisotropies in the hydrogen cluster explosions and explosions of methane and deuterated methane clusters, confirming the predicted dynamic acceleration effect expected of the lighter ion species. Furthermore we performed an experiment to study wavelength-scale particles (as opposed to the nanometer sized cluster particles usually employed in our experiments) with the intent of studying how Mie resonances affect strong field cluster interactions. Finally, we have started to implement plans to perform experiments on the irradiation of clusters with XUV pulses.

## Progress During the Past Year

We have an ongoing campaign to study high intensity laser interactions with exploding clusters (ie intensity  $\geq 10^{17}$  W/cm<sup>2</sup>). During the past year, with support from this BES grant, we have performed four activities in this area: we have concluded the study of the explosion of heteronuclear clusters, we have studied anisotropy in hydrogen cluster explosions, we have examined hot electron production from micron scale polystyrene spheres, and we have continued the construction and characterization of an experiment that will allow us to irradiate clusters with intense short wavelength (100-10 nm) femtosecond pulses.

### *Study of dynamic enhancement of ion energies from explosions of methane clusters*

Our work on this topic has been motivated by a series of results published in recent years. Over the last several years, there has been much activity in studying high intensity, ultrashort laser pulse interactions with atomic clusters. The most dramatic consequence of this unique interaction has been the observation of high

charge states and very fast ions. The ejection of ions with many keV of energy from exploding clusters can be exploited to drive nuclear fusion, and we have studied this phenomena quite extensively over the past few years under funding from this grant. When we proposed this grant we asked the question of whether mixed species, heteronuclear clusters like  $\text{CD}_4$ , will behave in the same manner as single species clusters under intense ultrafast laser irradiation. Theoretical results suggest that explosions of clusters with mixed atomic species may be more complicated and exhibit some interesting differences. The motivation for studying Coulomb explosions of mixed species clusters has been advanced recently through molecular dynamic simulations by Last and Jortner which indicate that the energies of lighter deuterons from exploding heteronuclear clusters, like  $\text{D}_2\text{O}$  or  $\text{CD}_4$ , could be increased through a dynamical effect in which the light ions will outrun the heavier ions, exploding in an outer shell with a higher average energy beyond what would be expected from the naïve estimate of ion energy based on initial potential energy as in the simple Coulomb explosion picture.

In our work during the past couple of years, we performed an experimental confirmation of this dynamic enhancement of light ion energies from exploding heteronuclear clusters using methane ( $\text{CH}_4$ ) and fully deuterated methane ( $\text{CD}_4$ ). Considering only the initial potential energy, the deuterons and protons from the same sized  $\text{CH}_4$  and  $\text{CD}_4$  clusters would acquire the same explosion energy upon irradiation. However, if the predicted kinematic enhancement of the light ion energies occurs, then the effect should be stronger in the case of  $\text{CH}_4$  compared to  $\text{CD}_4$  and be detectable through a study of these two molecular clusters under identical cluster formation and irradiation conditions. By comparing ion energy spectra we indeed observe a clear enhancement in the explosion energy of protons compared to deuterons. In our experiment a pulsed supersonic gas jet directed through a skimmer produced a low density cluster beam. The energies of the ions created by the laser-cluster interaction were determined by measuring the time of flight (TOF) of the ions in a field free drift tube. The laser was focused using an  $f/4.9$  refractive graded index yielding intensity of  $\sim 3 \times 10^{17} \text{ W/cm}^2$ . Measured ion distribution from both methane and deuterated methane clusters are shown in figure 1. The difference in masses between  $\text{H}^+$  and  $\text{D}^+$  causes a clearly apparent isotope effect with the

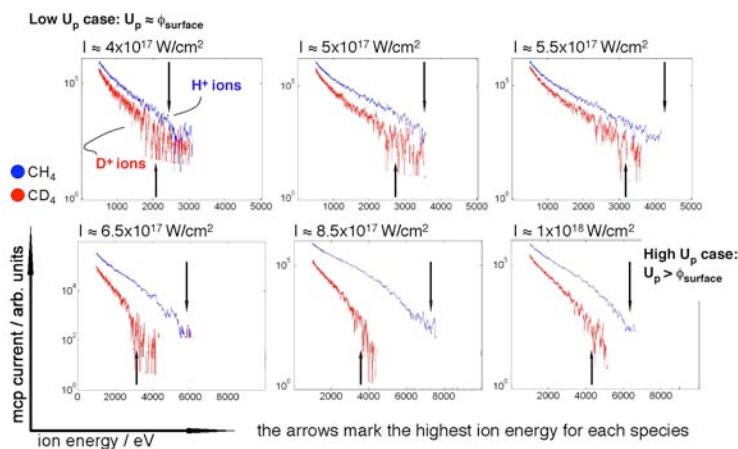


Figure 1: Measured ion spectra from  $\text{CH}_4$  and  $\text{CD}_4$  clusters at a range of laser intensities.

lighter protons ejected with higher energy. Figure 1 illustrates data for a range of laser intensities. At the lowest intensities, we see very little difference between the proton and deuteron data. This would be consistent with the fact that the laser ponderomotive energy is below that required to extract all the electrons and drive a Coulomb explosion. In this case we expect a plasma-like explosion and, as the data illustrate, expect no difference between the two isotopes. At the highest intensities, however, the Coulomb explosion mechanism dominates and the dynamic enhancement becomes more prominent.

### Studies of anisotropy in explosions of hydrogen clusters

Our second set of experiments during the past year represented a finalization of experiments begun somewhat earlier. In particular, we examined the explosions of clusters in the regime intermediate to the standard, pure Coulomb explosion where all electrons are ejected by the laser field, and a hydrodynamic explosion, where most electrons are retained in the cluster by space-charge forces. To derive information on this intermediate regime, we examined the anisotropy of ions ejected from laser irradiated hydrogen clusters. We chose to study the ion spatial distributions in hydrogen because any anisotropy must arise from the electron dynamics and not by differing charge states.

In our experiments we did indeed observe a clear asymmetry with ion energies ejected from  $H_2$  clusters. In particular we measured an enhancement of ion energies along the laser polarization direction. We conducted measurements for both short (40fs) and long (250fs) pulses attempting to access the pure Coulomb and intermediate interaction regimes. We find that the measured ion energies from irradiation with the short pulse can be reasonably well explained using a complete vertical ionization model. However, we find that higher ion energies were attained with the longer pulse, which we interpret as evidence for the vacuum heating of cluster electrons. The mean energies as a function of polarization angle for two pulse durations are shown in figure 2. In both cases the maximum ion energy is observed along the laser polarization. This is in contradiction to a pure Coulomb explosion model and indicates that the laser extracted electrons pull the ions along. The increase in ion energy with the longer pulse is an indication that vacuum heating is at work.

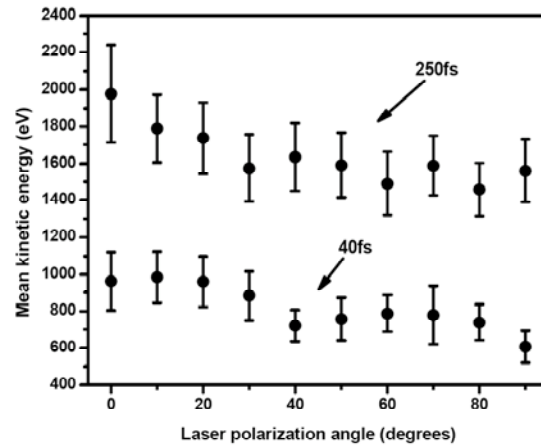


Figure 2: Angular distribution of the mean ion energies from  $H_2$  clusters irradiated with 40fs and 250fs laser pulse.

### Hot electron production from wavelength scale particles

In addition to exploring nanometer scale clusters, we are exploring other, unique cluster targets. In particular, we have begun a campaign under this grant to study hot electron generation and x-ray production from targets coated with microspheres. This work is motivated by the possibility that spheres with size comparable to the wavelength of the incident laser radiation can result in electric field enhancements through well known Mie resonances. This past year we investigated hard x-ray (>100 keV) generation from copper and fused silica targets coated with a partially covering layer of microspheres. When a spherical object is illuminated with light of a wavelength similar to the diameter of the object, a complicated electric field pattern arises due to interference between the incident and scattered waves as shown in figure 3. Substantial field enhancements can exist for certain sphere sizes.

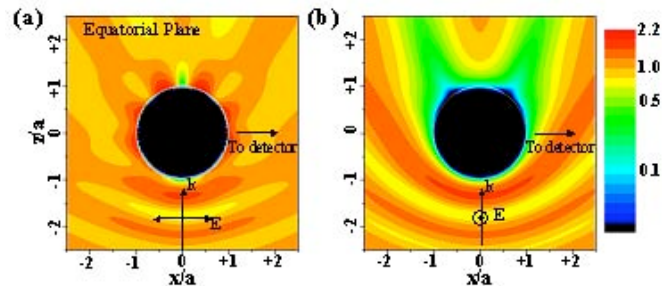


Fig. 3. Calculated electric field plot for an ionized, micron-diameter plasma sphere for laser polarization (a) parallel and (b) perpendicular to the page.

X-ray yield from illumination of sphere coated targets by 400 nm, 100 fs pulses at intensity of  $2 \times 10^{17} \text{ W/cm}^2$  at two photon energies as a function of sphere size is illustrated in figure 4. We see a clear peak in the x-ray yield for spheres with size 260 nm diameter. This roughly corresponds to the sphere size in which we expect a maximum in the electric field from Mie resonances and indicates that these Mie resonances can play an important role in producing hot electrons.

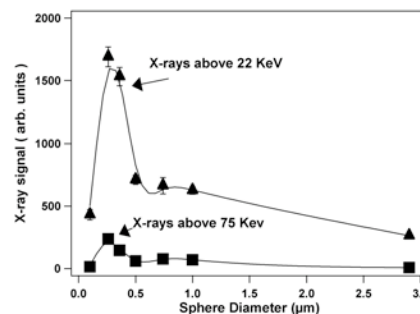


Figure 4: X-ray yield as a function of sphere size measured with filtered NaI detectors.

## Future Research Plans

Our future plans encompass the study of XUV pulse interactions with clusters. During this year we have completed construction of a separate beamline and chamber on the THOR laser which will allow us to generate high order harmonics with the full 0.7 J of laser energy and focus these harmonics into a cluster jet with an XUV mirror. This new beamline on THOR is illustrated in figure 5. We have conducted initial high harmonic generation studies with this new chamber. The goal is to focus pulses of up to 1  $\mu\text{J}$  of energy in the 40 – 15 nm range into a low density jet of clusters. We have arranged this to allow studies both with rare gas clusters and metal clusters. This will allow us to tune the excitation wavelength to near the giant dipole resonance of the cluster microplasma. Such experiments will lead the way to future experiments on the LCLS.

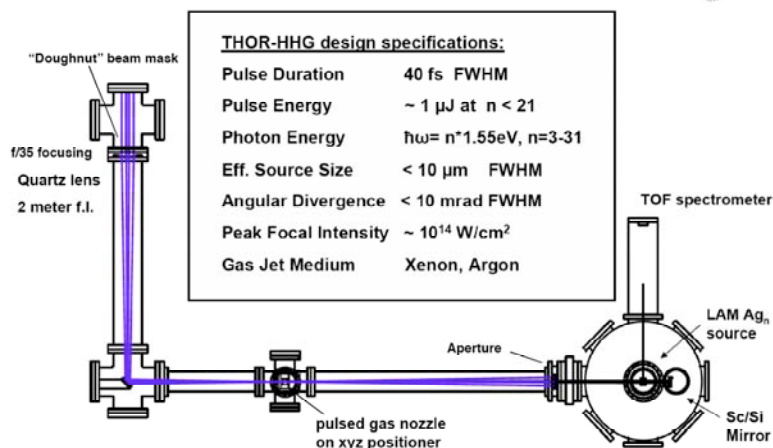


Figure 5: Schematic and specs of the new HHG cluster beamline on the THOR 20 TW laser

## Papers published on work supported by this grant during the past three years:

- 1) H. A. Sumeruk, S. Kneip, D. R. Symes, I. V. Churina, A. V. Belolipetski, T. D. Donnelly, and T. Ditmire, "Control of Strong-Laser-Field Coupling to Electrons in Solid Targets with Wavelength-Scale Spheres" to be published.
- 2) M. Hohenberger, D. R. Symes, K. W. Madison, A. Sumeruk, and T. Ditmire, "Dynamic Acceleration Effects in Explosions of Laser Irradiated Heteronuclear Clusters", *Phys. Rev. Lett.* **95**, 195003 (2005).
- 3) F. Buergens, K. W. Madison<sup>1</sup>, D. R. Symes, R. Hartke, J. Osterhoff, W. Grigsby, G. Dyer and T. Ditmire, "Angular distribution of neutrons from deuterated cluster explosions driven by fs-laser pulses", *Phys. Rev. E*, **74**, 016403 (2006)
- 4) R. Hartke, D. R. Symes, F. Buergens, L. Ruggles, J. L. Porter, T. Ditmire, "Neutron Detector Calibration using a table-top laser heated plasma neutron source" *Nuc. Inst. And Methods A* **540**, 464 (2005).
- 5) T.D. Donnelly, J. Hogan, A. Mugler, M. Schubmehl, N. Schommer, Andrew J. Bernoff, S. Dasnurkar and T. Ditmire, "Using ultrasonic atomization to produce an aerosol of micron-scale particles", *Rev. Sci. Instr.* **76**, 113301 (2005).
- 6) K. W. Madison, R. Fitzpatrick, P. K. Patel, D. Price, T. Ditmire, "The role of laser pulse duration in Coulomb explosions of deuterium cluster targets" *Phys. Rev. A* **70**, 053201 (2004).
- 7) K. W. Madison, P. K. Patel, D. Price, A. Edens, M. Allen, T. E. Cowan, J. Zweiback, and T. Ditmire, "Fusion neutron and ion emission from laser induced explosions of deuterium and deuterated methane clusters" *Phys. Plas.* **11**, 270 (2004).
- 8) T. Ditmire, S. Bless, G. Dyer, A. Edens, W. Grigsby, G. Hays, K. Madison, A. Maltsev, J. Colvin, M. J. Edwards, R. W. Lee, P. Patel, D. Price, B. A. Remington, R. Sheppherd, A. Wootton, J. Zweiback, E. Liang and K. A. Kielty, "Overview of future directions in high energy-density and high-field science using ultra-intense lasers" *Rad. Phys. And Chem.* **70**, 535 (2004).
- 9) K. W. Madison, P. K. Patel, M. Allen, D. Price, T. Ditmire, "An investigation of fusion yield from exploding deuterium cluster plasmas produced by 100 TW laser pulses" *J. Opt. Soc. Am. B* **20**, 113 (2003).
- 10) J. W. G. Tisch, N. Hay, K. J. Mendham, E. Springate, D. R. Symes, A. J. Comley, M. B. Mason, E. T. Gumbrell, T. Ditmire, R. A. Smith, J. P. Marangos, M. H. R. Hutchinson, "Interaction of intense laser pulses with atomic clusters: Measurements of ion emission, simulations and applications" *Nuc. Inst. Meth. B – Beam Interacts with Materials and Atoms* **205**, 310 (2003).

# Ultracold Molecules: Physics in the Quantum Regime

John Doyle

Harvard University

17 Oxford Street

Cambridge MA 02138

doyle@physics.harvard.edu

## 1. Program Scope

Our research encompasses a unified approach to the trapping of both atoms and molecules. Our goal is to extend our very successful work with CaH to NH and approach the ultracold regime. We plan to trap and cool  $10^{11}$  NH molecules loaded directly from a molecular beam. Elastic and inelastic collisional cross sections will be measured and cooling to the ultracold regime will be attempted. To date, no molecule-molecule collisional cross sections have been measured for ultracold heteronuclear molecules. Theory has now begun to offer predictions for NH. We note that as part of this work, we are continuing to develop an important trapping technique, buffer-gas loading. This method was invented in our lab and its significant advantages (large numbers of trapped atoms and molecules as well as general applicability) indicate that further development is warranted.

## 2. Recent Progress

The milestones for this project are:

- x-spectroscopic detection of ground-state NH molecules via LIF
- x-production of NH in a pulsed beam
- x-spectroscopic detection of ground-state NH molecules via absorption
- x-injection of NH beam into cryogenic buffer gas (including LIF and absorption detection)
- x-realization of 4 T deep trap run in vacuum
- x-injection of NH molecules into cryogenic trapping region
- x-loading of NH molecules into cryogenic buffer gas with 4 T deep trap
- x-trapping of NH
- o-measurement of spin-relaxation rate of NH with He
- o-removal of buffer gas after trapping of NH
- o-measurement of elastic and inelastic cross sections
- o-attempt evaporative cooling

NH, like many of the diatomic hydrides, has several advantages for molecular trapping including large rotational constant and relatively simple energy level structure. Some of the several key questions before us when this project began were: Could we produce enough NH using a pulsed beam? Is it possible to introduce a large number of NH molecules into a buffer gas? Would the light collection efficiency be enough for us to adequately detect fluorescence from NH? Could we get absorption spectroscopy to work so that absolute number measurements could be performed? Could we achieve initial loading of NH into the magnetic trap? We have now answered these questions, all to the positive.

There are important questions left. Will the spin relaxation rates with helium be low enough for us to remove the buffer gas? Will the NH-NH collision rates be adequate for evaporative cooling or will another method (like sympathetic or laser cooling) be necessary to cool NH into the ultracold regime. There is strong indication that the answer to the first is “yes.” Recent theoretical calculations by Krems and coworkers (motivated by our experiment) indicate that NH will survive

in the low-field-seeking state for several hundred thermalization times before it spin relaxes. The final question is still open and, indeed, answering this question is the key stated goal of this work.

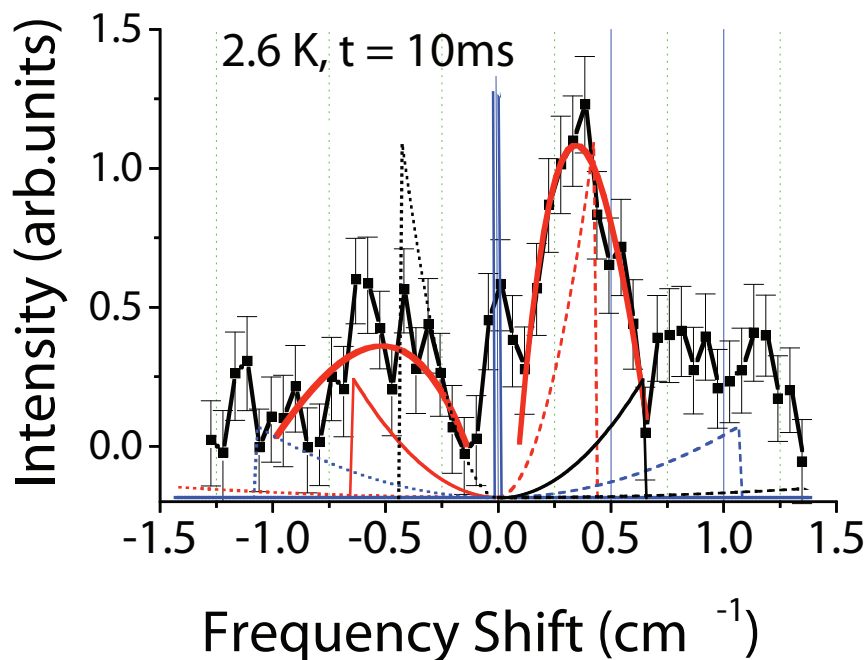


Figure 1: Spectra of trapped NH molecules at 2.6 K. Thick lines are guides to the eye. Thin lines are 0-th order simulated spectra for various transitions. Data is consistent with a trapped distribution of NH low-field seekers.

### Summary of Status of Project

The heart of the apparatus is a beam machine that we use to produce pulsed NH in a supersonic beam (see figure 2). (We are in the supersonic regime only to maximize NH flux; 3 dimensional translational cooling and rotational cooling are provide by the buffer gas.) The design of the pulsed source is based on the production of OH via DC discharge as executed by Nesbitt. In short, we have a pulsed valve and a slit plate with a layer of BN in between. A voltage between the plates and the nozzle of the pulsed valve produces a discharge whenever we allow gas into the nozzle. This is done by opening the pulsed valve, with a solenoid, for times about 1 ms.

This beam is directed toward our trapping magnet, the bore of which forms a cryogenic buffer-gas cell. This was constructed with a small entrance orifice of a few mm in diameter to allow the beam of NH to enter, thus buffer-gas cooling the NH. Several windows exist for the the introduction and collection of light. In this initial setup the magnet (and, therefore, the buffer gas) can be cooled to as low as around 2.5 K.

The basic experimental procedure is as follows. The pulse valve of our NH source is opened for about one millisecond. During this time a jet of ammonia exits the valve, entering the discharge region near the jaws, creating a beam of ammonia, NH and other species. This long pulse beam travels about 10 cm to the face of the cell where approximately all of the molecules heading toward the entrance orifice enter the cell. The NH are then cooled by the buffer gas in the cell. In our latest experiments we have been using fluorescence spectroscopy to detect the NH in the trapping region. We have been able to observe the NH molecules fall into the trap and our data is consistent with

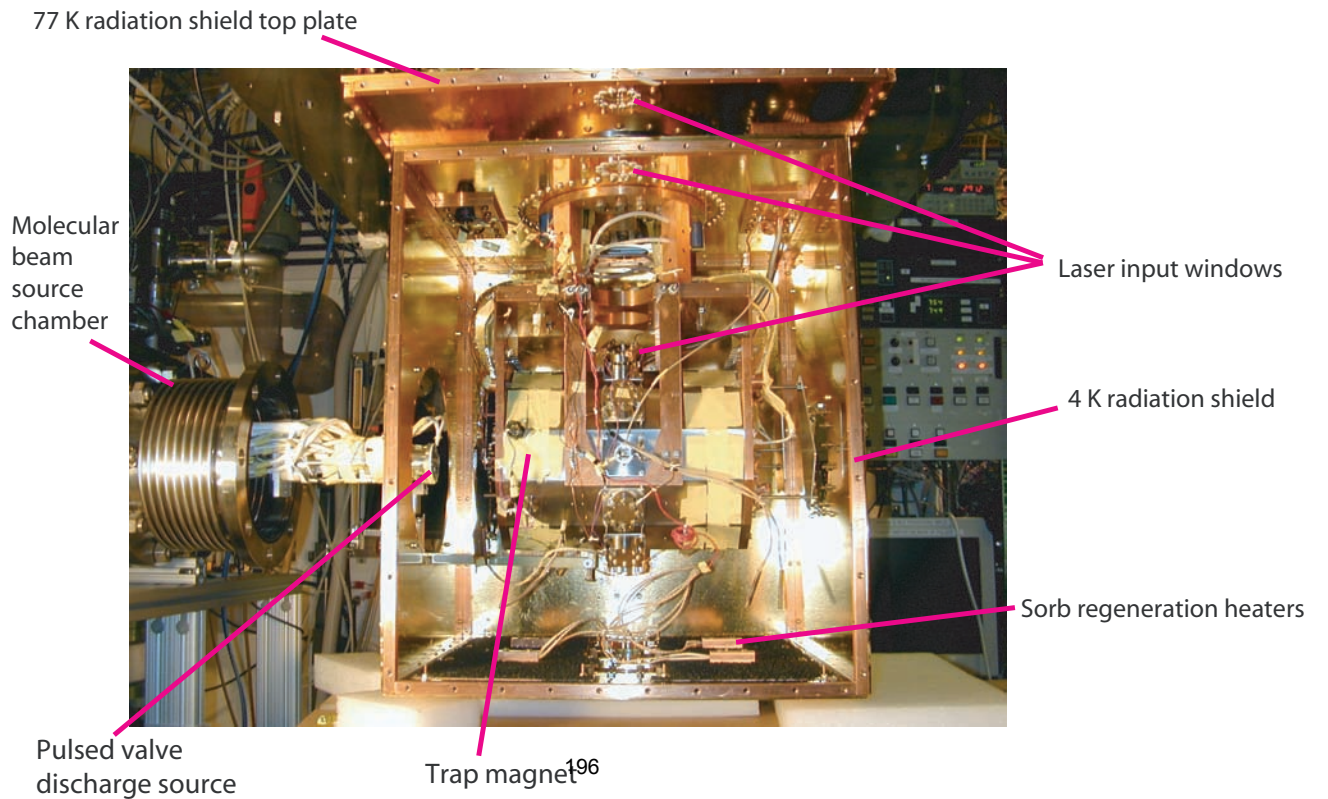
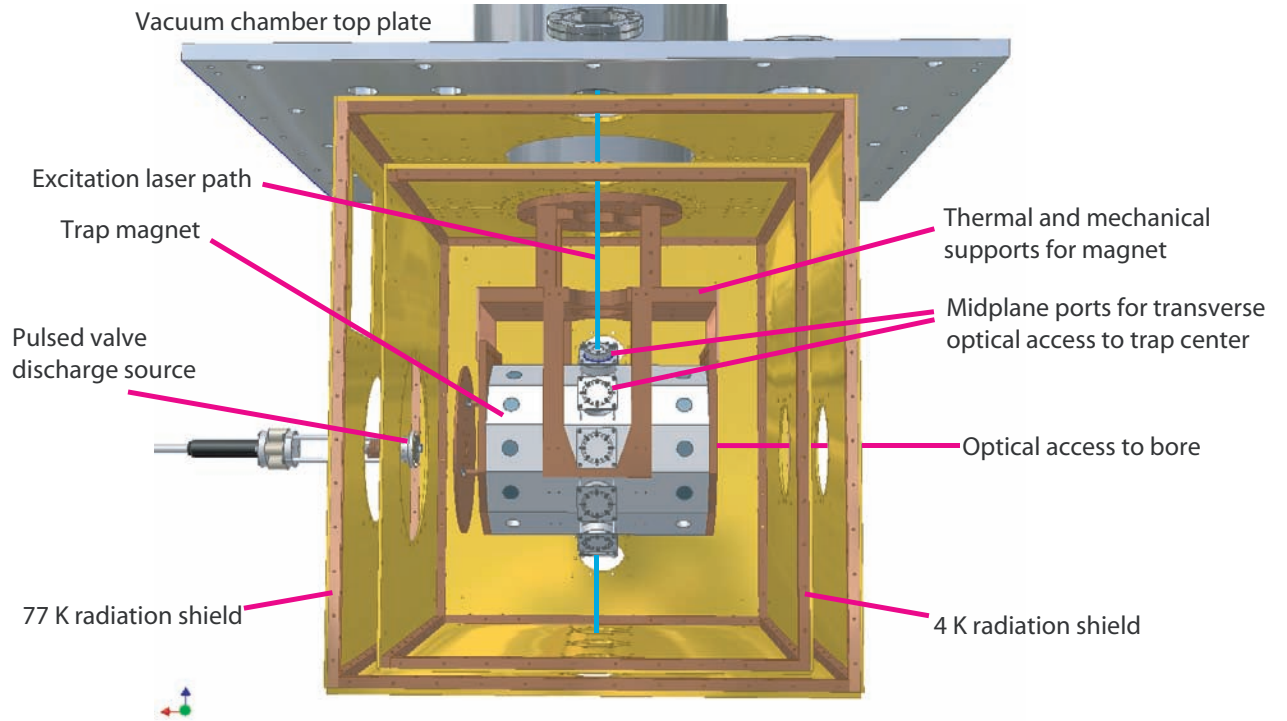
only low field seekers being present. In these test runs at high temperature (around 2.5 K), the lifetime of the trapped sample is short, only around 10 ms. This is consistent with our evaporation model for these low ratios of trap depth to temperature. We see no evidence of spin relaxation of NH, consistent with recent theory.

Since this data was taken, we undertook a major overhaul of our apparatus including installation of: a cryocooler, high-Tc magnet leads, entirely new cell, new He3 refrigerator, new molecular beam chamber, new pulsed valve source and several other devices. The key goal of these improvements is to lower the temperature of the trapping cell so as to trap the NH molecules with long lifetime. Lowering the cell temperature to 500 mK will greatly increase the lifetime of our trapped NH sample into the second range. These long lifetimes will immediately allow us to measure the fundamental NH-He spin relaxation cross section as well as prepare for removal of the buffer gas to observe NH-NH collisions. Other hoped for results of these improvements include much lower helium boil-off (due to the cryocooler) and higher reliability for our complex apparatus. The full apparatus is 80% debugged and we are hopeful for initial results on collisions by the end of the year.

### **3. Future Plans**

We continue on our program of trapping of NH. The next step is to buffer-gas load NH into the buffer-gas cell while the cell is inside the energized trap with the cell at lower temperatures, around 500 mK (instead of 2.5 K). In this way we should be able to spectroscopically determine the helium-NH spin relaxation rates.

Figure 2:



# Atomic Electrons in Strong Radiation Fields

J. H. Eberly  
Department of Physics and Astronomy  
University of Rochester, Rochester, NY 14627  
eberly@pas.rochester.edu

July 15, 2006

## Program Scope: Large Classical Ensemble Dynamics

Our underlying interest is in learning more about the ways that very intense laser light couples to atoms and molecules. To this end, we are studying the interaction of multi-electron atoms statistically by using ensembles of classical “atoms”, allowing us to pay detailed attention to the time-dependent response of atomic electrons to the strong forces that are acting: a combination of mutual e-e repulsion, the time-dependent external laser field and the Coulomb field of a nuclear core. We can study very strongly correlated few-electron behavior analogous to that seen experimentally in non-sequential double ionization (NSDI) of atoms and molecules [1, 2, 3, 4]. We have been reporting results on the average temporal dynamics of two electrons in a classical “atom” under peak pulse intensities between  $10^{14}$  and  $10^{16}$  watts/cm<sup>2</sup>. Our classical multi-electron “atom” is designed to have ionization thresholds similar to several noble gas atoms for which experimental results are available. Our modeling of a two-electron atom throughout a typical double ionization event [5, 6] follows several or many recollisions of one electron back into the other electrons in the atomic core region. We have recently demonstrated [7] that these techniques will be applicable to theoretical examination of NSTI (non-sequential triple ionization). Our recent Letter showed [8] that the classical theory predicts greatest correlated double ionization in the first recollision, in agreement with quantum predictions, although many recollisions can occur.

## Background

Strong and coherent radiation fields induce coherent responses in atomic electrons. Such coherence has opened a frontier in atomic physics where attosecond-timed features of electron motion can be predicted and controlled. One important counter-intuitive element of this new domain is that in such a strong and coherent field the photoionization process loses its one-way character and briefly becomes a multi-cycle process in which an electron periodically escapes the nucleus with high kinetic energy but is still able to be pulled back by the laser field.

The breakdown of radiative perturbation theory associated with such unconventional ionization processes is already reached in the vicinity of  $10^{12}$  watts/cm<sup>2</sup>. The conventional theory is a systematic extension of the Keldysh theory [9] of photoemission via tunneling. The experimental study of

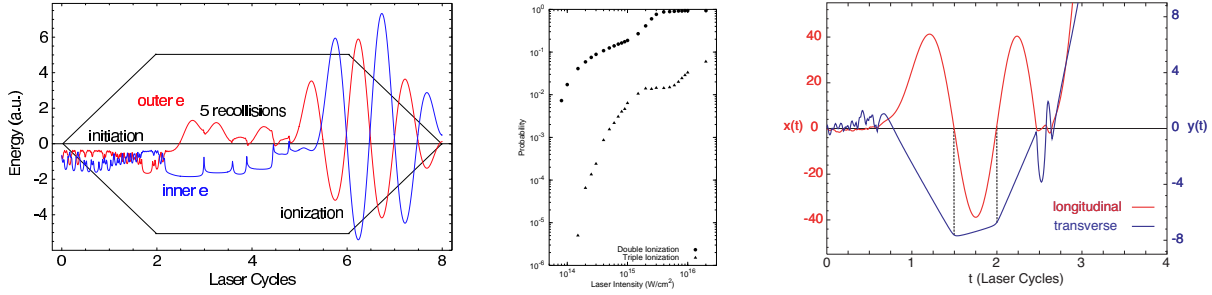


Figure 1: Left frame: energy trajectories for a single electron pair, showing the four episodes in a typical NSDI event – initiation, recollision, ionization, free jitter motion. The trapezoidal overlay indicates the turn-on and turn-off of the laser field envelope. Center frame: Classical correlation calculation showing that the “knee” signature is expected to appear in the triple as well as double non-sequential ionization ion count. Right frame: Time evolution showing first predictions of transverse motion of a recolliding electron. After turn-on of the field envelope, the “longitudinal” main motion  $x(t)$  (left scale), which consists of three wide quasi-sinusoidal swings and follows the laser field, is accompanied by transverse motion  $y(t)$  (right scale), which is a sequence of three straight-line drift segments prior to ionization. The vertical projection lines show that the timing of the abrupt changes in transverse drift direction come exactly at the times the main motion passes the position of the nucleus. This is a form of “Coulomb focusing”.

double ionization in the strong-field low-frequency “tunneling” regime has shown that for intensities that are two to four orders of magnitude greater than  $10^{12}$  watts/cm<sup>2</sup> modifications of existing theory are needed and in particular have led to the conclusion [1] that single active electron (SAE) theory is not adequate.

## Two-Electron Theory

For double ionization the exact solution of the time-dependent Schrödinger equation (TDSE) has been achieved only for helium. This numerically intensive result of the Taylor group [10] is generally accepted as the limit to what can be done theoretically for the foreseeable future in the NSDI experimental regime of near-780 nm wavelength. However, the physical model of recollision [11] can be used to suggest different approximations, one of which is the so-called “aligned electron approximation”, in which one extracts an advantage from the strong linearly polarized laser fields used in experiments, by introducing the ansatz of linear motion for the electrons, basically entraining their motion along the polarization direction, but providing a soft Coulomb core for their potential, to permit them to pass beside one another and sample both sides of the nucleus [12].

Under the aligned electron ansatz a variety of solutions of the TDSE for two coupled atomic electrons have been calculated and compared with experimental reports. The calculations can be done much more rapidly because of the dimensional restriction. Aligned-electron TDSE wave functions for two electrons are consistent with the NSDI “knee” in the ion-count data. For our purposes it is important that these two-electron wave functions can also be compared with classical ensemble calculations by comparing electron probability distributions as a function of time during the laser pulse for the same model parameters. The close match obtained thereby [13] provides strong evidence of the high proportion of classical rather than quantum correlation in the dynamics. The outcome of fully classical calculations [5, 6] is surprisingly satisfactory in modeling experimental findings, including prediction [15] of aspects of COLTRIMS longitudinal momentum distributions not well explained by approximate quantum S-matrix calculations.

## Recent Progress: Three-Electron Theory and Beyond the Aligned-Electron Ansatz

Classical theory of NSDI shares the interpretive framework of the well-known two-step “rescattering” scenario first proposed for NSDI by Corkum [11]. As the left frame of Fig. 1 shows, a typical classical double-ionization event is preceded by several or even many recollisions. This picture stands in contrast to the two-step quantum picture in which double ionization is deemed to occur in the very first recollision cycle.

Experimental study has begun to accumulate evidence for three- and higher multiple-electron ejection [14]. No method has been advanced to permit first-principles time-dependent quantum calculations to enter this domain. However, as we first proposed, we have been able to extend our classical theory in new directions, and we report here two preliminary successes so far.

In collaboration with S.L. Haan’s group in Calvin College we have dropped the aligned-electron ansatz completely and have been achieving control of truly 3d classical dynamics for two electrons, extending and improving understanding of NSDI. Preliminary results are being presented in conferences [15]. We expect to extend this work beyond two electrons.

An advance into completely new territory has been possible in classical three-electron theory, leading to the first results for NSTI (non-sequential triple ionization). One early finding [7] is that the same type of “knee” in the ion count data that characterizes NSDI is also predicted for NSTI, as shown in the central panel of Fig. 1. For triple ionization we have at the same time been able to extend the aligned electron theory by incorporating a transverse dimension. Explicit characteristics of transverse motion are now available for inspection in triple ionization, and one example is included in the right frame of Fig. 1. The laser has no direct impact transversely, so all transverse motion arises from electron correlation and nuclear attraction. Our classical dynamics allows this to be tracked during the ionization event, and the figure shows two curves, one for motion driven directly by the laser field, designated  $x(t)$  and the other for motion in a transverse plane, designated as  $y(t)$ . The caption explains that the transverse motion reveals an unexpected characteristic of Coulomb focusing, namely that it is not a gradual attraction of the electron to the nucleus, but rather a series of sharp impacts. This shows in yet one more way how the strong and phase-coherent laser, which forces the electron far from the nucleus almost all of the time without ionizing it, changes the way one should visualize high-field ionization events.

## Future Plans

We expect to explore the effects of electron correlation in very high-field environments by further extensions of statistical ensembles of Newtonian electrons. It is becoming steadily clearer that coherent-laser strong-field ionization is largely classically describable. Classical descriptions typically provide direct visualization, and assist interpretation. We expect this to be true of situations with more than two electrons in strong and coherent fields, where no quantum TDSE approach is expected to be feasible any time soon. We expect to continue to benefit from experimental input, as laboratory results on non-sequential multi-ionization have already begun to be reported [14].

## Acknowledgement

We have appreciated extended discussions with S.L. Haan and Phay J. Ho. Work supported by DOE Grant DE-FG02-05ER15713 is marked with \*\*\* in the listing below.

## References

- [1] D. N. Fittinghoff, P. R. Bolton, B. Chang and K. C. Kulander, *Phys. Rev. Lett.* **69**, 2642 (1992)
- [2] B. Walker *et al.*, *Phys. Rev. Lett.* **73**, 1227 (1994).
- [3] S. Augst, A. Talebpour, S.L. Chin, Y. Beaudoin, and M. Chaker, *Phys. Rev. A* **52**, 917(R) (1995); A. Talebpour *et al.*, *J. Phys. B* **30**, 1721 (1997); S. Larochelle, A. Talebpour and S. L. Chin, *J. Phys. B* **31**, 1201 (1998).
- [4] C. Guo, and G. N. Gibson, *Phys. Rev. A* **63**, R040701 (2001); M. J. DeWitt, E. Wells, and R. R. Jones, *Phys. Rev. Lett.* **87**, 153001 (2001); E. Wells, M. J. DeWitt, and R. R. Jones, *Phys. Rev. A* **66**, 013409 (2002).
- [5] Phay J. Ho, R. Panfili, S. L. Haan and J. H. Eberly, *Phys. Rev. Lett.* **94**, 093002 (2005)
- [6] Phay J. Ho, *Phys. Rev. A* **74**, 045401 (2005), arXiv:physics/0504037
- [7] \*\*\*Phay J. Ho and J.H. Eberly, arXiv: physics/0605026.
- [8] \*\*\*Phay J. Ho and J.H. Eberly, *Phys. Rev. Lett.* **95**, 193002 (2005), arXiv: physics/0507175.
- [9] L.V. Keldysh, *Zh. Eksp. Teor. Fiz.* **47**, 1945 (1964) [*Sov. Phys. JETP* **20**, 1307 (1965)].
- [10] See, for example, the report on helium in J. S. Parker *et al.*, *J. Phys. B* **36**, L393 (2003).
- [11] P. B. Corkum, *Phys. Rev. Lett.* **71**, 1994 (1993).
- [12] See J. Javanainen, J. H. Eberly and Q. Su, *Phys. Rev. A* **38**, 3430 (1987) and R. Grobe and J.H. Eberly, *Phys. Rev. Lett.* **68**, 2905 (1992).
- [13] R. Panfili, J. H. Eberly and S. L. Haan, *Opt. Express* **8**, 431 (2001). See also R. Panfili, S. L. Haan, and J. H. Eberly, *Phys. Rev. Lett.* **89**, 113001 (2002), and S. L. Haan, P. S. Wheeler, R. Panfili and J. H. Eberly, *Phys. Rev. A* **66**, 061402(R) (2002).
- [14] See L.F. DiMauro and P. Agostini, in *Adv. At. Mol. Opt. Phys.* **35**, edited by B. Bederson and H. Walther (Academic, 1995), and recent reports in A. Rudenko, et al., *Phys. Rev. Lett.* **93**, 253001 (2004), and S. Palaniyappan, et al., *Phys. Rev. Lett.* **94**, 243003 (2005).
- [15] \*\*\*S.L. Haan, L. Breen, A. Karim and J.H. Eberly, presentation at LPHYS-06 High-Field Seminar, July 24-28, 2006, Lausanne, Switzerland.

# Few-Body Fragmentation Interferometry

*Department of Energy 2006-2007*

James M Feagin

*Department of Physics  
California State University–Fullerton  
Fullerton CA 92834  
jfeagin@fullerton.edu*

We continue our work begun with DOE support to extract basic understanding and quantum control of few-body microscopic systems based on our long-time experience with more conventional studies of correlated electrons and ions. Although much has been achieved experimentally with quantum information and control with photons and quantum optics, there remains fundamental interest in establishing analogous tools with charged particles, especially correlated electrons and ions.<sup>1</sup> Key steps in this direction have been of course the successes with ion traps and with atom interferometry. We are thus motivated to consider few-body fragmentation detection from the more general perspective of reaction interferometry. We have accordingly continued to pursue the two parallel efforts, *detection interferometry* and *collective few-body excitations*. While we are keenly aware that many of the experiments we consider are difficult, we maintain a strong interest in our longtime overlap with various experimental groups in this country and in Europe.

## Two-Center Interferometry and Decoherence Effects

Advances in atom interferometry and ion trapping now afford systematic study of quantum interferences in mesoscopic systems with parameters that can be tracked from quantum towards macroscopic limits. For example, Pritchard and coworkers at MIT<sup>2</sup> have observed the interference fringes of a sodium atom passing through a Mach-Zehnder interferometer while scattering a photon. Likewise, Monroe and coworkers<sup>3</sup> at NIST in Boulder have engineered the external motion of a linearly trapped  ${}^9\text{Be}^+$  ion into a double-humped Schrödinger-cat superposition of two displaced coherent-state wavepackets. Besides their novelty in traditional AMO collision physics, such target systems allow one to study quantum correlations in well controlled environments with relatively few quantum parameters. Within the impulse approximation, we have developed a framework to connect these and related experiments including the observation of Young's fringes with photons scattered by a *pair* of trapped ions.<sup>4</sup> This work is an outgrowth of our general considerations of scattering interferometry and two-center interference effects from extended targets.<sup>5</sup>

We have been particularly interested in the coherent effects that result when a projectile scatters off a target atom and its displaced quantum image, a configuration which occurs when the target's external center-of-mass state is double humped.<sup>6</sup> We have thus considered the trapped-ion interferometry of a 'kicked-cat' state generated by photon scattering from a Schrödinger-cat state in analogy with scattering from the two arms of a Mach-Zehnder atom interferometer. We consider an incident photon  $\mathbf{k}_L$  resonantly scattered by an atom or ion

---

<sup>1</sup> J. Ullrich et al., Rep. Prog. Phys. **66**, 1463 (2003); J. Ullrich and V. P. Shevelko, Eds., *Many-Particle Quantum Dynamics in Atomic and Molecular Fragmentation*, Springer, New York (2003).

<sup>2</sup> M. S. Chapman et al., Phys. Rev. Lett. **75**, 3783 (1995); D. A. Kokorowski et al., Phys. Rev. Lett. **86**, 2191 (2001).

<sup>3</sup> C. Monroe et al., Science **272**, 1131 (1996).

<sup>4</sup> W. M. Itano et al., Phys. Rev. A **57**, 4176 (1998).

<sup>5</sup> J. M. Feagin and S. Han, Phys. Rev. Lett. **86**, 5039 (2001); Phys. Rev. Lett. **89**, 109302 (2002).

<sup>6</sup> J. M. Feagin, Phys. Rev. A **73**, 022108 (2006).

target with center-of-mass (CM) position  $\mathbf{C}$ , as depicted in Fig. 1. We assume for simplicity the photon encounter is impulsive and that the target's external CM motion is described by the initial wavefunction  $g_0(\mathbf{C})$  throughout the collision. The asymptotic photon-ion wave is then given by  $\psi \sim e^{i\mathbf{q}\cdot\mathbf{C}} g_0(\mathbf{C}) f_\gamma(\mathbf{k}) e^{ikr}/r$ , where  $\mathbf{k} \equiv k\hat{\mathbf{r}}$  and  $f_\gamma(k\hat{\mathbf{r}})$  is the *free-atom* resonance fluorescence amplitude. Here,  $\mathbf{q} \equiv \mathbf{k}_L - \mathbf{k}$  so that  $\hbar\mathbf{q}$  is a momentum transfer to the target by the scattered photon, and  $e^{i\mathbf{q}\cdot\mathbf{C}}$  is the momentum boost of the target external state due to the impulsive encounter once a photon detection direction  $\hat{\mathbf{r}}$  is selected. This boost and the resulting nonlocal phase shifts when the initial wavefunction  $g_0(\mathbf{C})$  is double humped are key elements of the interference effects we analyze. Consider for example the Schrödinger-cat superposition  $g_0(\mathbf{C}) = g_0^{(0)}(\mathbf{C} - \mathbf{C}_0) + g_0^{(1)}(\mathbf{C} - \mathbf{C}_1)$  describing the state of a *single* target atom or ion. If the component wavepackets  $g_0^{(n)}$  are relatively narrow compared to their separation  $\mathbf{d} \equiv \mathbf{C}_0 - \mathbf{C}_1$ , then the asymptotic *kicked-cat* state is approximately  $\psi \sim [e^{i\mathbf{q}\cdot\mathbf{C}_0} g_0^{(0)} + e^{i\mathbf{q}\cdot\mathbf{C}_1} g_0^{(1)}] f_\gamma(\mathbf{k}) e^{ik_L r}/r$ , which makes clear the photon-atom or -ion entanglement relative to the approximate photon scattering points  $\mathbf{C}_n$ . The scattered-photon states  $e^{i\mathbf{q}\cdot\mathbf{C}_n} f_\gamma(\mathbf{k}) e^{ik_L r}/r$  are not orthogonal and therefore will not fully discriminate which end of the kicked cat,  $g_0^{(0)}$  or  $g_0^{(1)}$ , the atom or ion was in when it scattered the photon. Thus, when allowed to recombine, the two ends of the cat will again interfere but with a visibility reduced by the partial overlap of these photon states.

### Einstein's Recoiling-Slit Experiment

The impulse approximation also provides a straightforward framework for describing photon two-slit interference with a trapped-ion source and thus a realization of Wootters and Zurek's seminal quantum discussion of Einstein's celebrated recoiling-slit experiment.<sup>7</sup> Wootters and Zurek revisited Einstein's gedanken experiment to analyze Young's double-slit interferometry to include in detail the photon which-path information stored in the recoiling entrance slit. They assumed an entrance slit cut into a spring-mounted plate that could be treated as a quantum oscillator under the action of a passing photon. They then considered alternative position and momentum measurements of the plate and the effect of the measurements on the photon interference. Wootters and Zurek thus exploited the underlying photon-plate entanglement to formulate quantitative statements about wave-particle duality, and their work became one of the first major publications on the subject.

We have thus considered photon scattering by a trapped ion as a modern realization of Wootters and Zurek's quantum analysis of the recoiling-slit experiment.<sup>8</sup> While a harmonically trapped ion provides a perfect quantum realization of a spring-mounted plate and entrance slit, we find that a coherent-state measurement of the recoiling ion, besides likely having experimental advantages, can mimic both position and momentum measurements of the ion in full

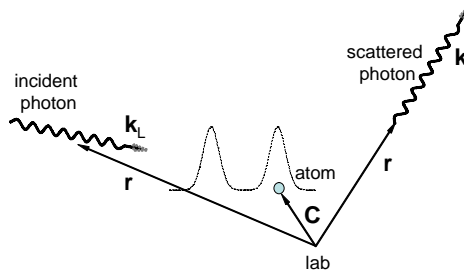


FIG. 1: Incident photon scattered by a two-center target.

<sup>7</sup> W. K. Wootters and W. H. Zurek, Phys. Rev. D **19**, 473 (1979).

<sup>8</sup> R. S. Utter and J. M. Feagin, Phys. Rev. A, submitted July (2006).

analogy with Wootters and Zurek. One readily identifies the resulting photon fringe visibility as the overlap of recoil-ion marker states describing a photon scattered towards one or the other slit. When the overlap vanishes, the direction of the scattered photon could in principle be determined via the photon-ion entanglement by a measurement of the recoil ion, blocking an interference effect. On the other hand, when the overlap is perfect, neither the direction of the recoiling ion nor of the scattered photon is discernable, and the interference is perfect. The intermediate stage of duality characterized by moderate overlap continues to warrant further study.

## Hardy Nonlocality

In parallel work, we have analyzed<sup>9</sup> the detection of a pair of recoiling reaction fragments, each by its own interferometer, to demonstrate Hardy's contradiction between quantum mechanics and local hidden variables.<sup>10</sup> Hardy's theorem sidesteps Bell's inequality by establishing the contradiction with just four measurement outcomes on two system fragments. Whereas Bell's theorem involves fully statistical violations of the quantum description, the Hardy result is simpler and hinges on essentially perfect correlations to establish nonlocality. Our interferometry is based on the projectile-target momentum entanglement and is independent of the identity and internal state of the fragments. Although no doubt a very difficult experiment, our approach is thus relatively straightforward, at least conceptually.

## Dichroism and Nondipolar Effects

Two-slit detection would also provide new probes of photoionization angular distributions. Even with the photo *single* ionization of an unoriented atom, we have demonstrated<sup>11</sup> that one could generate a circular dichroism analogous to the well established effect seen in photo *double* ionization<sup>12</sup> and thereby extract phase information on nondipolar amplitudes.

A related dichroism and nondipolar probe is expected in ordinary fluorescence in which a photon takes the role of the photoionized electron and is analyzed by two-port interferometry, as depicted in Fig. 2. Such an experiment is currently in progress by T. Gay and coworkers at the University of Nebraska and interference fringes have been observed with rubidium fluorescence photons. Our preliminary analysis indicates the technique may provide a useful method for

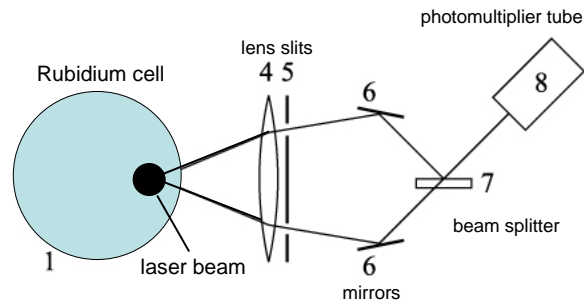


FIG. 2: Fluorescence interferometry experiment. The Rb (target) cell is 4 cm long, and the laser beam and therefore the reaction volume 20  $\mu\text{m}$  in diameter. The two slits are  $5^\circ$  apart at the laser beam.

<sup>9</sup> J. M. Feagin, Phys. Rev. A **69**, 062103 (2004).

<sup>10</sup> L. Hardy, Phys. Rev. Lett. **71**, 1665 (1993)

<sup>11</sup> J. M. Feagin, Phys. Rev. Lett. **88**, 043001 (2002).

<sup>12</sup> V. Mergel et al., Phys. Rev. Lett. **80**, 5301 (1998) and references therein; A. Knapp et al, J. Phys. B: At. Mol. Opt. Phys. **35**, L521 (2002). (*Feagin is a coauthor on these papers.*)

extracting electric and magnetic *quadrupole* contributions to dipole allowed transitions.

## Collective Coulomb Excitations

These projects continue to link to our more conventional longtime work in the AMO field of collective Coulomb excitations. For example, *multihit* detection of continuum electron pairs<sup>13</sup> has been extended to the photo double ionization of molecular hydrogen in the isotopic form D<sub>2</sub> including coincident detection of the deuterons.<sup>14</sup> Moreover, state-of-the-art *ab initio* computation of this four-particle process has been achieved by T. Rescigno and W. McCurdy and coworkers.<sup>15</sup> Also, F. Robicheaux and coworkers have applied a time-dependent close-coupling description to this problem.<sup>16</sup> Parallel to these achievements, we developed a model of molecular photo double ionization based closely on an analogous model cross section we established for helium.<sup>17</sup> These lowest-order approximations in the electron-pair angular momentum relative to a molecular axis have the advantage of providing approximate dynamical quantum numbers and propensity rules for excitation of certain molecular fragmentation configurations.<sup>18</sup> Departures from our model have recently been studied in detail experimentally by T. Reddish and A. Huetz and coworkers.<sup>19</sup> We have thus begun to examine higher-order corrections to our heliumlike description of D<sub>2</sub> fragmentation and intend to work closely with the LBNL group to compare with their extensive numerical predictions without the constraints inherent in analyzing experimental data.<sup>20</sup>

Two-center interference effects have been observed in the double ionization of aligned hydrogen molecules by fast heavy ion impact.<sup>21</sup> Moreover, electron interference fringes have now been extracted from molecular photoionization distributions.<sup>22</sup> We have thus also begun to extend our molecular photoionization model to include multicenter interference effects that come into play at higher energies.

## Publications and Recent Submissions

*Trapped-Ion Realization of Einstein's Recoiling-Slit Experiment*, R. S. Utter and J. M. Feagin, Phys. Rev. A, submitted July (2006). (*Utter is a CSUF masters degree candidate.*)

*Two-Center Interferometry and Decoherence Effects*, J. M. Feagin, Phys. Rev. A **73**, 022108 (2006).

*Hardy Nonlocality via Few-Body Fragmentation Imaging*, J. M. Feagin, Phys. Rev. A **69**, 062103 (2004).

*Fully Differential Cross Sections for Photo Double Ionization of Fixed-in-Space D<sub>2</sub>*, Th. Weber et al, Phys. Rev. Lett. **92**, 163001 (2004). (*Feagin is a coauthor.*)

---

<sup>13</sup> A. Knapp et al, J. Phys. B: At. Mol. Opt. Phys. **35**, L521 (2002). (*Feagin is a coauthor.*)

<sup>14</sup> Th. Weber et al., Phys. Rev. Lett. **92**, 163001 (2004) and references therein. (*Feagin is a coauthor.*)

<sup>15</sup> W. Vanroose, F. Martin, T. N. Rescigno and C. W. McCurdy, Phys. Rev. A **70**, 050703 (R) (2004); Science **310**, 1787 (2005).

<sup>16</sup> J. Colgan, M. S. Pindzola, and F. Robicheaux, J. Phys. B: At. Mol. Opt. Phys. **37**, L377 (2004).

<sup>17</sup> J. M. Feagin, J. Phys. B: At. Mol. Opt. Phys. **31**, L729 (1998); T. J. Reddish and J. M. Feagin, J. Phys. B: At. Mol. Opt. Phys. **32**, 2473 (1999).

<sup>18</sup> M. Walter, J. S. Briggs and J. M. Feagin, J. Phys. B: At. Mol. Opt. Phys. **33**, 2907 (2000).

<sup>19</sup> M. Gisselbrecht et al., Phys. Rev. Lett. **96**, 153002 (2006).

<sup>20</sup> W. McCurdy and T. Rescigno (LBNL), private communication.

<sup>21</sup> A. L. Landers, E. Wells, T. Osipov, K. D. Carnes, A. S. Alnaser, J. A. Tanis, J. H. McGuire, I. Ben-Itzhak, and C. L. Cocke, Phys. Rev. A **70**, 042702 (2004).

<sup>22</sup> L. Cocke (KSU), private communication.

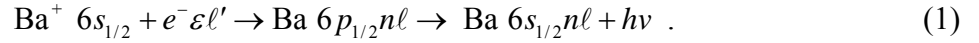
## Studies of Autoionizing States Relevant to Dielectronic Recombination

**T.F. Gallagher**  
**Department of Physics**  
**University of Virginia**  
**P.O. Box 400714**  
**Charlottesville, VA 22904-4714**  
 tfg@virginia.edu

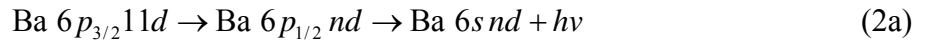
The focus of this program is doubly excited autoionizing states of atoms. The practical motivation of direct interest to the Department of Energy is that a systematic study of autoionization allows us to understand the reverse process, dielectronic recombination (DR), i.e., recombination of ions and electrons via intermediate autoionizing states. DR provides an efficient recombination mechanism for high temperature electrons, and it is important in high temperature laboratory and astrophysical plasmas.<sup>1,2</sup> Unlike radiative recombination (RR), DR terminates in excited bound states of atoms, so the the process is not the inverse of photoexcitation from the ground state but from an excited state.

During the past year we have worked on the effects of high frequency microwave fields on DR, the effects of small electric and magnetic fields on DR, and microwave resonance experiments and their interpretation

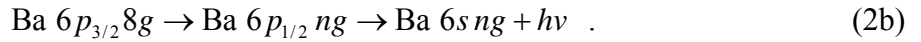
In Ba, the atom we have studied, DR is the recombination of a free electron with a Ba ion via an intermediate autoionizing state. This process can be written explicitly as



The incoming  $\varepsilon \ell'$  electron excites  $\text{Ba}^+$  from the  $6s_{1/2}$  to  $6p_{1/2}$  state and is itself captured in the  $n\ell$  orbit. If radiative decay to the bound  $6s_{1/2} n\ell$  state occurs, recombination has taken place. In our experiments we do not really study DR but a process which we term DR from a continuum of finite bandwidth. In DR from a continuum of finite bandwidth we replace the true continuum with a continuum of finite bandwidth, either the broad  $6p_{3/2} 11d$  or  $6p_{3/2} 8g$  ionizing state straddling the  $\text{Ba}^+ 6p_{1/2}$  limit.<sup>3</sup> We have examined the two processes



and



An atom in the  $6p_{3/2} 11d$  or  $6p_{3/2} 8g$  state makes the interchannel transition to the degenerate  $6p_{1/2} nd$  or  $6p_{1/2} ng$  state ( $20 < n < \infty$ ). If it decays radiatively to the bound  $6s_{1/2} nd$  or  $6s_{1/2} ng$  state, DR has occurred. The primary attractions of this technique are the energy resolution of  $\sim 0.5 \text{ cm}^{-1}$  ( $< 0.1 \text{ meV}$ ), the fact that the experiments can be done in zero electric and magnetic field, and that the partial wave of the entrance channel is well defined. The latter is different from true DR, and it gives us more detailed insight into the process. In the continuum of finite bandwidth experiments the  $11d$  or  $8g$  electron makes about twenty orbits and collides with the  $\text{Ba}^+$  core

twenty times before it autoionizes. Our experiments are similar to DR experiments done in storage rings,<sup>4</sup> in which the electrons have many opportunities to collide and recombine with the ions.

We have recently been exploring the enhancement of DR from a continuum of finite bandwidth by small electric and magnetic fields. The enhancement of the process of Eq. (2a) by an electric field requires that the field exceed the Inglis-Teller field of  $1/3n^5$ , due to the large quantum defect of the  $nd$  states.<sup>5</sup> Enhancement of the process of Eq. (2b), however, occurs at much smaller fields, and we have been concentrating on it.<sup>6</sup> We have observed several new phenomena. First, we have observed spectral holes in the DR signal when we apply small static fields, that is, the DR signal vanishes. We are now analyzing these data, and it appears that the holes occur at the locations of Ba  $6p_{3/2}n\ell$  states of  $\ell \geq 4$ . Holes appear because at the energies of these states atoms can return from the  $6p_{1/2}n\ell$  states to the  $6p_{3/2}n\ell$  states which autoionize rapidly. In true DR there would be incoming flux via all such states, and they would not appear as holes. However, in DR from a continuum of finite bandwidth and in storage ring experiments such spectral holes can be expected.

One of our interests in concentrating on DR from a continuum of finite bandwidth via the  $ng$  states, the process of Eq. (2b), is that the requisite electric fields are small, and the hydrogenic energy spacing between the Stark states,  $3nE$ , is small. Thus the magnetic field required to produce comparable shifts would be small, and it should be possible to observe a decrease in the DR signal when the magnetic field shift overwhelms the E field shift.<sup>7,8</sup> We have realized that there is another important effect as well, due to the fact that any atom which exhibits DR is not hydrogenic. In particular, at low fields the incomplete Stark manifolds have nearly degenerate low  $m$  Stark states.<sup>9</sup> As a consequence nearly an order of magnitude smaller magnetic fields should be required to mix them than might be expected on the basis of a hydrogenic model. We have started experiments to investigate this phenomenon, and the initial results appear to support the picture presented above.

We have examined several effects of microwave fields on DR. One of the more interesting observations is that we are able to observe above threshold recombination (ATR). Specifically, we are able to observe DR when the incoming energy is as much as  $10 \text{ cm}^{-1}$  above the  $6p_{1/2}$  limit, in spite of the fact that the ponderomotive energy due to the microwave field is only  $0.13 \text{ cm}^{-1}$  (4 GHz). From the Simpleman's model of above threshold ionization we would expect to see ATR only  $0.4 \text{ cm}^{-1}$  above the limit.<sup>10,11</sup> We have done calculations which indicate that the large energy range spanned by ATR is due to the fact that DR takes place in the Coulomb field of an ion. In other words, Volkov states are not the correct description.

In the past year we have worked on several aspects of the microwave spectroscopy of two electron atoms. First, we finished and published what we believe to be the first report of microwave spectroscopy of autoionizing states. In particular, we have observed the Ba  $5d_{3/2} ng$  ( $J = 2$ )  $\rightarrow$   $5d_{3/2} (n \pm 1)h$  ( $J = 3$ ) transitions for  $45 \leq n \leq 49$  using a delayed field ionization detection technique. The differences from the hydrogenic intervals are due to the first order quadrupole interaction and the second order dipole and quadrupole interactions between the ion core and the Rydberg electron. One of the more interesting results of this process is that we have realized that the commonly used core polarization representation of the second order dipole and quadrupole interactions breaks down for anisotropic cores.

The process of analyzing the data from our experiments led us to study carefully the previous work of Lundeen and his students on the intervals of the Rydberg states of two electron atoms. They had realized that the previously unexplained splitting of Ba  $6sn\ell$  states was due to admixtures of excited spin orbit ionic core states into the  $6s \text{ Ba}^+$  core.<sup>12,13</sup> We derived this result in a more systematic fashion and showed that the observed splittings were due only to the two lowest states of the ionic core, the 5d and 6p states. Furthermore, we demonstrated that it is possible to extract the dipole and quadrupole radial matrix elements connecting the 6s state to these two states in much the same way that the ionic core polarizabilities are extracted from the separations between the  $n\ell$  states, that is, it is possible to construct a graph in which the slope and intercept are the two matrix elements.

It is useful for us to be able to examine aspects of DR involving the high  $\ell$  states in low fields. Until now our choices in, for example, Ba were to use the  $6sng$  states, which requires four lasers, or two lasers and Stark switching, which typically entails kV/cm fields. In the past year we have discovered that we are able to transfer all the atoms from the Ba  $6snd$  states to the  $6sng$  states by two photon microwave transitions. A surprising aspect of the process is its inherently high resolution. To be specific, we are able to observe 100kHz wide lines for these transitions, in spite of the fact that they are occurring in the earth's magnetic field. The narrow linewidth results from the fact that the g factor for singlet states is always one, so all  $\Delta m = 0$  transitions are coincident in frequency. What is more interesting is that by applying fields of 1 V/cm we are able to observe the Stark states, and it should be possible to produce high  $\ell$  states by Stark switching with 1 V/cm fields instead of 1 kV/cm fields. This capability will enable us to probe autoionization of high angular momentum states in ways inconceivable only a year ago.

In the coming year we plan to finish the ongoing work on the enhancement of DR from  $ng$  states in combined E and B fields. We wish to verify that the nonhydrogenic B field enhancement ideas are correct and make measurements in higher B fields. We expect that, for a given E, as B is increased DR should increase, reach a maximum, and finally decline to a value equal to the  $E = 0$  value. We also plan to finish the experiments on ATR and begin to explore autoionization of higher  $\ell$  states in low fields.

## References

1. A. Burgess, *Astrophys. J.* 139, 776 (1964).
2. A.L. Merts, R.D. Cowan, and N.H. Magee, Jr., Los Alamos Report No. LA-62200-MS (1976).
3. J.P. Connerade, *Proc. R. Soc. London, Ser. A*, 362, 361 (1978).
4. T. Bartsch, S. Schippers, A. Muller, C. Brandau, G. Gwinner, A.A. Saghiri, M. Beutelspachier, M. Grieser, D. Schwalm, A. Wolf, H. Danared, and G.H. Dunn, *Phys. Rev. Lett.* 82, 3779 (1999).
5. L. Ko, V. Klimenko and T.F. Gallagher, *Phys. Rev. A*, 59, 2126 (1999).
6. E.S. Shuman, C.M. Evans, and T.F. Gallagher, *Phys. Rev. A* 69, 063402 (2004).
7. F. Robicheaux and M. S. Pindzola, *Phys. Rev. Lett.* 79, 2237 (1997).
8. V. Klimenko and T.F. Gallagher, *Phys. Rev. Lett.* 85, 3357 (2000).
8. V. Klimenko and T.F. Gallagher, *Phys. Rev. A* 66, 023401 (2002).
9. C. Fabre, Y. Kaluzny, R. Calabrese, L. Jun, P. Goy, and S. Haroche, *J. Phys. B* 17, 3217 (1984).
10. H. B. van Linden van den Heuvell and H. G. Muller, in *Multiphoton Processes*, edited by S. J. Smith and P. L. Knight (Cambridge University Press, Cambridge, 1988).
11. T.F. Gallagher, *Phys. Rev. Lett.* 61, 2304 (1988).
12. T.F. Gallagher, R. Kachru, and N.H. Tran, *Phys. Rev. A* 26, 2611 (1982).
13. E. L. Snow, R. A. Komara, M. A. Gearba, and S.R. Lundeen, *Phys. Rev. A* 68, 022510 (2003).
14. B. Edlen, in *Spectroscopy I*, edited by S. Flugge, *Handbuch der Physik*, Vol. 27 (Springer, Berlin, 1964).

## Publications 2004-2006

1. E.S. Shuman, C.M. Evans, and T.F. Gallagher, “ $\ell$  dependence of dielectronic recombination from a continuum of finite bandwidth in an electric field” *Phys. Rev. A* 69, 063402 (2004).
2. E.S. Shuman and T.F. Gallagher, “Resonant Enhancement of dielectronic recombination by a high frequency microwave field,” *Phys. Rev. A* 71, 033415 (2005).
3. E. S. Shuman and T. F. Gallagher, “Microwave Spectroscopy of autoionizing Ba  $5d_{3/2}n\ell$  states” *Phys. Rev. A* 73, 032511 (2006).
4. E. S. Shuman and T. F. Gallagher, “Ionic dipole and quadrupole matrix elements from nonadiabatic core polarization” *Phys. Rev. A* 74, 022502 (2006).

# Strongly-Interacting Quantum Gases

**Principal Investigator: Murray Holland**

murray.holland@colorado.edu

*440 UCB, JILA, University of Colorado, Boulder, CO 80309-0440*

## Program Scope

Dilute atomic gases have proved to be a fascinating system in which to study a variety of many-body phenomena. One of the primary goals at this time is to investigate the regime of strong interactions between the atoms. This topic contacts a diverse range of important quantum phenomena in many fields of physics. A strongly-correlated regime can be achieved either by increasing directly the effect of the interatomic interactions, or by decreasing, in a relative manner, the single-particle energies to allow the interaction effects to dominate.

In our program of research, we have been pursuing the development of an effective quantum field theory which describes superfluidity in dilute atomic gases in the presence of strong interactions. Some time ago, we produced a theoretical proposal pointing out the potential in dilute atomic gases to explore the crossover physics between Bose-Einstein condensation (BEC) and Bardeen-Cooper-Schrieffer (BCS) superfluidity. This has recently developed into a very active field of study in terms of both experiments and theory.

Our program encompasses this topic, along with other research directions which explore the role of strong many-body correlations. New research areas have been developed over the past few years and include atomtronics—an atom analogue of semiconductor devices—and ultracold atoms in rotating optical lattices. These systems share the common feature of the need to treat the interactions in a nonperturbative manner. They form interesting and controllable quantum systems for the development of many theoretical techniques originally introduced in the context of condensed matter physics.

## Ultracold bosons in rotating optical lattices

Recent observations of vortex lattices in rotating quantum gases have demonstrated in a dramatic way the superfluid properties of the Bose-Einstein condensate. As the rotation rate is increased, it is anticipated that the lattice should melt to form a vortex liquid, and the effect of quantum fluctuations and interactions should eventually allow the emergence of novel quantum states. Perhaps the most well known of these—the Laughlin wave function believed to be at the heart of the fractional quantum Hall

effect—should form near the critical rotation frequency for dynamic stability.

Although these effects are expected, the quantum Hall physics has never been observed in dilute quantum gases. The primary reason for this is technical in nature but also extremely difficult to avoid, since the parameter regime requires a combination of small numbers of atoms, at very low temperature, and with rapid rotation. This combination reduces the effect of single particle energies by bringing the quantum states corresponding to the lowest Landau level into degeneracy, and causing the residual interactions to completely dominate the form of the ground state wave function.

A potential way to overcome these practical difficulties is to use a rotating optical lattice as we recently showed (R. Bhat *et al.* 2006). We examined square two-dimensional systems at zero temperature comprised of strongly repulsive bosons with filling factors of less than one atom per lattice site. The entry of vortices into the system was characterized by jumps of  $2\pi$  in the phase winding of the condensate wave function. A lattice of size  $L \times L$  can have at most  $L - 1$  quantized vortices in the lowest Bloch band. In contrast to homogeneous systems, angular momentum is not a good quantum number since the continuous rotational symmetry is broken by the lattice. Instead, a quasi-angular momentum captures the discrete rotational symmetry of the system. Energy level crossings indicative of quantum phase transitions were observed when the quasi-angular momentum of the ground-state changed.

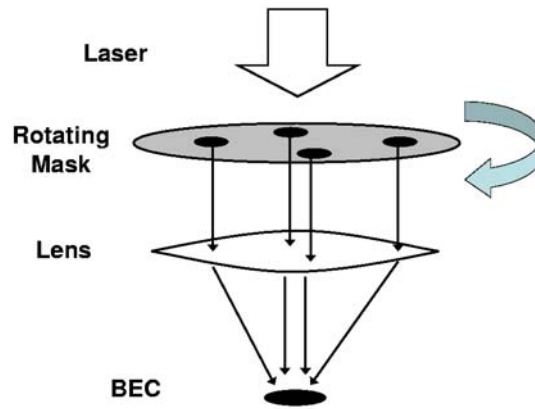


**Figure 1.** One way of making a rotating optical lattice (taken from the experimental group of E. Cornell). A laser beam passes through a rotating mask. A lens focuses the resulting lattice beam profile onto a stationary, trapped BEC. The lattice potential is imprinted via off-resonant interactions between the laser and the atoms.

## Atomtronics

The ubiquity of solid state electronic devices raises the question; to what degree can one do with atoms what one does with electrons in semiconductor devices? The versatility

of cold gases motivates taking this step from electronics to atomtronics.

The theoretical design and simulation of the atom analogue of semiconductor diodes and transistors was our first project aimed at establishing a conceptual framework for atomtronics (B.T. Seaman *et al.* preprint 2006). Our goal was to develop a macroscopic device which did not rely on single atom coherence, in direct analogy with the electronic situation which does not rely on electron coherence. More specifically, we used our knowledge of the superfluid and insulating phases of a Bose gas in a lattice to put together the ingredients needed for setting up diode configurations. We were able to simulate basic semiconductor device elements, including; batteries voltages and currents, the p-n junction, the diode, the field-effect transistor, and the bipolar transistor.

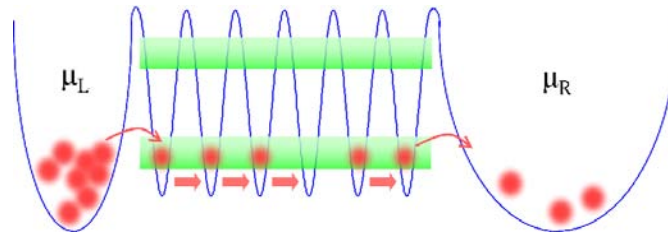


**Figure 1.** Schematic of atoms in a lattice connected to an atomtronic battery. A voltage is applied by connecting the system to two reservoirs, one of higher (left) and one of lower chemical potential (right). An excess (deficit) of atoms is generated in the left (right) part of the system respectively giving rise to a current from left to right. Different materials such as metals, insulators, n-type doped conductors, and p-type doped conductors, are made by the application of external potential fields to the optical lattice.

## Resonant superfluid crossover from BCS to BEC

We have continued our research into the description of resonances in ultracold quantum gases. Our aim is to develop the theory of Feshbach resonances as it applies to both broad and narrow resonances in a many-body quantum system. It is difficult to achieve the correct equation of state in the crossover from single to composite objects (for example the BCS to BEC crossover) in any mean-field theory. We are developing a discrete version of the quantum kinetic theory of the crossover, and this is applicable to resonance interactions of atoms in strongly confining optical lattices.

## Future work

In future work, we plan to examine the description of correlations beyond the pair form included in the superfluid description of Bardeen-Cooper-Schrieffer. These atom-molecule correlations are necessary in order to realize the correct mean-field potential on the Bose-Einstein condensation side of the crossover. The theory which has been

developed to date is almost entirely for the simplest cases of uniform systems, with no rotation and time-independent potentials, and a major goal is to relax these restrictions in future work.

### Publications in peer-reviewed journals on DOE supported research

- [1] M.L. Chiofalo, S. Giorgini, and M. Holland *Released momentum distribution of a Fermi gas in the BCS-BEC crossover*, accepted for Physical Review Letters (2006).
- [2] Rajiv Bhat, M. J. Holland, and L. D. Carr, *Bose-Einstein Condensates in Rotating Lattices*, Phys. Rev. Lett. **96**, 060405 (2006).
- [3] L. D. Carr, M. J. Holland, B. A. Malomed, *Macroscopic quantum tunneling of Bose-Einstein condensates in a finite potential well*, J. Phys. B: At. Mol. Opt. Phys. in press (2005).
- [4] C. A. Regal, M. Greiner, S. Giorgini, M. Holland, and D. S. Jin *Momentum distribution of a Fermi gas of atoms in the BCS-BEC crossover*, Phys. Rev. Lett. **95**, 250404 (2005).
- [5] B. T. Seaman, L. D. Carr, and M. J. Holland *Period doubling, two-color lattices, and the growth of swallowtails in Bose-Einstein condensates*, Phys. Rev. A **72**, 033602 (2005).
- [6] L. D. Carr and M. J. Holland *Quantum phase transitions in the Fermi-Bose Hubbard model*, Phys. Rev. A **72**, 033602 (2005).
- [7] B. T. Seaman, L. D. Carr, M. J. Holland *Nonlinear Band Structure in Bose Einstein Condensates: The Nonlinear Schrödinger Equation with a Kronig-Penney Potential*, Phys. Rev. A **71**, 033622 (2005).
- [8] B. T. Seaman, L. D. Carr, M. J. Holland *Effect of a potential step or impurity on the Bose-Einstein condensate mean field*, Phys. Rev. A **71**, 033609 (2005).
- [9] M. Holland *Atomic Beads on Strings of Light*, News and Views section, Nature **429**, 251 (2004).
- [10] L. D. Carr, R. Chiamonte, and M. J. Holland *End-point thermodynamics of an atomic Fermi gas subject to a Feshbach resonance*, Phys. Rev. A **70**, 043609 (2004).
- [11] Jelena Stajic, J. N. Milstein, Qijin Chen, M. L. Chiofalo, M. J. Holland, and K. Levin *Nature of superfluidity in ultracold Fermi gases near Feshbach resonances*, Phys. Rev. A **69**, 063610 (2004).
- [12] L. D. Carr and J. Brand *Pulsed atomic soliton laser*, Phys. Rev. A **70**, 033607 (2004).
- [13] S. G. Bhongale, J. N. Milstein, and M. J. Holland *Resonant formation of strongly correlated paired states in rotating Bose gases*, Phys. Rev. A **69**, 053603 (2004).
- [14] L.D. Carr and J. Brand *Spontaneous soliton formation and modulational instability in Bose-Einstein condensates*, Phys. Rev. Lett. **92**, 040401 (2004).
- [15] J. N. Milstein, C. Menotti, M. J. Holland *Feshbach resonances and collapsing Bose-Einstein condensates*, New Journal of Physics, Focus Issue on Quantum Gases **5**, 52 (2003).

## Using Intense Short Laser Pulses to Manipulate and View Molecular Dynamics

Robert R. Jones, Physics Department, University of Virginia,  
382 McCormick Road, P.O. Box 400714, Charlottesville, VA 22904-4714  
[rrj3c@virginia.edu](mailto:rrj3c@virginia.edu)

### I. Program Scope

This project focuses on the exploration and control of non-perturbative laser/molecule interactions. Intense non-resonant laser pulses can radically affect molecules, both in internal and external degrees of freedom. The energy and angular distributions of electrons, ions, and/or photons that are emitted from irradiated molecules contain a wealth of information regarding the molecular structure and dynamics in the field. However, a molecule's alignment with respect to the laser polarization axis is often a critical parameter in determining the effect of the field, and information encoded in photo-fragment distributions may only be interpretable if the molecular axis has a well-defined direction in the laboratory frame. Therefore, the random orientation of molecules in a gaseous sample poses a significant obstacle to understanding and manipulating strong-field molecular dynamics. Accordingly, we prepare aligned and/or oriented molecular targets for use in subsequent measurements.

### II. Recent Progress

We use intense short laser pulses to transiently align diatomic molecules for strong field ionization, dissociation, and high harmonic generation experiments. In the experiments, an alignment pulse (or pulses) drives a sequence of Raman transitions within each molecule, producing a rotational wavepacket whose evolution is characterized by periodic molecular alignment [1,2]. After a time-delay, the molecules are exposed to a second, more intense "signal" laser pulse, resulting in molecular ionization, fragmentation, and/or the emission of high harmonics. By selecting the appropriate time-delay and/or polarization angle between the alignment and signal lasers, we can systematically explore the efficiency of these strong-field processes as a function of the angle between the signal laser polarization and the molecular axis. In practice, the non-zero rotational temperature of the molecular sample, and the restriction on the maximum alignment laser intensity set by the molecular ionization threshold, limits the achievable degree of alignment. Thus, we work with preferentially, not perfectly, aligned ensembles.

During the past year, we have continued to explore (A) HHG from preferentially aligned room temperature diatomic molecules; (B) optimization of transient alignment of room temperature diatomic molecules using shaped laser pulses; and (C) two different methods for achieving field-free transient orientation of heteronuclear diatomics.

#### *A. High Harmonic Generation from Transiently Aligned Molecules in a Hollow-Core Fiber*

The HHG spectrum from a laser irradiated molecule depends on the molecule's electronic structure and on the spatial distribution of its nuclei. This dependence can be exploited i) to control HHG via intense laser manipulation of molecular structure; or conversely, ii) to probe molecular structure and dynamics with sub-Angstrom spatial and femtosecond temporal resolution [3-5]. The use of aligned rather than randomly oriented molecules is critical for both control and dynamical probe applications. HHG from aligned molecules is being explored in several labs[5,6], but to the best of our knowledge, ours is the only group utilizing a hollow-core waveguide [7] rather than a gas jet source for such studies. As noted below, there are a number of complications associated with the waveguide source, however, there are potential benefits as well. For example, quasi-phase matching of harmonics might be achieved by counter-propagating alignment and signal beams through the hollow fiber.

Generally, for room temperature  $N_2$ , we find that significantly higher harmonic emission (up to 2.5x) is observed from molecules preferentially aligned parallel rather than perpendicular to the intense laser field. In principle, this variation could be due to: i) the ionization rate anisotropy for molecules aligned parallel vs. perpendicular to the laser field [8]; ii) the anisotropy in the probability that a tunnel ionized electron will recollide with its parent ion; iii) the anisotropy in the probability that a recolliding electron will recombine with its parent ion and emit a high energy photon; and/or iv) a macroscopic effect associated with phase-matching or birefringence in the anisotropic molecular medium. We have performed additional measurements which allow us to rule out the first two of these possibilities. First, our characterization (via Coulomb explosion imaging) of the degree of room temperature alignment achieved in  $N_2$  with our laser pulses, coupled with previous measurements of the ionization rate anisotropy for  $N_2$  [8], indicate that the ionization probability in our waveguide is only a few percent larger for preferential alignment parallel as opposed to perpendicular to the drive laser polarization. Second, we have measured the HHG yield using an elliptically rather than linearly polarized drive laser, enabling us to translate the recolliding electron relative to the transverse location of the parent ion [4,5]. We find that the weak alignment of our sample has essentially no effect on the recollision probability. Thus, in the absence of phase-matching effects, the large alignment dependence of the harmonic yields can be attributed to the anisotropic recombination cross-section of the returning electron. Interestingly, we find that phase-matching can have a dramatic dependence on the alignment dependence of the harmonic yield. By slightly changing the spatial coupling of the alignment and signal beams into the fiber, we have observed a reversal of the signal enhancement in some harmonics, but not others. This reversal is pressure dependent and results in maximum harmonic signal for perpendicular rather than parallel alignment, precisely the opposite of the single molecule response. The precise origin of this effect is not completely understood. A manuscript detailing our observations is ready for submission to PRA.

Beyond spectral intensity variations, the harmonics emitted from molecules need not be linearly polarized along the drive laser field [9]. Instead, the polarization direction and ellipticity may show a pronounced variation as a function of harmonic order and the angle between the molecular axis and the fundamental laser field. Thus, aligned molecules could be used to produce coherent VUV radiation with well-defined, non-linear polarizations. Alternatively, a strong polarization dependence could be exploited as a sensitive time-resolved probe of molecular structure. We have been attempting to measure the polarization of harmonics from aligned molecules, but our experiments have been hampered by an extreme sensitivity of the HHG yield and polarization to nearly imperceptible variations in the coupling of the signal beam into the fiber and to the signal beam's polarization direction relative to the fiber. We are continuing to explore these effects.

### *B. Closed-Loop Optimization of Transient Alignment of Room Temperature Molecules*

Another focus of our program is the development of improved methods to transiently align molecular targets. In our recent CO ionization anisotropy measurements [i], we demonstrated that better alignment with reduced ionization background could be achieved by kicking molecules with two, time-delayed alignment pulses. More sophisticated pulse shapes have been suggested for improving the alignment further [10]. Accordingly, we explored the use of a laser pulse-shaper in conjunction with a genetic learning algorithm in a closed-loop optimal control scheme to search for the best laser pulse “shape” for aligning our room temperature samples at specific target times.

Interestingly, we have not found any pulse shapes that align molecules substantially better than a single, unshaped pulse. Note that technical limitations on the maximum temporal separation between pulse features prevents the algorithm from finding the well-known, “two-kicks separated

by the rotational revival period” solution mentioned above. However, we do find complex pulse shapes that cannot align molecules through purely impulsive interactions but are, nevertheless, just as effective as unshaped impulses.

In an attempt to understand the physics behind these solutions, we incorporated a genetic search algorithm into our rigid rotor code and asked it to find the most effective theoretical pulse shapes for alignment. Indeed, running under the same conditions used in the experiments, the simulation found complex laser fields that performed equivalently to transform limited pulses. More interestingly, a statistical analysis of the experimental and simulated search results shows that nearly identical linear combinations of pulse characteristics have the strongest correlation with alignment “fitness” in the two cases [11]. This comparison indicates that the simulation, with its assumption of an intensity-independent polarization anisotropy, accurately describes the experimental system even at intensities great enough to tunnel ionize the molecule. Moreover, it explicitly shows that because of the large parameter spaces explored, the direct comparison of closed-loop control experiment and simulation results is a powerful tool for evaluating the ability of the numerical code to describe the physical system. A manuscript describing these results is nearly ready for submission to PRA.

### *C) Field-Free Transient Orientation of Polar Molecules*

We are also actively exploring methods for transiently orienting polar molecules in field-free environments. Oriented molecular samples could have a number of strong-field physics applications. For example, one could measure anisotropies in tunneling ionization rates from different nuclei within a molecule. Furthermore, due to this ionization rate anisotropy, HHG from an oriented sample would presumably lead to the generation of both even and odd harmonics, providing greater flexibility for the synthesis of attosecond waveforms.

Optical-frequency laser pulses create periodically aligning, rotational wavepackets by driving Raman transitions between rotational states of the same parity ( $\Delta J = \pm 2$ ). Transient orientation of polar molecules requires the creation of a rotational wavepacket in which rotational states of both even and odd parity are coherently superimposed. We are investigating two different approaches for producing such wavepackets. First, we are attempting to use subpicosecond unipolar half-cycle pulses (HCPs) to directly drive  $\Delta J = \pm 1$  transitions between rotational levels of opposite parity [12]. Second, we are utilizing phase-coherent excitation with 400 nm and 800 nm laser pulses to induce asymmetric  $\Delta J = \pm 1, \pm 3$  Raman transitions (e.g. absorption of one  $\sim 400$  nm photon and emission of two  $\sim 800$  nm photons) within molecules.

In the HCP experiments, we aim to orient HBr molecules in a HBr:He supersonic expansion and probe the time-dependent orientation via Coulomb explosion with a time-delayed 30 fsec laser pulse. Estimates from our numerical simulations indicate that the molecules must be rotationally cooled to a few K if they are to be driven into an observable time-dependent orientation by HCPs with peak fields  $\sim 100$  kV/cm (i.e. the maximum HCP field produced to date using large aperture photoconductive emitters). We recently installed a Rydberg atom beam in the experimental chamber and, using HCP ionization for calibration, have confirmed that HCP fields  $> 50$  kV/cm are being produced in the laser/atom interaction region. We are now using transient laser alignment of the molecules to confirm that they have undergone sufficient rotational cooling for the orientation experiments. Once these tests are complete we will look for HCP orientation. If we are not successful, we will examine more complex orientation schemes. For example, our numerical

simulations (and those of others [13]) indicate that significant orientation enhancements can be achieved through the use of multiple, time-delayed HCPs or combined HCP and optical fields.

In the two-color experiments, we are working to transiently orient CO. Using phase-coherent, 800 nm + 400 nm pump pulses and a strong temporally overlapped Coulomb explosion probe, we have measured a strong phase-dependent variation in the number of multiply-charged ion fragments that explode toward/away-from the MCP detector in our ion spectrometer. However, we have yet to detect field-free molecular orientation at the rotational revival time. We now believe that the relatively weak orienting torque produced by the two-color field may be insufficient to overcome the large rotational kinetic energy of the room temperature molecules and the stronger alignment torques produced by the 800 nm and 400 nm beams individually. We are, therefore, developing a cold molecule source and plan to use a relatively weak 800 nm pulse to pre-align the cold molecules (in a plane) prior to their exposure to the two-color orienting field.

### III. Future Plans

As noted in the preceding section, we are continuing our efforts to transiently orient molecules using lasers and/or HCPs. In addition, we are developing a liquid-nitrogen-cooled, hollow-core fiber source that will enable us to measure HHG yields with counter-propagating alignment and signal beams. By cooling the fiber we should be able to better align the molecules within it. We hope to exploit the large delay-dependence of the harmonic emission, which in the counter-propagating geometry will produce a periodic variation in HHG efficiency down the fiber, to explore quasi-phase matching in the presence of substantial ionization.

### IV. Publications from Last 3 Years of DOE Sponsored Research (August 2003- August 2006)

i) D. Pinkham and R.R. Jones, "Intense Laser Ionization of Transiently Aligned CO," *Physical Review A* **72**, 023418 (2005).

ii) E. Wells, K.J. Betsch, C.W.S. Conover, M.J. DeWitt, D. Pinkham, and R.R. Jones, "Closed-Loop Control of Intense-Laser Fragmentation of S<sub>8</sub>," *Physical Review A* **72**, 063406 (2005).

iii) E. Wells, I. Ben-Itzhak, and R.R. Jones, "Ionization of Atoms by the Spatial Gradient of the Pondermotive Potential in a Focused Laser Beam," *Physical Review Letters* **93**, 23001 (2004).

### References

1. T. Seideman, *Phys. Rev. Lett.* **83**, 4971 (1999).
2. F. Rosca-Pruna and M.J.J. Vrakking, *Phys. Rev. Lett.* **87**, 163601 (2001).
3. M. Lein *et al.*, *Phys. Rev. A* **66**, 023805 (2002).
4. H. Nikura *et al.*, *Nature* **417**, 917 (2002).
5. Itatani *et al.*, *Nature* **432**, 867 (2004).
6. S. Baker *et al.*, *Science* **312**, 424 (2006).
7. A. Rundquist *et al.*, *Science* **280**, 1412 (1998).
8. I.V. Litvinyuk *et al.*, *Phys. Rev. Lett.* **90**, 233003 (2003).
9. B. Zimmerman, M. Lein, J.M. Rost, *Phys. Rev. A* **71**, 033401 (2005).
10. Leibscher, Averbukh and Rabitz, *Phys. Rev. Lett.* **90**, 213001 (2003).
11. J.L. White, B.J. Pearson, P.H. Bucksbaum, *J. Phys. B* **37**, L399 (2004).
12. M. Machholm and N.E. Henriksen, *Phys. Rev. Lett.* **87**, 193001 (2001).
13. E. Gershnel, I. Sh. Averbukh and R.J. Gordon, *Phys. Rev. A* **73**, 061401 (2006).

# Theory of threshold effects in low-energy atomic collisions

J. H. Macek

*Department of Physics and Astronomy,  
University of Tennessee, Knoxville, Tennessee and  
Oak Ridge National Laboratory, Oak Ridge, Tennessee  
email:jmacek@utk.edu*

## 1 Program scope

Threshold phenomena in ion-atom and atom-atom collisions relate to the dynamics of atoms at ultracold temperatures, of the order of a few microkelvin or even nanokelvin degrees while higher temperature processes are of more practical interest. Our projects bridge the region between ultracold temperatures and room temperatures by following features in atomic cross sections as they evolve with energy.

We have also investigated the occurrence of novel bound states, called Efimov states, in three-body neutral species. One part of our work relates these states to more readily studied effects of three-body recombination of bosons at ultra-cold temperatures. A second part of this project has investigated the possibility of forming Efimov states of fermions.

The projects listed in this abstract are sponsored by the Department of Energy, Division of Chemical Sciences, through a grant to the University of Tennessee. The research is carried out in cooperation with Oak Ridge National Laboratory under the ORNL-UT Distinguished Scientist program.

## 2 Recent progress

Calculations of elastic scattering and rearrangement collisions at energies below a few eV employ a wave representation of relative motion. Very accurate calculations of spin exchange in proton-hydrogen collisions in the  $10^{-4}$ -10 eV energy range have been made for benchmark purposes [1]. Structure in integral cross sections corresponding to conventional shape resonances and zero angle glory oscillations as well a novel type of structure, namely Regge oscillations, were identified.

These latter structures are new and were only found by us in the last two years. An important question is whether such structures are general. . To investigate this question we computed the integrated elastic scattering cross sections for protons scattering from helium, neon and argon gas atoms [2]. In all cases we find that there are Regge oscillations in the elastic scattering cross sections.

Regge oscillations are identified by separating integrated cross sections into standard semi-classical contributions and purely quantal contributions. These latter contributions  $q_m(E)$  are represented by

$$q_m(E) = \frac{2\pi}{\mu E} \text{Re} \left\{ \frac{f(\lambda_m(E))\lambda_m(E)}{1 + \exp[i2\pi\lambda_m(E)]} \right\}, \quad (1)$$

where  $\mu$  is the reduced mass,  $\lambda_m(E)$  is an energy-dependent eigenvalue formally identical to a complex value of angular momentum parameter  $\ell = \lambda - 1/2$  in the radial Schrödinger equation, and  $f(\lambda_m(E))$  is a parameter that is computed once  $\lambda_m(E)$  is found.

At half-integral values of  $\lambda_m(E)$  the denominator  $1 + \exp[i2\pi\lambda_m(E)]$  becomes infinite corresponding to a pole in  $q_m(E)$ . For positive  $E$  the values of  $\lambda_m(E)$  are complex numbers with both real and imaginary parts, thus  $q_m(E)$  maximizes near where the real part of  $\lambda_m(E)$  is half-integral. The contribution of  $q_m(E)$  to the total cross section oscillates as a function of  $E$  as  $\text{Re}[\lambda_m(E)]$  goes through successive integer values.

To verify that oscillations seen in computed integrated cross sections are due to the Regge contributions we have developed an accurate semiclassical method to compute  $\lambda_m(E)$  and  $f(\lambda_m(E))$ . For the case of proton-Helium scattering the contributions of the oscillatory terms computed directly using partial waves and the sum  $Q(E) = \sum_m q_m(E)$  over Regge trajectories are shown in Fig. (1). The two calculations agree very well showing that some oscillations in the total cross sections are indeed Regge oscillations similar to those found in proton-hydrogen atom cross sections.

To see if Regge oscillations appear for electron impact we have collaborated with the Clark-Atlanta theory group to search for Regge oscillations with Thomas-Fermi potentials. In this case we find that  $Q(E)$  is smooth therefore Regge oscillations are unlikely to occur in electron-atom integrated cross sections.

At nano-kelvin temperatures where atom-atom interactions can be characterized by scattering lengths  $a_\ell$  and effective ranges  $r_\ell$ , novel three-body

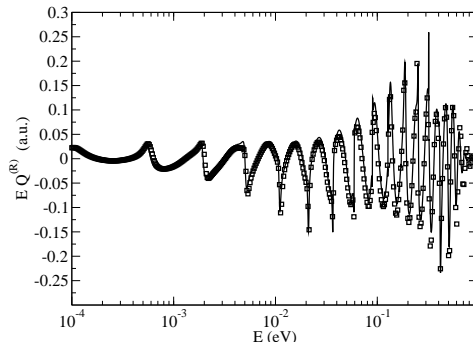


Figure 1: Comparison of  $EQ(E)$  for  $H^+ + He$  elastic scattering computed using a partial wave sum (squares) compared with the sum over Regge trajectories (solid curve).

states bound in an effective hyper-radial  $1/R^2$  potential, known as Efimov states, can form for sufficiently large  $a_0$  provided the atoms are bosons. We have shown that such states do not form for atoms that are fermions if only s-wave interactions are involved [3]. Alternatively, if p-wave interactions with large values of  $a_1$  are present, then we show that three-body Efimov states can occur for total orbital angular momentum  $L = 1$ , total spin  $S = 1/2$ , and odd parity. In this case we find that the effective three-body hyper-radial potential at large values of the hyper-radius  $R$  is given by

$$V_{\text{eff}}(R) = -\frac{t_0^2 + 1/4}{2\mu R^2} \quad (2)$$

where  $\mu$  is a mass parameter and  $R$  is the hyper-radius and  $t_0 = 0.6668$ . This effective potential has an infinite number of weakly bound states owing to the  $1/R^2$  behaviour at large distances. These are the Efimov states for fermions.

The Efimov states are related to the phase shift for the scattering of an atom  $A$  from a weakly bound diatomic molecule  $A_2$ . The phase shift varies logarithmically with the two-body scattering length  $a_0$ . In the case of bosons interacting via s-wave interactions, the hidden crossing theory shows that the three-body recombination rate oscillates with logarithmic phase that relates closely to the energies of loosely bound Efimov states. We have verified that this important conclusion holds for exact calculations [4] thus

recombination measurements provide an experimental means to investigate the Efimov effect.

### 3 Future plans

We will continue our study of the "Regge" oscillations in cross sections for atomic process and will examine Regge trajectories for Thomas-Fermi potentials applicable to electron impact and photoabsorption processes.

We will extend our study of three-particle interactions at the threshold to include both boson and fermion species. Exact recombination cross sections for fermion interactions computed using contact psuedo-potentials will be compared with approximate values based upon the hidden crossing theory. Structure in these cross sections, Stuekelburg oscillations in particular, will be examined. The relation of psuedo-potentials to realistic atom-atom interactions will also be considered.

### 4 References to DOE sponsored research that appeared in 2003-2005

1. Regge Oscillations in Integral Cross Sections for Proton Impact on Atomic Hydrogen, J. H. Macek, P. S. Krstic, and S.Yu. Ovchinnikov *Phys. Rev. Lett.* **93**, 183203 (2004).
2. Oscillations in the Integral Elastic Cross Sections for Scattering of Protons on Inert Gasses. S. Yu. Ovchinnikov, P. S. Krstic and J. H. Macek, *Phys. Rev. A* (2006) accepted for publication.
3. Properties of Pseudopotentials for Higher Partial Waves J. H. Macek and J. Sternberg, *Phys. Rev. Lett.* **97**, 023201 (2006).
4. Solution for boson-diboson elastic scattering at zero energy in the shape-independent model J. H. Macek, Serge Ovchinnikov and Gustavo Gasaneo, *Phys. Rev. A* **72**, 032709 (2005).

# Photoabsorption by Atoms and Ions

Steven T. Manson, Principal Investigator

*Department of Physics and Astronomy, Georgia State University, Atlanta, Georgia 30303*  
([smanson@gsu.edu](mailto:smanson@gsu.edu))

## ***Program Scope***

The goals of this research program are: to provide a theoretical adjunct to, and collaboration with, the various atomic and molecular experimental programs that employ third generation light sources, particularly ALS and APS; and to generally enhance our understanding of the photoabsorption process. To these ends, calculations are performed employing and enhancing cutting-edge methodologies to provide deeper insight into the physics of the experimental results; to provide guidance for future experimental investigations; and seek out new phenomenology. The general areas of programmatic focus are: manifestations of nondipole effects in atomic and molecular photoionization; photodetachment of inner and outer shells of negative ions; and photoionization of positive ions in ground and excited states. Flexibility is maintained to respond to opportunities that present themselves as well.

## ***Recent Progress***

### 1. Nondipole Effects in Atoms

Up until relatively recently, the conventional wisdom was that nondipole effects in photoionization were of importance only at photon energies of tens of keV or higher, despite indications to the contrary more than 35 years ago [1]. The last decade has seen an upsurge in experimental and theoretical results [2] showing that nondipole effects in photoelectron angular distributions could be important down to hundreds [3] and even tens [4] of eV. Our recent work included looking at the term (LS) dependence of nondipole effects in open-shell atoms [5]. Using the example of Mn, which exhibits very strong the  $3s \rightarrow 3d$  quadrupole resonances owing to the open  $3d$  subshell, very large nondipole effects were found in  $4s$  photoionization. The resulting nondipole angular distribution parameter,  $\gamma_{4s}$ , reached absolute values greater than 6 in the resonance region, making the nondipole contribution to the angular distribution at least as important as the dipole. Furthermore, the parameters differed both quantitatively and qualitatively depending upon the final state coupling of  $\text{Mn}^+ 3p^5 4s$ ,  $^7S$  or  $^5S$ . This type of difference should be exhibited in resonance regions of open-shell atoms throughout the periodic system and provide excellent cases for experimental scrutiny.

In addition, a combined calculational and laboratory investigation has provided the first experimental evidence for a quadrupole Cooper minimum, a phenomenon that had been predicted to exist much earlier [6], in studies of nondipole effects in Xe  $5s$  and  $5p$  [6]. While the evidence is much “cleaner” for the  $5s$  case, the  $5p$  case shows how much can be learned by a careful analysis of a combined theoretical and experimental investigation.

### 2. Photodetachment of Negative Ions

Negative ion photodetachment serves as a “laboratory” for the study of electron-electron correlation since many-electron interactions generally dominate both the

structure and dynamics of negative ions. In connection with our recent studies of inner-shell photoabsorption by  $\text{He}^-$  [8,9] and  $\text{Li}^-$  [10,11], the R-Matrix code was enhanced to deal with photodetachment—particularly the final-state wave function which was beyond the then-extant R-Matrix code. Using this experience we have moved on to the  $\text{C}^-$  ion which is of interest for a number of reasons: there was significant theoretical disagreement for the photodetachment cross section of the ground state of  $\text{C}^-$ ;  $\text{C}^-$  is one of the few negative ions to have a bound excited state; and there is experimental data on the cross section for K-shell photodetachment of  $\text{C}^-$ . Previously, we have looked at the valence photodetachment of the ground  $^4\text{S}$  state [12]. More recently, the photodetachment of the excited  $^2\text{D}$  state was considered [13]. In this calculation, which agrees well with experiment for both  $\sigma$  and  $\beta$  (unfortunately only at a single energy) a more limited previous R-Matrix calculation is corrected and the disagreements are reconciled. In addition, many examples of the Auger decay of shape resonances are found, and a detailed exposition of the photodetachment process leading to the lowest 13 states of neutral C is presented.

We have also looked at inner-shell ( $2p$ ) photodetachment of  $\text{Na}^-$ , which has been the subject of experimental investigation [14]. Our preliminary results [15] are in general agreement with the measurement except for a significant resonance that theory predicts to be a Feshbach resonance is not seen in the experiment; unfortunately the experiment could only look at the  $\text{Na}^+$  production channel. We are continuing to work on the problem to find the source of the discrepancy.

### 3. Photoionization of Positive Ions

Experimental studies of the photoionization of positive ions have seen a recent upsurge owing to the availability of facilities such as ALS and APS [16]. The study of transition metal ions is an extremely challenging problem owing to the unfilled  $3d$  subshell, which often exhibits rather different characteristics in initial and final states of the photoionization process. We have started this line of inquiry with the study of  $\text{Sc}^{++}$ , the simplest of the systems, a single  $3d$  electron outside a closed-shell Ar-like core, and a system that has been investigated experimentally [17]. Our very preliminary *ab initio* non-relativistic results, obtained using a modified R-matrix formulation, show excellent agreement with experiment, both as to the energies and the shapes of the various autoionizing structures. The key to getting agreement was that the calculation is *balanced*, i.e., that the same level of correlation is included in both initial and final states of the photoionization process; using the automatic procedure included in the R-matrix package leads to unbalanced results that are in poor agreement with experiment.

### ***Future Plans***

Fundamentally our future plans are to continue on the paths set out above. In the area of nondipole effects Hg will be investigated to try to unravel the combined effects of electron-electron correlation and relativistic interactions. In addition, the search for cases where nondipole effects are likely to be significant, as a guide for experiment, will continue. The study of the photodetachment of  $\text{C}^-$  shall move on to the photoabsorption in the vicinity of the K-shell edge of both the ground  $^4\text{S}$  and excited  $^2\text{D}$  states in order to understand how the slight excitation of the outer shell affects the inner-shell photoabsorption and to pave the way for experiment, in addition to further study of  $\text{Na}^-$ .

Finally, the study of the photoionization of the 3d transition metal ions shall continue with the introduction of relativity and the investigation of other transition metal systems, along with the continuation of our studies of the Be sequence.

***Publications Citing DOE Support Since September, 2003***

"Nondipole Effects in the Photoionization of Xe  $4d_{5/2}$  and  $4d_{3/2}$ : Evidence for Quadrupole Satellites," O. Hemmers, R. Guillemin, D. Rolles, A. Wolska, D. W. Lindle, K. T. Cheng, W. R. Johnson, H. L. Zhou and S. T. Manson, *Phys. Rev. Letters* **93**, 113001-1-4 (2004).

"Photodetachment of the Outer Shell of  $C^-$  in the Ground State," H.-L. Zhou, S. T. Manson, A. Hibbert, L. Vo Ky, N. Feautrier and J. C. Chang, *Phys. Rev. A* **70**, 022713-1-7 (2004).

"Experimental Investigation of Nondipole Effects in Photoemission at the Advanced Light Source," R. Guillemin, O. Hemmers, D. W. Lindle and S. T. Manson, *Radiation Phys. Chem.* **73** 311-327 (2005).

"Nondipole Effects in the Photoabsorption of Electrons in Two-Center Zero-Range Potentials," A. S. Baltenkov, V. K. Dolmatov, S. T. Manson and A. Z. Msezane, *J. Phys. B* **37**, 3837-3846 (2004).

"Photoionization of the Ground-State Be-Like  $B^+$  Ion Leading to the  $n=2$  and  $n=3$  States of  $B^{2+}$ ," D.-S. Kim and S. T. Manson, *J. Phys. B* **37**, 4013-4024 (2004).

"Nondipole Effects in Xe  $4d$  Photoemission," O. Hemmers, R. Guillemin, D. Rolles, A. Wolska, D. W. Lindle, K. T. Cheng, W. R. Johnson, H. L. Zhou and S. T. Manson, *J. Electron Spectrosc.* **144-147**, 51-52 (2005).

"Photoionization of the Excited  $1s^2 2s 2p^1 \ ^3P$  States of Be-like  $B^+$ ," D.-S. Kim and S. T. Manson, *Phys. Rev. A* **71**, 032701-1-12 (2005).

"Photoabsorption By Atoms and Ions," S. T. Manson, in *The Physics of Ionized Gases* in, Eds. L. Hadzievski, T. Grozdanov and N. Bibic (AIP, Melville, New York, 2004), pp. 49-58.

"Photoionization of the Ground-State Be-Like  $C^{+2}$  Ion Leading to the  $n=2$  and  $n=3$  States of  $C^{3+}$ ," D.-S. Kim and S. T. Manson, *J. Phys. B* **37**, 4707-4718 (2004).

"Gigantic Enhancement of Atomic Nondipole Effects: the  $3s \rightarrow 3d$  Resonance in Ca," V. K. Dolmatov, D. Bailey and S. T. Manson, *Phys. Rev. A* **72**, 022718-1-6 (2005).

"Photodetachment of the Outer Shell of  $C^-$  in the Excited  $^2D$  State", H.-L. Zhou, S. T. Manson, A. Hibbert, L. Vo Ky and N. Feautrier, *Phys. Rev. A* **72**, 032723-1-12 (2005).

“Theoretical and Experimental Demonstration of the Existence of Quadrupole Cooper Minima,” P. C. Deshmukh, T. Banerjee, H. R. Varma, O. Hemmers, R. Guillemin, D. Rolles, A. Wolska, S. W. Yu, D. W. Lindle, W. R. Johnson, and S. T. Manson, *Phys. Rev. Letters* (submitted).

“Strong Final-State Term-Dependence of Nondipole Photoelectron Angular Distributions from Half-Filled Shell Atoms,” V.K. Dolmatov and S. T. Manson, *Phys. Rev. A* (submitted).

### **References**

- [1] M. O. Krause, *Phys. Rev.* **177**, 151 (1969).
- [2] O. Hemmers, R. Guillemin and D. W. Lindle, *Radiation Phys. and Chem.* **70**, 123 (2004) and references therein.
- [3] O. Hemmers, R. Guillemin, E. P. Kanter, B. Kraessig, D. W. Lindle, S. H. Southworth, R. Wehlitz, J. Baker, A. Hudson, M. Lotrakul, D. Rolles, W. C. Stolte, I. C. Tran, A. Wolska, S. W. Yu, M. Ya. Amusia, K. T. Cheng, L. V. Chernysheva, W. R. Johnson and S. T. Manson, *Phys. Rev. Letters* **91**, 053002 (2003).
- [4] V. K. Dolmatov and S. T. Manson, *Phys. Rev. Letters* **83**, 939 (1999).
- [5] V. K. Dolmatov and S. T. Manson, *Phys. Rev. A* (submitted).
- [6] L. A. LaJohn and R. H. Pratt, *Radiation Phys. and Chem.* **61**, 365 (2001); **71**, 665 (2004); and references therein.
- [7] P. C. Deshmukh, T. Banerjee, H. R. Varma, O. Hemmers, R. Guillemin, D. Rolles, A. Wolska, S. W. Yu, D. W. Lindle, W. R. Johnson, and S. T. Manson, *Phys. Rev. Letters* (submitted).
- [8] H. L. Zhou, S. T. Manson, L. VoKy, A Hibbert and N. Feautrier, *Phys. Rev. A* **64**, 012714 (2001).
- [9] N. Berrah, J. Bozek, G. Turri, G. Ackerman, B. Rude, H.-L. Zhou and S. T. Manson, *Phys. Rev. Letters* **88**, 093001 (2002).
- [10] H. L. Zhou, S. T. Manson, L. VoKy, N. Feautrier and A. Hibbert, *Phys. Rev. Letters* **87**, 023001 (2001).
- [11] N. Berrah, J. D. Bozek, A. A. Wills, H.-L. Zhou, S. T. Manson, G. Akerman, B. Rude, N. D. Gibson, C. W. Walter, L. VoKy, A. Hibbert and S. Fergusson, *Phys. Rev. Letters* **87**, 253002 (2001).
- [12] H.-L. Zhou, S. T. Manson, A. Hibbert, L Vo Ky, N. Feautrier and J. C. Chang, *Phys. Rev. A* **70**, 022713 (2004).
- [13] H.-L. Zhou, S. T. Manson, A. Hibbert, L. Vo Ky and N. Feautrier, *Phys. Rev. A* **72**, 032723 (2005).
- [14] A. M. Covington, A Aguilar, V T Davis, I Alvarez, H C Bryant, C Cisneros, M Halka, D Hanstorp, G Hinojosa, A S Schlachter, J S Thompson and D J Pegg *J. Phys. B* **34**, L735 (2001); D. J. Pegg, private communication (2005).
- [15] H.-L. Zhou, S. T. Manson, A. Hibbert and T. Gorczyca, *Bull. Am. Phys. Soc.* **51(3)**, 151 (2006).
- [16] J. B. West, *J. Phys. B* **34**, R45 (2001) and references therein.
- [17] S. Schippers, A. Müller, S. Ricz, M. E. Bannister, G. H. Dunn, A. S. Schlachter, G. Hinojosa, C. Cisneros, A. Aguilar, A. M. Covington, M. F. Gharaibeh, and R. A. Phaneuf, *Phys. Rev. A* **67**, 032703 (2003).

## ELECTRON/PHOTON INTERACTIONS WITH ATOMS/IONS

Alfred Z. Msezane (email: [amsezane@cau.edu](mailto:amsezane@cau.edu))

Clark Atlanta University, Department of Physics and CTSPS  
Atlanta, Georgia 30314

### Program Scope

We develop methodologies for calculating Regge pole trajectories and residues for both singular and nonsingular potentials, important in heavy particle collisions, chemical reactions and atom-diatom systems. Methods are developed for calculating the GOS, useful in probing the intricate nature of the valence- and open-shell as well as inner-shell electron transitions. Standard codes are used to generate sophisticated wave functions for investigating CI mixing and relativistic effects in atomic ions. The wave functions are utilized in exploring correlation effects in dipole and non-dipole photoionization studies. The use of Regge trajectories to probe deeper into the near-threshold energy region of negative ions, reveals new and interesting manifestations and a better understanding of the underlying physics in this region.

### A. Complex Angular Momentum Methods and Applications to Collisions

#### A.1 QUB Collaboration, UTK TEAM, CAU TEAM

Over several years with our national/international collaborators we have been developing sophisticated methods for calculating Regge poles trajectories for both singular and non-singular scattering potentials. However, last year Macek et al. [1] presented the novel and elegant Mulholland method, implemented within the complex angular momentum (CAM) representation of scattering, to calculate integral elastic scattering cross sections and demonstrated the approach by explaining the observed oscillations in proton-H scattering. Subsequently, an important collaboration was formed, viz. the above. Two papers have now been produced [2, 3].

#### Regge Oscillations in Electron-Atom Elastic Cross-Sections?

In quantum scattering, the presence of a sufficiently narrow resonance allows the collision partners to form a long-lived intermediate complex. In order to preserve the total angular momentum this complex must rotate as it decays back into its constituent parts. Rotation of the complex takes scattering into angular regions not readily accessible to a direct scattering mechanism, and alters the appearance of the differential cross section (DCS). We have considered a system trapped in such a resonance state and allow it to decay at zero scattering angle, which through the optical theorem can be related to the total cross section (TCS). Here we show that for the resonance to contribute to the TCS the following additional resonance conditions must be satisfied: (i) Several rotations of the complex (Regge trajectory, viz. imaginary part versus the real part of the complex angular momentum, stays close to the real axis) and (ii) Coherent addition of forward scattering sub-amplitudes (real part of Regge pole is close to an integer). We exploit the recent CAM approach [1] for a detailed analysis of Regge trajectories and their contributions to the DCS and the TCS in electron-atom scattering for the case of  $Z = 75$  using the model Thomas-Fermi potential [3]. We conclude with a brief discussion of the dependence of the Regge trajectories and the cross-sections upon the nuclear charge  $Z$ .

#### A.2. Regge Pole Analysis of Near-Threshold Structure in Negative Ion Cross Sections of $\text{Ag}^-$ and $\text{Cu}^-$

Generally, no physical understanding is gained through summing a partial wave series which possesses a large number of numerically significant terms. Regge poles studies are essential for understanding the behavior of the DCS's and TCS's in atomic and molecular physics and short wave length collisions. In this representation scattering DCS's can be described using usually a small number of interfering physically significant amplitudes. The Regge pole trajectories determine the essential structure of a system by yielding both the bound states and the resonances as well as the scattering amplitudes. Regge trajectories provide insight into the dynamics of scattering by breaking down the scattering process into its sub-components, manifested through the partial cross sections. These are represented in terms of the individual Regge poles.

Within the Mulholland representation of the total cross sections as implemented through the CAM formalism in the description of the proton-H integral cross sections to explain the observed low energy oscillations [1] and in the recent investigation of Regge oscillations in electron-atom scattering [2], Regge pole trajectories have been exploited, for the first time ever, and used to analyze and interpret in a simple and transparent manner the near threshold behavior of the cross sections for negative ions, including the attendant resonance structure [4]. The results for  $\text{Ag}^-$  and  $\text{Cu}^-$  are contrasted, with interesting revelations; the near-threshold behavior of  $\text{Au}^-$  agrees with the measurement [5], while that of  $\text{Cu}^-$  disagrees (We approach threshold as  $E \rightarrow +0$ ,  $E$  is the electron energy).

### A.3. Dramatic Enhancement of the Near-Threshold Cross Sections of Negative Ions $\text{Cs}^-$ and $\text{Rb}^-$

We use Regge trajectories within the Mulholland formulation of the integral elastic cross sections to probe deeper into the near-threshold energy regime of the  $\text{Cs}^-$  and  $\text{Rb}^-$  negative ions for possible new manifestations. We find dramatic enhancement of the near-threshold total elastic cross section of the negative ion  $\text{Cs}^-$ , dominated entirely by a d-wave partial cross section deep down to the near threshold region (approximately  $E = 0.03$ ). But, surprisingly much deeper, the  $L=0$  partial cross section becomes the dominant component with considerably reduced amplitude, thereby yielding an unexpected s-wave Wigner threshold behavior. This calls for both experimental and theoretical investigations and demonstrates a clear case where the bound state of  $\text{Cs}^-$  is “squeezed” out into the continuum by the potential to preserve the total angular momentum because of insufficient energy to excite the appropriate resonance level. The results for  $\text{Rb}^-$  also exhibit interesting structures near threshold, including a very narrow resonance, coming from the  $L=4$  trajectory. The Regge pole trajectories are appropriate for analyzing the structure in the total and partial elastic cross sections (Here also we approach threshold as  $E \rightarrow +0$ ,  $E$  is the electron energy).

## B. Generalized Oscillator Strengths (GOS's) for Atomic Transitions

The GOS is important in various areas, including obtaining the correct spectral assignments and optical oscillator strengths, probing the intricate nature of the valence-shell and inner-shell electron excitations and exploring the excitation dynamics.

### B.1 Generalized Oscillator Strengths for the 3d Electrons of Cs, Ba and Xe: Effects of Spin-Orbit Activated Interchannel Coupling

We have investigated for the first time ever the use of the spin-orbit interaction to probe correlation effects in the GOS of the 3d subshells of Cs, Ba and Xe, viz. we study how the GOS's of the Cs, Ba, and Xe  $3d_{3/2}$  and  $3d_{5/2}$  levels are affected by the intradoublet correlations. The calculations are carried out using the Hartree-Fock approximation and within the framework of a modified version of the spin-polarized random phase approximation with exchange, which takes into account multielectron correlation effects. The effects of relaxation of the excited electrons due to the creation of the 3d vacancy are also accounted for. Our results for Cs, Ba, and Xe, obtained for values of the momentum transfer  $q$  from 0 to 4 a.u. and energy transfer  $\omega$  from 0.1 to 8 Ry, demonstrate the strong interaction between the components of the spin-orbit doublet of the 3d electrons in Cs, Ba, and Xe. This leads to the appearance of an additional maximum in the GOS for the  $3d_{5/2}$  subshell, due to the action of the  $3d_{3/2}$  electrons. Additionally, for the dipole transition in Cs and Ba, the  $3d_{5/2}$  subshell perturbs the  $3d_{3/2}$  strongly for  $q = 4$  a.u. only, while in Xe, the perturbation is at approximately  $\omega = 58$  Ry for all considered  $q$  values. It is concluded that the intradoublet correlations are generally very important in the dipole, monopole and quadrupole transitions, but particularly in the dipole transition.

### B.2 Generalized Oscillator Strengths for Ar: Experiment and Theory Interplay

Fan and Leung [6] measured *inter alia* the lowest nondipole discrete transition in Ar, which subsequently was attributed, contrary to the experimental interpretation, to the combined monopole, the dominant component, and quadrupole contributions. Recently, the GOS's for the valence-shell excitation of Ar have been measured at 2500 eV [7]. Of great interest and accomplishment in the measurement is that the electric monopole and quadrupole excitations were measured separately and compared with our theoretical prediction [8]. While there was general agreement between the measurement and our calculation on the quadrupole excitation of the 3p-4p excitation, the experimental GOS profile for the monopole excitation exhibits, contrary to our prediction, a second maximum at a higher value of the momentum transfer squared.

Following the measurement we recalculated (this summer) the GOS's for both the monopole and quadrupole transitions and found still only one minimum as before, rather than the two found by the experiment. This calls for both experimental and theoretical examinations for resolution.

### C. US-Africa Advanced Studies Institute on Photon Interactions

The NSF and African Laser Centre (ALC) funded Advanced Studies Institute was held in Durban, South Africa, November 3-12, 2005, immediately following the World Conference on Physics and Sustainable Development, also held in Durban the preceding week, thus enabling some participants to contribute to and learn from that important meeting. It brought together from the US and Africa approximately 60 advanced graduate students and postdoctoral researchers and 20 lecturers, including 4 from Europe. The African participants came from mainly the institutions that constitute the ALC, a virtual center of excellence that links scientists and laser infrastructure in at least six African nations; it is one of the strongest combinations of human and physical infrastructure for science in Africa. The general theme of the intensive set of lectures was light-matter interactions, incorporating various fields being actively studied in the US and Africa, including Atomic, Molecular, and Optical Physics, Physical Chemistry, and Materials Science. The Institute's main aims were *inter alia* to educate, foster and enhance collaborations among the participants and expose them to the latest cutting-edge research in photon interactions; it focused the sophisticated experimental and theoretical methodologies to uncovering new and fundamental manifestations in photon interactions. The Institute was fortunate indeed to have the opening lecture "Laser Spectroscopy for Environmental and Medical Diagnostics" delivered by Professor Sue Svanberg of Lund University and Chairman of the 2005 Nobel Committee on Physics.

Here I sincerely express my gratitude to the many members of this Group, whose competitive research drove the NSF proposal and for the success of the Institute. They took time from their busy schedules and traveled many miles to South Africa to deliver outstanding lectures. The participation of postdoctoral fellows and graduate students is also greatly acknowledged. In this regard, I particularly thank Drs. H. Kapteyn and M. Murnane for recommending two of their graduate students, especially Dr. Ra'an'an Tobey, then a graduate student. He has since exhibited strong leadership, consistent with NSF's goals of developing a more globally-engaged cadre of scientific leaders, by assembling an international collaboration on the important material  $\text{VO}_2$  involving the University of Colorado, UC Berkeley, Oxford University and iThemba Labs, South Africa. He is currently at iThemba Labs to support the African Nanosciences Network, whose primary interests are in developing nanosciences to impact the lives of ordinary people through cheap health and energy.

### Continuing Investigations

We have now forged collaborations with the Oakridge/University of Tennessee group under Dr. Macek and the Queen's University of Belfast group of Dr. Sokolovski on the development and application of the CAM theory, particularly in chemical reactions and electron-atom/ion collisions. Other research activities continue, such as GOS investigations and inner-shell studies as well as probing correlations.

### References

- [1] J.H. Macek, P.S. Krstic and S. Yu. Ovchinnikov, Phys. Rev. Lett. **93**, 183203 (2004)
- [2] D. Sokolovski, Z. Felfli, S. Yu. Ovchinnikov, J.H. Macek and A.Z. Msezane, Phys. Rev. A, Submitted (2006)
- [3] Z. Felfli, L. Watkins, D. Sokolovski, S. Yu. Ovchinnikov, J.H. Macek and A.Z. Msezane, Proc. of Neural, Parallel & Scientific Computations, Eds. S.K. Aityan et. al. (Dynamic Publishers Inc, Atlanta, 2006)
- [4] Z. Felfli, L. Watkins, D. Sokolovski and A.Z. Msezane, Phys. Rev. A, Submitted (R) (2006)
- [5] R.C. Bilodeau, M. Scheer and H.K. Haugen, J. Phys. B 31, 3885 (1998)
- [6] X. W. Fan and K. T. Leung, Phys. Rev. **A62**, 062703 (2000)
- [7] L.-F. Zhu, et al., Phys. Rev. **A73**, 042703 (2006)
- [8] A. Z. Msezane, et al., Phys. Rev. **A65**, 054701(2002); M. Amusia, et al., Phys. Rev. **A67**, 022703 (2003)

**Note: Paper No.11 below was at No.10 of the TOP 25 Hottest Papers in ADNDT for Second Quarter, 2005**

### Some Publications 2004 – 2006

1. “Energy levels and Lifetimes of High Angular Momentum and High Spins Levels  $3s3p3d (^4F_1)$  in Ti X,” G. P. Gupta and A. Z. Msezane, *Physica Scripta* **70**, 235 (2004).
2. “Semiclassical Approach to Regge Poles Trajectories Calculations for Nonsingular Potentials: Thomas-Fermi Type,” S. M. Belov, N. B. Avdonina, Z. Felfli, M. Marletta, A. Z. Msezane, and S. N. Naboko, *J. Phys.* **A37**, 6943 (2004).
3. “Spin Polarization of Photoelectrons from 3d Electrons of Xe, Cs and Ba”, M. Ya. Amusia, L.V. Chernysheva, N.S. Cherepkov, Z. Felfli and A.Z. Msezane, *Phys. Rev.* **A70**, 062709 (2004)
4. “A Semiclassical CAM Theory and PADÉ Reconstruction for Resonances, Rainbows and Reaction Thresholds”, D. Sokolovski and A.Z. Msezane, *Phys. Rev.* **A70**, 032710 (2004)
5. “Confinement Resonances in Photoelectron Angular Distributions from Endohedral Atoms”, M. Ya. Amusia, A.S. Baltenkov, V.K. Dolmatov, S.T. Manson and A.Z. Msezane, *Phys. Rev.* **A70**, 023201 (2004)
6. “Generalized Oscillator Strengths for Inner – Shell Electron Transitions”, Zhifan Chen and Alfred Z. Msezane, *Phys. Rev.* **A70**, 032714 (2004)
7. “Nondipole Effects in Photoabsorption of Electrons in Two – Center Zero – Range Potentials” A.S. Baltenkov, V.K. Dolmatov, S.T. Manson and A.Z. Msezane, *J. Phys.* **B37**, 3837 (2004)
8. “Effects of Spin- Orbit Activated Interchannel Coupling on Dipole Photoelectron Angular Distribution Asymmetry Parameters ”, M. Ya. Amusia, A.S. Baltenkov, L. V. Chernysheva, Z. Felfli, S. T. Manson, and A. Z. Msezane, *J. Phys.* **B37**, 937 (2004).
9. “Superluminal Tunnelling as a Quantum Measurement Effect”, D. Sokolovski, A.Z. Msezane and V.R. Shaginyan *Phys. Rev.* **A71**, 064103 (2005)
10. “Non-dipole Effects in Spin Polarization of Photoelectrons from 3d Electrons of Xe, Cs and Ba”, M.Ya. Amusia, N.A. Cherepkov, L.V. Chernysheva, Z. Felfli and A.Z. Msezane, *J. Phys.* **B38**, 1133 (2005)
11. “Large Scale CIV3 Calculations of Fine-Structure Energy Levels, Oscillation Strengths and Lifetimes in Fe XIV and Ni XVI”, G.P. Gupta and A.Z. Msezane, *Atomic Data Nuclear Data Tables* **89**, 1 (2005)
12. “Dramatic Distortion of Xe 4d Giant Resonance by the  $C_{60}$  Fullerene Shell”, M. Ya. Amusia, A.S. Baltenkov, L.V. Chernysheva, Z. Felfli and A.Z. Msezane, *J. Phys.* **B38**, L169 (2005)
13. “Modification of the Xe 4d Giant Resonance by the  $C_{60}$  Shell in Molecular  $Xe@C_{60}$ ”, M. Ya. Amusia, A.S. Baltenkov, L.V. Chernysheva, Z. Felfli and A.Z. Msezane, *Journal of Experimental and Theoretical Physics* **102**, 53 (2006)
14. “Random Phase Approximation with Exchange for Inner-Shell Electron Transitions”, Zhifan Chen and A.Z. Msezane, *Phys. Rev.* **A72**, 050702 (R) (2005)
15. “Minima in Generalized Oscillator Strengths and the Approach to High Energy Limit”, N.B. Avdonina, D. Fursa, A.Z. Msezane and R.H. Pratt, *Phys. Rev.* **A71**, 062711 (2005)
16. “Soft X-ray Emission Lines of Fe XV in Solar Flare Observations and the Chandra Spectrum of Capella”, F.P. Keenan, J.J. Drake, S. Chung, N.S. Brickhouse, K.M. Aggarwal, A.Z. Msezane, R.S.I. Ryans and D.S. Bloomfield, *Astrophysical Journal* **449**, 1203 (2006)
17. “Oscillator Strengths and Lifetimes in Kr XXV”, G.P. Gupta and A.Z. Msezane, *Physica Scripta* **73**, 556 (2006)
18. “Photoelectron Spectra of  $N@C_{60}$  Molecule on Crystalline Si Surface”, A.S. Baltenkov, U. Becker, S.T. Manson and A.Z. Msezane, *Phys. Rev.* **B73**, 075404 (2006)
19. “Universal Cause of High-Tc Superconductivity and Anomalous Behavior of Heavy Fermion Metals”, V.R. Shaginyan, M.Ya. Amusia, A.Z. Msezane and K.G. Popov, in *New Topics in Superconductivity Research* (NOVA, Publishers, 2006) Ed. B.P. Martins pp.
20. “Soft X-ray Emission Lines of Fe XV in Spectra of the Sun and Capella”, J.J. Drake, F.P. Keenan, S. Chung, N.S. Brickhouse, K.M. Aggarwal, A.Z. Msezane, R.S.I. Ryans and D.S. Bloomfield (AIP Conference Proceeding 774 On X-Ray Diagnostics of Astrophysical Plasma) Eds. R.K. Smith, 2005, pp. 349-35.
21. “Near Threshold Behavior of Angular Anisotropy Parameters in Negative Ions Photo-Detachment”, M.Ya. Amusia, A.S. Baltenkov, L.V. Chernysheva, Z. Felfli and A.Z. Msezane, *Phys. Rev.* **A72**, 032727 (2005)
22. “Random Phase Approximation with Exchange for Inner-Shell Electron Photoionization”, Zhifan Chen and A.Z. Msezane, in *Contemporary Problems in Mathematical Physics*, Eds. J. Gavaerts, M.N. Hounkonnou and A.Z. Msezane (World Scientific, 2006) pp xxx
23. Generalized Oscillator Strengths for the 3d Electrons of Cs, Ba, and Xe: Effects of Spin-Orbit-Activated Interchannel Coupling”, M. Ya. Amusia, L.V. Chernysheva, Z. Felfli, A.Z. Msezane, *Phys. Rev.* **A73**, 062716 (2006)

# Theory and Simulations of Nonlinear X-Ray Spectroscopy of Molecules

Shaul Mukamel

*Department of Chemistry, University of California, Irvine, CA 92697-2025*

*Electronic mail: smukamel@uci.edu*

New sources of x-ray radiation such as the free-electron laser are expected to reach the level of intensity, coherence, as well as spectral and temporal resolution required for performing coherent nonlinear spectroscopic measurements. These techniques should provide a wealth of information, inaccessible in linear (x-ray absorption fine structure (EXAFS) and x-ray absorption near edge (XANES)) spectroscopy. They could directly probe the interaction between core excitations at different sites, disentangle congested spectral features by projecting the signal on multiple axes, and monitor electron dynamics in real time. Theoretical simulations are required in order to connect specific spectral features with the electronic structure, local to the absorbing atom. Simulations of these novel nonlinear multidimensional signals can assess the sensitivity and predict the information content of various techniques. Developing new pulse sequences and methodologies for the simulation of nonlinear x-ray response in many-electron systems is the major focus of this research program.

## Simulation of x-ray absorption near-edge spectra and x-ray fluorescence spectra of optically excited molecules

The accurate theoretical description of linear and nonlinear X-ray spectra requires suitable ab initio methods. Mean-field techniques such as time-dependent density-functional theory (TDDFT) or time-dependent Hartree-Fock (TDHF) are routinely used to simulate optical spectra of molecules with up to hundreds of atoms. The deep-core approximation describes the high-lying core excitations by the optical excitations of a model system with modified nuclear charges. The sum-over-state expressions for the nonlinear x-ray response can then be readily evaluated with input from standard implementations of TDDFT and TDHF. The performance of these methods and the deep-core approximation were tested in x-ray absorption and fluorescence spectra of molecules in the ground and in optically excited states. The calculated XANES spectra of optically excited methanol, benzonitrile, hydrogen sulphide and titanium tetrachloride, and the fluorescence of optically excited methanol closely reproduced the experimental spectra, surpassing the accuracy of other available (e.g. the transition potential) approaches. These results can be used to simulate ultrafast optical pump/x-ray probe experiments.

## The role of multiple core-hole coherence in X-ray four-wave-mixing spectroscopies

Nonlinear response functions and the associated multi-time correlation functions provide a compact and universal description of the nonlinear response of many-particle systems. The response of the active space of valence electrons to an instantly-switched core-hole was calculated starting with the deep-core Hamiltonian of Noziers and De Dominicis. Correlation-function expressions were derived for the coherent nonlinear response of molecules to three resonant ultrafast pulses in the x-ray regime. The ability to create two-core-hole states with controlled attosecond timing in four-wave-mixing and pump probe techniques should open up new windows into the response of valence electrons, which are not available from incoherent x-ray Raman and fluorescence. The corresponding sum-over-state expressions for the third order response were implemented using the deep-core approximation. They require the excited electronic states of the molecule with 0, 1, and 2 core-holes. Closed expressions for the

necessary four-point correlation functions were derived for the simplified electron-boson model by using the second order cumulant expansion in the fluctuating potentials. Valence excitations are treated as quasiboson oscillators, an approximation which has been successfully used to describe vibrational motions in optical electronic excitations in terms of nuclear wave packets. The information obtained from multidimensional nonlinear techniques could be used to test and refine the electron boson model, and establish an anharmonic- oscillator picture for electronic excitations. The role of the Fermi Edge Singularities in nonlinear X-ray Spectroscopy will be studied.

Simulations of all-X-ray pump-probe signals of conjugated molecules will be carried out using the sum-over-state formalism. The excited electronic states with various core-holes were obtained at the TDDFT level; an approach already successfully applied to simulate the linear absorption. The interaction between multiple core excitations should lead to off diagonal cross peaks in two-dimensional correlation plots. The effects of different features (e.g. Degree of delocalization, dipole-selection rules) of valence excitations on the signal, and the optimal pulse parameters will be the focus of future investigations

The sum-over-state approach to the nonlinear response is conceptually straightforward but computationally expensive. Its accuracy is limited by the unavoidable truncation of the excited-states manifold. An alternative approach is being developed. Unlike the sum-over-states approach, which uses the electronic transitions obtained from the linear TDDFT response, the new method employs the direct real time-integration of the nonlinear TDDFT equations of the system perturbed by the external X-ray field. As a result, the time-evolution of the reduced single electron density matrix underlying the nonlinear response is obtained directly, avoiding the calculation of excited states. An electronic wave- packet picture for the spectra will then be established. The off diagonal elements of the density matrix should reveal the electronic coherence size associated with the response.

#### Anomalous continuous-time random-walk spectral diffusion in coherent third order optical response

Recursive relations were derived for nonlinear optical response functions of a two-level chromophore undergoing stochastic frequency fluctuations described by a continuous time random walk. Stationary ensembles were constructed, and signatures of anomalous relaxation in the photon echo signal were discussed for a two –state- jump modulation with a power-law waiting time density function  $\psi(t) \sim t^{-\alpha-1}$ . Stretched-exponential decay of the photon echo signal was predicted for  $0 < \alpha < 1$  and power law asymptotics for  $1 < \alpha < 2$ . These results can be used to analyze nonlinear spectra of disordered systems, polymers and glasses.

#### Generalized TDDFT response functions for spontaneous charge-density fluctuations and nonlinear response

Time-ordered superoperators were used to develop a unified description of nonlinear density response and spontaneous fluctuations of many-electron systems. The  $p$ 'th order density response functions are decomposed into  $2^{p+1}$  non-causal *Liouville space pathways*. Individual pathways are symmetric to the interchange of their space, time, and superoperator indices and can thus be calculated as functional derivatives. Other combinations of these pathways represent spontaneous density fluctuations and the response of such fluctuations to an external field. The causality paradox of time-dependent density-functional theory (TDDFT) was naturally resolved and shown to be intimately connected with the nonretarded nature of density fluctuations.

## Coherent-control of pump-probe signals of molecular aggregates by adaptive pulse polarizations

Various schemes for the simplification of the pump-probe spectrum of excitons by pure polarization-pulse-shaping were investigated in a simulation study. The state of light is manipulated by varying the phases of two perpendicular polarization components of the pump, holding its total spectral and temporal intensity profiles fixed. Genetic and iterative Fourier transform algorithms were used to search for pulse phase functions that optimize the ratio of the signal at two frequencies. New features were extracted from the congested pump-probe spectrum of a helical pentamer by selecting a combination of Liouville- space pathways. Tensor components which dominate the optimized spectra were identified.

### Publications Resulting from the Project

1. A Mechanical Force Accompanies FRET, A. Cohen and S. Mukamel, *J. Phys. Chem. B.*, 107, 3633-3638 (2003).
2. One-dimensional Transport with Dynamic Disorder, V. Barsegov, Y. Shapir and S. Mukamel, *Phys. Rev. E.* 68, 011101 (2003).
3. Self-Consistent Density Matrix Algorithm for Electronic Structure and Excitations of Molecules and Aggregates, S. Mukamel and O. Berman, *J. Chem. Phys.*, 119, 12194-12204 (2003).
4. Conformations and photophysics of stilbene dimer" A. Ruseckas, E.B. Namdas, J.Y. Lee, S. Mukamel, S. Wang, G. Bazan and V. Sundstrom, *J. Phys. Chem. A.* 107, 8029-8034 (2003).
5. Size Scaling of Intramolecular Charge Transfer Driven Optical Properties of Substituted Polyenes and Polyyenes, J.Y. Lee, B.J. Mhin, S. Mukamel, and K. S. Kim *J. Chem. Phys.* 119(14) 7519-7524 (2003).
6. Probing Exciton Dynamics Using Raman Resonances in Femtosecond X-Ray Four Wave Mixing, S. Tanaka and S. Mukamel, *Phys. Rev. A.* 67, 033818 (2003)
7. Nonlinear Response of Classical Dynamical Systems to Short Pulses, C. Dellago and S. Mukamel, *Bull. Kor. Chem. Soc.* 24, 1097-1101 (2003)
8. Multipoint Fluorescence Quenching Time Statistics for Single Molecules with Anomalous Diffusion, V. Barsegov and S. Mukamel, *J. Phys. Chem.*, 108, 15-24 (2004)
9. Simulation of x-ray absorption near edge spectra of electronically excited ruthenium tris-2,2'-bipyridine, S. Mukamel and L. Campbell, *J. Chem. Phys.* 121(24), (2004)
10. Simulation of Optical and X-ray Sum Frequency Generation Spectroscopy of 1-dimensional Molecular Chain, S. Tanaka and S. Mukamel, *J. Electron Spectrosc. Relat. Phenom.* 136,185 (2004)
11. Ligand Effects on the X-ray Absorption of a Nickel Porphyrin Complex, L. Campbell, S. Tanaka, and S. Mukamel, *Chem. Phys.* 299, 225-231 (2004)

- 12.** Superoperator Many-body Theorey of Molecular Currents: Non-equilibrium Green Functions in Real Time, U. Harbola and S. Mukamel in Theory and Applications of Computational Chemistry: The First 40 years. (Editors) C.E. Dykstra, G. Frenking, K.S. Kim and G.E. Scuseria, 373-396, Elsevier, Amsterdam (2005).
- 13.** The Role of Water on Electron-Initiated Processes and Radical Chemistry: Issues and Scientific Advances, B.C. Garrett, et.al, Chem. Rev. 105, 355-389 (2005).
- 14.** Generalized TDDFT Response Functions for Spontaneous Density Fluctuations and Nonlinear Response: Resolving the Causality Paradox in Real Time, S. Mukamel, Phys. Rev. A 71, 024503 (2005).
- 15.** Multiple Core-Hole Coherence in X-Ray Four-Wave-Mixing-Spectroscopies, S. Mukamel, Phys. Rev. B 72, 235110 (2005)
- 16.** Simulation of XANES and X-ray Flourescence Spectra of Optically Excited Molecules, R. K. Pandey and S. Mukamel, J. Chem, Phys 124, 094106 (2006)
- 17.** Anomalous continuous-time-random-walk spectral diffusion in coherent third order optical response, F. Sanda, S. Mukamel, Phys. Rev. E 73, 011103 (2006)
- 18.** Coherent-Control of Pump-Probe Signals of Helical Structures by Adaptive Pulse Polarizations, D. Voronine, D. Abramavicius, S. Mukamel, J. Chem. Phys. 124, 034104 (2006).

## Nonlinear Photoacoustic Spectroscopies Probed by Ultrafast EUV Light

Keith A. Nelson  
Department of Chemistry  
Massachusetts Institute of Technology  
Cambridge, MA 02139  
Email: [kanelson@mit.edu](mailto:kanelson@mit.edu)

Henry C. Kapteyn  
JILA  
University of Colorado and National Institutes of Technology  
Boulder, CO 80309  
E-mail: [kapteyn@jila.colorado.edu](mailto:kapteyn@jila.colorado.edu)

Margaret M. Murnane  
JILA  
University of Colorado and National Institutes of Technology  
Boulder, CO 80309  
E-mail: [murnane@jila.colorado.edu](mailto:murnane@jila.colorado.edu)

### Program Scope

This project is aimed at direct spectroscopic access to mesoscopic (nanometer) length scales and ultrafast time scales in condensed matter, with the objective of revealing the length and time scales associated with dynamical events in condensed matter. The primary effort in the project is directed toward nonlinear time-resolved spectroscopy with coherent soft x-ray, or extreme ultraviolet (EUV), wavelengths. Time-resolved four-wave mixing, or transient grating, measurements are conducted in order to directly define an experimental length scale as the interference fringe spacing formed by two crossed excitation pulses. [1] Dynamics are recorded through measurement of time-resolved coherent scattering, or diffraction, of probe pulses from the induced grating pattern. Measurements of the dynamical responses at various transient grating fringe spacings (i.e. grating wavevectors) can provide both correlation length and time scales for the processes under study. For most complex materials, especially those in which dynamical responses span a wide range of time scales (e.g. polymer relaxation dynamics, dipole or spin glass polarization or magnetization dynamics, etc.), we know little about the correlation length scales involved or whether they are associated with the dynamical time scales. For example, it is far from clear whether the faster and slower components of polymer relaxation dynamics should be associated with motions on shorter and longer lengths scales (e.g. molecular end groups and segments or whole polymer backbones) respectively. It is tempting to imagine such an association, but the intuitive connection is challenged by the fact that nearly identical multiscale and temperature-dependent dynamics are observed in supercooled liquids composed of small molecules, aqueous solutions, and atomic ions, none of which have extended structural elements but some or all of which may still have long correlation lengths. In these and many other complex condensed matter systems, direct experimental measurements of length and time scales are needed for elucidation of the underlying mechanisms of dynamical processes.

Continued progress in high harmonic generation [2] has yielded femtosecond soft x-ray pulses with nanojoule energies and excellent spatial coherence and focusability. The possibility of intensity levels comparable to those used in much of condensed matter nonlinear spectroscopy encourages the effort to extend the spectroscopic methods to EUV wavelengths. EUV transient grating measurements will provide fringe spacings in the range of a few tens of nanometers, permitting direct assessment of condensed matter correlation lengths that are almost all in the mesoscopic range. These correlation lengths have eluded study with optical wavelengths, since the shortest transient grating fringe spacing is on the order of the wavelength.

The key experiments are aimed at generation and time-resolved detection of acoustic waves whose wavelength and orientation match those of the transient grating pattern. Optical absorption of the crossed excitation pulses gives rise to spatially periodic heating and thermal expansion which launches the acoustic response. [1] Acoustic wave characterization permits direct determination of structural relaxation time scales  $\tau$  that are a significant fraction of the acoustic oscillation period, i.e. acoustic absorption is maximized when  $\omega\tau = 1$  where  $\omega$  is the acoustic frequency. It also permits assessment of correlation length scales  $d$ , i.e. acoustic scattering increases dramatically as  $qd \gg 1$  where  $q = 2\pi/\Lambda$  is the acoustic wavevector magnitude and  $\Lambda$  the acoustic wavelength. Transient grating measurements with optical wavelengths have permitted study of acoustic waves with wavelengths in the micron range and frequencies in the MHz range. With soft x-ray wavelengths, acoustic waves with wavelengths of a few tens of nanometers and frequencies in the 100-GHz range will be reached. This will provide access to picosecond structural relaxation dynamics and nanometer structural correlation lengths in a wide range of complex materials. In polymers and other glass-forming liquids, the full range of relaxation dynamics obtained through EUV and optical experiments will permit direct determination of multiscale relaxation dynamics across a very wide range, and the connections between these and nanometer correlation lengths will be tested.

EUV probing of acoustic responses also offers important advantages relative to optical probing because the shorter wavelengths mean correspondingly greater acoustically induced phase shifts and therefore correspondingly greater sensitivity to the acoustic displacements. Demonstration of facile EUV detection of dynamical acoustic responses is a central element of the experimental program and a prerequisite to high-wavevector photoacoustic measurements.

Strong absorption of EUV wavelengths at bulk material surfaces will lead to generation of surface acoustic waves whose characterization will yield dynamic shear and longitudinal modulus properties at ultrahigh frequencies. A parallel set of experiments has been undertaken to extract a subset of this information, the longitudinal component, for some materials including those that can be deposited as thin films. In these measurements, a thin metal film is irradiated by a sequence of femtosecond optical pulses, and temporally periodic thermal expansion of the film launches an acoustic wave into and through an underlying material layer and a second metal film. The acoustic frequency is given by the repetition rate of the optical pulse sequence. The acoustic wave is detected optically upon reaching the back of the sample. This approach resembles traditional ultrasonics, with photoacoustic rather than piezoelectric transducers. It is not as generally applicable as the EUV transient grating method since it must be possible to fabricate the multilayer metal-sample-metal structure with suitable sample thicknesses, often submicron since ultrahigh-frequency acoustic waves are strongly absorbed and/or scattered by many complex materials. However, for those materials that are amenable, this approach provides a useful segue to the EUV measurements.

## Recent Progress

Significant new progress has been made in the use of light in the EUV region of the spectrum to probe acoustic dynamics. Highly coherent EUV light can be generated through high-order harmonic generation of an ultrafast light pulse. The short wavelength, femtosecond duration, and high spatial coherence of this source make it ideal for probing coherent surface acoustic waves, making it possible to probe higher frequencies and shorter scale-lengths than similar experiments using visible-wavelength light. In 2004 we demonstrated the use of EUV light to probe the dynamics of lithographically structured samples. [3] In 2004-5, we extended this technique to the use of transient-grating excitation, and applied it to the dynamics of surface acoustic waves on homogeneous thin films. [4] Using visible or near-IR light in the transient grating geometry, we generated narrowband acoustic waves that propagated along the sample surface. These waves were then probed using EUV. These experiments implemented the transient grating photoacoustic technique at very high frequencies, making it possible to extract thin-film dispersion characteristics and film thickness values in the range of a few tens of nanometers with high accuracy. The EUV transient grating configuration yields excellent signal and signal-to-noise levels, since it is >700x more sensitive than at optical wavelengths due to the fact that the acoustic surface deformation corresponds to a much larger change in phase of the reflected wave at shorter probe wavelengths.

In 2005-6, we implemented the first EUV dynamic holography setup, and used it to study the dynamics of longitudinal acoustic wave packets in thin films. [5] In this experiment, EUV light illuminates a large region of the sample surface, a small portion of which is impulsively excited by a pump beam. Light scattering from the small dynamically varying portion of the sample interferes with light reflected from the unperturbed portions of the sample, and the interference pattern forms a Gabor hologram. In a pump-probe configuration, the time dependent holographic intensity directly accesses the surface dynamics. In this configuration, we monitored acoustic wavepackets undergoing multiple reflections at a buried film/substrate interface. This experiment demonstrates phase-sensitive probing of surface deformation with femtosecond time resolution.

In parallel experiments in which a sequence of optical pulses is used for photoexcitation of high-frequency acoustic waves, earlier results showed that tunable longitudinal waves in the 40-400 GHz frequency range could be generated at one side of a sample and detected interferometrically at the opposite side after traversal through. [6,7] The time of flight and signal strength yield the acoustic speed and attenuation rate respectively. In the last year a comprehensive study of acoustic attenuation in amorphous silica, a prototype disordered solid, was conducted. Frequencies up to 300 GHz, corresponding to acoustic wavelengths as short as 20 nm, were used. The results indicate that the attenuation, which is proportional approximately to the square of the acoustic wavevector, is due primarily to intrinsic structural disorder. Weaker contributions due to temperature-dependent activated processes also may be discerned.

During the past year the measurements have been extended to supercooled liquids, in which important high-frequency density relaxation dynamics have only been probed indirectly through measurement of dielectric relaxation or molecular orientation dynamics. We have observed acoustic waves at frequencies up to 50 GHz after traversal through glycerol and other liquids. These experiments are still under way, but it is clear

that fast structural relaxation dynamics may now be monitored directly. Liquid samples of submicron thickness should permit observation of acoustic waves with frequencies over 100 GHz, completely covering the fast relaxation dynamics of interest in many cases.

### Future Plans

In 2006, we plan to extend the current experiments in a variety of directions. We can use EUV radiation to excite dynamics in materials, to probe smaller scale lengths. We also plan to extend the dynamic holographic imaging to measure thermal transport phenomena in structured samples where the length scales are less than the phonon mean free path.

Using multiple-pulse optical excitation of tunable acoustic waves, a thorough frequency and temperature dependent study of supercooled liquid dynamics is planned. This work can extend up to the 100-200 GHz frequency range and down to several GHz. Using complementary methods, we can examine the response in roughly the 30 MHz – 3 GHz range. Work is under way to conduct measurements over this entire range in supercooled liquids at variable temperatures, permitting critical testing of theoretical predictions of relationships between fast and slow relaxation dynamics.

### References

1. “Impulsive stimulated light scattering from glass-forming liquids: I. Generalized hydrodynamics approach; II. Salol relaxation dynamics, nonergodicity parameter, and testing of mode coupling theory,” Y. Yang and K.A. Nelson, *J. Chem. Phys.* **103**, 7722-7731; 7732-7739 (1995).
2. “Phase-matched generation of coherent soft-x-rays,” A. Rundquist, C. Durfee, Z. Chang, S. Backus, C. Herne, M. M. Murnane and H. C. Kapteyn, *Science* **280**, 1412 – 1415 (1998).
3. “Nanoscale photothermal and photoacoustic transients probed with extreme ultraviolet radiation,” R.I. Tobey, E.H. Gershgoren, M.E. Siemens, M.M. Murnane, H.C. Kapteyn, T. Feurer, and K.A. Nelson, *Appl. Phys. Lett.* **85**, 564-566 (2004).
4. “Transient grating measurement of surface acoustic waves in thin metal films with extreme ultraviolet radiation,” R.I. Tobey, M.E. Siemens, M.M. Murnane, H.C. Kapteyn, D.H. Torchinsky and K.A. Nelson, *Appl. Phys. Lett.*, accepted for publication, 2006.
5. M.E. Siemens, R.I. Tobey, O. Cohen, M. M. Murnane, H. C. Kapteyn, and K.A. Nelson, “Ultrafast extreme ultraviolet holography: Dynamic monitoring of surface deformation“, to be submitted to *Optics Letters* (2006).
6. “Generation of ultrahigh frequency tunable acoustic waves,” J. D. Choi, T. Feurer, M. Yamaguchi, B. Paxton, and K. A. Nelson, *Appl. Phys. Lett.*, **87**, 081907 (2005).
7. “Ultrahigh frequency acoustic phonon generation and spectroscopy with Deathstar pulse shaping,” J.D. Beers, M. Yamaguchi, T. Feurer, B. Paxton, and K.A. Nelson, *Ultrafast Phenomena XIV*, S. DeSilvestri, T. Kobayashi, T. Kobayashi, K.A. Nelson, and T. Okada, eds. (Springer-Verlag, Berlin 2005), pp. 236-238.

# Single Molecule Fluorescence in Inhomogeneous Environments

Lukas Novotny (*novotny@optics.rochester.edu*)

*University of Rochester, Institute of Optics, Rochester, NY, 14627.*

## 1 Program Scope

In this project we study antenna-coupled light emission and absorption. We use a single molecule as an elementary light emitting device. In the weak-coupling regime, the interaction with the antenna influences the molecule's fluorescence rate and its excited-state lifetime. Our goal is to control these interactions using carefully designed metal nanostructures acting as optical antennas. Antenna mediated interactions open up the opportunity to observe and study new selection rules originating from the highly confined interaction. A quantitative understanding of single molecule fluorescence in inhomogeneous environments is important for the development of nanoscale sensors and biomolecular assays, for the developing field of nanoplasmonics, and for the emerging concept of optical antennas employed in surface enhanced spectroscopy and microscopy.

## 2 Recent Progress

In the past project period we studied the fluorescence rate of a single molecule as a function of its distance to a laser-irradiated gold nanoparticle. The local field enhancement leads to an increased excitation rate whereas nonradiative energy transfer to the particle leads to a decrease of the quantum yield (quenching). Because of these competing effects previous experiments showed either fluorescence enhancement or fluorescence quenching. By varying the distance between molecule and particle we showed the first experimental measurement demonstrating the continuous transition from fluorescence enhancement to fluorescence quenching. This transition cannot be explained by treating the particle as a polarizable sphere in the dipole approximation. The choice of a simple gold nanoparticle allowed us to quantitatively compare the experimental data with theoretical calculations. We achieved almost perfect agreement without using any adjustable parameters.

In order to formulate the problem we consider a single molecule located at  $\mathbf{r}_m$  that is represented by a two-level system with transition dipole moment  $\mathbf{p}$  and transition frequency  $\omega$ . For weak excitation (no saturation) the fluorescence rate  $\gamma_{em}$  is a two-step process which involves the excitation rate  $\gamma_{exc}$  and the emission probability represented by the apparent quantum yield  $q_a = \gamma_r/\gamma$ , with  $\gamma_r$  and  $\gamma$  being the radiative decay rate and the total decay rate, respectively.  $q_a$  is simply the likelihood of a radiative transition from excited to ground state. In principle,  $\gamma_{em}$  has to be evaluated at the excitation frequency and  $q_a$  at the emission frequency. However, because we excite the molecules at the peak of their emission spectrum, a single-frequency approximation is justified. The fluorescence rate can then be written as

$$\gamma_{em}(\omega) = \gamma_{exc} \frac{\gamma_r}{\gamma} = \gamma_{exc} \left[ 1 - \frac{\gamma_{nr}/\gamma_o}{\gamma/\gamma_o} \right], \quad (1)$$

where  $\gamma_o$  is the free-space decay rate,  $\gamma_{nr} = \gamma - \gamma_r$  is the nonradiative decay rate and  $\gamma_{exc} \propto |\mathbf{p} \cdot \mathbf{E}|^2$  is the excitation rate depending on the local excitation field  $\mathbf{E}(\mathbf{r}_m, \omega)$ .

We carried out the experiment schematically shown in Fig. 1a [13]. Single molecule samples were prepared by spin coating a 1 nM solution of Nile Blue on a cleaned glass coverslip. The sample was then overcoated with a thin layer (20 nm or 2 nm) of polymethyl methacrylate (PMMA). The thickness was determined by razor-blade scratching and subsequent imaging with atomic force microscopy (AFM). Spin casting of the PMMA layer resulted in molecules with different out-of-plane dipole orientations. A microscope objective with NA=1.4 was used to focus a radially polarized laser-beam with wavelength  $\lambda = 637\text{nm}$  on the sample

surface. Confocal fluorescence rate images were acquired by raster-scanning the sample in the focal plane of the laser beam and recording the fluorescence rate for each image pixel. The fluorescence rate patterns allowed us to identify molecules with vertical dipole moments (oriented perpendicular to sample surface). A spherical gold nanoparticle with diameter  $d = 80\text{nm}$  was attached to the end of a pointed optical fiber as shown by the SEM image in the inset of Fig. 1a. The supporting fiber was attached to a tuning-fork crystal whose resonance frequency was used in a feedback loop to maintain a constant distance  $z$ . Finally, the attached gold particle was positioned into the center of the laser focus by maximizing the backscattered light from the gold particle. Near-field fluorescence images were obtained by raster-scanning the sample while maintaining a constant particle-sample separation. Distance curves of the fluorescence rate were recorded by positioning the gold particle over a previously determined, vertically-oriented molecule and recording the emission rate as a function of particle-sample distance. Fig. 1b shows the calculated field distribution resulting from a classically emitting molecule located 2 nm underneath the surface and faced by a 80 nm gold particle.

Fig. 2a shows the fluorescence rate of a vertically oriented molecule as a function of particle-sample distance  $z$ . Experimental data (dots) are shown together with the theoretical curve derived from MMP calculations (c.f. Fig. 1b). No adjustable parameters are used in this calculation and the agreement between theory and experiment is surprisingly good. The fluorescence enhancement reaches a maximum at a distance of  $z \approx 5\text{nm}$ . For shorter distances fluorescence is quenched. In the experiments, the fluorescence background is  $\approx 4\text{ kHz}$  and originates from different sources such as gold luminescence. The background changes slightly with distance  $z$  which is likely the reason for the slight deviation between theory and experiment. Other sources of error are calibration tolerances and the fact that the molecule's orientation is not perfectly vertical. Interestingly, for distances  $z < 2\text{nm}$  the measured fluorescence rate drops more rapidly than the theoretical curve which is indicative for nonlocal effects (failure of local dielectric constants) and other surface related effects such as contamination. In Fig. 2b we show a typical fluorescence rate image of a vertically-oriented molecule acquired at  $z \approx 2\text{nm}$ . The molecule shows up as a donut pattern due to fluorescence quenching in the center of the image. As shown in Fig. 2c, the same pattern is predicted by our calculations.

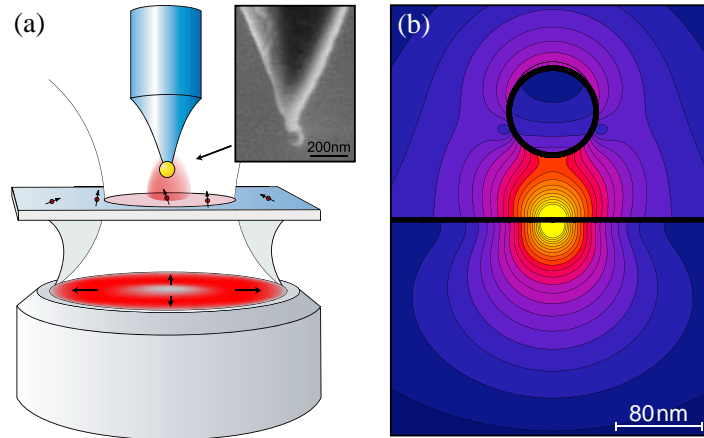


Figure 1: (a) Sketch of the experimental arrangement. See text for details. Inset: SEM image of a gold particle attached to the end of a pointed optical fiber. (b) Field distribution ( $|\mathbf{E}|^2$ , factor of 2 between successive contourlines) of an emitting dipole ( $\lambda = 650\text{nm}$ ) located 2 nm underneath the surface of a glass substrate and faced by a gold particle separated by a distance of  $z = 60\text{nm}$  from the glass surface.

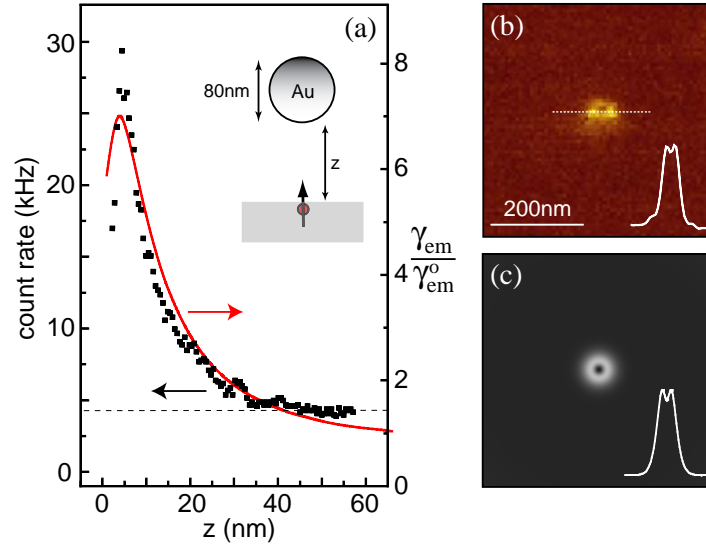


Figure 2: (a) Fluorescence rate as a function of particle-surface distance  $z$  for a vertically oriented molecule (solid curve: theory, dots: experiment). The horizontal dashed line indicates the background level. No adjustable parameters are used. (b) Fluorescence rate image of a single molecule acquired for  $z \approx 2\text{nm}$ . The dip in the center indicates fluorescence quenching. (c) Corresponding theoretical image.

### 3 Future Plans

In a next step we are planning to use gold nanorods as optical antennas because the theoretically predicted field enhancement is much stronger than the one of gold nanoparticles. We have started with the synthesis of gold nanorods. We will also study single molecules with a weaker quantum yield. For such molecules the quantum yield can be increased close to an optical antenna and hence the overall fluorescence enhancement becomes very strong. Our goal is to understand and control the different parameters involved in fluorescence enhancement. This understanding will help us to develop novel spectroscopic tools providing ultrahigh spatial resolution.

### 4 DOE sponsored publications (2003-2006)

- [1] A. Bouhelier, M. Beversluis, A. Hartschuh, and L. Novotny, "Near-field second-harmonic generation induced by local field enhancement," *Phys. Rev. Lett.* **90**, 13903 (2003).
- [2] M. R. Beversluis, A. Bouhelier, and L. Novotny, "Continuum generation from single gold nanostructures through near-field mediated intraband transitions," *Phys. Rev. B* **68**, 115433 (2003).
- [3] A. Bouhelier, M. R. Beversluis, and L. Novotny, "Characterization of nanoplasmonic structures by locally excited photoluminescence," *Appl. Phys. Lett.* **83**, 5041 (2003).
- [4] A. Bouhelier, M. R. Beversluis, and L. Novotny, "Near-field scattering of longitudinal fields," *Appl. Phys. Lett.* **82**, 4596 (2003).
- [5] A. Bouhelier, J. Renger, M. Beversluis, and L. Novotny, "Plasmon coupled tip-enhanced near-field microscopy," *J. Microsc.* **210**, 220 (2003).
- [6] A. Hartschuh, H. N. Pedrosa, L. Novotny, and T. D. Krauss, "Simultaneous fluorescence and Raman scattering from single carbon nanotubes," *Science* **301**, 1354 (2003).

- [7] A. Hartschuh, M. R. Beversluis, A. Bouhelier, and L. Novotny, "Tip-enhanced optical spectroscopy," *Phil. Trans. R. Soc. Lond. A* **362**, 807 (2004).
- [8] J. R. Zurita-Sanchez, J.-J. Greffet, and L. Novotny, "Near-field friction due to fluctuating fields," *Phys. Rev. A* **69**, 022902 (2004).
- [9] A. Bouhelier, A. Hartschuh, M. R. Beversluis, and L. Novotny, "Near-field optical microscopy in the nanosciences," in *Microscopy for Nanotechnology*, N. Yao and Z. L. Wang (eds.), Springer Verlag (2005).
- [10] A. Hartschuh, H. N. Pedrosa, J. Peterson, L. Huang, P. Anger, H. Qian, A. J. Meixner, M. Steiner, L. Novotny, and T. D. Krauss, "Single carbon nanotube optical spectroscopy," *ChemPhysChem* **6**, 1–6 (2005).
- [11] A. Hartschuh, H. Qian, A. J. Meixner, N. Anderson and L. Novotny, "Nanoscale optical imaging of excitons in single-walled carbon nanotubes," *Nano Lett.* **5**, p. 2310 (2005).
- [12] L. Novotny and S. J. Stranick, "Near-field optical microscopy and spectroscopy with pointed probes," *Ann. Rev. Phys. Chem.* **57**, 303–331 (2005).
- [13] P. Anger, P. Bharadwaj, and L. Novotny, "Enhancement and quenching of single molecule fluorescence," *Phys. Rev. Lett.* **96**, 113002 (2006).
- [14] N. Anderson, A. Bouhelier and L. Novotny, "Near-field photonics: tip-enhanced microscopy and spectroscopy on the nanoscale," *J. of Optics A: Pure & Applied Optics* **8**, S227 (2006).  
A. Hartschuh, H. Qian, A.J. Meixner, N. Anderson and L. Novotny, "Nanoscale optical imaging of single-walled carbon nanotubes," *J. Lumin.* **204**, 119-120 (2006).
- [15] L. Novotny and A. Bouhelier, "Near-field optical excitation and detection of surface plasmons," in *Surface Plasmon Nanophotonics*, M. Brongersma (ed.), Kluwer Academic Press, in press (2006).

# Electron-Driven Excitation and Dissociation of Molecules

A. E. Orel  
Department of Applied Science  
University of California, Davis  
Davis, CA 95616  
aeorel@ucdavis.edu

## Program Scope

This program will study how energy is interchanged in electron-polyatomic collisions leading to excitation and dissociation of the molecule. Modern *ab initio* techniques, both for the electron scattering and the subsequent nuclear dynamics studies, are used to accurately treat these problems. This work addresses vibrational excitation, dissociative attachment, and dissociative recombination problems in which a full multi-dimensional treatment of the nuclear dynamics is essential and where non-adiabatic effects are expected to be important.

## Recent Progress

We have carried out a number of calculations studying low-energy electron scattering from polyatomic systems, and vibrational excitation and dissociative attachment in a diatomic system. Much of this work has been done in collaboration with the AMO theory group at Lawrence Berkeley Laboratory headed by T. N. Rescigno and C. W. McCurdy. As a result of this collaboration, one of my students is working on experiments with the AMO experimental group headed by A. Belcamen. He is currently carrying out experiments on dissociative attachment of NO, a system where we have carried out calculations to support this work.

## Dynamics of Low-Energy Electron Attachment to Formic Acid

There has been recent experimental work showing that low-energy electrons (<2 eV) can fragment gas phase formic acid (HCOOH) molecules through resonant dissociative attachment processes. The principal reaction products of such collisions were found to be formate ions (HCOO<sup>-</sup>) and hydrogen atoms [1,2]. We have carried out *ab initio* calculations for elastic electron scattering from formic acid using the complex Kohn variational method. We identified the responsible negative ion state as a transient  $\pi^*$  anion with the electron temporarily trapped in the CO antibonding  $\pi$  orbital. However, the OH bond must be broken to form the formate ion. Also, since the products have A' symmetry and the resonance is A'', symmetry considerations dictate that the associated dissociation dynamics are intrinsically polyatomic. We found that the reaction follows a complicated path, first stretching both CO bonds, followed by a rotation of the hydrogen atom attached to the carbon out of plane, and then the OH bond starts to dissociate. A second anion surface, connected to the first by a conical intersection, is involved in the dynamics and the transient anion must necessarily deform to nonplanar geometries to couple to this state, before it can dissociate to the observed stable products.

The results of the calculation are described in a paper published in Physical Review Letters (Publication 6).

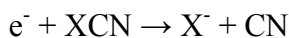
## Elastic Scattering of Low-energy Electrons by Tetrahydrofuran

We have carried out *ab initio* calculations for elastic electron scattering by tetrahydrofuran (THF) using the complex Kohn variational method. Studies of low-energy electron collisions with tetrahydrofuran (THF: C<sub>4</sub>H<sub>8</sub>O) are of particular value in gaining a better understanding of the dynamics of energy deposition in DNA, because THF can be viewed as a sugar-like component of the backbone of DNA. Absolute cross section measurements for electron collisions with gaseous THF have only recently appeared. Zecca et al. [3] reported total cross sections for positron and electron scattering from THF at energies below 21 eV and found a broad shape resonance in the total electron scattering cross section, peaked at ~7.5 eV. At the same time, Milosavljevic *et al.* [4] reported the first absolute differential cross sections for elastic scattering of electrons from THF for incident electron energies between 20 and 60 eV. To the best of our knowledge, only one previous theoretical study of low-energy electron scattering has been performed by Bouchiha and collaborators [5], which focused on the electron resonant states that may lead to dissociative electron attachment at incident electron energies of up to 10 eV using the R-matrix method. They found no shape resonances in this investigation, but reported a few core-excited resonances in the energy region spanning the first eight excited states. We carried out fixed-nuclei calculations at the equilibrium geometry of the target molecule for incident electron energies up to 20 eV. The calculated momentum transfer cross sections clearly reveal the presence of broad shape resonance behavior in the 8-10 eV energy range, in agreement with recent experiments. The calculated differential cross sections at 20 eV, which include the effects of the long-range electron-dipole interaction, are also found to be in agreement with the most recent experimental findings.

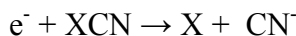
The results of the calculation are described in a paper published in Journal of Physics B (Publication 7).

## Dissociative attachment of ClCN and BrCN

We have completed our studies of the dissociative attachment of ClCN and BrCN. These systems (and the analogous pseudohalogens, such as HCN) have the interesting property that since both fragments have positive electron affinities, two fragmentation channels are open. These are:



or



where X is Cl or Br. The channel producing X<sup>-</sup> was suggested to proceed through the negative ion <sup>2</sup>Σ resonance state, formed by the addition of an electron to a σ\* antibonding orbital. The second channel, producing CN<sup>-</sup>, had been explained as a two-step mechanism. The first step is the transition to the <sup>2</sup>Π resonance, which is the addition of the electron to a π\* antibonding orbital with energy transfer from the C-N stretching mode into the dissociative X-CN mode [6].

The calculations reveal a much more complicated situation. Although the path to CN<sup>-</sup> is direct, proceeding through the lowest <sup>2</sup>Σ anion resonance, the path to Cl<sup>-</sup> proceeds through the second <sup>2</sup>Σ anion resonance. There are also two <sup>2</sup>Π resonances. The lowest

lying  $^2\Pi$  anion resonance correlates diabatically to an excited state of the negative ion fragments and does not cross the neutral. Therefore, this state can not directly lead to product. There is a second  $^2\Pi$  resonance that dissociates to  $CN^-$ . Coupling between these two resonances also allows the dissociative attachment to  $CN^-$  to occur.

We have calculated the four resonance curves, autoionization widths and couplings between the two  $^2\Pi$  resonances in all three dimensions - as a function of the X - CN internuclear distances, as a function of the C--N stretch and of the bend coordinate. For all states, as the C--N distance is increased or decreased (keeping the X - CN distance constant) the energy of the state increases, which can be fit to a Morse function. Bending reduces the symmetry from  $C_{\infty v}$  to  $C_s$ . This allows coupling between channels arising from  $\sigma^*$  and  $\pi^*$  antibonding orbitals, the  $\Sigma$  and one component of the degenerate  $\Pi$  resonance states. Such coupling will affect the cross section by allowing the  $^2\Sigma$  and the  $^2\Pi$  pathways to mix.

The Multiconfiguration Time-Dependent Hartree method (MCTDH) of the Heidelberg group [7] was used to compute the dynamics in three dimensions. Significant changes going from one (X-CN) to two dimensions (X-CN and C-N stretch) were found, but the addition of the bend caused only minor changes in the dissociative attachment cross section.

The results of the calculation are being prepared for submission to Journal of Chemical Physics (Publication 8).

## FUTURE PLANS

### Dissociative Attachment in Halogenated Molecules

There have been no theoretical systematic studies of dissociative attachment in organic molecules. There have been some such experimental studies, but these have been limited [8,9,10]. We have begun a series of calculations on mono-substituted organic compounds to look for general trends and to better understand what controls the energy flow leading to dissociation in these systems. We have chosen the systems, HCCCl, H<sub>3</sub>CCCl, H<sub>5</sub>CCCl, showing a series from triple, double to single bond respectively.

We will begin with ClCCH, chloroacetylene. This can be studied as a pseudo-diatomic, varying the Cl--C internuclear separation and keeping all other bond distances fixed. We can then investigate an intriguing possibility with this system. There has been some experimental evidence of dramatic effects in the DA cross section due to coupling between channels arising from  $\sigma^*$  and  $\pi^*$  antibonding orbitals [11]. Of course, for ClCCH in its linear configuration, these channels can not mix. However, mixing can occur if the molecule is bent. We are investigating this effect by carrying out the scattering for the bent structure. We are also looking at variations as other bonds are modified. This can be combined into a multi-dimensional study of the dissociation dynamics. If the dynamics are only studied in one-dimension, that is, as a function of the C-Cl bond distance, the physics of the energy transfer process is lost. The effect of the double vs. the triple C--C bond is combined with the effect of the increased symmetry in the linear HCCCl system which does not allow the  $\Sigma/\Pi$  mixing to occur. However, if the system is studied in

multiple dimensions, such that this mixing can occur, a more direct comparison is possible. This is a case where it is critical to go beyond the usual one-dimensional picture to truly understand the dissociation dynamics and energy flow within the modes of the system. We then plan to consider H<sub>3</sub>CCCl, the double-bond case and H<sub>5</sub>CCCl, the single bond case.

## REFERENCES

1. A. Pelc, W. Sailer, P. Scheier, N. J. Mason and T. D. Mark, *Eur. Phys. J. D* **20**, 411 (2002).
2. A. Pelc *et al*, *Chem. Phys. Lett*, **361**, 277 (2002).
3. A. Zecca, C. Perazzolli and M. J. Brunger, *J. Phys. B*, **38**, 2079 (2005).
4. A. R. Milosavljevic, A. Giuliani, D. Sevic, M. J. Hubin-Franskin and B. P. Marinkovic, *Eur. Phys. J. D* **35**, 411 (2005).
5. D. Bouchiha, J. D. Gorfinkiel, L. G. Caron, and L. *J. Phys. B*, **39**, 975 (2006).
6. F. Bruning, I. Hahndorf, A. Stamatovic, and E. Illenberger, *J. Phys. Chem.*, **100**, 19740 (1996), *Phys. Rev. A*, **11**, 1314 (1975).
7. M. H. Beck, A. Jackle, G. A. Worth and H. -D. Meyer, *Phys. Rep.*, 324 (2000).
8. D. M. Pearl and P. D. Burrow, *J. Chem. Phys.*, **101**, 2940 (1994).
9. K. Aflatooni and P. D. Burrow, *J. Chem. Phys.*, **113**, 1455 (2000).
10. G. A. Gallup, K. Aflatooni and P. D. Burrow, *J. Chem. Phys.*, **118**, 2562 (2003).
11. M. Allan and L. Andric, *J. Chem. Phys.*, **105**, 3559 (1996).

## PUBLICATIONS

1. *Ab initio* study of low-energy electron collisions with ethylene  
C. S. Trevisan, A. E. Orel, and T. N. Rescigno  
*Phys. Rev. A*, **68**, 062707 (2003).
2. Low-energy electron scattering of NO : *Ab initio* analysis of the <sup>3</sup>Σ<sup>-</sup>, <sup>1</sup>Δ and <sup>1</sup>Σ<sup>+</sup> shape resonances in the local complex potential model, Z. Zhang, W. Vanroose, C. W. McCurdy, A. E. Orel, and T. N. Rescigno  
*Phys. Rev. A*, **69**, 062711 (2004).
3. *Ab initio* study of low-energy electron collisions with tetrafluoroethene C<sub>2</sub>F<sub>4</sub>,  
C. S. Trevisan, A. E. Orel, and T. N. Rescigno,  
*Phys. Rev. A*, **70**, 012704 (2004).
4. A nonlocal *ab initio* model of dissociative electron attachment and vibrational excitation of NO, C. S. Trevisan, Karel Houfek, Zhiyong Zhang, A. E. Orel, C. W. McCurdy, and T. N. Rescigno, *Phys. Rev. A*, **71**, 052714 (2005).
5. Resonant electron-CF collision processes, C. S. Trevisan, A. E. Orel, and T. N. Rescigno, *Phys. Rev. A*, **72**, 627720 (2005).
6. Dynamics of Low-Energy Electron Attachment to Formic Acid, T. N. Rescigno, C. S. Trevisan and A. E. Orel, *Phys. Rev. Lett.* **96** 213201 (2006).
7. Elastic Scattering of Low-energy Electrons by Tetrahydrofuran, C. S. Trevisan, A. E. Orel and T. N. Rescigno, *J. of Phys. B* **39** L255 (2006).
8. Dissociative Attachment of ClCN and BrCN, J. Royal and A. E. Orel, to be submitted *J. Chem. Phys.*

## “Low-Energy Electron Interactions with Interfaces and Biological Targets”

Thomas M. Orlando, *School of Chemistry and Biochemistry and School of Physics,*  
*Georgia Institute of Technology, Atlanta, GA 30332-0400*

*Thomas.Orlando@chemistry.gatech.edu*

**1. Program Scope:** The primary objectives of this program are to investigate the fundamental physics and chemistry involved in low-energy (1-100 eV) electron scattering with i) water co-adsorbed with rare gas solids, ii) molecular solids such as thin-films of water, iii) complicated biologically relevant molecules such as DNA, and iv) adsorbate covered surfaces such as Cl terminated Si(111)  $7\times 7$ . The program is primarily experimental and concentrates on electron initiated damage and energy exchange in the deep valence and shallow core regions of the collision partners.

**2. Recent Progress:** This is the first year of the renewal program which began in Nov. 2005. We have focused on three main tasks:

**Project 1. Low-energy (5 –250 eV) electron stimulated desorption of cluster ions from water adsorbed on rare-gas overlayers.** This task examines the roles of hole transfer, Auger decay and intermolecular Coulomb decay (ICD) in the electron stimulated production and desorption of water cluster ions. Specifically, we have carried out studies of water adsorbed on graphite and graphite containing rare gas (Xe and Ar) spacer layers. The white peaks in Figure 1 are the cluster ion signal from 10 ML of water adsorbed on graphite. This signal is actually very small relative to the same coverage on many other substrates such as Pt(111) [1], ZrO<sub>2</sub> [2] and Si(111). However, an enormous increase in yield is found when water is adsorbed onto a few ML thick Xe overlayer pre-deposited on the graphite. Preliminary experiments also indicate that the threshold energy for forming the cluster ions is near 10 eV. This is a remarkably low energy relative to the two-hole state threshold near 22 eV but very close to the band-gap or ionization threshold of solid Xe. The low threshold energy and different intensity distribution indicates that the ESD of clusters from water adsorbed on rare gas overlayers may involve hole transfer from the substrate.

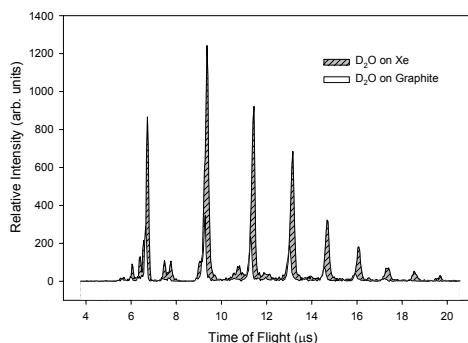


Figure 1. Cluster ion distribution observed during 100 eV pulsed electron beam bombardment of 10 ML of water on clean graphite (white peaks) and of submonolayer coverages of water on 3 ML of a Xe spacer layer adsorbed on the graphite.

The increased yields, low threshold energy and different intensity distributions are also likely due to differences of wetting behavior, the geometric structure of the adsorbed water/clusters as well as the electronic structure and hole transfer probabilities at the surface and interface. The rare gases will allow us to examine the differences between

isolated molecules (low coverage), clusters (medium coverage) and “solids” (high coverage).

**Project 2. A theoretical and description and experimental demonstration of diffraction in electron stimulated desorption (DESD).** Diffraction in electron-stimulated desorption has revealed a propensity for  $\text{Cl}^+$  desorption from rest atom vs. adatom areas and unfaulted vs. faulted zones of Cl terminated Si(111)-(7×7) surfaces. We associate the  $15 \text{ eV} \pm 1 \text{ eV}$  threshold with ionization of Si-Cl  $\sigma$ -bonding surface states and formation of screened 2-hole states with Si 3s character. Similar specificity is observed from A and B reconstructions. This can be due to reduced screening in unfaulted regions and increased hole localization in Si back-bonds within faulted regions. This has been published in D. Oh, M. T. Sieger and T. M. Orlando, “Zone specificity in the low-energy electron stimulated desorption of  $\text{Cl}^+$  from reconstructed Si(111)-7×7 surfaces” *Surf. Sci. Lett.* (2006).

**Project 3. Low-energy electron-induced damage of DNA: Neutral fragments yields.** A unique aspect of our program is the application of sensitive resonance enhanced multiphoton ionization (REMPI) detection of the desorbing neutral molecular and atomic fragments in combination with in situ Fourier Transform Infrared Reflection (FTIR) and ex-situ gel electrophoresis analysis of the remaining products. A diagram of an apparatus we have built and tested is shown below. This UHV system is equipped with a vacuum ultraviolet (VUV) laser source for single photon ionization of the primary neutral desorption products. The coherent VUV photons are generated by non-linear, third harmonic generation in rare gas (either Kr, Xe or Ar) expansions. When using Xe and 355 nm excitation, direct ionization using 118 nm light only or 118 nm + 355 nm can be employed. The latter increases sensitivity but also leads to greater fragmentation. The right hand frame in Figure 2 is data obtained using VUV detection of the neutrals during pulsed electron beam irradiation of a thin-film of DNA.

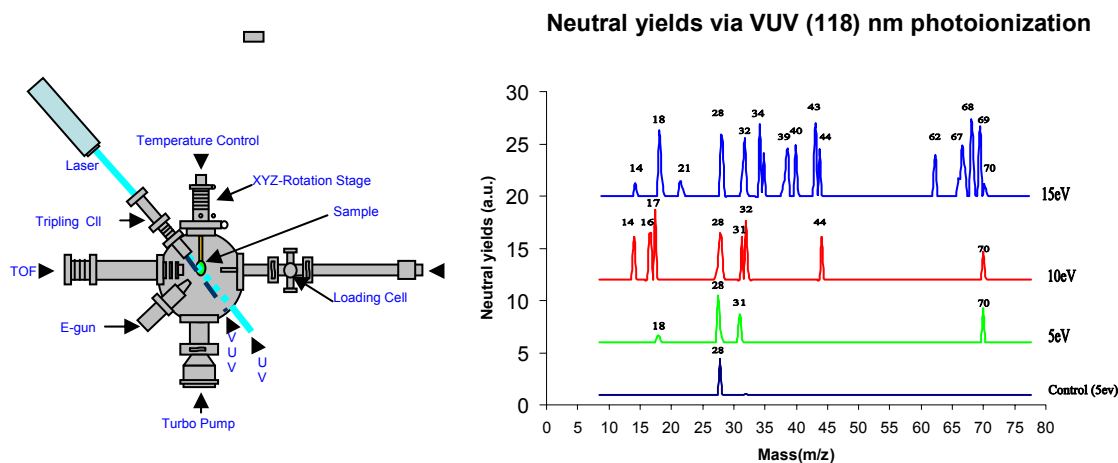


Figure 2. Schematic of the ultrahigh vacuum system constructed for studies of low-energy electron-induced damage of DNA and biologically relevant molecules. The novel aspects of this apparatus involve the Vacuum

Ultraviolet (VUV) light source, a cryogenically cooled sample chamber and a liquid dosing capability. The sample transfer stage can be retracted so that ex-situ gel electrophoresis of the DNA deposit can be carried out. The right-hand side of the Figure shows preliminary data on VUV detection of the neutral products desorbed from the surface during pulsed electron beam irradiation.

Neutral products which may correlate with the  $-HOCH_2$  terminal group on the 5' sugar end and a large base-pair fragment seem to dominate at low energies. Once the excitation exceeds the ionization threshold, multiple fragments, including sugar and base-pair fragments are observed. This is consistent with previous work which indicates DEA leads to damage of the sugar, phosphate groups and base pairs. Most studies of DEA induced damage of DNA concentrate on monitoring the negative ion desorption products [3,4]. Though these are very useful, complimentary data on the quantum-state distributions of the neutral yields will assist in the assignments of the resonances involved in DNA damage. In addition, we have modified the code used to describe DESD on single crystal surfaces, to model diffraction effects during electron scattering with DNA.

**Future Plans:** We intend to examine the physics governing the large enhancement in cluster ions from rare-gas overlayers by examining the:

- threshold energy necessary for the formation of each cluster ion
- the kinetic energy distribution of each cluster ion
- the yield dependence on rare gas identity and overlayer thickness
- the yield dependence on water coverage and presence of any isotope effect

We will also continue to emphasize experimental and theoretical studies of electron scattering with DNA and constituents of DNA.

**Publications from this program (2004-2006):**

1. T. M. Orlando, D. Oh, M. T. Sieger, and C. Lane, "Electron collisions with complex targets: diffraction effects in stimulated desorption", *Physica Scripta*, T110, 256 (2004).
2. J. Herring, A. Alexandrov, and T. M. Orlando, "The stimulated desorption of cations from pristine and acidic low-temperature ice surfaces" *Phys. Rev. Lett.* 92, 187602-1 (2004).
3. B. C. Garrett, et. al. including T. M. Orlando, "Role of Water in Electron-Initiated Processes and Radical Chemistry: Issues and Scientific Advances" *Chem. Rev.*, 105, 355 (2005).
4. J. Herring-Captain, G. A. Grieves, M. T. Sieger, A. Alexandrov, H. Chen and T. M. Orlando "Electron-stimulated desorption of  $H^+$ ,  $H_2^+$ , and  $H^+(H_2O)_n$  from nanoscale water thin-films" *Phys. Rev. B.* 72, 035431 (2005).

5. D. Oh, M. T. Sieger and T. M. Orlando, "Zone specificity in the low-energy electron stimulated desorption of Cl<sup>+</sup> from reconstructed Si(111)-7×7 surfaces" *Surf. Sci. Lett.* (in press 2006).
6. J. Herring-Captain, A. Alexandrov, and T. M. Orlando "Probing the interaction of hydrogen chloride on low-temperature water ice surfaces using electron stimulated desorption", *J. Chem. Phys.* (submitted).

**References:**

- 1.) J. Herring-Captain, G. A. Grieves, M. T. Sieger, A. Alexandrov, H. Chen and T. M. Orlando "Electron-stimulated desorption of H<sup>+</sup>, H<sub>2</sub><sup>+</sup>, and H<sup>+</sup>(H<sub>2</sub>O)<sub>n</sub> from nanoscale water thin-films," *Phys. Rev. B.* 72, 035431 (2005).
- 2.) T. M. Orlando, A. Alexandrov, and J. Herring, "Electron-stimulated Desorption of H<sup>+</sup>, H<sub>2</sub><sup>+</sup>, OH<sup>+</sup> and H<sup>+</sup>(H<sub>2</sub>O) from Water Covered Zirconia Surfaces," *J. Phys. Chem.* 118, 8898, (2003).
- 3.) B. Boudaiffa, et. al., "Resonant Formation of DNA Strand Breaks by Low-Energy (3-20 eV) Electrons," *Science*, 287, 1658 (2000).
- 4.) X. Pan, P. Cloutier, D. Hunting, and L. Sanche, "Dissociative Electron Attachment to DNA," *Phys. Rev. Lett.* 90, 208102-1 (2003).

# Photoelectron-vibrational coupling in nonlinear molecules

Erwin D. Poliakoff, Chemistry Department, Louisiana State University, Baton Rouge, LA 70803, [epoliak@lsu.edu](mailto:epoliak@lsu.edu)  
Robert R. Lucchese, Chemistry Department, Texas A&M University, College Station, TX 77843, [lucchese@mail.chem.tamu.edu](mailto:lucchese@mail.chem.tamu.edu)

## **Program scope**

Our research focuses on photoelectron scattering in the anisotropic fields of polyatomic molecules, and both theory and experiment are coordinated in this effort. Specifically, the experiments employ vibrationally resolved photoelectron spectroscopy, while theory uses Schwinger variational scattering theory and related static-exchange methods. The current emphasis is on relatively complex polyatomic systems. As the molecular architecture grows more complex, the photoelectron-molecular scattering can be manifested in rich new continuum structures that bear little resemblance to what is known for well-studied simple systems. As a result, new phenomena are likely to emerge as molecular architectures grow more complex, and the phenomena are studied with sufficient resolution to expose molecular aspects of the scattering, as can be accomplished via vibrationally-resolved photoelectron spectroscopy.

## **Recent progress**

Using high resolution photoelectron spectroscopy, we have studied how vibrational and electronic motion are coupled for a wide variety of polyatomic systems. Before this program was initiated, there were no studies which probed such coupling over a continuous range of photon energies, so these investigations are uncovering new phenomena and revealing underlying systematic behaviors that were neither understood or even anticipated. We have studied linear triatomics [ $\text{CS}_2$ ,  $\text{CO}_2$ ,  $\text{N}_2\text{O}$ ,  $\text{OCS}$ ], planar systems [ $\text{BF}_3$ ,  $\text{C}_6\text{F}_6$ , 1,3,5- $\text{C}_6\text{H}_3\text{F}_3$ , 1,4- $\text{C}_6\text{H}_4\text{F}_2$ ,  $\text{C}_2\text{Cl}_4$ ,  $\text{C}_2\text{F}_4$ , and  $\text{C}_2\text{F}_3\text{Cl}$ ], and tetrahedral molecules [ $\text{SiF}_4$  and  $\text{CF}_4$ ]. This work concentrates on polyatomics because they allow us to interrogate how resonances respond to mode-specific geometry changes. Studies of more complex molecules such as those listed requires high resolution, and this necessitated developing a supersonic molecular beam source which was compatible with the Scienta analyzer endstation at beamline 10.0.1.3 at the Advanced Light Source. The results on these polyatomics were made possible by the use of the supersonic beam assembly.

This research also relies extensively on state-of-the-art theory. In addition to calculations in support of the experimental effort, significant effort has been devoted to code development this year. In particular, we have developed a parallel version of the polyatomic photoionization code. This code has been tested for the simultaneous use of up to 32 cpus. In addition to parallelization, significant changes in the form of the partial-wave expansion have been made and the fundamental numerical procedures have been improved. This has allowed for better converged results, and will form the basis for the implementation of multichannel calculations in the near future. Calculations on the photoionization of more complex molecules have been greatly facilitated by these developments.

We use a recent example to illustrate the types of data that are obtained, as well as the insights which can be gleaned from them. Specifically, we just completed an extensive study of the energy dependence of the vibrational branching ratios in  $\text{C}_6\text{F}_6$   $b_{2u}^{-1}$  photoionization. In this study, we show that a new type of continuum photoelectron localization is manifested, and is likely to be commonplace for aromatic systems generally. Specifically, we show that the electron ejected via the  $b_{2u} \rightarrow ke_{2g}$  channel is trapped in a quasibound shape resonance state at a photon energy of 18 eV, and that the electron is localized along the C-C  $\sigma$ -backbone of the benzene ring. This new result emerges clearly from vibrationally resolved photoelectron spectroscopy measurements, and is corroborated from adiabatic static model-exchange scattering (ASME) calculations that treat the continuum photoelectron in a physically reasonable and computationally tractable framework. There are important differences between the current investigation and all previous studies. First, there are many more vibrational degrees of freedom that can and have been probed for hexafluorobenzene than in the previously studied systems, thereby enabling a very unambiguous picture of the photoelectron scattering dynamics in the molecular framework. Figure 1 shows photoelectron spectra for  $\text{C}_6\text{F}_6^+(\text{C}^2\text{B}_{2u})$  at two selected photon energies. It is obvious that there are significant differences in the relative intensities. In order to understand the underlying physics, it is instructive to map the vibrational branching ratios as a function of energy.

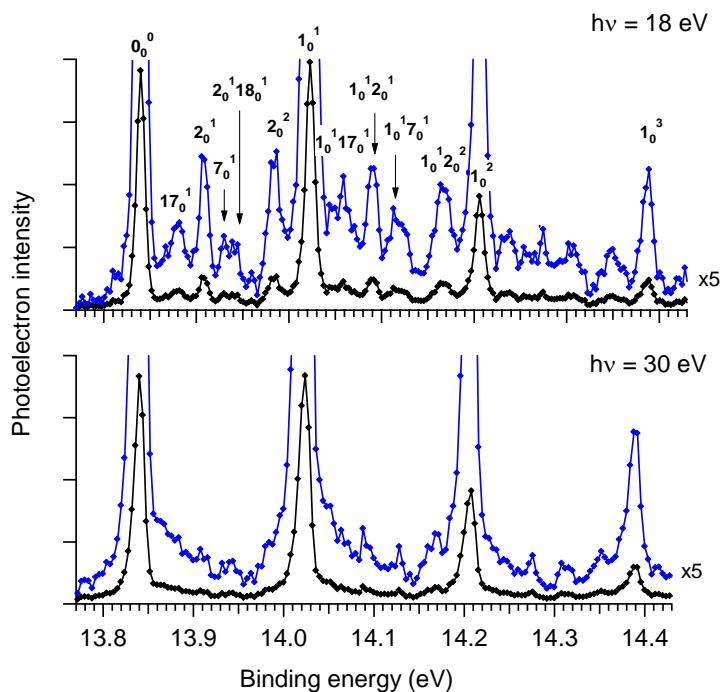


**Figure 1.** Vibrationally resolved photoelectron spectra for  $C_6F_6^+(C^2B_{2u})$  at two photon energies. Note the large number of vibrational levels enhanced in the 18 eV spectrum in the top frame. At this energy, there is a  $b_{2u} \rightarrow ke_{2g}$  shape resonance, which exhibits the new and unanticipated behavior.

Vibrational branching ratios are obtained by measuring the relative intensities of the various vibrational excitations of interest relative to the ground vibrational levels. Figure 2 shows vibrational branching ratio curves for modes 1, 2, and 17; pictorial representations of the vibrations are also displayed.

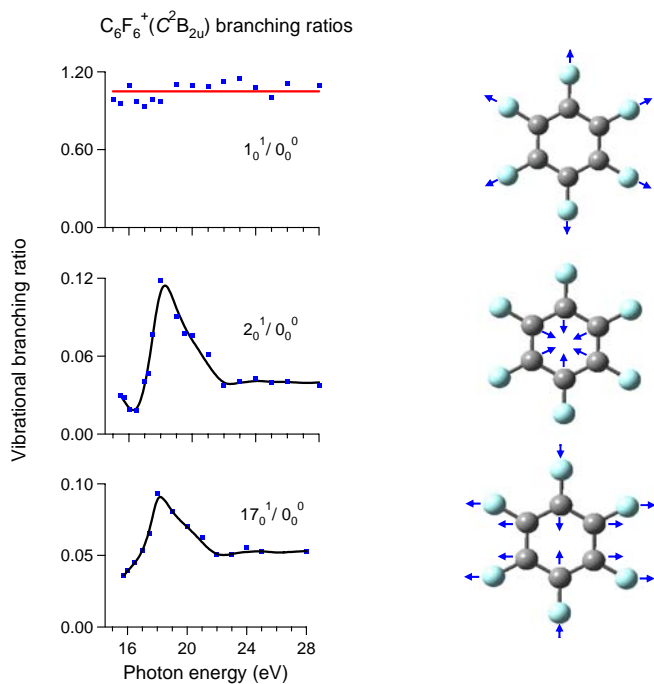


**Figure 2.** Vibrational branching ratios for selected vibrations. Note that mode 1 is flat while modes 2 and 17 clearly show the resonance at 18 eV. This provides information on the localization of the exiting photoelectron.

The most striking result is that the vibrational branching ratio curve for  $\nu_1$  (the C-F stretching mode) is very different from the other two. In particular, the curve for  $\nu_1$  appears very Franck-Condon, i.e., flat, while the other

two show a pronounced peak centered at  $h\nu \approx 18$  eV. The contrast between the curve for  $\nu_1$  and those for  $\nu_2$  and  $\nu_{17}$  provides a clue as to the nature of the resonance localization. Namely, the curves are consistent with the quasibound resonance wave function being localized along the in-plane benzene backbone of the molecule. The  $\nu_1$  vibrational mode corresponds to the C-F stretching motion. Because it does not distort the molecule in the region where the photoelectron is trapped, it is not expected to affect the resonance. On the other hand, both the  $\nu_2$  and the  $\nu_{17}$  modes distort the benzene backbone of the molecule, and thus are expected to affect the resonance significantly, as is observed.

It is possible to corroborate the above interpretation with the use of theory. The ASME results for  $C_6F_6$  show that there are two resonances in this energy range, and the results for them are shown in Fig. 3. The localization of the quasibound photoelectron is quite different for the two resonances. The resonances are calculated to appear at  $h\nu = 18.5$  and 21.0 eV. The lower energy resonance is the one responsible for the behavior seen in Fig. 2

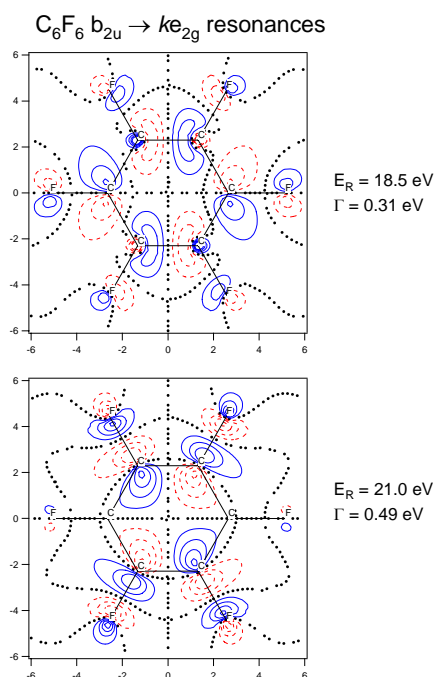


**Figure 3.** Contour maps of the continuum wavefunction showing two shape resonances. These were obtained from ASME calculations.

Note that the lower wavefunction does indeed have most of the electron density localized along the carbon backbone of the molecule, while the higher energy resonance has a “ring-like” node along the C-C framework. This is exactly what is suggested by the vibrational branching ratio curves.

These results have significant implications, as they indicate that photoelectron-vibrational interactions can emerge in ways not contemplated previously, and in so doing, shed light on the photoelectron trapping in larger systems. Indeed, the current observations indicate that the photoelectron trapping in larger polyatomics can occur in ways that have no parallels in simpler systems that have been studied. For example, the description suggested by the vibrational branching ratio curves is that the photoelectron is launched from a valence electron orbital into a ring in the plane of the carbon atoms. This continuum behavior is similar to bound valence electrons in one sense, in that bound  $\pi$  electrons are well known to arrange into ring-like orbitals. However, the observed continuum behavior is very different from bound valence electronic states in that the observed localization is in the plane of the aromatic ring, not above and below the plane, as is observed for  $\pi$ -networks of aromatic molecules. Moreover, these results belie the highly localized picture of shape resonance. Indeed, from the earliest reports of shape resonances, such as in  $SF_6$ , the view of shape resonances was that they are localized, rather than delocalized, and the current results show how this picture will evolve as the molecular framework is adjusted to accommodate more exotic localization patterns.

### Future plans

Most of the near-term future work will focus on VUV photoelectron spectroscopy, and we plan to extend our current studies in a few ways. First, the improvements made to the Schwinger variational code will be applied to all of the systems studied experimentally. This effort is already underway for  $C_6F_6$ . Second, we intend to study vibrationally resolved aspects of the photoelectron dynamics for *nonresonant* processes, such as Cooper minima. Third, we will begin studying larger nonaromatic ring structures. All of these new directions flow directly from the recent results, which demonstrate the feasibility and desirability of such studies.

### Publications:

- E.E. Doomes, P.N. Floriano, R.W. Tittsworth, R.L. McCarley, and E.D. Poliakoff, *Anomalous XANES spectra of octadecanethiol adsorbed on Ag(111)*, J. Phys. Chem. B **107**, 10193 (2003)
- E.E. Doomes, R.L. McCarley, E.D. Poliakoff, *Correlations between heterocycle ring size and X-ray spectra*, J. Chem. Phys. **119**, 4399 (2003)
- G.J. Rathbone, E.D. Poliakoff, J.D. Bozek, R.R. Lucchese, P. Lin, *Mode-specific photoelectron scattering effects on  $CO_2^+(C^2\Sigma_g^+)$  vibrations*, J. Chem. Phys. **120**, 612 (2004)
- G.J. Rathbone, R.M. Rao, E. D. Poliakoff, K. Wang, V. Mckoy, *Vibrational branching ratios in photoionization of CO and  $N_2$* , J. Chem. Phys. **120**, 778 (2004)
- G.J. Rathbone, E.D. Poliakoff, John D. Bozek, R.R. Lucchese, *Observation of the symmetry-forbidden  $5\sigma_u \rightarrow k\sigma_u$   $CS_2$  transition: A vibrationally driven photoionization resonance*, Phys. Rev. Lett. **92**, 1430021-1430024 (2004)
- G.J. Rathbone and E.D. Poliakoff, J.D. Bozek, R.R. Lucchese, *Intrachannel vibronic coupling in molecular photoionization*, Can. J. Chem. **82**, 1043-1051 (2004)
- G.J. Rathbone, E.D. Poliakoff, J.D. Bozek, R.R. Lucchese, *Electronically forbidden ( $5\sigma_u \rightarrow k\sigma_u$ ) photoionization of  $CS_2$ : Mode-specific electronic-vibrational coupling*, J. Chem. Phys. **122**, 064308 (2005).
- G.J. Rathbone, E.D. Poliakoff, J.D. Bozek, D. Toffoli, R.R. Lucchese, *Photoelectron trapping in  $N_2O$   $7\sigma \rightarrow k\sigma$  resonant ionization*, J. Chem. Phys. **123**, 014307/1-9 (2005).
- E.D. Poliakoff and R.R. Lucchese, *Evolution of photoelectron-vibrational coupling with molecular complexity*, Physica Scripta (in press)
- A. Das, E.D. Poliakoff, R.R. Lucchese, J.D. Bozek, *Launching a particle on a ring:  $b_{2u} \rightarrow ke_{2g}$  ionization of  $C_6F_6$* , J. Chem. Phys. (in preparation)
- A. Das, E.D. Poliakoff, J.D. Bozek, R. Montuoro, R.R. Lucchese, *Quasibound continuum states in  $SiF_4$   $5a_1^{-1}$  photoionization: Photoelectron-vibrational coupling*, J. Chem. Phys. (in preparation)
- A. Das, E.D. Poliakoff, R. Montuoro, R.R. Lucchese, J.D. Bozek, *Vibrationally resolved photoionization dynamics of  $CF_4$  in the  $D^2A_1$  state*, J. Chem. Phys. (in preparation)
- A. Das, E.D. Poliakoff, J.D. Bozek, R. Montuoro, R.R. Lucchese, *Evidence for a single-channel "window" resonance in  $BF_3^+(E^2A_1')$* , J. Chem. Phys. (in preparation)

# Control of Molecular Dynamics: Algorithms for Design and Implementation

Herschel Rabitz and Tak-San Ho, Princeton University  
Frick Laboratory, Princeton, NJ 08540, hrabitz@princeton.edu, tsho@princeton.edu

## A. Program Scope

This research is concerned with developing concepts for the systematic study of controlled quantum phenomena. Theoretical studies and simulations play central roles guiding the achievement of control over quantum dynamics, especially in conjunction with the use of optimal control theory and its realization in closed-loop learning experiments. Recent laboratory control advances have opened up many questions and possibilities for new directions in the field. The research in this program involves several interrelated components aiming at developing a deeper understanding of the principles of quantum control and providing new algorithms to extend the laboratory control capabilities.

## B. Recent Progress

In the past year several projects were pursued whose results are summarized below.

1. **The topology of optimally controlled quantum mechanical transition probability landscapes<sup>1</sup>** This work explored the topological structure of quantum mechanical transition probability landscapes. For controllable quantum systems based on the Euler-Lagrange variational equations derived from a cost function only requiring extremizing the transition probability, it was shown that the corresponding variational equations are automatically satisfied as a mathematical identity for control fields that either produce transition probabilities of zero or unit value. Similarly, the variational equations were shown to be inconsistent (i.e., they have no solution) for any control field which produces a transition probability different from either of these two extreme values. An upper bound was shown to exist on the norm of the functional derivative of the transition probability with respect to the control field anywhere over the landscape. Moreover, it was shown that the trace of the Hessian, evaluated for a control field producing a transition probability of a unit value, is bounded from below and the Hessian at a transition probability of unit value has an extensive null space and only a finite number of negative eigenvalues. Collectively, these findings showed that (a) the transition probability landscape extrema consist of values corresponding to no control or full control, (b) approaching full control involves climbing a gentle slope with no false traps in the control space and (c) an inherent degree of robustness exists around any full control solution. Although full controllability may not exist in some applications, the analysis

provides a basis to understand the evident ease of finding controls that produce excellent yields in simulations and in the laboratory.

2. **Optimal control landscapes for quantum observables**<sup>2</sup> In this work, quantum systems for optimal control were characterized by an evolving density matrix and a Hermitian operator associated with the observable of interest and the optimal control landscape was the observable as a functional of the control field. The features of interest over this control landscape consisted of the extremum values and their topological character. For controllable finite dimensional quantum systems with no constraints placed on the controls, this study showed that there is only a finite number of distinct values for the extrema, dependent on the spectral degeneracy of the initial and target density matrices. The consequences of these findings for the practical discovery of effective quantum controls in the laboratory was discussed.
3. **Revealing the key variables and states in optimal control of quantum dynamics**<sup>3</sup> In this study, sensitivity analysis of the wave function was shown to be useful for identifying the key variables and states in the calculations based on optimal control theory (OCT). The analysis calls for little extra effort beyond that of performing the original control calculation. An application of the analysis to a model multilevel control problem was carried out. This work showed that wave function sensitivity analysis is effective for identifying the key controls and states in an OCT calculation. A Hessian analysis of the OCT objective may similarly be performed as another measure of assessing the key control variables. The simplicity of the method's implementation makes it a convenient tool for extracting additional dynamical information. The formulation of these tools could also be expanded to further explore control sensitivity of the wave function throughout the control field pulse duration.
4. **Quantum optimal control of molecular isomerization in the presence of a competing dissociation channel**<sup>4</sup> In this investigation, the quantum optimal control of isomerization in the presence of a competing dissociation channel was simulated on a two-dimensional model. The control of isomerization of a hydrogen atom was achieved through vibrational transitions on the ground-state surface as well as with the aid of an excited-state surface. It was found that (1) suppression of the competing dissociation dynamics during the isomerization control on the ground-state surface becomes easier with an increase in the spatial separation between the isomerization and dissociation regions and with a decrease in the dissociation channel width and (2) isomerization control first involving transfer of amplitude to an excited-state surface is less influenced by the dissociation channel configuration on the ground-state surface, even in cases where the excited-state surface allows for a moderate spreading of the excited wave packet.

5. **Quantum observable homotopy tracking control**<sup>5</sup> This work proposed a new tracking method where the target observable at the final dynamical time follows a predefined track with respect to a homotopy tracking variable. The procedure calculated the series of control fields required to accomplish observable homotopy tracking by solving a first-order differential equation in terms of the homotopy tracking variable for the evolution of the control field. It was shown that controls produced by this technique render the desired track without encountering field singularities. This work also extended the technique to the case where the field-free Hamiltonian and dipole moment operator change with the tracking variable in order to explore the control of new physical systems along the track. Several simulations were performed illustrating the various uses for this quantum tracking control technique.
6. **The single-molecule dye laser**<sup>6</sup> This work explored the feasibility of inducing lasing action in a single dye molecule using an optical microcavity. A single-molecule light source was proposed, in which a microcavity-coupled dye molecule is pumped by multiple energy donors via an intermolecular resonance energy transfer mechanism. Using a quantitative model based on realistic parameters for microcavities and for organic dyes, it was showed that stimulated emission may become dominant over spontaneous fluorescence under optimal yet technically reachable conditions, suggesting the likelihood of achieving a single-molecule lasing photon source with the proposed device. Lasing of a single dye molecule generates signals much brighter than spontaneous fluorescence, and may find applications in a wide range of fields from physics and chemistry to biology.

## C. Future Plans

The research in the coming year will mainly focus on identifying the principles of quantum control for open quantum systems and its future prospects in the laboratory. Via detailed control landscape analysis, we aim to describe how and why the presence of an environment can influence the optimal control. The analysis will further provide insights into the classes of quantum control experiments expected to be most successful in the future. Other research plans include the following explorations of: (1) the effect of spatial and orientation inhomogeneities during control, (2) the relationships between the control of homologous quantum systems, and (3) the prospects of combining the capabilities of high throughput photonic reagent and chemical reagent apparatus for optimal performance of controlling molecular dynamics. Finally, we plan to develop rigorous, nonperturbative mathematical frameworks and efficient computational procedures for the study of optimal control of molecular collision dynamics, including elastic, inelastic, and reactive scattering in the presence of intense shaped laser pulses.

## D. References

1. The topology of optimally controlled quantum mechanical transition probability landscape, H. Rabitz, T.-S. Ho, M. Hsieh, B. Kosut, and M. Demiralp, *Phys. Rev. A.*, (2006), in press.
2. Optimal control landscapes for quantum observables, H. Rabitz, M. Hsieh, and C. Rosenthal, *J. Chem. Phys.* **124**, 204107 (2006)
3. Revealing the key variables and states in optimal control of quantum dynamics, M. Artamonov, T.-S. Ho, and H. Rabitz, *Chem. Phys. Lett.* **421**, 81 (2006).
4. Quantum optimal control of molecular isomerization in the presence of a competing dissociation channel, M. Artamonov, T.-S. Ho, and H. Rabitz, *J. Chem. Phys.* **124**, 064306 (2006)
5. Quantum observable homotopy tracking control, A. Rothman, T.-S. Ho, and H. Rabitz, *J. Chem. Phys.* **123**, 134104 (2005)
6. The single-molecule dye laser, Z. S. Wang, H. A. Rabitz, and M. O. Scully, *Laser Physics*, **15**, 118 (2005).
7. Observable-preserving control of quantum dynamics over a family of related systems, A. Rothman, T.-S. Ho, and H. Rabitz, *Phys. Rev. A* **72**, 023416 (2005)
8. Quantum control of molecular motion including electronic polarization effects with two stage toolkit, G. Balint-Kurti, F. Manby, Q. Ren, M. Artamonov, T.-S. Ho, and H. Rabitz, *J. Chem. Phys.*, **122**, 084110 (2005).
9. Quantum control of ozone isomerization, M. Artamonov, T.-S. Ho, and H. Rabitz, *Chem. Phys.*, **305**, 213-222 (2004).
10. Generalized monotonically convergent algorithms for solving quantum optimal control equations in product spaces, Y. Ohtsuki, G. Turinici, and H. Rabitz, *J. Chem. Phys.*, **120**, 5509 (2004).
11. Efficient extraction of quantum Hamiltonian information from optimal laboratory data, J. M. Geremia and H. A. Rabitz, *Phys. Rev. A*, **70**, 023804 (2004).
12. Efficient algorithms for the laboratory discovery of optimal quantum controls, G. Turinici, C. Le Bris, and H. Rabitz, *Phys. Rev. E*, **70**, 016704 (2004).
13. Mechanism analysis of controlled quantum dynamics in the coordinate representation, R. Sharp and H. Rabitz, *J. Chem. Phys.*, **121**, 4516-4527 (2004).

## **A Dual Bose-Einstein Condensate: Towards the Formation of Heteronuclear Molecules**

### **Principal Investigator:**

Dr. Chandra Raman  
Assistant Professor  
School of Physics  
Georgia Institute of Technology Atlanta, GA 30332-0430  
craman@gatech.edu

### **Program Scope:**

This research program explores quantum gases of atoms and molecules. Our goal is the study of superfluidity and correlated quantum effects in low temperature gases. As an experimentalist, one can manipulate the trapping potential (either optically or magnetically) as well as the microscopic interactions to realize a number of low temperature physical systems, from superfluids to superconductors and low temperature magnets.

Our work has a two-fold thrust. Our “atomic” approach explores superfluidity and novel effects of coherent matter waves using single component (i.e., atomic) Bose-Einstein condensates (BECs). We are also pursuing heteronuclear molecular quantum gases. Our approach is to use sympathetic cooling to form a dual BEC, then to create molecules by magneto-association using a number of recently predicted Feshbach resonances (these have been supported by new experimental data from Tiemann’s group PRA 72, 062505 (2005)). The eventual goal of the molecular effort is to create a dipolar superfluid, a novel strongly correlated quantum system.

Our experiment centers on the production of large atom-number sodium Bose-Einstein condensates (5-10 million atoms). Our method is naturally suited to efficient sympathetic cooling of Rb and the study of Na-Rb mixtures, through the large Na sample available from a high-flux Zeeman slowed atomic beam. Our apparatus is flexible enough that we eventually hope to explore superfluidity and related quantum effects in any of the systems  $^{23}\text{Na}$ ,  $^{85}\text{Rb}$ ,  $^{87}\text{Rb}$ , as well as mixtures (and molecules) of Na and Rb. These mixtures have not been magnetically trapped to date.

### **Recent Progress:**

- **Axicon Lens for Coherent Matter Waves.** In this work, we report on the realization of a conical lens, or “axicon” for Bose-Einstein condensates (BECs) using the dipole force exerted by a focused, blue-detuned laser beam. To our knowledge this is the first observation of the far-field pattern of an axicon using neutral atoms. In our experiment, the atoms expand radially outward in the form of an extremely thin, circular ring in spite of significant interactions between atoms. This is in marked contrast to the conventional BEC expansion, which is characterized by strong spatial dispersion and a broad final velocity distribution.

We have performed numerical solutions of the Gross-Pitaevskii equation confirming that this interplay between the external and internal forces can be exploited to tailor the expansion of a BEC using light fields. Our work, which has been submitted to Optics Express, is an important step toward the utilization of BECs as coherent matter wave sources for applications to coherent atom optics, holography and interferometry.

- **Detecting Curve Crossings.** We have discovered a powerful algebraic method of finding level crossings in physical systems by mapping it to the problem of locating the roots of a polynomial. The idea is to use the discriminant of a matrix to locate the curve crossings without actually computing the eigenvalues. In spite of limited information, one can use this to identify points in the parameter space where the Born-Oppenheimer approximation breaks down. This has implications in performing searches for Feshbach resonances. Our work has been submitted to Physical Review Letters.
- **Vortex Matter.** We have demonstrated a new method to directly detect the sense of rotation of a rapidly rotating Bose-Einstein condensate. We used Bragg scattering of laser light to map out the velocity distribution of a BEC, and obtained signatures of the microscopic velocity field. Our method is more general than time-of-flight imaging, which relies on the spatial scaling of the density distribution during expansion. This work has recently appeared as a Rapid Communication in Physical Review A [Phys. Rev. A 73, 041605(R) (2006)].
- **Dynamics of rotating Bose-Einstein condensates probed by Bragg scattering.** The time-of-flight technique is a destructive method and cannot be used for *in-situ* observation of the dynamics of a rotating condensate. However, the Bragg method couples out a small fraction of the atoms, and therefore, can be used as a non-destructive probe. Non-destructive methods would have far-reaching applications to the examination of vortex dynamics and superfluid turbulence.

In this work we examined the feasibility of non-destructive measurements by applying a sequence of two 0.5 ms duration Bragg pulses separated by a variable time  $\tau$ . We observed two diffracted stripes on either side of the undiffracted cloud in the center. This indicated that the Bragg process is indeed non-destructive, and does not disrupt the rotation. However, due to the accumulated potential energy during the time  $\tau$ , the diffracted cloud from the first pulse had a tilt angle and shape which is different from pulse 2. In fact, the tilt angle reverses sign after very short hold times  $\tau > 2.5$  ms compared with the trap oscillation period of  $\tau_{\text{osc}} = 32$ ms, a dynamical effect arising from a combination of rotation of the cloud and the three-dimensional harmonic potential. Our observations led us to understand the limitations of this non-destructive method. This work has been accepted to appear in a focus issue of the Journal of Mathematics and Computers in Simulation.

## Future Plans:

**Dual-species BEC.** We are currently integrating Rb into our BEC apparatus. We are currently implementing a dual atom source, followed by dual-species Zeeman slowing and magneto-optical trapping. Our experiments will focus on:

- Mixtures of  $^{23}\text{Na}$  with  $^{85}\text{Rb}$  or  $^{87}\text{Rb}$ . We expect to trap  $10^{10}$  Na atoms and  $10^8$  Rb atoms, allowing for efficient sympathetic cooling of the latter by the former.
- Feshbach resonances. Using optical traps, we can explore magnetic feshbach resonances in a wide range of magnetic fields up to 1.2 kGauss. A number of resonances below 1 kGauss have been predicted for heteronuclear collisions of  $^{23}\text{Na}$ - $^{87}\text{Rb}$  as well as  $^{23}\text{Na}$ - $^{85}\text{Rb}$  by Tiemann's group.
- A dual BEC provides opportunities for studying mixtures of two quantum fluids. Mixtures of atoms are profoundly influenced by the interplay between *self*-interaction and *mutual* interaction and can exhibit new quantum phenomena. We have proposed a new scheme for tailoring the spatial density profiles of each component condensate using species-selective light fields.
- $^{85}\text{Rb}$  BEC. Sympathetic cooling is likely to solve many of the difficulties that have been present thus far with producing  $^{85}\text{Rb}$  condensates. This is an attractive system due to its easily tunable interactions and due to the spin-2 ground state. The latter results in a 5 component vector order parameter which has not been observed in cold gases.

## Papers acknowledging DoE support in the past year:

1. M. Bhattacharya and C. Raman: *Detecting Curve Crossings without looking at the Spectrum*, submitted to Physical Review Letters. Available as e-print at <http://arxiv.org/abs/physics/0604213>.
2. S. R. Muniz, D. S. Naik and C. Raman: *Axicon Lens for Coherent Matter Waves*, submitted to Optics Express. Available as e-print at <http://arxiv.org/abs/cond-mat/0606540>.
3. S. R. Muniz, D. S. Naik, M. Bhattacharya and C. Raman: *Dynamics of rotating Bose-Einstein condensates probed by Bragg scattering*, accepted for publication in a refereed, focus issue of the Journal of Mathematics and Computers in Simulation (2006).
4. S. R. Muniz, D. S. Naik and C. Raman: *Bragg Spectroscopy of Vortex Lattices in Bose-Einstein condensates*. Rapid Communication in Phys. Rev. A **73**, 041605(R) (2006).
5. D. S. Naik, S. R. Muniz, and C. Raman: *Metastable Bose-Einstein condensate in a linear potential*. Rapid Communication in Phys. Rev. A **72**, 051606(R) (2005).

## Ultrafast X-ray Coherent Control

D. A. Reis<sup>1</sup> and P. H. Bucksbaum<sup>2</sup>

<sup>1</sup>*FOCUS Center, Physics Department, University of Michigan Ann Arbor, MI 48109-1040*

*dreis@umich.edu*

<sup>2</sup>*PULSE Center, Stanford University, Stanford, CA 94304*

*phb@slac.stanford.edu*

*Grant DEFG02-00ER15031*

### Program Scope

This is a program to develop ultrafast x-ray physics at synchrotrons and linear accelerators. The research is carried out at the Advanced Photon Source sector 7, with the MHATT-XOR collaboration (previously MHATT-CAT); and at the Stanford Linear Accelerator Center, with the SPPS collaboration and the Stanford Ultrafast Science Center. Our research concentrates on ultrafast and coherent dynamical processes in solids and molecular systems. Along with new science, we are developing new ultrafast methodology that will be utilized on future generation ultrafast x-ray sources such as LCLS. Ultrafast science probes dynamics on the atomic and molecular scale of bond vibration in a molecule or optical phonons in a solid. This is typically on the order of 100 fsec, but can in some cases be as long a few picoseconds. x rays are ideal probes of motion on these scales because of their short wavelength, and there has been much progress towards producing ultrafast x-ray pulses for transient dynamical studies.

Early efforts in the field concentrated on laser-generated plasmas, which can produce x-ray bursts as short as a few hundred femtoseconds. These sources are quite weak, however, and this has limited their use to a few very high contrast problems, such as crystalline melting. Electron beam-based x-ray sources can be much brighter. The challenge therefore has been to make these accelerator-based x-ray pulses short, so that they can record more than the time-averaged motion of transiently excited materials.

Third generation synchrotron pulses, which are 30–100 psec in duration, are tantalizingly close to the required duration, and so we and others have been working with them to learn about dynamics of transient molecular and solid state processes. Techniques that we and others have developed include picosecond x-ray streak cameras; X-ray switches based on x-ray transmission through or reflection from transiently excited crystals; and methods to shorten the electron bunches in the synchrotron.

We have also been key participants in the Stanford Sub-Picosecond Pulse Source, which produces sub-100 fsec x-ray pulses from compressed electrons traversing an undulator in the SLAC Final Focus Test Beam facility. The SPPS team has compressed 30 GeV electrons at SLAC, shortening the bunch length to about 80 fsec. The ultrafast pulses of x rays produced in the undulator have now been used in two different experiments which we describe below. This physics defines the frontier of ultrafast x-ray science that will be explored at LCLS.

## Recent Progress

SPPS: In April 2006 SPPS was decommissioned to make room for construction of the LCLS. SPPS has proven to be an incredibly important source for ultrafast x-ray science over the past 3 years, both as a staging ground for future LCLS experiments as well as a laboratory where we have performed the most detailed experiments to date on ultrafast laser-matter interactions (including carrier induced bond-softening in semimetals and nonthermal melting in semiconductors). Our first three research papers concern the synchronization of laser pulses with the x rays produced at the SPPS (Cavalieri *et al.*, 2005) and the dynamics of ultrafast disordering in laser-excited solids via single-shot femtosecond x-ray diffraction (Gaffney *et al.*, 2005; Lindenberg *et al.*, 2005). Our experiences on SPPS have culminated in the first ever measurements of the inter-atomic potential energy surface of a highly excited solid (Fritz *et al.*, 2006). This seminal experiment was also the first to utilize our single-shot electron beam timing diagnostic to perform pump-probe experiments with sub-jitter resolution.

To achieve femtosecond x-ray bursts SPPS utilized electron bunch compression techniques similar to those planned for LCLS. While this allows for the production of ultrashort x-ray bursts, the best synchronization of the electron pulse to an external laser has been at the picosecond level. The synchronization problem can limit the time-resolution in a laser pump-x-ray probe experiment and therefore, if left unchecked, it will be a severe limitation for the LCLS and other future accelerator based sources. One solution, which was used in the early ultrafast disordering experiments on SPPS, is to utilize a noncollinear geometry and collect the data all in a single shot. The noncollinear geometry provides a time-sweep between the pump and probe and allows for the dynamics to be recorded using a temporal-spatial encoding. In the case of ultrafast disordering, the effect on the Bragg scattering is so dramatic that such a technique can be utilized with the relatively large flux of the SPPS ( $\sim 10^6$  9 keV photons per sub-100 fs pulse).

Not all experiments can be done in a single shot, so we need a mechanism to determine relative arrival time between x rays and the laser on every shot. We have demonstrated that spatially resolved electrooptic sampling (EOS) of the electron bunch field is a non-invasive measurement of the pump-probe delay on every shot (as well as a bunch length diagnostic). In this manner, a series of shots can be taken in a random sampling fashion, and later rearranged according to arrival time. This post-binning makes more traditional, repetitive pump-probe measurements possible. Using the single-shot disordering experiment mentioned above as an independent measurement of the x-ray arrival time, we were able to show that we could correlate the EOS to the arrival time of the x rays to within 60 fs, rms. In these experiments, we use a single pulse from the laser oscillator to probe the relativistically enhanced ( $\gamma=60,000$ ) electric field near the electron bunch just before it radiates x rays in the undulator. A synchronized oscillator pulse is then amplified and used for the excitation of the InSb crystal. So long as the path lengths remain stable, the pulses should be locked to each other. We have demonstrated this technique to measure the details of the inter-atomic potential energy surface of a highly excited bismuth film.

In the Bi experiment, an ultrafast laser pulse was used to promote a large fraction of the valence electrons into the conduction band of a thin bismuth film, during a few tens of femtoseconds. The presence of such a dense electron-hole plasma significantly alters the interatomic potential before the atoms have a chance to move. Following this excitation, the atoms move in very large amplitude coherent motion which was measured via x-ray diffraction. From this, we were able to follow the equilibrium position and curvature of the double-well potential as function of carrier density and time over the first few picoseconds of excitation. These are the two key parameters that determine the Peierls distorted structure. The experiments were in excellent agreement with our previous optical experiments and density functional theory (Murray *et al.*, 2005), which indicates that we are very close to a solid-solid phase transition. Whether we can coherently drive this transition without melting the material remains an important question that we hope to answer in the near future.

APS: One of the main goals of our experimental progress at APS continues to be the control x-ray diffraction in order to produce a femtosecond switch for x rays. In our earlier work at APS, we used coherent control of vibrational excitations, on the picosecond time-scale, as a means to exchange energy between two distinct diffracted beams in the anomalous transmission of x rays. But, we also used this new phenomenon to study the dynamics of the dense electron hole plasma generated in semiconductors following ultrafast laser-excitation. Over the past few years our emphasis had shifted to SPPS. However, we have still been active utilizing APS and its  $\sim 100ps$  x rays to study the thermal, mechanical and electronic properties of thin films and interfaces (Lee *et al.*, 2005). These experiments centered on the zone center coherent acoustic phonons generated through the deformation potential. However, the path to equilibration is much more complicated, involving processes that occur from tens of femtoseconds to microseconds. We are currently looking at the initial cooling of the electrons through the emission of phonons with wavevectors spanning the entire Brillouin zone, through time-resolved x-ray diffuse scattering. Little is known about these processes, especially at high excitation densities, except indirectly by optical means. X-ray diffuse scattering provides an important tool in understanding the full phonon dynamics. These experiments are primarily limited by flux and temporal resolution; consequently, and perhaps ultimately single-shot experiments are planned for LCLS.

Our work has also been recently highlighted in (Broge *et al.*, 2005; Reis *et al.*, to be published, 2006; Reis and Lindenberg, to be published, 2006).

## Future Plans

While SPPS has been decommissioned there is still much work to be done at SLAC in the short lead up to LCLS. We plan, in collaboration with the new PULSE center, to continue our electrooptic experiments following the first bunch compressor for LCLS, which will be installed later this year.

At APS, we continue our work on x-ray diffuse scattering, and interface physics. We have also been actively studying potential science opportunities for ultrafast compressed x-ray pulses at the APS, where, accelerator physicists have been looking at the possibility of generating high brightness picosecond x rays using an insertion device. We are very encouraged by their work, which suggests that 1ps FWHM pulses can be produced for every bunch in the storage ring, or at reduced rep-rate in the very near future. This would indeed be a major development for 3rd generation sources, and would be complementary to 4th generation machines. We have collaborated with APS machine physicists to study this problem. We have also been actively involved in the development of two laser laboratories at the PULSE center, which will give us the capability to investigate strong field alignment, and ultrafast molecular structure.

### Publications 2005–2006

- Broge, D., E. Peterson, and P. H. Bucksbaum, 2005, Spectrally resolved transient alignment of molecular iodine, DAMOP.
- Cavalieri, A. L., D. M. Fritz, S. H. Lee, P. H. Bucksbaum, D. A. Reis, J. Rudati, D. M. Mills, P. H. Fuoss, G. B. Stephenson, C. C. Kao, D. P. Siddons, D. P. Lowney, *et al.*, 2005, Phys. Rev. Lett. **94**, 114801.
- Fritz, D. M., D. A. Reis, B. Adams, R. A. Akre, J. Arthur, C. Blome, P. H. Bucksbaum, A. L. Cavalieri, S. Engemann, S. Fahy, R. W. Falcone, P. H. Fuoss, *et al.*, 2006, submitted to Nature .
- Gaffney, K. J., A. M. Lindenberg, J. Larsson, K. Sokolowski-Tinten, C. Blome, O. Synnergren, J. Sheppard, C. Caleman, A. G. MacPhee, D. Weinstein, D. P. Lowney, T. Allison, *et al.*, 2005, Physical Review Letters **95**(12), 125701 (pages 5), URL <http://link.aps.org/abstract/PRL/v95/e125701>.
- Lee, S. H., A. L. Cavalieri, D. M. Fritz, M. C. Swan, R. S. Hegde, M. Reason, R. S. Goldman, and D. A. Reis, 2005, Phys. Rev. Lett. **95**(24), 246104 (pages 4), URL <http://link.aps.org/abstract/PRL/v95/e246104>.
- Lindenberg, A. M., J. Larsson, K. Sokolowski-Tinten, K. J. Gaffney, C. Blome, O. Synnergren, J. Sheppard, C. Caleman, A. G. MacPhee, D. Weinstein, D. P. Lowney, T. K. Allison, *et al.*, 2005, Science **308**, 392.
- Murray, E. D., D. M. Fritz, J. K. Wahlstrand, S. Fahy, and D. A. Reis, 2005, Phys. Rev. B **72**(6), 060301 (pages 4), URL <http://link.aps.org/abstract/PRB/v72/e060301>.
- Reis, D. A., K. J. Gaffney, B. Torralva, and G. H. Gilmer, to be published, 2006, MRS bulletin .
- Reis, D. A., and A. M. Lindenberg, to be published, 2006, in *Light Scattering in Solids IX*, edited by M. Cardona and R. Merlin (Springer-Verlag).

## “Atomic Physics Based Simulations of Ultra-cold Plasmas”

**F. Robicheaux**

*Auburn University, Department of Physics, 206 Allison Lab, Auburn AL 36849  
(robicfj@auburn.edu)*

### **Program Scope**

This theory project focuses on the study of atomic processes that occur in ultra-cold plasmas. We have investigated plasmas without magnetic fields[1] and in strong magnetic fields[2,3]. The results of our studies of atomic processes in strongly magnetized plasmas are of direct relevance to the two collaborations (ALPHA and ATRAP) that are attempting to create cold anti-hydrogen. The results of our studies of plasmas without magnetic fields were used to interpret the results from several experimental groups. Some of the techniques we developed have been used to study collision processes in ions, atoms and molecules.

### **Recent Progress 2005-2006**

*Three body recombination in strong magnetic fields:* Recent experiments have demonstrated the formation of anti-hydrogen when anti-protons traverse a positron plasma. The dominant formation mechanism is TBR which occurs when two positrons collide in the field of the anti-proton so that one loses enough energy to become bound. The strong magnetic field introduces new and interesting features into the process. In previous studies, the guiding center approximation was used for the light particles; this removes the cyclotron motion which allows for much larger time steps in the calculation. We removed this approximation[10] so that we could study the magnetic moments of the atoms formed by three body recombination. The next stage anti-hydrogen experiments will attempt to trap the atoms using the effect of a spatially varying magnetic field on the magnetic moment. The expectation was that the atoms would be easily trapped because TBR gives highly excited atoms with large magnetic moments. The calculations confound these expectations because the majority of atoms are formed in high-field seeking states.

*Photon-atom processes in strong magnetic fields:* We performed two studies of highly excited atoms in strong magnetic fields interacting with photons. The first[11] was a theoretical study of radiative cascade in strong magnetic fields. Our calculation was fully quantum mechanical and was focused on the basic mechanism for changing the radiative cascade. The radiative decay of individual states can be strongly affected by the magnetic field because it can mix states with different angular momenta. However, the radiative cascade from a group of atoms does not show large effects unless the magnetic field is strong enough to qualitatively change the character of the states. The second study[13] was a joint project with an experimental group to investigate whether it is possible to stimulate radiative cascade with and without strong magnetic field. The idea was to make a large energy transition so photoionization was one of the competing channels. We found that it was possible to find laser intensity such that by far most of the atoms were driven to lower levels and few atoms were ionized. However, this only worked in

weak magnetic fields. In strong magnetic fields, the stimulated photon emission was suppressed to the point that photo-ionization was strongest channel.

*Double charge transfer:* Hessels and co-workers proposed the formation of anti-hydrogen by a two step process. In the first step, a Rydberg atom enters a positron plasma where charge transfer occurs to give Rydberg positronium. The Rydberg positronium then can travel to a region of anti-protons where a second charge transfer occurs to give Rydberg anti-hydrogen. This process was observed experimentally but the statistics were low. The original proposal included calculations but for no magnetic field whereas the experiments are performed in strong magnetic fields; the experimentalists noted that new calculations, that included a strong B, were needed. We carried out the calculation of both stages of this process[8] to understand how a strong magnetic field affects each stage. We found, and understood, two surprising results. First, the positronium are either emitted randomly or mostly perpendicular to the B-field for relevant strengths and binding energies. Second, the magnetic moment of the resulting anti-hydrogen was not randomly oriented but was most likely to result in high-field seeking states.

*Molecules:* In Ref. [6], we computed the charge transfer in collisions of p or  $\text{He}^{2+}$  with  $\text{H}_2^+$  molecular ion. In particular, we investigated the dependence on the angle of the molecular ion relative to the projectile's velocity. The motivation was calculations performed by Cheng and Esry that did not agree with the results of experiments performed at KSU. Our calculations qualitatively agreed with the calculations of Cheng and Esry. In Refs. [4,7,12], we report on calculations of electron scattering from the simplest molecule  $\text{H}_2$  and molecular ion  $\text{H}_2^+$ . In particular, we focused on ionization and excitation since these are the most difficult processes to describe theoretically. These calculations extend our methods for computing atomic processes to molecules where the lack of spherical symmetry greatly complicates the calculation.

*Two electron continua:* Recent experiments have suggested that the double photoionization of some atoms result in cross sections that oscillate near threshold. We performed calculations[9] near threshold for double photoionization of He from the ground state and model calculations from excited states. This is a computationally challenging problem because the cross section needs to be found at several energy points and the size of the calculation roughly scales like the inverse of the energy above threshold. Substantial convergence checks need to be performed because the oscillation is a small fraction of the cross section. We did not observe oscillations. In Ref. [5], we give the results of calculations of electron impact ionization from excited states of H and H-like ions ( $\text{Li}^{2+}$  and  $\text{B}^{4+}$ ). We compared fully quantum calculations with distorted wave perturbation theory and a completely classical calculation. This is important because ionization from the ground state is not a one step process in many plasmas; the ionization occurs by electron impact excitation to high n states followed by a subsequent ionization. Not surprisingly, we found that the perturbative calculations improved as the charge increased and n decreased. However, we found that the classical calculations did not approach the quantum calculations quickly with increasing n. Fully quantum calculations are time consuming and can be converged only for  $n < 6$ . Many plasma modeling programs use simple approximations for ionization out of high n states

based on mixed classical/quantum calculations whose validity is now suspect. Our conclusion is that electron impact ionization of highly excited ions is an urgent, open question.

Finally, this program has several projects that are strongly numerical but only require knowledge of classical mechanics. This combination is ideal for starting undergraduates on publication quality research. Since 2004, 5 undergraduates have participated in this program. Daniel Phalen completed the quantum scattering calculation of Ref. [6] during the summer of 2004. Chris Norton and Michael Wall completed the double charge exchange calculation[8] during spring of 2005; they are now working on a time dependent quantum problem. Michael Wall was one of 5 undergraduates invited to give a talk on their research at the undergraduate session of the DAMOP 2006 meeting. Michelle Zhang and Christine Taylor completed a project (submitted to PRA) to simulate the motion of an anti-hydrogen atom interacting with the complicated magnetic fields in the proposed anti-hydrogen traps in order to test ideas about measuring whether or not the anti-hydrogen atoms are trapped; they are now studying the motion of the anti-protons through the complicated magnetic and electric fields in the actual experiments. In addition to these undergraduates, this grant supports the investigations of Turker Topcu who is a graduate student; he has completed the investigation of radiative cascade in strong B[11], the component of Ref. [9] related to model double photoionization near threshold, model quantum calculations of electron impact ionization of Rydberg atoms ( $n \sim 25$ ) (submitted to PRA), and is in the process of calculating the time dependent escape of Rydberg electrons in parallel electric and magnetic fields.

### **Future Plans**

*Ultra-cold plasmas* Recent experiments by S. Bergeson's group at BYU and G. Raithel's group at U. Michigan have uncovered interesting behavior of ultra-cold plasmas with cylindrical symmetry. The BYU experiments have  $B \sim 0$  while the UM experiments are in high B. We have developed programs to study these systems but have applied them to specific problems. We plan to: (1) simulate the expansion of ultracold plasma in cylindrical symmetry with and without high B and compare to experiment and our previous results for spherical symmetry and (2) simulate TBR in an expanding ultracold plasma in strong B and the properties of the atoms.

*Anti-hydrogen motivated calculations* The next generation of anti-hydrogen experiments are aimed at trapping the anti-hydrogen. To address possible issues, we will investigate processes that arise from this goal. In particular, we plan to: (1) develop a program to compute the radiative recombination rate in strong magnetic field and also use it for ion charges other than 1 in order to determine the effect on electron cooling of ions in storage rings, (2) complete the study of the motion and possible center of mass cooling of anti-hydrogen due to radiative cascade, and (3) study three body recombination in the presence of oppositely charged light species which can halt the process through charge transfer.

*Related problems* In many plasma simulations, electron scattering from highly excited atoms is treated by a classical approximation but this may be inaccurate[5]. Recent calculations have found interesting classical, chaotic dynamics for a highly excited electron in parallel electric and magnetic fields. We plan to: (1) complete

the study of model quantum calculations with reduced dimensionality in order to treat very high  $n$  and understand how the quantum results approach the classical and (2) investigate the time dependent quantum evolution of a Rydberg electron in parallel electric and magnetic fields.

#### **DOE Supported Publications (2003-2006)**

- [1] F. Robicheaux and J.D. Hanson, Phys. Plasmas **10**, 2217 (2003).
- [2] F. Robicheaux and J.D. Hanson, Phys. Rev. A **69**, 010701 (2004).
- [3] F. Robicheaux, Phys. Rev. A **70**, 022510 (2004).
- [4] M.S. Pindzola, F. Robicheaux, J.A. Ludlow, J. Colgan, and D.C. Griffin, Phys. Rev. A **72**, 012716 (2005).
- [5] D.C. Griffin, C.P. Balance, M.S. Pindzola, F. Robicheaux, S.D. Loch, J.A. Ludlow, M.C. Witthoef, J. Colgan, C.J. Fontes, and D.R. Schultz, J. Phys. B **38**, L199 (2005).
- [6] D.J. Phalen, M.S. Pindzola, and F. Robicheaux, Phys. Rev. A **72**, 022720 (2005).
- [7] M.S. Pindzola, F. Robicheaux, and J. Colgan, J. Phys. B **38**, L285 (2005).
- [8] M.L. Wall, C.S. Norton, and F. Robicheaux, Phys. Rev. A **72**, 052702 (2005).
- [9] U. Kleiman, T. Topcu, M.S. Pindzola, and F. Robicheaux, J. Phys. B **39**, L61 (2006).
- [10] F. Robicheaux, Phys. Rev. A **73**, 033401 (2006).
- [11] T. Topcu and F. Robicheaux, Phys. Rev. A **73**, 043405 (2006).
- [12] M.S. Pindzola, F. Robicheaux, S.D. Loch, and J.P. Colgan, Phys. Rev. A **73**, 052706 (2006).
- [13] A. Wetzels, A. Gurtler, L.D. Noordam, and F. Robicheaux, Phys. Rev. A **73**, 062507 (2006).

## High Harmonic Generation in Discharge-Ionized Plasma Channels

Jorge J. Rocca,

*Electrical and Computer Eng Department, Colorado State University, Fort Collins, CO 80523-1373*  
*rocca@engr.colostate.edu*

Henry C. Kapteyn

*JILA/Physics Department, University of Colorado, Boulder, CO 80309-0440*  
*kapteyn@jila.colorado.edu*

### Program Description

We are investigating aspects of the development and use of compact coherent soft x-ray sources based on fast capillary discharges and high order harmonic up-conversion, and soft x-ray laser amplification. These sources are very compact, yet can generate soft x-ray radiation with peak spectral brightness several orders of magnitude larger than a synchrotron beam line. In relation to source development, we are exploring the generation of high harmonics in a *pre-ionized* medium created by a capillary discharge. The use of pre-ionized nonlinear media may make it possible to generate coherent light at  $> 1$  KeV photon energy, by reducing ionization-induced defocusing of the incident laser. Using this new technique we have recently dramatically extended the photon energy created by high-order harmonic generation in xenon from the highest value previously demonstrated, 75 eV, to 150 eV.

### High harmonic generation from ions in a capillary discharge

High-order harmonic generation (HHG) coherently up-converts laser light from the visible and infrared into the extreme-ultraviolet region of the spectrum. The highest photon energy that can be produced via this interaction is predicted by the cutoff rule to be  $h\nu_{\max} = I_p + 3.17U_p$ , where  $I_p$  is the ionization potential of the atom and  $U_p \propto I_L \lambda^2$  is the ponderomotive energy of the electron in the laser field. Here  $I_L$  is the peak laser intensity and  $\lambda$  is the wavelength of the driving laser field. From this rule, the range of photon energies that are generated in HHG is determined by the laser intensity. However, in most experiments to date, the maximum observed HHG photon energy has been limited not by the available laser intensity, but by the intensity at which the target atoms are nearly completely ionized. This is because ionization of the nonlinear medium by the driving laser leads to severe ionization-induced defocusing of the driving laser limiting the maximum obtainable laser intensity. The intensity at which an atom (or ion) ionizes depends directly on the ionization potential of the atom. Because ions have much higher ionization potentials than neutrals, significantly higher energy photons can be generated from ions than from neutrals. The use of a capillary discharge to create a preformed plasma with a tailored level of ionization allows HHG from ions while avoiding ionization losses of the driving laser and ionization-induced defocusing. This leads to the generation of higher photon energies from ions with higher ionization potentials and an increase in efficiency of the entire generation process. Additionally, the radial electron density profile of the capillary discharge plasma is concave, producing an index waveguide. This plasma waveguide combats additional ionization-induced defocusing of the laser and allows for a decreased laser intensity near the walls of the capillary, making it possible to guide the higher intensities required for shorter wavelength generation without damaging the walls.

With this objective we have developed and characterized a discharge-ionized gas-filled capillary channel in which both the degree of ionization and the electron density profile can be tailored for propagation of an intense ultrashort laser pulse. Using a two-temperature one-dimensional Lagrangian hydrodynamic/atomic code developed at CSU we have predicted the characteristics of the capillary plasmas and the discharge parameters that are required to optimize the degree of ionization and the guiding for HHG. Current pulses of several microsecond duration and 5-150 A amplitude were used to create plasma channels in 175-250  $\mu\text{m}$  diameter capillary tubes. Time-resolved, visible spectroscopy of the discharge plasma confirms the model prediction that the level of ionization can be readily tuned by adjusting the amplitude of the discharge current. In these discharges the dynamics of the plasma is dominated by ohmic heating and heat conduction losses. Shortly after the initiation of the current pulse the plasma expands as a result of the larger temperature increase in the axial region of the plasma due to ohmic heating. The outer region of the plasma remains colder due to heat conduction to the capillary walls. This generates a radial electron density profile with minimum on axis and maximum at the capillary wall. This concave electron density profile gives origin to an index of refraction distribution with maximum on axis that guides the laser light. This profile is exactly opposite of the divergent profile created through optical field ionization by the driving laser. Experimentally, this waveguide has efficiently guided laser pulses with peak intensities over  $10^{15}$   $\text{W}/\text{cm}^2$  over lengths of 5 cm through a plasma formed from 6 Torr Ar. This capillary discharge can reliably operate at repetitions rates up to 100 Hz, which is unprecedented for a discharge designed for laser guiding.

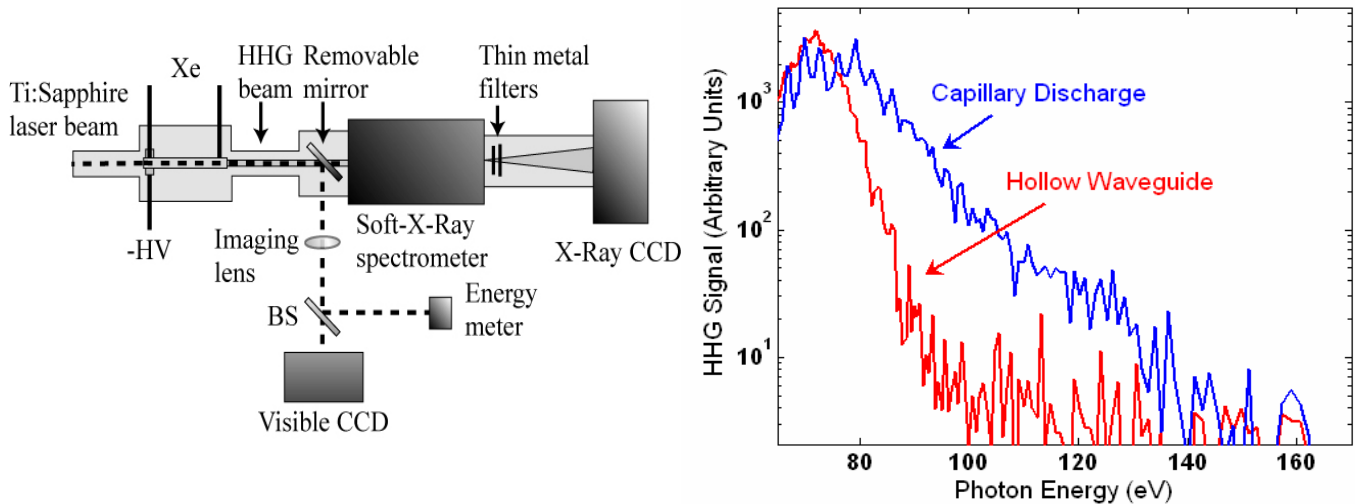


**Figure 1.** (left) Schematic of the experimental setup. (right) The high harmonic spectrum obtained with 5 A current pulses in 2.9 Torr Xe is shown in blue. In red, the spectrum obtained in neutral xenon without the discharge. The harmonic cutoff is extended by more than 50 eV by using the discharge. The flux at high photon energies is also dramatically enhanced.

## Results

We have investigated the up-conversion of laser pulses from a 10 Hz CPA Ti:Sapphire laser system ( $\lambda = 800$  nm) in a Xe plasma column created by a 5 cm long, 175  $\mu\text{m}$  inner diameter capillary discharge. The experimental setup is shown on the left of Figure 1. Laser pulses of 28 fs in duration and 5 mJ energy were focused to a diameter of  $\sim 100$   $\mu\text{m}$  at the entrance of the

capillary. Holes drilled 3 mm from either end of the capillary served as gas inlets allowing us to keep a constant gas pressure over the length of the capillary while maintaining vacuum at the entrance and exit of the discharge. Typically the discharge was operated with 2-4 Torr of xenon. Figure 1 (right) shows the harmonic spectrum obtained when a 5 A current pulse is used to preionize 2.9 Torr of xenon. Also shown is the spectrum obtained under the same conditions without the discharge. The highest photon energy extends to 150 eV when the capillary discharge is used to prepare a preformed, ionized plasma. This is significantly higher than the cutoff observed in the hollow waveguide without the discharge, and constitutes a dramatic extension over the highest previously reported harmonic generated from xenon, 75 eV. We also have achieved an enhancement of the harmonic flux near 90 eV of nearly 2 orders of magnitude. Figure 2 (top) shows the dependence of the highest harmonics on the time during the discharge current pulse at which the laser is injected. The highest harmonics are only generated for several microseconds after the peak of the current pulse. Time-resolved visible spectroscopy measurements, shown in the bottom of Figure 2, of the emission of the discharge plasma show that at this time the plasma is nearly completely ionized. This is in agreement with the computer simulations of the discharge. Furthermore, calculations of the ionization rates of the laser pulse predict that the highest harmonics (>75 eV) cannot be generated from neutral xenon. These calculations combined with the model of the discharge and visible spectroscopy show that the harmonics are generated entirely from Xe ions.

Another prominent feature of this data is that, in the 45–85 eV spectral region, the individual harmonic peaks are much better resolved when the discharge is used to preionize the xenon. This is seen in the left of Figure 3. Without the discharge, the lack of resolved harmonic peaks results from self-phase modulation of the fundamental laser pulse that would be expected to accompany the rapid ionization of the neutral xenon by the laser. When the discharge preionizes the xenon atoms, phase modulation of the laser is dramatically reduced leading to better resolved harmonic peaks. Spectral measurements of the laser pulses exiting the capillary show significant spectral broadening and blueshifting without the discharge, as shown in the right side of Figure 3. In contrast, when the discharge is on, the fundamental laser spectrum shows a very small change in spectrum from that observed from an evacuated capillary.

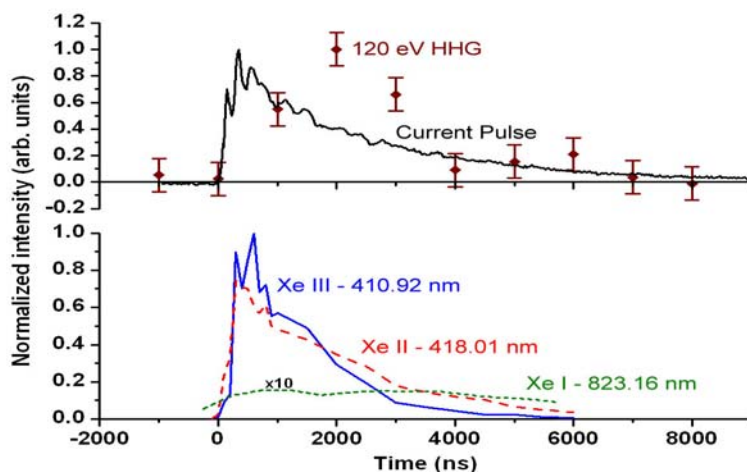


**Figure 2.** (top) Time evolution of the harmonic signal at 120 eV (diamonds). The capillary discharge current pulse is shown for reference (black). (bottom) Time evolution of visible emission lines from Xe I (823.16 nm), Xe II (418.01 nm), and Xe III (410.92 nm). This data shows that at the time during the current pulse that the highest harmonics are generated, the plasma is essentially completely ionized.

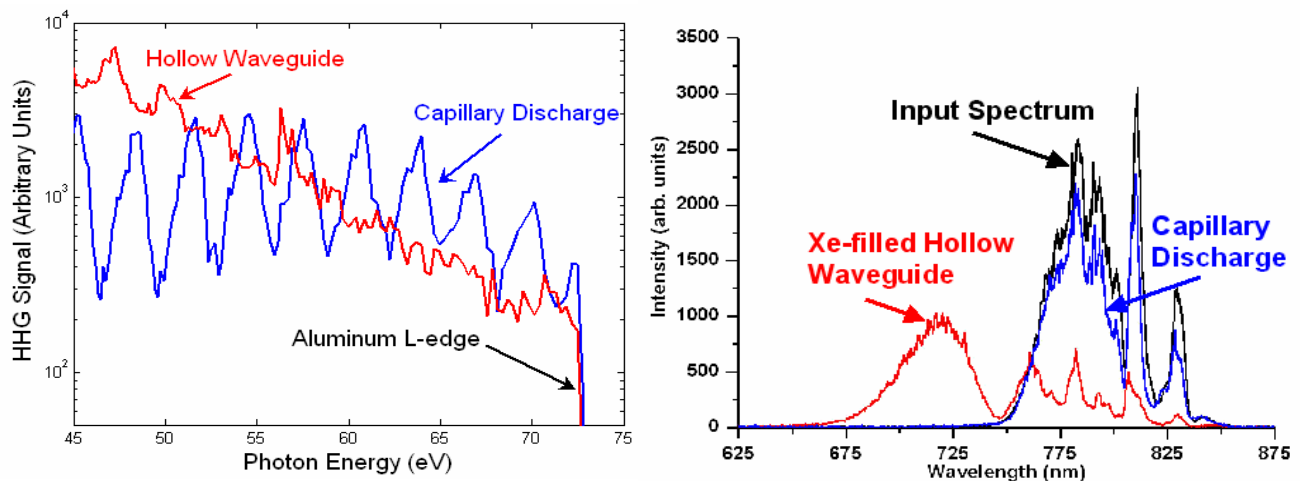


**Figure 3.** (left) Comparison of harmonic spectra obtained in the capillary discharge plasma and in a hollow waveguide. Individual harmonic peaks are much better resolved when the discharge is used due to the reduction of self-phase modulation of the driving laser pulse. The sharp edge at 72 eV is due to an aluminum filter used to reject the driving laser. (right) Spectrum of the driving laser entering and exiting the waveguides. The hollow waveguide spectrum is heavily blue shifted while the spectrum of the laser exiting the discharge is very similar to the input spectrum.

### Future plans

During the next year of the project we will continue investigate generation of high harmonics from ions in these discharge-created waveguides with lighter gases that have higher ionization potentials, such as argon and neon. The use of these higher ionization potential gases within the discharge will lead to significantly higher photon energies. In addition, quasi-phase matching methods within the plasma waveguide such as modulated guides and the use of two color driving laser pulses will be investigated.

### Journal publications from DOE sponsored research 2005-06

1. D.M. Gaudiosi, B. Reagan, T. Popmintchev, M. Grisham, M. Berrill, O. Cohen, B.C. Walker, M.M. Murnane, H.C. Kapteyn, J.J. Rocca, "High-Order Harmonic Generation from Ions in a Capillary Discharge", *Physical Review Letters*, **96**, 203001 (2006).
2. M.A. Larotonda, Y. Wang, M. Berrill, B.M. Luther, J.J. Rocca, Mahendra Man Shakya, S. Gilbertson, and Zenghu Chang, "Pulse duration measurements of grazing incidence pumped high repetition rate Ni-like Ag and Cd transient soft x-ray lasers". *Optics Letters*, in press (2006)
3. S. Heinbuch, M. Grisham, D. Martz, and J.J. Rocca, "Demonstration of a desk-top size high repetition rate soft x-ray laser", *Optics Express*, **13**, 4050, (2005).
4. Y. Wang, B.M. Luther, M. Berrill, M. Marconi, J.J. Rocca, "Capillary discharge-driven metal vapor plasma waveguides", *Physical Review E*, **72**, 026413, (2005)
5. B.M. Luther, Y. Wang, M. Berrill, D. Alessi, M.C. Marconi, M.A. Larotonda, and J.J. Rocca, "Highly ionized Ar plasma waveguides generated by a fast capillary discharge", *IEEE Transactions on Plasma Science*, **33**, 582, (2005).
6. Y. Wang, B.M. Luther, F. Pedacci, M. Berrill, F. Brizuela, M. Marconi, M.A. Larotonda, V.N. Shlyaptsev, and J.J. Rocca, "Dense Capillary Discharge Plasma Waveguide Containing Ag Ions", *IEEE Transactions on Plasma Science*, **33**, 584, (2005).

# DYNAMICS OF FEW-BODY ATOMIC PROCESSES

**Anthony F. Starace**

*The University of Nebraska  
Department of Physics and Astronomy  
116 Brace Laboratory  
Lincoln, NE 68588-0111*

*Email: astarace1@unl.edu*

## PROGRAM SCOPE

The goals of this project are to understand and describe processes involving energy transfers from electromagnetic radiation to matter as well as the dynamics of interacting few-body, quantum systems. Investigations of current interest are in the areas of high energy density physics, attosecond physics, strong field physics, and double photoionization processes. In some cases our studies are supportive of and/or have been stimulated by experimental work carried out by other investigators funded by the DOE AMO physics program.

## RECENT PROGRESS

### A. Non-Dipole Effects in Double Photoionization of He

In recent years two major themes in both experimental and theoretical studies of atomic photoionization have been the analysis of nondipole (or retardation) effects in single-electron photoionization (both in the soft x-ray and the vuv regions) and the analysis of double photoionization (especially in the vuv energy region). Surprisingly, there have not been as yet any analyses of nondipole effects on double photoionization. In part this is because nearly all experimental measurements have been carried out with linear polarization in the orthogonal plane geometry (i.e., photoelectrons are detected in the plane perpendicular to the photon wave vector). For this case, non-dipole effects vanish. One year ago we completed an analysis of nondipole effects on the triply differential cross section (TDCS) for double photoionization of He (see publications [4], [5], and [7]). Specifically, we have derived a general parameterization for the double photoionization amplitude of He taking into account both dipole (E1) and quadrupole (E2) components of the electron-photon interaction operator. Nondipole effects originate from the interference of the E1 and E2 amplitudes. Our numerical results show that these effects are significant in double photoionization of He even for excess energies as low as 80 eV and that they should be observable in experiments with current state-of-the-art capabilities.

For the case of linearly polarized light, we have analyzed [4, 7] our parameterized formulas for the TDCS and proposed two experimental geometries for which the nondipole effects are maximal, one for equal energy sharing and one for unequal energy sharing. For the case of circularly polarized light, we analyzed [5, 7] the influence of nondipole interactions on the circular dichroism (CD) effect in double photoionization of He. We have shown analytically that there exists a nonzero CD effect for the case of equal energy sharing. We have also predicted unusual asymmetries of the TDCS for the case of elliptically polarized light. We have proposed two experimental arrangements for measuring each of these effects, which together provide a polarization sensitive means of measuring nondipole effects in double photoionization. Our numerical estimates indicate that CD effects are significant for electron energies as low as 40 eV.

Recently, we have analyzed non-dipole effects on double-differential cross sections, have parametrized these in terms of four dynamical parameters, and have proposed experimental configurations to best measure these effects [8]. We have also made predictions for non-dipole effects on TDCSs at high excess energies that give improved agreement with experiments using linearly polarized light [10]. An invited talk on our work was presented at an international conference in Buenos Aires in summer 2005 [9].

### **B. GeV Electrons from Ultra Intense Laser Interactions with Highly Charged Ions**

We have investigated in great detail recently [11] the interaction of intense laser radiation with highly charged hydrogenic ions using a three-dimensional relativistic Monte Carlo simulation. This work extended an earlier investigation [S.X. Hu and A.F. Starace, *Phys. Rev. Lett.* **88**, 245003 (2002)] in which it was demonstrated that free electrons cannot be accelerated to GeV energies by the highest intensity lasers because they are quickly expelled from the laser pulse before it reaches peak intensity. We showed that highly charged ions exist that (1) have deep enough potential wells that tunneling ionization is insignificant over the duration of an intense, short laser pulse, and (2) have potentials that are not too deep, so that the laser pulse is still able to ionize the bound electron when the laser field reaches its peak intensity. We showed that when the ionized electron experiences the peak intensity of the laser field, then it is accelerated to relativistic velocity along the laser propagation direction (by the Lorentz force) within a tiny fraction of a laser cycle. Within its rest frame it then “rides” on the peak laser amplitude and is accelerated to GeV energies before being expelled from the laser pulse. Our recent work [11] includes an extensive set of calculations to demonstrate the dependence of the ionized electron energy spectrum on the experimentally controllable parameters. These include the target ion and the laser intensity, frequency, duration, and, especially, the focal properties.

### **C. Elliptic and Circular Dichroism in Two-Photon Double Ionization of Atoms**

Recent advances in generating vuv light of higher intensity (than provided by synchrotrons) make possible studies of multi-electron ejection due to multiphoton interactions of atomic electrons with vuv radiation. Two-photon double ionization (TPDI) of He has recently attracted much attention, as its study provides new insights into two-electron ejection dynamics. However, so far all studies of TPDI have been limited to the case of linearly polarized light. Within the past year, we have investigated how the shape of the photoelectron angular distribution in TPDI [i.e., of the triply-differential cross section (TDCS)] depends upon the

handedness of (in general elliptically-polarized) vuv radiation. We have derived an *ab initio* parametrization of the two-photon double ionization amplitude from an  $s^2$  subshell of an atom in a  $^1S$ -state and used it to predict two light polarization effects on photoelectron angular distributions that do not exist in single-photon double ionization: (i) elliptic dichroism and (ii) circular dichroism at equal energy sharing. Our estimates for He show large magnitudes for these effects, which provide a means for polarization control of double ionization by vuv light. A manuscript on this work has recently been submitted to *Physical Review Letters*.

#### **D. CWDVR Method for Atomic Systems in Short Laser Pulse Fields**

Very recently, we have been developing an efficient and accurate grid method for solving the time-dependent Schrödinger equation for an atomic system interacting with an intense laser pulse. Instead of the usual finite difference (FD) method, the radial coordinate is discretized using the discrete variable representation (DVR) constructed from Coulomb wave functions. For an accurate description of the ionization dynamics of atomic systems, we have found that the Coulomb wave function discrete variable representation (CWDVR) method needs 3-10 times fewer grid points than the FD method owing to the fact that the CWDVR grid points are distributed unevenly but more effectively. The other important advantage of the CWDVR method is that it treats the Coulomb singularity accurately and gives a good representation of continuum wave functions. The time propagation of the wave function is implemented using the well-known Arnoldi method. We have tested the method for treating multiphoton ionization of both the  $H$  atom and the  $H^-$  ion in intense laser fields. The short-time excitation and ionization dynamics of  $H$  interacting with an abruptly introduced static electric field has also investigated. For a wide range of field parameters, ionization rates calculated using the CWDVR method are found to be in excellent agreement with those of other accurate theoretical calculations. A report on this work will soon be submitted for publication.

#### **FUTURE PLANS**

Our group is currently carrying out research on the following projects: (1) Analysis of doubly differential two-photon, double ionization cross sections for He; (2) Development of an effective range theory approach for laser-assisted electron-atom scattering; and (3) Analysis of attosecond pulse interactions with atomic systems using the newly developed CWDVR method described in Sec. D above.

#### **PUBLICATIONS STEMMING FROM DOE-SPONSORED RESEARCH (July 2003 – June 2006)**

- [1] M. Masili and A.F. Starace, “Static and Dynamic Dipole Polarizability of the He Atom Using Wave Functions Involving Logarithmic Terms,” *Phys. Rev. A* **68**, 012508 (2003).
- [2] G. Lagmago Kamta and A.F. Starace, “Elucidating the Mechanisms of Double Ionization Using Intense Half-Cycle, Single-Cycle, and Double Half-Cycle Pulses,” *Phys. Rev. A* **68**, 043413 (2003).

- [3] A.Y. Istomin, N.L. Manakov, and A.F. Starace, “Perturbative Analysis of the Triply Differential Cross Section and Circular Dichroism in Photo Double Ionization of He,” *Phys. Rev. A* **69**, 032713 (2004).
- [4] A.Y. Istomin, N.L. Manakov, A.V. Meremianin, and A.F. Starace, “Non-Dipole Effects in Photo Double Ionization of He by a VUV Photon,” *Phys. Rev. Lett.* **92**, 063002 (2004).
- [5] A.Y. Istomin, N.L. Manakov, A.V. Meremianin, and A.F. Starace, “Circular Dichroism at Equal Energy Sharing in Photo Double Ionization of He,” *Phys. Rev. A* **70**, 010702(R) (2004).
- [6] A.V. Flegel, M.V. Frolov, N.L. Manakov, and A.F. Starace, “Circularly Polarized Laser Field-Induced Rescattering Plateaus in Electro-Atom Scattering,” *Phys. Lett. A* **334**, 197 (2005).
- [7] A.Y. Istomin, N.L. Manakov, A.V. Meremianin, and A.F. Starace, “Nondipole Effects in the Triply-Differential Cross Section for Double Photoionization of He,” *Phys. Rev. A* **71**, 052702 (2005).
- [8] A.Y. Istomin, A.F. Starace, N.L. Manakov, A.V. Meremianin, A.S. Kheifets, and I. Gray, “Parametizations and Dynamical Analysis of Angle-Integrated Cross Sections for Double Photoionization Including Nondipole Effects,” *Phys. Rev. A* **72**, 052708 (2005).
- [9] A.Y. Istomin, N.L. Manakov, A.V. Meremianin, and A.F. Starace, “Non-Dipole Effects in Double Photoionization of He,” in *Ionization, Correlation, and Polarization in Atomic Collisions*, ed. A. Lahmam-Bennani and B. Lohmann (A.I.P., Melville, NY, 2006), pp. 18-23.
- [10] A.Y. Istomin, A.F. Starace, N.L. Manakov, A.V. Meremianin, A.S. Kheifets, and I. Bray, “Nondipole Effects in Double Photoionization of He at 450 eV Excess Energy,” *J. Phys. B* **39**, L35 (2006).
- [11] S.X. Hu and A.F. Starace, “Laser Acceleration of Electrons to GeV Energies Using Highly Charged Ions,” *Phys. Rev. E* **73**, 066502 (2006).
- [12] L.Y. Peng, Q. Wang, and A.F. Starace, “Photodetachment of H<sup>-</sup> by a Short Laser Pulse in Crossed Static Electric and Magnetic Fields,” *Phys. Rev. A* **74**, xxx (2006).

# **FEMTOSECOND AND ATTOSECOND LASER-PULSE ENERGY TRANSFORMATION AND CONCENTRATION IN NANOSTRUCTURED SYSTEMS**

DOE Grant No. DE-FG02-01ER15213

Mark I. Stockman, Pi

Department of Physics and Astronomy, Georgia State University, Atlanta, GA 30303

E-mail: [mstockman@gsu.edu](mailto:mstockman@gsu.edu), URL: <http://www.phy-astr.gsu.edu/stockman>

Report for the Grant Period of 2005-2006 (Publications 2004-2006)

## **1 Program Scope**

The program is aimed at theoretical investigations of a wide range of phenomena induced by ultrafast laser-light excitation of nanostructured or nanosize systems, in particular, metal/semiconductor/dielectric nanocomposites and nanoclusters. Among the primary phenomena are processes of energy transformation, generation, transfer, and localization on the nanoscale and coherent control of such phenomena.

## **2 Recent Progress**

### **2.1 SPASER: Effect, and Prospective Devices [1, 2]**

We have earlier introduced a novel concept of SPASER (Surface Plasmon Amplification by Stimulated Emission of Radiation) [3]. Spaser is predicted to generate ultrashort (10-100 fs) ultraintense (optical electric field  $\sim 10^8$  V/cm or greater) pulses of local optical fields at nanoscale. When realized experimentally spaser may completely change the nanooptics.

Recently, we have shown theoretically that the efficient nanolens, which is a self-similar aggregate of a few metal nanosphere, in an active medium of semiconductor quantum dots is an efficient spaser [2]. This spaser possesses a sharp hot spot of local fields in its nanofocus between the minimum-radius nanospheres. A related recent development has been an experiment by a group of L. Eng of Technical University of Dresden (Germany) where the principles of spaser have been confirmed [4].

### **2.2 Nanofocusing of Optical Energy in Tapered Plasmonic Waveguides [5, 6]**

We have predicted theoretically that surface plasmon polaritons propagating toward the tip of a tapered plasmonic waveguide are slowed down and asymptotically stopped when they tend to the tip, never actually reaching it (the travel time to the tip is logarithmically divergent). This phenomenon causes accumulation of energy and giant local fields at the tip. There are various prospective applications of this proposed effect in nanooptics and nanotechnology. Because there is transfer from micro- to nanoscale of not only energy, but also coherence (phase), these results allow for full coherent control on the nanoscale.

### **2.3 Coherent Control of Ultrafast Energy Localization on Nanoscale [7, 8]**

Our research has significantly focused on problem of controlling localization of the energy of ultrafast (femtosecond) optical excitation on the nanoscale. We have proposed and theoretically developed a distinct approach to solving this fundamental problem [7, 9-13]. This approach, based on the using the relative phase of the light pulse as a functional degree of freedom, allows one to control the spatial-temporal distribution of the excitation energy on the nanometer-femtosecond scale. We have shown that using even the simplest phase modulation, the linear chirp, it is possible to shift in time and spatially concentrate the linear local optical fields, but the integral local energy does not depend on the phase modulation. In contrast, for nonlinear responses, the integral local energy efficiently can be coherently controlled. It is difficult to overestimate possible applications of this effect, including nano-chip computing, nanomodification (nanolithography), and ultrafast nano-sensing. Recently, we have shown [8] that using two-pulse (interferometric) coherent control in a complex random nanosystem it is possible to localize the ultrafast

optical fields in with spatial resolution of down to 2 nm. In specially designed V-shape nanoantennas, it is possible to move the “hot spot” of plasmonic excitation to a given nanometric hot spot along a 30 nm extension of this nanoantenna [8].

Following our pioneering work, there has recently been an explosion of activity on both theoretical [14-17] and experimental [18-21] investigations of the ultrafast coherent control on the nanoscale. This field will rapidly grow into one of the most important in the nanoscience with application to the nanoscale computations, sensing, spectroscopy, etc. It will require our increased attention to stay at the forefront.

## **2.4 Efficient Nanolens [2, 22, 23]**

As an efficient nanolens, we have proposed a self-similar linear chain of several metal nanospheres with progressively decreasing sizes and separations [24]. The proposed system can be used for nano-optical detection, Raman characterization, nonlinear spectroscopy, nano-manipulation of single molecules or nanoparticles, and other applications. Recently, we have shown [2] that this nanolens surrounded by an active medium of nanocrystal quantum dots can be an efficient spaser. Another development has been a theory of the second-harmonic generation in an efficient nanolens (a linear self-similar aggregate of a few metal nanospheres) [23]. The second harmonic local fields form a very sharp nanofocus between the smallest spheres where these fields are enhanced by more than two orders of magnitude. This effect can be used for diagnostics and nanosensors.

## **2.5 Second Harmonic Generation on Nanostructured Surfaces [25]**

This research resulted from an international collaboration with the group of Prof. Joseph Zyss (France). [25-27]. Based on the spectral-expansion Green’s function theory, we theoretically describe the topography, polarization, and spatial-coherence properties of the second-harmonic (SH) local fields at rough metal surfaces. We have recently investigated this class of phenomena to predict and describe giant fluctuations of local SH fields in random nanostructures [25].

## **2.6 Strong Field Effects in Nanostructures: Forest Fire Mechanism of Dielectric Breakdown [28, 29]**

This research is a result of an extensive international collaboration (UK, Germany, Canada, and the USA). We have described the interaction of ultrashort infrared laser pulses with clusters and dielectrics. Rapid ionization occurs on a sub-laser wavelength scale below the conventional breakdown threshold. It starts with the formation of nanodroplets of plasma that grow like forest fires, without any need for heating of the electrons promoted to the conduction band. This effect is very important for the physics of laser damage of semiconductors and dielectrics by a moderate-intensity radiation. This research has recently been extended to include some effects of the nanostructured plasmas generated in the process of the photoinduced damage (modification) of the solids.

## **2.7 Theory of Coherent Near-Field Optical Microscopy [30, 31]**

We have developed theory of phase-sensitive near-field scanning optical microscopy (in collaboration with the group of Dr. Victor Klimov, LANL). It is possible to determine the spectral phase of the surface plasmon resonances in metal nanoparticles. In turn, this allows us to determine the positions of these resonances with unprecedented resolution. Recently the interference near-field spectroscopy that we proposed and developed was used [32] for further studies of plasmonic nanosystems with proper reference to our work.

## **2.8 Nanoplasmonics at Metal Surface: Enhanced Relaxation and Superlensing [33, 34]**

We have considered a nanoscale dipolar emitter (quantum dot, atom, fluorescent molecule, or rare earth ion) in a nanometer proximity to a flat metal surface. There is strong interaction of this emitter with unscreened metal electrons in the surface nanolayer that causes enhanced relaxation due to surface plasmon excitation and Landau damping. For the system considered, conventional theory based on metal as continuous dielectric fails both qualitatively and quantitatively.

In a recent development [34], we have considered a principal limitations on the spatial resolution on the nanoscale of the “Perfect Lens” introduced by Pendry, also known as the superlens. In the conventional, local electrodynamics, the superlens builds a 3d image in the near zone without principal limitations on the spatial resolution. We have shown that there is a principal limitation on this resolution, ~5 nm in practical

terms, which originates from the spatial dispersion and Landau damping of dielectric responses of the interacting electron fluid in metals.

## 2.9 Theory of SERS [35]

We have revisited theory of one of the most important phenomena in nanoplasmonics, Surface Enhanced Raman Scattering. This theory shows that the predicted levels of enhancement in the red spectral region are still several orders of magnitude less than the enhancement factors  $\sim 10^{13} - 10^{14}$  observed experimentally. The difference may be due to the effects not taken into account by the theory: self-similar enhancement [24] or chemical enhancement [36].

## 2.10 Excitation of Surface Plasmon Polaritons (SPPs) by Free Electron Impact [37]

We have provided theoretical support and interpretation for the experimental investigation of the SPP generation by free-electron impact. This effect can be used as a basis of a novel method to visualize eigenmodes of plasmonic nanosystem by exciting them with an electron microscope beam.

## 3 Future Plans

We will develop both the theory in the directions specified above and the collaborations with the experimental and theoretical groups that we have developed. Among the future projects, we will consider attosecond effects of the carrier-envelope phase. We will also consider mechanical effects of the  $\omega - 2\omega$  interference in nanosystems. Yet another direction will be theory of full spatio-temporal control on the nanoscale.

## 4 Publications Resulting from the Grant

The major articles published by our group during this Report (2004-2006) period are indicated by bold typeface at the corresponding headings above.

## References

1. D. J. Bergman and M. I. Stockman, *Can We Make a Nanoscopic Laser?*, *Laser Phys* **14**, 409-411 (2004).
2. K. Li, X. Li, M. I. Stockman, and D. J. Bergman, *Surface Plasmon Amplification by Stimulated Emission in Nanolenses*, *Phys. Rev. B* **71**, 115409-1-4 (2005).
3. D. J. Bergman and M. I. Stockman, *Surface Plasmon Amplification by Stimulated Emission of Radiation: Quantum Generation of Coherent Surface Plasmons in Nanosystems*, *Phys. Rev. Lett.* **90**, 027402-1-4 (2003).
4. J. Seidel, S. Grafstroem, and L. Eng, *Stimulated Emission of Surface Plasmons at the Interface between a Silver Film and an Optically Pumped Dye Solution*, *Phys. Rev. Lett.* **94**, 177401-1-4 (2005).
5. M. I. Stockman, in *Plasmonics: Metallic Nanostructures and Their Optical Properties II*, edited by N. J. Halas and T. R. Huser, *Delivering Energy to Nanoscale: Rapid Adiabatic Transformation, Concentration, and Stopping of Radiation in Nano-Optics* (SPIE, Denver, Colorado, 2004), Vol. 5512, p. 38-49.
6. M. I. Stockman, *Nanofocusing of Optical Energy in Tapered Plasmonic Waveguides*, *Phys. Rev. Lett.* **93**, 137404-1-4 (2004).
7. M. I. Stockman, D. J. Bergman, and T. Kobayashi, *Coherent Control of Nanoscale Localization of Ultrafast Optical Excitation in Nanosystems*, *Phys. Rev. B* **69**, 054202-10 (2004).
8. M. I. Stockman and P. Hewageegana, *Nanocalibrated Nonlinear Electron Photoemission under Coherent Control*, *Nano Lett.* **5**, 2325-2329 (2005).
9. M. I. Stockman, S. V. Faleev, and D. J. Bergman, *Coherent Control of Femtosecond Energy Localization in Nanosystems*, *Phys. Rev. Lett.* **88**, 67402-1-4 (2002).
10. M. I. Stockman, S. V. Faleev, and D. J. Bergman, *Coherently Controlled Femtosecond Energy Localization on Nanoscale*, *Appl. Phys. B* **74**, S63-S67 (2002).
11. M. I. Stockman, S. V. Faleev, and D. J. Bergman, *Coherently-Controlled Femtosecond Energy Localization on Nanoscale*, *Appl. Phys. B* **74**, 63-67 (2002).
12. M. I. Stockman, D. J. Bergman, and T. Kobayashi, in *Proceedings of SPIE: Plasmonics: Metallic Nanostructures and Their Optical Properties*, edited by N. J. Halas, *Coherent Control of Ultrafast Nanoscale Localization of Optical Excitation Energy* (SPIE, San Diego, California, 2003), Vol. 5221, p. 182-196.
13. M. I. Stockman, S. V. Faleev, and D. J. Bergman, in *Ultrafast Phenomena XIII, Coherently-Controlled Femtosecond Energy Localization on Nanoscale* (Springer, Berlin, Heidelberg, New York, 2003).
14. M. Sukharev and T. Seideman, *Phase and Polarization Control as a Route to Plasmonic Nanodevices*, *Nano Lett.* **6**, 715-719 (2006).

15. M. Sukharev and T. Seideman, *Coherent Control Approaches to Light Guidance in the Nanoscale*, J. Chem. Phys. **124**, - (2006).
16. T. Brixner, F. J. G. d. Abajo, J. Schneider, C. Spindler, and W. Pfeiffer, *Ultrafast Adaptive Optical near-Field Control*, Phys. Rev. B **73**, 125437 (2006).
17. T. Brixner, F. J. G. d. Abajo, J. Schneider, and W. Pfeiffer, *Nanoscope Ultrafast Space-Time-Resolved Spectroscopy*, Phys. Rev. Lett. **95**, 093901 (2005).
18. A. Kubo, K. Onda, H. Petek, Z. Sun, Y. S. Jung, and H. K. Kim, *Femtosecond Imaging of Surface Plasmon Dynamics in a Nanostructured Silver Film*, Nano Lett. **5**, 1123-1127 (2005).
19. A. Kubo, K. Onda, H. Petek, Z. Sun, Y. S. Jung, and H. K. Kim, in Ultrafast Phenomena XIV, edited by T. Kobayashi, T. Okada, T. Kobayashi, K. A. Nelson and S. D. Silvestri, *Imaging of Localized Silver Plasmon Dynamics with Sub-Fs Time and Nano-Meter Spatial Resolution* (Springer, Niigata, Japan, 2004), Vol. 79, p. 645-649.
20. P. v. d. Walle, L. Kuipers, and J. L. Herek, in Ultrafast Phenomena XV, *Coherent Control of Light in Metal Nanostructures* (Pacific Grove, California, 2006), p. Paper TuD3.
21. M. Bauer, D. Bayer, T. Brixner, F. J. G. d. Abajo, W. Pfeiffer, M. Rohmer, C. Spindler, and F. Steeb, in Ultrafast Phenomena XV, *Adaptive Control of Nanoscopic Photoelectron Emission* (Pacific Grove, California, 2006), p. Paper ThB3.
22. M. I. Stockman, K. Li, X. Li, and D. J. Bergman, in Plasmonics: Metallic Nanostructures and Their Optical Properties II, edited by N. J. Halas and T. R. Huser, *An Efficient Nanolens: Self-Similar Chain of Metal Nanospheres* (SPIE, 2004), Vol. 5512, p. 87-99.
23. K. Li, M. I. Stockman, and D. J. Bergman, *Enhanced Second Harmonic Generation in a Self-Similar Chain of Metal Nanospheres*, Phys. Rev. B **72**, 153401-1-4 (2005).
24. K. Li, M. I. Stockman, and D. J. Bergman, *Self-Similar Chain of Metal Nanospheres as an Efficient Nanolens*, Phys. Rev. Lett. **91**, 227402-1-4 (2003).
25. M. I. Stockman, *Giant Fluctuations of Second Harmonic Generation on Nanostructured Surfaces*, Chem. Phys. **318**, 156-162 (2005).
26. M. I. Stockman, D. J. Bergman, C. Anceau, S. Brasselet, and J. Zyss, *Enhanced Second-Harmonic Generation by Metal Surfaces with Nanoscale Roughness: Nanoscale Dephasing, Depolarization, and Correlations*, Phys. Rev. Lett. **92**, 057402-1-4 (2004).
27. M. I. Stockman, D. J. Bergman, C. Anceau, S. Brasselet, and J. Zyss, in Complex Mediums V: Light and Complexity, edited by M. W. McCall and G. Dewar, *Enhanced Second Harmonic Generation by Nanorough Surfaces: Nanoscale Depolarization, Dephasing, Correlations, and Giant Fluctuations* (SPIE, 2004), Vol. 5508.
28. L. N. Gaier, M. Lein, M. I. Stockman, P. L. Knight, P. B. Corkum, M. Y. Ivanov, and G. L. Yudin, *Ultrafast Multiphoton Forest Fires and Fractals in Clusters and Dielectrics*, J. Phys. B: At. Mol. Opt. Phys. **37**, L57-L67 (2004).
29. L. N. Gaier, M. Lein, M. I. Stockman, G. L. Yudin, P. B. Corkum, M. Y. Ivanov, and P. L. Knight, *Hole-Assisted Energy Deposition in Dielectrics and Clusters in the Multiphoton Regime*, J Mod Optic **52**, 1019-1030 (2005).
30. A. A. Mikhailovsky, M. A. Petruska, M. I. Stockman, and V. I. Klimov, *Broadband near-Field Interference Spectroscopy of Metal Nanoparticles Using a Femtosecond White-Light Continuum*, Opt. Lett. **28**, 1686-1688 (2003).
31. A. A. Mikhailovsky, M. A. Petruska, K. Li, M. I. Stockman, and V. I. Klimov, *Phase-Sensitive Spectroscopy of Surface Plasmons in Individual Metal Nanostructures*, Phys. Rev. B **69**, 085401-1-6 (2004).
32. K. Lindfors, T. Kalkbrenner, P. Stoller, and V. Sandoghdar, *Detection and Spectroscopy of Gold Nanoparticles Using Supercontinuum White Light Confocal Microscopy*, Phys. Rev. Lett. **93**, 037401-1-4 (2004).
33. I. A. Larkin, M. I. Stockman, M. Achermann, and V. I. Klimov, *Dipolar Emitters at Nanoscale Proximity of Metal Surfaces: Giant Enhancement of Relaxation in Microscopic Theory*, Phys. Rev. B **69**, 121403(R)-1-4 (2004).
34. I. A. Larkin and M. I. Stockman, *Imperfect Perfect Lens*, Nano Lett. **5**, 339-343 (2005).
35. M. I. Stockman, in Springer Series Topics in Applied Physics, edited by K. Kneipp, M. Moskovits and H. Kneipp, *Surface Enhanced Raman Scattering – Physics and Applications* (Springer-Verlag, Heidelberg New York Tokyo, 2006).
36. J. Jiang, K. Bosnick, M. Maillard, and L. Brus, *Single Molecule Raman Spectroscopy at the Junctions of Large Ag Nanocrystals*, J. Phys. Chem. B **107**, 9964-9972 (2003).
37. M. V. Bashevoy, F. Jonsson, A. V. Krasavin, N. I. Zheludev, Y. Chen, and M. I. Stockman, *Generation of Traveling Surface Plasmon Waves by Free-Electron Impact*, Nano Lett. **6**, 1113-1115 (2006).

# Laser-Produced Coherent X-Ray Sources

Donald Umstadter

*212 Ferguson, University of Nebraska, Lincoln, NE 68588*  
*dpu@unlserve.unl.edu*

## 1 Program Scope:

In this project, we experimentally and theoretically explore the physics of novel x-ray sources, which are based on the interactions of ultra-high-intensity laser light with matter. The x-ray source design parameters are angstrom-wavelength, femtosecond-duration, and a footprint small enough to fit in a university laboratory. A promising approach to reach this goal involves the nonlinear or relativistic Thomson scattering of intense laser light from a relativistic electron beam. In this process, eV-energy laser light is Doppler-shifted into keV-energy x-rays. Moreover, because the electron beam is accelerated by the ultra-high gradient of a laser wakefield—driven by a pulse from the same laser system—the combined length of both the accelerator and wiggler regions is millimeter length scale. Such sources have applications as novel tools in chemistry, biology, physics and material science for the study of ultrafast processes, such as inner shell excitations and optically-induced phase transitions. They also have industrial applications to non-destructive testing, submicron-resolution imaging of cracks, remote sensing and advanced nuclear fusion.

## 2 Recent Progress:

We have investigated laser-driven x-ray sources both experimentally as well as theoretically. Two types of sources were demonstrated: one based on Thomson scattering [11], in which the laser light pulse acts directly as the wiggler, and another based on betatron oscillations, in which an ion channel—produced in the wake of the laser pulse—acts as the wiggler [16]. We have also demonstrated that it is possible to condition an MeV electron beam optically which would enable the generation of ultrashort duration, hard x-ray pulses [10]. The results are found to agree with a novel electromagnetic field model that we developed, which provides an exact solution for the field distribution at the focus for a laser beam of arbitrary spot size and pulse duration [1, 2, 3, 4, 5]. Last, we now have—in our newly renovated laboratory—an operational laser system with 100-TW peak power, 25-fs pulse duration and 10-Hz repetition rate.

### 2.1 Experiment

#### 2.1.1 Laser based synchrotron radiation

Beams of x rays in the keV energy range were produced from the interaction of a intense laser with plasma. Here, energetic electrons are accelerated by a laser wakefield, and experience betatron oscillations in an ion channel formed in the wake of the intense femtosecond laser pulse. The experiment was performed at the Laboratoire d'Optique Appliquée with a laser delivering energies up to 1 J on target in 30 fs (FWHM) pulses, with a linear horizontal polarization. The laser beam was focused with an f/18 off-axis parabolic mirror onto the edge of a supersonic

helium gas jet (diameter 3 mm). The vacuum-focused intensity  $I_L = 3 \times 10^{18} \text{ W cm}^2$ , for which the corresponding normalized vector potential  $a_0 = 1.2$ . We observed an intense, broadband beam of x-ray radiation in the keV spectral range, and confined in the forward direction within a 50-mrad cone (FWHM). The spectral distribution of the radiation was measured from 1 keV to 10 keV by placing a set of Be, Al, Cu, and Ni filters in front of the detector. The spectrum depicted decreases exponentially from 1 to 10 keV. The total number of photons (integrated over the bandwidths of the filters and over the divergence of the x-ray beam) is found to be more than  $10^8$  photons (per shot/solid angle at 0.1% BW). The most important feature of the observed x-ray emission is its collimation in a low divergence beam centered onto the laser axis. Recorded for x-ray energies above 1 keV and for  $n_e = 8 \times 10^{18} \text{ cm}^{-3}$ , the beam divergence is found to be 20 mrad (FWHM).

### 2.1.2 Conditioning of laser-produced electron beams

The interaction of a laser-produced electron beam with an ultraintense laser pulse in free space is studied. We show that the optical pulse with  $a_0 = 0.5$  imparts momentum to the electron beam, causing it to deflect along the laser propagation direction. The observed 3-degree angular deflection is found to be independent of polarization and in good agreement with a theoretical model for the interaction of free electrons with a tightly focused Gaussian pulse, but only when longitudinal fields are taken into account. This technique was used to temporally characterize a subpicosecond laser-wakefield-driven electron bunch.

Optical manipulation of the electron trajectories can be applied to conditioning laser-produced electron beams. Since the magnitude of the deflection depends on the electron energy for a fixed laser intensity, a quasi-monochromatic, low-emittance, ultrashort-pulse electron beam can be obtained by using a suitable aperture downstream of the interaction region. Applications include high temporal resolution electron diffraction, shock and laboratory astrophysics, and electron beam injection for accelerators.

### 2.1.3 Facilities Development

Last, we have just completed the construction of a high-power-laser facility at UNL nominally operating at peak power of 100 TW, a pulse duration of 25 fs, and a repetition rate of 10 Hz. Achievement of these laser parameters should allow us to meet the future x-ray source requirements. The pulse duration of both the laser and the x-rays are 25 fs. Besides x-ray source development, this laser has other applications in high-field physics, because, when focused, it can reach an unprecedented level of intensity of  $6 \times 10^{22} \text{ W/cm}^2$ , which produces a relativistic mass shift—due to the electron’s quiver motion—of seventy times the electron rest mass. The system is extremely stable (short-term stability of the order of 1% and long-term stability  $\sim 5\%$ ), attributes that will make it viable for reproducible experimental results and applications.

To support the stringent demands of such a state-of-the-art laser system, our 5,000-sq-ft laboratory has undergone a multi-million-dollar renovation to provide it with a high degree of stability in terms of temperature ( $< \pm 0.5$  degree C), humidity ( $< 5\%$ ), and vibration. The 1,300-sq-ft target room is also radiation shielded.

## 2.2 Theory

Current electron beam sources that might be used for ultrafast structural analysis suffer from two limitations: (1) Because of space-charge broadening, low-energy e-beams from laser-triggered photocathodes have limited charge and relatively long duration; (2) Because of nonlinearity, high-energy electrons from wakefields lack controllable energy spreads. In order to design a

source that might overcome these limitations, we have numerically simulated our experimental study (discussed in Sec. 2.1.2) on acceleration of electrons by a laser in vacuum. We showed that quasi-monoenergetic and ultra-short duration electron bunches could be produced by deflecting a laser-accelerated electron beam by a synchronized high-intensity laser pulse. In the simulation, a laser of intensity  $10^{19}$  W/cm<sup>2</sup> produces a deflected electron beam of charge  $7 \times 10^8$  electrons and energy  $2.4 \pm 0.5$  MeV. Currently we are simulating the requirements for using MeV electron beams for ultrafast electron diffraction. The crucial parameters are the beam current and divergence in order to obtain measurable diffraction and permit single-shot operation with sub-100 fs resolution.

These investigations of laser acceleration of electrons by laser light in vacuum prompted the development of an exact solution for the fields of a focused laser for arbitrary spot size and pulse duration. We found theoretically that, in comparison with monochrome fields, the inclusion of longer wavelengths reduces the fraction of laser energy in the focus from 86.5% to 72.7% in a single-cycle Ti:Sapphire laser pulse. Thus, unlike light with long pulse duration (many optical cycles), the transverse distribution of the field is found to depend on the longitudinal field profile [1, 2, 3, 4, 5].

### 3 Future Plans

Using our new laser facility, we propose to develop high-brightness and ultrafast x-ray sources, driven all-optically, with the overall goal of obtaining femtosecond pulses of quasi-monochromatic keV x-rays to permit the study of ultrafast dynamics in materials with atomic resolution. We will also explore the use of ultrashort laser-produced and optically-conditioned electron bunches as an alternative to x-ray probes, with a view to extending current electron microscopy and diffraction techniques to more energetic electrons, thus permitting the use of a large number of electrons per bunch, without the loss of ultrafast resolution. The results of the proposed radiation-generation experiments will be analyzed in detail by the use of quasi-analytical models as well as particle-in-cell simulations, with a view towards developing a detailed understanding of the complex nonlinear physics governing high-intensity laser-produced plasmas. Besides the goals elaborated in the project scope (Sec. 1), a near-term goal is to demonstrate the generation of an x-ray intensity that is sufficient to study nonlinear (two-photon) atomic processes.

### References

- [1] S. Sepke and D. Umstadter, "Exact analytical solution for the vector electromagnetic field of Gaussian, attenuated Gaussian, and annular Gaussian laser modes," *Opt. Lett.* 31, 1447 (2006).
- [2] S. Sepke and D. Umstadter, "Analytical solutions for the electromagnetic fields of tightly focused laser beams of arbitrary pulse length," *Opt. Lett.* (accepted for publication, 2006).
- [3] S. Sepke and D. Umstadter, "Analytical solutions for the electromagnetic fields of attenuated and annular Gaussian laser modes Part I. Small F-number laser focusing," *JOSA B* (accepted for publication, 2006).
- [4] S. Sepke and D. Umstadter, "Analytical solutions for the electromagnetic fields of attenuated and annular Gaussian laser modes Part II. Large F-number laser focusing," *JOSA B* (accepted for publication, 2006).

- [5] S. Sepke and D. Umstadter, "Analytical solutions for the electromagnetic fields of flattened and annular Gaussian laser modes Part III. Arbitrary length pulses and spot sizes," *JOSA B* (accepted for publication, 2006).
- [6] D. Umstadter, S. Banerjee, S. Chen, S. Sepke, A. Maksimchuk, A. Valenzuela, A. Rousse, R. Shah, and K. Ta Phuoc, "Generation of ultrashort pulses of electrons, X-rays and optical pulses by relativistically strong light", AIP Conference Proceedings, SUPERSTRONG FIELDS IN PLASMAS: Third International Conference on Superstrong Fields in Plasmas, vol. 827, 86 (2006).
- [7] S. Sepke, Y.Y. Lau, J.P. Holloway, and, D. Umstadter, "Thomson Scattering and Ponderomotive Intermodulation within Standing Laser Beat Waves in Plasma," *Phys. Rev. E* 72, 026501 (2005).
- [8] D. Umstadter, S. Sepke, S.Y. Chen, "Relativistic Nonlinear Optics," *Advances in Atomic and Molecular Physics*, Chap. 7, 152 (2005).
- [9] D. Umstadter, "Einstein's impact on optics at the frontier," *Phys. Letts. A* 347, 121 (2005).
- [10] S. Banerjee, S. Sepke, R. Shah, A. Valenzuela, A. Maksimchuk, and D. Umstadter, "Optical Deflection and Temporal Characterization of an Ultrafast Laser-Produced Electron Beam," *Phys. Rev. Lett.* 95, 035004 (2005).
- [11] K. Ta Phuoc, F. Burgy, J.-P. Rousseau, V. Malka, A. Rousse, R. Shah, D. Umstadter, A. Pukhov and S. Kiselev, "Laser based synchrotron radiation," *Phys. Plasmas* 12, 023101 (2005).
- [12] T. Lin, A. Maksimchuk, D. Umstadter, "Electron angular distribution from ultrahigh-intensity-laser and solid targets interaction", *Quantum Electronics and Laser Science Conference, QELS '05*, vol. 3, 1816 (2005).
- [13] S. Chen, P. Zhang, W. Theobald, N. Saleh, M. Rever, A. Maksimchuk, D. Umstadter, D., "Observation of Relativistic Cross-Phase Modulation in High Intensity Laser-Plasma Interactions", *Quantum Electronics and Laser Science Conference, QELS '05*, vol. 3, 1558 (2005).
- [14] S. M. Sepke, S. Banerjee, R. Shah, A. Valenzuela, D. Umstadter, "Vacuum scattering technique for wakefield electron beam diagnostic and conditioning measurements ", *Quantum Electronics and Laser Science Conference, QELS '05* , vol. 3, 1819 (2005).
- [15] E. S. Dodd, J. K. Kim, and D. Umstadter, "Simulation of ultrashort electron pulse generation from optical injection into wake-field plasma waves," *Phys. Rev. E* 70, 056410 (2004).
- [16] A. Rousse, K. Ta Phuoc, R. Shah, A. Pukhov, F. Lefebvre, V. Malka, S. Kiselev, F. Burgy, J.-P. Rousseau, D. Umstadter, and D. Hulin, "Production of a keV X-Ray Beam from Synchrotron Radiation in Relativistic Laser-Plasma Interaction," *Phys. Rev. Lett.* 93, 135005 (2004).
- [17] D. Umstadter, "Relativistic Nonlinear Optics," *Encyclopedia of Modern Optics*, edited by Robert D. Guenther, Duncan G. Steel and Leopold Bayvel, Elsevier, Oxford, (2004), p. 289.



## Author Index

Acremann, Y. ....	148
Alabadi, H. ....	131,134,137
Alnaser, A.S. ....	89,96,97,104,105,108,110
Arms, D.A. ....	67,76
Bandrauk, A.D. ....	106
Bannister, M.E. ....	7,131,134,139
Beck, D. ....	155
Becker, K.H. ....	159
Belkacem, A. ....	118,119,122.1
Ben-Itzhak, I. ....	87,88,89
Berrah, N. ....	148,163
Bing, S. ....	108
Bocharova, I. ....	105
Bohn, J. L. ....	41
Bozek, J. ....	148
Braaten, E. ....	34
Bucksbaum, P. ....	148,260
Buth, C. ....	78,82
Carnes, K. D. ....	87,88,89
Cavalieri, A. ....	148
Chakraborty, H.S. ....	108,113
Chang, Z. ....	87,89,92,96,108,109,110
Chapman, H. ....	148
Chatzakis, I. ....	110
Cheng, S. ....	79
Chu, S.I. ....	167
Cocke, C. L. ....	87,89,96,97,104,105
Corkum, P.B. ....	106
Côté, R. ....	28
Cundiff, S. ....	171
Dalgarno, A. ....	175
Dantus, M. ....	178
DeMille, D. ....	182
DePaola, B.D. ....	52,87
DiMauro, L. ....	185
Ditmire, T. ....	189
Dooley, P.W. ....	106
Doyle, J. ....	193
Duan, Z. ....	92
Dufresne, M.E. ....	67,76
Dunford, R.W. ....	67,76,77,78,79,82
Ederer, D.L. ....	67,76,77,78
Eberly, J.H. ....	197
Esry, B.D. ....	72,87,88,89
Falcone, R.W. ....	119,148
Fayer, M. ....	148

## Author Index

Feagin, J.M. ....	201
Feuerstein, B. ....	112
Fogle, Jr., M.R. ....	131,134,137,139
Fritz, D. ....	148
Gaffney, K. ....	148,149,151
Gallagher, T.F. ....	205
Ghimire, S. ....	89,96
Gilbertson, S. ....	94
Glover, T.E. ....	94
Gordon, A. ....	81
Gould, P. ....	25
Greene, C. ....	68
Habib, A. ....	110
Hajdu, J. ....	148,150
Hale, J.W. ....	131,139
Harris, S. ....	148
Hastings, J. ....	148
Havener, C.C. ....	131,134,137,139
Head-Gordon, M. ....	119
Hedman, B. ....	148
Herman, P. ....	148
Herschbach, D. ....	23
Hertlein, M. ....	118,122.1
Ho, T-S. ....	253
Hodgsen, K. ....	148
Höhr, C.M. ....	67,76,77,78
Holland, M. ....	209
Isberg, J. ....	148
Jin, D. ....	44
Jones, R.R. ....	213
Kanter, E.P. ....	67,76,77,78,79,80
Kapteyn, H.C. ....	60,268
Kärtner, F.X. ....	81
Kasevich, M. ....	148
Klimov, V. ....	114
Kochur, A.G. ....	79
Krässig, B. ....	67,76,78,79,80
Krause, H.F. ....	4,131,132,136,137,139
Krejčík, P. ....	148
Kristic, P.S. ....	140
Landahl, E. C. ....	67,76,77,78
Landers, A. ....	105
Lee, K.F. ....	106
Lee, R. ....	148
Lee, T. ....	142
Légaré, F. ....	106

## Author Index

Leonard, M. ....	89
Leone, S. ....	119
Li, C. ....	92
Lin, C. D. ....	87,100
Lindenberg, A. ....	148,149
Litvinyuk, I.V. ....	87,89,96,97,104,105
Lucchese, R.R. ....	249
Lundeen, S.R. ....	8
Lunning, J. ....	148
Macek, J.H. ....	131,142,217
Manson, S.T. ....	221
Marhajan, C.M. ....	89,96,97,104,105
Mashiko, H. ....	94
McCurdy, C.W. ....	118,123
McKoy, V. ....	15
Meyer, F.W. ....	3,131,132,136,139
Minami, T. ....	141,142
Moon, E. ....	92
Msezane, A.Z. ....	225
Mukamel, S. ....	229
Murnane, M.M. ....	60
Nelson, K.A. ....	233
Neumark, D.M. ....	119
Niederhausen, T. ....	112,113
Nilsson, A. ....	148,149
Novotny, L. ....	237
Obreshkov, B. ....	113
Orel, A.E. ....	241
Orlando, T.M. ....	245
Osipov, T. ....	89,105
Ovchinnikov, S.Y. ....	142
Peterson, E.R. ....	76,77,78,79
Phaneuf, R.A. ....	19
Poliakoff, E.D. ....	249
Pratt, S.T. ....	78.
Rabitz, H. ....	253
Raithel, G. ....	48
Raman, C. ....	257
Ranitovic, P. ....	89,96,97,104,105
Ray, D. ....	105
Reinhold, C.O. ....	131,140,141
Reis, D.A. ....	148,260
Rescigno, T.N. ....	118,123
Richard, P. ....	87,108,109,110
Robicheaux, F. ....	264
Rocca, J.J. ....	268

## Author Index

Rohringer, N. ....	67,76,81
Rose-Petruck, C.G. ....	56
Rudati, J. ....	67,77
Santra, R. ....	67,76,77,78,81,82
Sayler, A.M. ....	88,89
Schoenlein, R.W. ....	119,127
Schultz, D.P. ....	131,141,142
Seideman, T. ....	63
Siegmann, H. ....	148
Shan, B. ....	108,109,110
Southoff, N. ....	1
Southworth, S.H. ....	67,76,77,78,79,80
Starace, A.F. ....	272
Stockman, M.I. ....	276
Stöhlker, T. ....	79
Stohr, J. ....	148,149,150
Stotler, D.P. ....	2
Tarnovsky, V. ....	159
Thomas, J.E. ....	37
Thomas, T.D. ....	11
Thumm, U. ....	87,108,112
Tong, X.M. ....	89,96,104
Ulrich, B. ....	89,96,105
Umstadter, D. ....	280
Van der Spoel, D. ....	148
Vane, C.R. ....	131,133,134,136,137,139
Vergara, L.I. ....	131,132
Villeneuve, D.M. ....	106
Wang, P.Q. ....	88,89,104
Weber, P. ....	148
Wehlitz, R. ....	80
Woody, N. ....	108
Ye, J. ....	32
Young, L. ....	67,76,77,78,79,80,82
Zamkov, M. ....	104,108,109,110
Zhang, H. ....	131,132

## Registered Participants (as of 8/17/2006)

Bannister, Mark E.  
Oak Ridge National Laboratory  
Physics Division, P.O. Box 2008  
Oak Ridge, TN 37831  
E-Mail: bannisterme@ornl.gov  
Phone: (865) 574-4700

Beck, Donald  
Michigan Technological University  
Physics Department  
Houghton, MI 49931  
E-Mail: donald@mtu.edu  
Phone: (906) 487-2019

Becker, Kurt  
Stevens Institute of Technology  
Department of Physics  
Hoboken, NJ 07030  
E-Mail: kbecker@stevens.edu  
Phone: (201) 216-5671

Belkacem, Ali  
Lawrence Berkeley National Laboratory  
Mail Stop: 2R0300  
Berkeley, California 94720  
E-Mail: abelkacem@lbl.gov  
Phone: (510) 486-7778

Ben-Itzhak, Itzhik  
J.R. Macdonald Laboratory, Kansas State University  
Physics Department, Cardwell Hall  
Manhattan, KS 66506  
E-Mail: ibi@phy.ksu.edu  
Phone: (785) 532-1636

Berrah, Nora  
Western Michigan University  
Physics Department, Everett Tower  
Kalamazoo, MI 49008  
E-Mail: nora.berrah@wmich.edu  
Phone: (269) 387-4955

Bohn, John  
University of Colorado  
JILA, UCB 440  
Boulder, CO 80309  
E-Mail: bohn@murphy.colorado.edu  
Phone: (303) 492-5426

Braaten, Eric  
Ohio State University  
191 W Woodruff Ave  
Columbus, OH 43210  
E-Mail: braaten@mps.ohio-state.edu  
Phone: (614) 688-4228

Bucksbaum, Philip H.  
Stanford University  
Pulse Center, Photon Sciences, SLAC  
Menlo Park, CA 94025  
E-Mail: phb@slac.stanford.edu  
Phone: (650) 926-5337

Casassa, Michael  
DOE/BES SC22.11  
19901 Germantown Road  
Germantown, MD 20585-1290  
E-Mail: michael.casassa@science.doe.gov  
Phone: (301) 903-0448

Chu, Shih-I  
University of Kansas  
Department of Chemistry, Malott Hall  
Lawrence, KS 66044  
E-Mail: sichu@ku.edu  
Phone: (785) 864-4094

Cocke, C.L.  
J.R. Macdonald Laboratory, Kansas State University  
Physics Department, Cardwell Hall  
Manhattan, KS 66506  
E-Mail: cocke@phys.ksu.edu  
Phone: (785) 532-1609

Conover, Charles  
Colby College/National Science Foundation  
Department of Physics and Astronomy  
5860 Mayflower Hill Drive  
Waterville, ME 04901  
E-Mail: cconover@nsf.gov  
Phone: (207) 859-5864

Côté, Robin  
University of Connecticut  
Physics Department U-3046  
2152 Hillside Road  
Storrs, CT 06269  
E-Mail: rcote@phys.uconn.edu  
Phone: (860) 486-4912

## Registered Participants

Crisp, Michael  
Office of Fusion Energy Sciences  
U.S. Department of Energy  
1000 Independence Ave, SW  
Washington, DC 20585  
E-Mail: Michael.Crisp@Science.doe.gov  
Phone: (301) 903-4883

Cundiff, Steve  
University of Colorado  
JILA, UCB 440  
Boulder, CO 80309  
E-Mail: cundiffs@jila.colorado.edu  
Phone: (303) 492-6807

Dalgarno, Alexander  
Harvard-Smithsonian Center for Astrophysics  
60 Garden St  
Cambridge, MA 02138  
E-Mail: adalgarno@cfa.harvard.edu  
Phone: (617) 495-4403

Dantus, Marcos  
Michigan State University  
58 Chemistry Building  
East Lansing, MI 48864  
E-Mail: dantus@msu.edu  
Phone: (517) 355-9715 x314

DeMille, David  
Yale University  
Physics Department, P.O. Box 208120  
New Haven, CT 06520  
E-Mail: david.demille@yale.edu  
Phone: (203) 432-3833

DePaola, Brett D.  
J.R. Macdonald Laboratory, Kansas State University  
Physics Department, Cardwell Hall  
Manhattan, KS 66506  
E-Mail: depaola@phys.ksu.edu  
Phone: (785) 532-6777

DiMauro, Louis  
The Ohio State University  
Department of Physics  
Columbus, OH 43210  
E-Mail: dimauro@mps.ohio-state.edu  
Phone: (614) 688-5726

Ditmire, Todd  
University of Texas  
Department of Physics  
Austin, TX 78712  
E-Mail: tditmire@physics.utexas.edu  
Phone: (512) 471-3296

Doyle, John  
Harvard University  
17 Oxford Street  
Cambridge, MA 02138  
E-Mail: doyle@physics.harvard.edu  
Phone: (617) 495-3201

Dunford, Robert  
Argonne National Laboratory  
9700 S. Cass Ave  
Argonne, IL 60439  
E-Mail: dunford@anl.gov  
Phone: (630) 252-4052

Eberly, Joseph H.  
University of Rochester  
Wilson Blvd.  
Rochester, NY 14627  
E-Mail: eberly@pas.rochester.edu  
Phone: (585) 275-4351

Esry, Brett  
JR Macdonald Lab, Kansas State University  
Department of Physics, Cardwell Hall  
Manhattan, KS 66506  
E-Mail: esry@phys.ksu.edu  
Phone: (785) 532-1620

Feagin, Jim M.  
California State University Fullerton  
800 North State College Blvd  
Fullerton, CA 92834  
E-Mail: jfeagin@fullerton.edu  
Phone: (714) 278-3366

Gould, Phillip  
University of Connecticut  
Physics Dept., U-3046  
2152 Hillside Rd.  
Storrs, CT 06269  
E-Mail: phillip.gould@uconn.edu  
Phone: (860) 486-2950

## Registered Participants

Greene, Chris  
University of Colorado  
JILA, UCB 440  
Boulder, CO 80309  
E-Mail: chris.greene@colorado.edu  
Phone: (303) 492-4770

Hilderbrandt, Richard  
DOE/BES SC22.11  
19901 Germantown Road  
Washington, DC 20585  
E-Mail: richard.hilderbrandt@science.doe.gov  
Phone: (301) 903-0035

Jin, Deborah  
University of Colorado  
JILA, UCB 441  
Boulder, CO 80309-0440  
E-Mail: jin@jilau1.colorado.edu  
Phone: (303) 492-7746

Kanter, Elliot P.  
Argonne National Laboratory  
9700 S. Cass Avenue  
Argonne, IL 60439  
E-Mail: kanter@anl.gov  
Phone: (630) 252-4050

Klimov, Victor  
Los Alamos National Laboratory  
MS J567  
Los Alamos, NM 87545  
E-Mail: klimov@lanl.gov  
Phone: (505) 665-8284

Krause, Herbert F.  
Oak Ridge National Laboratory  
Physics Division, P.O. Box 2008  
Oak Ridge, TN 37831  
E-Mail: krausehf@ornl.gov  
Phone: (865) 574-5049

Lucchese, Robert  
Texas A&M University  
Department of Chemistry  
College Station, TX 77843  
E-Mail: lucchese@mail.chem.tamu.edu  
Phone: (979) 845-0187

Herschbach, Dudley  
Harvard University  
Department of Chemistry,  
12 Oxford Street  
Cambridge, MA 02138  
E-Mail: herschbach@chemistry.harvard.edu  
Phone: (617) 495-3218

Holland, Murray  
University of Colorado  
JILA, UCB 440  
Boulder, CO 80309  
E-Mail: murray.holland@colorado.edu  
Phone: (303) 492-4172

Jones, Robert R.  
University of Virginia  
Physics Department, Box 400714  
Charlottesville, VA 22904  
E-Mail: rrj3c@virginia.edu  
Phone: (434) 924-3088

Kapteyn, Henry C.  
University of Colorado  
JILA, 440 UCB  
Boulder, CO 80309  
E-Mail: kapteyn@colorado.edu  
Phone: (303) 492 6763

Kraessig, Bertold  
Argonne National Laboratory  
9700 S. Cass Ave  
Argonne, IL 60525  
E-Mail: kraessig@anl.gov  
Phone: (630) 252-9230

Lin, Chii Dong  
JR Macdonald Lab, Kansas State University  
Dept. of Physics, Cardwell Hall  
manhattan, KS 66506  
E-Mail: cdlin@phys.ksu.edu  
Phone: (785) 532-1617

Lundeen, Stephen  
Colorado State University  
Dept. of Physics  
Fort Collins, CO 80523  
E-Mail: lundeen@lamar.colostate.edu  
Phone: (970) 491-6647

## Registered Participants

Macek, Joseph H.  
Univiversity Tennessee  
Oak Ridge National Laboratory  
401 Nielsen Physics Bldg.  
Knoxville, TN 37996  
E-Mail: jmacek@utk.edu  
Phone ☎865) 974-0770

Marceau, Diane  
DOE/BES SC22.1  
19901 Germantown Road  
Germantown, MD 20874  
E-Mail: diane.marceau@science.doe.gov  
Phone: (301) 903-0235

McKoy, Vincent  
California Institute of Technology  
1200 E. California Blvd.  
Pasadena, CA 91125  
E-Mail: mckoy@caltech.edu  
Phone: (626) 395-6545

Msezane, Alfred Z.  
Clark Atlanta University  
223 James P Brawley Drive, SW (Box 92)  
Atlanta, GA 30314  
E-Mail: amsezane@ctsps.cau.edu  
Phone: (404) 880-8663

Murnane, Margaret M.  
University of Colorado  
JILA, 440 UCB  
Boulder, CO 80309  
E-Mail: murnane@colorado.edu  
Phone: (303) 492-6763

Orlando, Thomas M.  
Georgia Institute of Technology  
1160 Bramlett Forest Trail  
Lawrenceville, GA 30045  
E-Mail: thomas.orlando@chemistry.gatech.edu  
Phone: (404) 894-822

Poliakoff, Erwin  
Louisiana State University  
Department of Chemistry  
Baton Rouge, LA 70803  
E-Mail: epoliak@lsu.edu  
Phone: (225) 578-2933

Manson, Steven  
Georgia State University  
Department of Physics and Astronomy  
Atlanta, GA 30303  
E-Mail: smanson@gsu.edu  
Phone: (404) 651-3082

McCurdy, C. William  
U. C. Davis and  
Lawrence Berkeley National Laboratory  
One Cyclotron Rd.  
Berkeley, CA 94720  
E-Mail: cwmccurdy@lbl.gov  
Phone: (510) 486-4283

Meyer, Fred W.  
Oak Ridge National Laboratory  
P.O. Box 2008  
Oak Ridge, TN 37831  
E-Mail: meyerfw@ornl.gov  
Phone: (865) 574-04705

Mukamel, Shaul  
University of California, Irvine  
516 Rowland Hall #433A  
Irvine, CA 92697  
E-Mail: smukamel@uci.edu  
Phone: (949) 824-7600

Orel, Ann E.  
Department of Applied Science  
UC Davis  
One Shields Ave.  
Davis, CA 95616  
E-Mail: aeorel@ucdavis.edu  
Phone: (530) 752-6025

Phaneuf, Ronald A.  
University of Nevada  
Department of Physics, 220  
Reno, NV 89557  
E-Mail: phaneuf@physics.unr.du  
Phone: (775) 784-6818

Raithel, Georg  
University of Michigan  
450 Church St.  
Ann Arbor, MI 48109  
E-Mail: graithel@umich.edu  
Phone: (734) 647-9031

## Registered Participants

Raman, Chandra  
Georgia Institute of Technology  
837 State St.  
Atlanta, GA 30332  
E-Mail: craman@gatech.edu  
Phone: (404) 894-9062

Reis, David A.  
University of Michigan  
450 Church Street  
Ann Arbor, MI 48109  
E-Mail: dreis@umich.edu  
Phone: (734) 763-9649

Rescigno, Thomas N.  
Lawrence Berkeley National Laboratory  
1 Cyclotron Rd. MS-50F  
Berkeley, CA 94720  
E-Mail: tnrescigno@lbl.gov  
Phone: (510) 486-8652

Richard, Patrick  
JR Macdonald Lab, Kansas State University  
Department of Physics, Cardwell Hall  
Manhattan, KS 66506  
E-Mail: richard@phys.ksu.edu  
Phone: (785) 539-5670

Robicheaux, Francis  
Auburn University  
206 Allison Lab  
Auburn University, AL 36849  
E-Mail: robicfj@auburn.edu  
Phone: (334) 844-4366

Rocca, Jorge  
Colorado State University  
ERC, 1320 Campus Delivery  
Fort Collins, CO 80523-1320  
E-Mail: rocca@engr.colostate.edu  
Phone: (970) 491-8371

Rose-Petruck, Christoph G.  
Brown University  
324 Brook Str, Box H  
Providence, RI 02912  
E-Mail: Christoph\_Rose-Petruck@brown.edu  
Phone: (401) 863-1533

Santra, Robin  
Argonne National Laboratory  
Physics Division, P.O. Box 2008  
Argonne, IL 60439  
E-Mail: rsantra@anl.gov  
Phone: (630) 252-4994

Sauthoff, Ned  
Oak Ridge National Laboratory  
ITER Project Office  
Oak Ridge, TN 37831  
E-Mail: sauthoffnr@ornl.gov  
Phone: (865) 574-5947

Schoenlein, Robert  
Lawrence Berkeley National Laboratory  
1 Cyclotron Rd. MS: 2-300  
Berkeley, CA 94720  
E-Mail: rwschoenlein@lbl.gov  
Phone: (510) 486-6557

Schultz, David R.  
Oak Ridge National Laboratory  
Physics Division, MS 6372, Bldg. 6010  
Oak Ridge, TN 37831  
E-Mail: schultzd@ornl.gov  
Phone: (865) 576-9461

Seideman, Tamar  
Northwestern University  
2145 Sheridan Road  
Evanston, IL 60208  
E-Mail: seideman@chem.northwestern.edu  
Phone: (847) 467-4979

Smith, Augustine  
Morehouse College  
830 Westview Dr SW  
Atlanta, GA 30314  
E-Mail: asmith@morehouse.edu  
Phone: (404) 215-2615

Southworth, Steve H.  
Argonne National Laboratory  
Bldg. 203, 9700 S. Cass Ave.  
Argonne, IL 60439  
E-Mail: southworth@anl.gov  
Phone: (630) 252-3894

## Registered Participants

Starace, Anthony F.  
The University of Nebraska  
Department of Physics & Astronomy, 116 Brace Lab  
Lincoln, NE 68588  
E-Mail: [astarace1@unl.edu](mailto:astarace1@unl.edu)  
Phone: (402) 472-2795

Stockman, Mark I.  
Georgia State University  
Department of Physics and Astronomy  
Atlanta, GA 30303  
E-Mail: [mstockman@gsu.edu](mailto:mstockman@gsu.edu)  
Phone: (404) 651-2779

Stotler, Daren P.  
Princeton University  
Princeton Plasma Physics Lab  
Princeton, NJ 08543  
E-Mail: [dstotler@pppl.gov](mailto:dstotler@pppl.gov)  
Phone: (609) 243-2063

Thomas, T. Darrah  
Oregon State University  
153 Gilbert Hall  
Corvallis, OR 97331  
E-Mail: [T.Darrah.Thomas@oregonstate.edu](mailto:T.Darrah.Thomas@oregonstate.edu)  
Phone: (541) 737-6711

Thomas, John  
Duke University  
Physics Department  
Durham, NC 27708  
E-Mail: [jet@phy.duke.edu](mailto:jet@phy.duke.edu)  
Phone: (919) 660-2508

Umstadter, Donald  
University of Nebraska, Lincoln  
212 Ferguson Hall  
Lincoln, NE 68522  
E-Mail: [dpu@unlserve.unl.edu](mailto:dpu@unlserve.unl.edu)  
Phone: (402) 472-8115

Ye, Jun  
University of Colorado  
JILA. UCB 440  
Boulder, CO 80309  
E-Mail: [ye@jila.colorado.edu](mailto:ye@jila.colorado.edu)  
Phone: (303) 735-3171

Young, Linda  
Argonne National Laboratory  
9700 S. Cass Ave.  
Argonne, IL 60439  
E-Mail: [young@anl.gov](mailto:young@anl.gov)  
Phone: (630) 252-8878